

**THE CATALYTIC ASYMMETRIC FISCHER INDOLIZATION
AND BEYOND**

Inaugural-Dissertation

zur

Erlangung des Doktorgrades

der Mathematisch-Naturwissenschaftlichen Fakultät

der Universität zu Köln

vorgelegt von

Steffen Müller

aus Einbeck

Köln 2012

Berichterstatter:

Prof. Dr. Benjamin List

Prof. Dr. Hans-Günther Schmalz

Prof. Dr. Neil K. Garg

Tag der mündlichen Prüfung: 24.01.2012

Für meine Familie

*“Wenn es gelingt, in dem dunkeln Gebiete der organischen Natur
auf einen lichten Punkt zu treffen, der uns wie einer der Eingänge erscheint,
durch die wir vielleicht auf die wahren Wege zur Erforschung
und Erkennung dieses Gebietes gelangen können,
so hat man immer Ursache sich Glück zu wünschen,
selbst wenn man sich der Unerschöpflichkeit des vorgesetzten Gegenstandes bewusst ist.“*

Friedrich Wöhler & Justus von Liebig
Annalen der Pharmacie **1832**, 3, 249.

Die vorliegende Arbeit entstand von Februar 2008 bis November 2011 am Max-Planck Institut für Kohlenforschung in Mülheim an der Ruhr unter der Anleitung von Prof. Dr. Benjamin List.

Für die Möglichkeit diese Arbeit in seinem Arbeitskreis anzufertigen und die interessante Themenstellung bin ich Herrn Prof. Dr. Benjamin List zu herzlichstem Dank verpflichtet. Durch seine kontinuierliche Unterstützung, das mir von ihm entgegengebrachte Vertrauen und die mir gewährten Freiheiten hat er diese Arbeit ermöglicht. Dafür gebührt ihm mein tiefster Dank.

Weiterhin danke ich Herrn Prof. Dr. Hans-Günther Schmalz für die freundliche Übernahme des Korreferats, Herrn Prof. Dr. Axel Klein für die Übernahme des Prüfungsvorsitzes sowie Herrn Dr. Martin Klußmann für die Übernahme des Prüfungsbeisitzes.

Mein Dank gilt außerdem all denjenigen, die Teile dieser Arbeit sorgfältig Korrektur gelesen haben: Dr. Martin Klußmann, Dr. Kevin M. Jones, Dr. Shikha Gandhi, Olga Lifchits, Manuel Mahlau, Kristina Zumbansen und Dr. Matthew J. Webber.

Ferner möchte ich mich bei allen Mitarbeitern der Arbeitsgruppe für die angenehme Arbeitsatmosphäre bedanken. Besonderer Dank gilt Dr. Matthew J. Webber, Ilija Čorić und Dr. Beatrice Bechi für die produktive Zusammenarbeit in einigen Teilgebieten dieser Arbeit, meinen ehemaligen Auszubildenden Matthias Miosga und Jens Truckenbrodt für ihren großen Einsatz sowie Hendrik van Thienen, Pascal Walkamp, Simone Marcus, Marianne Hannappel und Arno Döhring für die ausgezeichnete Organisation des Laborbetriebs. Herzlichster Dank gebührt ebenfalls Adrienne Hermes für die Unterstützung in administrativen Angelegenheiten.

Herzlich bedanke ich mich auch bei allen Mitarbeiterinnen und Mitarbeitern der Service Abteilungen für ihre großartige Unterstützung.

Ich danke dem Fonds der Chemischen Industrie für die Gewährung eines Kekulé-Stipendiums.

Mein größter Dank gebührt meiner Familie für Ihre fortwährende Unterstützung und Ihr unendliches Vertrauen. Vielen Dank.

Table of Contents

Table of Contents	I
Abstract	V
Kurzzusammenfassung.....	VI
List of Abbreviations	VII
1 Introduction	1
2 Background	4
2.1 Asymmetric Catalysis	4
2.2 Asymmetric Organocatalysis.....	5
2.2.1 Historical Development.....	5
2.2.2 Organizing the Chaos	7
2.3 Asymmetric Brønsted Acid Catalysis.....	8
2.3.1 General Brønsted Acid Catalysis	9
2.3.2 Specific Brønsted Acid Catalysis	11
2.4 Pericyclic Reactions.....	14
2.4.1 Cycloaddition Reactions	15
2.4.2 Sigmatropic Rearrangements.....	15
2.4.3 Electrocyclizations	17
2.4.4 Group Transfer Reactions	20
2.4.5 The Woodward-Hoffman Rules of Orbital Symmetry.....	21
2.5 The Fischer Indole Synthesis	23
2.5.1 Historical Background	23
2.5.2 Some Recent Developments	24
2.5.3 Chiral Indole Derivatives from Fischer Indolizations.....	26
2.6 Pyrazolines	30
2.7 Acetals in Nature and Organic Chemistry	31

3 Objectives of This PhD Work	35
3.1 Synthesis of SPINOL-Derived Phosphoric Acids and Disulfonimides	35
3.2 The Catalytic Asymmetric Fischer Indolization	36
3.3 Development of a Catalytic Asymmetric 6π Electrocyclization	38
3.4 Kinetic Resolution of Homoaldols via Intramolecular Transacetalization	40
4 Results and Discussion	42
4.1 Synthesis of SPINOL-Derived Phosphoric Acids and Disulfonimides	42
4.1.1 Synthesis of Racemic and Enantiomerically Pure SPINOL.....	42
4.1.2 Synthesis of Phosphoric Acids from Racemic SPINOL.....	43
4.1.3 Synthesis of Phosphoric Acids from Enantiomerically Pure SPINOL.....	47
4.1.4 Synthesis of SPINOL-Derived Disulfonimides.....	50
4.1.5 Structural Comparison of SPINOL-Derived Catalysts with their BINOL Analogs.....	52
4.1.5.1 Phosphoric Acids.....	53
4.1.5.2 Disulfonimides	54
4.1.6 Summary	55
4.2 The Catalytic Asymmetric Fischer Indolization	56
4.2.1 Synthesis of Chiral Indolenines via the Fischer Indole Synthesis.....	56
4.2.1.1 N-Acyl Enehydrazines as Potential Substrates	58
4.2.1.2 N,N'-Diphenylenehydrazines as Potential Substrates	62
4.2.1.3 The Thermal Approach	65
4.2.2 Synthesis of 3-Substituted Tetrahydrocarbazoles	74
4.2.2.1 N-Acyl Enehydrazines as Potential Substrates	75
4.2.2.2 The Thermal Approach	77
4.2.2.3 The Cation Exchange Approach.....	83
4.2.2.4 The Catalytic Asymmetric Fischer Indolization.....	88
4.2.2.5 Formal Synthesis of (S)-Ramatroban.....	93
4.2.3 Summary	94
4.3 Development of a Catalytic Asymmetric 6π Electrocyclization	96
4.3.2 Catalytic Asymmetric 6 π Electrocyclization of α,β -Unsaturated Arylhydrazones	102
4.3.3 Enantioselective Synthesis of 2-Pyrazolines from Enones and Phenylhydrazine.	105
4.3.4 Mechanistic considerations	108

4.3.5 Diastereoselective Alkylations of 2-Pyrazolines.....	111
4.3.6 Summary	116
4.4 Kinetic Resolution of Homoaldols via a SPINOL-Derived Phosphoric Acid	
Catalyzed Asymmetric Intramolecular Transacetalization	117
4.4.1 Optimization of Reaction Conditions	117
4.4.2 Resolution of Secondary Homoaldols	122
4.4.3 Resolution of Tertiary Homoaldols	125
4.4.4 Mechanistic Considerations	127
4.4.5 Applications of Resolved Homoaldols.....	131
4.4.6 Summary	133
4.5 Synthesis of Substrates	135
4.5.1 Substrates for the Indolization of Cyclohexanone-derived Phenylhydrazones....	135
4.5.1.1 Synthesis of 4-Substituted Cyclohexanones	135
4.5.1.2 Synthesis of N-Substituted N-Arylhydrazines	137
4.5.1.3 Synthesis of Arylhydrazones.....	138
4.5.2 Substrates for the Catalytic Asymmetric 6 π Electrocyclization	141
4.5.2.1 Synthesis of α,β -Unsaturated Ketones	141
4.5.2.2 Synthesis of α,β -Unsaturated Arylhydrazones	142
4.5.3 Synthesis of Racemic Acetal Protected Aldehyde Homoaldols	143
5 Summary.....	146
6 Outlook	155
6.1 SPINOL-Derived Catalysts.....	155
6.2 The Catalytic Asymmetric Fischer Indolization	157
6.3 The Catalytic Asymmetric 6π Electrocyclization	158
6.4 STRIP-Catalyzed Kinetic Resolution of Homoaldols	159
7 Experimental Part.....	162
7.1 General Experimental Conditions	162
7.2 Synthesis of BINOL-, H₈-BINOL-, VAPOL- and TADDOL-Derived Catalysts.....	166
7.3 Synthesis of SPINOL-Derived Phosphoric Acids and Disulfonimides	168

7.3.1 SPINOL-Derived Phosphoric Acids.....	168
7.3.2 SPINOL-Derived Disulfonimides	188
7.4 The Catalytic Asymmetric Fischer Indolization	193
7.4.1 Indolenines and Indolines	193
7.4.1.1 Indolenines from Enehydrazines	193
7.4.1.2 Fischer Indolizations of Phenylhydrazones from α -Branched Aldehydes.....	194
7.4.2 Tetrahydrocarbazoles.....	198
7.4.2.1 Synthesis of Hydrazines.....	198
7.4.2.2 Synthesis of Ketones.....	206
7.4.2.3 Synthesis of Hydrazones.....	219
7.4.2.4 Synthesis of Tetrahydrocarbazoles with Different Protecting Groups.....	237
7.4.2.5 Enantioselective Synthesis of 3-Substituted Tetrahydrocarbazoles.....	245
7.4.2.6 Large Scale Indolization and Formal Synthesis of (S)-Ramatroban	257
7.5 Catalytic Asymmetric 6π Electrocyclization.....	260
7.5.1 Synthesis of α,β -Unsaturated Ketones	260
7.5.2 Synthesis of α,β -Unsaturated Arylhydrazones.....	266
7.5.3 Synthesis of 2-Pyrazolines	274
7.5.4 Derivatizations of 2-Pyrazolines.....	285
7.6 STRIP-Catalyzed Kinetic Resolution of Homoaldols	290
7.6.1 Synthesis of Racemic Homoaldols.....	290
7.6.2 Kinetic Resolution of Racemic Homoaldols.....	304
7.6.3 Transformations of Resolved Homoaldols	323
7.7 X-Ray Crystal Structure Data	327
8 Bibliography	361
9 Appendix.....	375
9.1 Erklärung	375
9.2 Lebenslauf	376

Abstract

The synthesis of new chiral Brønsted acids and their application in the catalytic asymmetric Fischer indolization, a catalytic asymmetric 6π electrocyclization, and the kinetic resolution of homoaldols are presented. In the course of this work, synthetic routes to novel spirocyclic C_2 -symmetric phosphoric acids and disulfonimides were developed. These structures represent new and complementary tools for enantioselective catalysis. In the realization of a catalytic asymmetric Fischer indolization, catalyst poisoning by the basic ammonia by-product was identified as the major challenge associated with the utilization of only substoichiometric amounts of a chiral Brønsted acid promoter. Different potential solutions to this problem were explored, eventually leading to the first catalytic asymmetric Fischer indolization. This reaction enabled the efficient and highly enantioselective synthesis of 3-substituted tetrahydrocarbazoles from 4-substituted cyclohexanone-derived phenylhydrazones in the presence of a 5 mol% loading of a novel spirocyclic chiral phosphoric acid and an ion exchange resin as ammonia scavenger. Inspired by this project, another class of hydrazones, derived from α,β -unsaturated ketones, was employed as substrates for the first catalytic asymmetric 6π electrocyclization. The chiral Brønsted acid-catalyzed cyclization of these substrates – isoelectronic to the 6π electrocyclization of the pentadienyl anion – afforded 2-pyrazolines in high yields and enantioselectivities. The synthetic utility of the obtained products was exemplified by the development of some highly diastereoselective subsequent transformations. Furthermore, one of the newly developed spirocyclic phosphoric acids was identified as a highly efficient catalyst for the kinetic resolution of γ -hydroxy acetals via an intramolecular transacetalization reaction. The combination of a kinetic resolution and a parallel kinetic resolution renders this methodology highly efficient for both secondary and tertiary homoaldols. The versatility of this process was amongst others demonstrated in the enantioselective synthesis of a γ -butyrolactone natural product.

Kurzzusammenfassung

Die Synthese neuer chiraler Brønsted-Säuren und deren Verwendung in der katalytisch-asymmetrischen Fischer Indolisierung, einer katalytisch-asymmetrischen 6π Elektrocyclisierung sowie in der kinetischen Racematspaltung von Homoaldolen werden vorgestellt. Im Rahmen dieser Arbeit wurden Syntheserouten zu neuen, spirocyclischen, C_2 -symmetrischen Phosphorsäuren und Disulfonimiden als komplementäre Werkzeuge für die asymmetrische Katalyse erschlossen. Bei der Realisierung einer katalytisch-asymmetrischen Fischer Indolisierung stellte sich die Deaktivierung des Katalysators durch basisches Ammoniak, das als Nebenprodukt der Reaktion anfällt, als Hauptproblem für die Verwendung substöchiometrischer Mengen chiraler Brønsted-Säuren heraus. Es wurden unterschiedliche Lösungsansätze für dieses Problem untersucht, von denen schließlich einer zur Entwicklung der ersten katalytisch-asymmetrischen Fischer Indolisierung führte. Diese Reaktion ermöglichte die effiziente und hochgradig enantioselektive Synthese 3-substituierter Tetrahydrocarbazole. Die Indolisierung der Hydrazone 4-substituierter Cyclohexanone gelang in Gegenwart von 5 Mol-% einer neuen spirocyclischen chiralen Phosphorsäure und einem Ionenaustauscher zur Entfernung des Ammoniaks. In Anlehnung an dieses Projekt wurde eine andere Klasse von Hydrazonen, abgeleitet von α,β -ungesättigten Ketonen, in der ersten katalytisch-asymmetrischen 6π Elektrocyclisierung eingesetzt. Die von einer chiralen Brønsted-Säure katalysierte Cyclisierung dieser Substrate – isoelektronisch zur 6π Elektrocyclisierung des Pentadienylanions – lieferte 2-Pyrazoline in hohen Ausbeuten und Enantioselektivitäten. Der synthetische Nutzen der erhaltenen Produkte wurde in der Entwicklung hochgradig diastereoselektiver Derivatisierungen veranschaulicht. Außerdem stellte sich eine neu entwickelte spirocyclische Phosphorsäure als hervorragender Katalysator für die kinetische Racematspaltung von γ -Hydroxyacetalen mittels einer extrem leistungsstarken intramolekularen Transacetalisierung heraus. Durch die Kombination einer kinetischen Racematspaltung und einer parallelen kinetischen Racematspaltung ist diese Methode gleichsam effizient für sekundäre und tertiäre Homoaldole. Die erhaltenen Homoaldole wurden unter anderem in der enantioselektiven Naturstoffsynthese eines γ -Butyrolactons weiterverwendet.

List of Abbreviations

Ac	acetyl
aq.	aqueous
Ar	aryl
atm	atmosphere
BINAP	2,2'-bis(diphenylphosphino)-1,1'-binaphthyl
BINOL	1,1'-bi-naphthol
Bn	benzyl
Boc	<i>tert</i> -butyloxycarbonyl
bp	boiling point
Bu	butyl
Bz	benzoyl
c	concentration
Cat.	catalyst
Cbz	carbobenzyloxy
CC	column chromatography
CG50	Amberlite CG50
CI	chemical ionisation
COD	1,5-cyclooctadiene
conc.	concentrated
conv.	conversion
Cy	cyclohexyl
d	day(s) or doublet
dba	dibenzylideneacetone
DET	diethyl tartrate
DME	dimethoxyethane
DMF	<i>N,N</i> -dimethylformamide
DMSO	dimethylsulfoxide
DPP	diphenyl phosphate
dr	diastereomeric ratio
ee	enantiomeric excess
EI	electron impact
<i>ent</i>	enantiomer(ic)
eq	equation
equiv	equivalent(s)
er	enantiomeric ratio
ESI	electrospray ionisation
Et	ethyl
FDA	U.S. Food and Drug Administration
FMO	frontier molecular orbital
GC	gas chromatography
h	hour(s)
H ₈ -BINOL	5,5',6,6',7,7',8,8'-octahydro-1,1'-bi-2-naphthol
HOMO	highest occupied molecular orbital
HPLC	high performance liquid chromatography
HRMS	high resolution mass spectrometry

<i>i</i>	<i>iso</i>
LUMO	lowest unoccupied molecular orbital
M	molar (mol·L ⁻¹)
m	multiplet
<i>m</i>	<i>meta</i>
<i>m/z</i>	<i>atomic mass units per charge</i>
<i>m</i> CPBA	<i>meta</i> -chloroperoxybenzoic acid
Me	methyl
min	minute(s)
MOM	methoxymethyl
mp	melting point
MsOH	methanesulfonic acid
<i>n</i>	<i>normal</i>
n.d.	not determined
NCS	<i>N</i> -chlorosuccinimide
NMP	<i>N</i> -methyl-2-pyrrolidone
NOE	nuclear Overhauser effect
PCC	pyridinium chlorochromate
PG	protecting group
PIB	<i>para</i> -iodobenzyl
Ph	phenyl
NPhthal	phthalimidoyl
Pr	propyl
pybox	pyridine bis(oxazoline)
q	quartet
quant.	quantitative
r.t.	room temperature
<i>rac</i>	racemic
s	singlet
sat.	saturated
sept	septet
SPINOL	1,1'-spirobiindane-7,7'-diol
STRIP	6,6'-bis(2,4,6-triisopropylphenyl)-1,1'-spirobiindan-7,7'-diyl hydrogenphosphate
T	temperature
t	time or triplet
TADDOL	$\alpha,\alpha,\alpha',\alpha'$ -tetraaryl-1,3-dioxolan-4,5-dimethanol
TBACl	tetrabutylammonium chloride
TBHP	<i>tert</i> -butyl hydroperoxide
Tf	trifluoromethanesulfonyl
TFAA	trifluoroacetic anhydride
THF	tetrahydrofuran
TLC	thin layer chromatography
TMEDA	<i>N,N,N',N'</i> -tetramethylethylenediamine
TMS	trimethylsilyl
TRIP	3,3'-bis(2,4,6-triisopropylphenyl)-1,1'-binaphthyl-2,2'-diyl hydrogenphosphate
Ts	<i>para</i> -toluolsulfonyl
VAPOL	2,2'-diphenyl-(4-biphenanthrol)

1 Introduction

Chirality, the property of an object or system not being superposable with its mirror image, is a three dimensional phenomenon omnipresent in nature. Like amino acids, which occur almost exclusively as a single stereoisomer, the majority of chiral compounds in nature are produced with a strong preference for one enantiomer. While the origin of homochirality is still subject of speculation,^[1] its consequences for life are fairly well understood. A significant contribution to this awareness originated from the use of chiral compounds as therapeutic agents.

The use of natural products as medicinal agents can be traced back almost 5000 years, though of course without a scientific rationale at that time. In a Chinese book about herbs, the powdered roots of the plant *Dichroa febrifuga* are described to benefit the treatment of “fevers”. Modern analysis revealed several alkaloids with antimalarial activity to be present in the plant extract, amongst others β -dichroine (**1**) (Figure 1).^[2]

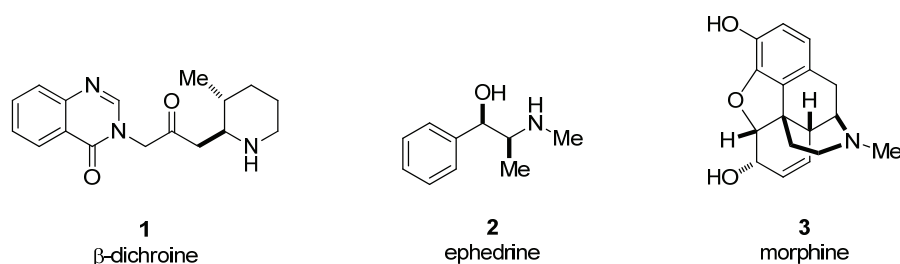


Figure 1. Enantiomerically pure natural products historically used for the treatment of diseases.

Other examples of natural products which were identified as biologically active ingredients of early medicinal plants are the stimulant ephedrine (**2**) from the gymnosperm shrub *Ephedra sinica*, and the potent analgesic morphine (**3**), a constituent of the dried seed capsule juice of the poppy *Papaver somniferum* (Figure 1). These chiral molecules share the common feature that nature produces them enantioselectively so that their use can be considered as treatment with single enantiomer drugs. Of course the awareness of chirality was lacking back then and it was only in the middle of the 19th century when the fundamental work by Pasteur,^[3] van't Hoff^[4] and LeBel^[5] set the basis for modern stereochemistry.^[6] At around the same time the enantiospecific action by enzymes on substrates was studied by Emil Fischer. He concluded that enzymes can only act on

substrates if the two fit like a lock and key.^[7] However, in the following century these fundamental findings of stereospecific interactions were largely ignored by pharmaceutical companies who had started to prepare synthetic drugs. Although many of these new structures were chiral, the separate investigation of each enantiomer played only a minor role and companies were not much interested in producing single enantiomer drugs unless nature provided them. Hence, the vast majority of chiral synthetic drugs were introduced as racemates during the 20th century.^[8] Only recently has the FDA and other international regulatory agencies issued strict guidelines concerning the development of new chiral drugs.^[9] Finally, after 5000 years of single enantiomer therapeutics and 100 years of racemic drugs, the development of stereochemically homogeneous drugs is common practice.

Consequently the global demand for chiral, non racemic compounds is continuously increasing. The soaring number of applications for enantiomerically pure molecules, most importantly in drug development, but also in agrochemicals, food industry and new materials is evidenced by a predicted annual market growth for chiral fine chemicals sold as single enantiomers of more than 10% and a total market value of US\$ 7000 million in 2002.^[10] The strongest driving force for this development is by far the pharmaceutical industry, accounting for more than 80% of the complete market.^[10a] The traditional ways to access these valuable products are resolution or diastereoselective chemical synthesis. The later involves an already enantiomerically enriched precursor such as a chiral auxiliary, mainly derived from the chiral pool. However, these methods involve some severe drawbacks as the resolution of a racemate can usually only provide a maximum yield of 50% of the desired enantiomer, and the auxiliary approach requires stoichiometric amounts of a suitable and readily available chiral precursor and generates equimolar quantities of by-products. Despite these drawbacks, resolution and chiral pool chemistry accounted for 55% of the US\$ 7000 million in revenues worldwide from chiral products in 2002.^[10b]

An alternative to these classical approaches is asymmetric catalysis.^[11] In asymmetric catalysis each molecule of a chiral, non racemic catalyst can transfer the chiral information to a theoretically infinite number of product molecules by being continuously regenerated during the reaction. In this respect, asymmetric catalysis can be considered the biomimetic approach to enantiomerically enriched products, since nature uses the same concept in the

stereoselective biosynthesis by enzymes. Only recently have chemical methods been developed to a level at which enantioselectivities comparable to that of enzymes (approaching 100% enantiomeric excess) can be achieved in certain transformations. In appreciation of these achievements and the recognition of asymmetric catalysis as future technology, the 2001 Nobel prize for chemistry was awarded to William Knowles and Ryoji Noyori "*for their work on chirally catalysed hydrogenation reactions*" and to K. Barry Sharpless "*for his work on chirally catalysed oxidation reactions*".^[12]

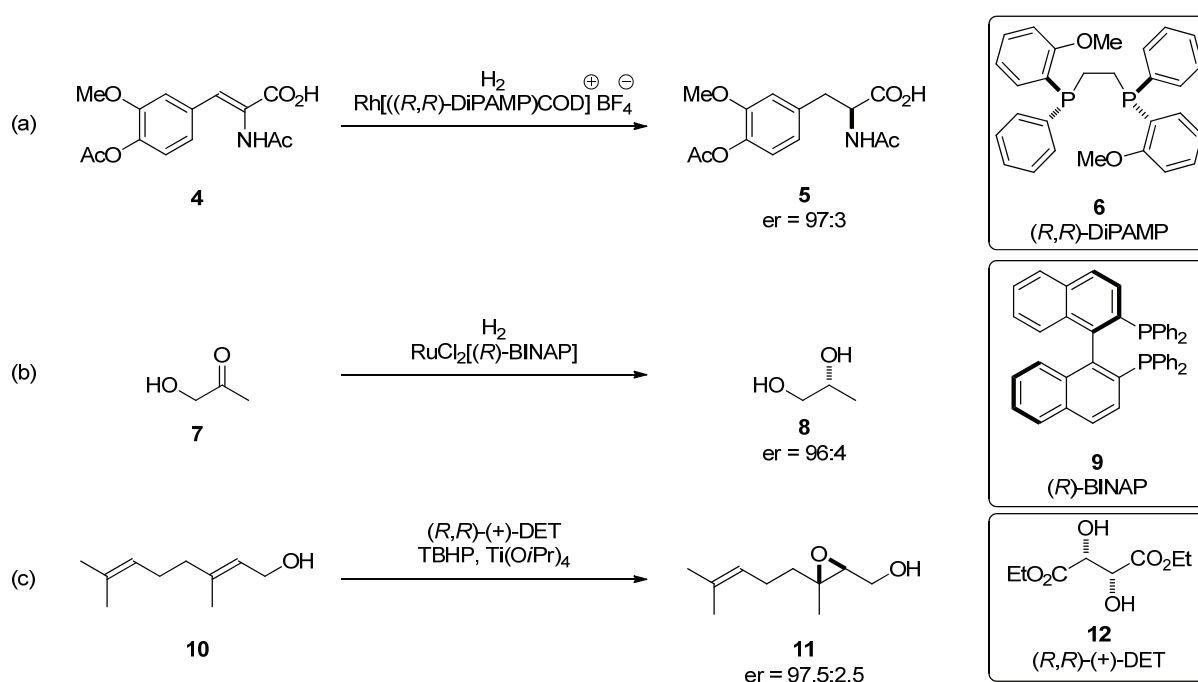
The early days of asymmetric catalysis were dominated by metal based catalysts and biocatalysts mainly represented by enzymes.^[13] Only recently has the potential of small, low molecular weight organic molecules as enantioselective catalysts been uncovered. Driven by an unprecedented interest in the development of new organocatalysts, this field was rapidly established as a complementary tool and now constitutes the third pillar of asymmetric catalysis.^[14] The work described in this thesis deals with a subgroup of organocatalysts, namely chiral organic Brønsted acids. These intriguing structures exhibit the possibility of using the most simple and probably most versatile catalytically active species, a simple proton, in the proximity of a chiral environment. Considering the number of chemical reactions amenable to Brønsted acid catalysis, this field of research offers seemingly boundless opportunities to be explored.

The following chapters review some of the most important and most recent developments in this area and provide background information about the underlying principles and reactions which were addressed in the course of the work described. Afterwards, the investigations conducted in the course of this PhD work, including catalyst design as well as the application of chiral Brønsted acids to long standing challenges in asymmetric catalysis such as the catalytic asymmetric Fischer indolization and the enantioselective catalysis of a 6π electrocyclozation are described. These seemingly unrelated projects will turn out to share unexpected parallels and reveal their common history, dating back more than 100 years.

2 Background

2.1 Asymmetric Catalysis

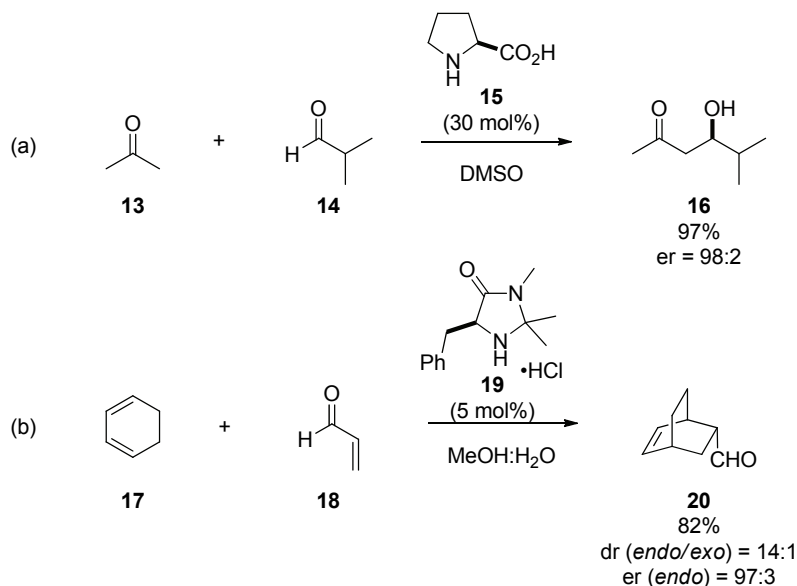
Asymmetric catalysis is characterized by the development and application of chiral, non racemic catalysts to transform achiral or racemic starting materials into enantioenriched compounds. What seemed to be an academic curiosity in the 1960s when the first reports appeared, has turned into one of the most investigated fields of research on the cutting edge of organic synthesis and organometallic chemistry today. In appreciation of their pioneering contributions to this new area of chemistry, the 2001 Nobel prize for chemistry was awarded to William Knowles and Ryoji Noyori who developed catalytic asymmetric reductions (Scheme 1a and b), and K. Barry Sharpless, who applied asymmetric catalysis to epoxidations (Scheme 1c) and hydroxylation reactions.



Scheme 1. Representative examples of landmark developments in asymmetric catalysis: Catalytic asymmetric hydrogenations by Knowles (a),^[15] Noyori (b)^[16] and asymmetric epoxidation by Sharpless (c).^[17]

After the recognition of asymmetric catalysis as future technology, many research groups in academia and industry joined the field and developed new catalysts for a variety of transformations.^[18] For around 40 years these man-made catalysts were mainly designed based on (transition) metals as the active principle.^[13] Only very recently the landmark

reports by List and MacMillan awakened the awareness that also purely organic molecules are able to act as highly enantioselective catalysts. While List *et al.* reported the proline (**15**) catalyzed direct asymmetric aldol reaction (Scheme 2a),^[19] the group of MacMillan employed chiral oxazolidinone salt **19** in enantioselective Diels-Alder reactions (Scheme 2b).^[20]



Scheme 2. Enantioselective catalysis of the direct aldol reaction (a), and a Diels Alder reaction (b) using metal free catalysts.^[19,20]

These impressive results together with the widespread strong interest in asymmetric catalysis as a whole resulted in the explosive growth of a new area in catalysis research, namely asymmetric organocatalysis. This field now constitutes, besides metal- and bio-catalysis, the third pillar of asymmetric catalysis.

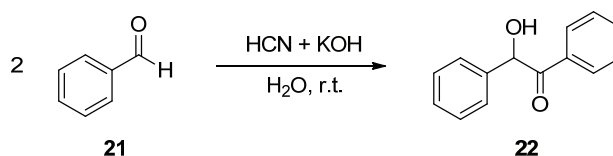
2.2 Asymmetric Organocatalysis

2.2.1 Historical Development

The development of asymmetric organocatalysis during the last decade was in every respect breathtaking. Based on some isolated examples of poorly understood reactions the field has grown into a multifaceted and blossoming area of seemingly unlimited opportunities within a few years. Especially its only very recent development is particularly

surprising in light of the long standing awareness of the potential of organic molecules as catalysts.^[21]

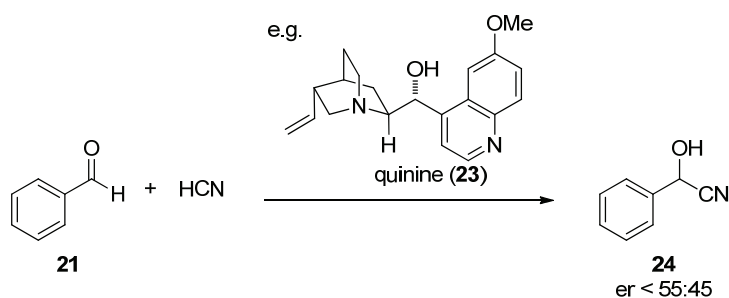
In 1832 Wöhler and Liebig studied the oil of bitter almonds and found that besides benzaldehyde (**21**), the oil was also containing hydrocyanic acid. When a sample of this oil was treated with potassium hydroxide, the formation of benzoin (**22**) was observed (Scheme 3).^[22]



Scheme 3. Cyanide-catalyzed benzoin-addition observed by Wöhler and Liebig.^[22]

In retrospect this observation can be explained by the nowadays well known cyanide-catalyzed benzoin reaction of benzaldehyde to form the α -hydroxy ketone **22**. Since the intermediate of this reaction is the potassium salt of the corresponding cyanohydrin, it is up to individual interpretation whether or not this particular example fulfils all the strict requirements to be considered purely organocatalytic in the light of today's standards. However, this work contributed to the awareness that organic entities like cyanide can act as nucleophilic catalysts.

The first example of an enantioselective organocatalytic reaction goes back to 1912, when Breiding reported the cinchona alkaloid **23** promoted addition of hydrogen cyanide to benzaldehyde (**21**) (Scheme 4).^[23] Although the reported enantioselectivities were low, the conceptual novelty of these insightful experiments should turn out to find the appreciation of generations of chemists in the following decades.^[24]



Scheme 4. Breiding's organocatalytic asymmetric cyanohydrin synthesis.^[23]

Following up on Breeding's work, chemists in the 20th century developed scattered examples of organocatalytic asymmetric transformations of which some were already reaching remarkable levels of enantioselectivity. Some key developments which are worth being mentioned in this context are the cinchona alkaloid-catalyzed addition of methanol to ketenes by Pracejus,^[25] and the proline-catalyzed intramolecular aldol reaction reported by Hajos and Parish as well as by Eder, Sauer and Wiechert.^[26] However, the general awareness of the potential of small organic molecules as enantioselective catalysts was only rising at the end of the last century when an increasing interest in the development of organocatalytic enantioselective transformations could be recognized. Eventually the field recorded an explosive growth after the landmark studies by the groups of List and MacMillan (see Scheme 2) and is currently amongst the most studied areas in organic chemistry.^[27]

2.2.2 Organizing the Chaos

One of the reasons accounting for the impressive interest in this emerging area as evidenced by the increasing number of publications each year (Figure 2)^[28] are definitely the advantages which organocatalysts offer over their metal-based or bio-derived counterparts. Organocatalysts are usually air and moisture stable and thus can be used under aerobic atmosphere in wet solvents. Since they do not contain toxic metals they are often supposed to be safer and more environmentally benign. Most importantly, however, seems the fact that organic chemists are, as a matter of course, more familiar with purely organic molecules, which do not involve d-orbitals or relativistic effects, rather than with transition metals, rendering the use of purely organic molecules as catalysts intuitively more attractive to them.

Remarkably multifaceted in catalyst classes employed as well as in reaction types described, the flood of scientific contributions in this area can be assigned to a small number of different categories. Berkessel and Gröger suggested the classification according to the mode of interaction between the substrate and the catalyst into *covalent catalysis*, in which covalent adducts between the substrate and the catalyst are formed, and *non-covalent catalysis*, which is characterized by non-covalent interactions such as hydrogen bonding between the substrate and the catalyst.^[27a]

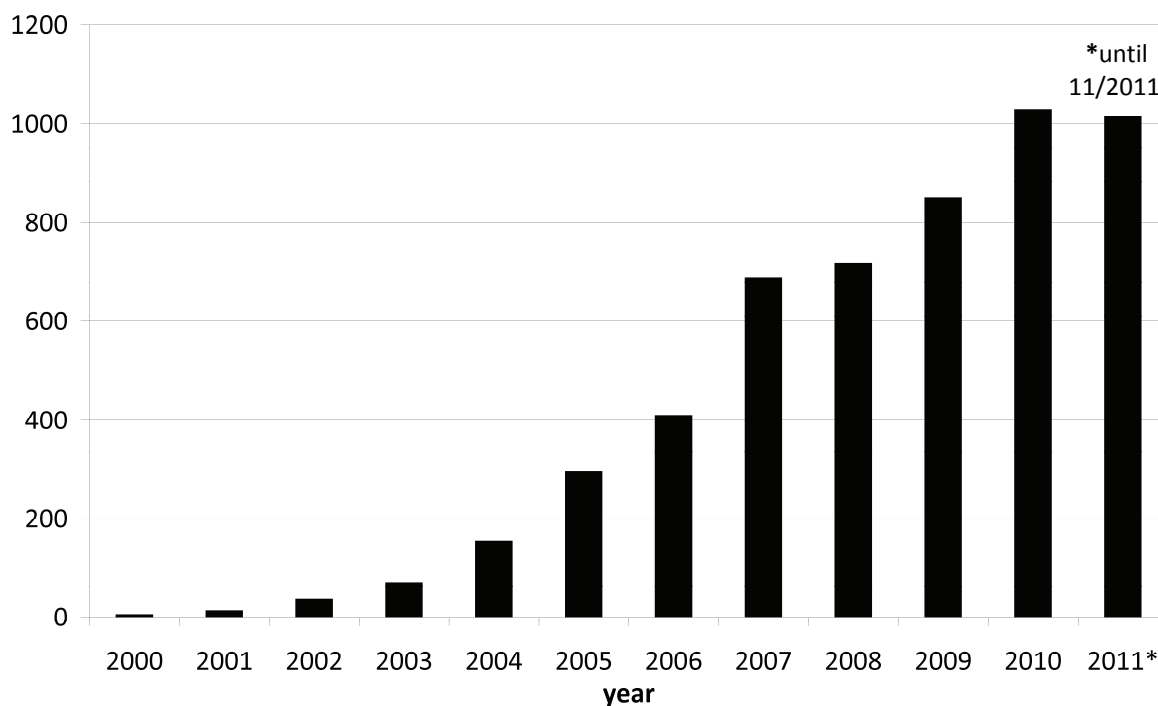


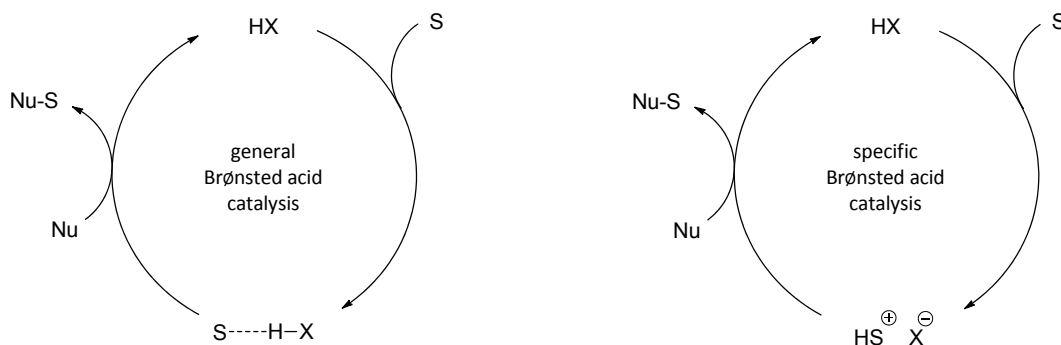
Figure 2. Annual number of publications containing the concept “organocatalysis”.^[28]

Another complementary way of classifying the vast majority of organocatalysts by their mode of action has been suggested by our group. According to this categorization, organocatalysts can either act by accepting an electron pair from or donating it to the substrate, the so called *Lewis acid catalysis* and *Lewis base catalysis*, or by accepting or donating a proton, the so called *Brønsted base catalysis* and *Brønsted acid catalysis*.^[29] Correspondingly, the studies conducted within this work are being best described as non-covalent catalysis with chiral Brønsted acids.

2.3 Asymmetric Brønsted Acid Catalysis

In 1923 the Danish chemist Johannes Nicolaus Brønsted and the English chemist Thomas Martin Lowry independently introduced a novel definition for acids and bases.^[30,31] According to the later so called Brønsted-Lowry theory, an acid is a molecule which is able to donate a proton, whereas a base is the corresponding counterpart which is able to accept a proton. In terms of catalysis this definition can be refined by the differentiation between general Brønsted acids and specific Brønsted acids.^[32] A general Brønsted acid catalyst activates the substrate (S) for nucleophilic attack (Nu) by hydrogen bond donation and

proton transfer occurs to the transition state in the rate determining step (Scheme 5, left). In the case of specific Brønsted acids the proton completely dissociates from the acid, resulting in the formation of an ion pair by reversible protonation of the substrate (S) in a pre-equilibrium (Scheme 5, right). In both cases this activation has a LUMO lowering effect and the activated functional group becomes more Lewis-acidic.

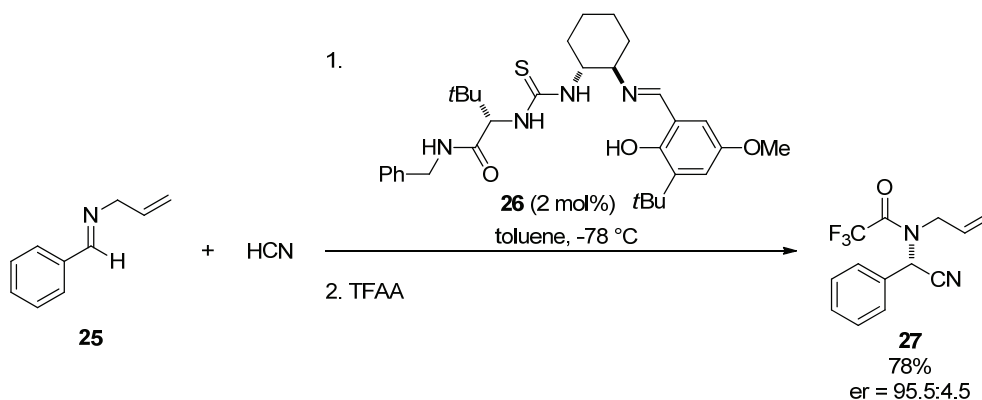


Scheme 5. Schematic catalytic cycles for general (left) and specific Brønsted acid catalysis (right).

To which one of these categories a given reaction belongs depends on the inherent difference in pK_a values of substrate and catalyst. Additionally, in many cases the assignment to either of these may be ambiguous.^[33]

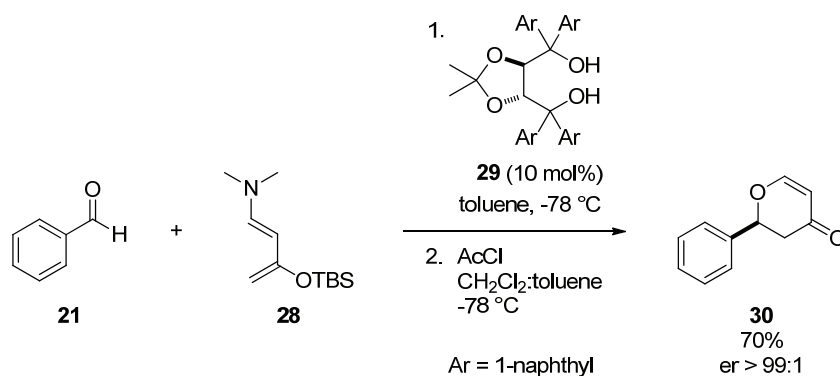
2.3.1 General Brønsted Acid Catalysis

Although nature has always used general Brønsted acid catalysis in the enzyme-mediated enantioselective synthesis of organic molecules, highly enantioselective man-made catalysts based on this activation mode were reported only very recently. In 1998 Jacobsen and co-workers coincidentally found that chiral thioureas like **26**, which were originally designed as ligands for metal catalysts, were highly efficient in promoting the asymmetric Strecker reaction between allyl imines **25** and hydrogen cyanide.^[34] The best catalyst identified promoted the 1,2-addition in good yields and enantioselectivities for a variety of aromatic and aliphatic imines (Scheme 6).



Scheme 6. Thiourea **26** catalyzed asymmetric Strecker reaction by Jacobsen and co-workers.^[34]

The first successful application of chiral diols as enantioselective hydrogen bonding catalysts was reported by the group of Rawal. Based on their observation that certain hetero Diels-Alder reactions were accelerated in alcoholic solvents,^[35] the group discovered that chiral TADDOL **29** was an efficient catalyst to promote this reaction highly enantioselectively (Scheme 7).^[36]

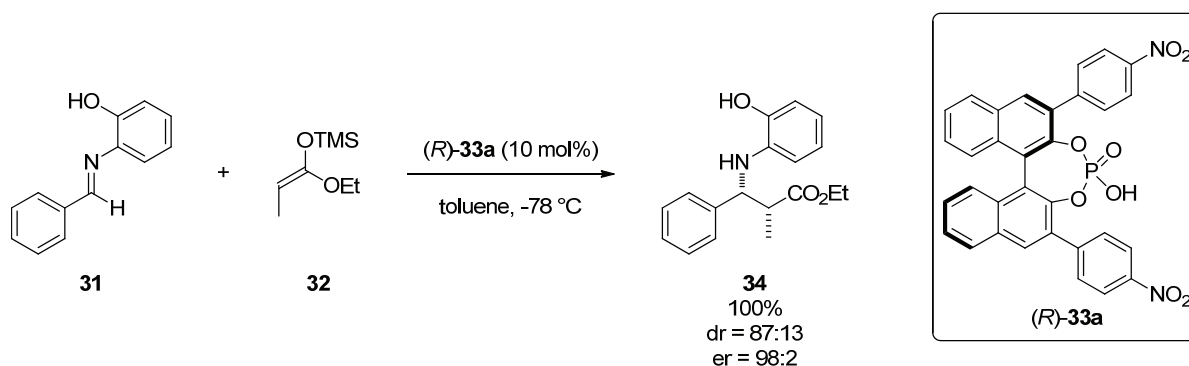


Scheme 7. TADDOL **29** catalyzed hetero Diels-Alder reaction between benzaldehyde (**21**) and diene **28** by Rawal and co-workers.^[36]

These examples illustrate the potential of chiral hydrogen bond donors to act as enantioselective catalysts in asymmetric transformations. Of course the groups of Jacobsen and Rawal have not been the only chemists working in this field and wonderful contributions including chiral catalysts based on thioureas, guanidinium and amidinium ions, squareimides, diols and many others more were published by numerous research groups around the world.^[32,37] However, while the area of general Brønsted acid catalysis is characterized by rather weak acids, a switch to specific Brønsted acid catalysis can be observed when going to stronger acids typically operating at pK_a (in DMSO) ≤ 4 .^[38]

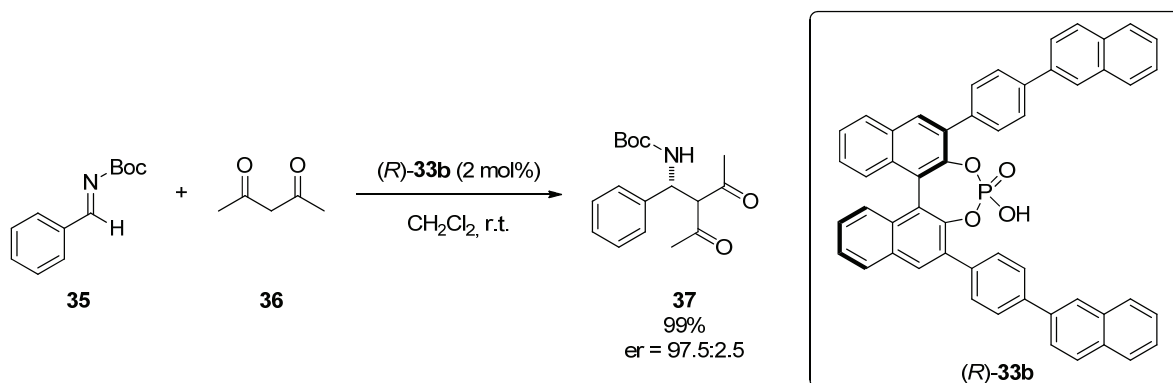
2.3.2 Specific Brønsted Acid Catalysis

Strong Brønsted acids like hydrochloric acid, polyphosphoric acid or *para*-toluenesulfonic acid have served as versatile catalysts in organic chemistry for decades. However, the successful development of chiral analogs providing access to products with high enantiomeric ratios was only accomplished recently. In 2004 the research group of Akiyama reported the use of BINOL-derived phosphoric acid (*R*)-**33a** as an efficient catalyst for the Mannich reaction between aryl imines of type **31** and silyl ketene acetal **32**.^[39] The corresponding β -amino esters like **34** were obtained in high yields and enantioselectivities (Scheme 8).



Scheme 8. Chiral phosphoric acid (*R*)-**33a** catalyzed Mannich reaction developed by Akiyama and co-workers.^[39]

At the same time, the group of Terada reported a similar phosphoric acid catalyst (*R*)-**33b**, differing only in the substituents in 3- and 3'-position, to efficiently catalyze the Mannich reaction between acetyl acetone (**36**) and aromatic *N*-Boc-imines **35** in impressive chemical and optical yield (Scheme 9).^[40]



Scheme 9. Chiral phosphoric acid (*R*)-**33b** catalyzed Mannich reaction as reported by Terada *et al.* in 2004.^[40]

Later on in 2010 Ishihara and co-workers reinvestigated this reaction and found that not the phosphoric acid, but rather its calcium salt, which was accidentally formed and not recognized as such, was accounting for the results obtained by the group of Terada.^[41] However, after these initial reports, chiral phosphoric acid catalysis received considerable attention and it was found that a large number of reactions, mainly involving imine substrates, were amenable to this kind of enantiofacial discriminating activation. This development came along with the synthesis and identification of new phosphoric acid catalysts. Besides the simple variation of the 3,3'-substituents of the BINOL backbone, some different chiral scaffolds were also investigated. In the course of this endeavour Akiyama and co-workers designed a new chiral TADDOL-derived phosphoric acid **38** as catalyst for Mannich type reactions,^[42] the VAPOL phosphoric acid (*R*)-**39** was used by Antilla *et al.* for imine amidations,^[43] and the group of Gong was the first to report high enantioselectivities with H₈-BINOL-derived phosphoric acid (*R*)-**40a** and applied it to the enantioselective Biginelli reaction (Figure 3).^[44] Furthermore, the chiral phosphoric acid **41** consisting of two BINOL-moieties was reported by Du and co-workers as catalyst for the transfer hydrogenation of quinolines^[45] and the dimeric phosphoric acid **42** was applied to a three component 1,3-dipolar cycloaddition by the group of Gong (Figure 3).^[46]

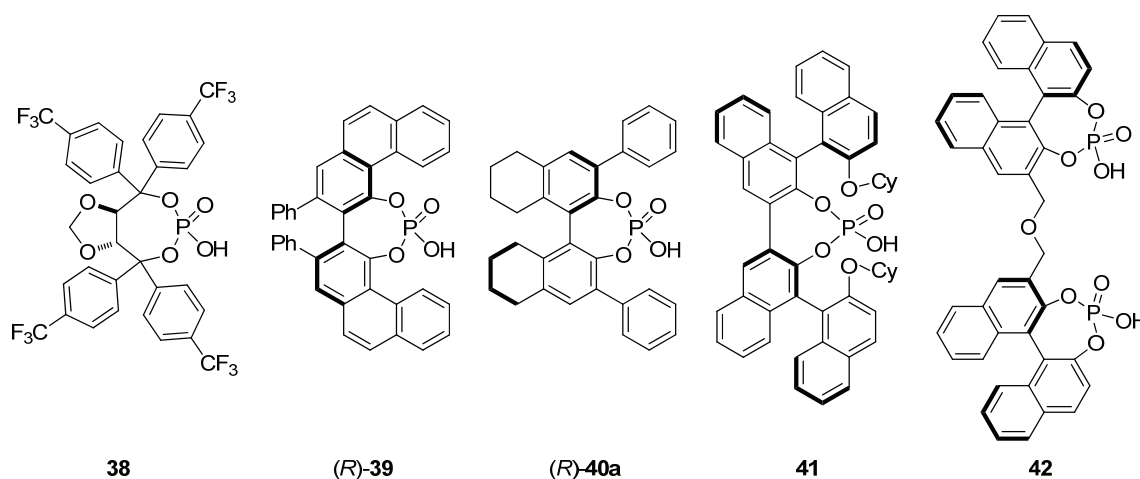


Figure 3. Overview of new chiral phosphoric acid motifs developed between 2004 and 2008.

In order to enable the efficient activation of different substrate classes, strong chiral Brønsted acids other than phosphoric acids were developed. The group of Terada developed phosphordiamidic acids of type **43** as catalysts for Mannich reactions of *N*-acyl imines with 1,3-dicarbonyl compounds.^[47] Based on the strongly acidifying effect of triflyl groups,^[48]

Yamamoto *et al.* designed the chiral *N*-triflyl phosphoramidate (*S*)-**44a** which was shown to be considerably more acidic than simple phosphoric acids and was used to activate enones for asymmetric Diels-Alder reactions with siloxydienes.^[49] A development towards an increased acidity is the dicarboxylic acid **45** which was used by Maruoka and co-workers in the context of enantioselective Mannich reactions of *N*-Boc-imines with diazo compounds.^[50]

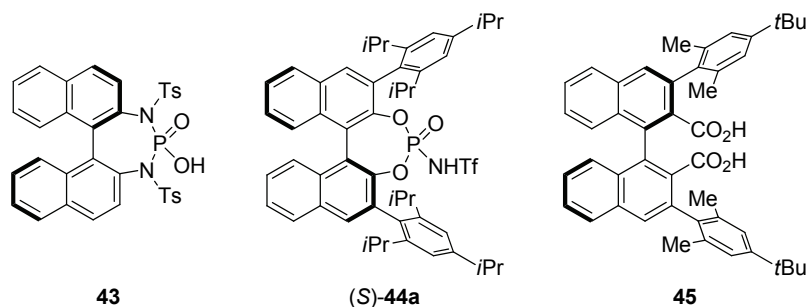


Figure 4. Successfully introduced strong chiral Brønsted acids other than phosphoric acids.

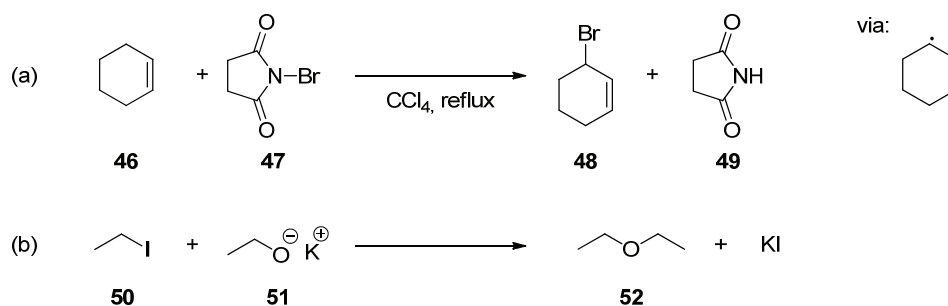
In light of the vast number of reactions which have already been successfully elaborated with these organic catalysts, the structural diversity of chiral strong Brønsted acidic catalysts can still be considered as quite limited. Besides the already above mentioned transformations, numerous other reactions including Friedel-Crafts reactions,^[51] Pictet-Spengler reactions,^[52] aza-ene type reactions,^[53] Strecker reactions,^[54] Baeyer-Villiger oxidations,^[55] Kabachnik-Fields reactions^[56] and many others more have been conducted enantioselectively by using chiral Brønsted acids.^[57] Notably, in the vast majority of these cases the BINOL-derived phosphoric acids **33** or their structurally closely related H₈-BINOL-derivatives **40** proved to be the catalyst of choice.

In summary, one can say that chiral phosphoric acids have emerged as extremely powerful organocatalysts over the last few years. Especially the BINOL-derived derivatives proved to be privileged structures, in particular for the activation of imine substrates. However, in light of the huge number of reactions which are amenable to Brønsted acid acceleration, the potential of strong chiral Brønsted acids has hardly been exhausted yet. One class of reactions which has only marginally been dealt with in this context are pericyclic reactions.

2.4 Pericyclic Reactions

In light of their large number, the classification of organic reactions may, upon first inspection, appear as an ambitious undertaking. However, every transformation in organic chemistry can be classified into one of only three distinct categories, namely radical, ionic and pericyclic reactions.^[58]

Radical reactions are characterized by the action of single electrons, usually generated by homolytic bond cleavage. A prominent example of this type of reaction is the Wohl-Ziegler bromination (Scheme 10a).^[59]



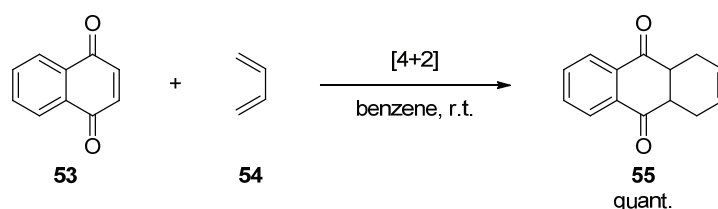
Scheme 10. (a) Wohl-Ziegler bromination of cyclohexene (**46**), a radical reaction.^[59c] (b) Williamson's ether synthesis, an ionic reaction.^[60]

The most abundant class of organic reactions are of ionic nature. These reactions are typically characterized by the action of paired electrons, although ironically, at least some of the reactions are known to proceed via single electron transfer.^[61] In an ionic transformation the nucleophilic reaction partner provides both electrons for the formation of the new bond. Examples of this reaction type are nucleophilic substitutions, e.g. in Williamson's ether synthesis (Scheme 10b).^[60]

The third class of organic reactions are the so called pericyclic reactions. Pericyclic reactions have a cyclic transition state in which the reorganization of electrons, all bond making and bond breaking events, occur simultaneously in a concerted manner. Generally there are four different reaction types which belong to this class, namely cycloadditions, sigmatropic rearrangements, electrocyclizations and group transfer reactions.

2.4.1 Cycloaddition Reactions

Cycloaddition reactions are characterized by two π -electron containing components reacting together to form two new σ -bonds at their termini, which are thereby incorporated into a new ring. A famous example is the Diels-Alder reaction,^[62] which is a [4+2] cycloaddition (Scheme 11).

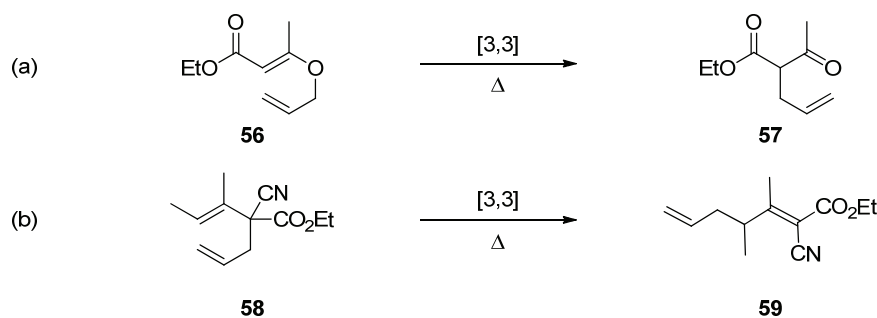


Scheme 11. Diels-Alder reaction of α -naphthoquinone (**53**) and butadiene (**54**).^[62]

Cycloaddition reactions are extremely useful in organic synthesis, since their chemo-, regio- and diastereoselectivity can easily be predicted by the Woodward-Hoffman rules and the FMO-theory (*vide infra*). Additionally, rather complex structures can reliably be assembled from simple starting materials in a single step. Consequently cycloaddition reactions are also the best studied pericyclic reactions in terms of asymmetric catalysis for both metal-based and metal-free catalyst systems. However, since cycloaddition reactions are not the subject of this thesis, they will not be discussed further at this point.^[63]

2.4.2 Sigmatropic Rearrangements

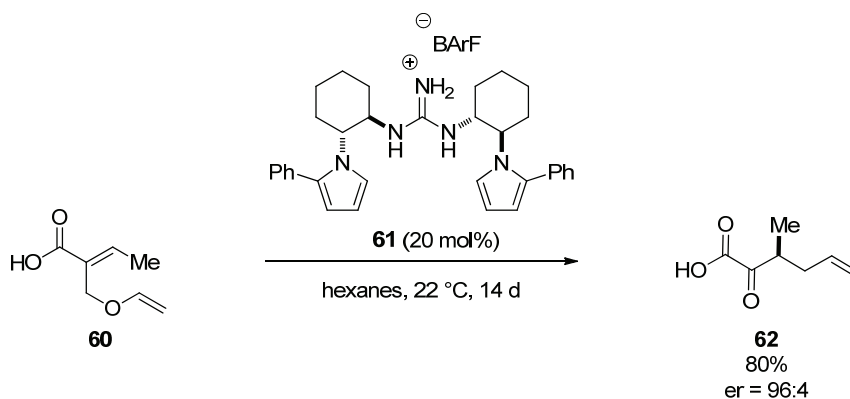
Sigmatropic rearrangements are intramolecular pericyclic reactions characterized by the overall movement of a σ -bond and the reorganization of the π -electrons in the periphery. The particular classification of sigmatropic rearrangements depends on the number of atoms between the position of the former σ -bond and the newly formed one. Famous examples are the Claisen-rearrangement of allyl vinyl ethers or the Cope rearrangement of 1,5-hexadienes. Already in 1912, Claisen reported that upon heating allyl vinyl ethers like **56** undergo a rearrangement to give *C*-allylated carbonyl compounds like **57** (Scheme 12a).^[64]



Scheme 12. (a) Claisen rearrangement of allyl vinyl ether **56**.^[64] (b) Cope rearrangement of the substituted 1,5-cyclohexadiene **58**.^[65]

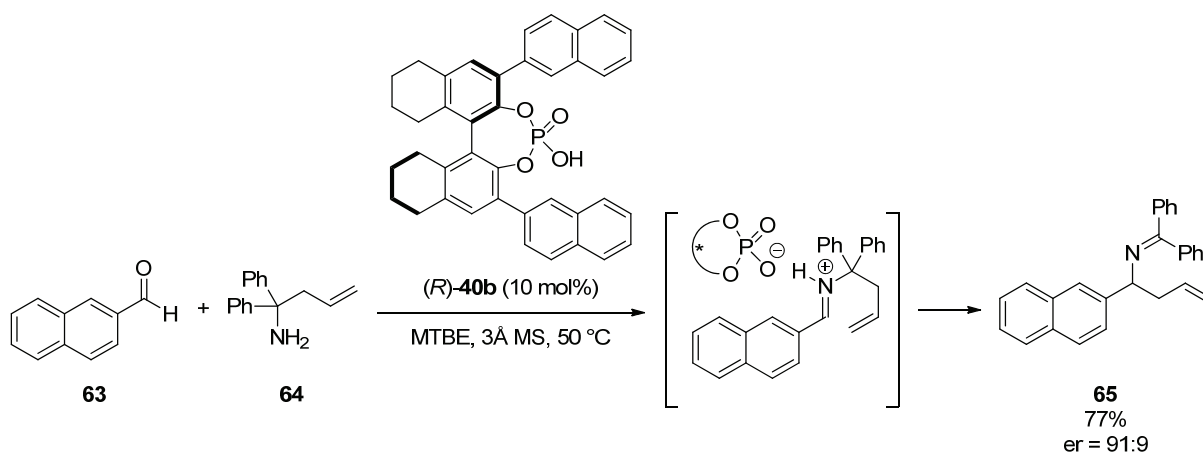
The corresponding reaction of the purely carbon based 1,5-diene **58** was discovered almost 30 years later by Cope and is since then referred to as the Cope rearrangement.^[65] According to the naming convention, both transformations can be classified as [3,3]-sigmatropic rearrangements.

An attractive feature which renders sigmatropic rearrangements powerful tools in organic synthesis is the remarkable substrate induced diastereoselectivity usually observed. As a result a large number of auxiliary based approaches for this type of stereoselective C-C-bond construction have been developed. More recently, efficient catalytic asymmetric methods have emerged, mainly relying on metal-based Lewis-acid catalysts.^[66] The first examples of metal-free systems for asymmetric sigmatropic rearrangements employed secondary amines,^[67] cinchona alkaloids^[68] and chiral Brønsted acids as catalysts. In 2008 the group of Jacobsen reported an enantioselective Claisen rearrangement catalyzed by the chiral guanidinium-salt **61**.^[69] In the presence of hydrogen-bonding catalyst **61** (20 mol%) allyl vinyl ethers like **60** rearranged under mild conditions, although at a low rate, to give the rearranged product of type **62** in high yields and enantioselectivities (Scheme 13).



Scheme 13. Chiral guanidinium-ion **61** catalyzed Claisen rearrangement.^[69]

In the same year, Rueping and Antonchick reported an enantioselective aza-Cope rearrangement, which was efficiently catalyzed by a chiral phosphoric acid.^[70] The reaction sequence consists of two subsequent steps. In the first step, allylamine **64** condenses with the aldehyde **63**. The resulting imine is then protonated by the phosphoric acid catalyst (*R*)-**40b** and the iminium ion undergoes the rearrangement in the chiral environment of the counteranion to give product **65** in good yield and enantioselectivity (Scheme 14).



Scheme 14. Aza-Cope rearrangement catalyzed by chiral phosphoric acid (*R*)-**40b**.^[70]

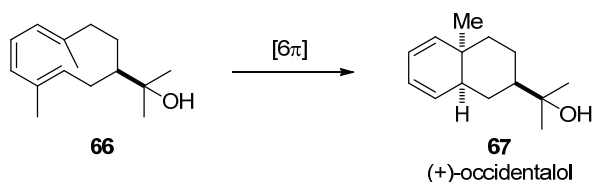
Although sigmatropic rearrangements are much less developed than cycloaddition reactions with respect to catalytic asymmetric variants, considerable progress has been made over the last years. The development of new efficient catalytic systems is advancing and novel metal free catalysts seem to bear high potential to significantly contribute to this development.

2.4.3 Electrocyclizations

Electrocyclizations involve the concerted cycloisomerization of a conjugated π -electron system. They are, in contrast to cycloadditions, which describe the reaction of two different components, unimolecular reactions. In the course of an electrocyclization two ends of a conjugated π -system react to form a new σ -bond at the overall expense of one π -bond. They are classified according to the number of π -electrons involved in the transition

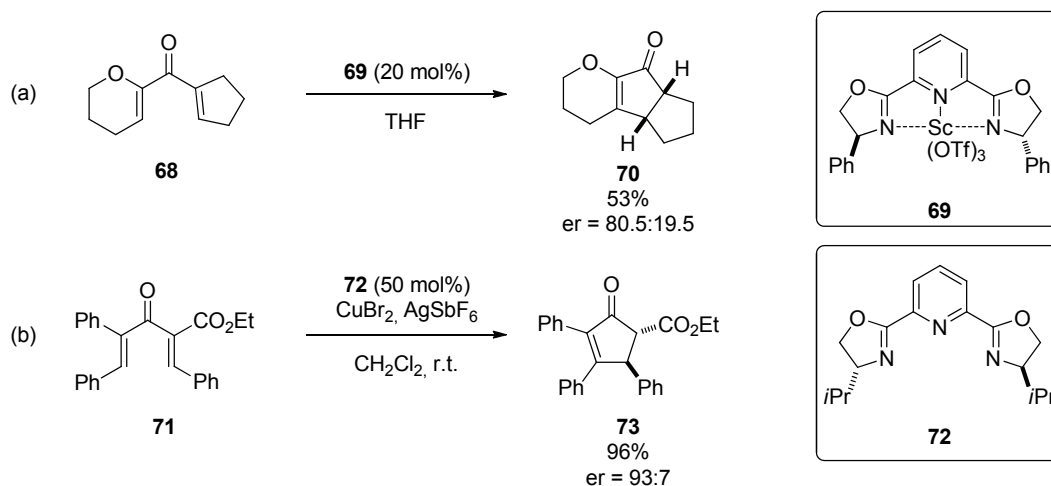
state. It is assumed that electrocyclizations play an important role in the biosynthesis of many natural products.^[71]

One example of a biosynthetic electrocyclization can be found in the synthesis of the eudesman-type sesquiterpene (+)-occidentalol (**67**), which was isolated from the wood of *Thuja occidentalis*.^[72] In the final step of the biosynthesis, the 1,3,5-decatriene **66** undergoes a 6π electrocyclization to form the natural product **67**.^[73]



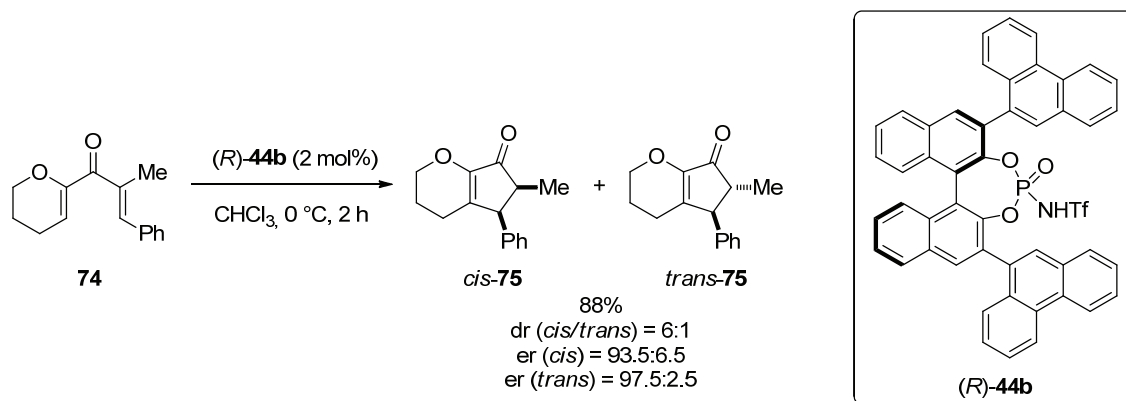
Scheme 15. Proposed 6π electrocyclization in the biosynthesis of (+)-occidentalol (**67**).

Inspired by nature, chemists frequently use electrocyclization strategies in the biomimetic synthesis of natural products.^[71] However, methods for influencing the rate of these reactions or their stereochemical outcome by means of catalysis are scarce and limited to a few notable exceptions. The Nazarov 4π electrocyclization is an important method for the construction of five membered ring carbocycles from divinyl ketones.^[74] The development of catalytic asymmetric versions of this reaction was pioneered by the research groups of Trauner and Aggarwal, who independently discovered that chiral Lewis acids were able to promote this reaction if a suitable ligand is used. Both groups identified chiral pybox ligands as the most efficient. While Trauner *et al.* used scandium complex **69** as catalyst (Scheme 16a),^[75] Aggarwal employed the copper complex of ligand **72** to promote the reaction (Scheme 16b).^[76] Whilst both methods have obvious drawbacks including moderate yields and enantioselectivities or high catalyst loadings, these reports represent the first examples of catalytic asymmetric electrocyclizations and the starting point for the development of more efficient protocols.^[75b]



Scheme 16. Catalytic asymmetric Nazarov cyclizations developed by the groups of Trauner (a) and Aggarwal (b).

The Nazarov cyclization was also the first electrocyclic reaction which was successfully promoted by a purely organic catalyst in an enantioselective manner. The group of Rueping applied the chiral *N*-triflyl phosphoramidate (*R*)-**44b** to the electrocyclic cyclization of divinyl ketones of type **74** and obtained the corresponding cyclopentenones **75** in high yields and good stereoselectivities (Scheme 17).^[77]

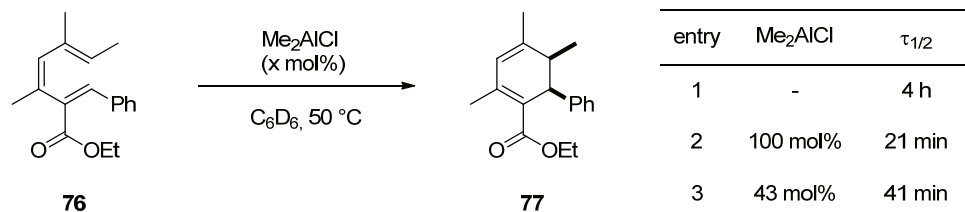


Scheme 17. Organocatalytic Nazarov cyclization developed by Rueping and co-workers.^[77]

Following up on this work, several groups reported on the use of new catalysts and other substrates in this transformation.^[78] However, the Nazarov 4π electrocyclic cyclization remained the only electrocyclic reaction which was found to be catalyzable in an asymmetric fashion.

The general feasibility of catalyzing 6π electrocyclic reactions was demonstrated by Bergmann, Trauner and co-workers only very recently. Supported by theoretical calculations they found that the electrocyclic cyclization of triene **76** could be significantly accelerated in the

presence of dimethylaluminum chloride as Lewis-acidic catalyst even at substoichiometric loadings (Scheme 18).^[79]

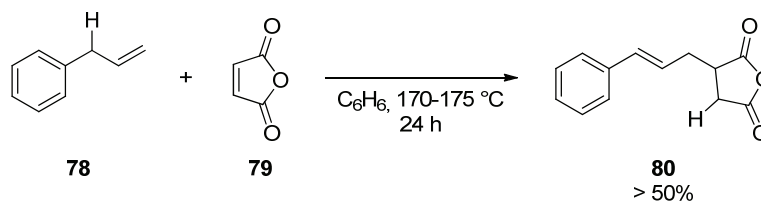


Scheme 18. Rate acceleration of the 6π electrocyclization of triene **76** in the presence of a Lewis acid catalyst.^[79]

Although these results suggested opportunities to overcome present limitations in the asymmetric catalysis of electrocyclizations different from the Nazarov reaction, further developments remained elusive.

2.4.4 Group Transfer Reactions

Group transfer reactions are the fourth and last class of pericyclic reactions. In the course of a group transfer reaction, a new σ-bond is formed at the expense of a π-bond. Due to only few transformations falling into this category, they are only of minor relevance from a synthetic chemist's viewpoint. The most frequently utilized group transfer reaction is the ene reaction, also known as Alder-ene reaction. One of the first Alder-ene reactions reported was the addition of allyl benzene (**78**) to maleic anhydride (**79**) under harsh reaction conditions to give the succinic anhydride **80** (Scheme 19).^[80]



Scheme 19. One of the first ene reactions discovered by Alder and co-workers.^[80]

Since the initial discovery in 1943, ene reactions have been studied extensively and numerous variations including other substrate classes and catalytic methods, requiring less harsh reaction conditions have been developed. Catalytic asymmetric ene reactions are usually promoted by chiral Lewis acids, but also first organocatalytic versions have been

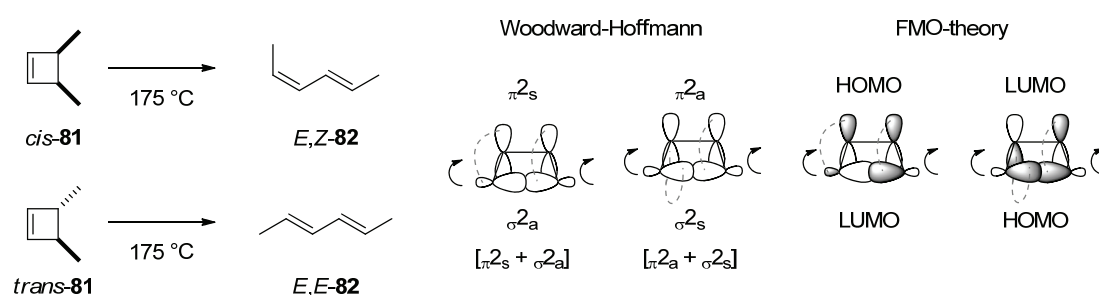
developed.^[81] However, since group transfer reactions are not a subject of this thesis, they will not be discussed further at this point.

2.4.5 The Woodward-Hoffman Rules of Orbital Symmetry

While radical and ionic reactions were reasonably well understood in the middle of the last century, their pericyclic counterparts were not even recognized as an individual class at that time. Although some pericyclic reactions like the Diels-Alder reaction were already known, their unusual behaviour in terms of reaction rates, regio- and stereoselectivity continued to puzzle chemists, who were trying to bring the experimental observations in line with a reasonable mechanism. In 1962, Doering, partially desperate by this undertaking, even called pericyclic reactions “*no-mechanism*” reactions.^[82] This situation changed when Woodward made another observation in the course of the synthesis of Vitamin B₁₂ which was hard to explain with common theories at that time. However, Woodward and Hoffmann recognized a higher principle between these “*no-mechanism*” reactions which set the basis for their rules of the conservation of orbital symmetry, also known as the Woodward-Hoffmann rules.^[83]

The Woodward-Hoffmann rules are based on the theory of molecular orbitals and the underlying developments and reasonings are far reaching and thus will not find appropriate space to be discussed in detail here. However, the essence of their groundbreaking work can be condensed in only a few rules, which can help to reliably predict and explain the course of pericyclic reactions. The key statement of the Woodward-Hoffmann rules is that the orbital symmetry in a pericyclic reaction is conserved. As a consequence, pericyclic reactions occurring from the electronic ground state are allowed when the number of $(4q+2)_s$ and $(4r)_a$ components is odd ($q = 0, 1, 2, 3, \dots$; $r = 0, 1, 2, 3, \dots$; $s = \text{suprafacial}$; $a = \text{antarafacial}$). Accordingly a pericyclic reaction occurring from the first excited electronic state is allowed when the number of $(4q+2)_s$ and $(4r)_a$ components is even. An illustrative example for these rules are the ring openings of the isomeric 3,4-dimethylcyclobutenes **81**. While *cis*-3,4-dimethylcyclobutene (*cis*-**81**) opens under thermal conditions to give the *E,Z*-2,4-hexadiene (*E,Z*-**82**), the corresponding *trans* isomer *trans*-**81** gives under the same conditions

exclusively the *E,E*-2,4-hexadiene (*E,E*-**82**) (Scheme 20).^[84] This result can be explained by applying the aforementioned rules. The ring opening of the cyclobutenes involves four electrons, of which two are forming the C-C single bond and the others are forming the C-C double bond. Thus, the entire system consists of two $(4q+2)$ components and zero $(4r)$. In order for the reaction to proceed under thermal conditions, one of the $(4q+2)$ has to be dealt with as suprafacial $(4q+2)_s$, whereas the other component has to be antarafacial $(4q+2)_a$. This situation can be realized in two ways, either by a $[\pi 2_a + \sigma 2_s]$ or by a $[\pi 2_s + \sigma 2_a]$ system. In both cases the outcome is the same in that the two substituents on the cyclobutene rotate in the same direction, resembling a conrotatory ring opening.



Scheme 20. Electrocyclic ring opening of the two isomeric 3,4-dimethylcyclobutenes *cis*-**81** and *trans*-**81**.

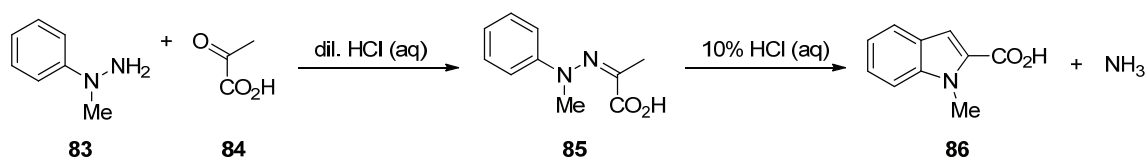
A related approach to explain the stereoselectivity of this ring opening is the discussion in terms of frontier molecular orbitals (FMOs). This concept goes back to the fundamental work by Fukui who found that the reactivity of organic compounds could be well approximated by only looking at the highest occupied molecular orbital (HOMO) and the lowest unoccupied molecular orbital (LUMO), which resemble the frontier molecular orbitals.^[85] In general, bond-making and bond-breaking events occur when a (partially) occupied orbital interacts with a (partially) unoccupied orbital which is similar in energy. Applying this concept to the ring opening of the two isomeric 3,4-dimethylcyclobutenes **81** shows that the ring opening has to occur conrotatory in order to cause bonding interactions to form the π -orbitals present in the dienes **82** (Scheme 20). Whether the rotation at one side of the cyclobutene preferentially occurs inwards or outwards is of course arbitrary for the discussed examples. However, this torquoselectivity^[86] is the element which has to be controlled in order to render pericyclic reactions asymmetric.

Altogether the Woodward-Hoffmann rules and Fukui's FMO-theory contributed significantly to the understanding of pericyclic reactions. Both concepts rely on the theory of molecular orbitals and have individual advantages regarding their application. While the Woodward-Hoffmann rules provide an easy applicable tool to predict the inherent stereochemistry of pericyclic reactions, the rational origin of this selectivity is easier traceable on the basis of the FMO-theory.

2.5 The Fischer Indole Synthesis

2.5.1 Historical Background

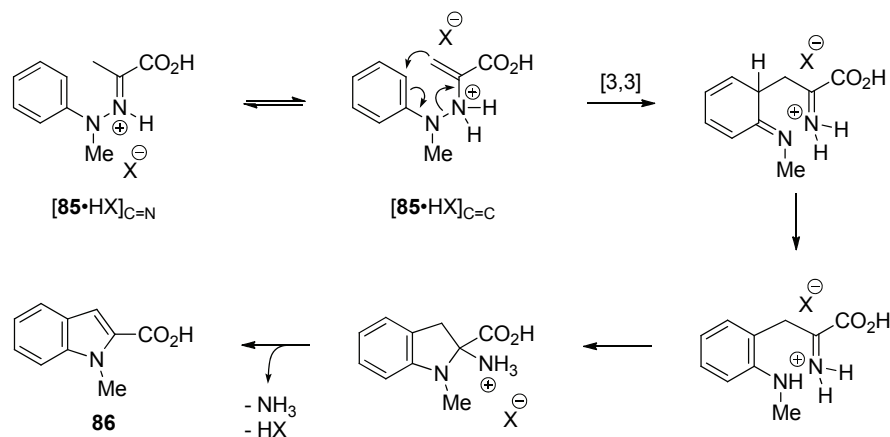
In 1883 the German chemist Emil Fischer was studying the chemistry of phenylhydrazones, including their synthesis and chemical properties under different conditions. Amongst the hydrazones investigated, he found one particular compound which was behaving differently from all the others. When Fischer heated up hydrazone **85** derived from 1-methyl1-phenylhydrazine (**83**) and pyruvic acid (**84**) in hydrochloric acid, he obtained a new compound which, according to his analyses, was generated from the hydrazone **85** by formal loss of ammonia.^[87] However, the structure of the newly obtained product remained unclear until Fischer and Hess, one year after the initial discovery, identified the mysterious new compound as indole-3-carboxylic acid (**86**) (Scheme 21).^[88]



Scheme 21. The Fischer indole synthesis discovered in 1883.

After its discovery, this new method for the synthesis of indole derivatives attracted considerable attention amongst synthetic chemists and found multiple applications. However, the reaction mechanism, though subject of numerous speculations which eventually turned out to be wrong, remained unsettled for forty more years. In 1924 Robinson and Robinson finally suggested a mechanistic scenario, which is widely accepted until today.^[89] According to their proposal, hydrazone **85** is protonated under acidic

conditions (HX). The protonated hydrazone $[85 \cdot \text{HX}]_{\text{C}=\text{N}}$ exists in equilibrium with the corresponding enehydrazine $[85 \cdot \text{HX}]_{\text{C}=\text{C}}$ which undergoes a [3,3]-sigmatropic diaza-Claisen rearrangement. Rearomatization by proton shift is followed by a 5-exo-trig cyclization. Subsequent elimination of ammonia generates the aromatic indole **86** and liberates the acid promoter (Scheme 22).



Scheme 22. Generally accepted mechanism of the Fischer indole synthesis proposed by Robinson and Robinson.

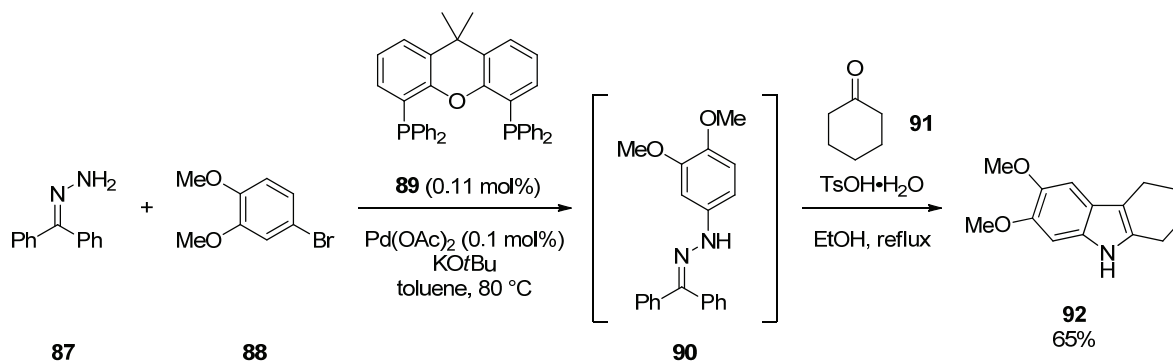
Notably, the Fischer indole synthesis was the first method for the synthesis of indole derivatives available. Due to its high relevance the reaction has been investigated intensively leading to the advancement of the method. While Fischer originally found the reaction to be catalyzed by hydrochloric acid, various other catalysts were found equally effective later on. Examples include Brønsted acids like formic acid, acetic acid, sulfuric acid or polyphosphoric acid, as well as Lewis acids like zinc chloride, boron trifluoride, platinum chloride or copper chloride.^[90]

2.5.2 Some Recent Developments

The huge diversity of indole-containing scaffolds in natural products and pharmaceutically relevant compounds caused massive interest in the *de novo* synthesis of these molecules and, as a matter of course, alternative synthetic strategies for the assembly of indole derivatives were developed.^[91] Despite these recent developments, the venerable Fischer indole synthesis has maintained its prominent role as the method of choice for the synthesis of indoles derivatives for almost 130 years and still constitutes a very active area of

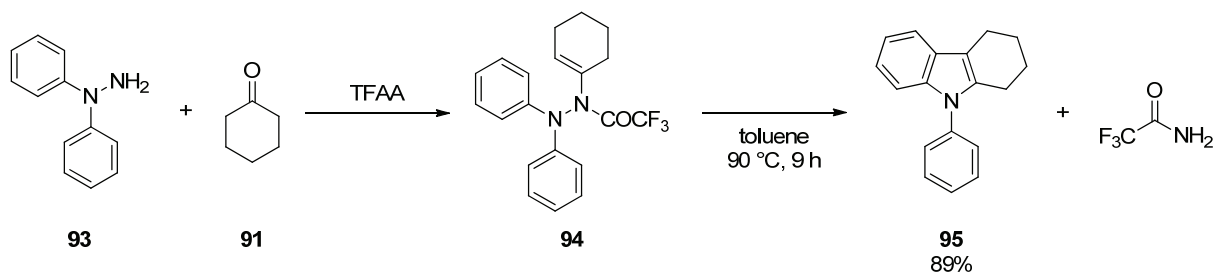
research with more than 700 publications over the last 15 years.^[91c] Some reasons for the popularity of the Fischer indole synthesis are the operational simplicity, high levels of reproducibility, scalability, broad substrate scope, high atom economy and low cost starting materials. More recent developments focussed on some remaining limitations.

In contrast to the required carbonyl components, which are usually easy to handle and commercially available, phenylhydrazines are relatively unstable and only few derivatives can be purchased directly. Recently Buchwald and co-workers developed an elegant method to circumvent this limitation by using a reaction sequence of Pd-catalyzed cross coupling and Fischer indolization. In the first step, the benzophenone hydrazone (**87**) is coupled with aryl bromide **88** in the presence of a palladium Xantphos complex. The resulting *N*-aryl benzophenone hydrazone **90** can be directly treated with an enolizable carbonyl compound and *para*-toluenesulfonic acid to achieve a hydrazone transfer followed by Fischer indolization (Scheme 23).^[92] The high yields generally obtained and the easy accessibility of the starting materials render this reaction an attractive complement to the traditional approach.



Scheme 23. A palladium-catalyzed method for the preparation of indoles via the Fischer indolization.

Another drawback of the Fischer reaction is that typically rather harsh reaction conditions operating at elevated temperatures and employing at least stoichiometric amounts of acid are required to efficiently facilitate the reaction. An alternative to these classic reaction conditions was suggested by Naito *et al.*, who found that *N*-trifluoroacetyl enehydrazines like **94** are sufficiently activated to undergo a thermal Fischer indolization at moderate temperature and without the need for an additional catalyst (Scheme 24).^[93]

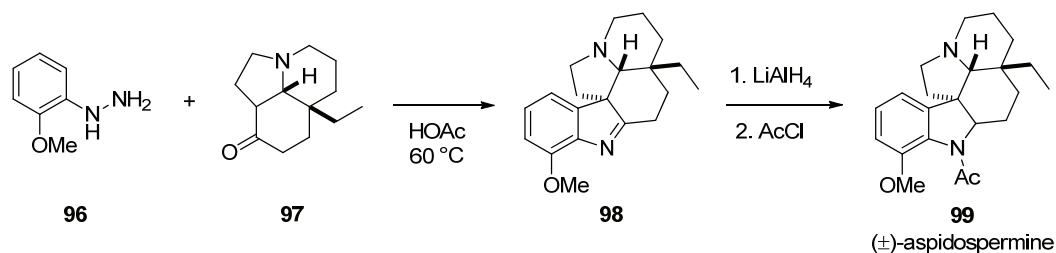


Scheme 24. Thermal Fischer indolization of *N*-trifluoroacetyl enehydrazine **94**.

Although the enehydrazine substrate **94** has to be prepared in an additional step from the corresponding hydrazine **93** and ketone **91**, the indolization process is very facile, in some cases even proceeding at room temperature. Notably the by-product generated with this method is trifluoroacetamide rather than ammonia.

2.5.3 Chiral Indole Derivatives from Fischer Indolizations

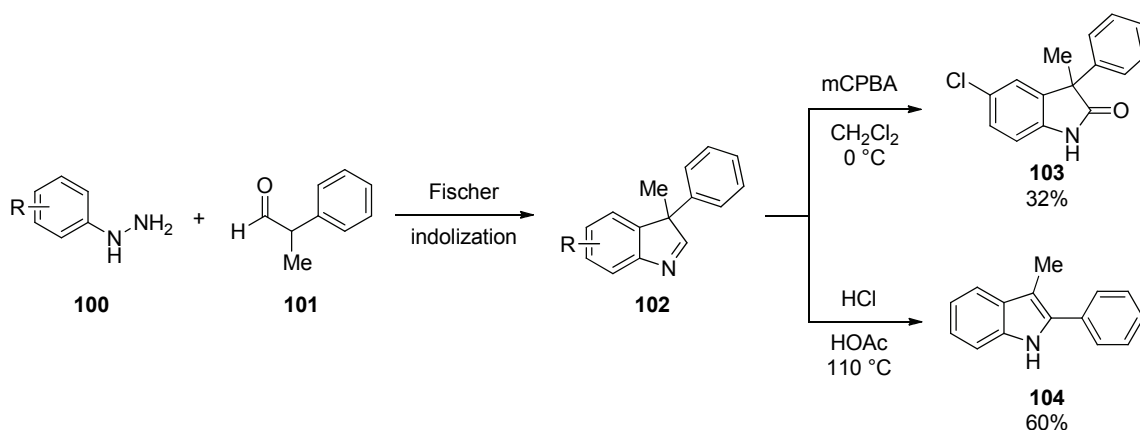
Even though the parent indole is an achiral molecular entity, the generation of chiral products in the course of a Fischer indolization is by no means uncommon. The utilization of α -branched carbonyl compounds for instance can lead to the formation of indolenines with a quaternary stereocenter in the 3-position. In their synthesis of (\pm)-aspidospermine (**99**), Stork and co-workers took advantage of this reactivity. The Fischer indolization between hydrazine **96** and the complex cyclohexanone **97** gave the indolenine **98** which was converted into the target **99** by imine reduction and *N*-acetylation (Scheme 25).^[94]



Scheme 25. Last steps in Stork's total synthesis of (\pm)-aspidospermine (**99**).

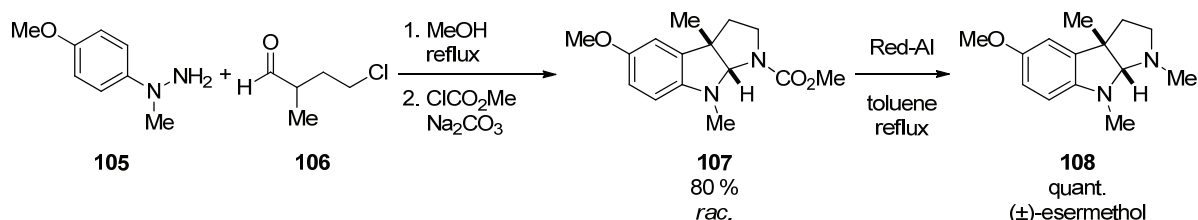
While unsymmetric ketones like **97** can generally react via two different enehydrazines, resulting in two different products, α -branched aldehydes do not display this issue of regioselectivity and are therefore more common reaction partners for the formation of indolenines in Fischer indolization reactions. The relatively easy generation of all-carbon

quaternary stereocenters in combination with the high synthetic value provided by the indolenine products makes this strategy so attractive. The group of Liu investigated transformations of indolenines other than reductions and found that the indolenines of type **102** can likewise be converted to the corresponding oxindoles **103** via a *m*CPBA-mediated oxidation.^[95] Also achiral 2,3-disubstituted indoles like **104** can be accessed from the same precursors via an acid promoted Wagner-Meerwein rearrangement (Scheme 26).^[96]



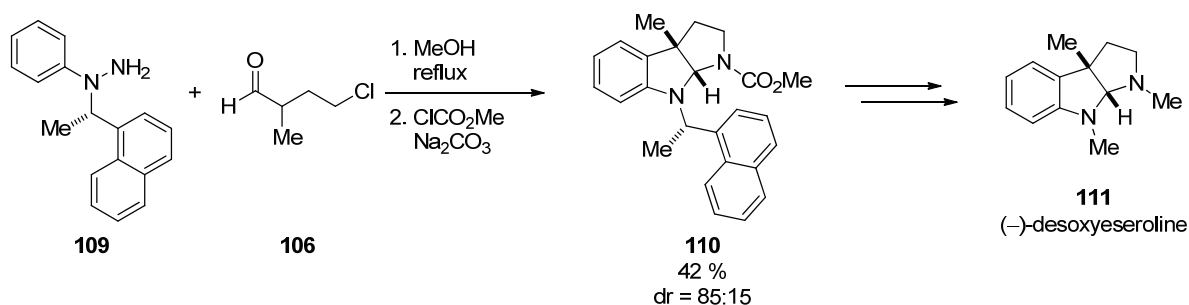
Scheme 26. Oxidation and Wagner-Meerwein rearrangement of indolenines **102** obtained via the Fischer indolization.

Another elegant application of the Fischer indole synthesis which leads to chiral products was pioneered by the group of Grandberg. They found that the use of α -branched carbonyl groups with an electrophile in the γ -position leads to the formation of pyrroloindolines, most likely occurring via an intramolecular substitution of the chloride by a nitrogen atom either prior or subsequent to the rearrangement step.^[97] This method was further elaborated by Nishida *et al.* in their synthesis of pyrroloindoline alkaloids like esermethol (**108**) (Scheme 27).^[98]



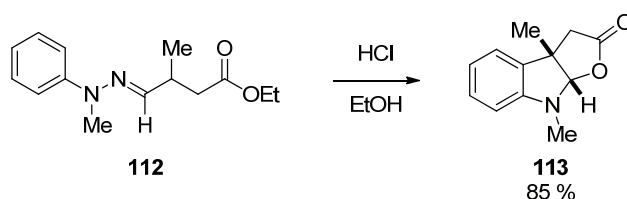
Scheme 27. Synthesis of chiral pyrroloindolines via the Fischer indolization in the total synthesis of (\pm)-esermethol (**108**).

The same group also reported the first attempts to conduct this reaction stereoselectively, relying on an auxiliary based diastereoselective Fischer indolization. For this purpose they introduced phenylhydrazine **109**, bearing a chiral benzyl protecting group and applied it to the Fischer indolization with α -methyl- γ -chlorobutanal (**106**). The pyrroloindoline **110** was obtained in 42% yield and 85:15 dr and was further converted to the natural product (–)-desoxyeseroline (**111**) (Scheme 28).^[99]



Scheme 28. Diastereoselective Fischer indolization in the synthesis of (–)-desoxyeseroline (**111**).

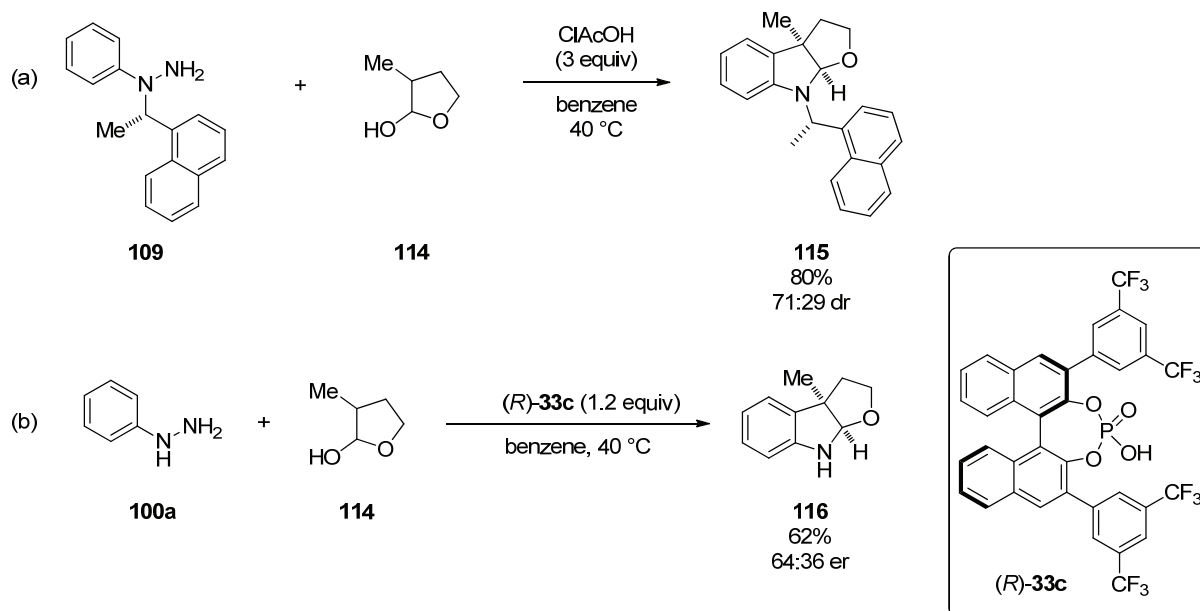
A related approach relying on the interception of the indolenine product with an internal nucleophile was introduced by Rosenmund and Sadri in 1979. They employed phenylhydrazones of type **112** derived from α -branched aldehydes tethered to an ester in the γ -position in the indolization. In the course of the reaction, the ester is hydrolyzed and the resulting acid attacks the indolenine in intramolecular fashion to form the final racemic lactone **113** (Scheme 29).^[100]



Scheme 29. Synthesis of chiral lactone-fused indoline **113**.^[100]

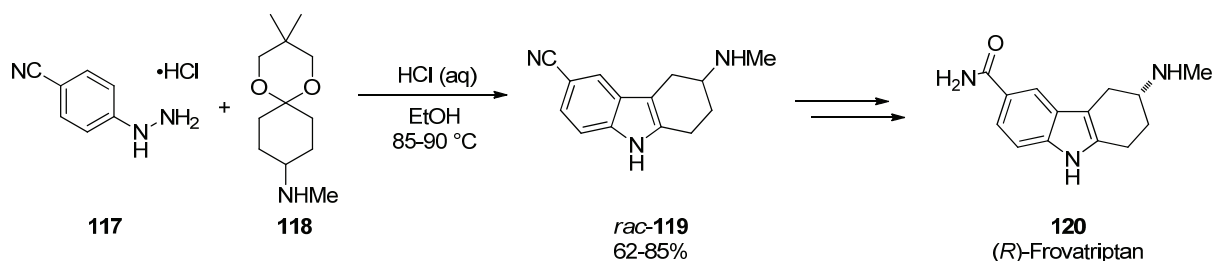
Recently, Neil Garg and co-workers further elaborated this concept and reported the synthesis of furoindolines by the utilization of α -branched lactols as latent γ -hydroxyaldehyde equivalents in their “interrupted Fischer indolization”.^[101] In an extension of this methodology the same group used the auxiliary introduced by Nishida *et al.*^[99] to render the same transformation diastereoselectively (Scheme 30a).^[102] The desired product **115** was obtained in good yield albeit only low diastereoselectivity. Additionally noteworthy

are their attempts towards the utilization of chiral phosphoric acid catalysts in this transformation. However, the only reported example involved an excess of the chiral BINOL-derived phosphoric acid (*R*)-**33c** (1.2 equivalents) and furnished the desired product **116** with low enantioselectivity (Scheme 30b).



Scheme 30. Diastereoselective interrupted Fischer indolization (a) and chiral phosphoric acid (*R*)-**33c**-promoted enantioselective Fischer indolization (b).

Another important class of chiral products which are routinely produced via the Fischer indole synthesis are tetrahydrocarbazoles. In particular 3-aminotetrahydrocarbazoles possess multiple biological activities and are used as drugs for the treatment of several diseases like asthma or coronary artery disease.^[103] One example is the 3-methylamino tetrahydrocarbazole Frovatriptan (**120**) which is used as the (*R*)-enantiomer for the treatment of migraine headaches (Scheme 31).



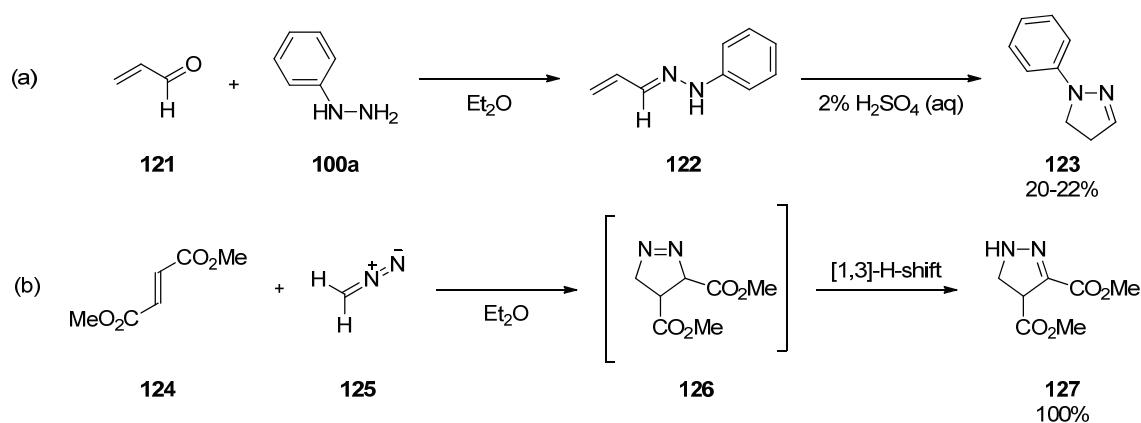
Scheme 31. A devised industrial synthesis of Frovatriptan (**120**).

An industrial route which was devised in 1998 includes the synthesis of the racemic 3-aminotetrahydrocarbazole **119** by Fischer indolization of the acetal protected

cyclohexanone **118** with phenylhydrazine **117**. Racemate resolution and further functional group manipulations finally give the enantiomerically pure drug **120** (Scheme 31).^[104] Although Frovatriptan (**120**) is used as a single enantiomer drug, the core of the molecule is built up in a racemic synthesis and resolution is used to obtain the pure desired enantiomer. This procedure is not only disadvantageous with regard to the additional step required for the resolution, but also in terms of product yield, since half of the product has to be discarded. A potential alternative to construct the new stereocenter enantioselectively would be an asymmetric Fischer indolization. However, not a single report of an enantioselective Fischer indolization which employs substoichiometric amounts of a chiral promoter was known in the literature prior to the investigations reported herein.

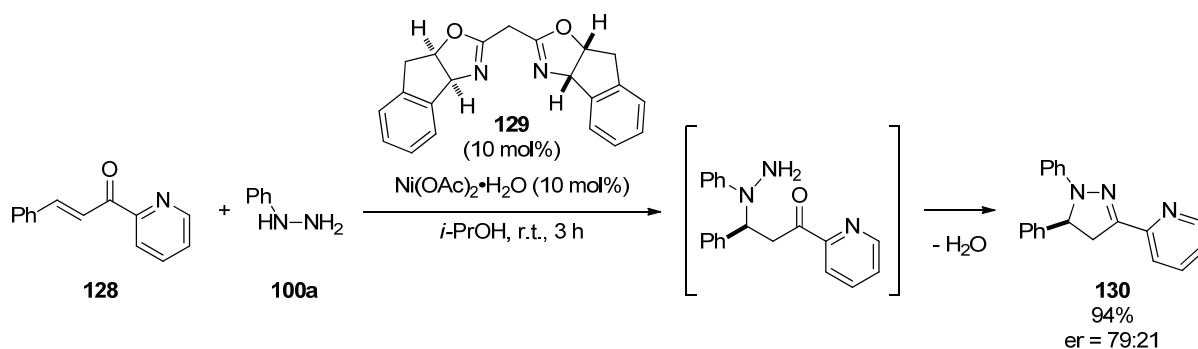
2.6 Pyrazolines

Possessing numerous potent biological activities, such as antidepressant, anticancer, anti-inflammatory, antibacterial, and antiviral activity, pyrazolines are interesting synthetic targets.^[105] One of the first methods for the synthesis of pyrazolines was discovered by Emil Fischer and Otto Knoevenagel in 1887. Upon treating the hydrazone **122**, derived from phenylhydrazine (**100a**) and acrolein (**121**), with diluted sulfuric acid they obtained phenylpyrazolin **123** (Scheme 32a).^[106] Few years later Buchner *et al.* were investigating the reaction between diazoacetate and olefins and obtained pyrazolines via [2+3]-dipolar cycloadditions,^[107] while von Pechmann used the same reaction to trap diazomethane (**125**), which he had just discovered, with dimethyl fumarate (**124**) (Scheme 32b).^[108]



Scheme 32. Syntheses of pyrazolines via cyclization of α,β -unsaturated hydrazone **122** (a) and [2+3]-dipolar cycloaddition (b).

Today, more than 100 years after their discovery, these two synthetic strategies are among the most general approaches to access pyrazolines.^[109] Several elegant catalytic asymmetric versions of the Buchner–von Pechmann type cycloaddition have been reported, mainly relying on Lewis-acid catalysts such as oxazaborolidines,^[110] bisoxazolidine complexes of nickel, zinc, magnesium^[111] and copper^[112] as well as Ti-^[113] and Zr-BINOLate systems.^[114] In contrast, Fischer’s reaction has not received much attention in this regard. In 2007 Kanemasa and Yanagita reported an enantioselective conjugate addition-cyclocondensation cascade between different aryl hydrazines of type **100a** and 3-phenyl-1-(2-pyridyl)-1-propenone (**128**). In the presence of a chiral nickel complex, optically enriched pyrazolines such as **130** were obtained in moderate enantioselectivities (Scheme 33).^[115]



Scheme 33. Catalytic asymmetric synthesis of pyrazolines via a conjugate addition intramolecular condensation sequence.

However, in contrast to the mechanism of this reaction, the Fischer pyrazoline synthesis proceeds by condensation between enones and hydrazines to give the corresponding often isolable hydrazone, which then cyclizes to the pyrazoline.^[116] Although this pathway is frequently used for the synthesis of pharmaceutically relevant molecules, no catalytic asymmetric version has been reported.

2.7 Acetals in Nature and Organic Chemistry

Emil Fischer’s fundamental contributions to organic chemistry were largely connected to phenylhydrazine (**100a**), which he described for the first time in 1875.^[117] The discovery of the Fischer indole and pyrazoline syntheses occurred in the course of his studies on phenylhydrazines. Also for his studies on the structural and stereochemical elucidation of

sugars, which Fischer was awarded the Nobel prize in 1902 for, phenylhydrazine turned out to be of essential value for derivatizing the molecules of interest. One of the sugars Fischer elucidated the configuration of was D-glucose (**131**).

Glucose occurs in nature mostly in polymeric form either as cellulose (**132**) or as amylose (**133**) (Figure 5, left). These two biopolymers differ only in the absolute configuration of their acetal stereocenter which represents the linkage between the monomeric units, and yet the chemistry of these two compounds is entirely different. While amylose can easily be hydrolyzed in slightly acidic media and thus can be easily digested by humans, the chemical depolymerisation of cellulose is challenging. In fact, the realization of this process to unlock renewable feedstocks for fine chemical production is a major subject of modern research.

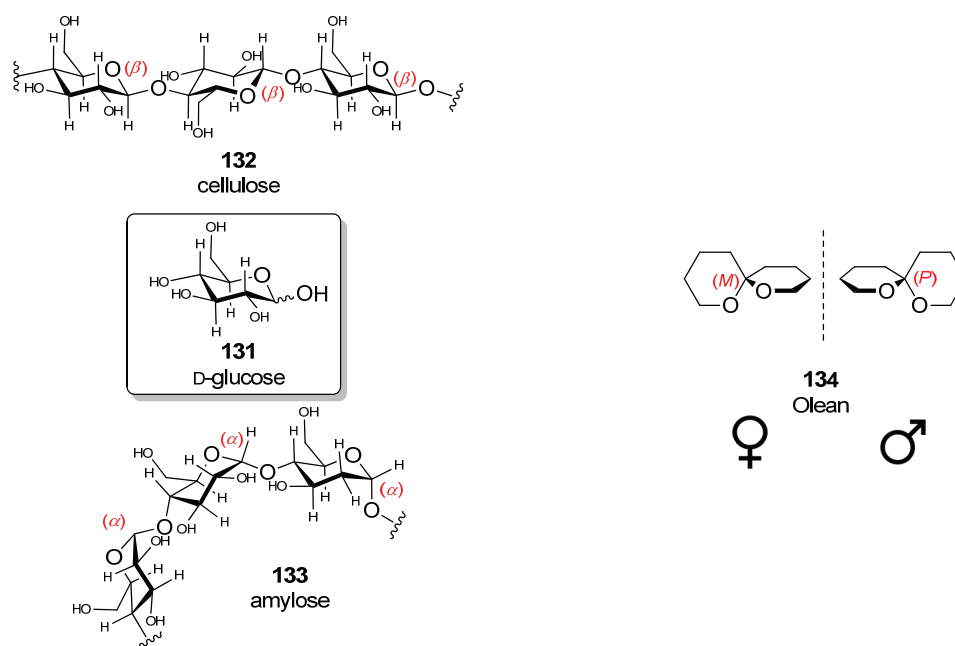
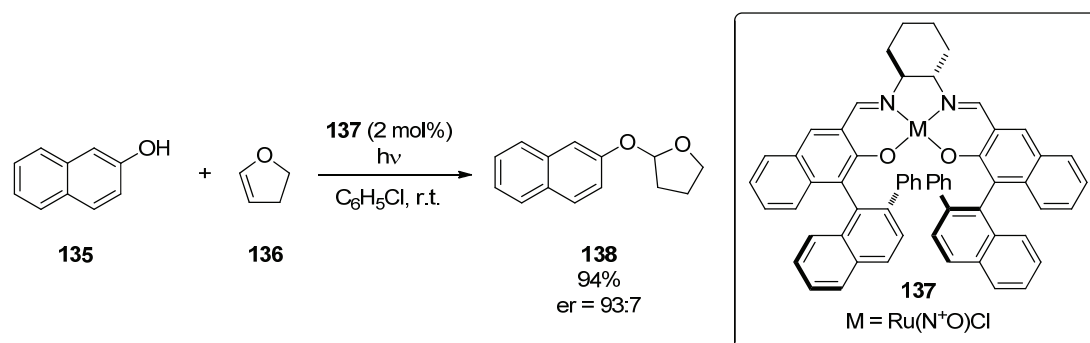


Figure 5. Stereostructures of D-glucose (**131**) and polymers derived thereof (left) and Olean (**134**), the olive fruit flies' sex-pheromone (right).

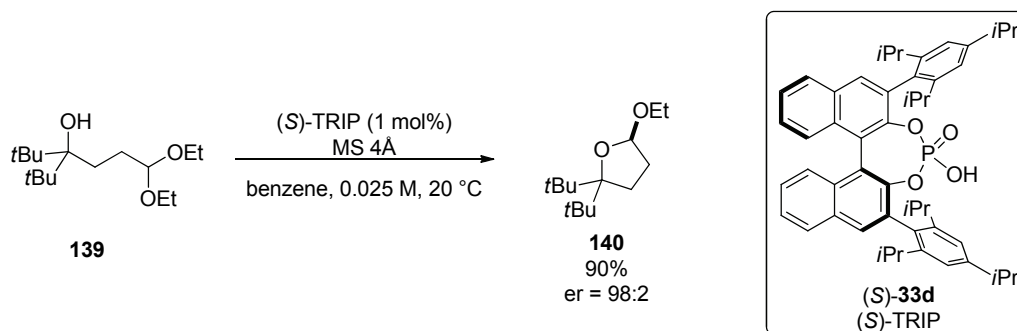
Another illustrative example of the importance of the absolute configuration of acetal stereocenters is Olean (**134**), the sex-pheromone of the olive fruit fly. Both enantiomers of this spirocyclic ketal occur in nature, but while the (M)-enantiomer acts only on the female flies, its antipode is acting on the males (Figure 5, right).

The most important strategy for the synthesis of acetals is the Brønsted acid-mediated addition of heteroatom nucleophiles to carbonyl compounds with extrusion of one molecule of water. This type of reaction in combination with the importance of controlling the absolute stereochemistry of acetal stereocenters make chiral Brønsted acid catalysis a perfect platform for the development of catalytic asymmetric acetalization reactions. The first developments towards this direction involved the use of chiral phosphoric acids for the synthesis of *N,N*-acetals via the addition of amides to imines,^[118] and the reaction between aldehydes and *ortho*-amino arylamides.^[119] An extension of this methodology is the chiral Brønsted acid promoted enantioselective synthesis of *N,O*-acetals via alcohol addition to imines as reported by Antilla *et al.*,^[120] or the addition of aldehydes to salicylamides developed by our group.^[121] However, the catalytic asymmetric construction of *O,O*-acetals has remained a formidable challenge for a long time. Until recently the only reported example involved the addition of alcohols to cyclic enol ethers in the presence of the chiral Ru-salen complex (**137**), giving acetal **138** in good yield and enantioselectivity (Scheme 34).



Scheme 34. Catalytic asymmetric synthesis of *O,O*-acetal **138** via the addition of 2-naphthol (**135**) to dihydrofuran (**136**).

In 2010, our group reported the intramolecular transacetalization of γ -hydroxyacetals such as **139** catalyzed by the chiral phosphoric acid TRIP (**33d**). Using only 1 mol% of the catalyst the cyclic lactoethers **140** were obtained in high yields and enantioselectivities with the acetal stereocenter as the only stereogenic element (Scheme 35).^[122]



Scheme 35. Catalytic asymmetric intramolecular transacetalization.

Although upon first inspection the products of this reaction may appear less valuable as chiral building blocks, the inherent 1,4-dioxygenation pattern in this particular oxidation state makes them acetal protected aldehyde homoaldols. This structural motif, often bearing an additional chiral center at the carbon atom attached to the alcohol, is present in many natural products and pharmaceutically relevant compounds.

3 Objectives of This PhD Work

3.1 Synthesis of SPINOL-Derived Phosphoric Acids and Disulfonimides

Chiral phosphoric acids have emerged as powerful organocatalysts over recent years^[57] and since the pioneering works by the groups of Akiyama^[39] and Terada^[40] an impressive number of reactions have successfully been developed based on these catalyst systems. Surprisingly, the vast majority of these reactions involve BINOL-derived catalysts with varying 3,3'-substituents. These catalysts are readily accessible from the commercially available enantiomerically pure BINOL (**141**) and H₈-BINOL (**142**) and are tuneable with regard to steric and electronic properties via the 3,3'-substituents. While these two scaffolds are structurally very similar, the VAPOL-(**143**)-derived catalyst, which is the third most frequently used type of chiral phosphoric acid, offers a different geometry but suffers from lacking tunability (Figure 6).

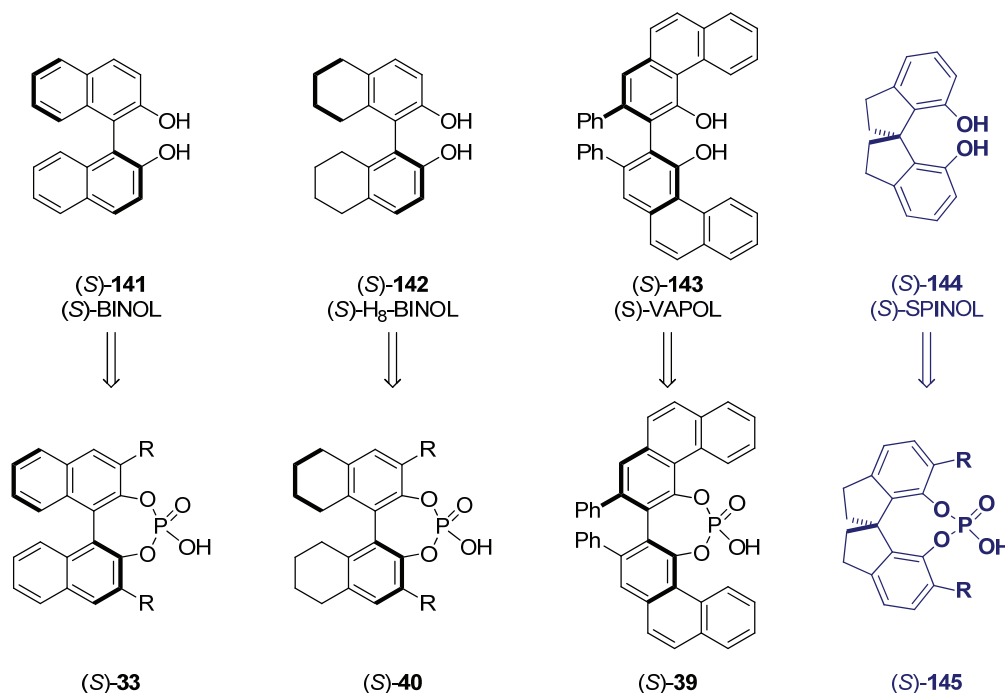
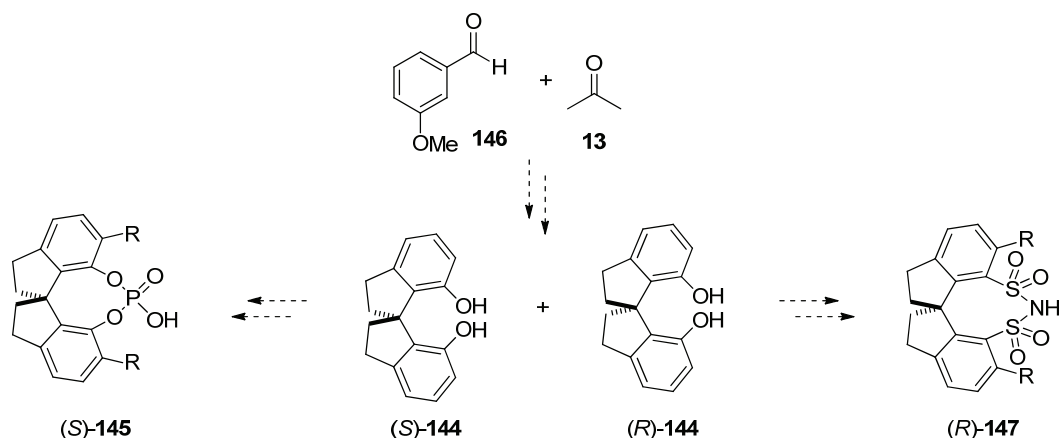


Figure 6. Different C₂-symmetric diols and phosphoric acids derived thereof.

In order to provide new and potentially complementary tools for asymmetric Brønsted acid catalysis, one goal of this PhD work was the development of novel catalysts. In this light the C₂-symmetric spirobiindane SPINOL (**144**), originally introduced by Birman and co-workers in 1999, appeared to be an interesting scaffold.^[123] Since this first report,

SPINOL-derived ligands have found applications mainly in asymmetric metal catalysis.^[124] Furthermore two applications in metal free catalysis were reported at the outset of our own studies. The group of Zhou used a SPINOL-derived amine in asymmetric aldol reactions,^[125] and Fu and co-workers reported the use of a related phosphine as a nucleophilic catalyst.^[126]

The SPINOL-backbone was envisioned to be also a promising motif for the development of new and complementary phosphoric acids of type **145**, since these catalysts would be structurally different from established catalysts and at the same time allow for modifications by introduction of different 6,6'-substituents. Therefore one of the goals of this PhD work was to develop a route to SPINOL-derived phosphoric acids **145** and probe their performance as catalysts (Scheme 36).



Scheme 36. Envisioned synthesis of SPINOL-derived phosphoric acids **145** and disulfonimides **147**.

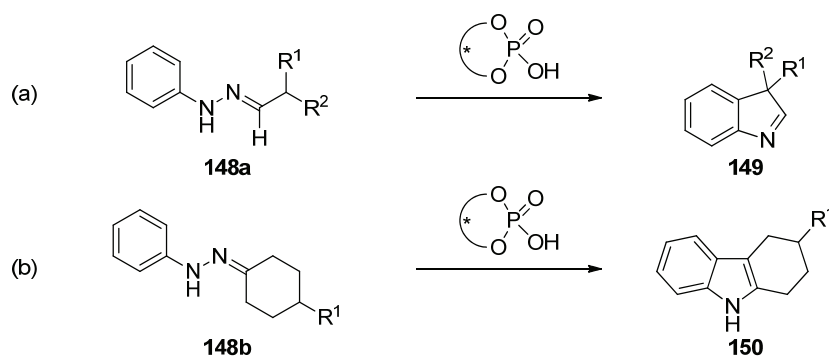
Besides the phosphoric acids **145**, also the corresponding SPINOL-derived disulfonimides **147** became interesting synthetic targets after our group had identified BINOL-disulfonimides as powerful organic Lewis-acids.^[127]

3.2 The Catalytic Asymmetric Fischer Indolization

Indoles are widely distributed heterocyclic compounds in nature and their synthesis has attracted massive attention. Of the numerous methods available for the construction of indoles, the over 120 years old Fischer indolization, an acid-mediated rearrangement of phenylhydrazones, still remains their epitome. Remarkably, catalytic asymmetric Fischer

indolizations have so far remained elusive. Therefore the second goal of this PhD work was the development of such a reaction.

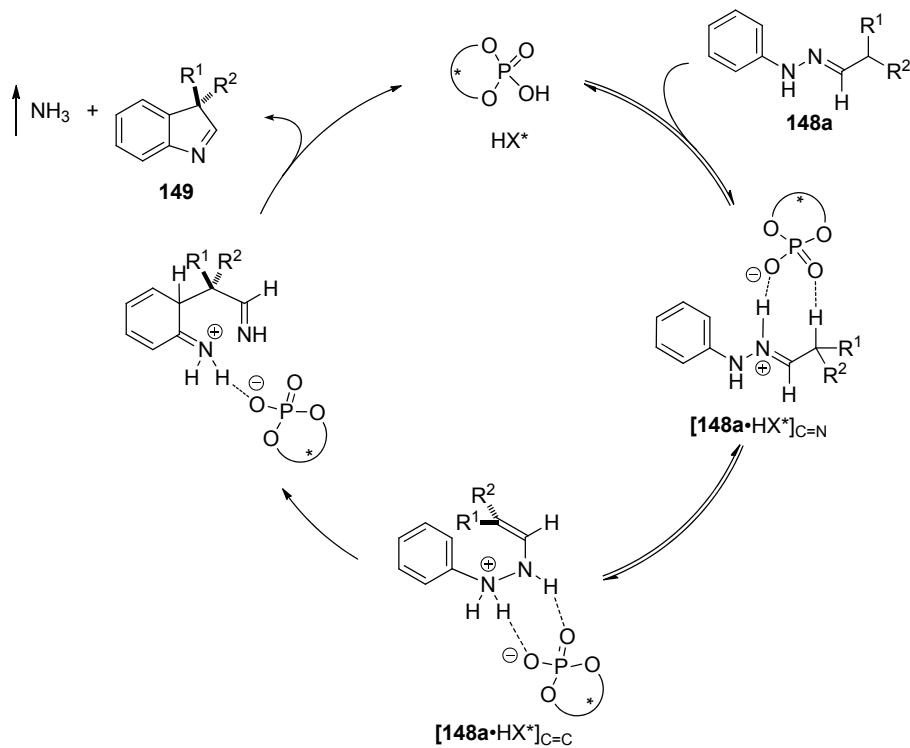
The targeted transformations involved the indolization of phenylhydrazones **148a** and **148b**, derived from α -branched carbonyl compounds as well as from 4-substituted cyclohexanones. Chiral phosphoric acids or related strong chiral Brønsted acids were envisioned to be suitable catalysts to promote these reactions enantioselectively to give indolenines **149** with an all carbon quaternary stereocenter in the 3-position (Scheme 37a), and 3-substituted tetrahydrocarbazoles **150** in enantiomerically enriched form (Scheme 37b). The latter reaction was inspired by the work of the Seidel-group, who had reported the desymmetrization of 4-substituted cyclohexanones in the catalytic asymmetric Friedländer condensation with *ortho*-amino benzaldehydes.^[128] We envisioned this strategy to be applicable in a similar fashion to the Fischer indole synthesis.



Scheme 37. Planned synthesis of indolenines **149** (a) and tetrahydrocarbazoles **150** (b) via catalytic asymmetric Fischer indolizations.

The proposed catalytic cycle is based on the widely accepted mechanism of the Fischer indolization as proposed by Robinson and Robinson.^[89] Accordingly the chiral Brønsted acid (HX^*) accelerates the hydrazone-enehydrazine equilibration. In the key step, the protonated enehydrazine $[148a \cdot HX^*]_{C=C}$ undergoes the irreversible [3,3]-sigmatropic rearrangement as the cation of a chiral hydrogen bond assisted ion pair with the chiral phosphate anion. After rearomatization and ring closure the desired indolenine **149** is formed along with ammonia as the by-product. The continuous removal of the ammonia due to its volatility at ambient temperature should eventually regenerate the active catalyst (Scheme 38). A similar mechanism was proposed for the indolization of 4-substituted cyclohexanone derived phenylhydrazones **148b**. But while in the case of α -branched

carbonyl compounds the chiral hydrazone is converted to an achiral enehydrazine in the transition state, in the case of cyclohexanone derived hydrazones the reaction had to proceed via a dynamic kinetic resolution of the chiral starting material **148b**.

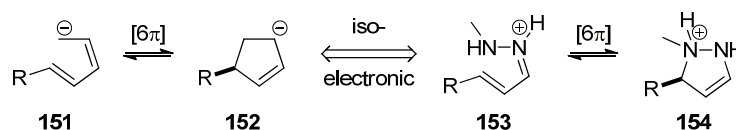


Scheme 38. Proposed catalytic cycle for the Fischer indolization of phenylhydrazones **148a** derived from α -branched aldehydes.

3.3 Development of a Catalytic Asymmetric 6π Electrocyclization

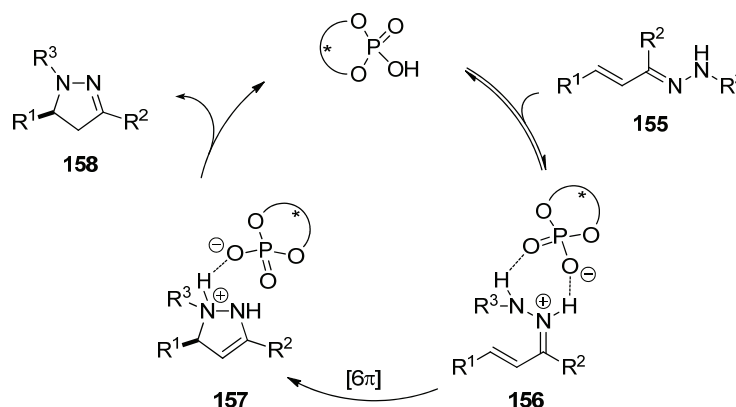
Electrocyclizations, cycloadditions, and sigmatropic rearrangements are the most prominent classes of pericyclic reactions. Due to their synthetic utility, these reactions have become very popular in synthetic organic chemistry and the development of catalytic asymmetric versions has been a logical consequence. Compared to cycloadditions and sigmatropic rearrangements, which are now well established in asymmetric catalysis, electrocyclizations remain largely unexplored in this respect and at the outset of these studies not a single example of a catalytic asymmetric 6π electrocyclization had been reported.

Stimulated by the project on the catalytic asymmetric Fischer indolization, the cyclization of α,β -unsaturated hydrazones into the corresponding 2-pyrazolines represented another appealing potential application for asymmetric Brønsted acid catalysis. Also this reaction is known to be acid-catalyzed as originally discovered by E. Fischer.^[106] Considering a protonated hydrazone as the reactive species, we realized the isoelectronic relationship between this process and the 6π electrocyclization of the pentadienyl anion **151** (Scheme 39). Interestingly, it turned out that our reasoning was not entirely new and that Huisgen had discussed this analogy already 20 years earlier.^[129]



Scheme 39. Isoelectronic 6π electrocyclizations.

Although truly catalytic versions of Fischer's pyrazoline synthesis are scarce, we reasoned that a chiral Brønsted acid catalysis strategy might be applicable. The proposed catalytic cycle involves the protonation of the α,β -unsaturated hydrazone **155** by the catalyst to give the diaza-analog of the pentadienyl anion **156** which can undergo the cyclization as the cation of a chiral hydrogen bond assisted ion pair.

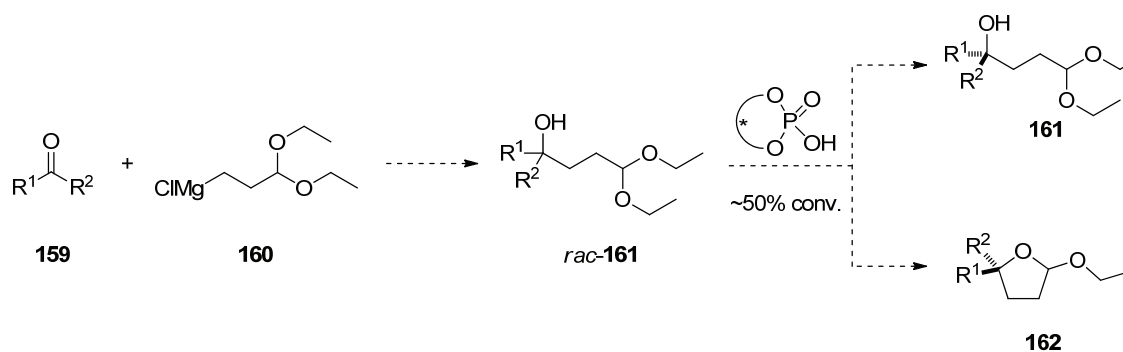


Scheme 40. Proposed catalytic cycle for the 6π electrocyclization of α,β -unsaturated hydrazones **155**.

We hypothesized that it might be possible to control the torquoselectivity of the 6π electrocyclization by the proper choice of the chiral counteranion. After the cyclization the intermediary 3-pyrazoline isomerizes to give the thermodynamically favoured 2-pyrazoline **158** and the active catalyst is regenerated. The realization of this process was another objective of this work.

3.4 Kinetic Resolution of Homoaldols via Intramolecular Transacetalization

γ -Hydroxycarbonyl compounds, or homoaldols, represent a versatile motif for organic synthesis that can be easily transformed into a vast array of important chiral compounds such as γ -lactones, tetrahydrofurans, pyrrolidines, and others. Consequently, various homoenolate equivalents have been developed, but their use in enantioselective homoaldol reactions invariably relies on stoichiometric chiral ligands or auxiliaries.^[130] Recently *N*-heterocyclic carbenes opened up a new route for the organocatalytic generation of homoenolates.^[131] However, their application in asymmetric homoaldol reactions is still rather underdeveloped.^[132] Strategically different approaches include catalytic enantioselective reduction of γ -ketoesters^[133] and dynamic kinetic resolution of racemic γ -hydroxyamides using combined enzymatic and transition-metal catalysis.^[134] Tertiary homoaldols, however, are not accessible by these methods. Therefore the last goal of this PhD work was the development of an efficient, mild and general kinetic resolution of homoaldols based on the Brønsted acid-catalyzed intramolecular transacetalization which was discovered by our group.^[122] From this previous work it was already known that the addition of Grignard reagent **160**, which can be prepared from the commercially available chloride, to symmetric ketones **159** ($R^1 = R^2$) afforded the achiral acetal protected homoaldols. For this work, the addition of the same Grignard reagent to aldehydes and unsymmetric ketones to produce the racemic homoaldols *rac*-**161** in a one step synthesis appeared reasonable.



Scheme 41. Envisioned kinetic resolution of acetal protected homoaldols *rac*-**161** via intramolecular transacetalization.

Since the previous method turned out to be unsuitable for the kinetic resolution of unsymmetric homoaldols, the task of this part of the PhD work was the development and identification of a new catalyst system, which would allow an efficient resolution of these readily available and synthetically versatile γ -hydroxy acetals.

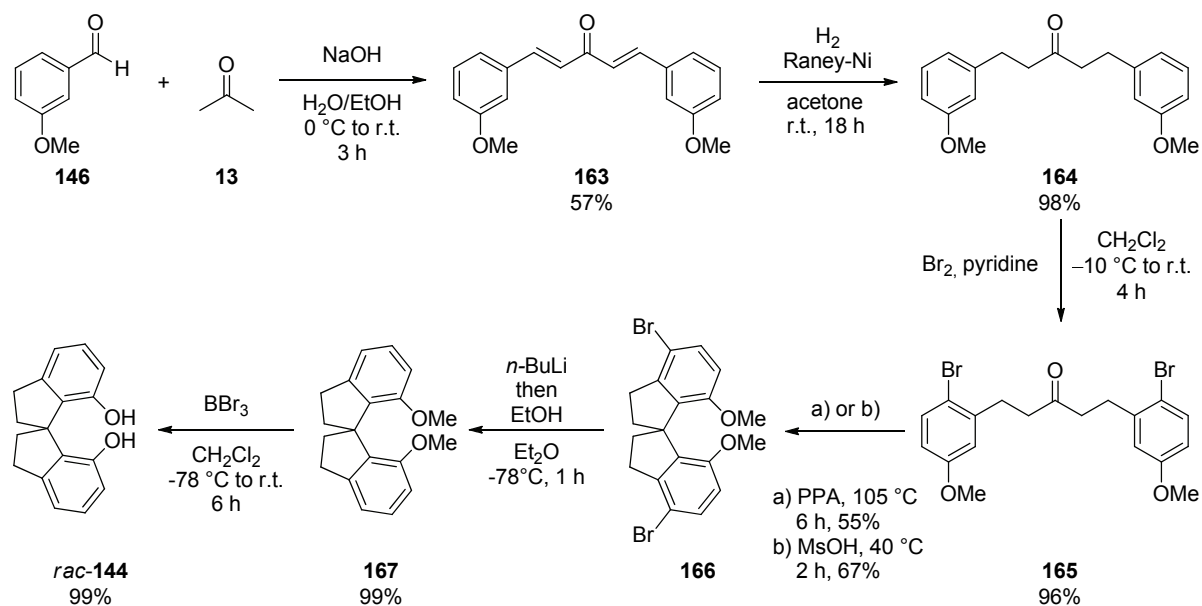
4 Results and Discussion

4.1 Synthesis of SPINOL-Derived Phosphoric Acids and Disulfonimides

The first part of this thesis describes the synthesis of SPINOL-derived phosphoric acids and disulfonimides as complementary tools for asymmetric Brønsted and Lewis acid catalysis. Unlike in the case of BINOL-derived catalysts, the C₂-symmetric 1,1'-spirobiindane-7,7'-diol (SPINOL, **144**) was not commercially available and had to be synthesized.

4.1.1 Synthesis of Racemic and Enantiomerically Pure SPINOL

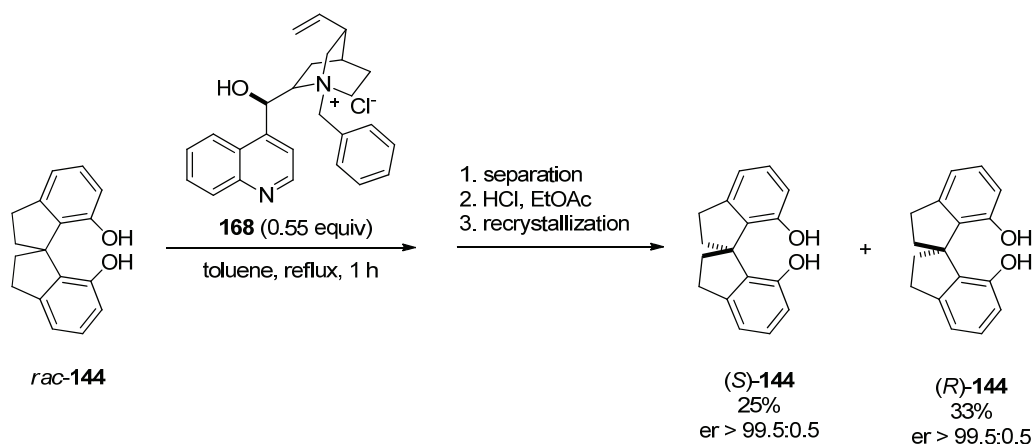
The synthesis of racemic SPINOL (*rac*-**144**) was first reported by Birman *et al.*^[123] and we started our work following the reported protocol. The synthesis starts with a double Claisen-Schmitt condensation between 3-methoxybenzaldehyde (**146**) and acetone (**13**), to afford the dienone **163** in 57% yield. It was then treated with Raney-Ni under an atmosphere of hydrogen to give the ketone **164** in quantitative yield. Subsequent bromination with bromine in the presence of pyridine is necessary to introduce a protecting group *para* to the methylether in order to direct the following cyclization into the *ortho*-position.



Scheme 42. Synthesis of racemic SPINOL (*rac*-**144**).

When the cyclization of dibromide **165** was conducted in polyphosphoric acid as described by Birman and co-workers, the spirocycle **166** was obtained in only 55% yield, whereas treatment of ketone **165** with MsOH afforded the desired product **166** with an increased yield of 67%. The debromination on a large scale (> 1g) was best achieved by a lithium halogen exchange followed by a protic workup. The final *O*-demethylation with BBr₃ afforded racemic SPINOL (*rac*-**144**) in an overall yield of 35% over six steps (Scheme 42).

For the resolution of diol *rac*-**144** the method developed by the groups of Deng, Zhou and Ye was followed.^[135] Accordingly, racemic SPINOL (*rac*-**144**) was treated with *N*-benzylcinchonidinium chloride (**168**) and the precipitating 1:1 inclusion complex of the ammonium salt **168** and (*S*)-SPINOL ((*S*)-**144**) was separated from the (*R*)-SPINOL containing solution. After removal of the residual ammonium salt by treatment with HCl and subsequent recrystallization both enantiomers were obtained in virtually enantiomerically pure form in 25% and 33% yield, respectively.

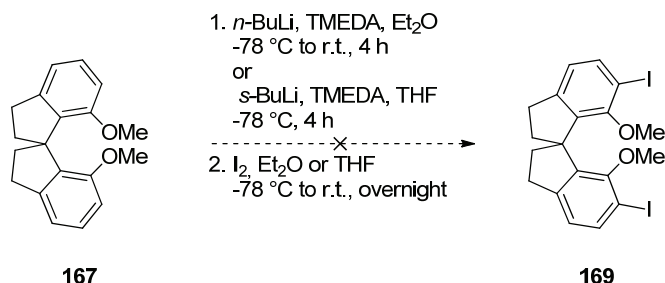


Scheme 43. Resolution of racemic SPINOL (*rac*-**144**) using the method developed by the groups of Deng, Zhou and Ye.

4.1.2 Synthesis of Phosphoric Acids from Racemic SPINOL

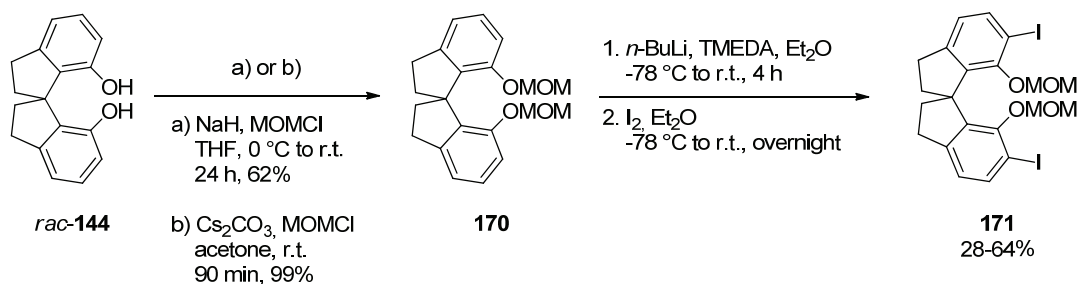
For the synthesis of the targeted SPINOL-derived phosphoric acids **145**, the racemic as well as the enantiomerically pure diol **144** was now available. However, in order to obtain both enantiomers of the potential catalysts with a minimum number of synthetic manipulations, the synthesis was first conducted with racemic starting material, relying on enantiomer separation of the final phosphoric acids via preparative chiral HPLC.

To enable the introduction of different 6,6'-substituents these positions had to be functionalized accordingly. Attempts to conduct a directed *ortho*-lithiation iodination sequence on the stage of the dimethylether **167** did not lead to the corresponding diiodide **169** (Scheme 44).



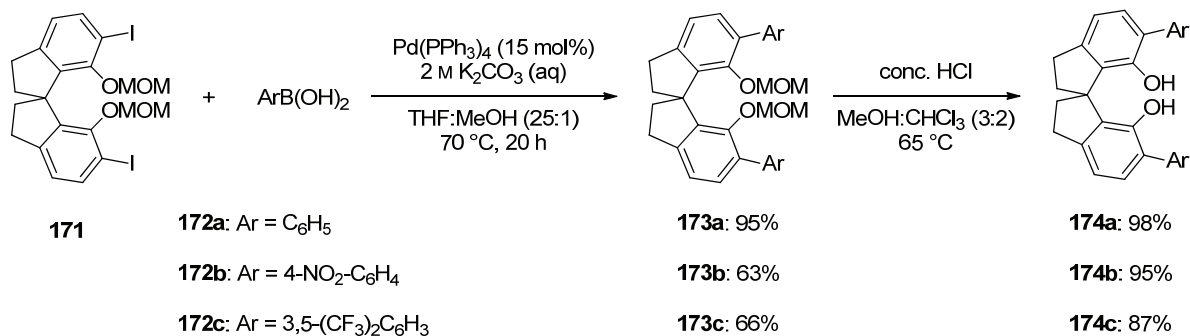
Scheme 44. Attempted 6,6'-functionalization of methylether **167**.

In 2007 Zhou *et al.* had reported this reaction to be successful starting from the MOM-protected SPINOL **170**.^[136] Following their procedure for the MOM-protection of diol *rac*-**144** with sodium hydride and chloromethyl methyl ether gave the desired product **170** in 62% yield. This result was improved to quantitative yield by using caesium carbonate as the base in acetone as the solvent. With intermediate **170** the iodination was successful, although the desired product **171** was obtained in varying yields of 28-64%, along with significant amounts of mono-iodinated product when the procedure reported by the group of Zhou was employed (Scheme 45).



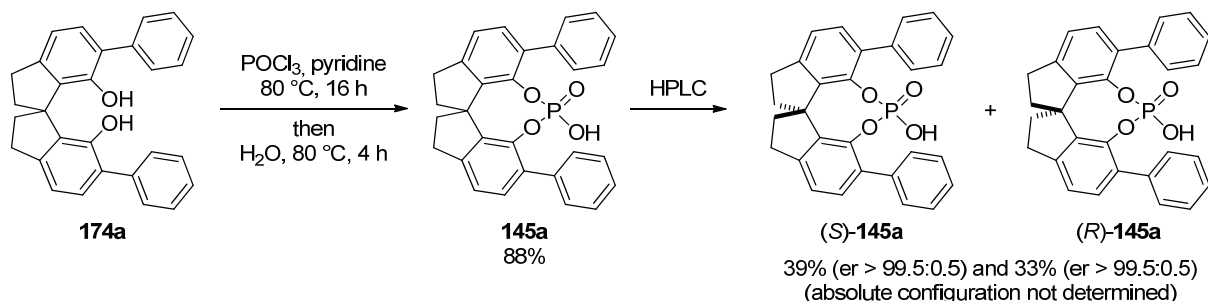
Scheme 45. Synthesis of diiodide **171** from SPINOL (*rac*-**144**).

With key intermediate **171** in hand, structural diversity was introduced by using Suzuki-Miyaura cross couplings with different boronic acids **172a-c**. The method reported by Zhou and co-workers worked well for differently substituted phenylboronic acids and the coupling products **173a-c** were obtained in 63-95% yield. MOM-deprotection was achieved with concentrated hydrochloric acid and afforded the desired diols **174a-c** in $\geq 87\%$ yield (Scheme 46).



Scheme 46. Suzuki-Miyaura couplings of diiodide **171** with boronic acids **172a-c** and subsequent MOM-deprotection.

For the final steps in the synthesis of the first SPINOL-derived phosphoric acids, the diols **174a-c** were treated with POCl₃ in pyridine followed by hydrolysis according to a standard procedure used for the BINOL-analogs.^[39,40] However, under standard conditions the reaction between the diol **174a** and POCl₃ proceeded only sluggishly and elevated temperature and prolonged reaction time were required to reach full conversion to the acid chloride. Surprisingly, even the hydrolysis of the phosphoric acid chloride proved difficult under standard reaction conditions and was only achieved by using elevated temperatures (Scheme 47).

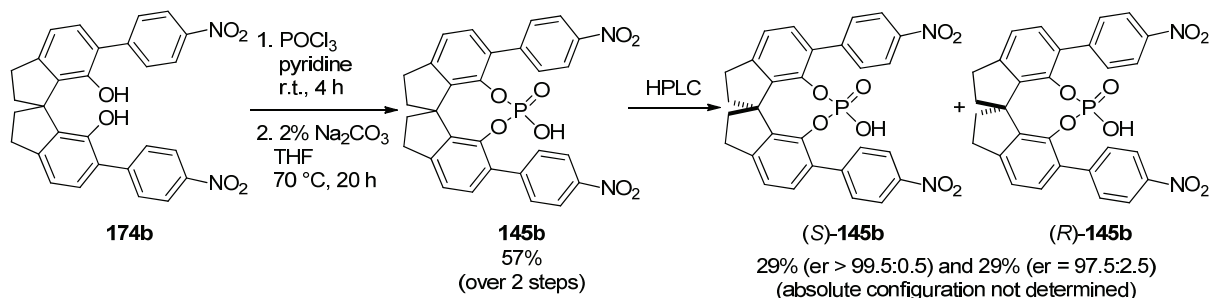


Scheme 47. Synthesis and resolution of SPINOL-derived phosphoric acid **145a**.

The resolution of **145a** was achieved by preparative HPLC and two enantiomerically pure fractions (39% and 33% yield) of unknown configuration were obtained.

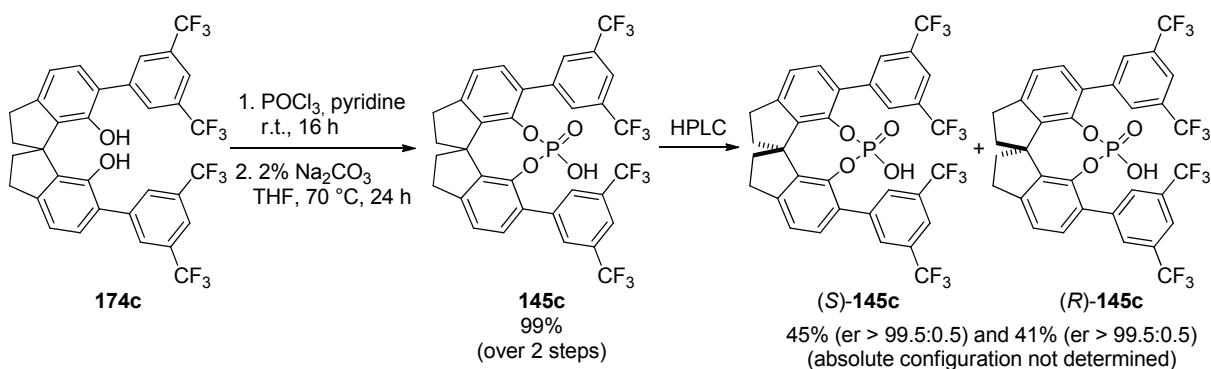
The synthesis and resolution of phosphoric acid **145b** was achieved in a similar manner. Diol **174b** was converted to the corresponding phosphoric acid chloride by treatment with POCl₃ in pyridine. In this case the crude acid chloride was isolated and hydrolyzed with aqueous sodium carbonate solution in refluxing THF to afford the racemic acid **145b** in 57% yield from diol **174b**. Resolution by preparative HPLC gave 29% of one

enantiomerically pure acid and 29% of the second enantiomer with 97.5:2.5 er (Scheme 49). The absolute configurations were not determined.



Scheme 48. Synthesis and resolution of SPINOL-derived phosphoric acid **145b**.

The same route was also used to obtain the phosphoric acids **(S)-145c** and **(R)-145c**. In this case the separation by preparative HPLC was more efficient and gave both enantiomers with >99.5:0.5 er in 45% and 41% yield, respectively (Scheme 49).

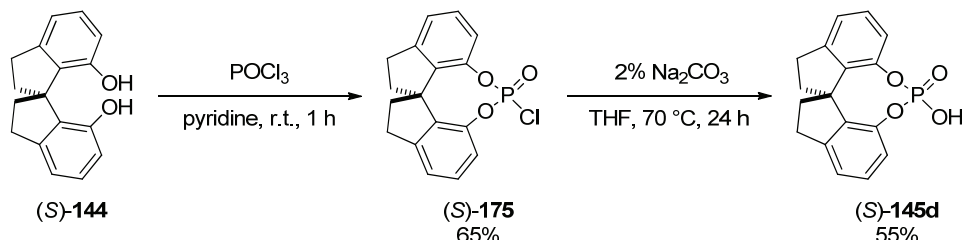


Scheme 49. Synthesis and resolution of SPINOL-derived phosphoric acid **145c**.

Although the resolution via HPLC on the stage of the final phosphoric acids is beneficial in terms of step economy and at the same time provides potential catalysts of high purity, it turned out that most racemic phosphoric acids were poorly soluble and the resolution via HPLC was not very efficient. Only phosphoric acid **145c** proved to be well suited for this kind of resolution, allowing for column loadings of >30 mg per run with a run time <10 min. The usually observed insufficient separation of the enantiomers and the small amount of material which could be separated in a single run suggested the syntheses to be better conducted starting from already resolved SPINOL.

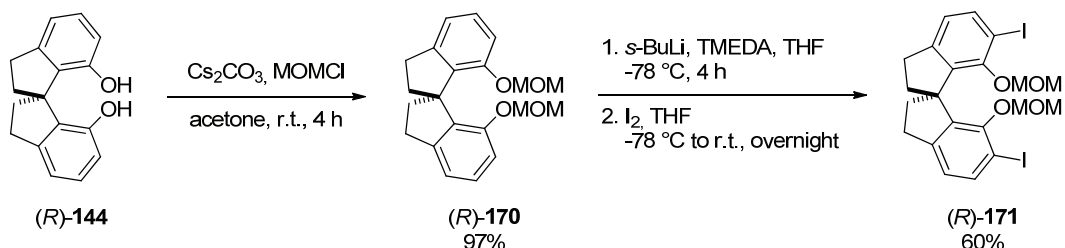
4.1.3 Synthesis of Phosphoric Acids from Enantiomerically Pure SPINOL

The unsubstituted SPINOL-phosphoric acid (*S*)-**145d** was obtained after treatment of the resolved diol (*S*)-**144** (see Scheme 43) with POCl₃ and hydrolysis of the crude acid chloride under previously established conditions (Scheme 50).



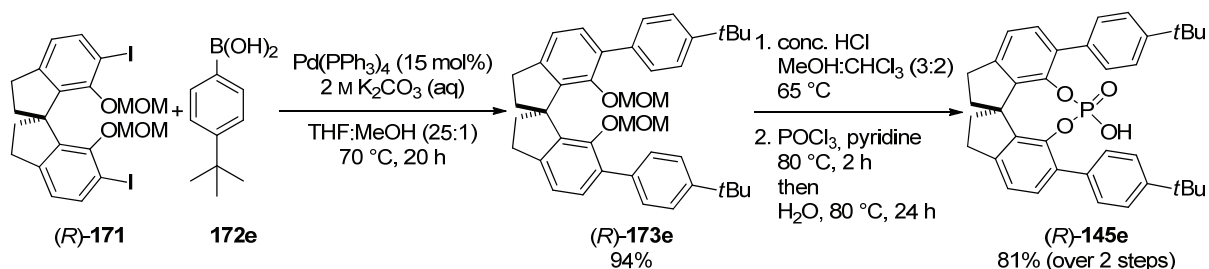
Scheme 50. Synthesis of (*S*)-SPINOL hydrogenphosphate ((*S*)-**145d**).

For the introduction of 6,6'-substituents, the same strategy of MOM-protection and *ortho*-lithiation iodination sequence was used as before in the racemic series (see Scheme 45). However, by replacing *n*-butyllithium for *s*-butyllithium and a switch in solvent from diethyl ether to tetrahydrofuran the reproducibility of the iodination step was improved and gave diiodide (*R*)-**171** in 60% yield from the MOM-protected diol (*R*)-**170** (Scheme 51).



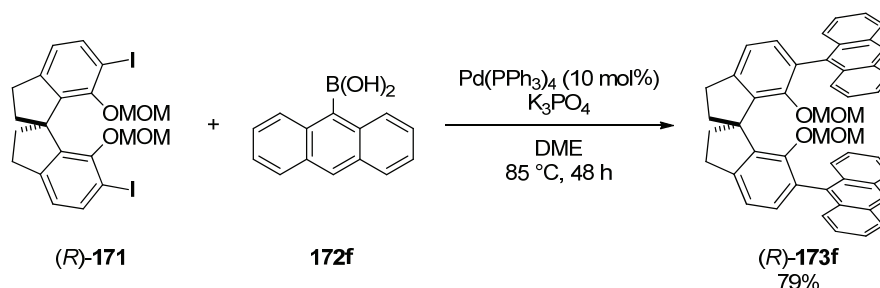
Scheme 51. MOM-Protection and diiodination of (*R*)-SPINOL ((*R*)-**144**) under optimized reaction conditions.

The 6,6'-bis-4-(*tert*-butyl)phenyl substituted phosphoric acid (*R*)-**145e** was accessible in good overall yield over three steps from the diiodide (*R*)-**171** by Suzuki coupling, MOM-deprotection and phosphorylation as already described for the synthesis of related racemic phosphoric acids (Scheme 52).



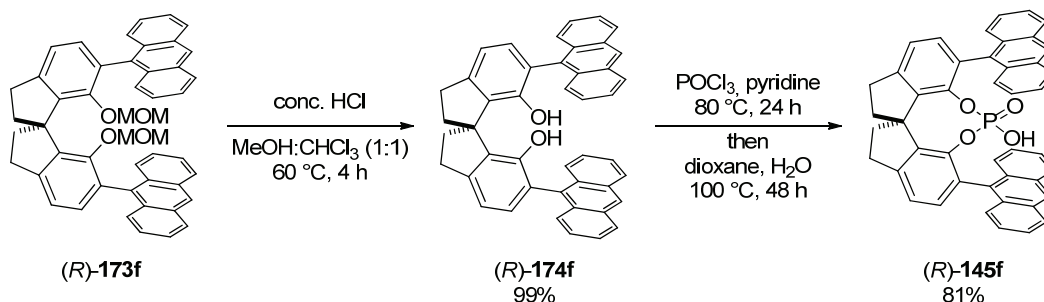
Scheme 52. Synthesis of (R) -SPINOL-derived phosphoric acid (R) -**145e**.

Another frequently utilized 3,3'-substituent in BINOL-derived catalysts is the 9-anthracenyl moiety. Attempts to access the SPINOL analog of this phosphoric acid using the established method failed on the stage of the palladium-catalyzed coupling between diiodide (R) -**171** and 9-anthracenylboronic acid (**172f**). After individual optimization for this boronic acid, the best results were obtained when potassium phosphate was used as the base and the reaction was conducted in dimethoxyethane as the solvent.^[137] Under these conditions the coupling product (R) -**173f** was obtained in 79% yield (Scheme 53).



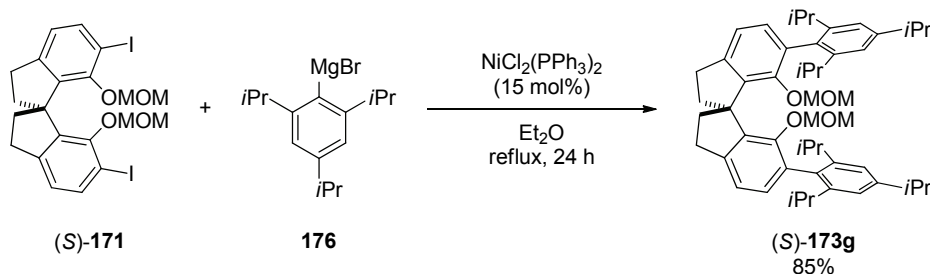
Scheme 53. Suzuki coupling of diiodide (R) -**171** with 9-anthracenyl boronic acid (**172f**).

The subsequent deprotection with concentrated hydrochloric acid worked as before and afforded diol (R) -**174f** in quantitative yield. When the substituted SPINOL (R) -**174f** was submitted to POCl_3 in the presence of pyridine at elevated temperature, the desired phosphoric acid chloride precipitated as a colorless solid. Due to its poor solubility in a variety of different solvents the hydrolysis of the acid chloride proved challenging and was finally achieved by diluting the crude reaction mixture with 1,4-dioxane, followed by quenching with water and heating to 100 °C for 48 hours until a clear solution was obtained again (Scheme 54).



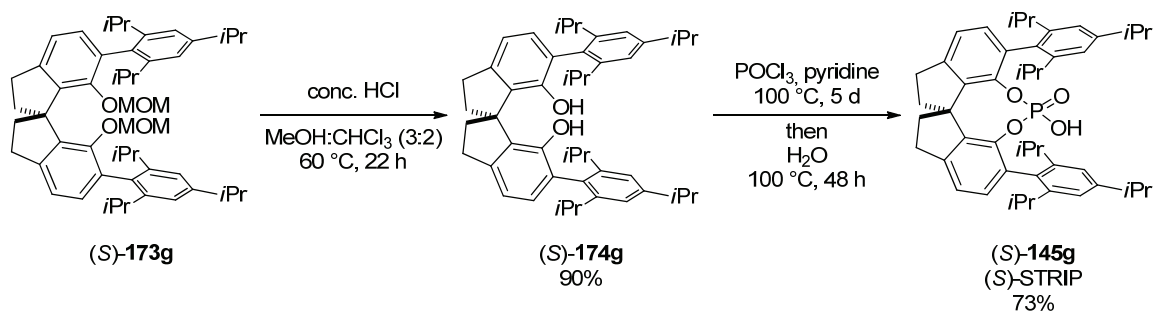
Scheme 54. Synthesis of bis-(9-anthracenyl)-substituted phosphoric acid (*R*)-**145f**.

One of the most successfully employed phosphoric acids with respect to highly enantioselective applications is 3,3'-bis(2,4,6-triisopropylphenyl)-1,1'-binaphthyl-2,2'-diyl hydrogenphosphate (**33d**, TRIP).^[138] Consequently, the SPINOL-derived analog was another important synthetic target for us. It was already known from the synthesis of the BINOL-derived catalyst that the 2,4,6-triisopropylphenyl substituents have to be introduced via a Kumada coupling since Suzuki reactions are usually not successful.^[139] Accordingly, the diiodinated and MOM-protected SPINOL (*S*)-**171** was submitted to the Kumada cross coupling reaction with Grignard reagent **176** and the coupled product **173g** was obtained in 85% yield (Scheme 55).



Scheme 55. Kumada cross coupling of diiodide (*S*)-**171** and Grignard reagent **176**.

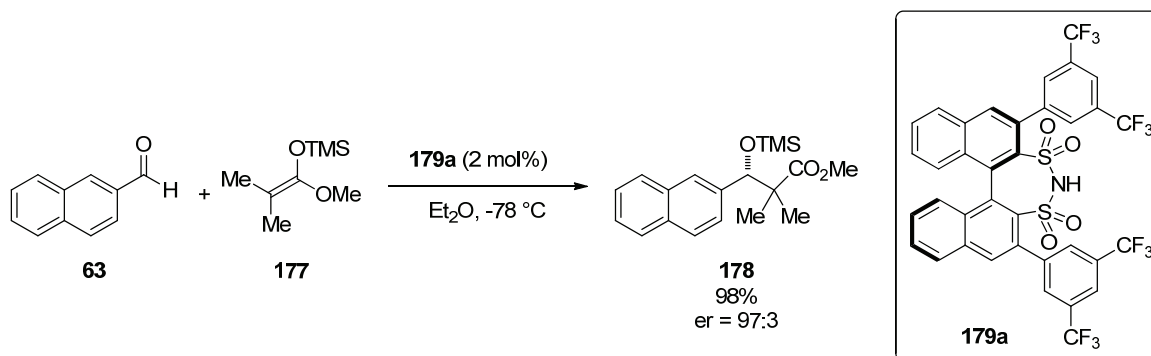
The last steps in the synthesis of (*S*)-STRIP ((*S*)-**145g**), the spirocyclic analog of TRIP (**33d**), started as usual with the deprotection of the coupling product (*S*)-**173g** under standard conditions to give the diol (*S*)-**174g** in 90% yield. In this case the phosphorylation as well as the subsequent hydrolysis of the intermediary acid chloride required forcing conditions including elevated temperatures and prolonged reaction times to give (*S*)-STRIP ((*S*)-**145g**) in 73% yield from the diol (*S*)-**174g**. This poor reactivity may be attributed to the steric congestion of the hydroxy groups caused by the bulky 6,6'-substituents (Scheme 56).



Scheme 56. Last steps in the synthesis of the spirocyclic TRIP analog STRIP ((S)-145g).

4.1.4 Synthesis of SPINOL-Derived Disulfonimides

In 2009 our group reported the development of the chiral BINOL-derived disulfonimide **179a** and its application to highly enantioselective Mukaiyama aldol reactions of silyl ketene acetals of type **177** with simple aldehydes like **63** (Scheme 57).^[127] Since these chiral disulfonimides are not only excellent Brønsted acids, but turn into strong Lewis acids upon silylation, they offer an attractive tool for strong chiral Brønsted acid catalysis as well as an entry for enantioselective organic Lewis acid catalysis.

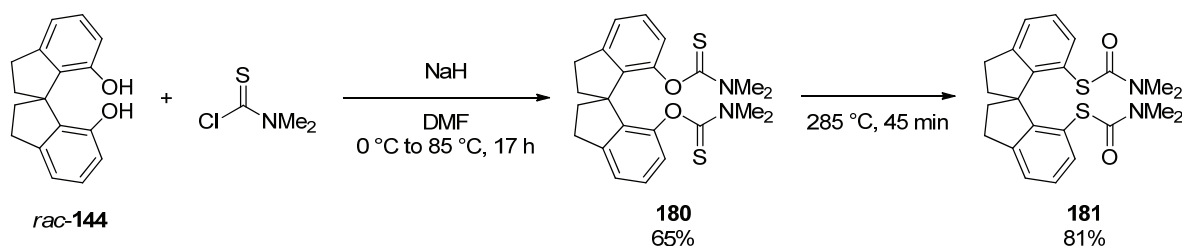


Scheme 57. Disulfonimide **179a** catalyzed Mukaiyama aldol reaction reported by our group.^[127]

In order to provide new and potentially complementary catalysts of this type, the synthesis of the related SPINOL-derived disulfonimides became another exciting objective. Since the enantiomers of the corresponding 3,5-bis(trifluoromethyl)phenyl substituted phosphoric acid **145c** were easily separable via preparative HPLC, the corresponding disulfonimide was assumed to behave equally well. This would allow to obtain both enantiomers of the catalyst in a minimum number of synthetic steps and so the synthesis

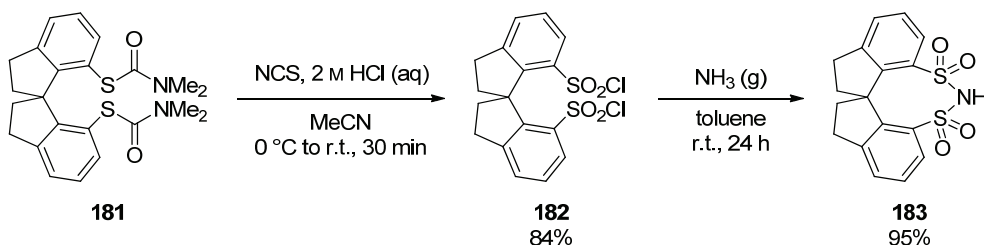
was started from racemic SPINOL (*rac*-**144**), using a modification of the route reported for the BINOL-derived catalyst **179a**.^[127,140,141]

Deprotonation of the diol *rac*-**144** with sodium hydride and treatment with dimethyl thiocarbamoyl chloride in DMF gave the *O*-arylthiocarbamate **180** in 65% yield. Careful optimization of the Newman-Kwart rearrangement^[142] revealed the reaction to be best conducted at 285 °C to afford 81% of the *S*-arylthiocarbamate **181** (Scheme 58).



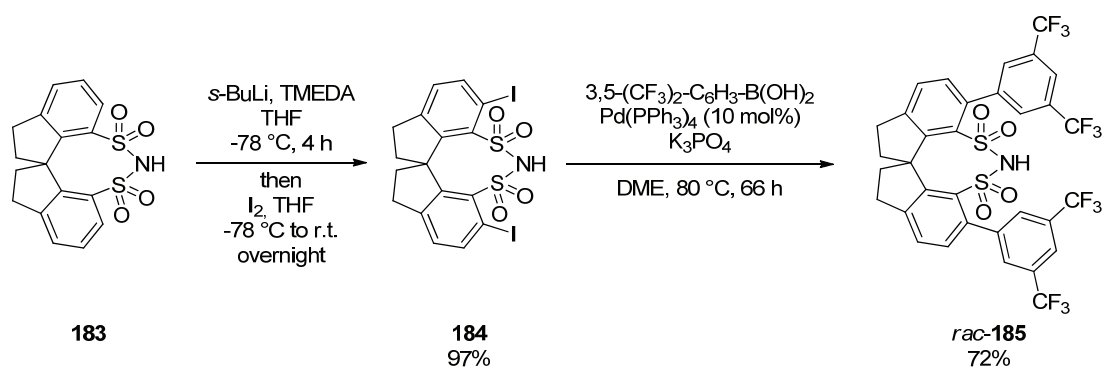
Scheme 58. Synthesis of *S*-arylthiocarbamate **181** from racemic SPINOL (*rac*-**144**).

Carbamate **181** was directly converted to the disulfonic acid chloride **182** by treatment with *N*-chlorosuccinimide and hydrochloric acid.^[143] When this acid chloride was dissolved in toluene and exposed to ammonia gas, the 6,6'-unsubstituted disulfonimide **183** was obtained (Scheme 59).



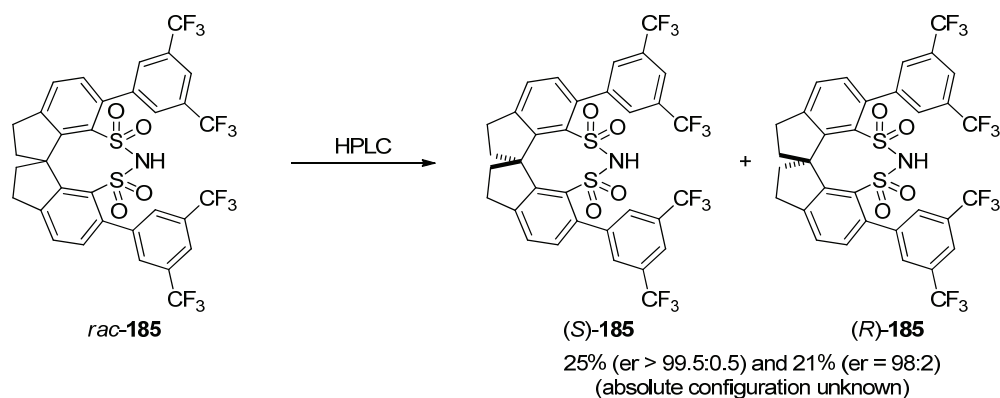
Scheme 59. Synthesis of the 6,6'-unsubstituted disulfonimide **183**.

The introduction of 6,6'-substituents was finally achieved by an efficient *ortho*-lithiation iodination sequence of disulfonimide **183** and subsequent Suzuki-Miyaura cross coupling of diiodide **184** with the corresponding arylboronic acid **172c** (Scheme 60).



Scheme 60. Introduction of 6,6'-substituents to disulfonimide **183** by iodination and palladium-catalyzed cross coupling.

Unfortunately, the separation of the two enantiomers of the substituted compound *rac-185* by preparative HPLC was not very efficient and afforded only one pure enantiomer in 25% yield along with the second enantiomer with 98:2 er in 21% yield (Scheme 61). This poor separation is the result of very similar retention times, resulting in insufficient separation of the two enantiomers and limitation of the processable amount of catalyst.



Scheme 61. Separation of spirocyclic disulfonimide *rac-185* by preparative HPLC.

4.1.5 Structural Comparison of SPINOL-Derived Catalysts with their BINOL Analogs

After the synthesis of the target molecules was accomplished and some representative X-ray structures were obtained, the structural differences and similarities of the new catalysts with their BINOL-derived counterparts were investigated. We were hoping that this comparison could later on be helpful in order to explain potentially different behaviour in catalysis and lead to a better understanding of the catalysts.

4.1.5.1 Phosphoric Acids

In comparison to BINOL-derived phosphoric acids and the majority of other previously reported phosphoric acid catalysts (see Figure 3), in which the acid functionality is embedded in a seven-membered ring, the SPINOL-analogs contain an eight-membered ring with the active motif. A comparison of X-ray structures of SPINOL-derived phosphoric acid **145a** (Figure 7) and a BINOL-based analog revealed further structural differences.

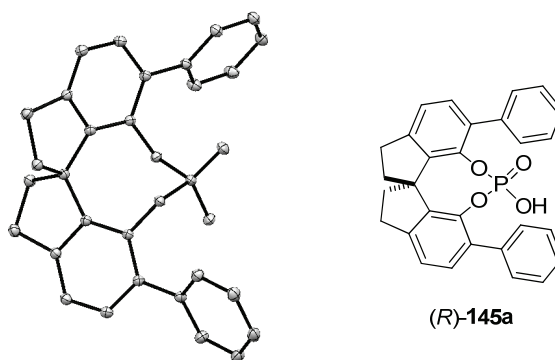


Figure 7. ORTEP plot of the X-ray crystal structure of SPINOL-derived phosphoric acid **145a**. Ellipsoids are drawn at 50% probability level.

The comparison of the crystal structures of phosphoric acid **145a** and the related BINOL-derived catalyst **33e**^[144] revealed the distances l between the outer corners of the 3,3'- and 6,6'-substituents to be very similar. Also the dihedral angle β of the catalyst backbones was very similar in both cases (Figure 8).

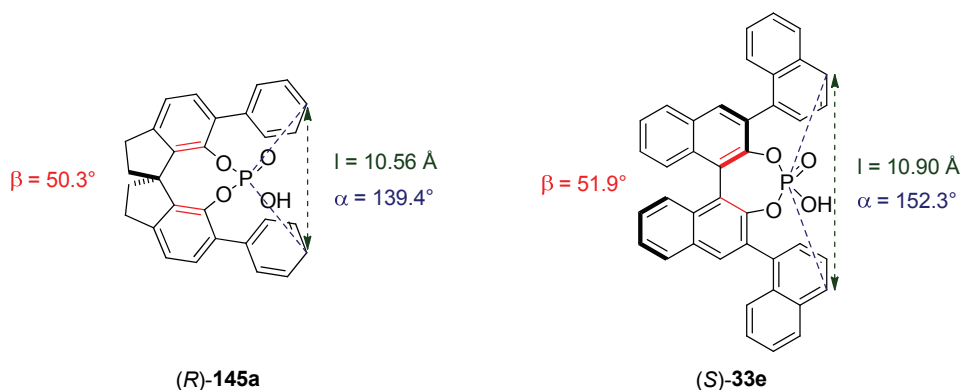


Figure 8. Structural comparison of SPINOL- and BINOL-derived phosphoric acids **145a** and **33e**.

However, the angle α which is spanned by the 6,6'- and 3,3'-substituents, respectively, and the phosphorous atom, representing the active center of the catalyst,

turned out to be significantly different and smaller in the spirocyclic acid **145a**. As a consequence, the chiral pocket in the SPINOL-derived catalyst **145a** is deeper than in the BINOL derivative **33e**. This difference may account for the reactivity differences encountered in the phosphorylation of the corresponding diols and the subsequent hydrolysis of the acid chlorides.

4.1.5.2 Disulfonimides

Chiral disulfonimides are relatively new catalysts and only little is known about their structure and their mode of action. Thus, the comparison of the X-ray structure of SPINOL-derived disulfonimide **185** (Figure 9) with its BINOL analog **179a** could be helpful in providing more insight into the structural requirements for a privileged catalyst.

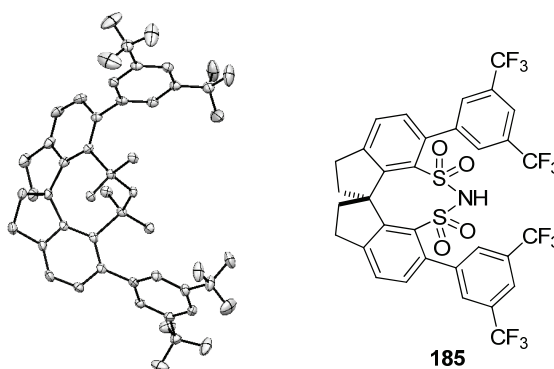


Figure 9. ORTEP plot of the X-ray crystal structure of SPINOL-derived disulfonimide **185**. Ellipsoids are drawn at 50% probability level.

Analysis of the X-ray structure of the spirocyclic disulfonimide **185** and the BINOL-derived catalysts **179a**^[140] revealed significant structural differences. While the dihedral angle β of the catalyst backbone of disulfonimide **185** ($\beta = 54.6^\circ$) is similar to the one of the corresponding phosphoric acid, the dihedral angle in the BINOL scaffold **179a** is significantly larger ($\beta = 65.2^\circ$), illustrating the higher flexibility of this backbone due to the biaryl axis (Figure 10).

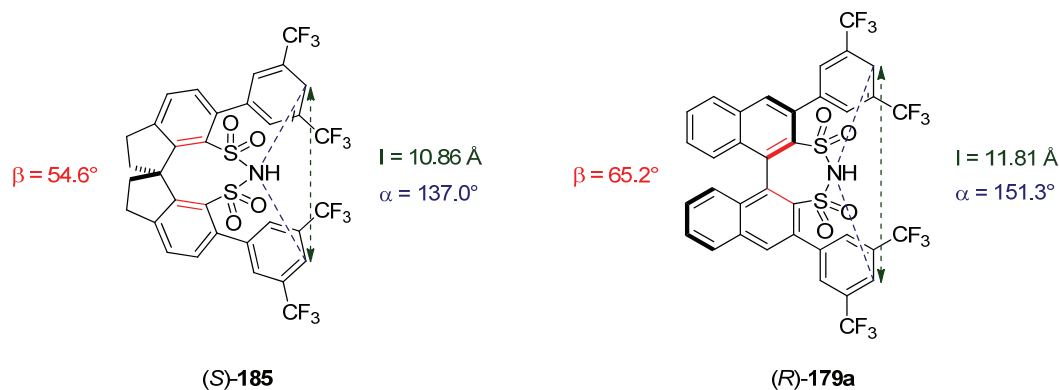


Figure 10. Structural comparison of SPINOL- and BINOL-derived disulfonimides (*S*)-**185** and (*R*)-**179a**.

Also the distances I between the outer corners of the substituents as well as the active angle α under which a potential substrate can approach the active center of the catalyst are smaller in the spirocyclic molecule **185**. Altogether the chiral pocket in disulfonimide **185** is notably smaller than that of catalyst **179a**.

4.1.6 Summary

In the first part of this thesis, the synthesis of novel SPINOL-derived phosphoric acids and disulfonimides as new tools for asymmetric Brønsted and Lewis acid catalysis is described. The new phosphoric acids were obtained in 12 steps from aldehyde **146** and acetone (**13**). It was shown that a racemic synthesis followed by resolution of the enantiomers by chiral HPLC can be a powerful strategy to obtain both enantiomers of the catalyst in pure form, if a sufficient method for the separation is available. The alternative strategy involved the literature known resolution of SPINOL (**144**) as common precursor. The developed route to disulfonimides of type **185** required 13 steps and was only conducted with racemic material and subsequent separation of the enantiomers via HPLC. The obtained X-ray structures of both catalyst classes allowed for a first comparison of their structural properties. It was shown that SPINOL-derived catalysts are geometrically different from their commonly used BINOL derivatives. In general the new spirocyclic structures provide a more compact chiral environment. How these structural differences translate into their behaviour as catalysts with respect to activity and enantioselectivity will be discussed in the following chapters.

4.2 The Catalytic Asymmetric Fischer Indolization

The importance of the Fischer indole synthesis as method of choice for the construction of indole derivatives and the lack of enantioselective protocols prompted us to develop a catalytic asymmetric version of this reaction using asymmetric Brønsted acid catalysis. The investigations described below include the indolization of arylhydrazones derived from α -branched carbonyl compounds to obtain indolenines with a quaternary stereocenter in the 3-position and the synthesis of 3-substituted tetrahydrocarbazoles from arylhydrazines and 4-substituted cyclohexanones.

4.2.1 Synthesis of Chiral Indolenines via the Fischer Indole Synthesis

Initial experiments were devoted to probe the potential of organic phosphoric acids to act as catalysts in this transformation. Accordingly, phenylhydrazine (**100a**) and 2-methylpentanal (**186**) were mixed in different solvents in the presence of 20 mol% of diphenylphosphate (DPP). In all cases the intermediary hydrazone **187** was formed quantitatively within minutes. In etheric solvents like dioxane and THF the indolization did not proceed under these reaction conditions (Table 1, entries 1 and 4), whereas in the case of dichloromethane, acetonitrile and toluene, around 20% of the desired product **188** was detected after 22 h (Table 1, entries 2, 3 and 5). However, prolonged reaction time did not lead to an improved yield and after increasing the reaction temperature to 40 °C the product slowly started to decompose and no further conversion was observed.

Table 1. DPP as catalyst for the Fischer indolization.^a

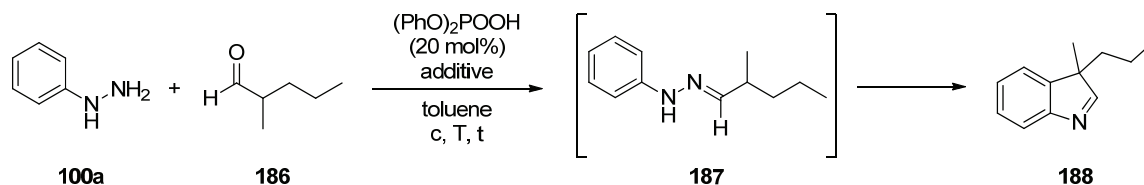
entry	solvent	t	yield of 188 ^b
1	1,4-dioxane	22 h	0%
2	CH ₂ Cl ₂	22 h	18%
3	MeCN	22 h	17%
4	THF	22 h	0%
5	toluene	22 h	18%

^aReactions were conducted in a sealed flask with 0.10 mmol phenylhydrazine (**100a**), 0.10 mmol aldehyde **186** and 20 mol% DPP in 0.5 mL of solvent. ^bDetermined by GC-MS.

These results were encouraging in that they proved the capability of organic phosphoric acids like DPP to promote the Fischer indolization. On the other hand the best conversions obtained were in the range of 20%, resembling the amount of catalyst loading. This lack of catalyst turnover can be explained by the poisoning of the catalyst with basic ammonia, which is generated as the stoichiometric by-product of the reaction. Apparently the acid-base equilibrium is in favour of the ammonium phosphate, thus inhibiting the loss of ammonia from the reaction mixture and the regeneration of the active catalyst.

In order to facilitate the catalyst turnover, the role of different additives was investigated next (Table 2).

Table 2. Screening of additives to facilitate the catalyst turnover.^a



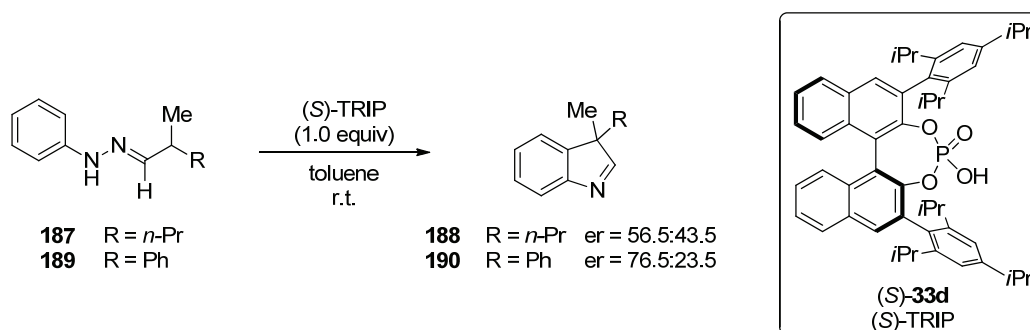
entry	additive	c	t	T	observation
1	aldehyde 186 (1 equiv)	0.2 M	48 h	40 °C	≈ 20% product formed
2	H ₂ O (1 equiv)	0.2 M	48 h	40 °C	≈ 20% product formed
3	PhOH (1 equiv)	0.2 M	48 h	40 °C	≈ 20% product formed
4	AcOH (1 equiv)	0.2 M	48 h	40 °C	≈ 20% product formed
5	(PhO) ₂ POOH (0.8 equiv)	0.2 M	48 h	40 °C	48% isolated yield
6	SiO ₂ (2 equiv)	0.5 M	16 h	r.t.	only hydrazone formation
7	MgSO ₄ (2 equiv)	0.5 M	16 h	r.t.	only hydrazone formation
8	Al ₂ O ₃ (2 equiv)	0.5 M	16 h	r.t.	only hydrazone formation
9	MS 3Å (30 mg)	0.5 M	16 h	r.t.	only hydrazone formation
10	MS 5Å (30 mg)	0.5 M	16 h	r.t.	≈ 20% product formed
11	CuCl (2 equiv)	0.5 M	4 h	r.t.	decomposition
12	CuCl ₂ (2 equiv)	0.5 M	4 h	r.t.	decomposition
13	CuSO ₄ ·5H ₂ O (2 equiv)	0.5 M	4 h	r.t.	decomposition
14	Ag ₂ CO ₃ (2 equiv)	0.5 M	4 h	r.t.	decomposition
15	AgNO ₃ (2 equiv)	0.5 M	4 h	r.t.	decomposition

^aReactions were conducted in a sealed flask with 0.10 mmol phenylhydrazine (**100a**), 0.10 mmol aldehyde **186** and 20 mol% DPP.

An additional equivalent of aldehyde as well as weakly Brønsted acidic additives did not affect the reaction (Table 2, entries 1-4). When a stoichiometric amount of DPP was used,

the reaction achieved high conversion and 48% of the product **188** was isolated (Table 2, entry 5). While 5Å molecular sieves did not influence the normal reaction outcome (Table 2, entry 10), additives like SiO₂, MgSO₄, Al₂O₃ and 3Å molecular sieves seemed to completely inhibit the reaction and only hydrazone formation was observed in these cases (Table 2, entries 6-9). The use of copper and silver salts as additives, which were assumed to trap the liberated ammonia by complexation, resulted only in the rapid decomposition of the starting materials without traces of desired product being formed (Table 2, entries 11-15).

Although at this point no catalyst turnover was achieved with organic phosphoric acids, the general possibility of rendering the indolization enantioselectively had to be investigated. Therefore the preformed hydrazones **187** and **189** were treated with stoichiometric amounts of the chiral phosphoric acid (*S*)-TRIP ((*S*)-**33d**) in toluene. Indeed the desired products **188** and **190** were obtained in scalemic form with an encouraging enantioselectivity of 76.5:23.5 er in the case of indolenine **190** (Scheme 62).



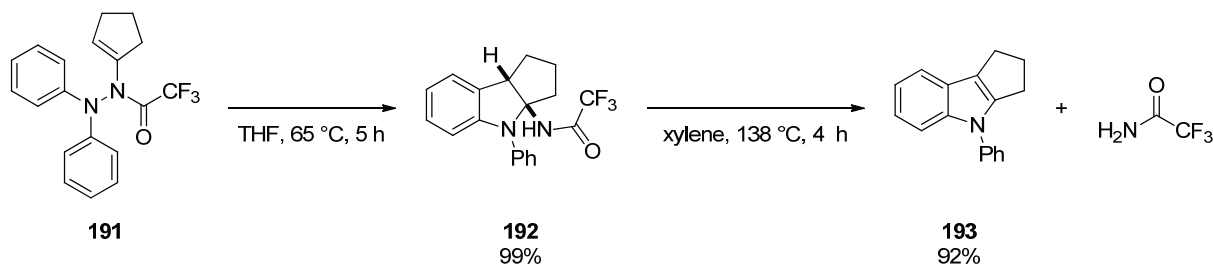
Scheme 62. Indolization with stoichiometric amounts of chiral phosphoric acid (*S*)-**33d**.

However, in order to enable the use of a chiral Brønsted acid at substoichiometric loadings, the problem of catalyst poisoning by ammonia had to be addressed.

4.2.1.1 *N*-Acyl Enehydrazines as Potential Substrates

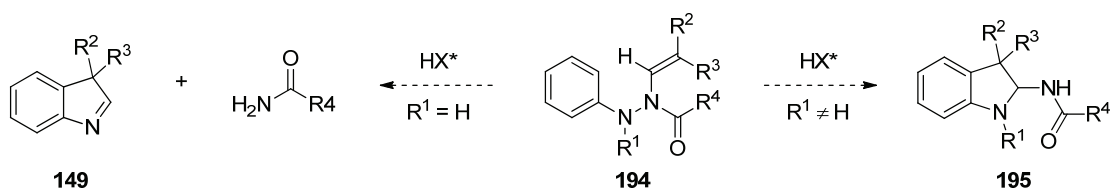
Our next approach to avoid the catalyst poisoning by ammonia was based on the work by Naito and co-workers.^[93] In 1999 this group found that the Fischer indolization of *N*-acyl enehydrazines is a very facile process. Certain substrates already reacted at only slightly elevated temperature without any catalyst to give the desired rearranged products in high yields (see also Scheme 24).^[93a] When enehydrazine **191** was heated to 65 °C in THF the

aminal product **192** was obtained. Upon further heating indoline **192** reacted under loss of trifluoroacetamide to give the indole **193** (Scheme 63).^[93a]



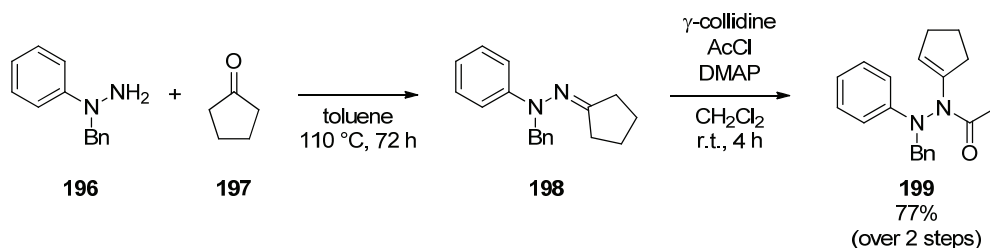
Scheme 63. Thermal Fischer indolization of *N*-acyl enehydrazine **191** reported by Naito and co-workers.^[93a]

Since the products obtained in this reaction are less basic than ammonia, it was rationalized that it should be possible to avoid catalyst poisoning with this class of substrates. Thus a catalytic asymmetric Fischer indolization of related substrates should be realizable if the rearrangement was still susceptible to Brønsted acid catalysis (Scheme 64).



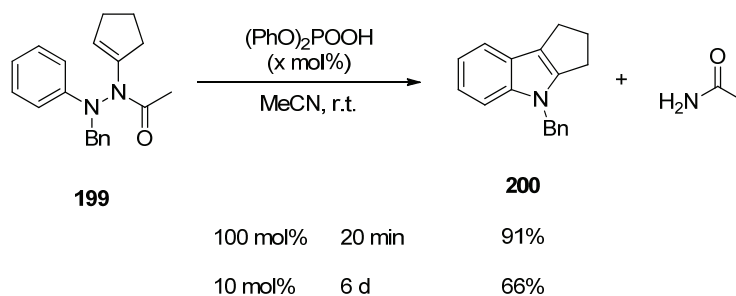
Scheme 64. Intended enantioselective Fischer indolization of *N*-acyl enehydrazines **194** derived from α -branched aldehydes.

To investigate if the rearrangement of *N*-acyl enehydrazines could be accelerated by Brønsted acids, the enehydrazine **199** derived from *N*-benzyl-*N*-phenylhydrazine (**196**) and cyclopentanone (**197**) was synthesized by condensation and acylation as described by Naito and co-workers (Scheme 65).^[93c]



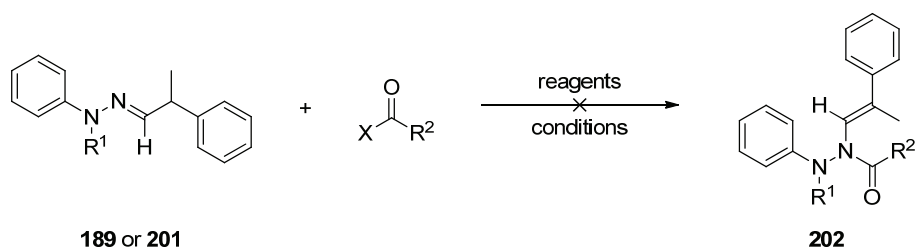
Scheme 65. Synthesis of *N*-acyl enehydrazine **199**.

When a solution of enehydrazine **199** in acetonitrile was treated with an equimolar amount of DPP at ambient temperature, the reaction reached complete conversion within 20 minutes and indole **200** was isolated in 91% yield. When only 10 mol% of DPP were used, the reaction rate decreased significantly. Strikingly though, the reaction did not stop and went to almost complete conversion within 6 days at room temperature to afford the desired product **200** in 66% yield (Scheme 66).



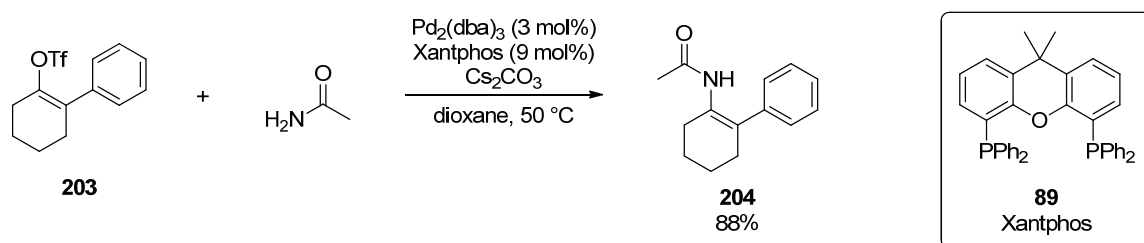
Scheme 66. Phosphoric acid-catalyzed indolization of *N*-acetyl enehydrazine **199**.

Encouraged by this result, we now aimed towards the synthesis of corresponding substrates derived from hydratropic aldehyde (**101**) and different phenylhydrazines. Therefore the preformed hydrazone **189** or **201** was treated with an acylating agent in the presence of a suitable base. However, all attempts to access the *N*-benzylated enehydrazines **202** failed. Depending on the reaction conditions, the starting material did not react or complex mixtures of products were obtained (Table 3, entries 1-9). When hydrazone **189** derived from unprotected phenylhydrazine was used (Table 3, entries 10 and 11), the acylation only took place at the free *NH*-group and again neither the desired product nor the double acylated product was formed. These results are in agreement with the work by Alcaide *et al.*, who also did not achieve the *N*-acylation of enehydrazines with acid chlorides.^[145] However, they found a similar product to be formed from the reaction of an azine with diphenylketene. Applied to our system, this procedure failed and again a complex mixture of products was obtained with no indication of the desired *N*-acyl enehydrazine (Table 3, entries 12).

Table 3. Attempted acylation of phenylhydrazones derived from hydratropic aldehyde.

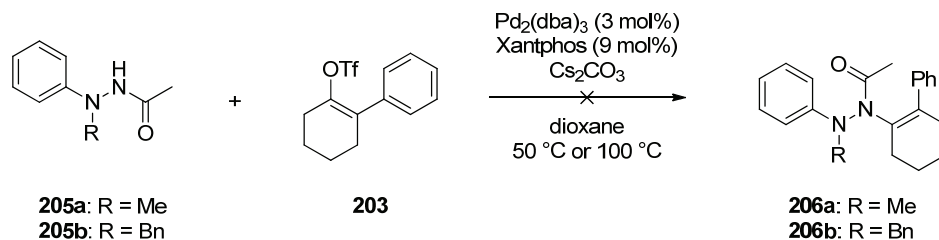
entry	hydrazone	R ¹	X-CO-R ²	reagents	conditions
1	201a	Bn	AcCl	γ -collidine	CH ₂ Cl ₂ , r.t.
2	201a	Bn	AcCl	γ -collidine, DMAP	CH ₂ Cl ₂ , r.t.
3	201a	Bn	AcCl	NEt ₃	benzene, r.t. to reflux
4	201a	Bn	AcCl	NEt ₃	THF, r.t. to 50 °C
5	201a	Bn	AcCl	pyridine	benzene, 0 °C to r.t. to reflux
6	201a	Bn	AcCl	-	CH ₂ Cl ₂ , -78 °C to r.t.
7	201a	Bn	Ac ₂ O	pyridine	neat, r.t. to 100 °C
8	201a	Bn	TFAA	γ -collidine	CH ₂ Cl ₂ , 0 °C to r.t.
9	201a	Bn	TFAA	NEt ₃	CH ₂ Cl ₂ , 0 °C
10	189	H	TFAA	γ -collidine	CH ₂ Cl ₂ , 0 °C
11	189	H	Boc ₂ O	NEt ₃ , DMAP	MeCN, r.t.
12	201b	Boc		-	benzene, reflux

Since it was not possible to achieve the acylation of hydrazones derived from α -branched aldehydes, the possibility to access the desired substrates for our Fischer indolization using a cross coupling methodology was investigated. In 2003 Wallace and co-workers reported the synthesis of enamides of type **204** via a palladium-catalyzed coupling of enol triflates **203** with amides (Scheme 67).^[146]

**Scheme 67.** Pd-Catalyzed amidation of enol triflates **203** by Wallace and co-workers.^[146]

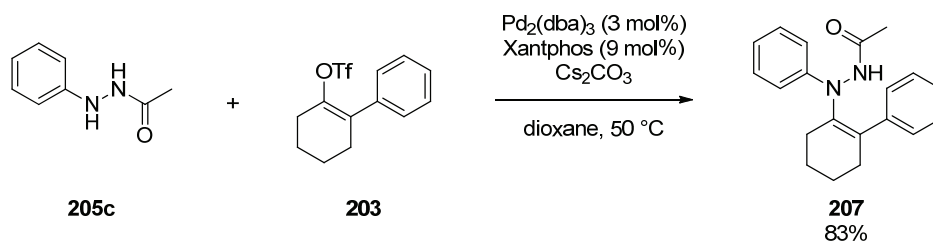
Based on this report it was hypothesized that it should be possible to replace the amide component in this reaction by a suitable *N*-acylated hydrazine. To probe whether or not this holds true, the *N*-alkylated acetylhydrazines **205a** and **205b** were submitted to the

coupling with enoltriflate **203**. Unfortunately, this reaction did not proceed under the reported conditions and elevated temperature only resulted in complex product mixtures, so that the targeted enehydrazines **206a** and **206b** were not obtained (Scheme 68).



Scheme 68. Attempted coupling between hydrazines **205a** and **205b** and enoltriflate **203**.

When instead of *N*-alkylated *N*-phenylhydrazines **205a** and **205b**, the non-protected *N*-phenyl-*N'*-acetylhydrazine **205c** was used, the reaction proceeded cleanly to give a new product in 83% yield. However, it turned out that in this case the coupling proceeded at the wrong nitrogen atom and the undesired regioisomer **207** was the product obtained (Scheme 69).

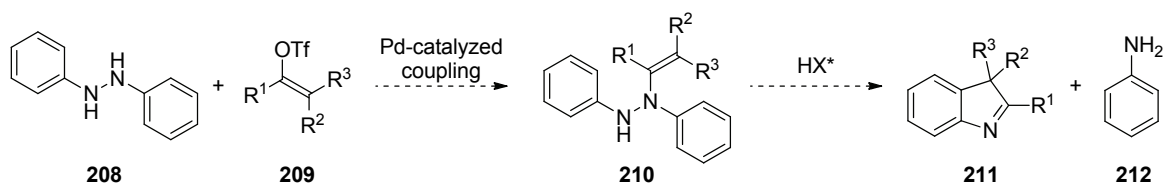


Scheme 69. Palladium-catalyzed coupling of phenylhydrazine **205c** and enoltriflate **203**.

Although all attempts to access *N*-acyl enehydrazines derived from α -branched carbonyl compounds remained fruitless, the outcome of this last coupling reaction opened up a new opportunity to access suitable substrates for the catalytic asymmetric Fischer indole synthesis.

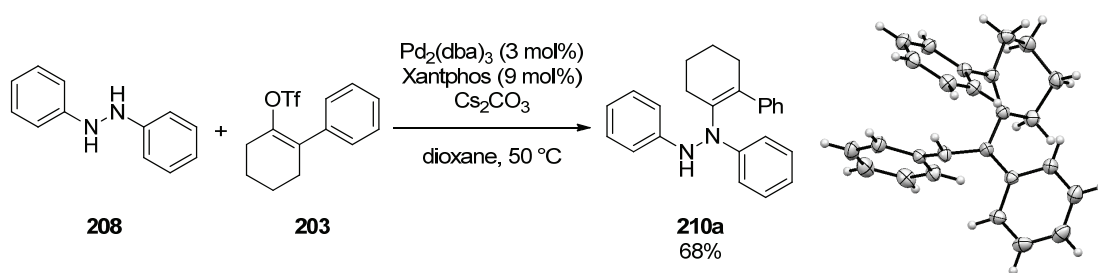
4.2.1.2 *N,N'*-Diphenylenehydrazines as Potential Substrates

The palladium-catalyzed coupling of hydrazine **205c** had shown that the reaction proceeded preferentially at the anilinic nitrogen of the hydrazine (Scheme 69). From this observation the use of the symmetric *N,N'*-diphenylhydrazine (**208**) appeared logical, since a coupling with this reagent should inevitably afford a preformed enehydrazine **210**, which could be a useful substrate for the Fischer indolization (Scheme 70).



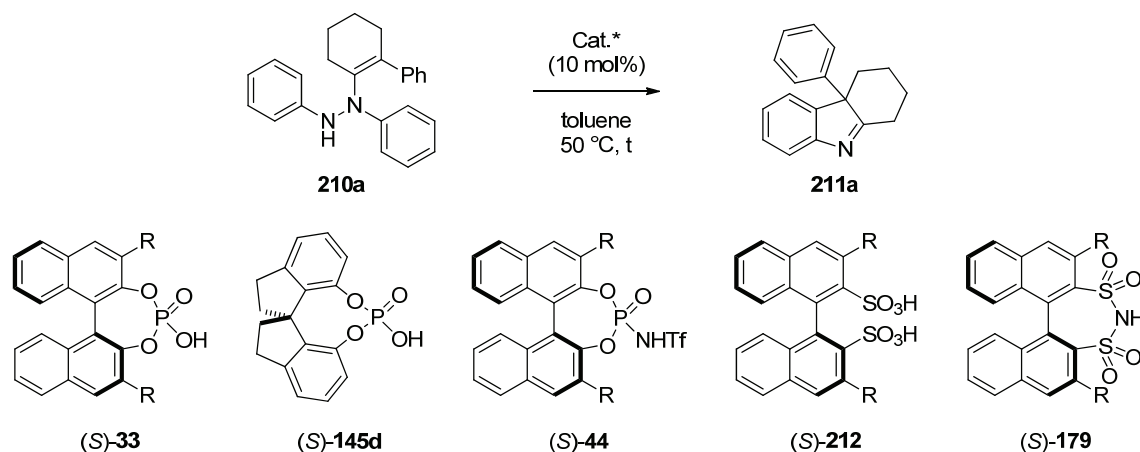
Scheme 70. Envisioned new strategy towards a catalytic asymmetric Fischer indole synthesis.

This type of indolization would produce aniline (**212**) as the stoichiometric by-product. Although aniline is a better proton scavenger than acetamide, it is still significantly less basic than ammonia ($\text{pKa}(\text{NH}_4^+) = 10.5$ vs. $\text{pKa}(\text{PhNH}_3^+) = 3.5$)^[147] and we were hoping that this difference in basicity could be sufficient to facilitate catalyst turnover in our reaction. As expected, the coupling between hydrazobenzene (**208**) and enol triflate **203** proceeded smoothly and delivered the desired coupling product **210a** in 68% yield (Scheme 71). The structure of enehydrazine **210a** was unambiguously proven by X-ray crystallography.



Scheme 71. Palladium-catalyzed coupling of hydrazobenzene (**208**) and enol triflate **203**, and X-ray crystal structure of the product **210a** (ORTEP plot, ellipsoids are drawn at 50% probability level).

With substrate **210a** in hand, its reactivity in the presence of substoichiometric amounts of different Brønsted acids was investigated. First the reaction was conducted with achiral DPP (20 mol%) at 50 °C in toluene. The reaction turned out to be messy and the formation of several side products was evidenced by TLC. Yet, 43% of the desired product were isolated after 70 h reaction time. Significantly, this example represented the first Fischer indolization which proceeded with measurable catalyst turnover in our hands (Table 4, entry 1).

Table 4. Catalytic asymmetric Fischer indolization of enehydrazine **210a**.^a

entry	Cat.*	R	t	yield ^b	er ^c
1 ^d	DPP	-	70 h	43%	-
2	(S)- 33f	9-anthracenyl	6 d	n.d.	72.5:27.5
3 ^e	(S)- 33f	9-anthracenyl	8 d	n.d.	69.5:30.5
4 ^f	(R)- 33c	3,5-(CF ₃) ₂ -C ₆ H ₃	6 d	n.d.	44:56
5	(S)- 33d	2,4,6- <i>i</i> Pr ₃ -C ₆ H ₂	6 d	n.d.	56.5:43.5
6	(S)- 145d	-	48 h	45%	50.5:49.5
7	(S)- 44c	9-anthracenyl	6 d	n.d.	69.5:30.5
8	(S)- 212	3,5-(CF ₃) ₂ -C ₆ H ₃	6 d	n.d.	58.5:41.5
9	(S)- 179	3,5-(CF ₃) ₂ -C ₆ H ₃	48 h	n.d.	n.d.

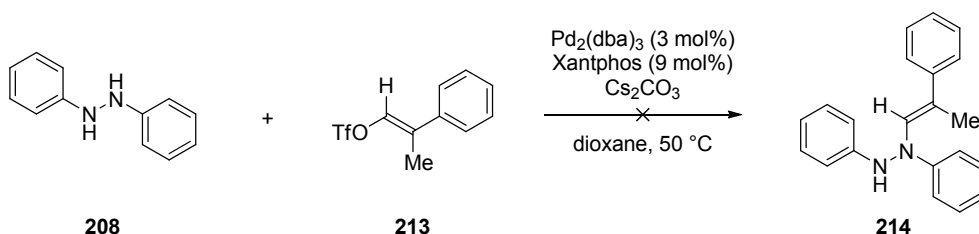
^aReactions were conducted with 0.050 mmol of substrate **210a** and 10 mol% of the catalyst in toluene (0.5 mL).

^bIsolated yield. ^cDetermined by HPLC analysis on a chiral stationary phase. The absolute configuration of the product was not determined. ^d20 mol% of DPP was used. ^e80 °C. ^f(R)-Enantiomer of the catalyst was used.

Furthermore, several classes of chiral Brønsted acids including phosphoric acids, *N*-triflyl phosphoramides, disulfonimides and disulfonic acids were tested as catalysts under the same reaction conditions. In all cases the starting material was completely consumed within 48 h. However, the reactions were usually messy and only traces of the product were detected along with several new compounds. Since the ratio of product to by-products did not change with prolonged reaction time, the formation of the side products from the decomposition of the enehydrazine **210a** rather than being intermediates of the indolization was a more likely explanation. The best enantioselectivity (er = 72.5:27.5) was obtained with phosphoric acid (S)-**33f**, but the desired product was only formed in minor quantities (Table 4, entry 2). Attempts to accelerate the reaction in order to favour the indolization over the decomposition of the starting material were unsuccessful. The reaction at 80 °C proceeded as before and the enantioselectivity dropped slightly to 69.5:30.5 er (Table 4, entry 3). The fastest and cleanest reaction was observed with the spirocyclic phosphoric acid (S)-**145d**,

giving the product in 45% yield but in racemic form (Table 4, entry 6). Disulfonimide (*S*)-**179** led to complete decomposition and not even traces of the product were detectable in the complex mixture of products (Table 4, entry 9).

In all these cases the instability of the starting material over the course of the reaction - also observable in the slow degradation of a pure crystalline sample - was clearly the limiting factor of this transformation. Additionally, the attempts to synthesize enehydrazines of type **214**, derived from α -branched aldehydes, failed under the previously used coupling conditions (Scheme 72). Although the starting materials were consumed, the desired product **214** could not be obtained from the reaction mixture.



Scheme 72. Attempted synthesis of aldehyde-derived enehydrazine **214**.

The lengthy synthesis of ketone-derived substrates like **210a**, their instability under the reaction conditions and the decreased atom economy compared to the classical process are severe drawbacks of this methodology. In light of the low enantioselectivities obtained in first test reactions and the unsuccessful attempts to extend this reaction to aldehyde-derived substrates, this approach was considered not promising enough to be followed up on.

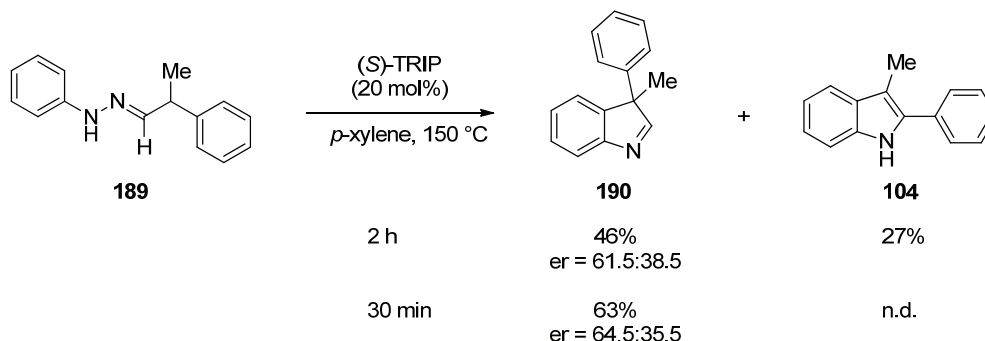
4.2.1.3 The Thermal Approach

Some of the results reported in this section were obtained in collaborative effort with B. Bechi.

All of our previous attempts to realize an enantioselective Fischer indole synthesis with only substoichiometric amounts of a chiral Brønsted acid at ambient or slightly elevated temperature failed due to lacking catalyst turnover or insufficient access to suitable substrates. Being aware that the major problem of the direct indolization of arylhydrazones

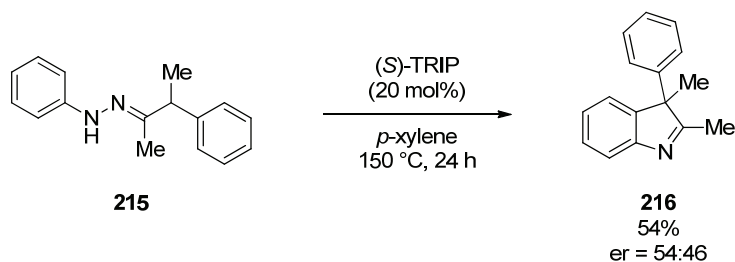
is the catalyst poisoning by the liberated ammonia, we were yet convinced that it should be possible to remove the volatile ammonia from the reaction mixture, even if the ammonium phosphate was the strongly favoured compound in the acid-base equilibrium. Our next approach was devoted to explore the possibility of achieving catalyst turnover in the indolization of simple arylhydrazones under more forcing reaction conditions.

In the next experiment, which was driven half by curiosity and half by desperation, a solution of hydrazone **189** in xylene was treated with 20 mol% of (*S*)-TRIP ((*S*)-**33d**) and heated to 150 °C. Surprisingly, after 2 h all of the starting material was consumed and the desired indolenine **190** was obtained in 46% yield as the major product, along with indole **104** in 27% yield, resulting from the Wagner-Meerwein rearrangement of **190**. Even more remarkable in light of the high reaction temperature was the fact that indolenine **190** was obtained with an enantiomeric ratio of 61.5:38.5 er (Scheme 73). Additionally, the formation of the undesired side product **104** could be largely avoided by reducing the reaction time to 30 min. In this case the yield of indolenine **190** could be increased to 63% with a comparable enantioselectivity of 64.5:35.5 er.



Scheme 73. Catalytic asymmetric Fischer indolization of hydrazone **189**.

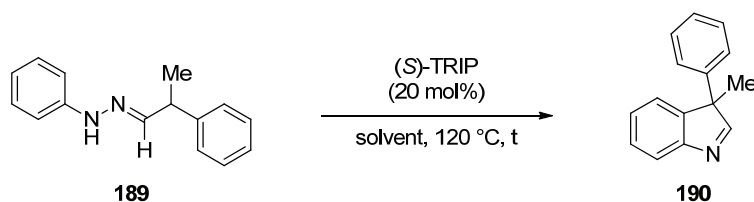
Also phenylhydrazone **215** derived from an α -branched ketone turned out to react under the same conditions and product **216** was isolated in 54% yield and 54:46 er after a reaction time of 24 h (Scheme 74).



Scheme 74. Indolization of hydrazone **215** derived from an α -branched ketone.

These results clearly suggested that catalyst turnover can be achieved if the generated ammonia is removed from the solution into the gas phase by the refluxing solvent. To identify milder reaction conditions in order to improve the chemical yield and the enantioselectivity of this process, the reaction temperature was modified next. Since the aldehyde-derived substrate **189** was more reactive than its ketone analog **215** and gave better results in terms of yield and enantioselectivity, this class of compounds was focussed on in the next experiments (Table 5).

Table 5. Solvent screening for the indolization of hydrazone **189**.^a



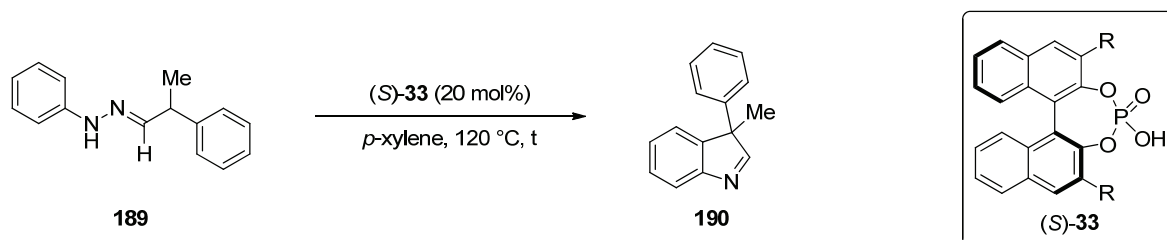
entry	solvent	t	yield ^b	er ^c
1	<i>p</i> -xylene	15 h	62%	66:34
2	toluene	14 h	75%	68.5:31.5
3	trifluorotoluene	4 h	55%	64.5:35.5
4	chlorobenzene	14 h	74%	79:21
5 ^d	DMF	36 h	52%	54:48
6	(<i>n</i> -Bu) ₂ O	19 h	52%	66:34
7 ^e	CH ₂ Cl ₂	7 d	42%	65.5:34.5

^aReactions were conducted in a sealed flask with 0.10 mmol of substrate **189** and 20 mol% the catalyst (*S*)-**33d** in 1.0 mL of solvent. ^bIsolated yield. ^cDetermined by HPLC analysis on a chiral stationary phase. The absolute configuration of the product was not determined. ^dThe reaction was stopped after 36 h despite incomplete conversion. ^eThe reaction was run in refluxing CH₂Cl₂ (5 mL) at 46 °C under atmospheric pressure.

However, when the reaction was conducted in xylene, a minimum temperature of 120 °C was found to be required to promote the indolization efficiently and avoid the degradation of the starting material over time. Under these reaction conditions the

indolization with (*S*)-TRIP ((*S*)-**33d**) as catalyst afforded the desired product in 62% yield with an enantiomeric ratio of 66:34 (Table 5, entry 1). Other aromatic solvents turned out to be suited as well and gave the product in 55-75% yield (Table 5, entries 2-4) with a promising enantioselectivity of 79:21 er in the case of chlorobenzene (Table 5, entry 4). Especially noteworthy was also the fast rate observable, when the reaction was conducted in trifluorotoluene (Table 5, entry 3). In contrast, the reaction in DMF was comparably slow and was stopped after 36 h to afford the indolenine **190** in 52% yield and almost racemic form (Table 5, entry 5). Also dibutylether seemed to be suitable for this reaction, affording the desired product in 52% yield and 66:34 er (Table 5, entry 6). The hypothesis that the removal of ammonia from the reaction mixture is facilitated by the refluxing solvent and not only a consequence of elevated temperatures was supported by the observation that even in boiling dichloromethane (46 °C) the product was isolated in 42% yield with an er of 65.5:34.5 after a prolonged reaction time of 7 days (Table 5, entry 7).

In parallel to the solvent screening, the role of different BINOL-derived phosphoric acids **33** as catalysts was investigated (Table 6). Notably, the yield of the reactions always exceeded 20% thus clearly evidencing catalyst turnover in all cases. The best enantioselectivities were obtained with the phenyl substituted catalyst (*S*)-**33h** and the 9-anthracenyl derivative (*S*)-**33f**, delivering the desired product in 78.5:21.5 er and 77.5:22.5 er, respectively (Table 6, entries 2 and 10). However, when the reaction was conducted with catalyst (*S*)-**33f** in chlorobenzene, indolenine **190** was obtained in a good yield of 75% after only 4 h reaction time, but with a disappointing enantioselectivity of only 64:36 er (Table 6, entry 11).

Table 6. Screening of BINOL-derived phosphoric acids as catalysts for the indolization of hydrazone **189**.^a

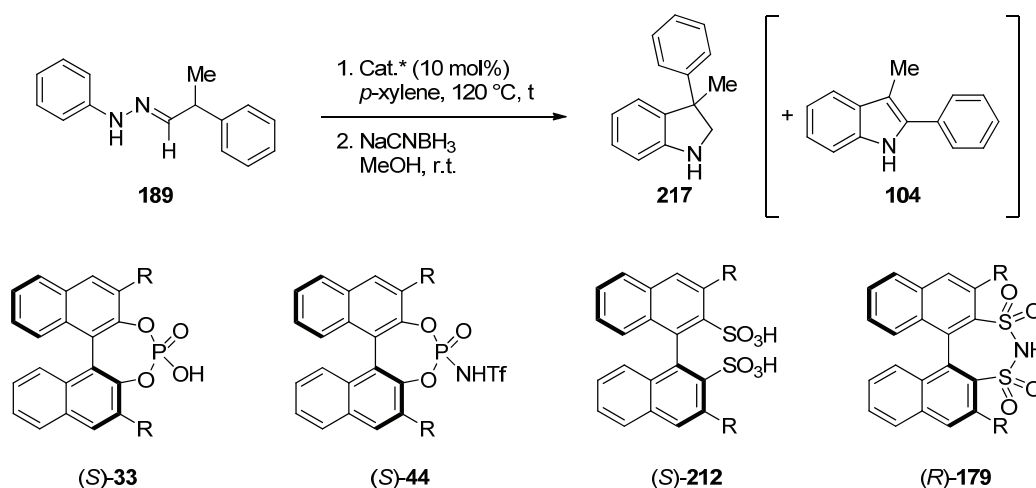
entry	Cat.*	R	t	yield ^b	er ^c
1	(S)- 33g	H	22 h	48%	54:46
2	(S)- 33h	C ₆ H ₅	24 h	31%	78.5:21.5
3	(S)- 33i	4-CH ₃ -C ₆ H ₄	48 h	38%	61.5:38.5
4	(S)- 33j	4- <i>t</i> Bu-C ₆ H ₄	21 h	51%	62:38
5	(S)- 33k	4-Ph-C ₆ H ₄	7 h	38%	58:42
6	(S)- 33l	2,6-(CH ₃) ₂ -C ₆ H ₃	3.5 h	59%	72.5:27.5
7 ^d	(R)- 33c	3,5-(CF ₃) ₂ -C ₆ H ₃	8 h	36%	46.5:53.5
8	(S)- 33e	1-naphthyl	40 h	38%	63.5:36.5
9	(S)- 33m	2-naphthyl	24 h	66%	62.5:37.5
10	(S)- 33f	9-anthracenyl	24 h	51%	77.5:22.5
11 ^e	(S)- 33f	9-anthracenyl	4 h	75%	64:36

^aReactions were conducted in a sealed flask with 0.100 mmol of substrate **189** and 20 mol% the catalyst in *p*-xylene (1.0 mL). ^bIsolated yield. ^cDetermined by HPLC analysis on a chiral stationary phase. The absolute configuration of the product was not determined. ^d(*R*)-enantiomer of the catalyst was used. ^eThe reaction was conducted on a 0.050 mmol scale in chlorobenzene (0.5 mL).

The results obtained from these experiments were encouraging in that they proved the feasibility of catalyst turnover as well as the general possibility of controlling the stereochemical outcome of the reaction by a chiral Brønsted acid. Nevertheless, the enantioselectivities obtained so far were only modest and the isolated yields varied significantly and were generally lower than expected from the monitoring of the reaction by TLC. Hence, the rather sensitive indolenine **190** was from now on converted into the more stable indoline **217** by an *in situ* reduction with sodium cyanoborohydride prior to isolation.^[148] This procedure was expected to grant higher yields and an improved reproducibility of the results. Furthermore, the following experiments were conducted with a synthetically more useful catalyst loading of 10 mol%. To enable comparison of this new protocol with the results obtained previously (see Table 6), phosphoric acids **33c**, **33d** and **33f** were reinvestigated as catalysts (Table 7, entries 1-3). As expected, the obtained yields were generally higher than before after comparable reaction times. However, the

enantioselectivities were diminished probably due to the lower catalyst loading (e.g. Table 6, entry 10 vs. Table 7, entry 1). When *N*-triflyl phosphoramidate **44c** was used as catalyst, the product was obtained with a low enantiomeric ratio of 56.5:43.5 (Table 7, entry 4). The relatively low yield of 38% can be explained by the formation of a significant amount of the Wagner-Meerwein product **104**. This side reaction turned out to be generally preferred for stronger Brønsted acids. With increasing acidity more of the rearranged product was formed, resulting in diminished yields of the desired indoline **217**, which in these cases was additionally formed with low enantioselectivities (Table 7, entries 4-6).

Table 7. Screening of different catalyst classes for the indolization of hydrazone **189**.^a



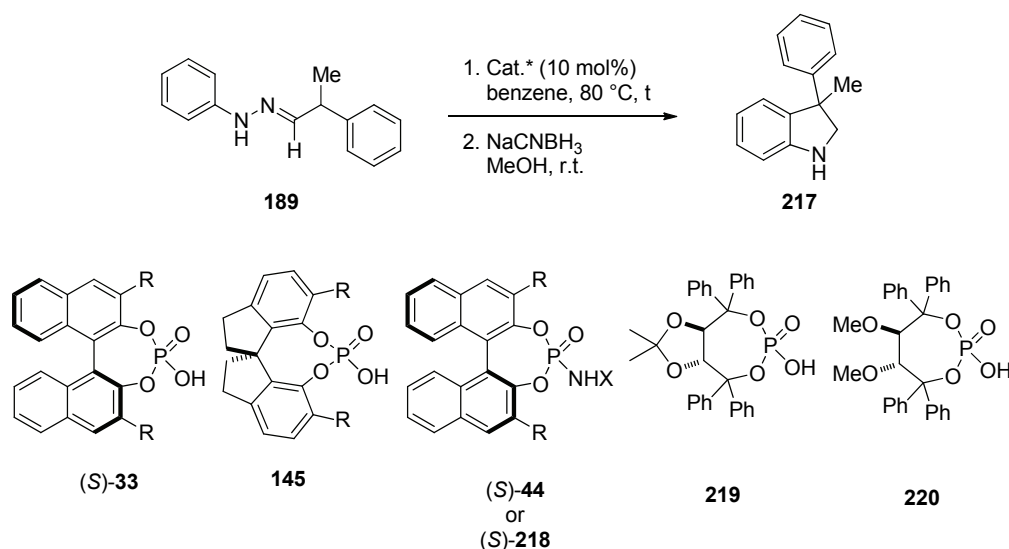
entry	Cat.*	R	t	yield ^b	er ^c	comment
1	(S)- 33f	9-anthracenyl	16 h	62%	65.5:34.5	
2	(S)- 33d	2,4,6- <i>i</i> Pr ₃ -C ₆ H ₂	16 h	59%	62.5:37.5	
3 ^d	(R)- 33c	3,5-(CF ₃) ₂ -C ₆ H ₃	16 h	51%	47:53	
4	(S)- 44c	9-anthracenyl	16 h	38%	56.5:43.5	some Wagner-Meerwein rearrangement 104
5	(S)- 212	3,5-(CF ₃) ₂ -C ₆ H ₃	16 h	23%	57:43	mainly Wagner-Meerwein rearrangement 104
6	(R)- 179a	3,5-(CF ₃) ₂ -C ₆ H ₃	16 h	n.d.	n.d.	only Wagner-Meerwein rearrangement 104

^aReactions were conducted in a sealed flask with 0.050 mmol of substrate **189** and 10 mol% the catalyst in *p*-xylene (0.5 mL). ^bIsolated yield. ^cDetermined by HPLC analysis on a chiral stationary phase. The absolute configuration of the product was not determined. ^d(*R*)-enantiomer of the catalyst was used.

With the clear indication that phosphoric acids were the catalysts of choice to promote the indolization with promising enantioselectivities without facilitating the undesired Wagner-Meerwein rearrangement, another problem of the reaction had to be addressed. So far the indolization under catalyst turnover had been successful only at

temperatures >100 °C. From our initial experiments it was known that the reaction itself proceeded even at ambient temperature, but catalyst turnover was the limiting factor here. Furthermore, more recent experiments had shown that turnover could be achieved if the generated ammonia was removed from the reaction mixture into the gas phase by the refluxing solvent, and aromatic solvents had provided the best results in terms of yields and enantioselectivities. Consequently, the use of lower boiling solvents such as benzene or the performance of the reaction under reduced pressure seemed to be good options to ensure catalyst turnover while running the reaction at lower temperatures in aromatic solvents. Since chiral phosphoric acids provided the best results so far, this type of catalysts was used preferentially in the following screenings.

Indeed the use of only 10 mol% of a chiral phosphoric acid in refluxing benzene (bp = 80 °C) was sufficient to promote the indolization of hydrazone **189**. After complete conversion of the starting material **189** the intermediary indolenine **190** was reduced to afford the indoline **217** as the final product. All BINOL-derived phosphoric acids afforded indoline **217** in good yields ($\geq 62\%$) in reasonable reaction times (Table 8, entries 1-7). The best enantioselectivity of 76.5:23.5 er was obtained with the 1-naphthyl substituted catalyst **33e** (Table 8, entry 3). Although the reaction proceeded faster when 20 mol% of the same catalyst were used, the final yield and enantioselectivity remained unaffected (Table 8, entry 4). The new SPINOL-derived catalyst **145c** gave only a low enantioselectivity of 56:44 er (Table 8, entry 8). The enantiomeric ratio obtained with (*R*)-STRIP ((*R*)-**145g**) was comparable to the reaction outcome with (*S*)-TRIP ((*S*)-**33d**), but the reaction rate was significantly lower with the spirocyclic catalyst (Table 8, entry 9). The *N*-triflyl phosphoramidate (*S*)-**44c** gave lower yields and enantioselectivities than the equally substituted phosphoric acid (Table 8, entry 10), which was in agreement with the results obtained before (see Table 7, entries 1 and 4). The *N*-phosphinyl phosphoramidate (*S*)-**218**^[121,149] showed decreased reactivity and gave the product **217** with an enantiomeric ratio of 60:40 (Table 8, entry 11). Phosphoric acids **219** and **220**, derived from TADDOLs, afforded the desired product **217** in good yields, albeit in racemic form (Table 8, entries 12 and 13).

Table 8. Indolization of hydrazone **189** with different phosphoric acids in refluxing benzene.^a

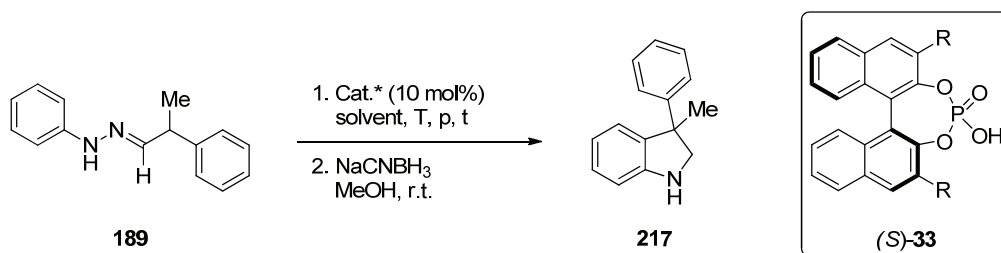
entry	Cat.*	R	t	yield ^b	er ^c
1	(S)-33f	9-anthracenyl	18 h	66%	59.5:40.5
2	(S)-33d	2,4,6- <i>i</i> Pr ₃ -C ₆ H ₂	48 h	84%	71.5:28.5
3	(S)-33e	1-naphthyl	42 h	72%	76.5:23.5
4 ^d	(S)-33e	1-naphthyl	12 h	77%	77:23
5	(S)-33n	1-pyrenyl	12 h	82%	59.5:40.5
6	(S)-33o	SiPh ₃	44 h	67%	58.5:51.5
7	(S)-33p	≡-Ph	52 h	62%	53:47
8	145c	3,5-(CF ₃) ₂ -C ₆ H ₃	20 h	80%	56:44
9	(R)-145g	2,4,6- <i>i</i> Pr ₃ -C ₆ H ₂	6 d	48%	74:26
10	(S)-44c [X = Tf]	1-naphthyl	22 h	53%	59:41
11	(S)-218 [X = P(O)(4-CF ₃ -C ₆ H ₄) ₂]	2,4,6- <i>i</i> Pr ₃ -C ₆ H ₂	72 h	57%	60:40
12	219	-	24 h	71%	53.5:46.5
13	220	-	20 h	83%	50:50

^aReactions were conducted in a flask equipped with a reflux condenser with 0.100 mmol of substrate **189** and 10 mol% of the catalyst in benzene (2.0 mL). ^bIsolated yield. ^cDetermined by HPLC analysis on a chiral stationary phase. The absolute configuration of the product was not determined. ^d20 mol% of catalyst were used.

While (S)-TRIP ((S)-**33d**) afforded the best yield for this transformation, BINOL-derived phosphoric acid (S)-**33e** gave the highest enantioselectivity of 76.5:23.5 er. To further improve these results, the performance of these two catalysts in different solvents was investigated next. Based on our previous screening experiments apolar aprotic solvents with boiling points similar to that of benzene like *n*-hexane (bp = 69 °C) and cyclohexane (bp = 81 °C) appeared promising. Furthermore toluene was used as an alternative aromatic solvent under reduced pressure (p = 190 mbar) to keep the boiling point at 65 °C. As a

general trend it was observed that TRIP (**33d**) usually gave higher yields (Table 9, entry 1-3), whereas catalyst **33e** gave slightly higher enantioselectivities (Table 9, entries 4-8). The best enantiomeric ratio of er = 78:22 was obtained with phosphoric acid **33e** in toluene at 65 °C and 190 mbar (Table 9, entry 6). The use of solvent mixtures had detrimental effects on both, yield and enantioselectivity (Table 9, entries 7 and 8).

Table 9. Solvent screening for the catalytic asymmetric Fischer indolization of hydrazone **189**.^a

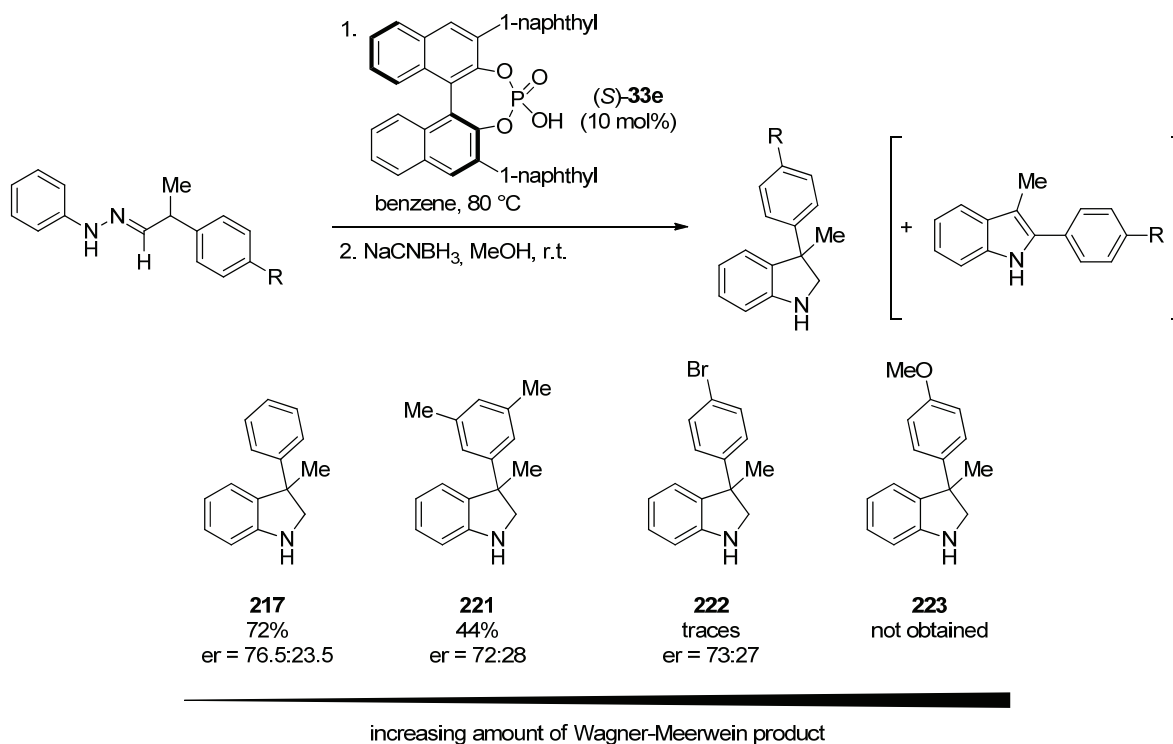


entry	Cat.*	solvent	T	p	t	yield _b	er ^c
1	R = 2,4,6- <i>i</i> Pr ₃ -C ₆ H ₂	<i>n</i> -hexane	69 °C	1 atm	48 h	79%	73.5:26.5
2	R = 2,4,6- <i>i</i> Pr ₃ -C ₆ H ₂	cyclohexane	81 °C	1 atm	40 h	89%	73.5:26.5
3	R = 2,4,6- <i>i</i> Pr ₃ -C ₆ H ₂	toluene	65 °C	190 mbar	68 h	63%	63:37
4	R = 1-naphthyl	<i>n</i> -hexane	69 °C	1 atm	67 h	53%	72:28
5	R = 1-naphthyl	cyclohexane	81 °C	1 atm	37 h	57%	76:24
6	R = 1-naphthyl	toluene	65 °C	190 mbar	68 h	56%	78:22
7	R = 1-naphthyl	benzene:CH ₂ Cl ₂ (3:1)	60 °C	1 atm	40 h	27%	72.5:27.5
8	R = 1-naphthyl	cyclohexane:CH ₂ Cl ₂ (3:1)	60 °C	1 atm	40 h	10%	74:26

^aReactions were conducted in a flask equipped with a reflux condenser with 0.100 mmol of substrate **189** and 10 mol% the catalyst in 2.0 mL of solvent. ^bIsolated yield. ^cDetermined by HPLC analysis on a chiral stationary phase. The absolute configuration of the product was not determined.

From our screening experiments the 1-naphthyl substituted phosphoric acid **33e** had been identified as the most promising catalyst with regard to the enantioselectivity. Although the results obtained so far left much to be desired, we were curious about the generality of our method. Since the reactions in benzene at 80 °C and in toluene at 65 °C under reduced pressure gave comparable results, the preliminary substrate scope was determined in benzene as the solvent for practical reasons. The reaction of substrate **189** worked as before and gave the desired product **217** in 72% yield with an enantiomeric ratio of 76.5:23.5. Comparable enantioselectivities were obtained for substituted indolines **221**

and **222** (Scheme 75). However, it turned out, that substitutions on the aromatic moiety of the aldehyde component, which increase the electron density of the aromatic ring by inductive and/or mesomeric effects facilitate the degradation of the intermediary indolenine via the Wagner-Meerwein pathway. Thus, indoline **223** was not obtained, but only the corresponding rearranged aromatic indole.



Scheme 75. Preliminary substrate scope of the catalytic asymmetric Fischer indolization of α -branched aldehyde-derived phenylhydrazones.

Notably, this method represents what is to the best of our knowledge the first catalytic asymmetric Fischer indolization. However, the only moderate enantioselectivities obtained during our optimization studies and the problems encountered with increasing complexity of new substrates rendered this system challenging in terms of further advancements at this point. Instead, further investigations were conducted on another, potentially less problematic substrate class.

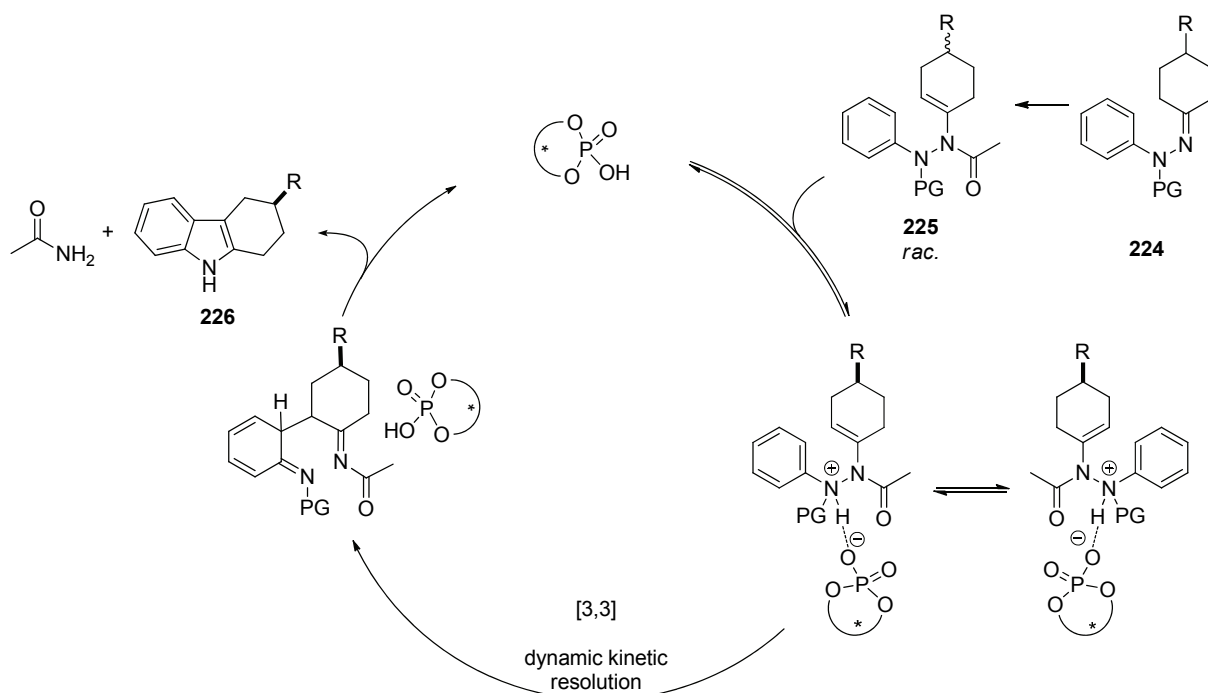
4.2.2 Synthesis of 3-Substituted Tetrahydrocarbazoles

The studies on the catalytic asymmetric Fischer indolization of phenylhydrazones derived from α -branched aldehydes did not lead to a high yielding and highly

enantioselective method for the synthesis of the desired indolenines. Yet, the findings helped to identify the major challenges in the development of a catalytic asymmetric Fischer indolization in general and suggested different solutions. These insights set the starting point for the following investigations.

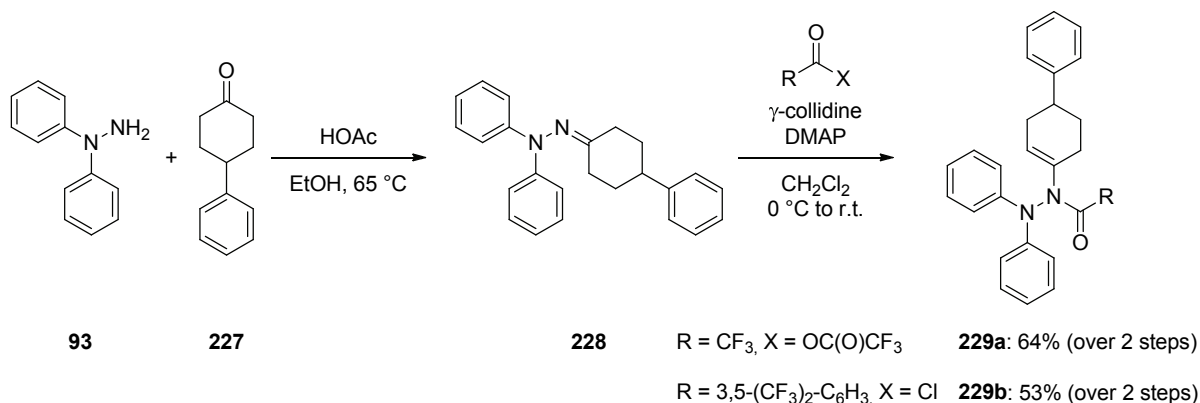
4.2.2.1 *N*-Acyl Enehydrazines as Potential Substrates

The phosphoric acid-catalyzed indolization of *N*-acyl enehydrazine **199** was found to be a facile process and catalyst turnover was achieved by the replacement of ammonia by the less basic acetamide as the leaving group (see Scheme 66). The realization of an enantioselective variant of this reaction failed due to lacking access to the requisite starting materials. At this point, it was hypothesized that it should be possible to synthesize *N*-acyl enehydrazines of type **225** from cyclohexanone-derived phenylhydrazones **224**. Although these substrates are already chiral, the two enantiomers were supposed to equilibrate in the presence of the phosphoric acid catalyst. Hence the indolization could occur via a dynamic kinetic resolution, giving the enantioenriched products **226** along with acetamide as the non-basic by-product (Scheme 76).



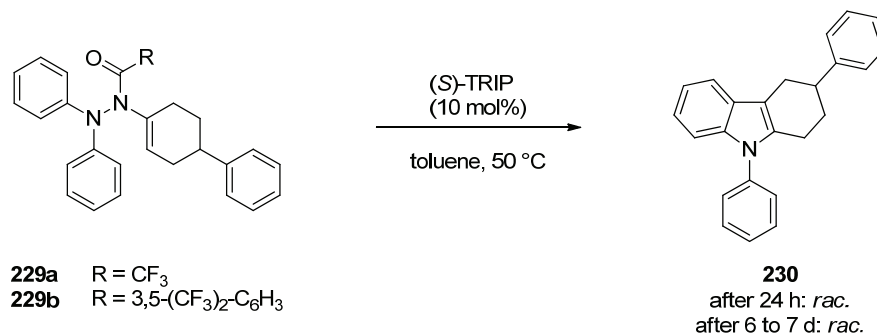
Scheme 76. Proposed catalytic cycle for the enantioselective Fischer indolization of *N*-acyl enehydrazines **225** via a dynamic kinetic resolution.

To probe this hypothesis, two different *N*-acylated enehydrazines were synthesized from 1,1-diphenyl hydrazine (**93**) and 4-phenylcyclohexanone (**227**) via hydrazone formation and subsequent base-mediated acylation. The trifluoroacetylated and a benzoylated enehydrazines **229a** and **229b** were obtained in good overall yields of 64% and 53%, respectively (Scheme 77).



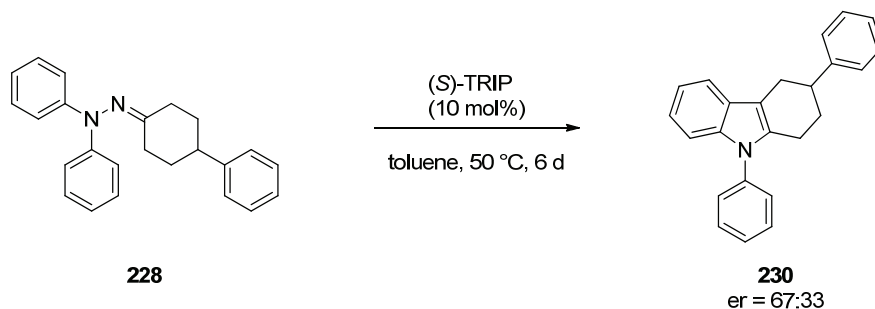
Scheme 77. Synthesis of *N*-acyl enehydrazines **229a** and **229b**.

With these new and promising substrates in hand, their reactivity in the presence of a chiral phosphoric acid was investigated. For first experiments (*S*)-TRIP (*S*)-**33d**, 10 mol%) was chosen as our benchmark catalyst and the reactions were conducted at 50 °C in toluene. Similar to other enehydrazines before, both substrates **229a** and **229b** proved to be rather unstable under the reaction conditions and led to complex mixtures of products over the course of 6-7 days of reaction time. However, pure samples of the desired tetrahydrocarbazole **230** could be obtained from the mixtures via preparative TLC after 24 h and at the end of the reaction. Surprisingly, in all cases the obtained product was entirely racemic, suggesting that in each case both enantiomeric enehydrazines undergo the Fischer indolization with a very similar rate, irrespective of their absolute configuration.



Scheme 78. (*S*)-TRIP-Catalyzed indolization of enehydrazines **229a** and **229b**.

In a control experiment, hydrazone **228** was submitted to exactly the same reaction conditions to probe if TRIP (**33d**) could induce some enantioselectivity in related cyclizations. Delightfully, in this case the tetrahydrocarbazole **230** was obtained with an enantiomeric ratio of 67:33, of course again in minor quantities due to lacking catalyst turnover (Scheme 79).



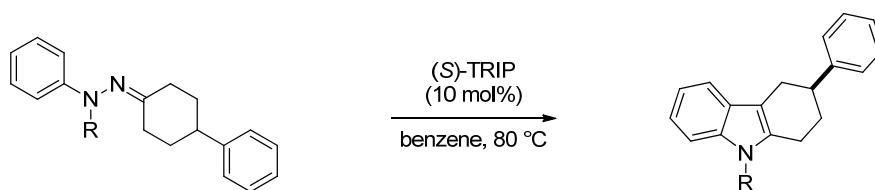
Scheme 79. (S)-TRIP-Catalyzed Fischer indolization of hydrazone **228**.

This promising result in combination with the instability observed for the *N*-acyl enehydrazines **229a** and **229b** under our reaction conditions prompted us again to concentrate on the thermal removal of ammonia, rather than on its replacement by a less basic leaving group.

4.2.2.2 The Thermal Approach

In the Fischer indolization of hydrazones derived from α -branched aldehydes refluxing benzene was found to be a suitable reaction medium to efficiently facilitate the reaction under relatively mild conditions and ensure catalyst turnover by loss of ammonia from the reaction mixture. Consequently, these reaction conditions were also applied to the phenylhydrazones derived from 4-phenylcyclohexanone.

First experiments were directed towards the identification of a suitable protecting group for the phenylhydrazine. Therefore the different hydrazones **228**, **231** and **233** were submitted to the reaction conditions with 10 mol% of (S)-TRIP as the catalyst. Unfortunately, the unprotected hydrazone **231** proved to be highly unstable in the presence of the catalyst and afforded a complex mixture of products with no indication of the desired product being formed (Table 10, entry 1).

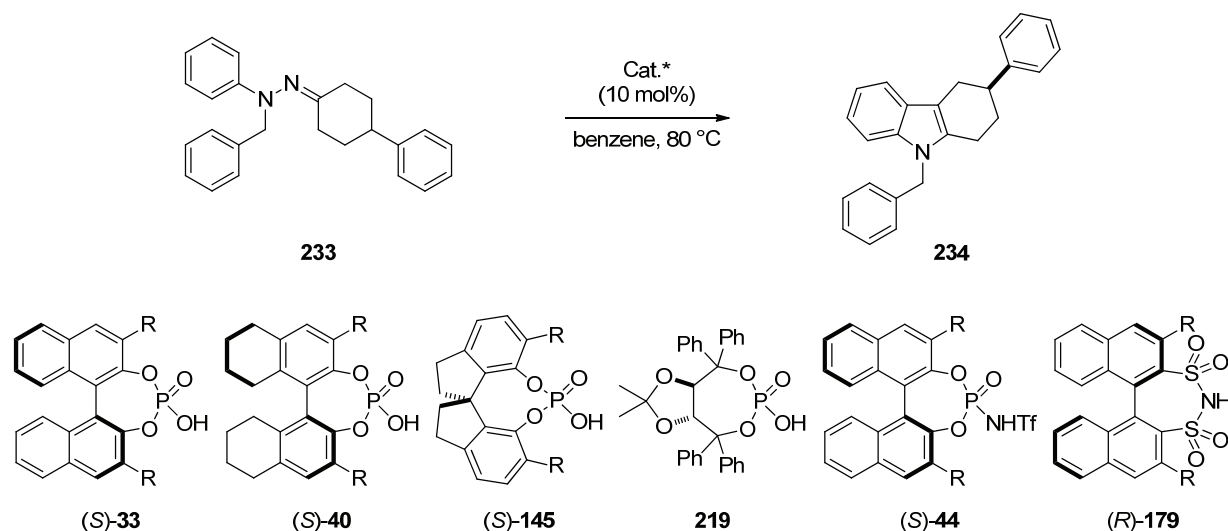
Table 10. Identification of a suitable protecting group.^a

entry	substrate	product	R	t	yield ^b	er ^c
1	231	232	H	72 h	n.d.	n.d.
2 ^d	228	230	Ph	22 h	40%	64:36
3	233	234	Bn	48 h	74%	51:49

^aReactions were conducted in a flask equipped with a reflux condenser with 0.100 mmol of substrate and 10 mol% the catalyst (*S*)-**33d** in benzene (1.0 mL) and stopped after the indicated time, irrespective of conversion. ^bIsolated yield. ^cDetermined by HPLC analysis on a chiral stationary phase. ^dThe absolute configuration of the product was not determined.

The phenyl substituted hydrazone **228** reacted cleanly to afford the desired product **230** in 40% yield and with an enantiomeric ratio of 64:36 after 22 h (Table 10, entry 2). Also the benzyl protected substrate **233** provided a clean reaction and tetrahydrocarbazole **234** was isolated in 74% yield after 48 h, albeit in racemic form (Table 10, entry 3). Nevertheless we decided to further investigate the indolization of substrate **233**, given its good reactivity and the advantages of a *N*-benzyl- over a *N*-phenyl protecting group in terms of deprotection.

Consequently the next step was the examination of different catalysts to see if the indolization of the benzylated hydrazone **233** was catalyzable in enantioselective manner at all. For this purpose the preformed hydrazone **233** was reacted with different types of chiral Brønsted acids in refluxing benzene. Delightfully, it was found that other BINOL-derived phosphoric acids afforded non-racemic product **234** (Table 11, entries 1-11), with the best enantiomeric ratio of 78.5:21.5 obtained for the 9-anthracenyl substituted catalyst **33f** (Table 11, entry 5). Interestingly, the extension of the 9-anthracenyl substituent by another aromatic moiety resulted in an almost complete loss of enantioselectivity (Table 11, entries 10 and 11). The catalysts **40c** and **40d** based on a H₈-BINOL backbone gave inferior results compared to their BINOL counterparts (Table 11, entries 12 and 13).

Table 11. Preliminary catalyst screening for the indolization of hydrazone **233**.^a

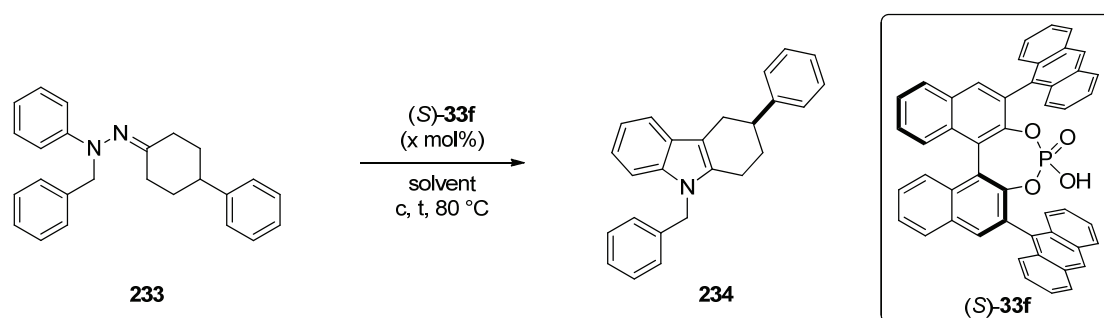
entry	Cat.*	R	t	yield ^b	er ^c
1 ^d	(S)-33h	C ₆ H ₅	20 h	n.d.	57:43
2 ^d	(S)-33k	4-C ₆ H ₅ -C ₆ H ₄	20 h	n.d.	47.5:52.5
3	(S)-33e	1-naphthyl	96 h	81%	69.5:30.5
4	(S)-33m	2-naphthyl	20 h	42%	54.5:45.5
5	(S)-33f	9-anthracenyl	24 h	66%	78.5:21.5
6	(S)-33p	9-phenanthryl	24 h	96%	75.5:24.5
7 ^{d,e}	(R)-33o	SiPh ₃	96 h	32%	43.5:56.5
8 ^d	(S)-33c	3,5-(CF ₃) ₂ -C ₆ H ₃	96 h	64%	55.5:44.5
9 ^d	(S)-33l	2,6-(CH ₃) ₂ -C ₆ H ₄	66 h	17%	77.5:22.5
10 ^d	(S)-33q		64 h	34%	52:48
11 ^d	(S)-33r		66 h	19%	56:44
12	(S)-40c	1-naphthyl	24 h	21%	65.5:34.5
13	(S)-40d	9-phenanthryl	24 h	27%	72.5:27.5
14 ^d	(S)-145g	2,4,6- <i>i</i> Pr ₃ -C ₆ H ₂	72 h	17%	71:29
15 ^d	145c	3,5-(CF ₃) ₂ -C ₆ H ₃	68 h	n.d.	48:52
16 ^d	219	-	96 h	19%	47:53
17	(S)-44c	9-anthracenyl	18 h	36%	48.5:51.5
18	(R)-179a	3,5-(CF ₃) ₂ -C ₆ H ₃	16 h	98%	48:52

^aReactions were conducted in a flask equipped with a reflux condenser with 0.100 mmol of substrate **233** and 10 mol% the catalyst in benzene (1.0 mL) and stopped after the indicated time, irrespective of conversion.

^bIsolated yield. ^cDetermined by HPLC analysis on a chiral stationary phase. ^dReaction was conducted in a sealed vial. ^e(*R*)-Enantiomer of the catalyst was used.

The use of (*S*)-STRIP ((*S*)-**145g**) resulted in an improved enantiomeric ratio of 71:29 er (Table 11, entry 14) when compared to TRIP (**33d**, er = 51:49). SPINOL- and TADDOL-derived phosphoric acids **145c** and **219** as well the *N*-triflyl phosphoramidate **44c** gave almost racemic products in this screening (Table 11, entries 15-17). Notably, disulfonimide **179a** proved to be highly reactive and gave the desired product in quantitative yield, albeit in racemic form (Table 11, entry 18).

Amongst the catalysts tested, the 9-anthracenyl substituted phosphoric acid (*S*)-**33f** gave the highest enantioselectivity so far. In further optimizations the reaction solvent, the catalyst loading and the optimal concentration were determined (Table 12). It turned out that all aromatic solvents performed very similar (Table 12, entries 1-8), giving the product **234** in enantioselectivities between 77.5:22.5 er (Table 12, entries 6 and 7) and 80:20 er (Table 12, entry 1). Aliphatic and etheric solvents resulted in slightly reduced yields (Table 12, entries 9-11), with a small improvement in enantioselectivity to 81.5:18.5 er in the case of cyclohexane (Table 12, entry 9). The reaction also worked well in acetonitrile and 1,2-dichloroethane, giving the tetrahydrocarbazole **234** in good yields, albeit only modest enantioselectivities (Table 12, entries 12 and 13). Since benzene provided the best compromise between reactivity and enantioselectivity, the optimization of concentration and catalyst loading was conducted in this solvent. An increase in concentration to 0.2 M resulted in a slightly diminished enantioselectivity (Table 12, entry 14), and in more dilute reaction mixtures the reaction rate decreased (Table 12, entries 15 and 16). Hence the catalyst loading was studied at 0.1 M concentration of hydrazone **233** in benzene. While an increased catalyst loading of 20 mol% resulted in a diminished enantioselectivity of 76:24 er (Table 12, entry 17), a catalyst loading of 5 mol% turned out to be as efficient as the use of 10 mol% of catalyst (*S*)-**33f** (Table 12, entry 18).

Table 12. Screening of solvent, concentration and catalyst loading.^a

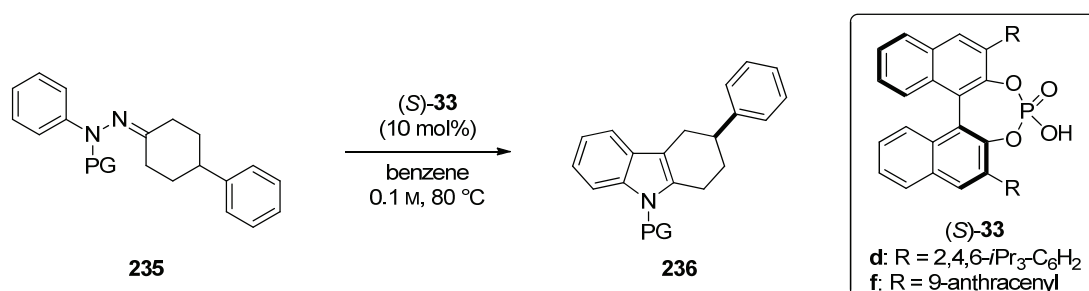
entry	solvent	x mol%	c	t	yield ^b	er ^c
1	benzene	10 mol%	0.1 M	24 h	22%	80:20
2	toluene	10 mol%	0.1 M	22 h	18%	79.5:20.5
3	<i>o</i> -xylene	10 mol%	0.1 M	24 h	45%	79.5:20.5
4	<i>m</i> -xylene	10 mol%	0.1 M	24 h	33%	77.5:22.5
5	<i>p</i> -xylene	10 mol%	0.1 M	24 h	33%	79.5:20.5
6	mesitylene	10 mol%	0.1 M	24 h	24%	77.5:22.5
7	chlorobenzene	10 mol%	0.1 M	24 h	46%	77.5:22.5
8	trifluorotoluene	10 mol%	0.1 M	24 h	23%	79:21
9	cyclohexane	10 mol%	0.1 M	24 h	17%	81.5:18.5
10 ^d	<i>n</i> -hexane	10 mol%	0.1 M	44 h	14%	72:28
11	1,4-dioxane	10 mol%	0.1 M	22 h	14%	76.5:23.5
12	acetonitrile	10 mol%	0.1 M	22 h	36%	63:37
13	1,2-dichloroethane	10 mol%	0.1 M	28 h	40%	71.5:28.5
14	benzene	10 mol%	0.2 M	24 h	20%	79:21
15	benzene	10 mol%	0.05 M	72 h	43%	76:24
16	benzene	10 mol%	0.02 M	72 h	38%	80:20
17	benzene	20 mol%	0.1 M	72 h	56%	76:24
18	benzene	5 mol%	0.1 M	24 h	33%	80:20

^aReactions were conducted in a sealed tube with 0.050 mmol of substrate **233** and 10 mol% of catalyst (*S*)-**33f** and stopped after the indicated time, irrespective of conversion. ^bIsolated yield. ^cDetermined by HPLC analysis on a chiral stationary phase. ^dReaction was conducted at 70 °C.

Since the variation of solvent, concentration and catalyst loading did not lead to a significantly improved enantioselectivity, the benzyl protecting group was modified next in order to obtain higher enantioselectivities. All substrates were run in parallel with the 9-anthracenyl substituted phosphoric acid (*S*)-**33f** and (*S*)-TRIP ((*S*)-**33d**) in benzene at 80 °C. For practical reasons, the reactions were conducted in sealed vials with a catalyst loading of 10 mol% at 80 °C in benzene. The replacement of the benzyl protecting group by a Cbz-group or a benzhydryl residue gave the desired product in only low enantioselectivities for both catalysts (Table 13, entries 1 and 2). Structurally modified benzyl groups gave generally

better enantiomeric ratios with the 9-anthracenyl substituted catalyst **33f** (Table 13, entries 3-14). Significantly, bulky substituents *para* to the benzylic methylene group resulted in slightly increased enantioselectivities compared to the parent benzyl group (Table 13, entries 9-14), with the highest enantiomeric ratio of 83.5:16.5 obtained for the 4-phenylbenzyl and 4-iodobenzyl group (Table 13, entries 11 and 14). However, synthetically more useful enantioselectivities than 83.5:16.5 *er* could not be achieved under these reaction conditions.

Table 13. Variation of the protecting group.^a

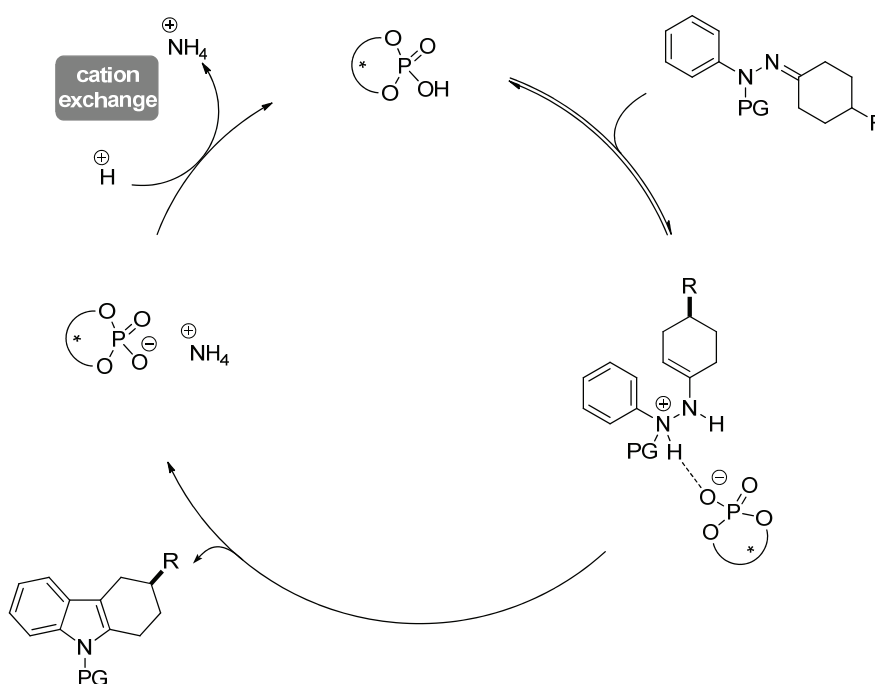


entry	substrate	PG	t	catalyst (S)-33d		catalyst (S)-33f	
				yield ^b	<i>er</i> ^c	yield ^b	<i>er</i> ^c
1	235a	Cbz	44 h	n.d.	46.5:53.5	n.d.	52.5:47.5
2	235b	(C ₆ H ₅) ₂ CH	48 h	13%	58:42	28%	60.5:39.5
3	235c	β-naphthyl-CH ₂	60 h	30%	55.5:44.5	32%	82.5:17.5
4	235d	2-Me-C ₆ H ₄ -CH ₂	62 h	25%	56:44	24%	79.5:20.5
5	235e	3,5-Me ₂ -C ₆ H ₃ -CH ₂	60 h	22%	61.5:38.5	28%	79:21
6	235f	3,5-(MeO) ₂ -C ₆ H ₃ -CH ₂	60 h	24%	57.5:42.5	33%	79.5:20.5
7	235g	3,5-(CF ₃) ₂ -C ₆ H ₃ -CH ₂	60 h	12%	62:38	21%	77.5:22.5
8	235h	3,5-F ₂ -C ₆ H ₃ -CH ₂	67 h	22%	59.5:40.5	23%	79:21
9	235i	4-Me-C ₆ H ₄ -CH ₂	62 h	29%	52:48	34%	80:20
10 ^d	235j	4- <i>t</i> Bu-C ₆ H ₄ -CH ₂	67 h	33%	58.5:41.5	28%	81.5:18.5
11	235k	4-Ph-C ₆ H ₄ -CH ₂	67 h	34%	56:44	36%	83.5:16.5
12	235l	4-F-C ₆ H ₄ -CH ₂	62 h	27%	48.5:51.5	29%	81:19
13	235m	4-Br-C ₆ H ₄ -CH ₂	60 h	23%	50:50	33%	82.5:17.5
14	235n	4-I-C ₆ H ₄ -CH ₂	62 h	24%	51.5:48.5	31%	83.5:16.5

^aReactions were conducted in a sealed tube with 0.050 mmol of substrate **235** and 10 mol% the catalyst and stopped after the indicated time, irrespective of conversion. ^bIsolated yield. ^cDetermined by HPLC analysis on a chiral stationary phase.

4.2.2.3 The Cation Exchange Approach

Although by varying the protecting group the stereochemical outcome of the reaction was influenced, the obtained enantioselectivities had to be improved more significantly in order to provide a highly enantioselective and thus synthetically more useful methodology. However, the most promising way to increase the enantioselectivity was invariably correlated with the lowering of the reaction temperature. This, on the other hand, would require another efficient method to remove the ammonia from the reaction mixture to avoid catalyst poisoning. So far, our approaches to address this problem included either the replacement of ammonia by another less basic leaving group, or the removal of ammonia from the reaction mixture by the refluxing solvent. While the first approach suffered mostly from the poor stability of the requisite substrates, the ammonia removal under reflux conditions worked reasonably well only at elevated temperatures, since in this case the system had to work against the equilibrium between the free ammonia and the strongly favoured ammonium phosphate.

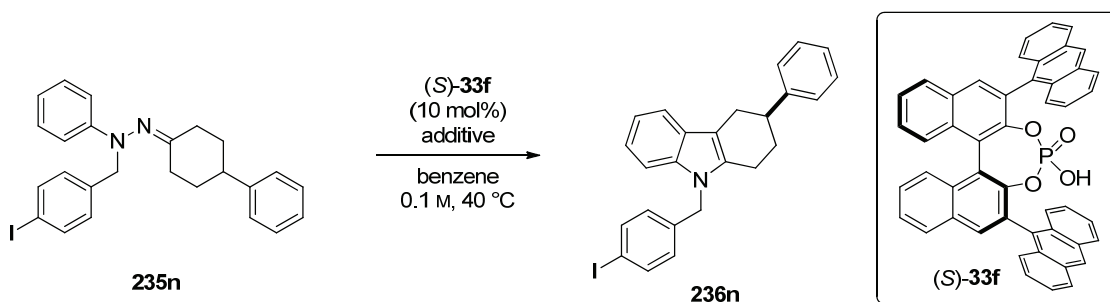


Scheme 80. Proposed catalytic cycle reliant on the cation exchange of the ammonium phosphate.

At this point, we hypothesized that it might be possible to take advantage of the equilibrium and benefit from the efficient conversion of ammonia to the ammonium ion, if it was possible to use a cation exchange process to replace the ammonium ion by a proton. In

the envisioned catalytic cycle, the equilibration between the hydrazone and enehydrazine is accelerated by the phosphoric acid catalyst. After the [3,3]-sigmatropic rearrangement followed by product formation and extrusion of ammonia, the ammonium phosphate is formed. Possibly, this indolization-inactive species could be converted back to the active catalyst by cation exchange (Scheme 80).

Usually, cation exchange is accomplished by polymeric resins, which are functionalized with carboxylic or sulfonic acid groups. In these cases, a competition between the different acids and anionic species, respectively, in our reaction, of which only the chiral phosphate anion would be able to induce an enantioselective reaction, appeared likely. To probe this hypothesis and explore the potential of this method, the Fischer indolization of hydrazone **235n**, bearing the optimized protecting group, was conducted in the presence of 10 mol% of BINOL-derived phosphoric acid (*S*)-**33f** and different acidic additives as potential reagents to facilitate the cation exchange in benzene at 40 °C. When no additive was used, the desired tetrahydrocarbazole **236n** was obtained with a significantly improved enantiomeric ratio of 89.5:10.5 er at this temperature, but as expected the conversion remained low even after 7 days of reaction time (Table 14, entry 1). Weak carboxylic acids like acetic acid, pivalic acid and different benzoic acids had almost no influence on the conversion of the reaction, but the enantiomeric ratio of the product decreased with these additives (Table 14, entries 2-7). Remarkably, the strongly acidic cation exchange resin Amberlyst 15 resulted in the full conversion of hydrazone **235n** after 5 days (Table 14, entries 8 and 9). Unfortunately, also the enantioselectivity of the process turned out to be influenced by the resin. The more of the resin was used, the lower was the enantiomeric ratio of the final product, evidencing the above discussed competition of different anionic species in the reaction mixture. When the weakly acidic cation exchange resin Amberlite CG50 was used, it turned out that the conversion was highly dependant on the amount of resin used (Table 14, entries 10-12). With a resin loading of 20 equivalents of carboxylic functions per substrate molecule complete conversion was achieved after 5 days. More significantly, the enantiomeric ratio of the final product **236n** (er = 88:12) was only slightly inferior to the one obtained without any additive (Table 14, entry 12).

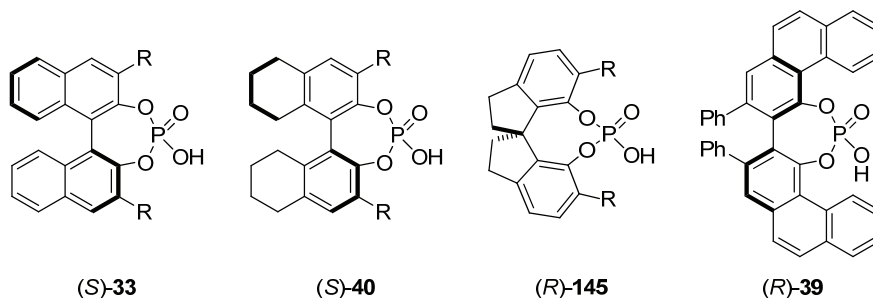
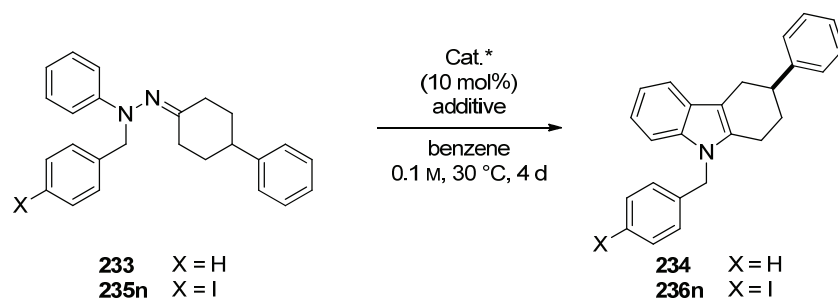
Table 14. Screening of acidic additives.^a

entry	additive	t	er ^b	conversion ^c	
				complete	incomplete
1	-	7 d	89.5:10.5		X
2	AcOH (1 equiv)	7 d	76:24		X
3	<i>t</i> BuCO ₂ H (1 equiv)	7 d	82.5:17.5		X
4	C ₆ H ₅ CO ₂ H (1 equiv)	7 d	74.5:25.5		X
5	4-NO ₂ -C ₆ H ₄ CO ₂ H (1 equiv)	7 d	74:26		X
6	4-MeO-C ₆ H ₄ CO ₂ H (1 equiv)	7 d	81:19		X
7	2-MeO-C ₆ H ₄ CO ₂ H (1 equiv)	7 d	82.5:17.5		X
8	Amberlyst 15 (10 mg) (≈ 1.88 equiv R-SO ₃ H)	5 d	82:18	X	
9	Amberlyst 15 (20 mg) (≈ 3.76 equiv R-SO ₃ H)	5 d	77.5:22.5	X	
10	Amberlite CG 50 (10 mg) (≈ 4 equiv R-CO ₂ H)	5 d	89.5:10.5		X
11	Amberlite CG 50 (20 mg) (≈ 8 equiv R-CO ₂ H)	5 d	89:11		X
12	Amberlite CG 50 (50 mg) (≈ 20 equiv R-CO ₂ H)	5 d	88:12	X	

^aReactions were conducted in a sealed tube with 0.025 mmol of substrate **235n** and 10 mol% of catalyst **(S)-33f** and stopped after the indicated time. ^bDetermined by HPLC analysis on a chiral stationary phase. ^cDetermined by TLC.

Driven by these exciting findings, the Fischer indolization of the benzyl protected hydrazone **233** was reinvestigated with different phosphoric acid catalysts in the presence of Amberlite CG50. To better understand the role of the ion exchange resin, some experiments with achiral diphenylphosphate as the catalyst were conducted at 50 °C. When 1 equivalent of DPP was used, the reaction reached complete conversion after 4 h and gave racemic tetrahydrocarbazole **234** in 83% yield (Table 15, entry 1). As expected, a dramatic decrease in the reaction rate was observable when catalytic amounts (5 mol%) of the same catalyst were used. After fast initial product formation (monitored by TLC) the reaction rate

decreased dramatically and after 48 h, a yield of only 9% was observed (Table 15, entry 2). As expected the addition of Amberlite CG50 restored the catalyst reactivity and the yield improved to 63% under otherwise identical reaction conditions (Table 15, entry 3). Although ion exchange resins have previously been used as catalysts for Fischer indolizations,^[150] this resin alone was incapable of catalyzing the reaction, giving only traces of the indolization product at 50 °C (Table 15, entry 4). This result is in perfect agreement with the unperturbed enantioselectivities observed previously (see Table 14). In order to further improve our method, different chiral acid catalysts, including BINOL-, H₈-BINOL-, VAPOL- as well as SPINOL-derived phosphoric acids were screened again. The reactions were run at 30 °C with a catalyst loading of 5 mol% and were stopped after 4 days, irrespective of the conversion. Accordingly, the yields obtained varied significantly between 11% (Table 15, entry 14) and 98% (Table 15, entries 15 and 16). As before, the BINOL-derived phosphoric acid **33f** bearing 9-anthracenyl substituents in the 3,3'-positions afforded the product in a good yield of 75% with a promising 85:15 er (Table 15, entry 10). Eventually, when the catalyst backbone was changed from BINOL to SPINOL, the novel spirocyclic phosphoric acid **145f** was found to be the optimal catalyst in terms of yield and enantioselectivity, giving the desired product in 98% yield and 93.5:6.5 er (Table 15, entry 16). This result was even further improved when the finding from our previous protecting group screening, that bulky substituents in the 4-position of the benzyl group had a beneficial effect on the enantioselectivity, was included. We ultimately opted for the use of the 4-iodobenzyl protecting group, supposing that this entity would be analogous to the parent benzyl group in terms of deprotection, while at the same time granting advantageous crystalline properties of starting materials and products as well as offering a handle for the synthesis of compound libraries by means of cross coupling reactions.^[151] Finally, tetrahydrocarbazole **236n** was obtained in 98% yield and 95:5 er (Table 15, entry 18) when the reaction of hydrazone **235n** was conducted in the presence of 4Å molecular sieves as a supplementary additive.

Table 15. Catalyst screening in the presence of a cation exchange resin.^a

entry	Cat.*	R	additive	X	yield ^b	er ^c
1 ^{d,e}	DPP		-	H	83%	-
2 ^{e,f}	DPP		-	H	9% ^g	-
3 ^{e,f}	DPP		CG50	H	63%	-
4 ^{e,f}	-		CG50	H	<5% ^g	-
5	(S)-33d	2,4,6- <i>i</i> Pr ₃ -C ₆ H ₂	CG50	H	25%	54.5:45.5
6	(S)-33j	4- <i>t</i> Bu-C ₆ H ₄	CG50	H	20%	40.5:59.5
7	(S)-33c	3,5-(CF ₃) ₂ -C ₆ H ₃	CG50	H	50%	59.5:40.5
8	(S)-33e	1-naphthyl	CG50	H	43%	70.5:29.5
9	(S)-33p	9-phenanthryl	CG50	H	50%	83:17
10	(S)-33f	9-anthracenyl	CG50	H	75%	85:15
11	(S)-40c	1-naphthyl	CG50	H	42%	61.5:38.5
12	(S)-40d	9-phenanthryl	CG50	H	66%	74:26
13	(R)-145g	2,4,6- <i>i</i> Pr ₃ -C ₆ H ₂	CG50	H	24%	80:20
14	(S)-145e	4- <i>t</i> Bu-C ₆ H ₄	CG50	H	11%	43.5:56.5
15	145c	3,5-(CF ₃) ₂ -C ₆ H ₃	CG50	H	98%	48.5:51.5
16	(R)-145f	9-anthracenyl	CG50	H	98%	93.5:6.5
17	(R)-39	-	CG50	H	52%	49.5:50.5
18	(R)-145f	9-anthracenyl	CG50 + MS 4Å	I	98%	95:5

^aReactions were conducted on a 0.050 mmol scale. Where indicated Amberlite CG50 (100 mg) and MS 4Å (25 mg) were added. ^bIsolated yields unless otherwise stated. ^cDetermined by HPLC analysis on a chiral stationary phase. ^d1 Equivalent of DPP was used, 4 h reaction time. ^e50 °C. ^f48 h. ^gDetermined by ¹H NMR spectroscopy. DPP = diphenylphosphate. CG50 = Amberlite CG50.

Due to the good crystalline properties of product **236n** and the presence of the iodine in the molecule, it was possible to unambiguously determine the absolute

configuration of the product by X-ray structure analysis (Figure 11). According to this analysis, the stereocenter in the 3-position of tetrahydrocarbazole **236n** had the *S* configuration.

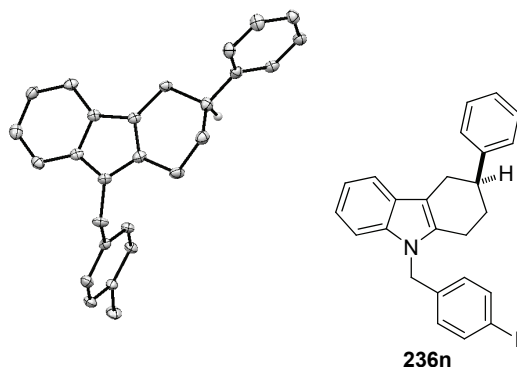
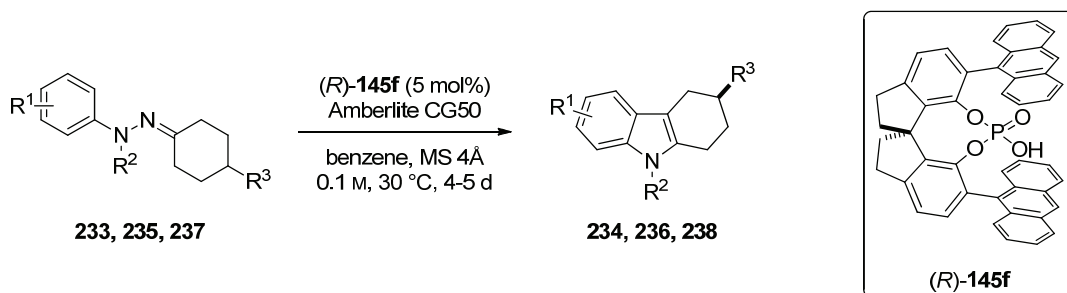


Figure 11. ORTEP plot of the X-ray crystal structure of tetrahydrocarbazole **236n**. Ellipsoids are drawn at 50% probability level.

4.2.2.4 The Catalytic Asymmetric Fischer Indolization

Some of the results reported in this section were obtained in collaborative effort with M. J. Webber.

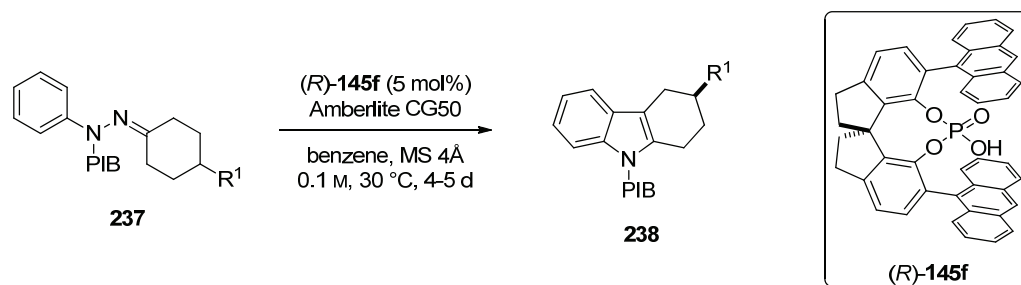
At this point the identified reaction conditions finally allowed to obtain the desired product **236n** in a high yield and with high enantioselectivity in the presence of only 5 mol% of a chiral Brønsted acid. To explore the generality of this method, the substrate scope of our reaction was investigated next. The *N*-benzyl protected hydrazone **233** and the iodinated analog **235n** reacted smoothly to give the products **234** and **236n** in 94% and 99% yield and enantiomeric ratios of 94:6 and 95:5, respectively (Table 16, entries 1 and 2). Different *para*-substituents at the hydrazine moiety furnished 6-substituted tetrahydrocarbazoles **238a-c** in good yields, regardless of their electronic properties, albeit with slightly reduced enantioselectivity (Table 16, entries 3-5). Also the 3,5-dimethyl substituted hydrazone **237d** reacted similarly (Table 16, entry 6). When 3-methyl substituted phenylhydrazones **237e** and **237f** were employed, the reaction proceeded with a synthetically useful regiocontrol (6:1). In both cases the 7-methyl carbazole derivatives **238e** and **238f** were obtained as the major regioisomers with enantiomeric ratios of 96:4 and 93:7, respectively (Table 16, entries 7 and 8).

Table 16. Substrate scope of the catalytic asymmetric Fischer indolization – variation of the hydrazine moiety.^a

entry	product	yield ^b	er ^c
1	234 $\text{R}^1 = \text{H}, \text{R}^2 = \text{Bn}$	94%	94:6
2	236n $\text{R}^1 = \text{H}, \text{R}^2 = 4\text{-iodobenzyl (PIB)}$	99%	95:5
3	238a $\text{R}^1 = \text{Me}, \text{R}^2 = \text{PIB}$	99%	92.5:7.5
4	238b $\text{R}^1 = \text{OMe}, \text{R}^2 = \text{PIB}$	96%	87.5:12.5
5	238c $\text{R}^1 = \text{Br}, \text{R}^2 = \text{PIB}$	82%	87.5:12.5
6	238d $\text{R}^1 = \text{Me}, \text{R}^3 = \text{C}_6\text{H}_5$	90%	88:12
7	238e $\text{R}^1 = \text{H}, \text{R}^3 = \text{C}_6\text{H}_5$	91% ^d	96:4
8	238f $\text{R}^1 = \text{H}, \text{R}^3 = 2\text{-naphthyl}$	90% ^d	93:7

^aReactions were run on a 0.100 mmol scale with Amberlite CG50 (200 mg) and MS 4Å (50 mg). ^bIsolated yield. ^cDetermined by HPLC analysis on a chiral stationary phase. ^d6:1 mixture of regioisomers (determined by ¹H NMR). PIB = 4-iodobenzyl.

The reaction furthermore tolerated different substitutions on the ketone moiety. All hydrazones **237g-m** in which R^1 was an aromatic group were transformed to the tetrahydrocarbazoles **238g-m** in high yields (88-99%) and with good enantioselectivities between 94:6 and 96:4 er, irrespective of the electronic or steric nature of the substituent (Table 17, entries 1-7). Aliphatic groups in this position were also tolerated (Table 17, entries 8-10). The desired products **238n-p** were obtained in good yields (70-98%) with a notably high enantioselectivity of 95:5 er in the case of the small methyl substituent (Table 17, entry 8). Switching to more sterically demanding alkyl substituents, diminished enantioselectivity was observed (Table 17, entries 9 and 10).

Table 17. Substrate scope of the catalytic asymmetric Fischer indolization – variation of the ketone moiety.^a

entry	product	yield ^b	er ^c
1	238g R ¹ = 4- <i>t</i> Bu-C ₆ H ₄	89%	94.5:5.5
2	238h R ¹ = 4-MeO-C ₆ H ₄	94%	96:4
3	238i R ¹ = 4-F-C ₆ H ₄	99%	94.5:5.5
4	238j R ¹ = 3,5-Me ₂ -C ₆ H ₃	88%	94:6
5	238k R ¹ = 3,5-(MeO) ₂ -C ₆ H ₃	98%	94.5:5.5
6	238l R ¹ = 3-Cl-C ₆ H ₄	97%	94:6
7	238m R ¹ = 2-naphthyl	99%	94.5:5.5
8	238n R ¹ = Me	70%	95:5
9	238o R ¹ = cyclohexyl	98%	91.5:8.5
10	238p R ¹ = <i>t</i> -Bu	90%	80:20
11	238q R ¹ = OBz	99%	98.5:1.5
12 ^d	238r R ¹ = NPhthal	99%	93.5:6.5
13	238s	11% ^e	80.5:19.5
14 ^f	238t	62% ^e	90.5:9.5

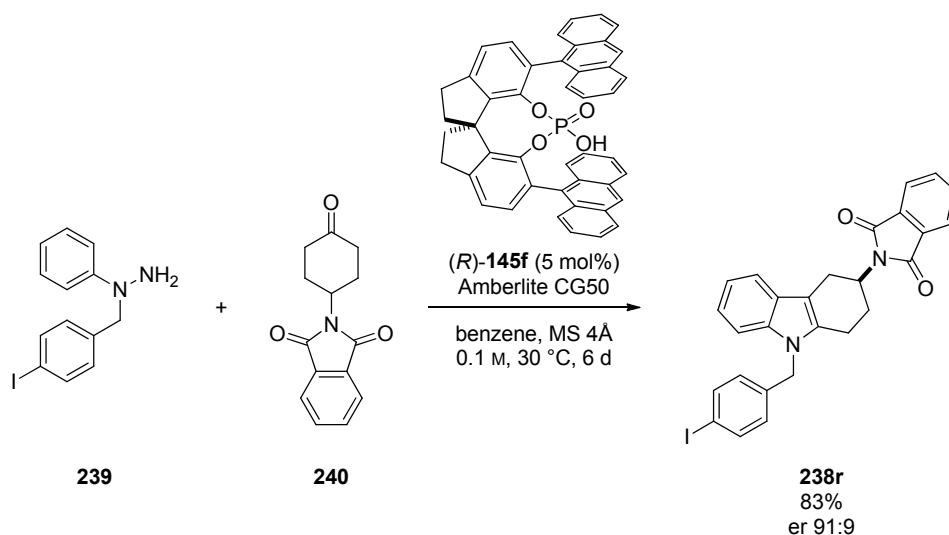
^aReactions were run on a 0.100 mmol scale with Amberlite CG50 (200 mg) and MS 4Å (50 mg). ^bIsolated yield.

^cDetermined by HPLC analysis on a chiral stationary phase. ^d6 d. ^eIncomplete conversion of starting material. ^f8 d at 50 °C. PIB = 4-iodobenzyl.

Heteroatom-substituted substrates **237q** and **237r** were well tolerated and both gave the desired products **238q** and **238r** in 99% yield (Table 17, entries 11 and 12). Particularly noteworthy is the high enantioselectivity of 98.5:1.5 er observed in the benzoyloxy-substituted product **238q** (Table 17, entry 11). The synthesis of tetrahydrocarbazole **238s** bearing a quaternary stereogenic center proved challenging in terms of conversion and

enantioselectivity (Table 17, entry 13). Although cyclopentanone-derived hydrazone **237t** also showed reduced reactivity, conducting the reaction at elevated temperatures and with a prolonged reaction time gave **238t** in 62% yield and with 90.5:9.5 er (Table 17, entry 14).

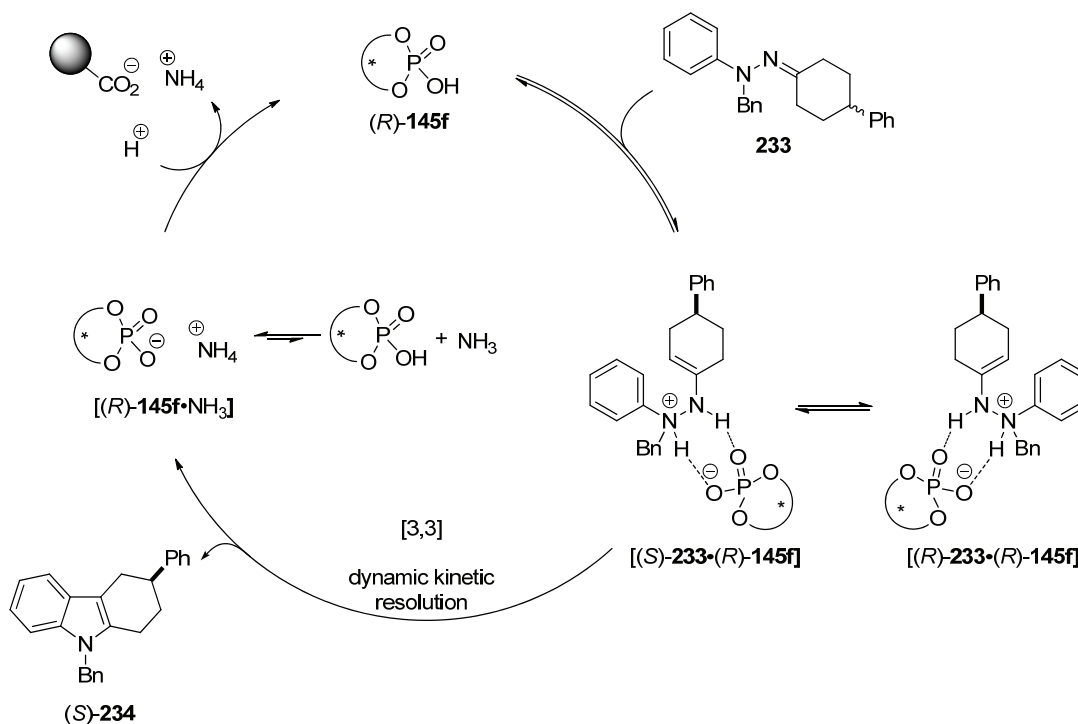
Given the biological relevance of 3-amino-tetrahydrocarbazoles,^[152] also the possibility of obtaining product **238r** in a one pot procedure from the corresponding phenyl hydrazine **239** and 4-*N*-phthalimidocyclohexanone (**240**) was investigated. In this reaction the desired product **238r** was obtained in 83% yield with an enantiomeric ratio of 91:9 er (Scheme 81). Thus the results obtained were comparable to those obtained when starting from the pre-formed hydrazone **237r**.



Scheme 81. Enantioselective synthesis of tetrahydrocarbazole **238r** from hydrazine **239** and ketone **240**.

In agreement with the widely accepted mechanism of the Fischer indolization,^[89] we propose that catalyst **145f** accelerates the hydrazone-enehydrazine tautomerisation. In 2011 the research groups of Houk and Garg had shown that in certain Fischer indolizations hydrazones without a protecting group can be protonated at either of the two nitrogen atoms, resulting in two different reaction pathways.^[153] In this respect the benzyl group in our system is considered to be essential in rendering the anilinic nitrogen sufficiently basic to ensure enehydrazine protonation at this position. This would allow the reaction to proceed via a distinct pathway involving a chiral hydrogen bond assisted ion pair for the dual activation of the substrate. Supposingly, one of the diastereomeric ion pairs [*(R)*-**233**·*(R)*-**145f**] and [*(S)*-**233**·*(R)*-**145f**] undergoes the irreversible [3,3]-sigmatropic rearrangement at a

higher rate to give product (*S*)-**234** by means of a dynamic kinetic resolution, and the ammonium salt of the catalyst [(*R*)-**145f**·NH₃] (Scheme 82). Ultimately, the active catalyst (*R*)-**145f** is regenerated by cation exchange with the resin.



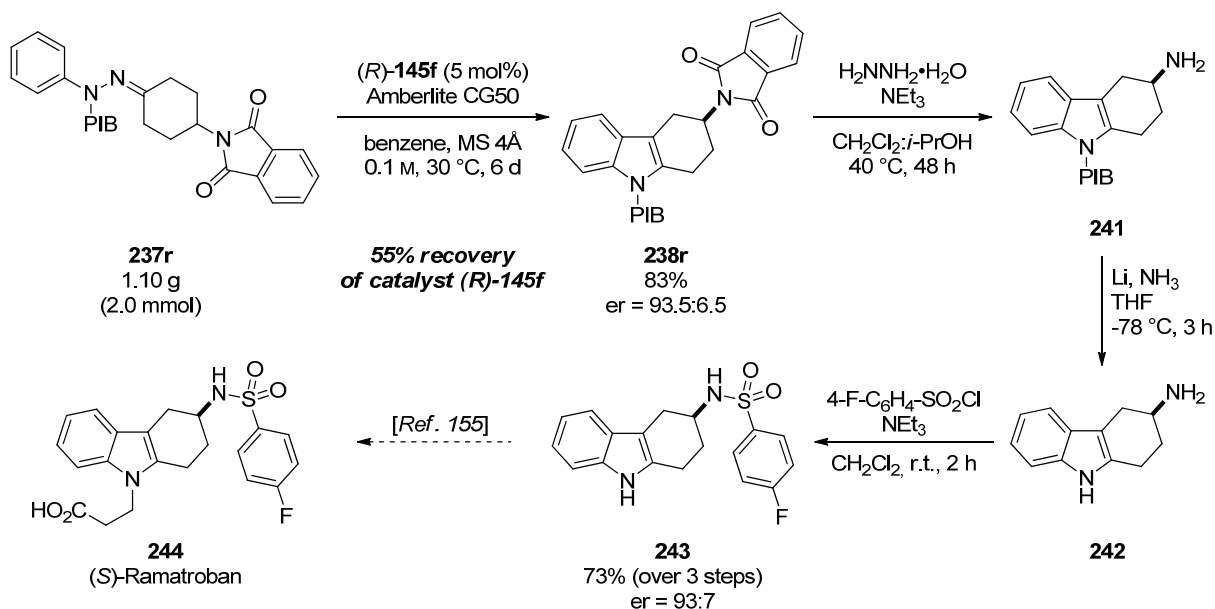
Scheme 82. Suggested mechanistic scenario for the catalytic asymmetric Fischer indolization of hydrazone **233**.

Alternatively, the preferred formation of only one enehydrazone enantiomer from the hydrazone and subsequent rearrangement can also be envisioned. However, in mechanistic studies Hughes found that the hydrazone-enehydrazone isomerisation becomes rate determining in the Fischer indolization only under extremely acidic reaction conditions.^[154] In light of these results, the alternative mechanistic scenario seems less likely.

4.2.2.5 Formal Synthesis of (*S*)-Ramatroban

Some of the results reported in this section were obtained in collaborative effort with M. J. Webber.

To briefly demonstrate the utility of the developed method, a formal synthesis of the thromboxane receptor antagonist Ramatroban (**244**) was targeted.^[152a,155] Commonly this enantiomerically pure drug is obtained via resolution of a racemic precursor in the course of the synthesis. Hence, the development of an efficient catalytic asymmetric synthesis would constitute a major improvement in terms of atom and step economy. Indolization of hydrazone **237r** on a 2.0 mmol scale proceeded without compromising yield or enantioselectivity and allowed 55% recovery of the catalyst (*R*)-**145f**. Starting from tetrahydrocarbazole **238r**, deprotection of the phthalimide was accomplished by treatment with hydrazine. Subsequent debenzoylation of amine **241** was easily achieved under Birch conditions to give the fully deprotected material **242**, which was directly sulfonlated without intermediate purification to give the literature known intermediate **243**^[155] in good overall yield and without erosion of the initial enantiomeric ratio (Scheme 83).



Scheme 83. Formal synthesis of (*S*)-Ramatroban (**244**) using the catalytic asymmetric Fischer indolization as key step.

Comparison of the optical rotation of sulfonamide **243** with literature data revealed the intermediate **243** to have the *S* configuration.^[155] This is in accordance with the absolute configuration of **236n** as determined by X-ray structure analysis (see Figure 11).

4.2.3 Summary

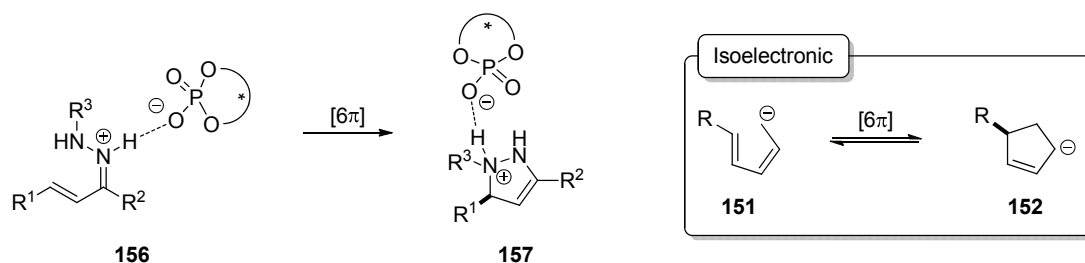
The catalytic asymmetric Fischer indolization of two different substrate classes has been studied. First investigations were devoted to the development of a Fischer indolization utilizing α -branched carbonyl compounds as substrates to give chiral indolenines bearing a quaternary stereocenter in the 3-position. Catalyst poisoning by the liberated ammonia was identified as the major challenge in the realization of such a process with substoichiometric amounts of a chiral Brønsted acid. As a possible solution the use of *N*-acyl enehydrazines which liberate non-basic acetamides as the stoichiometric by-product was suggested. It was shown that the indolization of these substrates is generally amenable to Brønsted acid catalysis, but suitable substrates were not easily accessible and turned out to be rather unstable compounds. An alternative solution was the removal of the generated ammonia by the refluxing solvent. With this procedure the Fischer indolization afforded chiral indolenines with enantioselectivities up to 76.5:23.5 er. The main limitation of this methodology was the requirement of a relatively high reaction temperature of 80 °C at which only moderate enantioselectivities were obtained. Furthermore, the undesired Wagner-Meerwein rearrangement of the indolenine products at this temperature limited the substrate scope significantly.

As a second substrate class, the catalytic asymmetric Fischer indolization of arylhydrazones derived from 4-substituted cyclohexanones was investigated. In the course of these studies, a cation exchange resin was identified as a powerful tool for the efficient removal of ammonia from the reaction mixture and a new SPINOL-derived chiral phosphoric acid was found to be a privileged catalyst for this transformation. This combination culminated in the development of a general, mild and efficient method to access enantiomerically enriched 3-substituted tetrahydrocarbazoles via a dynamic kinetic resolution of the corresponding hydrazones, representing the first catalytic asymmetric

Fischer indolization.^[156] The desired products were obtained in high yields up to 99% and enantiomeric ratios of up to 98.5:1.5. Furthermore, the synthetic utility of this methodology was demonstrated in the formal synthesis of the thromboxane receptor antagonist Ramatroban. The application of this novel cation exchange resin based technique to the indolization of hydrazones derived from α -branched aldehydes remained to be studied.

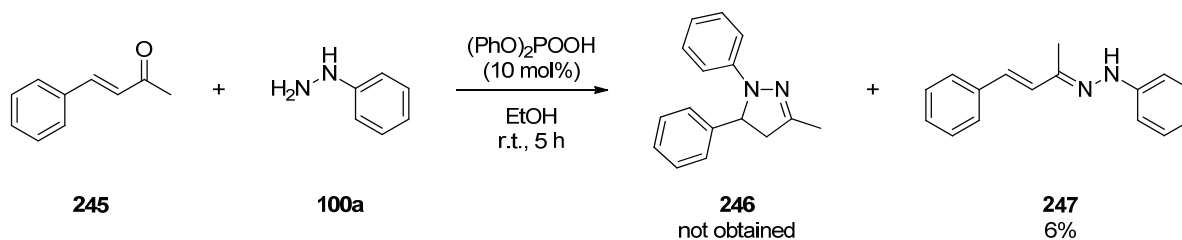
4.3 Development of a Catalytic Asymmetric 6π Electrocyclization

Inspired by our studies on the Fischer indolization we also became interested in the reaction of hydrazones derived from α,β -unsaturated carbonyl compounds. Emil Fischer probably went along similar lines, when he discovered this efficient acid-mediated synthesis of 2-pyrazolines in 1887.^[106] Later on Huisgen recognized the isoelectronic relationship between this transformation and the 6π electrocyclization of the pentadienyl anion.^[129] Although truly catalytic versions of Fischer's pyrazoline synthesis were scarce, the possibility to apply chiral Brønsted acid catalysis in order to control the torquoselectivity of this 6π electrocyclization appeared tempting.



Scheme 84. Proposed chiral Brønsted acid-catalyzed 6π electrocyclization in the synthesis of 2-pyrazolines and the isoelectronic process of the pentadienyl anion **151**.

In first experiments it was examined whether or not it was possible to conduct the Fischer pyrazoline synthesis in the presence of only substoichiometric amounts of an organic phosphoric acid. Therefore, an ethanolic solution of benzylideneacetone (**245**) and phenylhydrazine (**100a**) was treated with 10 mol% of diphenylphosphate (Scheme 85).

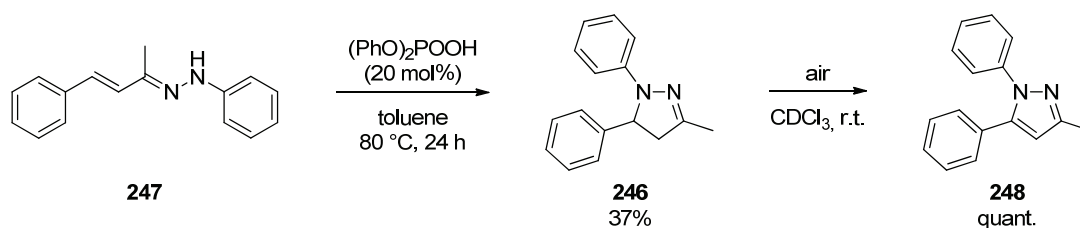


Scheme 85. Attempted DPP-catalyzed Fischer pyrazoline synthesis and isolation of hydrazone **247**.

After 5 h at room temperature the enone **245** was completely consumed and a new product had formed. Most of this new compound decomposed during the purification by column chromatography. Upon analysis of a small pure fraction obtained, corresponding to a

yield of 6%, the new compound turned out to be the hydrazones **247** rather than the expected pyrazoline **246** (Scheme 85).

The same results were obtained when the reaction was conducted in dichloromethane, acetonitrile, toluene or diethylether. In all cases the intermediary hydrazone formed readily at room temperature but no further reaction to the desired product **246** was observed. However, when the preformed hydrazone **247** was treated with 20 mol% of DPP in toluene at 80 °C, the desired pyrazoline **246** was obtained in 37% yield, but oxidized over night in chloroform to the fully aromatic achiral pyrazole **248** (Scheme 86).



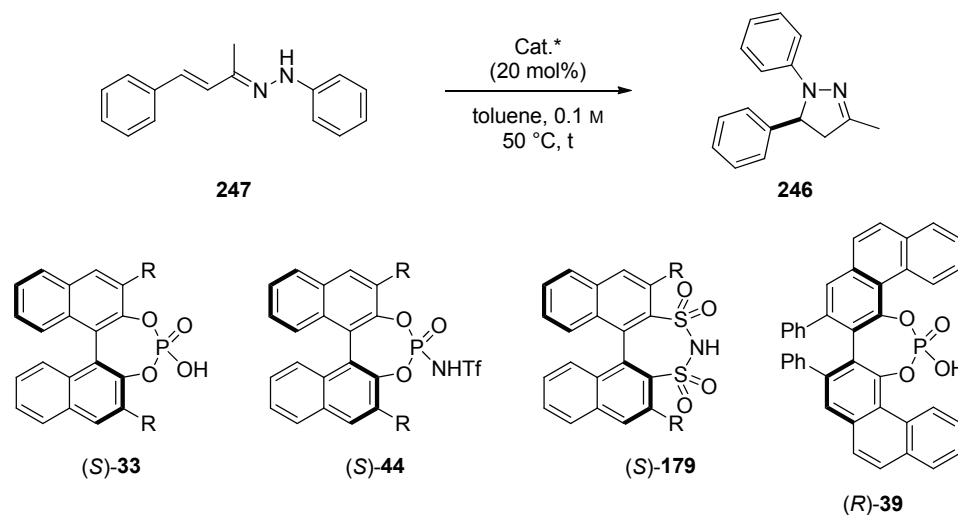
Scheme 86. DPP-catalyzed synthesis of pyrazoline **246** and its aerobic oxidation to pyrazole **248**.

Encouraged by these findings, it was concluded that the synthesis of 2-pyrazolines could generally be accomplished with only substoichiometric amounts of a Brønsted acid if preformed hydrazones were used as the starting material. Given the susceptibility of pyrazoline **246** towards oxidation, further experiments were conducted under an inert atmosphere to avoid this decomposition pathway. With a promising protocol in hand, the potential of different chiral Brønsted acids of promoting the cyclization of hydrazone **247** enantioselectively was studied.

All BINOL-derived chiral phosphoric acids afforded the 2-pyrazoline **246** in good yield. The reaction time was strongly dependent on the individual structure of the catalyst (Table 18, entries 1-12). The best enantiomeric ratio of 81:19 was obtained with the 9-anthracenyl substituted phosphoric acid (*S*)-**33f** (Table 18, entry 11). Furthermore noteworthy was the observation that the absolute configuration of the preferred product enantiomer was strongly dependent on the 3,3'-substituents of the catalyst (*cf.* e.g. Table 18, entries 8 and 11). When *N*-triflyl phosphoramides (*S*)-**44c-e** were used as catalysts, the desired product **246** was always obtained in high yields $\geq 90\%$, albeit only low enantioselectivities (Table 18, entries 13-15). The disulfonimides (*S*)-**179b** and (*S*)-**179c** afforded almost racemic product in

88% and 85% yield, respectively (Table 18, entries 16 and 17). With the VAPOL-derived phosphoric acid (*R*)-**39** as catalyst, pyrazoline **246** was obtained in 80% yield with an enantiomeric ratio of 41:59 er (Table 18, entry 18).

Table 18. Screening of different chiral Brønsted acid catalysts for the electrocyclicization of hydrazone **247**.^a

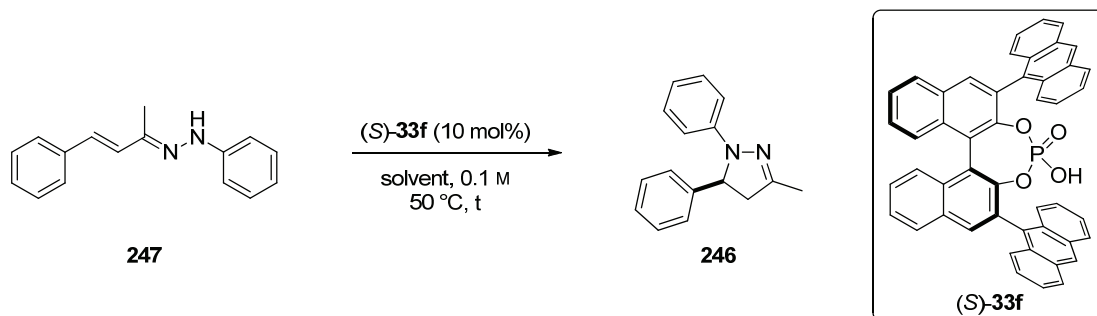


entry	Cat.*	R	t	yield ^b	er ^c
1	(<i>S</i>)- 33d	2,4,6- <i>i</i> Pr ₃ -C ₆ H ₂	70 h	79%	55.5:44.5
2 ^d	(<i>S</i>)- 33d	2,4,6- <i>i</i> Pr ₃ -C ₆ H ₂	50 h	90%	65.5:34.5
3 ^e	(<i>R</i>)- 33c	3,5-(CF ₃) ₂ -C ₆ H ₃	5 h	99%	77:23
4	(<i>S</i>)- 33h	C ₆ H ₅	5 h	85%	40:60
5	(<i>S</i>)- 33e	1-naphthyl	5 h	85%	28.5:71.5
6	(<i>S</i>)- 33m	2-naphthyl	6 h	91%	36.5:63.5
7	(<i>S</i>)- 33s	2,4,6-Me ₃ -C ₆ H ₂	4 h	80%	58:42
8	(<i>S</i>)- 33i	4-Me-C ₆ H ₄	6 h	91%	29.5:70.5
9	(<i>S</i>)- 33j	4- <i>t</i> Bu-C ₆ H ₄	4 h	99%	28:72
10	(<i>S</i>)- 33k	4-Ph-C ₆ H ₄	19 h	91%	33.5:66.5
11	(<i>S</i>)- 33f	9-anthracenyl	19 h	85%	81:19
12 ^d	(<i>S</i>)- 33p	9-phenanthryl	50 h	81%	67.5:32.5
13	(<i>S</i>)- 44c	9-anthracenyl	24 h	99%	44.5:55.5
14	(<i>S</i>)- 44d	4- <i>t</i> Bu-C ₆ H ₄	16 h	98%	42.5:57.5
15	(<i>S</i>)- 44e	3,5-(CF ₃) ₂ -C ₆ H ₃	16 h	90%	51.5:48.5
16	(<i>S</i>)- 179b	H	18 h	88%	54:46
17	(<i>S</i>)- 179c	2,4,6- <i>i</i> Pr ₃ -C ₆ H ₂	16 h	85%	54:46
18	(<i>R</i>)- 39	-	30 h	80%	41:59

^aReactions were run on a 0.025 mmol or 0.050 mmol scale with 20 mol% of the corresponding catalyst under an Ar atmosphere. ^bIsolated yield. ^cDetermined by HPLC analysis on a chiral stationary phase. ^d10 mol% of the catalyst were used. ^e(*R*)-enantiomer of the catalyst was used.

From this preliminary catalyst screening, the BINOL-derived phosphoric acid **33f** bearing 9-anthracenyl groups in the 3,3'-positions was identified as the most promising catalyst. Hence it was also used in the optimization of the reaction solvent. With 10 mol% of catalyst (*S*)-**33f** the reaction in toluene proceeded as before with 20 mol% and afforded pyrazoline **246** in 85% yield and with an enantiomeric ratio 81:19 (Table 19, entry 1). While in *p*-xylene and trifluorotoluene the desired product was obtained with slightly diminished enantioselectivities (Table 19, entries 2 and 5), benzene and especially chlorobenzene had beneficial effects on the stereochemical outcome of the reaction (Table 19, entries 3 and 4) and the enantiomeric ratio improved up to 85.5:14.5 in the case of chlorobenzene (Table 19, entry 4).

Table 19. Variation of the reaction solvent and catalyst loading.^a

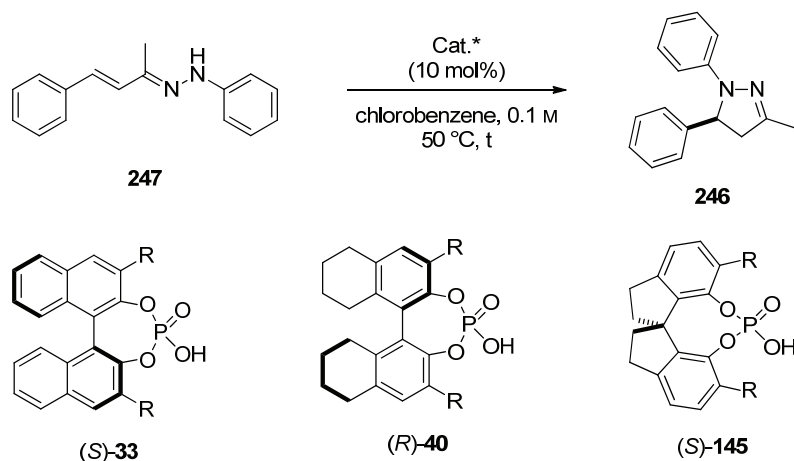


entry	solvent	t	yield ^b	er ^c
1	toluene	20 h	85%	81:19
2	<i>p</i> -xylene	44 h	83%	75.5:24.5
3	benzene	20 h	90%	84.5:15.5
4	chlorobenzene	20 h	74%	85.5:14.5
5	trifluorotoluene	45 h	66%	74.5:25.5
6	THF	72 h	64%	59:41
7	MeCN	24 h	51%	42:58
8	CHCl ₃	20 h	80%	66.5:33.5
9	EtOH	20 h	85%	45.5:54.5
10	EtOAc	72 h	68%	62:38
11	cyclohexane	72 h	29%	78:22
12 ^d	chlorobenzene	8 h	97%	84.5:15.5
13 ^e	chlorobenzene	24 h	87%	83.5:16.5
14 ^f	chlorobenzene	66 h	83%	77.5:22.5

^aReactions were run on a 0.025 mmol scale with 10 mol% of catalyst (*S*)-**33f** under an Ar atmosphere. ^bIsolated yield. ^cDetermined by HPLC analysis on a chiral stationary phase. ^d20 mol% of the catalyst was used. ^e5 mol% of the catalyst was used. ^f2 mol% of the catalyst was used.

The reaction seemed to be relatively robust with respect to different solvents. The etheric solvent THF, acetonitrile, chloroform, ethyl acetate and even the protic solvent ethanol afforded the product in decent yields, but the enantioselectivities were only moderate to low in these cases (Table 19, entries 6-10). Only in cyclohexane the cyclization of hydrazone **247** proceeded sluggishly, most likely because of the poor solubility of the substrate **247**, and 2-pyrazoline **246** was isolated in 29% yield with an enantiomeric ratio of 78:22 (Table 19, entry 11). Finally, the influence of the loading of catalyst **33f** was investigated in chlorobenzene. When 20 mol% of the phosphoric acid (*S*)-**33f** were used, the enantioselectivity of the product **246** was unperturbed (Table 19, entry 12), whereas the reduction to 5 mol% and 2 mol% came along with prolonged reaction times and diminished enantioselectivities (Table 19, entries 13 and 14).

Although the use of chlorobenzene had turned out to be beneficial for the stereochemical outcome of the reaction, the obtained enantioselectivity was still not optimal. Further optimizations included the reinvestigation of chiral Brønsted acid catalysts previously tested in toluene as well as other phosphoric acids with more sophisticated substituents. The unsubstituted BINOL-derived phosphoric acid (*S*)-**33g** as well its substituted analogs (*S*)-**33h**, (*S*)-**33o**, (*S*)-**33t**, and (*R*)-**33c** gave low enantioselectivities of 68.5:31.5 er or below (Table 20, entries 1-5). More surprising was the behaviour of catalysts (*S*)-**33q** and (*S*)-**33u**. While anthracene substituents gave the best results so far, the catalysts with modified anthracenyl groups gave disappointing enantioselectivities of 41:59 er (Table 20, entry 6) and 32:68 er (Table 20, entry 7), respectively. H₈-BINOL-based catalyst (*R*)-**40e** with 9-anthracenyl substituents was comparable to its BINOL-analog, though slightly inferior in terms of enantioselectivity (Table 20, entry 8). The benzhydryl substituted analog (*R*)-**40f** afforded pyrazoline **246** with a detrimental enantioselectivity of 67.5:32.5 er (Table 20, entry 9), which was comparable to the performance of different SPINOL-derived catalysts **145a**, **145c** and **145d** (Table 20, entries 10-12).

Table 20. Screening of different catalysts for the cyclization of hydrazone **247** in chlorobenzene.^a

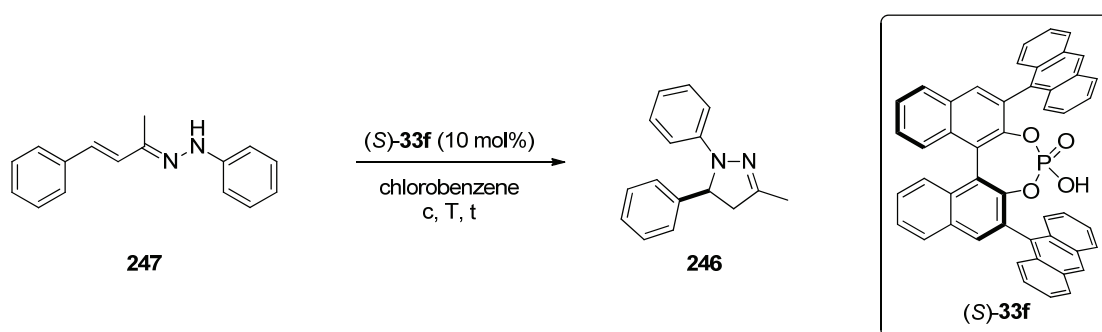
entry	Cat.*	R	t	yield ^b	er ^c
1	(S)-33g	H	14 h	88%	57.5:42.5
2	(S)-33h	C ₆ H ₅	6 h	85%	68.5:31.5
3	(S)-33o	SiPh ₃	48 h	51%	64.5:35.5
4	(S)-33t	3,5-Ph ₂ -C ₆ H ₃	17 h	99%	48:52
5 ^d	(R)-33c	3,5-(CF ₃) ₂ -C ₆ H ₃	6 h	88%	34:66
6	(S)-33q		24 h	80%	41:59
7	(S)-33u		32 h	66%	32:68
8	(R)-40e	9-anthracenyl	16 h	96%	16.5:83.5
9	(R)-40f	Ph ₂ CH	24 h	66%	67.5:32.5
10	(S)-145d	H	14 h	99%	61.5:38.5
11	145a	C ₆ H ₅	48 h	74%	63.5:36.5
12	145c	3,5-(CF ₃) ₂ -C ₆ H ₃	42 h	85%	60.5:39.5

^aReactions were run on a 0.025 mmol scale with 10 mol% of the corresponding catalyst under an Ar atmosphere. ^bIsolated yield. ^cDetermined by HPLC analysis on a chiral stationary phase. ^d(R)-enantiomer of the catalyst was used.

Unfortunately, no better catalyst for the cyclization of hydrazone **247** into the 2-pyrazoline **246** than the BINOL-derived phosphoric acid (S)-**33f** was identified.^[157] To obtain the best results possible, concentration and reaction temperature were finally optimized for this phosphoric acid and chlorobenzene as the solvent. It was found that our standard concentration of 0.1 M was already optimal and increased or decreased concentrations gave

inferior results (Table 21, entries 1-6). Variation of the temperature revealed that the reaction could also be conducted at temperatures as low as 30 °C without compromising the reactivity too much (Table 21, entries 7 and 8). Under these reaction conditions 2-pyrazoline **246** was obtained in 92% yield and with an enantiomeric ratio of 88:12 after 96 h reaction time (Table 21, entry 8).

Table 21. Fine tuning of the reaction conditions for the electrocyclicization of hydrazone **247** with catalyst (*S*)-**33f**.^a

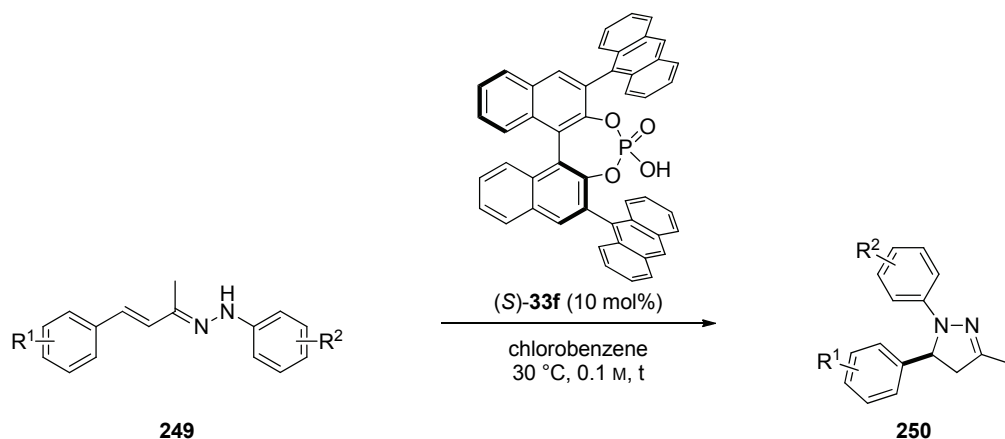


entry	c	T	t	yield ^b	er ^c
1	1.0 M	50 °C	16 h	96%	70.5:29.5
2	0.5 M	50 °C	16 h	90%	72.5:27.5
3	0.2 M	50 °C	16 h	93%	78:22
4 ^d	0.1 M	50 °C	16 h	99%	85:15
5 ^d	0.05 M	50 °C	16 h	99%	85:15
6 ^d	0.01 M	50 °C	25 h	99%	82.5:17.5
7 ^d	0.1 M	40 °C	26 h	99%	87.5:12.5
8 ^d	0.1 M	30 °C	96 h	92%	88:12

^aReactions were run on a 0.200 mmol scale with 10 mol% of catalyst (*S*)-**33f** under an Ar atmosphere. ^bIsolated yield. ^cDetermined by HPLC analysis on a chiral stationary phase. ^dReactions were run on a 0.025 mmol scale with 10 mol% of catalyst (*S*)-**33f** under an Ar atmosphere.

4.3.2 Catalytic Asymmetric 6 π Electrocyclization of α,β -Unsaturated Arylhydrazones

After careful optimization of the catalyst structure and the reaction conditions the developed protocol was applied to different substrates. Benzylideneacetone-derived phenylhydrazone **247** reacted as in the optimization studies and was obtained in 92% yield and with an enantiomeric ratio of 88:12 (Table 22, entry 1).

Table 22. Enantioselective 6π electrocyclization of α,β-unsaturated arylhydrazones.^a

entry	hydrazone	t	yield ^b	er ^c	
1		247	96 h	92%	88:12
2		249a : R ¹ = F	90 h	94%	94.5:5.5
3		b : R ¹ = Cl	7 d	96%	95:5
4		c : R ¹ = Br	109 h	95%	95:5
5 ^d		d : R ¹ = NO ₂	96 h	93%	96:4
6		e : R ¹ = CF ₃	9 d	88%	96.5:3.5
7		f : R ¹ = F	96 h	91%	93.5:6.5
8		g : R ¹ = Cl	96 h	95%	95.5:4.5
9		h : R ¹ = Br	96 h	94%	96:4
10 ^d		i : R ¹ = NO ₂	60 h	99%	97.5:2.5
11		j : R ¹ = Me	8 d	84%	85:15
12		k : R ¹ = OMe	8 d	92%	91:9
13 ^e		249l	96 h	85%	93:7
14		249m	75 h	93%	95:5
15		249n	93 h	90%	79:21
16		249o	36 h	91%	92.5:7.5
17 ^f		249p	40 h	88%	88.5:11.5

^aUnless otherwise noted, the reactions were run on a 0.10 mmol scale with 10 mol% of catalyst (S)-**33f** under an Ar atmosphere in chlorobenzene (1.0 mL) at 30 °C. ^bIsolated yield. ^cDetermined by HPLC analysis on a chiral stationary phase. ^dReaction was run at 40 °C. ^eReaction was run at 20 °C. ^fReaction was run at 50 °C.

The reaction turned out to be well suited for hydrazones bearing electron-withdrawing substituents at the aromatic ring of the enone part. All kinds of halogen atoms in the *para*-position of the aromatic ring were tolerated, giving the desired products **250a-c** in enantioselectivities of up to 95:5 er (Table 22, entries 2-4). Also the strongly electron-withdrawing nitro- and trifluoromethyl- groups behaved likewise well (Table 22, entries 5 and 6). *Meta*-substituents on the aromatic ring of the enone moiety of hydrazones **249f-k** gave similar results (Table 22, entries 7-12) with enantiomeric ratios of up to 97.5:2.5 (Table 22, entry 10). The electron-donating substituents in substrates **249l** and **249m** accelerated the reaction and were likewise well tolerated (Table 22, entries 13 and 14). The reaction also worked well with substituents on the phenylhydrazine component. While with the strongly electron-withdrawing fluorine substituent a diminished enantioselectivity was observed (Table 22, entry 15), the use of 4-methoxyphenylhydrazone **249o** resulted in a faster reaction and a good enantioselectivity of 92.5:7.5 er (Table 22, entry 16). Finally, 4-fluorophenylhydrazone **249p** also cyclized readily at slightly elevated temperature to give pyrazoline **250p** in 88% yield and with an enantiomeric ratio of 88:12 (Table 22, entry 17). Significantly, this compound is a patented COX-2 inhibitor.^[158]

The absolute configuration of the brominated pyrazoline **250h** was determined by X-ray structure analysis. The *S* configuration found for this compound was assumed to be representative for other derivatives.

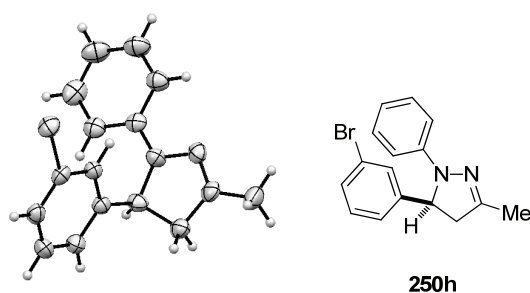


Figure 12. ORTEP plot of the X-ray crystal structure of pyrazoline **250h**. Ellipsoids are drawn at 50% probability level.

Besides the well working substrates discussed above, also some limitations of this methodology became noticeable. In the attempted reaction of hydrazone **251** derived from 2,6-dimethylphenylhydrazine, no conversion was observable. This lack of reactivity may be attributed to the steric hindrance caused by the additional methyl substituents. Also the

carbamate substituted hydrazones **252** and **253** and the tosylated derivative **254** did not afford any product under our reaction conditions. In these cases the electron withdrawing character of the substituents apparently reduces the electron density of the system and thus prevents the cyclization (Figure 13).

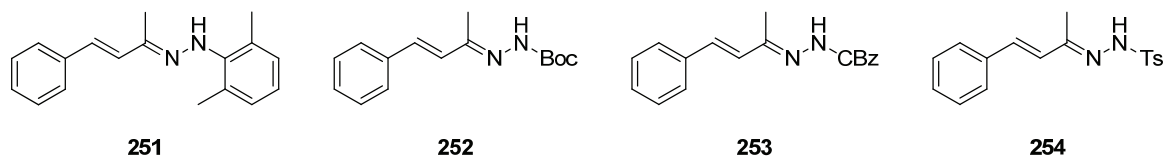


Figure 13. Unreactive hydrazone substrates **251-254**.

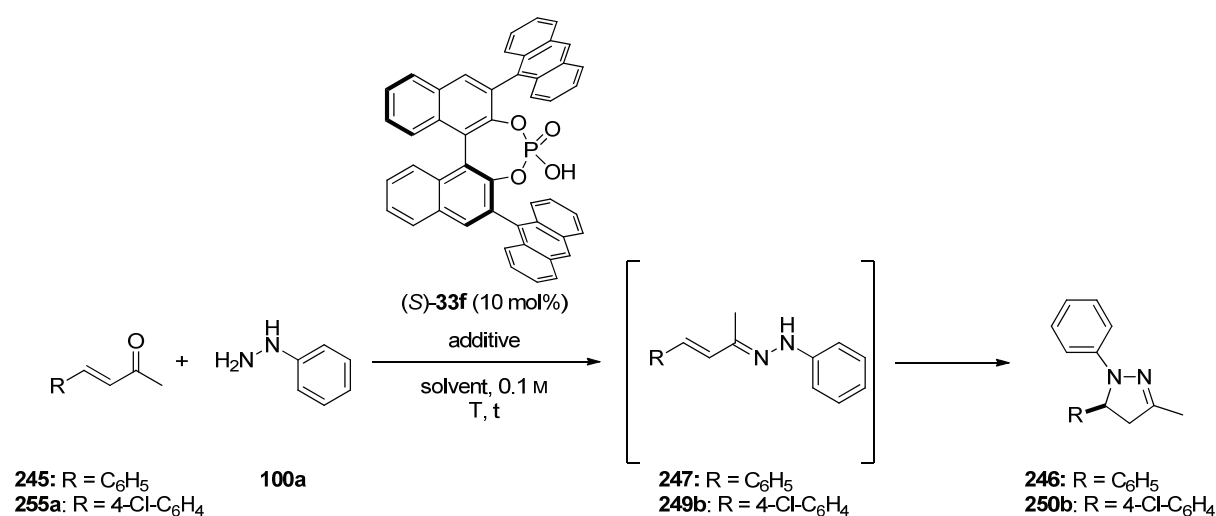
Another limitation of the method so far was the need for the preformed hydrazones. Most of these substrates turned out to be unstable towards column chromatography and purification had to be accomplished by crystallization. Consequently, only those hydrazones which were either stable towards chromatography or crystalline substrates could be used so far. Therefore, we next attempted to overcome this limitation by the development of an *in situ* method.

4.3.3 Enantioselective Synthesis of 2-Pyrazolines from Enones and Phenylhydrazine

In order to extend the developed methodology to a more general synthesis of 2-pyrazolines from α,β -unsaturated carbonyl compounds and hydrazines, also a direct method that does not require isolation of the hydrazone intermediates was investigated. First benzylideneacetone (**245**) and phenylhydrazine (**100a**) were reacted in the presence of catalyst (*S*)-**33f** (10 mol%) in toluene at 40 °C. The reaction turned out to be very slow under these reaction conditions and was stopped after 72 h to afford the desired product **246** in 48% yield and with a low enantiomeric ratio of only 56:44 (Table 23, entry 1). When the same reaction was run in the presence of 4Å molecular sieves to remove the liberated water from the reaction mixture, the enantiomeric ratio increased to 71.5:28.5. However, the reactivity remained low and after 72 h only 48% of the 2-pyrazoline **246** were isolated (Table 23, entry 2). The addition of other drying agents like 5Å molecular sieves, magnesium sulfate or sodium sulfate gave comparable results. The enantioselectivities of the desired product remained below the values expected from our previous results. Furthermore, the reaction rates decreased dramatically with this procedure (Table 23, entries 3-5). While the

diminished enantiomeric ratios could be explained by the presence of moisture in the reaction mixture (*cf.* Table 23, entries 1 and 2), the reason for the loss of reactivity remained unclear, especially since monitoring of the reaction by TLC indicated a relatively fast and quantitative hydrazone formation in all cases. To restore the reactivity and initial enantioselectivity of the process, the protocol was modified slightly.

Table 23. Optimization of reaction conditions for the enantioselective one-pot synthesis of 2-pyrazolines from enones and phenylhydrazine.^a



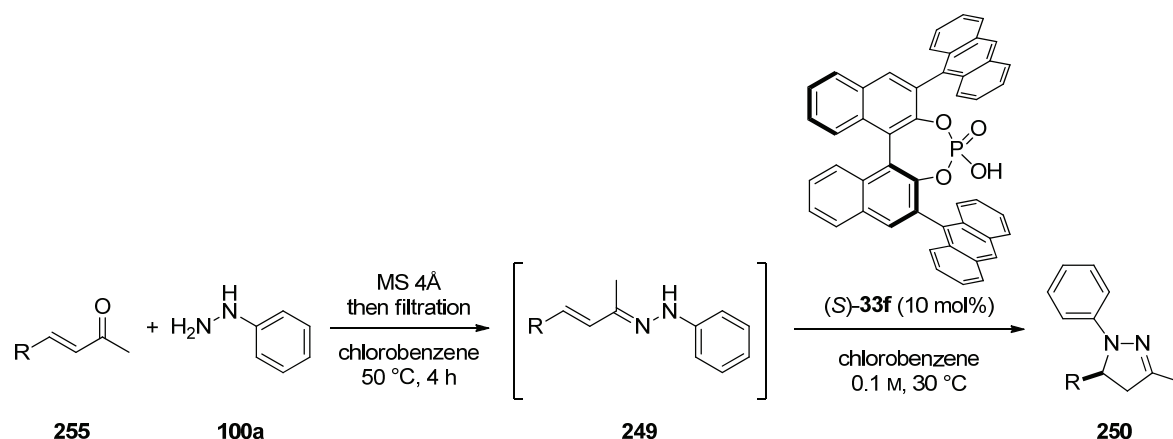
entry	enone	additive	solvent	T	t	yield ^b	er ^c
1	245 R = C ₆ H ₅	-	PhMe	40 °C	72 h	48%	56:44
2	245 R = C ₆ H ₅	MS 4Å	PhMe	40 °C	72 h	48%	71.5:28.5
3	255a R = 4-Cl-C ₆ H ₄	MS 5Å	PhCl	50 °C	48 h	13%	75.5:24.5
4	255a R = 4-Cl-C ₆ H ₄	MgSO ₄	PhCl	50 °C	48 h	74%	85.5:14.5
5	255a R = 4-Cl-C ₆ H ₄	Na ₂ SO ₄	PhCl	50 °C	48 h	34%	75:25
6 ^{d,e}	255a R = 4-Cl-C ₆ H ₄	MgSO ₄	PhCl	40 °C	25 h	77%	92.5:7.5
7 ^{d,f}	255a R = 4-Cl-C ₆ H ₄	MS 4Å	PhCl	40 °C	25 h	77%	91:9

^aThe reactions were run on with enone (0.100 mmol) and phenylhydrazine (**100a**, 0.100 mmol) with 10 mol% of catalyst (*S*)-**33f** and 30 mg of the corresponding additive under an Ar atmosphere. ^bIsolated yield. ^cDetermined by HPLC analysis on a chiral stationary phase. ^dEnone **255a** (0.105 mmol), phenylhydrazine (**100a**, 0.100 mmol), and the additive were stirred at 50 °C for 4 h, then the mixture was filtered into a vial containing catalyst (*S*)-**33f** and stirred at 40 °C for the indicated time. ^e20 equivalents of MgSO₄ (241 mg) were used. ^f30 mg of MS 4Å were used.

Given the facile formation of the hydrazone intermediates via condensation of the enone and the hydrazines in combination with a good reactivity observed when starting from the preformed hydrazones, enone **255a** and phenylhydrazine (**100a**) were now reacted in chlorobenzene at 50 °C in the presence of 20 equivalents of magnesium sulfate as the

water scavenger. After complete hydrazone formation the salt was removed by filtration and catalyst (*S*)-**33f** was added to the resulting solution of the hydrazone in chlorobenzene and stirred at 40 °C. Already after 25 h the reaction reached complete conversion and pyrazoline **250b** was isolated in 77% yield with an enantiomeric ratio of 92.5:7.5 (Table 23, entry 6). Since this procedure required huge amounts of the drying agent, we were delighted to find that 4 Å molecular sieves provided virtually identical results and allowed to reduce the amount of solid additive by almost 90% (Table 23, entry 7).

This procedure finally allowed conducting the electrocyclization under the reaction conditions developed previously without the isolation of the pure hydrazones. The yields and enantioselectivities obtained with this protocol were comparable to those reported earlier (Table 24, entries 1-3). Additionally, it was now possible to use enones of which the corresponding phenylhydrazones were not accessible before. The iodinated 2-pyrazoline **250q** was obtained in 89% yield with a high enantioselectivity of 95.5:4.5 er (Table 24, entry 4). Also the synthesis of pyrazoline **250r** bearing a quaternary stereocenter (Table 24, entry 5) or product **250s** with substituents in the 3-position other than methyl groups (Table 24, entry 6) was possible in high yields, although the enantiomeric ratios in these cases were only moderate. When aliphatic enone **255g** was subjected to the same reaction conditions, the cyclization proceeded only sluggishly even at elevated temperatures and gave a poor yield and enantioselectivity (Table 24, entry 7). Interestingly, this result was improved by using the more acidic but, in the case of aromatic hydrazones less selective, *N*-triflyl phosphoramidate analog of (*S*)-**44c** as catalyst. In this case, pyrazoline **250t** was obtained in 40% yield and with an enantiomeric ratio of 74.5:25.5 (Table 24, entry 8), thus illustrating the potential generality of our method.

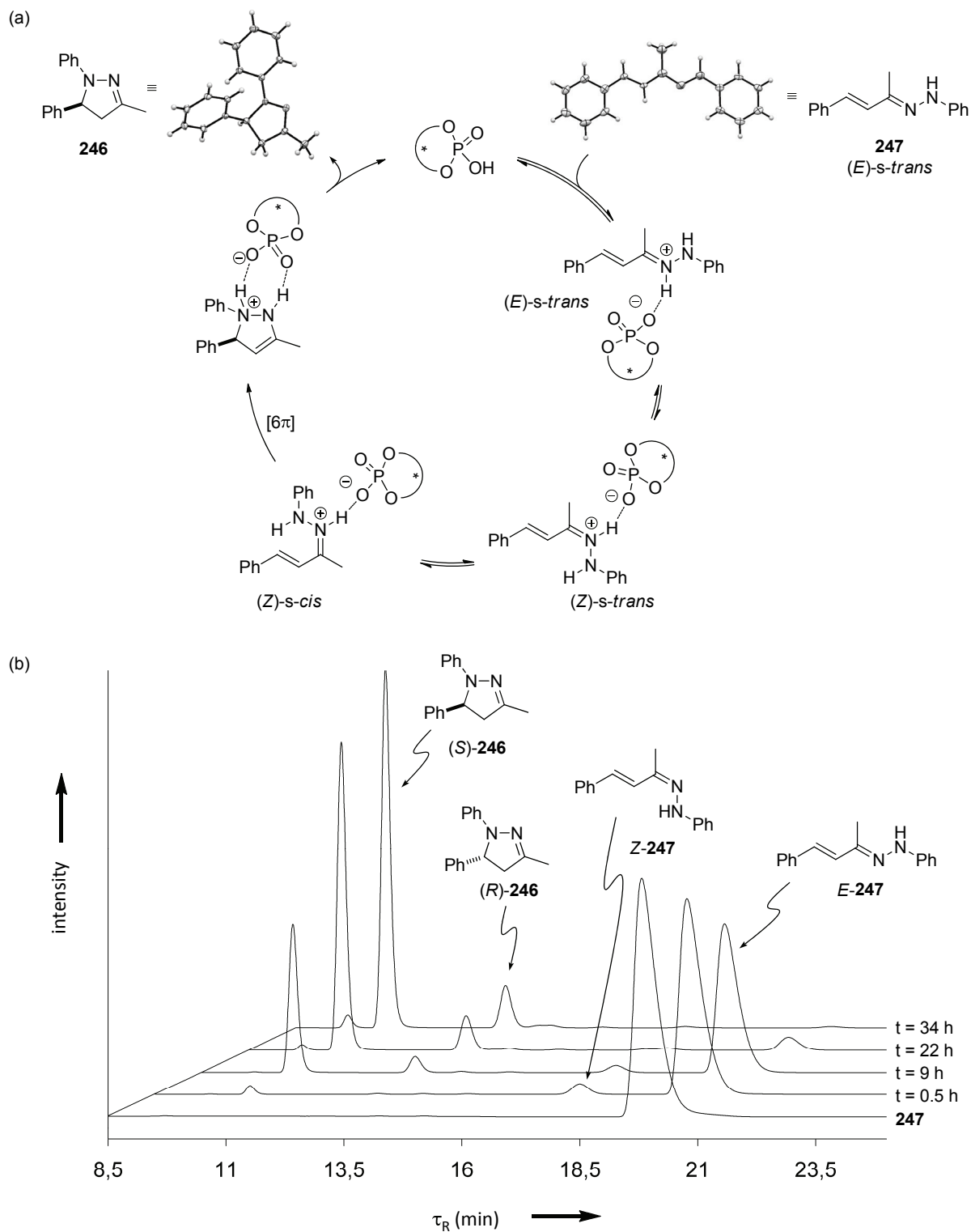
Table 24. Enantioselective synthesis of 2-pyrazolines starting from α,β -unsaturated ketones **255** and phenylhydrazine (**100a**).^a

entry	enone	product	t	yield ^b	er ^c
1	255a R = 4-Cl-C ₆ H ₄	250b	66 h	97%	93.5:6.5
2	255b R = 3-Br-C ₆ H ₄	250h	66 h	88%	95:5
3 ^d	255c R = 3-NO ₂ -C ₆ H ₄	250i	96 h	99%	96.5:3.5
4	255d R = 3-I-C ₆ H ₄	250q	70 h	89%	95.5:4.5
5	255e	250r	66 h	88%	60.5:39.5
6	255f	250s	6 d	67%	63.5:36.5
7 ^e	255g R = <i>n</i> -C ₅ H ₁₁	250t	24 h	18%	65.5:34.5
8 ^f	255g R = <i>n</i> -C ₅ H ₁₁	250t	24 h	40%	74.5:25.5

^aUnless otherwise noted, enone **255** (0.105 mmol), phenylhydrazine (**100a**, 0.100 mmol) and 4 Å molecular sieves (30 mg) were stirred for 4 h at 50 °C, then the mixture was filtered and the solution was treated with 10 mol% of catalyst (*S*)-**33f** and stirred under an Ar atmosphere in chlorobenzene (1.0 mL) at 30 °C. ^bIsolated yield. ^cDetermined by HPLC analysis on a chiral stationary phase. ^dReaction was run at 40 °C. ^eReaction was run at 100 °C with 0.110 mmol of enone **255g** and 20 mol% of catalyst (*S*)-**33f**. ^fReaction was run at 50 °C with 0.110 mmol of enone **255g** and 20 mol% of the 9-anthracenyl substituted BINOL-derived *N*-triflyl phosphoramidate (*S*)-**44c** as the catalyst.

4.3.4 Mechanistic considerations

In the course of the development of the catalytic asymmetric synthesis of 2-pyrazolines a Röntgen-structure of the α,β -unsaturated phenylhydrazone **247** was obtained. The analysis of this structure revealed that hydrazone **247** exists as the linear (*E*)-*s-trans*-conformer (*E*)-*s-trans*-**247** (Scheme 87a). To undergo the reaction, hydrazone **247** has to adopt the “cyclization-reactive” (*Z*)-*s-cis*-conformation, which requires both, C-C-single-bond rotation and C-N-double-bond isomerization.



Scheme 87. Proposed catalytic cycle and X-ray structures of hydrazone **247** and pyrazoline **246** (a) and HPLC traces of the reaction mixture at different times t (b) (reaction was run at 40 °C).

While the *s-trans* to *s-cis* isomerization should be a facile process even at room temperature and in the absence of any catalyst, the *E/Z*-isomerization of the hydrazone

bond requires acid catalysis. Indeed, in the absence of the catalyst (*S*)-**33f** only one peak for pure (*E*)-*s-trans*-**247** was detectable by HPLC (Scheme 87b). After the addition of phosphoric acid (*S*)-**33f**, a second peak of identical mass, as confirmed by LC-MS, emerged. This peak disappeared again during the course of the reaction, thus indicating an intermediate (Scheme 87b). Since the *E/Z*-isomerization of related α,β -unsaturated hydrazones is known to be catalyzed by phosphoric acid,^[159] this peak most likely corresponds to (*Z*)-**247**. After adopting an *s-cis*-conformation, the protonated intermediate [(*Z*)-**247**·(*S*)-**33f**] undergoes the 6π electrocyclization as the cation of a chiral hydrogen bond assisted ion pair and furnishes the 3-pyrazoline. Subsequent isomerization and deprotonation eventually gives the thermodynamically favoured 2-isomer **246** along with the liberated catalyst (*S*)-**33f**. Also the structure of the product **246** was unambiguously proven by X-ray crystallography (Scheme 87a).

While the need for the carbon-nitrogen double bond isomerization prior to the cyclization, as well as the formation of the thermodynamically favoured 2-pyrazoline after the carbon-nitrogen bond-forming step are requisite for product formation, one might argue about the key step of this mechanistic proposal: the 6π electrocyclization. Can the ring-closure not also be described by a different mechanism? Huisgen already raised this question in 1980 and came up with a simple answer: *'Cannot the formation of pyrazolines also be classified as a nucleophilic addition of the NH₂ group [...] to the electrophilic α,β -unsaturated imine? This is an alternative description of one and the same process, differing only in the choice of words and not in its meaning [...]. Like the electrocyclization of [the pentadienyl anion], that of [an α,β -unsaturated hydrazone] requires the two 90° rotations about the axes of the terminal bonds'*.^[129]

Are these two reaction modes really identical? In principle, one could imagine different transition states for both scenarios. In the case of a pericyclic 6π electrocyclization, both ends of the conjugated π -electron system fulfill a rotation in disrotatory fashion (Figure 14, left), whereas in the case of the nucleophilic attack, the nitrogen lone pair would interact with the LUMO of the conjugated carbon-carbon double bond in a Michael addition-like mechanism (Figure 14, right).

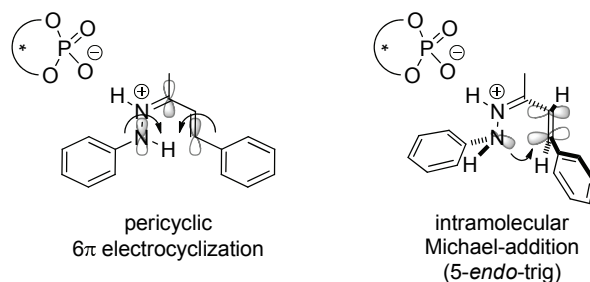


Figure 14. Possible transition states of two different mechanistic scenarios.

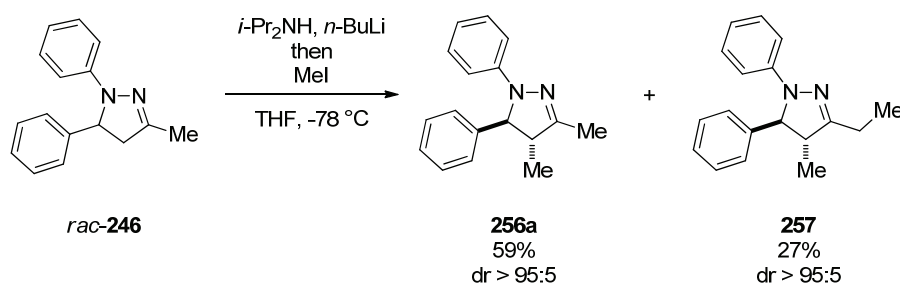
From the perspective of the synthetic chemist, the outcome is the same for both cases, because the structure of the substrates and products do not allow any conclusions concerning a possible torquoselectivity of the electrocyclization. In fact, depending on the mechanism, one could expect to obtain the 1,5-*cis*-configured product from the electrocyclization for steric reasons, whereas the nucleophilic addition should favor the corresponding *trans*-product. But due to the configurational lability of the *N*-stereocenter, the outcome of the reaction is the same for both. However, even if both scenarios could be envisioned, we believe that this reaction is best described as a 6 π electrocyclization for the following reasons. Firstly, the protonated hydrazone is the diaza analog of the pentadienyl anion and consequently their cyclizations are isoelectronic. Secondly, a nucleophilic 1,4-addition would involve a 5-*endo*-trig cyclization, which is a disfavored process according to Baldwin's rules,^[160] thus pointing towards the electrocyclic mechanism. Thirdly, in the case of a Michael-addition like mechanism, one would expect a dramatic drop of the reaction rate when a β,β -disubstituted acceptor is used instead of a monosubstituted double bond. In our reaction this additional substitution does not affect the rate of the reaction and pyrazoline **250r** bearing a quaternary stereocenter is formed as efficiently and rapidly as derivatives with a tertiary stereocenter (*cf.* Table 24, entries 2 and 5). Although these hints are in favour of the 6 π electrocyclization, the alternative nucleophilic 1,4-addition can not be ruled out at this point. The true mechanism may well turn out to be something between these two descriptions and theoretical studies are clearly needed to gain clarity.^[161]

4.3.5 Diastereoselective Alkylations of 2-Pyrazolines

Not only their manifold biological activities, but also their use as synthetic building blocks makes pyrazolines important and interesting molecules. With respect to

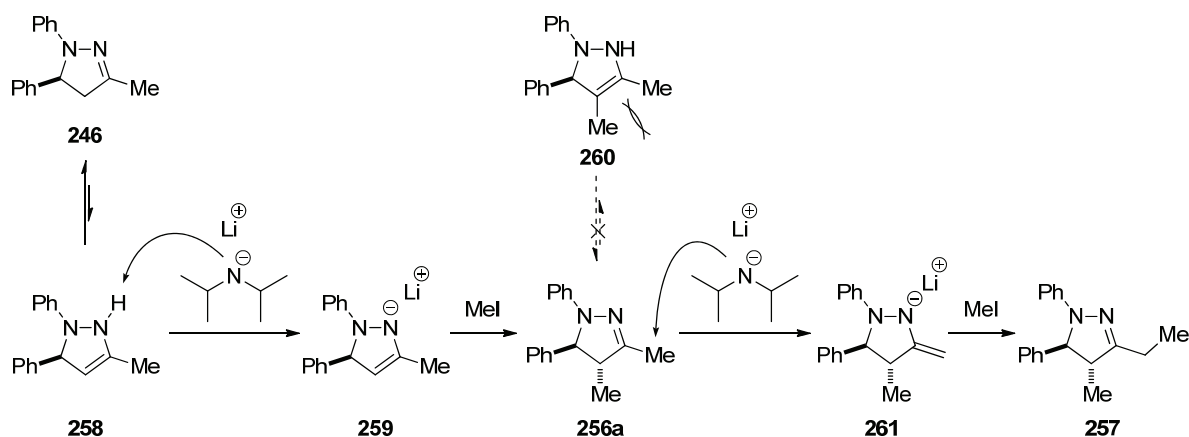
derivatization reactions, especially the high diastereoselectivities usually observed, are an attractive feature of this compound class in general.^[162] Strikingly though, to the best of our knowledge, no diastereoselective derivatizations of the 3-methyl-1,5-diarylpyrazolines obtained herein had been reported in the literature prior to our work. This fact, and the new opportunity to obtain these pyrazolines in optically active form, triggered our interest in possible further transformations. In particular, the substructure of a masked 1,3-diamine and the presence of five potentially acidic protons, which allows modifications of the pyrazoline core as well as the side chain in the 3-position, prompted us to investigate the follow-up chemistry of our products more closely.

While diastereoselective alkylations of 1,3,5-triarylpyrazolines had been reported to proceed in the 4-position of the heterocycle for obvious reasons,^[162d] the deprotonation of our substrates could be expected to occur at the 3-methyl group under kinetic conditions. Accordingly, a racemic sample of pyrazoline **246** was treated with lithium diisopropylamide at -78 °C followed by the addition of iodomethane. Surprisingly it turned out that rather than the 3-methyl group, the C4-methylene unit inside the pyrazoline ring had been alkylated under these conditions. The 4-methylated product **256a** was obtained as a single diastereoisomer (according to ¹H NMR analysis). After NMR-based structure elucidation and comparison with literature data,^[163] the new product was assigned as *trans*-3,4-dimethyl-1,5-diphenylpyrazoline (**256a**). The only moderate yield of the new product **256a** of 59% could be attributed to the formation of another compound under the reaction conditions. This by-product differed from pyrazoline **256a** by the presence of an additional methylene group and was isolated in 27% yield. It was identified as pyrazoline **257**, resulting from the double methylation of the substrate **246**. It is noteworthy that heterocycle **257** was also obtained as a single diastereoisomer (Scheme 88).



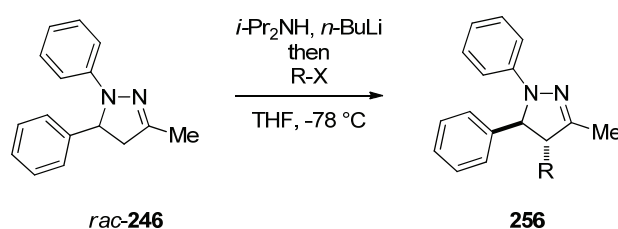
Scheme 88. Methylation products of 2-pyrazoline **246**.

This unexpected regioselectivity in the alkylation of pyrazoline **246** can be explained by the equilibrium between the 2-pyrazoline **246** and its tautomeric 3-pyrazoline **258** (Scheme 89). Although the 2-pyrazoline **246** is thermodynamically favoured, it seems as if the *NH*-proton of the 3-pyrazoline **258** is deprotonated, shifting the equilibrium to the lithiated compound **259**. Subsequently, the alkylating agent approaches the nucleophile from the sterically less congested face to afford the 4,5-*trans*-product **256a**. In the presence of remaining base, the alkylated 2-pyrazoline **256a** is again deprotonated. Since the formation of the corresponding tautomer **260** is now disfavoured due to a high allylic strain, the second deprotonation occurs on the methyl group in the 3-position and subsequent reaction of the deprotonated species **261** with another molecule of alkylating agent provides the observed by-product **257** (Scheme 89).



Scheme 89. Possible explanation for the regio- and diastereoselectivity observed in the alkylation of pyrazoline **246**.

By adjusting the stoichiometry of reagents, we were able to produce the 4-methylated 2-pyrazoline **256a** in 66% yield (Table 25, entry 1). Furthermore, substrate **246** was found to be readily alkylated by a variety of other alkylating agents. The products **256a-e** were obtained in satisfactory yields with perfect diastereocontrol (Table 25). The scope of alkylating agents includes primary alkyl halides, allyl halides, benzyl halides, chloromethoxymethylether, and even secondary alkyl halides, although in this case the product **256e** was obtained with a reduced yield of 43% (Table 25, entry 5).

Table 25. Diastereoselective C4-alkylations of pyrazoline **246**.^a

entry	product	R	X	yield ^b
1	256a	Me	I	66%
2	256b	allyl	Br	61%
3	256c	Bn	Br	60%
4	256d	CH ₂ OCH ₃	Cl	60%
5	256e	<i>i</i> -Pr	I	43%

^aThe reactions were run with pyrazoline **246** (0.423 mmol), LDA (1.7 equiv) and the corresponding alkylating agent (1.5 equiv) in THF (5 mL) at -78 °C. ^bIsolated yield.

The unambiguous proof of the *trans*-relationship between the substituents in the 4- and 5-position of the products was finally obtained from the X-ray crystal structure analysis of pyrazoline **256d** (Figure 15).

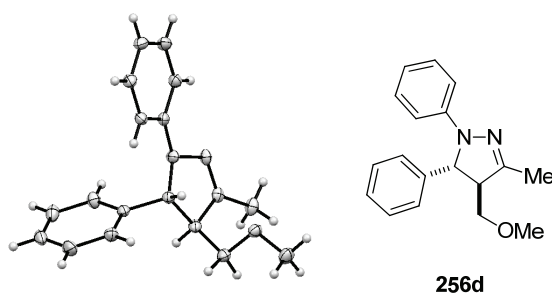
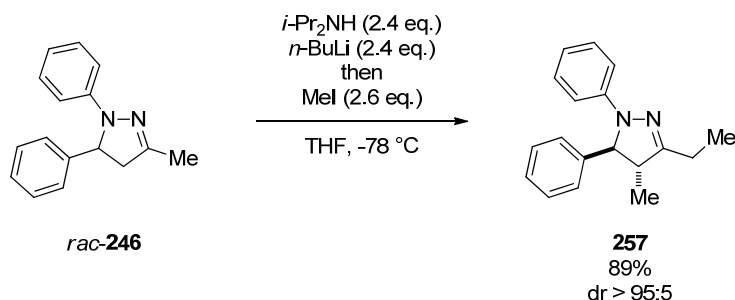


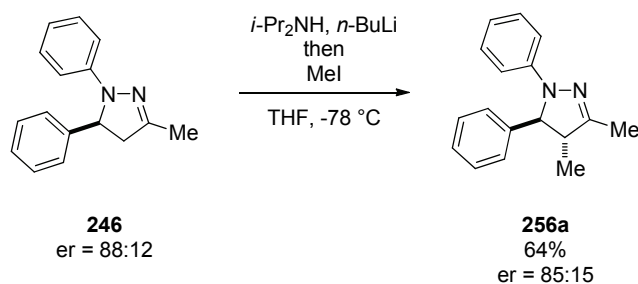
Figure 15. ORTEP plot of the X-ray crystal structure of pyrazoline **256d**. Ellipsoids are drawn at 50% probability level.

Since the only significant by-products of the alkylation reactions were the doubly alkylated products like **257**, the modification of the reaction conditions such that **257** could be obtained as the major product was a logical consequence. Indeed, when 2.4 equivalents of lithium diisopropylamide and an excess of methyl iodide were used, the two carbon-carbon bond-forming reactions, namely the diastereoselective methylation of the pyrazoline core and the sidechain homologization, were accomplished in one step. The desired product **257** was obtained in 89% yield, again as a single diastereoisomer (Scheme 90).



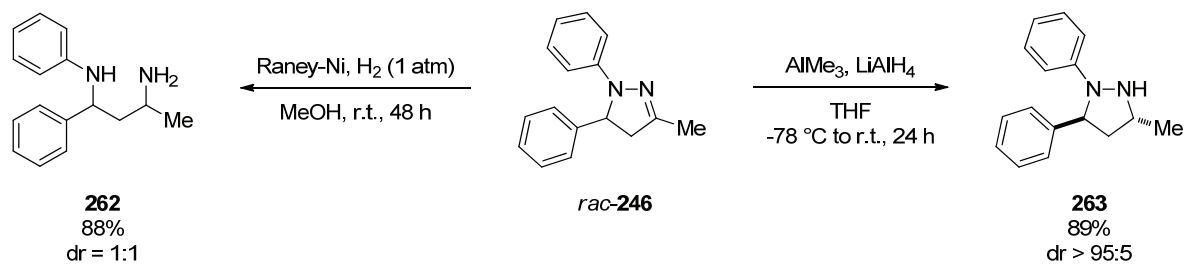
Scheme 90. One-pot diastereoselective C4-methylation and sidechain homologization of pyrazoline **246**.

Also an enantiomerically enriched sample of **246** was submitted to the methylation. Aware of the possibility that deprotonation of the pyrazoline at C4 could cause racemization by reversible intramolecular elimination, we were pleased to find that the enantiomeric ratio of **246** dropped only slightly and the desired product **256a** was obtained with 64% yield and with an enantiomeric ratio of 85:15 (Scheme 91).



Scheme 91. Diastereoselective C4-methylation of enantiomerically enriched 2-pyrazoline **246**.

Besides the alkylation of the 2-pyrazolines obtained with the Fischer synthesis, also the reduction of these compounds represented a desirable derivatization. A realization of such a reaction in a diastereoselective manner would give access to interesting 1,3-diamines or precursors thereof. Starting from 2-pyrazoline **246** it was found that the 1,3-diamine **262** can be easily accessed in a single step via reduction with Raney-Ni and hydrogen gas. Although this procedure provided the desired product **262** in a high yield of 88%, no diastereoselectivity was observed (Scheme 92). However, when 2-pyrazoline **246** was treated with lithium aluminium hydride in the presence of trimethyl aluminium, pyrazolidine **263** was obtained in 89% yield as a single diastereoisomer. Analysis of the NMR-spectra and comparison with literature data suggested the product to be the 3,5-*trans*-isomer **263**.^[164]



Scheme 92. Reduction of pyrazoline **246** with Raney-Ni and LiAlH₄.

Thus the enantioselective 6π electrocyclization of α,β -unsaturated hydrazones turned out to be a powerful tool to access optically active 2-pyrazolines. These compounds are not only interesting due to their pharmaceutical properties, but can further undergo highly diastereoselective transformations and as such serve as potentially useful synthetic building blocks.

4.3.6 Summary

A catalytic asymmetric version of the Fischer pyrazoline synthesis has been developed. Chiral Brønsted acids were shown to efficiently catalyze the cycloisomerization of α,β -unsaturated hydrazones to give pyrazolines in high yields and enantioselectivities. This procedure was expanded to a more general *in situ* protocol, which gives comparable yields and enantioselectivities while starting from simple enones and phenylhydrazine rather than from the preformed hydrazones. To the best of our knowledge, this reaction constitutes the first example of a catalytic asymmetric 6π electrocyclization.^[165,166] Based on the data obtained by monitoring the reaction by HPLC, as well as from crystal structure analyses, a mechanism for the reaction was proposed and alternative pathways were discussed. It was shown that the 2-pyrazolines obtained can undergo highly diastereoselective alkylation reactions with a broad variety of different alkylating reagents.^[167] Furthermore, the conversion of one of our products into a 1,3-diamine as well as a diastereoselective reduction to the corresponding fully saturated pyrazolidine has been demonstrated. These transformations allow both, the modification of the pyrazoline core and the side chain in the 3-position, and thus enable the creation of molecular diversity from readily available, optically active starting materials.

4.4 Kinetic Resolution of Homoaldols via a SPINOL-Derived Phosphoric Acid

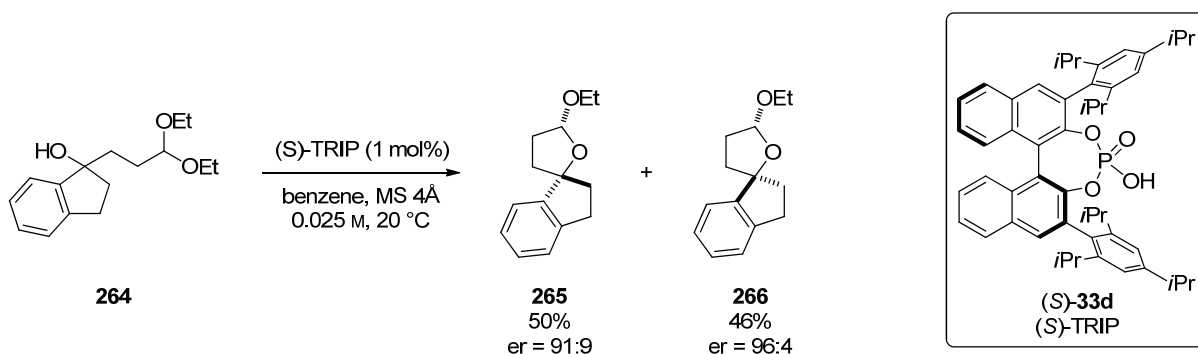
Catalyzed Asymmetric Intramolecular Transacetalization

Some of the results reported in this section were obtained in collaborative effort with I. Čorić.

Allowing for the enantioselective construction of *O,O*-acetal stereocenters, the chiral Brønsted acid-catalyzed intramolecular transacetalization discovered by our group is of high academic importance.^[122] On the other hand, the synthetic utility of the obtained products is rather limited due to a lack of methods for their stereoselective derivatization. However, an interesting feature of this transformation is the fact that the substrates are acetal protected γ -hydroxycarbonyl compounds, so called homoaldols. In comparison to lactoethers derived from achiral alcohols, chiral homoaldols are highly versatile synthetic building blocks, which are difficult to obtain by means of asymmetric catalysis. Therefore the development of a kinetic resolution of acetal protected homoaldols using the transacetalization strategy was aimed for.

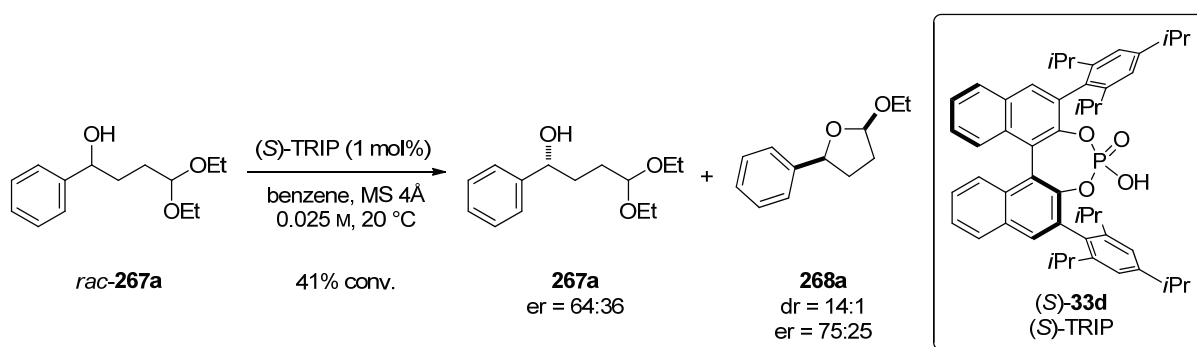
4.4.1 Optimization of Reaction Conditions

In the course of the studies on the catalytic asymmetric transacetalization one example of a chiral γ -hydroxy acetal was already explored as a substrate. Under the reported reaction conditions the tertiary alcohol **264** was found to undergo a parallel kinetic resolution and afforded the two diastereomeric lactoethers **265** and **266** in high yields and good enantiomeric ratios of 91:9 and 96:4, respectively (Scheme 93).^[122]



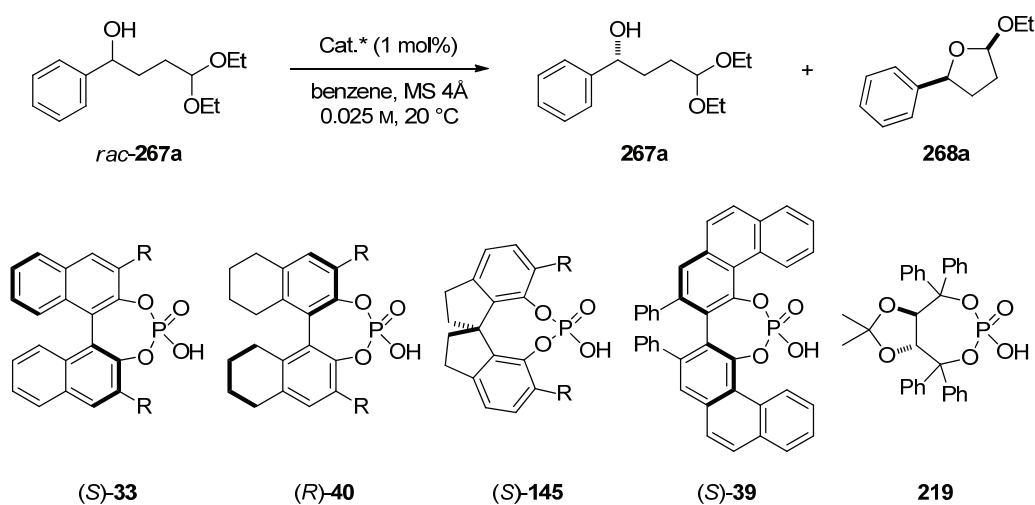
Scheme 93. TRIP-Catalyzed intramolecular transacetalization of tertiary homoaldol **264**.^[122]

However, the obtained enantioselectivities were not optimal and additionally the two products were inseparable, thus limiting the usefulness of the reaction as a resolution. In order to evaluate the potential of the described protocol to accomplish the kinetic resolution of other homoaldols, the secondary alcohol *rac*-**267a** was first submitted to identical reaction conditions. After 41% conversion the reaction was stopped and the mixture was analyzed. It was found that the product **268a** had formed as a 14:1 mixture with its diastereoisomer 5-*epi*-**268a** and the major isomer **268a** was obtained with a low enantiomeric ratio of 75:25. Accordingly also the enantiomeric ratio of the remaining starting material **267a** was also low (er = 64:36) (Scheme 94).



Scheme 94. TRIP-Catalyzed kinetic resolution of homoaldol *rac*-**267a**.

Even if these results suggested that a kinetic resolution of secondary homoaldols was generally possible by using the transacetalization strategy, a suitable catalyst for this transformation had to be identified to improve the efficiency of the process. When the 3,3'-substituents on the BINOL-backbone were changed to 9-anthracenyl groups, the obtained enantioselectivities dropped even further (*cf.* Table 26, entries 1 and 2). Neither the utilization of the 9-anthracenyl substituted H₈-BINOL catalyst (*R*)-**40e** nor by using the VAPOL- and TADDOL-derived phosphoric acids (*S*)-**39** and **219** were the results previously obtained with TRIP (**33d**) improved (Table 26, entries 3,5 and 6). However, when (*S*)-STRIP ((*S*)-**145g**), the SPINOL-derived analog of TRIP was tested as a catalyst, it was found that a remarkably good kinetic resolution had occurred. At a conversion of 51% the alcohol **267a** was found to have an enantiomeric ratio of 92:8 and at the same time the lactoether product **268a** was obtained with a good diastereomeric ratio of 21:1 and a high enantioselectivity of 95:5 er for the major diastereoisomer (Table 26, entry 4).

Table 26. Screening of different catalysts for the kinetic resolution of homoaldol *rac*-**267a**.^a

entry	Cat.*	conv. ^b	er (267a) ^b	er (268a) ^b	er (5- <i>epi</i> - 268a) ^b	dr ^b
1	(S)- 33d R = 2,4,6- <i>i</i> Pr ₃ -C ₆ H ₂	41%	64:36	75:25	93.5:6.5	14:1
2	(S)- 33f R = 9-anthracenyl	47%	58:42	61:39	83.5:16.5	17:1
3	(R)- 40e R = 9-anthracenyl	38%	44.5:55.5	38.5:61.5	21:79	17:1
4	(S)- 145g R = 2,4,6- <i>i</i> Pr ₃ -C ₆ H ₂	51%	8:92	5:95	<0.5:99.5	21:1
5	(S)- 39 -	41%	43:57	37.5:62.5	39:61	7:1
6	219 -	26%	51:49	55:45	66.5:33.5	7:1

^aThe reactions were run on a 0.025 mmol scale in benzene with MS 4Å (12.5 mg). ^bDetermined by HPLC analysis on a chiral stationary phase.

The relative configuration of the two diastereomeric products **268a** and 5-*epi*-**268a** was elucidated by nuclear Overhauser effect spectroscopy (NOESY) experiments. The major diastereoisomer was identified as the 2,5-*cis*-configured tetrahydrofuran **268a** as indicated by a strong NOE-signal between the CH₂-group of the ethoxy substituent and the *ortho*-protons of the phenyl group (Figure 16, left). In contrast, the minor diastereoisomer showed a characteristic NOE-signal between the acetal proton and the *ortho*-protons of the phenyl group and was thus assigned a 2,5-*trans* relationship (Figure 16, right).

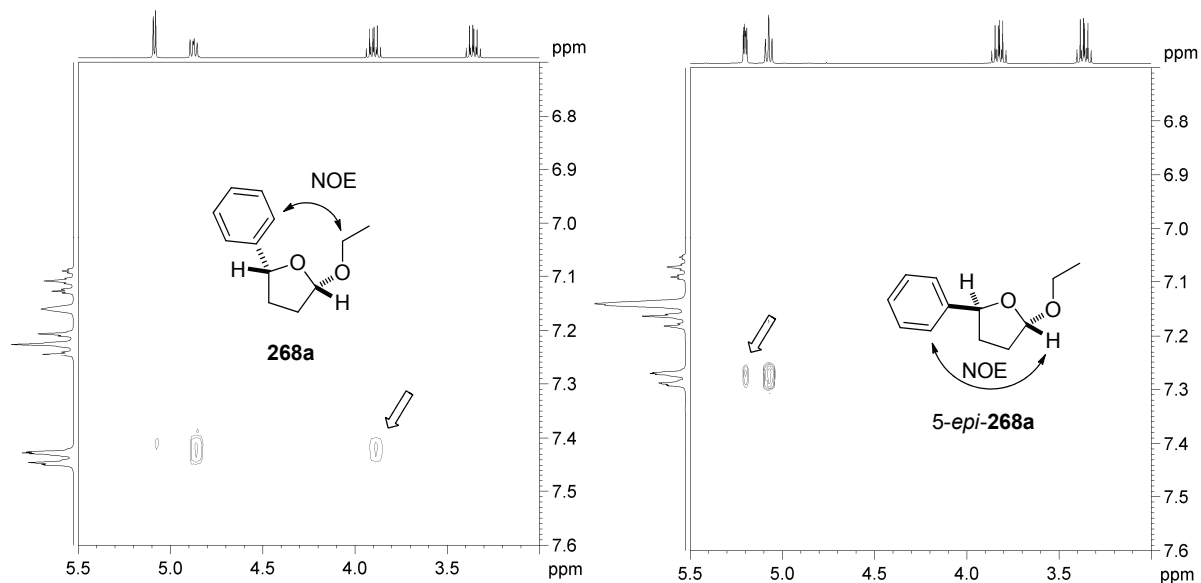
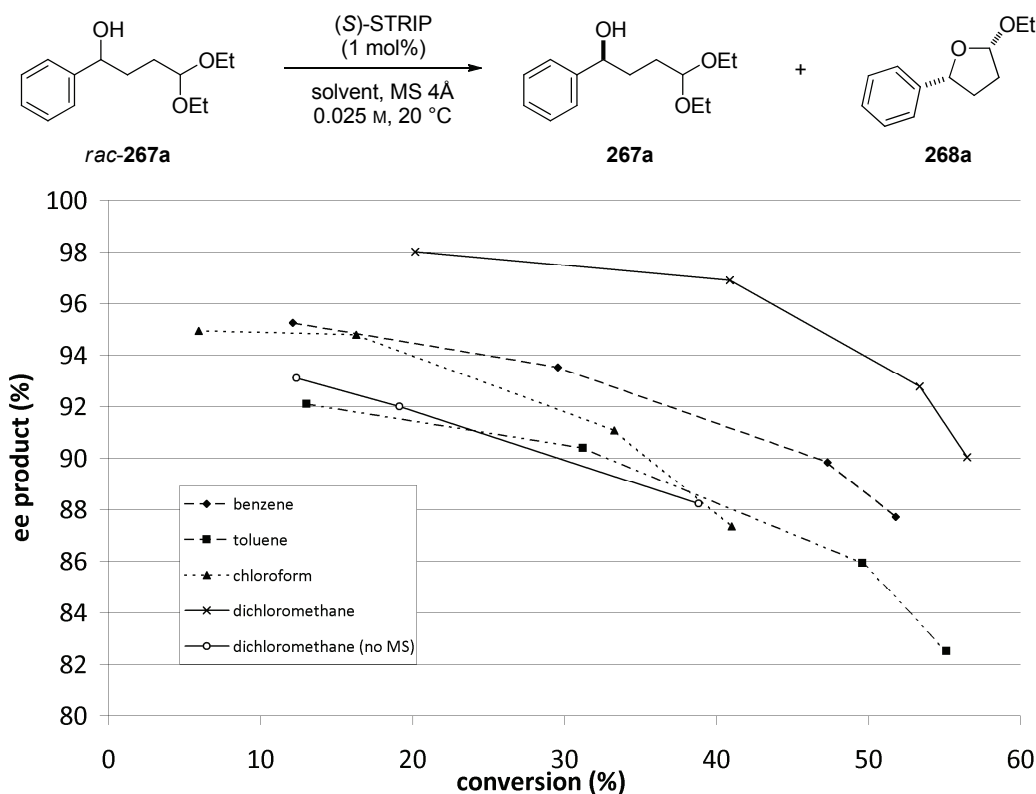


Figure 16. NOE Spectra of the two diastereomeric products **268a** and **5-epi-268a**.

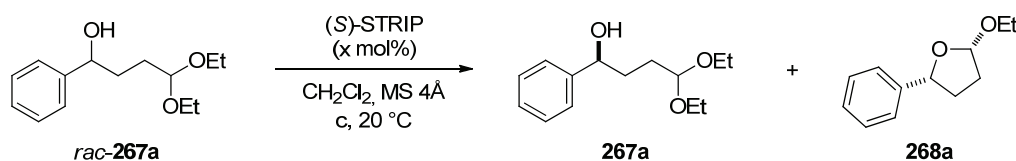
Having identified STRIP (**145g**) as a powerful catalyst for this transformation, the role of different solvents was investigated. Therefore the reaction was conducted at 20 °C in the presence of (*S*)-STRIP ((*S*)-**145g**, 1 mol%) and 4Å molecular sieves. To follow the progression of the reaction over time, samples were taken from the mixture after 2.5 h, 8 h, 20.3 h and 28.5 h and analyzed with respect to conversion and the enantiomeric ratio of the product **268a** (Scheme 95). In benzene and chloroform the enantiomeric ratio of the product **268a** at low conversion was around 97.5:2.5. The initial enantiomeric ratio of the product in chloroform diminished faster than in benzene with increasing conversion, whereas the overall reaction was faster in benzene. Reactivity-wise the aromatic solvents toluene and benzene were very similar, but the reaction in benzene was more enantioselective. By far the best result in terms of both, reaction rate and enantioselectivity was obtained when dichloromethane was used as the solvent. Also the influence of the molecular sieves becomes evident from Scheme 95. When the reaction was conducted in dichloromethane without molecular sieves the reaction became less enantioselective and slower (samples were taken after 3 h, 5.5 h and 18 h) than in the presence of this additive.



Scheme 95. Enantiomeric excess of lactoether **268a** with respect to conversion in different solvents with (S)-STRIP ((S)-**145g**) as catalyst.

With dichloromethane as the solvent of choice the influence of the catalyst loading was explored, speculating on the possibility of using less than 1 mol% of STRIP (**145g**). To ensure an acceptable reaction rate the concentration of the solution had to be increased when catalysts loadings below 1 mol% were used.

Table 27. Optimization of the catalyst loading.^a



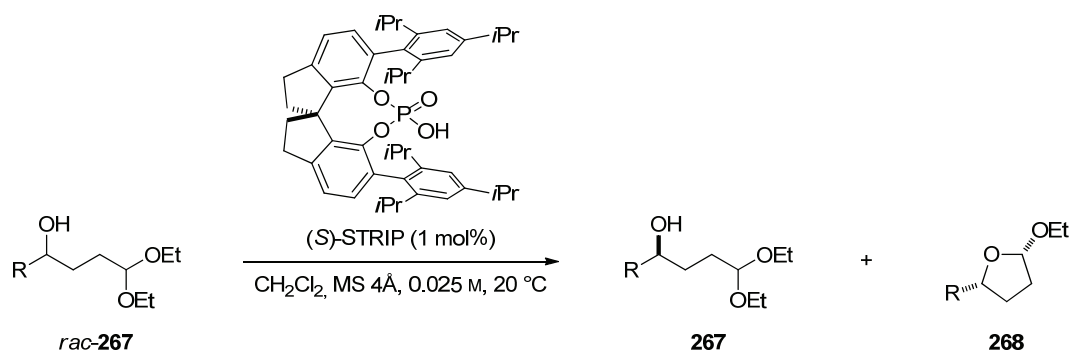
entry	(S)-STRIP (mol%)	c	t	conv. ^b	er (267a) ^b	er (268a) ^b	er (5- <i>epi</i> - 268a) ^b	dr ^b
1	1	0.025 M	20.3 h	53%	99:1	96.5:3.5	>99.5:0.5	16:1
2	0.5	0.1 M	19 h	55%	99:1	94:6	99.5:0.5	14:1
3	0.1	0.1 M	19 h	29%	68:32	94.5:5.5	87.5:12.5	36:1

^aThe reactions were conducted on a 0.050 mmol scale in CH₂Cl₂ with MS 4Å (25.0 mg). ^bDetermined by HPLC analysis on a chiral stationary phase.

Indeed the reaction turned out to also work well with 0.5 mol% of (*S*)-STRIP ((*S*)-**145g**), giving results only slightly inferior to those obtained when 1 mol% of the catalyst was used in a more dilute solution (cf. Table 27, entries 1 and 2). Even a catalyst loading of only 0.1 mol% was sufficient to provide the product **268a** with a good enantiomeric ratio of 94.5:5.5 at 29% conversion after 19 hours (Table 27, entry 3). Ultimately the scope of the kinetic resolution was explored with a catalyst loading of 1 mol%, given the slightly better results obtained in the optimization studies under these reaction conditions.

4.4.2 Resolution of Secondary Homoaldols

The exploration of various secondary homoaldols under the optimized reaction conditions revealed our resolution to be very general. Like the phenyl substituted homoaldol *rac*-**267a** (Table 28, entry 1), all homoaldols *rac*-**267b-f** with an aromatic group attached to the stereocenter were resolved very efficiently. Electron rich aromatics (Table 28, entry 2) were as well tolerated as electron deficient aromatic substituents (Table 28, entry 3). Also *meta*-substituted phenyl groups (Table 28, entry 4), polycyclic aromatic residues (Table 28, entry 5) and heterocycles (Table 28, entry 6) underwent the reaction smoothly. In all cases the cyclic acetal **268** as well as the starting alcohol **267** were obtained in high enantioselectivities at around 55% conversion. Usually the minor diastereoisomer of the product *5-epi*-**268** was separable from the major product **268** by simple column chromatography and was found to have the same configuration at the alcohol-derived stereocenter as the remaining starting material **267**. This means for example in the case of the heterocyclic substrate *rac*-**267f**, that the lactoether **268f** was obtained in a perfect theoretical yield of 50% with an enantiomeric ratio of 97.5:2.5. In a classical kinetic resolution this result corresponds to a selectivity factor of $s = 146$.^[168] A vinyl-substituent was also well tolerated (Table 28, entry 7). As expected from our previous screening results, a catalyst loading of 0.1 mol% was still sufficient to facilitate the kinetic resolution with high selectivities, albeit at a reduced rate as illustrated by substrate *rac*-**267g** (Table 28, entry 8). The results obtained with a bulky aliphatic residue were comparable to the previous examples (Table 28, entry 9).

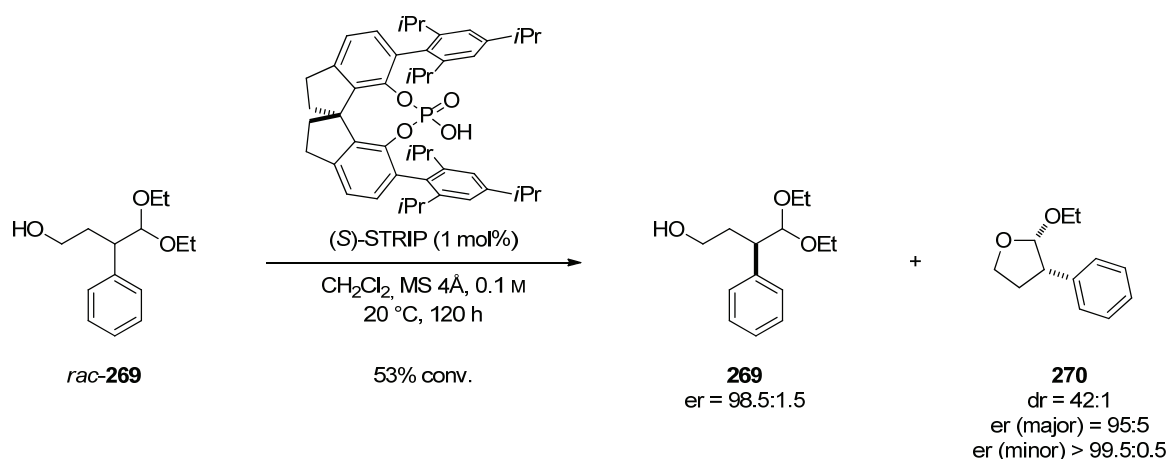
Table 28. STRIP-Catalyzed kinetic resolution of secondary homoaldols.^a

entry	product 268	t	conv. ^b	er (267) ^b	er (268) ^b	dr ^b
1	268a Ar = C ₆ H ₅	18 h	55%	98.5:1.5	97:3	13:1
2	268b Ar = 4-MeO-C ₆ H ₄	16 h	55%	98:2	97:3	12:1
3	268c Ar = 4-F-C ₆ H ₄	14 h	54%	97.5:2.5	96.5:3.5	13:1
4	268d Ar = 3,5-Me ₂ -C ₆ H ₃	16 h	52%	96:4	97:3	20:1
5	268e Ar = 2-naphthyl	16 h	54%	96.5:3.5	96.5:3.5	14:1
6	268f	14 h	53%	98.5:1.5	97.5:2.5	19:1
7	268g	14 h	56%	98:2	98:2	8:1
8 ^c	268g	70 h	56%	96.5:3.5	97:3	9:1
9	268h	4 h	55%	98:2	93.5:6.5	19:1
10	268i	10 h	68%	97:3	96.5:3.5	2.9:1
11 ^d	268j	1 h	54%	95:5	89:11	>50:1
12 ^d	268k	12 h	55%	96.5:3.5	89.5:10.5	44:1
13 ^d	268l	6 h	64%	97.5:2.5	85:15	8:1

^aReactions were performed on a 0.100 mmol scale with 4Å molecular sieves (50 mg). ^bDetermined by HPLC analysis on a chiral stationary phase. Only one enantiomer of the minor *trans* diastereomer could be detected, except for 5-*epi*-**268h** (er = 97:3), 5-*epi*-**268i** (er = 99.5:0.5), 5-*epi*-**268k** (er = 71:29), and 5-*epi*-**268l** (er = 83.5:16.5). ^cUsing 0.1 mol% of (S)-STRIP ((S)-**145g**) at a concentration of 0.1 M. ^dProduct diastereoisomers were not separable by column chromatography.

The reaction of linear-aliphatic-substituted homoaldol *rac*-**267i** illustrates a remarkable aspect of our reaction. The chiral catalyst (*S*)-**145g** is not only able to differentiate between the two enantiomers of the starting material, but also controls the configuration of the acetal stereocenter which is created in the transacetalization. Thus, even in cases where the enantiodifferentiation of the starting material is not very pronounced, the less reactive enantiomer is converted into the minor *trans*-diastereomer. This effect enabled us to obtain the major diastereomer of cyclic acetal **268i** with an enantiomeric ratio of 96.5:3.5 and again a perfect theoretical yield of 50% at 68% conversion (Table 28, entry 10). This result resembles the efficiency of a classic kinetic resolution operating at a selectivity factor of $s = 94$.^[168] Furthermore the STRIP-catalyzed kinetic resolution of homoaldols is also extendable to homoaldol substrates with a *cis*-double bond *rac*-**267j** (Table 28, entry 11) or an aromatic tether between the alcohol and the acetal moiety like in substrates *rac*-**267k** and *rac*-**267l** (Table 28, entries 12 and 13).

Remarkably our method also allowed the resolution of homoaldols with remote stereocenters. The primary alcohol *rac*-**269** was found to be less reactive than other previously used substrates and the reaction had to be run for 120 h at 0.1 molar concentration to achieve 53% conversion. However, the STRIP-catalyzed resolution provided lactoether **270** with 95:5 er as a 42:1 mixture with its diastereoisomer and the unreacted alcohol **269** with an enantiomeric ratio of 98.5:1.5 (Scheme 96).



Scheme 96. STRIP-catalyzed kinetic resolution of homoaldol *rac*-**269**.

Encouraged by the outstanding results the resolution provided for a variety of homoaldols, also the investigation of the analogous process for tertiary homoaldols was explored.

4.4.3 Resolution of Tertiary Homoaldols

While chemical resolutions of secondary alcohols are well studied,^[169] the related processes for tertiary alcohols still remain profoundly challenging. The methods developed for secondary alcohols are usually not easily extendable to resolutions of tertiary alcohols. Besides the limited number of biocatalytic processes,^[170,171] few nonenzymatic methods for the resolution of tertiary alcohols, including chiral reagents^[172] and catalytic methods with peptide-based catalysts^[173] and metal catalysts have been developed.^[174] Accordingly, we were extremely pleased to find that our method for the kinetic resolution of secondary homoaldols was very well applicable to the higher substituted analogs.

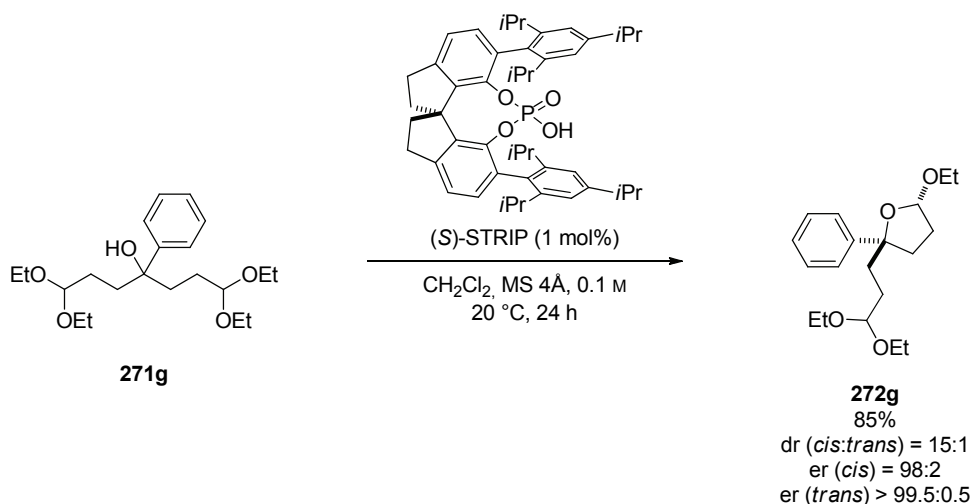
The resolution of homoaldol *rac*-**271a**, bearing a methyl-group and an aromatic substituent at the alcohol stereocenter proceeded as efficiently as with secondary homoaldols and both, cyclic acetal **272a** and acyclic acetal homoaldol **271a**, were obtained with excellent enantioselectivity (Table 29, entry 1). The outcome of the reaction is almost not affected with increasing size of the aliphatic substituent (Table 29, entry 2) resulting in a remarkable resolution of substrates with sterically similar substituents. Highly efficient enantiodifferentiation between aryl and bulky aliphatic groups (Table 29, entries 3-4) and even between aryl and benzyl groups (Table 29, entry 5) was observed, affording highly enantioenriched products with valuable quaternary stereocenters. Excellent results were also obtained with substrate *rac*-**271f** bearing only aliphatic substituents (Table 29, entry 6). In this case the product **272f** was obtained in a theoretical yield of 48% with an enantiomeric ratio of 99:1. This result is comparable with a classical kinetic resolution operating at a selectivity factor of $s > 300$.^[168]

Table 29. STRIP-Catalyzed kinetic resolution of tertiary homoaldols *rac*-**271**.^a

entry	product 272	t	conv. ^b	er (271) ^b	er (272) ^b	dr ^b
1	272a 	10 h	55%	96:4	98.5:1.5	9:1
2	272b 	12 h	55%	98.5:1.5	98.5:1.5	9:1
3	272c 	28 h	55%	92:8	97.5:2.5	7:1
4 ^c	272d 	24 h	57%	95:5	99:1	5:1
5 ^c	272e 	40 h	54%	97.5:2.5	99:1	11:1
6	272f 	3 h	51 %	96.5:3.5	99:1	18:1

^aReactions were performed on a 0.100 mmol scale with 4Å molecular sieves (50 mg). ^bDetermined by HPLC analysis on a chiral stationary phase. Only one enantiomer of the minor *trans* diastereomer could be detected, except for 5-*epi*-**272a** (er = 99.5:0.5), 5-*epi*-**272d** (er = 99.5:0.5), and 5-*epi*-**272f** (er = 96.5:3.5). ^cProduct diastereoisomers were not separable by column chromatography.

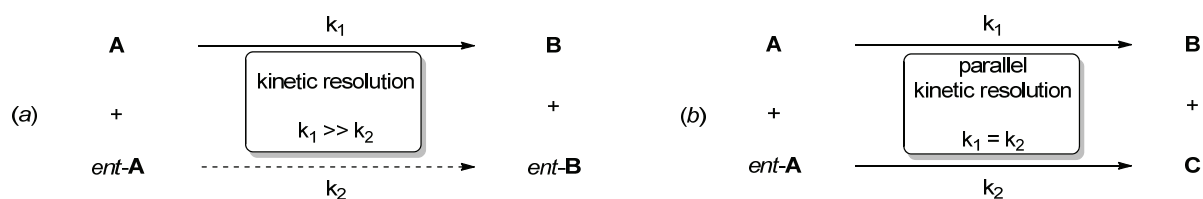
The exceptional enantioselectivity of this reaction was furthermore illustrated by a desymmetrization experiment. When a 0.1 M solution of achiral tertiary homoaldol **271g** in dichloromethane was submitted to otherwise identical reaction conditions, the desymmetrization product **272g** was obtained in 85% yield as a 15:1 mixture of diastereoisomers with an enantiomeric ratio of 98:2 for the major *cis*-isomer **272g** (Scheme 97).



Scheme 97. Desymmetrization of tertiary homoaldol **271g**.

4.4.4 Mechanistic Considerations

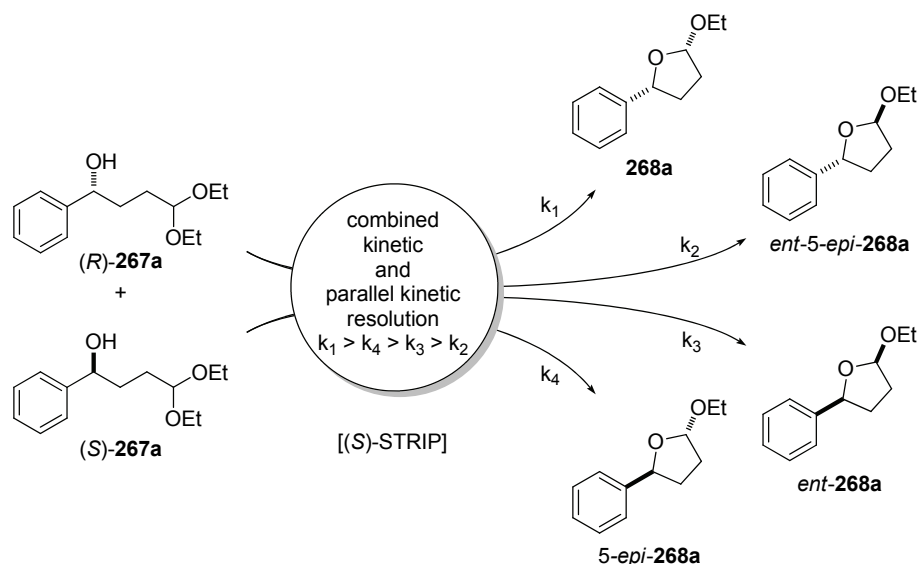
The high efficiency observed in the STRIP-catalyzed kinetic resolution of acetal protected homoaldols via intramolecular transacetalization is remarkable for a chemical resolution method. In almost all of the cases, both the lactoether product and the unreacted alcohol were obtained in high enantioselectivities in theoretical yields between 40-50%. The main feature of our reaction accounting for this highly efficient resolution is the presence of a combined kinetic and parallel kinetic resolution. In the ideal scenario of a classic catalytic kinetic resolution the reaction rates k_1 and k_2 of the two enantiomers of the racemic starting material *rac-A* are extremely different in the presence of a chiral catalyst. As a consequence, one enantiomer **A** undergoes the chemical reaction preferentially to form the product **B**, whereas the other enantiomer *ent-A* remains unreacted and *ent-B* is not formed (Scheme 98a). Thus a perfect kinetic resolution converts one enantiomer of the starting material to the enantiomerically pure product while the second enantiomer of the starting material remains unreacted and is also obtained as a single enantiomer at 50% conversion.



Scheme 98. Idealized schematic description of a kinetic resolution (a), and a parallel kinetic resolution (b).

In a catalyzed parallel kinetic resolution^[175] both enantiomers A and $ent-A$ of the starting material react with similar rates k_1 and k_2 but in the presence of a chiral catalyst two different products B and C are formed. The products B and C can be for instance regio- or diastereoisomers, but not enantiomers. Thus a perfect parallel kinetic resolution converts a racemic starting material $rac-A$ into two different products B and C , of which each is obtained in 50% yield as a single enantiomer (Scheme 98b).

In the STRIP-catalyzed kinetic resolution of homoaldols both of these two processes function in parallel (Scheme 99). The catalyst is able to distinguish between the two enantiomeric homoaldols (R)-**267a** and (S)-**267a** and preferentially activates one of them (k_1). Furthermore the catalyst provides high control over the configuration of the newly formed stereocenter, resulting in the formation of the desired lactoether **268a**.

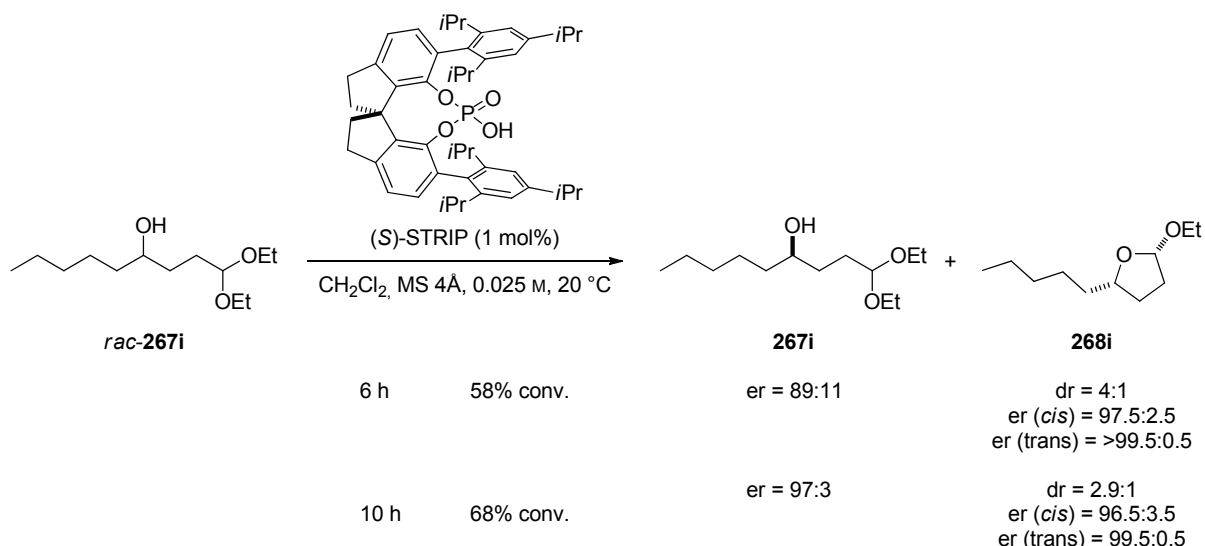


Scheme 99. Combination of a kinetic resolution and a parallel kinetic resolution in the (S)-STRIP-catalyzed kinetic resolution of homoaldol $rac-267a$.

Accordingly in cases where the enantiodifferentiation of the starting material is not very pronounced, the less reactive alcohol (S)-**267a** is preferentially converted into the

lactolether 5-*epi*-**268a** (k_4), the diastereomer of **268a**. Only in rare cases the less reactive enantiomer (*S*)-**267a** is converted into the enantiomer of the main product *ent*-**268a** (k_3), diminishing the enantioselectivity of the main product **268a**. Almost not observable is the formation of product *ent*-5-*epi*-**268a** (k_2), which is the enantiomer of the minor *trans*-diastereoisomer 5-*epi*-**268a** (Scheme 99).

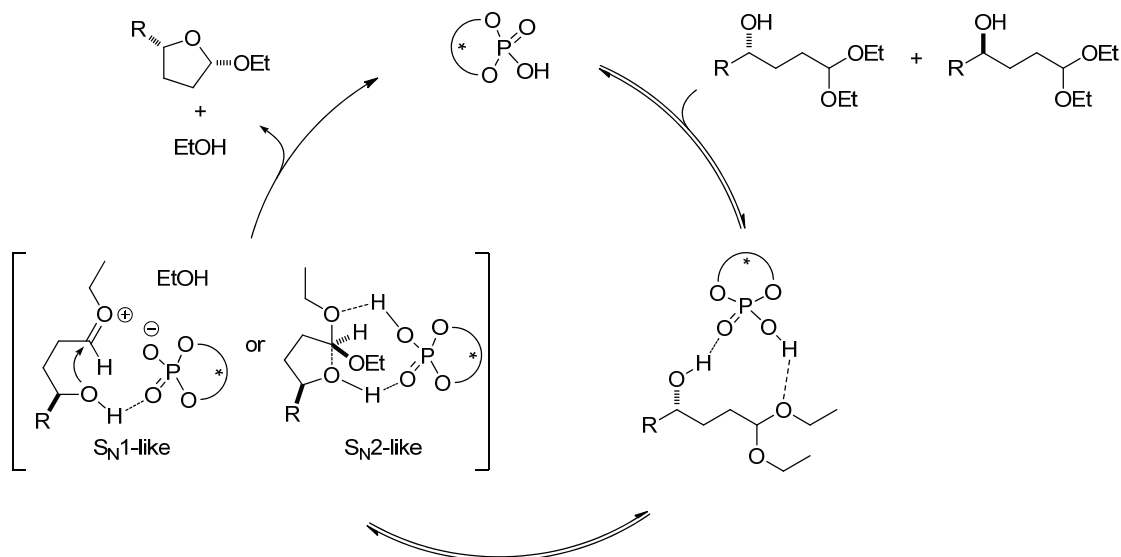
A good example to illustrate this cooperativeness of the two processes is the resolution of homoaldol *rac*-**267i** (Scheme 100). After 6 h reaction time 58% of the starting alcohol *rac*-**267i** is converted to the product **268i** with a diastereomeric ratio of 4:1. This result corresponds to a theoretical yield of 46% of the major diastereoisomer **268i** with a high enantiomeric ratio of 97.5:2.5. At the same time the unreacted starting material **267i** is obtained with only moderate enantioselectivity of 89:11 er. Since the chiral alcohol stereocenter is flanked by two very similar aliphatic chains, the differentiation of the two enantiomers by the catalyst is obviously only moderately efficient in this case. In a classic kinetic resolution an increased conversion would lead to an improved enantiomeric excess of the starting material at the expense of its chemical yield and the enantiomeric ratio of the product. Also in our reaction a higher conversion of 68% affords the remaining starting material **267i** with a high enantiomeric ratio of 97:3. Significantly though, the enantiomeric ratio of the major product diastereoisomer **268i** is almost not affected. Instead the diastereomeric ratio of the products decreased to 2.9:1. In this example, like for the vast majority of other substrates, the two diastereomeric products **268i** and 5-*epi*-**268i** were easily separable by column chromatography and the minor *trans*-diastereomer 5-*epi*-**268i** turned out to have the same absolute configuration at the alcohol-derived stereocenter as the remaining starting material **267i**. Thus the resolution of homoaldol *rac*-**267i** afforded the major product **268i** in a perfect theoretical yield of 50% with an enantiomeric ratio 96.5:3.5. The combined yield of remaining starting material **267i** and the minor *trans*-diastereomer 5-*epi*-**268i** accounts for the other 50% yield with an equally efficient resolution with respect to the alcohol stereocenter.



Scheme 100. Kinetic resolution of homoaldol *rac*-**267i** after different reaction times.

Only this synergistic combination of a kinetic resolution and a parallel kinetic resolution allows the reaction to proceed with a very high efficiency and enables the utilization of both, the unreacted starting material and the lactoether product in highly enantioenriched form for further transformations.

Although the transacetalization reaction itself is seemingly simple, different mechanistic scenarios are conceivable. A reasonable proposal involves the differentiation of the two enantiomers of the starting material by the chiral phosphoric acid by selective coordination to the substrate via a double hydrogen-bonding regime. Such a dual activation should increase the nucleophilicity of the alcohol oxygen atom and at the same enhance the electrophilicity of the acetal carbon atom. For the subsequent cyclization two mechanistic scenarios differing in the order of events appear plausible.^[122] In the S_N1 -like mechanism ethanol is liberated prior to the intramolecular attack of the alcohol function to the intermediary oxocarbenium ion. The catalyst substrate interaction in this case is best described as a hydrogen bond assisted ion pair. In contrast, a possible S_N2 -like mechanism involves the replacement of one acetal ethoxy group by the oxygen atom of the homoaldol in a Walden inversion.^[176] The stabilization of this concerted transition state may be best described as a hydrogen bonding interaction between the phosphoric acid and the substrate. After this ring closure the lactoether product is formed along with ethanol as the stoichiometric by-product and the active catalyst is regenerated.



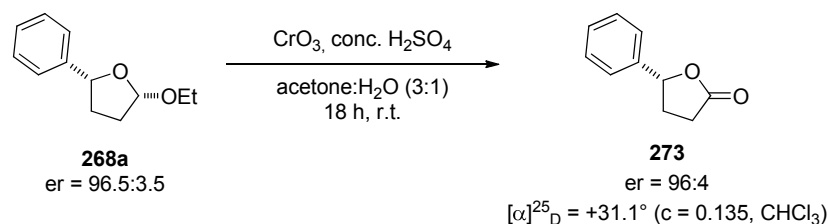
Scheme 101. Proposed catalytic cycle for the STRIP-catalyzed kinetic resolution of homoaldols.

While the S_N1 -type mechanism involves the formation of an energetically disfavoured oxocarbenium ion, the S_N2 -like mechanism appears to be questionable due to the required geometrical alignment of substrate and catalyst. Of course these two mechanistic scenarios are idealized descriptions and the true mechanism may comprise characteristics of both scenarios.

4.4.5 Applications of Resolved Homoaldols

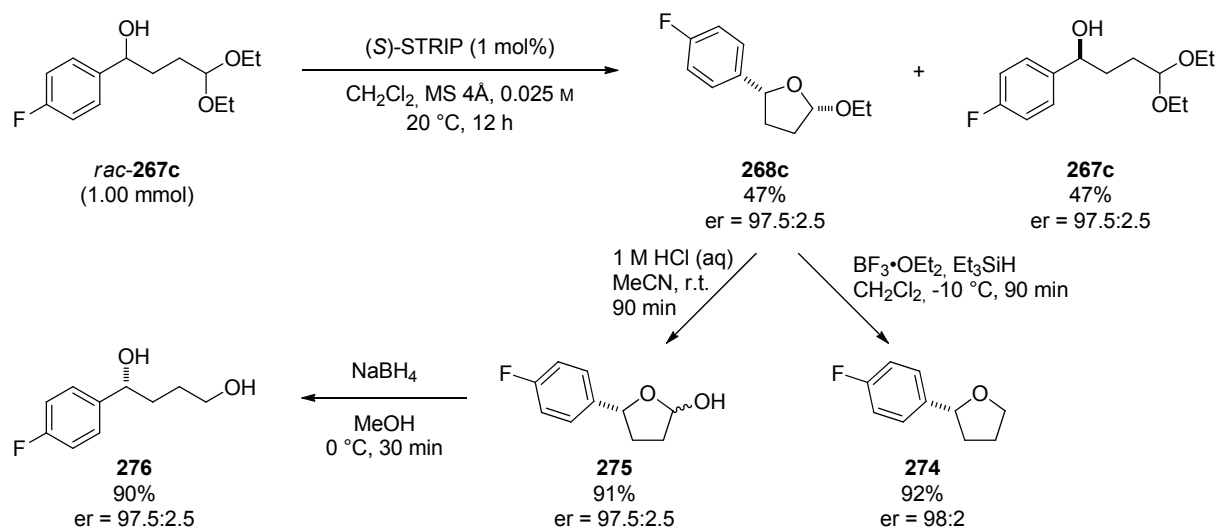
A drawback of the method described herein is a maximum theoretical yield of 50% of the desired enantiomer by virtue of it being a kinetic resolution. However, given the lack of general alternative methods to efficiently access enantiomerically enriched homoaldols and the immense synthetic importance of the products, the kinetic resolution via intramolecular transacetalization provides a powerful tool for obtaining highly enantiomerically enriched surrogates of γ -hydroxy aldehydes. To illustrate the potential of these structures to serve as valuable synthetic building blocks and to determine the absolute configuration of our products, some of the compounds obtained were derivatized. First a small sample of enantiomerically enriched cyclic acetal **268a** was submitted to a Jones oxidation. The reaction proceeded without compromising the initial enantioselectivity and comparison of

the optical rotation of the obtained γ -butyrolactone **273** with literature data^[177] revealed the product to have the *R* configuration (Scheme 102).



Scheme 102. Determination of the absolute configuration of lactoether **268a** by oxidation to the literature known γ -butyrolactone **273**.

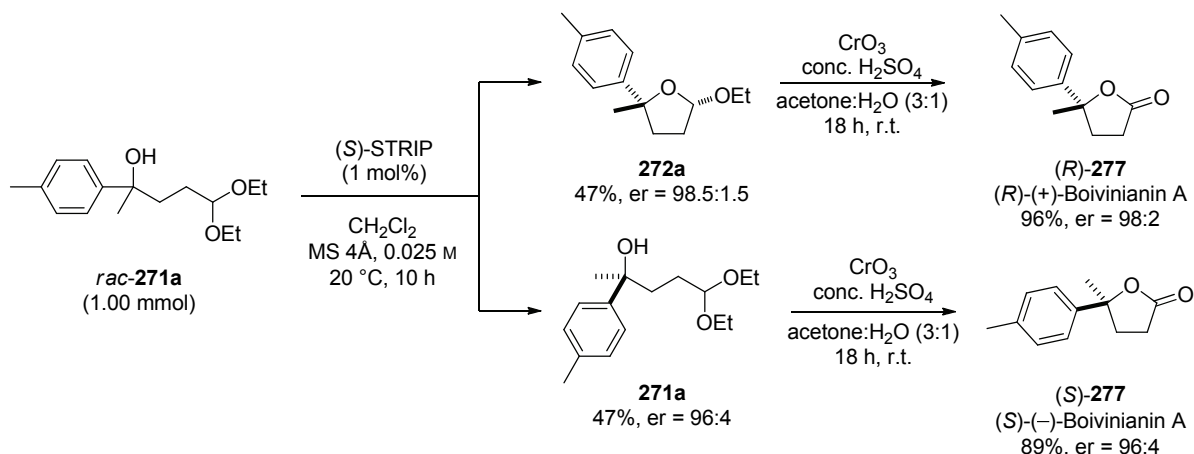
Furthermore the kinetic resolution of secondary alcohol *rac*-**267c** was conducted on a preparative 1.0 mmol scale. After 12 hours the cyclic acetal **268c** and the secondary alcohol **267c** were both obtained in 47% yield and with an enantiomeric ratio of 97.5:2.5. The lactoether **268c** was successfully reduced to the chiral tetrahydrofuran **274** in 92% yield and without erosion of enantioselectivity by using boron trifluoride and triethylsilane as the hydride source. Alternatively, the cyclic acetal **268c** can be hydrolyzed to give lactol **275**, which resembles the unprotected aldehyde homoaldol and thus is amenable to sodium borohydride reduction to afford the 1,4-diol **276** in high overall yield and unperturbed enantiomeric ratio (Scheme 103).



Scheme 103. Kinetic resolution of homoaldol *rac*-**267c** on a 1.00 mmol scale and derivatization of the cyclic acetal **268c** by reduction and substitution.

The resolution of tertiary alcohol *rac*-**271a** proceeded with comparable efficiency on a 1.0 mmol scale. The cyclic acetal **272a** and the tertiary alcohol **271a** were both obtained in 47% yield with enantioselectivities of 98.5:1.5 er and 96:4 er, respectively. Both homoaldols

272a and **271a** were converted into the γ -butyrolactone natural product Boivinianin A (**277**)^[178] in one step via simple Jones oxidation. In both cases the initial enantioselectivity of the quaternary stereocenter was entirely retained (Scheme 104). The absolute configuration of the lactones (*R*)-**277** and (*S*)-**277** was confirmed by comparison of the optical rotation with literature reported data.^[179]



Scheme 104. Enantioselective synthesis of both enantiomers of Boivinianin A **277**.

The demonstrated derivatizations represent only selected examples of a variety of known transformations including reductions,^[180] transacetalizations,^[181] eliminations to give dihydrofurans,^[182] substitutions,^[183] Friedel-Crafts reactions,^[184] acetal-ene reactions^[185] or oxidations.^[186] Regarding this rich chemistry of acetals, the transacetalization approach is not only a very general and reliable method for the kinetic resolution of homoaldols but at the same time provides extremely versatile synthetic building blocks with valuable stereocenters.

4.4.6 Summary

An efficient kinetic resolution of alcohols tethered to an acetal moiety, based on the previously reported catalytic asymmetric transacetalization reaction was developed by introducing the novel SPINOL-derived phosphoric acid STRIP (**145g**, 1 mol%) as a catalyst.^[122,187] This methodology is likewise well applicable to a wide range of secondary and tertiary alcohols. The racemic homoaldol substrates are easily accessible, mostly in one step from commercially available starting materials. The combination of a kinetic resolution

and a parallel kinetic resolution ensures that high enantioselectivities are obtained for the product and the unreacted starting material. It is noteworthy that this kinetic resolution represents a very atom-economic method which, unlike common alternative resolution methods, does not require any stoichiometric reagents and forms ethanol as the only by-product. The enantiomerically enriched product and unreacted starting material are conveniently acetal protected γ -hydroxy aldehydes. Accordingly they can be easily modified for example by oxidation, reduction or substitution. Along these lines the enantioenriched homoaldols were transformed into chiral tetrahydrofurans and 1,4-diols. Furthermore the method was applied to the enantioselective synthesis of both enantiomers of the γ -butyrolactone natural product Boivinianin A, bearing a quaternary stereocenter. Altogether this reaction resembles a practical, highly efficient, general, mild and atom economic method for the kinetic resolution of homoaldols and thus provides access to valuable synthetic intermediates.

4.5 Synthesis of Substrates

This section provides an overview of the methods used for the synthesis of the routinely employed substrates and is ordered according to the reaction in which the particular substrate was used.

4.5.1 Substrates for the Indolization of Cyclohexanone-derived Phenylhydrazones

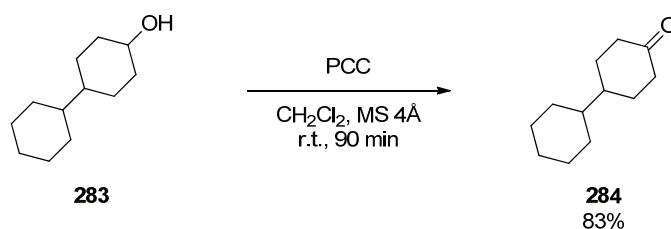
4.5.1.1 Synthesis of 4-Substituted Cyclohexanones

The synthesis of 4-aryl substituted cyclohexanones commenced with the addition of an aryl-Grignard reagent to commercially available 1,4-cyclohexanedione monoethyleneacetal (**278**). The resulting tertiary alcohols **279** were eliminated to the corresponding olefins **280** under acidic conditions using *para*-toluenesulfonic acid. After hydrogenation of the double bond with palladium on charcoal the desired 4-arylated cyclohexanones **282** were obtained after deprotection of acetal **281** with aqueous hydrochloric acid in refluxing THF (Table 30).

Table 30. Synthesis of 4-arylated cyclohexanones **282** from 1,4-cyclohexanedione monoethyleneacetal (**278**).

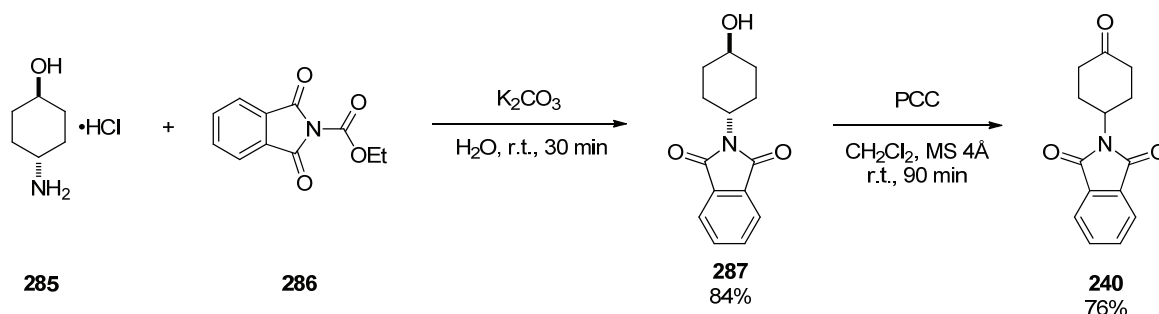
entry	Ar	X	279	yield	282	yield (from 279)
1	4-tBu-C ₆ H ₄	Br	279a	92%	282a	60%
2	4-MeO-C ₆ H ₄	Br	279b	90%	282b	71%
3	4-F-C ₆ H ₄	Br	279c	85%	282c	49%
4	3,5-Me ₂ -C ₆ H ₃	Br	279d	96%	282d	27%
5	3,5-(MeO) ₂ -C ₆ H ₃	Br	279e	88%	282e	60%
6	3-Cl-C ₆ H ₄	Cl	279f	87%	282f	26%
7	2-naphthyl	Br	279g	90%	282g	71%

The synthesis of 4-cyclohexyl cyclohexanone (**284**) was achieved from commercially available 4-cyclohexyl cyclohexanol (**283**) by a PCC-mediated oxidation in 83% yield (Scheme 105).



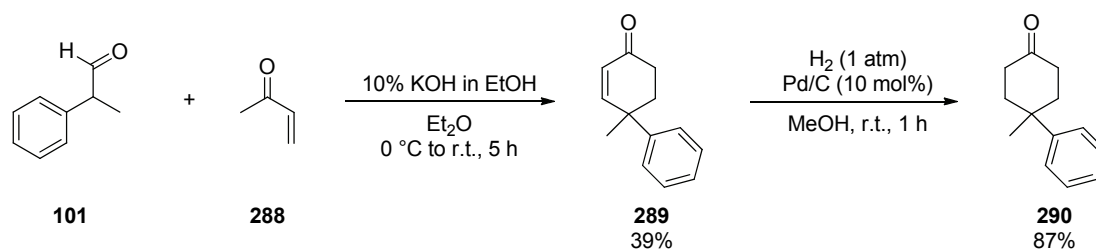
Scheme 105. Oxidation of 4-cyclohexyl cyclohexanol (**283**).

For the synthesis of *N*-phthalimido-4-aminocyclohexanone (**240**) a literature reported procedure was followed.^[188] Accordingly *trans*-aminocyclohexanol **285** was treated with *N*-carbethoxyphthalimide (**286**) in aqueous potassium carbonate solution to afford the cyclohexanol **287** in 84% yield. Subsequent oxidation using PCC provided 76% of cyclohexanone **240** (Scheme 106).



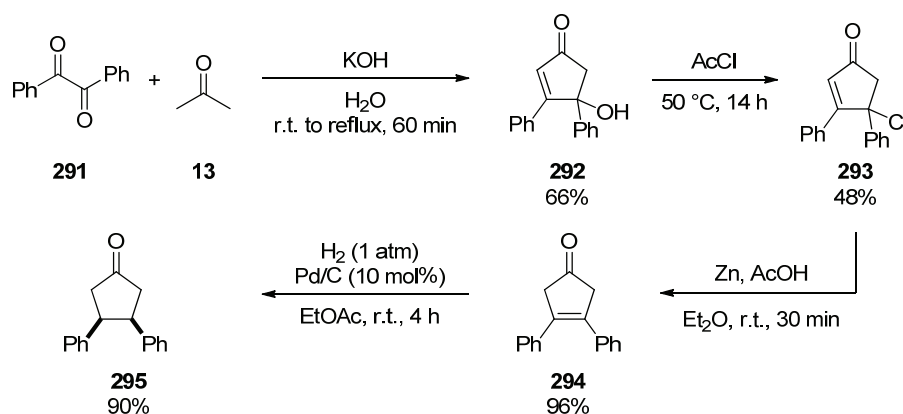
Scheme 106. Synthesis of *N*-phthalimido-4-aminocyclohexanone (**240**) from *trans*-4-aminocyclohexanol (**285**).

4-Methyl-4-phenylcyclohexanone **290** was obtained from hydratropic aldehyde (**101**) and methyl vinyl ketone (**288**) in a potassium hydroxide-mediated Michael-addition aldol-condensation cascade as reported by Zimmerman *et al.*,^[189] followed by subsequent hydrogenation of enone **289** over palladium on charcoal (Scheme 107).



Scheme 107. Synthesis of 4-methyl-4-phenylcyclohexanone **290**.

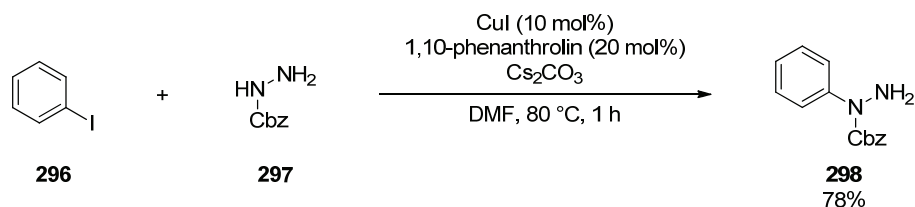
The synthesis of cyclopentanone **295** started with a literature reported potassium hydroxide-mediated aldol condensation-intramolecular aldol addition reaction of benzil (**291**) and acetone (**13**).^[190] The tertiary alcohol **292** was converted to the olefin **294** in a two step protocol by treatment with acetyl chloride and subsequent zinc-mediated chloride elimination as reported by Corey and Uda.^[191] Finally the cyclopentanone **295** was obtained by hydrogenation using hydrogen and palladium on charcoal (Scheme 108).



Scheme 108. Synthesis of *meso*-cyclopentanone **295**.

4.5.1.2 Synthesis of *N*-Substituted *N*-Arylhydrazines

The synthesis of *N*-carbobenzyloxy substituted phenylhydrazine **298** was accomplished by using a copper-catalyzed cross coupling between iodobenzene (**296**) and carbamate **297** as reported by Cho *et al.*^[192] and the desired product **298** was obtained in 78% yield (Scheme 109).

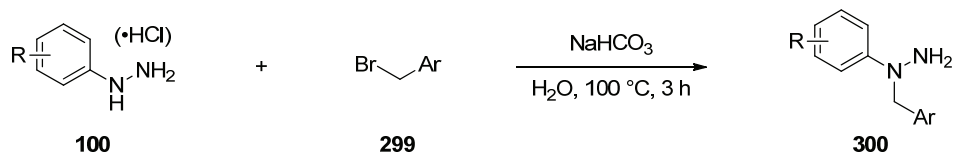


Scheme 109. Copper-catalyzed coupling between iodobenzene **296** and carbamate **297**.

The benzyl protection of arylhydrazines was accomplished by using a modification of the procedure reported by Perni and Gribble.^[193] An equimolar mixture of the corresponding arylhydrazine or its hydrochloride salt and benzyl bromide were heated to 100 °C in the presence of aqueous sodium bicarbonate (Table 31). Although this method also provided

significant amounts of the undesired regioisomeric N'-benzylated N-arylhydrazine, it was selected as the method of choice given its operational simplicity compared to alternative methods.^[194] The N-benzylated arylhydrazines were obtained in 34-73% yield.

Table 31. N-Benylation of arylhydrazines **100**.



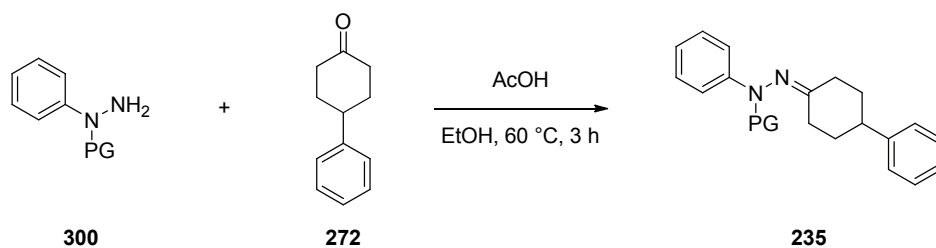
entry	hydrazine 100	R	bromide 299	Ar	product 300	yield
1	100a	H	299a	C ₆ H ₅	300a	53%
2	100a	H	299b	2-naphthyl	300b	44%
3	100a	H	299c	2-Me-C ₆ H ₄	300c	58%
4	100a	H	299d	3,5-Me ₂ -C ₆ H ₃	300d	43%
5	100a	H	299e	3,5-(MeO) ₂ -C ₆ H ₃	300e	61%
6	100a	H	299f	3,5-(CF ₃) ₂ -C ₆ H ₃	300f	73%
7	100a	H	299g	3,5-F ₂ -C ₆ H ₃	300g	62%
8	100a	H	299h	4-Me-C ₆ H ₄	300h	44%
9	100a	H	299i	4- <i>t</i> Bu-C ₆ H ₄	300i	54%
10	100a	H	299j	4-Ph-C ₆ H ₄	300j	50%
11	100a	H	299k	4-F-C ₆ H ₄	300k	57%
12	100a	H	299l	4-Br-C ₆ H ₄	300l	65%
13	100a	H	299m	4-I-C ₆ H ₄	239	61%
14	100b	4-Me	299m	4-I-C ₆ H ₄	300m	62%
15	100c	3,5-Me ₂	299m	4-I-C ₆ H ₄	300n	65%
16	100d	3-Me	299m	4-I-C ₆ H ₄	300o	49%
17	100e	4-OMe	299m	4-I-C ₆ H ₄	300p	44%
18	100f	4-Br	299m	4-I-C ₆ H ₄	300q	34%

4.5.1.3 Synthesis of Arylhydrazones

All arylhydrazones were synthesized by mixing equimolar amounts of the appropriate arylhydrazine and the corresponding ketone in the presence of catalytic amounts of acetic acid in hot ethanol. For the studies concerning the influence of the protecting group, the

corresponding *N*-protected-*N*-phenylhydrazines were condensed with 4-phenylcyclohexanone (**272**) to afford the desired hydrazones **235** (Table 32). While the unprotected hydrazone **231** turned out to be rather unstable and was accordingly only obtained in a low 12% yield (Table 32, entry 1), all protected derivatives were stable compounds and could be isolated in high yields (Table 32, entry 2-16).

Table 32. Synthesis of *N*-protected-*N*-phenylhydrazones of 4-phenylcyclohexanone (**227**).

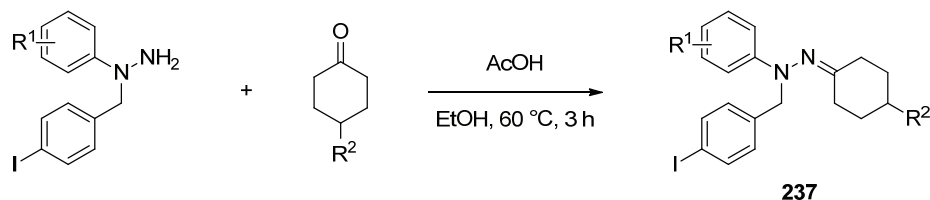


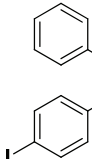
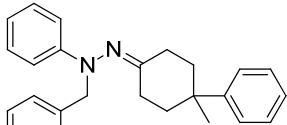
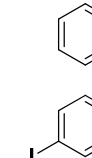
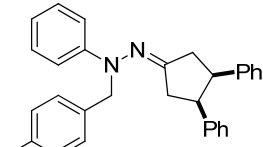
entry	product	PG	yield
1	231	H	12%
2	235a	Cbz	88%
3	233	C ₆ H ₅ -CH ₂	86%
4	235b	(C ₆ H ₅) ₂ CH	72%
5	235c	2-naphthyl-CH ₂	90%
6	235d	2-Me-C ₆ H ₄ -CH ₂	92%
7	235e	3,5-Me ₂ -C ₆ H ₃ -CH ₂	99%
8	235f	3,5-(MeO) ₂ -C ₆ H ₃ -CH ₂	95%
9	235g	3,5-(CF ₃) ₂ -C ₆ H ₃ -CH ₂	91%
10	235h	3,5-F ₂ -C ₆ H ₃ -CH ₂	80%
11	235i	4-Me-C ₆ H ₄ -CH ₂	80%
12	235j	4- <i>t</i> Bu-C ₆ H ₄ -CH ₂	64%
13	235k	4-Ph-C ₆ H ₄ -CH ₂	92%
14	235l	4-F-C ₆ H ₄ -CH ₂	64%
15	235m	4-Br-C ₆ H ₄ -CH ₂	93%
16	235n	4-I-C ₆ H ₄ -CH ₂	85%

In analogous manner the 4-iodobenzyl substituted arylhydrazones for the evaluation of the substrate scope were accessed by condensation of the corresponding *N*-4-iodobenzyl-*N*-arylhydrazines and the appropriate ketone. Most of the products directly precipitated from the reaction mixture and thus were obtained by simple filtration in a chromatography

free synthesis. This beneficial crystallinic property can at least to some extent be attributed to the 4-iodobenzyl protecting group.

Table 33. Synthesis of *N*-4-iodobenzyl-*N*-arylhydrazones of different ketones.

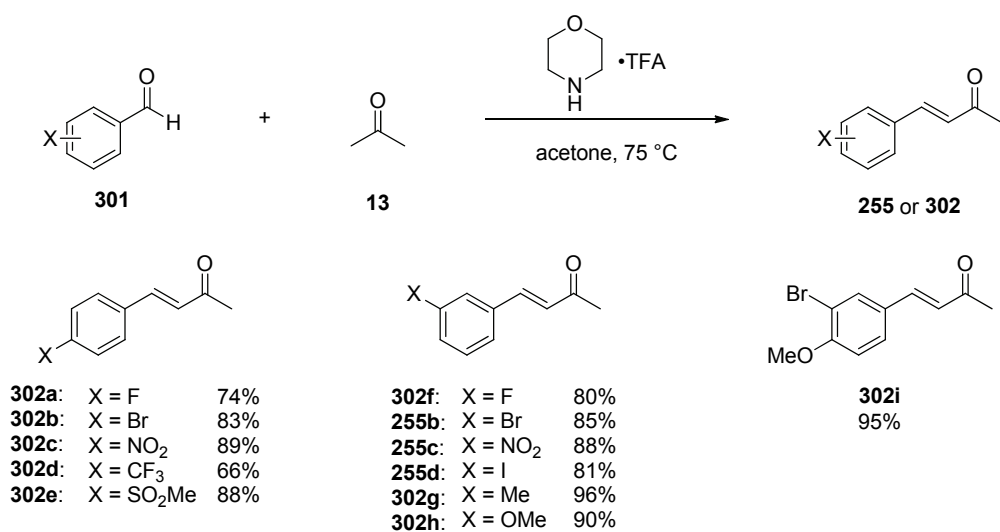


entry	product 237	R ¹	R ²	yield
1	237a	4-Me	C ₆ H ₄	83%
2	237b	4-MeO	C ₆ H ₄	72%
3	237c	4-Br	C ₆ H ₄	64%
4	237d	3,5-Me ₂	C ₆ H ₄	44%
5	237e	3-Me	C ₆ H ₄	49%
6	237f	3-Me	2-naphthyl	82%
7	237g	H	4- <i>t</i> Bu-C ₆ H ₄	83%
8	237h	H	4-MeO-C ₆ H ₄	60%
9	237i	H	4-F-C ₆ H ₄	81%
10	237j	H	3,5-Me ₂ -C ₆ H ₃	42%
11	237k	H	3,5-(MeO) ₂ -C ₆ H ₃	81%
12	237l	H	3-Cl-C ₆ H ₄	75%
13	237m	H	2-naphthyl	76%
14	237n	H	Me	34%
15	237o	H	cyclohexyl	28%
16	237p	H	<i>t</i> -Bu	49%
17	237q	H	OBz	54%
18	237r	H	NPhthal	79%
19	237s			84%
20	237t			79%

4.5.2 Substrates for the Catalytic Asymmetric 6π Electrocyclization

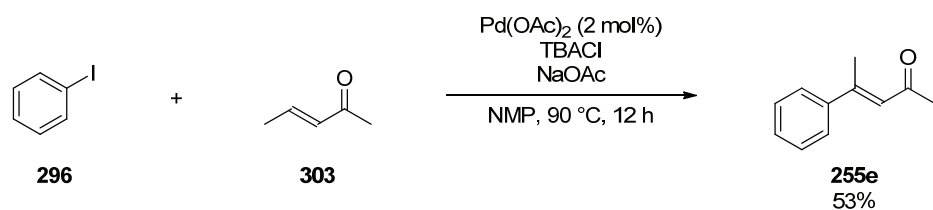
4.5.2.1 Synthesis of α,β -Unsaturated Ketones

Most of the α,β -unsaturated ketones required for the synthesis of the starting hydrazones as well as for the direct synthesis of enantiomerically enriched 2-pyrazolines were accessed by using a morpholinium trifluoroacetate-catalyzed aldol condensation of benzaldehydes **301** with acetone (**13**),^[195] unless they were commercially available. Especially for the mono-aldol condensation of acetone with different aldehydes on a laboratory scale this method has proven to be superior over commonly used hydroxide base-mediated reactions, since undesired side reactions can largely be avoided with this catalyst system. Accordingly, the enones were obtained in moderate to high yields by using this procedure (Scheme 110).



Scheme 110. Morpholinium trifluoroacetate-catalyzed aldol condensation of acetone (**13**) with benzaldehydes **301**.

For the synthesis of the β,β -disubstituted ketone **255e** a Heck coupling between iodobenzene (**296**) and 3-penten-2-one (**303**) was employed. Following a procedure originally developed for Heck reactions of crotonaldehyde,^[196] the starting materials were reacted in the presence of palladium acetate, tetrabutylammonium chloride (TBACl) and sodium acetate in *N*-methyl-2-pyrrolidone (NMP) to give the desired enone **255e** in 53% yield.

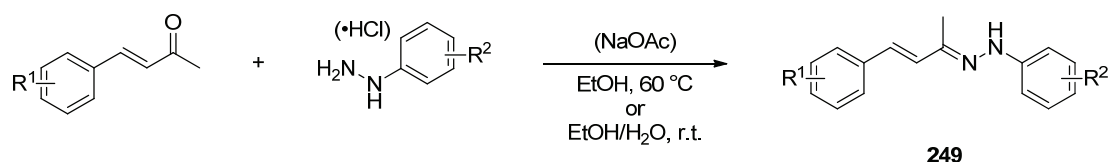


Scheme 111. Heck coupling of iodobenzene (**296**) and 3-penten-2-one (**303**).

4.5.2.2 Synthesis of α,β -Unsaturated Arylhydrazones

The condensation of arylhydrazines and α,β -unsaturated ketones was accomplished by mixing equimolar amounts of the starting materials in ethanol (Table 34).^[197]

Table 34. Condensation of enones and arylhydrazines.



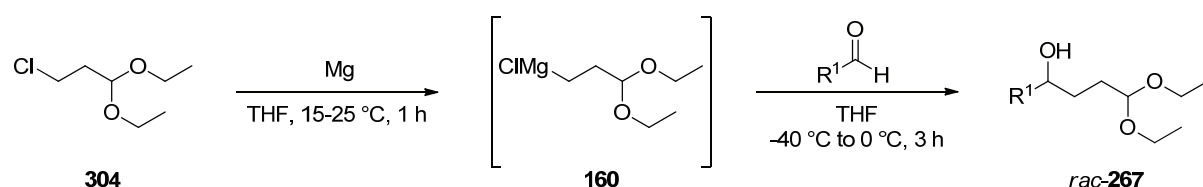
entry	product	R ¹	R ²	yield
1	247	H	H	82%
2	249a	4-F	H	74%
3	249b	4-Cl	H	63%
4	249c	4-Br	H	52%
5	249d	4-NO ₂	H	38%
6	249e	4-CF ₃	H	63%
7	249f	3-F	H	37%
8	249g	3-Cl	H	61%
9	249h	3-Br	H	41%
10	249i	3-NO ₂	H	28%
11	249j	3-Me	H	39%
12	249k	3-MeO	H	24%
13	249l	3,4-(OCH ₂ O)	H	68%
14	249m	3-Br, 4-MeO	H	81%
15	249n	H	4-F	21%
16	249o	3-Br	4-MeO	52%
17	249p	4-SO ₂ Me	4-F	51%

In cases where arylhydrazine hydrochlorides were used, the reaction was conducted in an ethanol-water mixture in the presence of sodium acetate to avoid acidic conditions and prevent pyrazoline formation (Table 34). Since most of the products were unstable towards purification by column chromatography, purification had to be accomplished by crystallization. Thus a low yield does not necessarily reflect a sluggish reaction but can be attributed to the high solubility of the product leading to a decreased isolated yield.

4.5.3 Synthesis of Racemic Acetal Protected Aldehyde Homoaldols

A striking feature of the STRIP-catalyzed kinetic resolution of homoaldols is the efficient and straightforward preparation of the racemic substrates. Most of the acetals which were submitted to the kinetic resolution were accessed in a single step from commercially available starting materials by addition of an organometallic reagent to the corresponding carbonyl compound. Along these lines the addition of the Grignard reagent **160** derived from alkyl chloride **304** to various aldehydes provided the racemic homoaldols *rac*-**267** in generally high yields (Table 35).^[122,198]

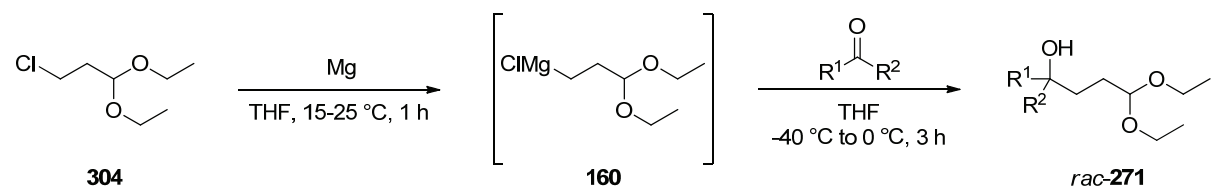
Table 35. Synthesis of racemic secondary homoaldols *rac*-**267** by addition of Grignard reagent **160** to different aldehydes.



entry	product	R ¹	R ²	yield
1	<i>rac</i> - 267a	C ₆ H ₅	H	92%
2	<i>rac</i> - 267b	4-MeO-C ₆ H ₄	H	95%
3	<i>rac</i> - 267c	4-F-C ₆ H ₄	H	90%
4	<i>rac</i> - 267d	3,5-Me ₂ -C ₆ H ₃	H	97%
5	<i>rac</i> - 267e	2-naphthyl	H	94%
6	<i>rac</i> - 267f	2-thiophenyl	H	97%
7	<i>rac</i> - 267g	<i>E</i> -C ₆ H ₄ -CH=CH	H	81%
8	<i>rac</i> - 267h	<i>t</i> -Bu	H	77%
9	<i>rac</i> - 267i	<i>n</i> -C ₅ H ₁₁	H	80%

In analogous manner, the tertiary homoaldols *rac*-**271** were synthesized by addition of the Grignard reagent **160** to various ketones (Table 36).^[122,198]

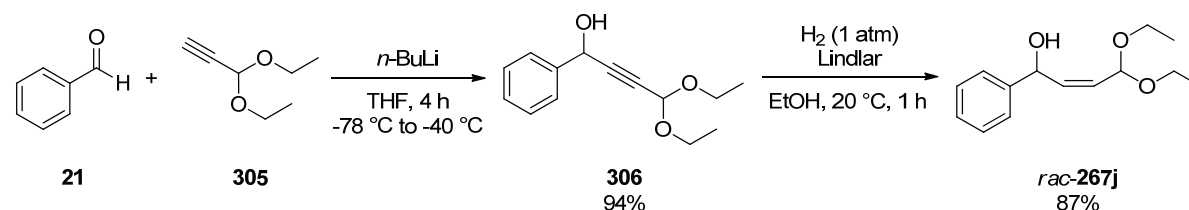
Table 36. Synthesis of racemic tertiary homoaldols *rac*-**271** by addition of Grignard reagent **160** to different ketones.



entry	product	R ¹	R ²	yield
1	<i>rac</i> - 271a	4-Me-C ₆ H ₄	Me	82%
2	<i>rac</i> - 271b	C ₆ H ₅	Et	97%
3	<i>rac</i> - 271c	C ₆ H ₅	<i>i</i> -Pr	96%
4	<i>rac</i> - 271d	C ₆ H ₅	(Me) ₂ CHCH ₂	95%
5	<i>rac</i> - 271e	C ₆ H ₅	C ₆ H ₅ CH ₂	68%
6	<i>rac</i> - 271f	<i>t</i> -Bu	Me	65%
7 ^a	<i>rac</i> - 271g	C ₆ H ₅	(EtO) ₂ CH(CH ₂) ₂	96%

^aThe Grignard reagent was added to benzoic acid methyl ester.

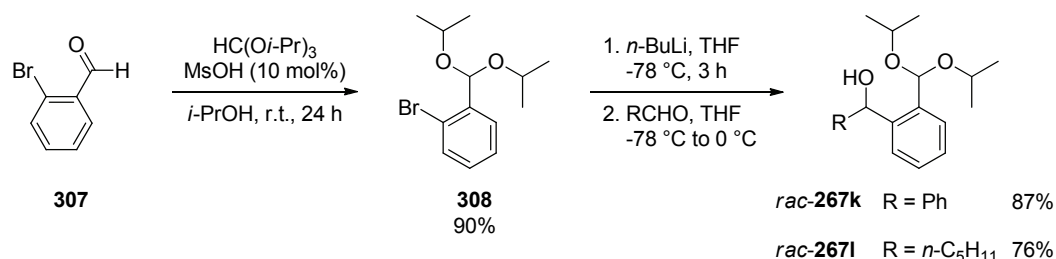
The synthesis of racemic homoaldol *rac*-**267j** bearing a *Z*-configured double bond tether commenced with the addition of an alkynyl lithium reagent derived from acetal **305** to benzaldehyde (**21**). The resulting alcohol **306** was partially hydrogenated over a Lindlar catalyst under standard reaction conditions to afford the homoaldol *rac*-**267j** in 82% overall yield (Scheme 112).



Scheme 112. Synthesis of allylic homoaldol *rac*-**267j** through benzaldehyde alkynylation and partial triple bond reduction.

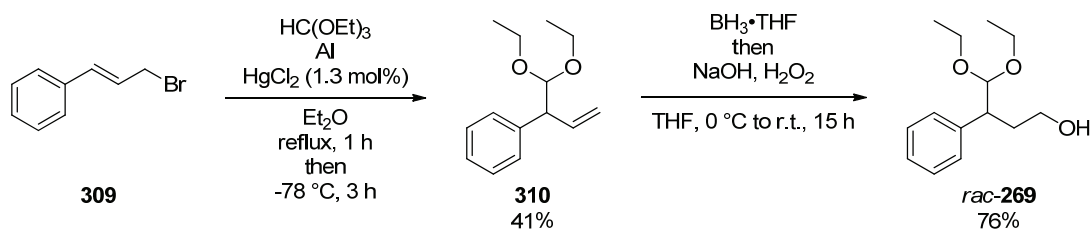
The construction of benzene-tethered homoaldols was also accomplished in two steps. First 2-bromobenzaldehyde (**307**) was converted into the diisopropyl acetal **308** by treatment with triisopropylorthoformate in the presence of methanesulfonic acid.

Subsequent halogen-lithium exchange and trapping of the organometallic species with the corresponding aldehydes provided the homoaldols *rac*-**267k** and *rac*-**267l** (Scheme 113).



Scheme 113. Synthesis of benzene-tethered homoaldols *rac*-**267k** and *rac*-**267l**.

Whereas all homoaldols so far were obtained by the addition of an acetal-containing organometallic reagent to a carbonyl compound, the synthesis of the primary alcohol *rac*-**269** was achieved differently. First cinnamyl bromide (**309**) was converted to the aluminium organic compound by aluminium halogen exchange. Subsequent treatment with triethylorthoformate resulted in the benzylic alkylation, caused by an allylic rearrangement, to give acetal **310** in 41% yield.^[199] After hydroboration with the borane-tetrahydrofuran adduct and oxidative workup with basic hydrogen peroxide solution the desired alcohol *rac*-**269** was obtained in 76% yield (Scheme 114).



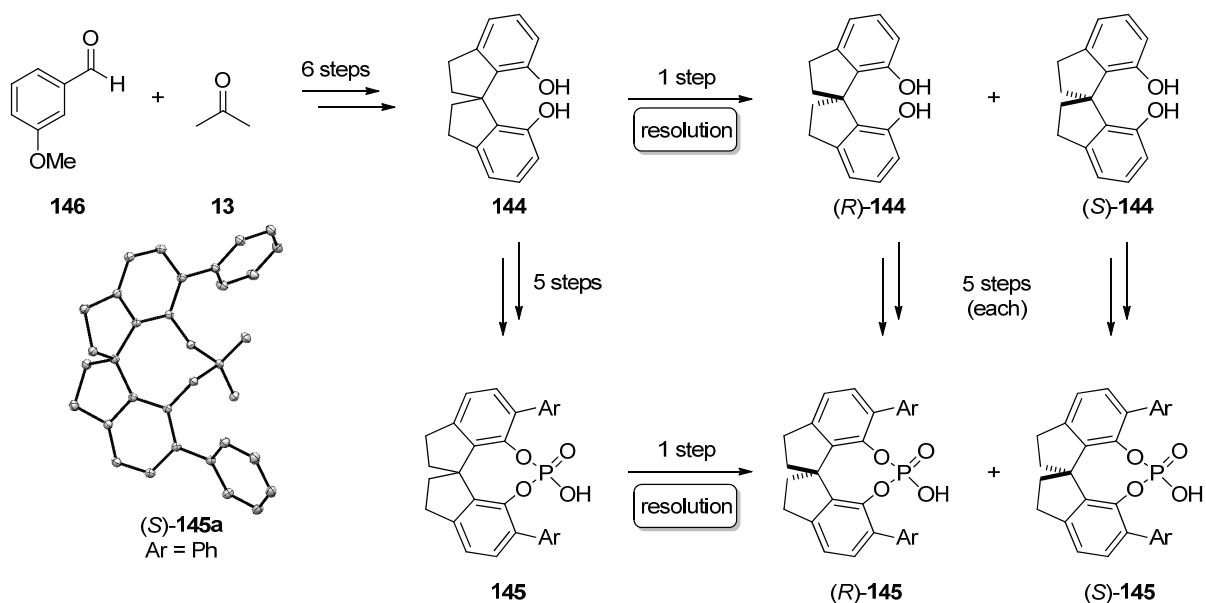
Scheme 114. Synthesis of primary alcohol *rac*-**269** from cinnamyl bromide (**309**).

5 Summary

The development of catalytic asymmetric versions of important and frequently utilized classic transformations in organic chemistry is one of the major challenges towards the establishment of asymmetric catalysis as the tool of choice for accessing enantiomerically pure compounds. Dedicated to this endeavor, our group is constantly aiming for classics in organic synthesis of which catalytic asymmetric protocols are elusive.

The work described in the previous chapters was dedicated to the development of SPINOL-derived phosphoric acids as complementary tools for asymmetric Brønsted acid catalysis and the application of chiral Brønsted acids in the development of the first catalytic asymmetric Fischer indolization, an unprecedented catalytic asymmetric 6π electrocyclozation and the kinetic resolution of homoaldols. All these transformations had not been achieved by means of asymmetric catalysis previously and the ultimate goal was the development of general and efficient protocols for these reactions, enabling access to valuable chiral products and synthetic intermediates.

The structural similarity of the commonly utilized BINOL- and H₈-BINOL-derived phosphoric acids on one side, and a lack of tunability of alternatives such as VAPOL hydrogenphosphate on the other side prompted us to develop new catalysts. For this purpose, the C₂-symmetric SPINOL (**144**) was considered to be a suitable platform since SPINOL-derived catalysts should provide a geometrically different environment while still exhibiting the possibility of structural diversification by introducing different substituents in the 6,6'-positions. The synthesis of a variety of chiral SPINOL-derived phosphoric acids **145** was achieved in 12 steps, starting from 3-methoxybenzaldehyde (**146**) and acetone (**13**). The two viable routes developed include a racemic synthesis of the catalysts followed by enantiomer separation by chiral HPLC, and alternatively the chemical resolution of SPINOL (**144**) and completion of the synthesis from the enantiomerically pure intermediate (Scheme 115).

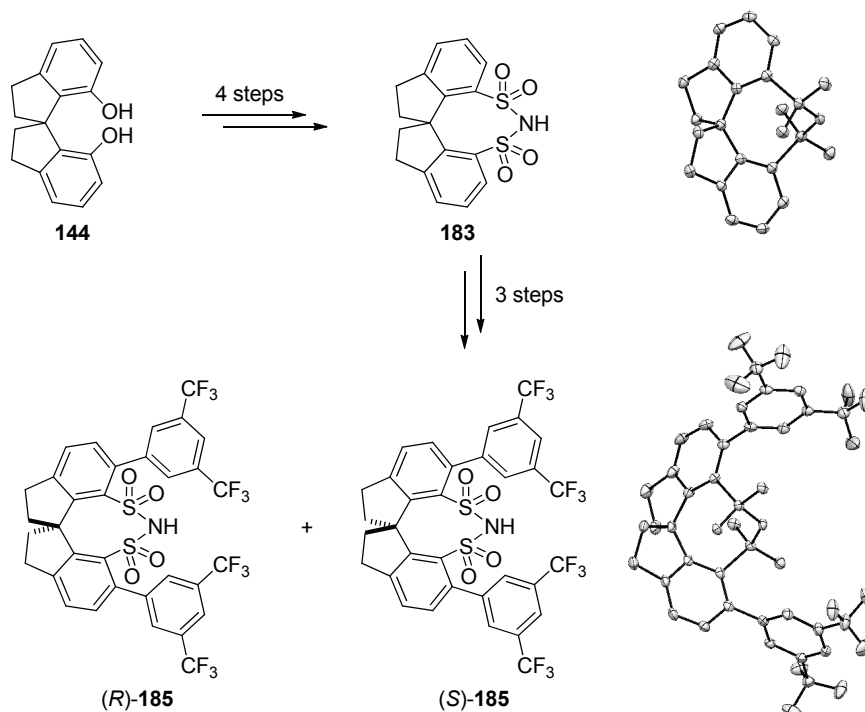


Scheme 115. Synthesis of SPINOL-derived phosphoric acids (**145**) and X-ray structure of one representative example (ORTEP plot, ellipsoids are shown at 50% probability level).

Altogether seven new chiral phosphoric acids were synthesized in this manner. A comparison of the structural properties of the new SPINOL-derived catalysts with commonly used BINOL phosphoric acids based on X-ray structure analysis revealed most importantly, that the spirocyclic hydrogenphosphates provide a more compact chiral environment than the axially chiral catalysts. In general, the phosphoric acid functionality in the SPINOL-derived catalysts is buried deeper in the chiral pocket created by the 6,6'-substituents. The applications of these catalysts reported herein underlined their complementary character for asymmetric Brønsted acid catalysis.

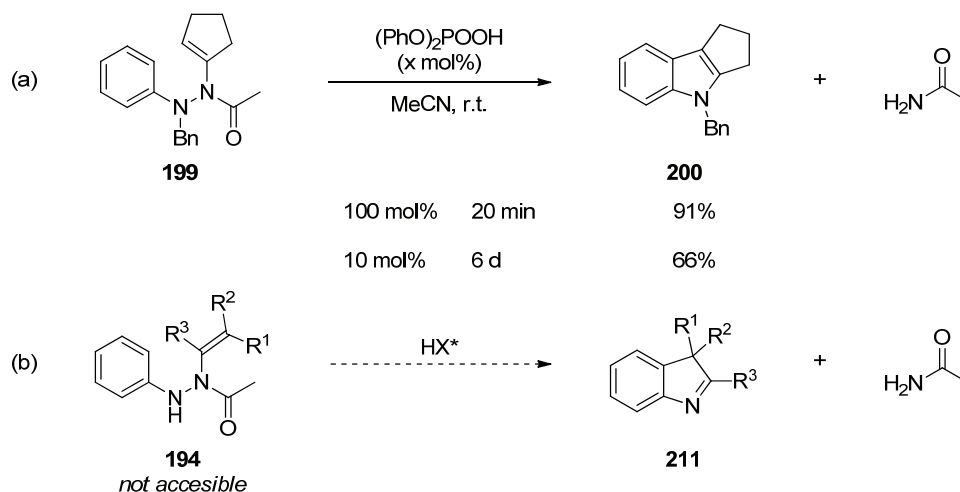
Furthermore, we enclosed a synthetic route to SPINOL-derived disulfonimides. Although disulfonimides in general showed only limited potential to act as efficient catalysts in any of the reactions studied in the course of this work, the encouraging results other co-workers in the group obtained with BINOL-derived disulfonimides prompted us to also seek access to the spirocyclic analogs thereof. The racemic disulfonimide **183** was obtained from SPINOL (**144**) in four steps and could be further converted to the 6,6'-disubstituted derivative **185**, which was obtained in optically pure form after enantiomer separation by HPLC in altogether 13 steps (Scheme 116). X-Ray crystallography allowed for a comparison of the structural properties of disulfonimide **185** with its BINOL-analog, again uncovering distinct differences between these two catalyst types. The performance of these new

catalysts was not investigated in the reactions described herein for reasons discussed above. However, the new disulfonimides were utilized by other group members with promising preliminary results.



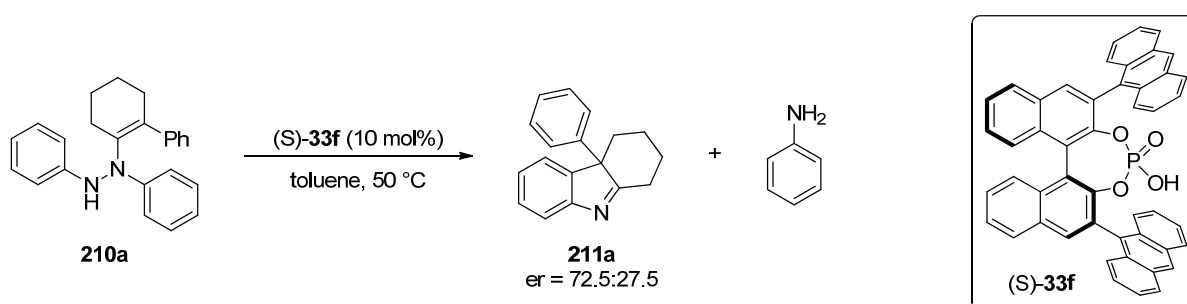
Scheme 116. Synthesis of SPINOL-derived disulfonimides and X-ray structure of representative examples (ORTEP plot, ellipsoids are shown at 50% probability level).

Our first application of enantioselective Brønsted acid catalysis occurred in the context of the development of the catalytic asymmetric Fischer indolization. Starting investigations addressed the indolization of phenylhydrazones derived from α -branched aldehydes. The generation of basic ammonia as stoichiometric by-product of the reaction, resulting in the poisoning of the acid catalyst by salt formation, was identified as the major problem associated with this process. Several possibilities to circumvent this inherent difficulty were explored. The use of *N*-acetyl enehydrazines as alternative substrates would result in the liberation of the much less basic acetamide as the by-product, and catalyst poisoning was assumed to be avoidable in this way. Indeed, the reaction of *N*-acetyl enehydrazine **199** was found to be amenable to Brønsted acid catalysis (Scheme 117a), but attempts to extend this reaction to substrates which give rise to chiral products **211** failed due to the difficulty of accessing the appropriate starting materials **194** (Scheme 117b).



Scheme 117. Attempted utilization of *N*-acetyl enehydrazines as substrates in the catalytic asymmetric Fischer indolization.

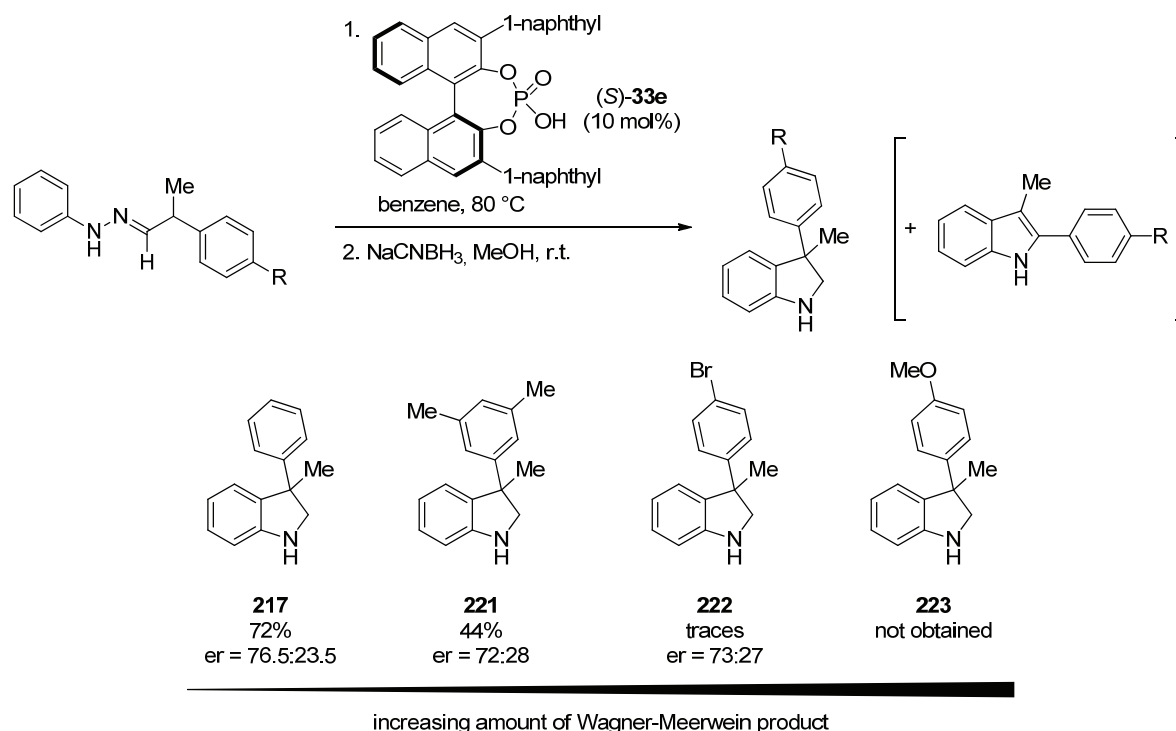
Though more basic than acetamide, aniline is still much less basic than ammonia and was thus considered an alternative leaving group. A corresponding test substrate **210a** was accessed via a palladium-catalyzed cross coupling and its indolization afforded heterocycle **211a** with enantioselectivities of up to 72.5:27.5 er (Scheme 118). Moreover, catalyst turnover was indeed observed in some cases. However, this particular substrate class turned out to be rather unstable under the reaction conditions required for the indolization, resulting in low yields and considerable decomposition of the starting material. Furthermore, the attempts to access corresponding substrates derived from α -branched aldehydes via the same route failed.



Scheme 118. Catalytic asymmetric Fischer indolization of enehydrazine **210a**.

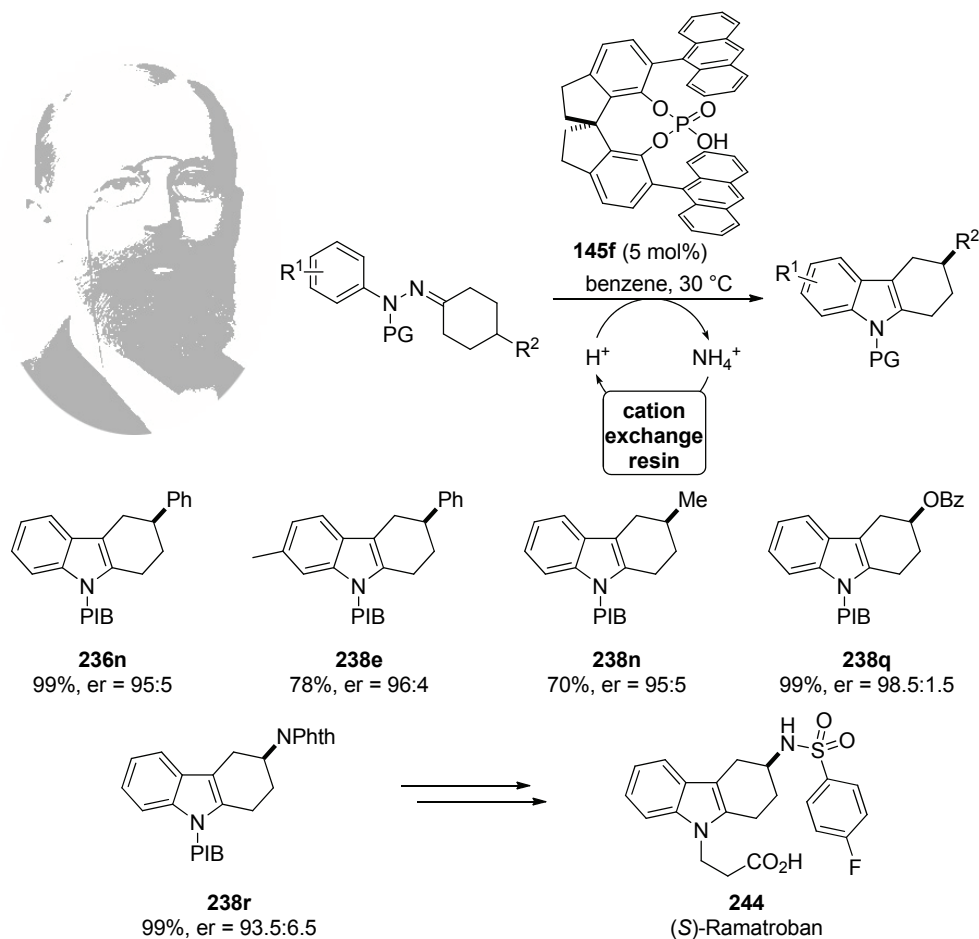
In light of these results, the classic approach generating ammonia as the by-product was again considered most promising and catalyst turnover was finally achieved by removing the liberated ammonia from the reaction mixture by the refluxing solvent. Under these conditions, indoline **217**, obtained after *in situ* reduction of the intermediary indolenine **190**, was afforded in a good yield of 72% and with a moderate enantioselectivity of 76.5:23.5 er.

However, the high temperature resulted in varying amounts of the rearranged Wagner-Meerwein by-product, depending on the particular substrate.



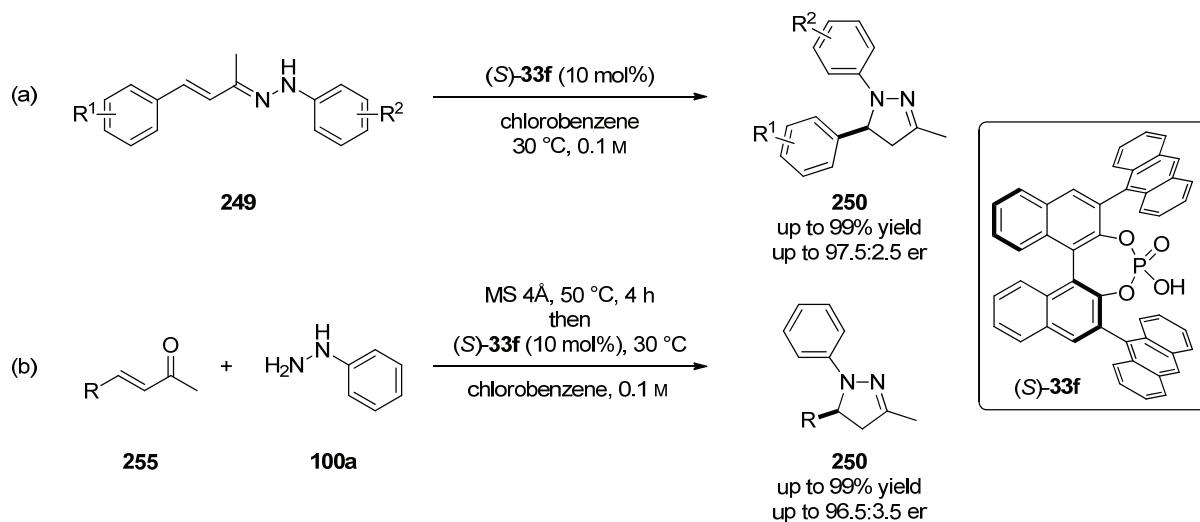
Scheme 119. The catalytic asymmetric Fischer indolization of α -branched aldehyde-derived phenylhydrazones.

The ultimate solution to the ammonia problem, which allowed the reaction to be conducted at low temperature, was finally found in connection with the work on the indolization of hydrazones derived from 4-substituted cyclohexanones. The use of a weakly acidic ion exchange resin facilitated catalyst turnover without diminishing the enantioselectivity of the reaction. In combination with the newly developed SPINOL-derived phosphoric acid **145f** (5 mol%), this method yielded 3-substituted tetrahydrocarbazoles in high yields and enantioselectivities for a wide range of different substrates (Scheme 120). Furthermore, this method was employed in the enantioselective formal synthesis of the thromboxane receptor antagonist (*S*)-Ramatroban (**244**).



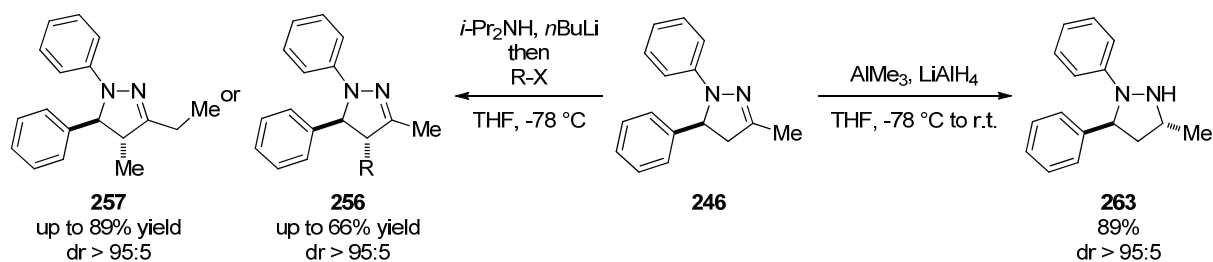
Scheme 120. Portrait of Emil Fischer and the catalytic asymmetric Fischer indolization. Enantioselective synthesis of 3-substituted tetrahydrocarbazoles and formal synthesis of (*S*)-Ramatroban (**244**). PIB = *para*-iodobenzyl.

Inspired by this work, we became also interested in the Fischer pyrazoline synthesis. Given its isoelectronicity to the 6π electrocyclization of the pentadienyl anion, this reaction was envisioned to be a suitable platform for the development of a catalytic asymmetric 6π electrocyclization. This process was finally realized by utilizing α,β -unsaturated arylhydrazones as starting materials and the BINOL-derived phosphoric acid **33f** (10 mol%) as a catalyst (Scheme 121a). The desired 2-pyrazolines were obtained in high yields and good enantioselectivities. Additionally, the method was extended to a similarly efficient direct protocol, forming the hydrazones *in situ* from the corresponding aromatic or aliphatic enones and arylhydrazines (Scheme 121b). Based on the data obtained by monitoring of the reaction by HPLC as well as from crystal structure analyses, a mechanism for the reaction was proposed and alternative pathways were discussed.



Scheme 121. Catalytic asymmetric 6π electrocyclization of α,β-unsaturated arylhydrazones **249** (a) and direct method for the synthesis of 2-pyrazolines **250** from enones **255** and phenylhydrazine (**100a**) (b).

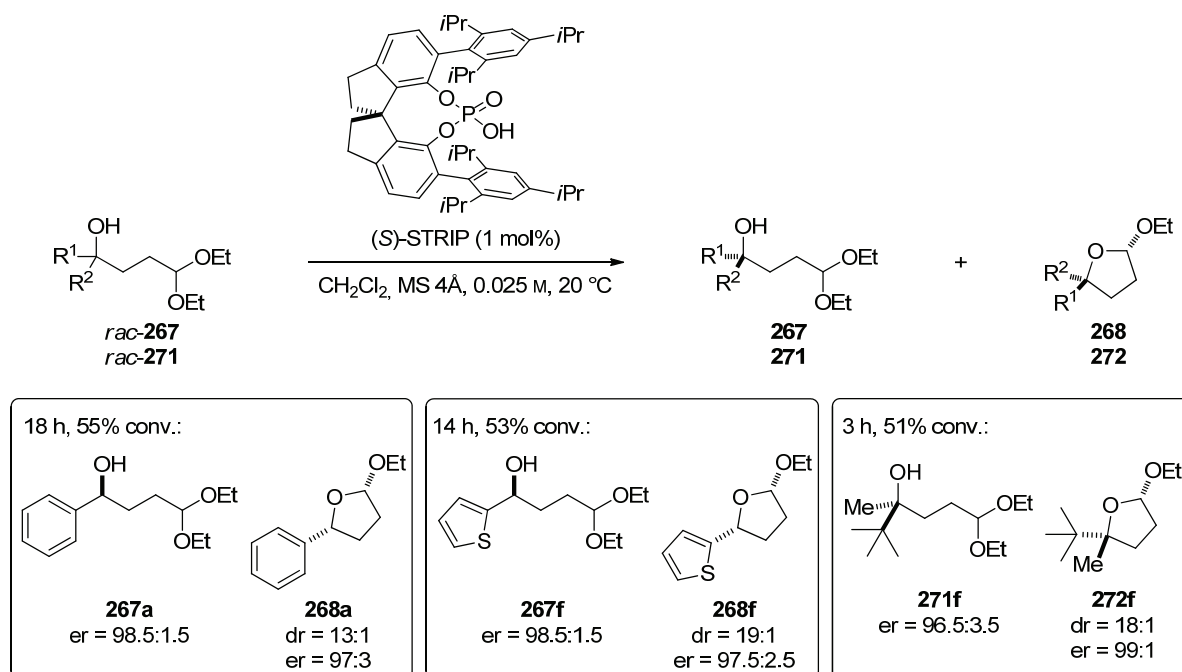
Additionally, the synthetic utility of the obtained 2-pyrazolines was demonstrated in highly diastereoselective alkylation reactions and a diastereoselective reduction (Scheme 122).



Scheme 122. Diastereoselective derivatizations of 2-pyrazoline **246**.

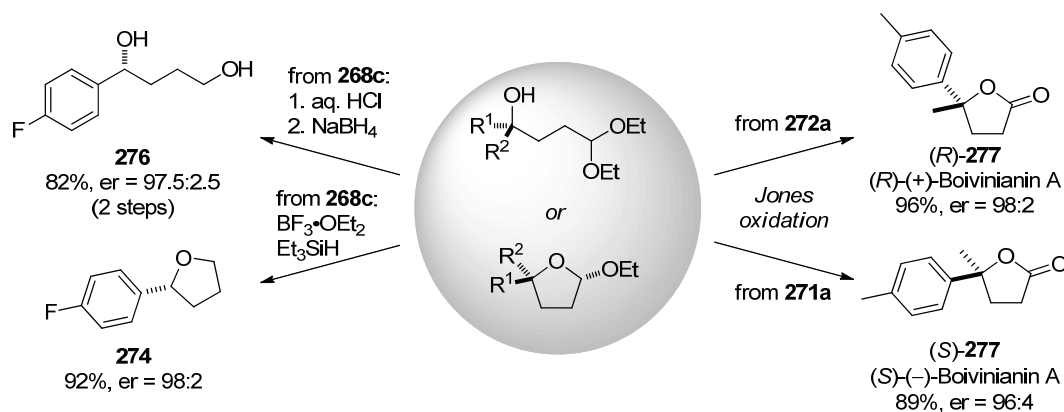
The last project of this work was devoted to the development of a kinetic resolution of homoaldols based on the catalytic asymmetric intramolecular transacetalization reaction. The conditions previously reported for the enantioselective transacetalization of achiral homoaldols resulted in disappointing results. However, when the BINOL-derived phosphoric acid TRIP (**33d**) was replaced by the newly developed spirocyclic analog STRIP (**145g**), an efficient resolution was observed. By further optimization of reaction parameters, the results were additionally improved. Eventually the developed method allowed for the highly efficient kinetic resolution of various secondary and tertiary acetal protected aldehyde homoaldols (Scheme 123). The combination of a kinetic resolution and a parallel kinetic resolution ensures that high enantioselectivities can be obtained for the product and the

unreacted starting material in almost all cases. The racemic homoaldol substrates are easily accessible, mostly in one step from commercially available starting materials. Other attractive features of this reaction are the high atom economy, the operational simplicity and the fact that no stoichiometric reagents are required.



Scheme 123. STRIP-Catalyzed kinetic resolution of homoaldols via intramolecular transacetalization.

The resolved homoaldols are extremely versatile synthetic intermediates and can easily be modified, for example by oxidation, reduction or substitution. This synthetic utility was illustrated by transforming the enantioenriched homoaldols into a chiral tetrahydrofuran **274**, a 1,4-diol **276** and the γ -butyrolactone natural product Boivinianin A (**277**).



Scheme 124. Utilization of the resolved homoaldols.

Altogether, the reactions developed in the course of this work constitute practical, highly efficient, general, mild and atom economic methods for the enantioselective synthesis of important heterocycles like indoles and pyrazolines as well as for the resolution of homoaldols. Notably, in many cases, the newly developed SPINOL-derived phosphoric acids were superior over BINOL-derived analogs and other derivatives, underlining their complementary character. We expect these findings to be of great value for new developments in the field of chiral Brønsted acid catalysis in terms of both catalyst design as well as reaction development.

Part of this work has been subject of publications in peer-reviewed scientific journals:

“A Catalytic Asymmetric 6π Electrocyclization: Enantioselective Synthesis of 2-Pyrazolines”, S. Müller, B. List, *Angew. Chem.* **2009**, *121*, 10160-10163; *Angew. Chem. Int. Ed.* **2009**, *48*, 9975-9978.

“Catalytic Asymmetric 6π -Electrocyclization: Accessing Highly Substituted Optically Active 2-Pyrazolines via Diastereoselective Alkylations”, S. Müller, B. List, *Synthesis* **2010**, 2171-2178.

“Kinetic Resolution of Homoaldols via Catalytic Asymmetric Transacetalization”, I. Čorić,† S. Müller,† B. List, *J. Am. Chem. Soc.* **2010**, *132*, 17370-17373. († these authors contributed equally)

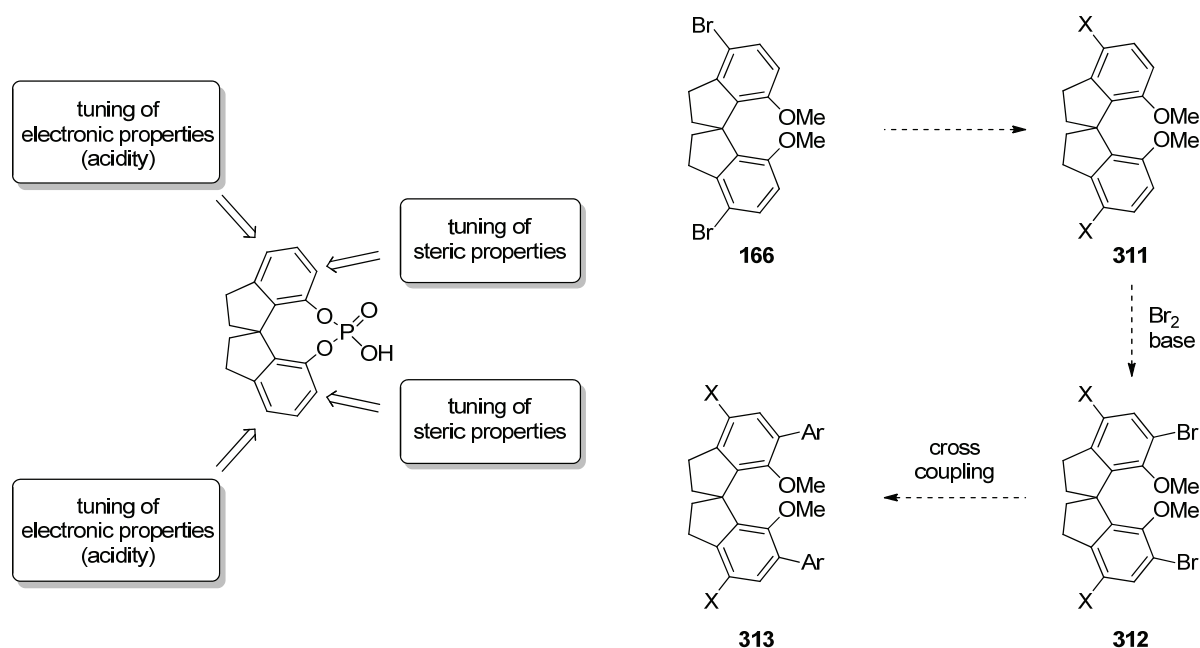
“The Catalytic Asymmetric Fischer Indolization”, S. Müller, M. J. Webber, B. List, *J. Am. Chem. Soc.* **2011**, *133*, 18534-18537.

6 Outlook

In light of the work described in the previous chapters it would be presumptuous to conclude that only little research in the discussed fields is left to be done. In fact the opposite is true. The presented results clearly illustrate the numerous formidable challenges and exciting opportunities to be met in the future in each of the projects described.

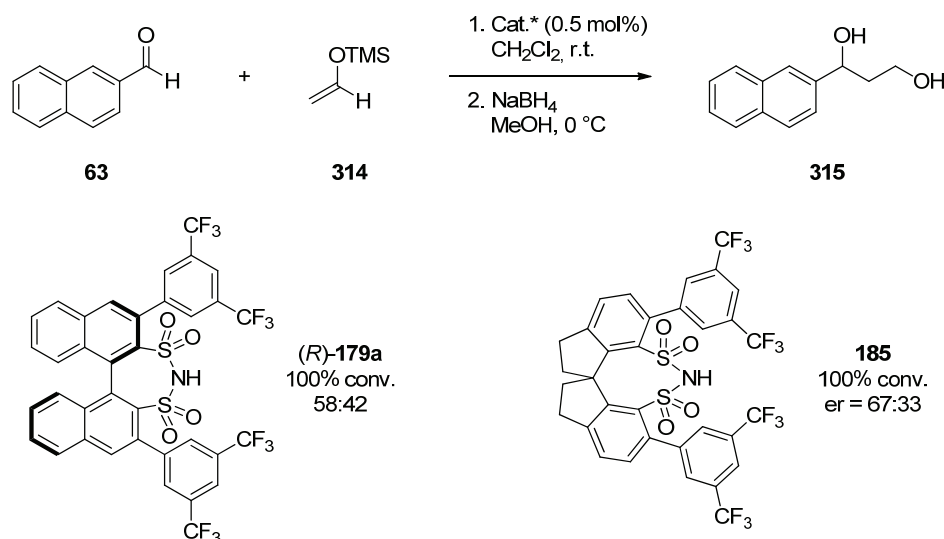
6.1 SPINOL-Derived Catalysts

The SPINOL-derived phosphoric acids were shown to behave in a complementary manner to analogs based on other backbones. Astonishingly, in many cases the particular SPINOL-derivative was superior over its BINOL- and H₈-BINOL analogs. However, besides the different geometrical environment these intriguing structures are providing, the SPINOL backbone offers an additional advantage which has not been investigated so far. Unlike in 2-naphthol based catalysts, the position *para* to the phenolic group is not occupied and thus allows a more efficient tuning of the electronic properties and consequently of the acidity of SPINOL-based acids by the introduction of suitable electron withdrawing or donating substituents (Scheme 125, left). The required synthetic precursor for this modification is obtained as an intermediate in the synthesis of racemic SPINOL (*rac*-**144**). The dibromide **166** is usually hydrodebrominated but it can likewise be envisioned to use the halogen atoms for further functionalizations to introduce appropriate groups with different electronic demands (e.g. CF₃, CN, Me). Depending on the nature of the group X, the product **311** may directly be brominated *ortho* to the methylethers via an electrophilic aromatic substitution without the need for changing the protecting group to yield compound **312**. This would enable the introduction of bulky *ortho*-substituents via cross coupling reactions to provide the compound **313** (Scheme 125, right). From the coupling product **313**, the completion of the synthesis of the phosphoric acids may be accomplished according to reported protocols.



Scheme 125. Possibilities for tuning of the properties of SPINOL-derived phosphoric acids (left) and envisioned synthetic route towards 4,4',6,6'-substituted catalysts from known intermediate **166** (right).

Besides phosphoric acid catalysis, especially enantioselective disulfonimide catalysis is a growing field of interest.^[200] So far, the reported catalysts exclusively rely on the BINOL motif. Given the beneficial effects observed in the phosphoric acid series and the generally viable route to SPINOL-derived disulfonimides disclosed herein, the detailed investigation of this catalyst class seems highly promising.



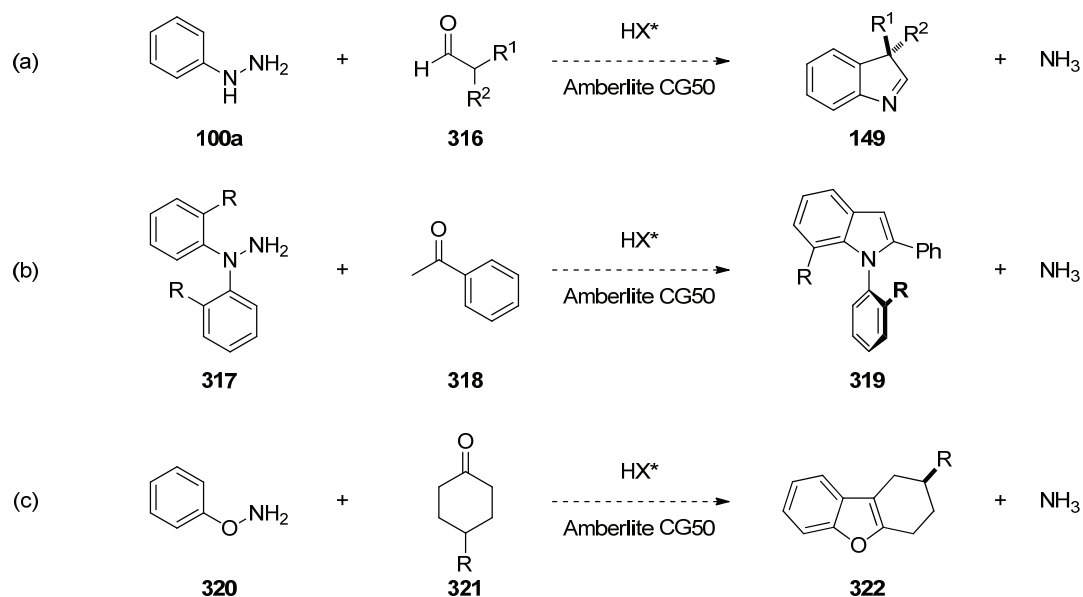
Scheme 126. Mukaiyama aldol reaction between 2-naphthaldehyde (**63**) and silyl enol ether **314** catalyzed by different disulfonimides.^[201]

First explorative experiments towards the utilization of SPINOL-derived disulfonimides as catalysts were already conducted in our group. For instance, in the Mukaiyama aldol reaction between 2-naphthaldehyde (**63**) and silyl enol ether **314**, the newly developed spirocyclic disulfonimide **185** was superior over its BINOL analog (*R*)-**179a** and afforded the diol **315** after reduction of the aldehyde in a promising enantiomeric ratio of 67:33 (Scheme 126).^[201]

Besides their use as Brønsted- or Lewis-acid catalysts, the application of the newly developed spirocyclic structures as chiral counteranions^[202] represents another field for potential applications.^[203]

6.2 The Catalytic Asymmetric Fischer Indolization

Regarding the catalytic asymmetric Fischer indolization, the identification of the ion exchange resin as powerful ammonia scavenger was one of the most exciting findings. Since this discovery was made on a very late stage of this work, the generality of this concept remains to be investigated in the context of the Fischer indolization of phenylhydrazones derived from α -branched aldehydes **316** (Scheme 127a). Furthermore, we envision our method to inspire the development of other catalytic asymmetric Fischer indolizations like for instance in the synthesis of axially chiral indoles **319** (Scheme 127b). Also a route to helically chiral indoles is conceivable, just like the application of the ion exchange technology to Garg's interrupted Fischer indolization.^[101,102] Besides this, there are numerous other reactions which could potentially benefit from the ion exchange resin in terms of rate acceleration and facilitation of catalyst turnover. One other example is the synthesis of chiral benzofurans from *O*-aryl hydroxylamines **320** and 4-substituted cyclohexanones **321** in a Fischer indolization like reaction (Scheme 127c).^[204] These reactions are representatives for transformations in which the developed method may pave the way for the realization of a catalytic asymmetric protocol.



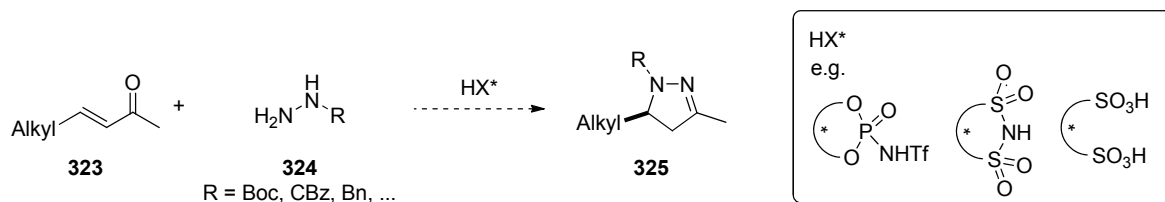
Scheme 127. Some potential future applications of the ion exchange resin technology in enantioselective Brønsted acid catalysis: synthesis of chiral indolenines (a), catalytic asymmetric Fischer indolization in the synthesis of axially chiral indoles (b), and enantioselective synthesis of chiral tetrahydrobenzofurans (c).

In fact, several chiral phosphoric acid-catalyzed reactions require the addition of acidic co-catalysts such as acetic acid or achiral phosphoric acids to render the system sufficiently reactive.^[205] However, in some cases these additives were also found to detrimentally influence the stereochemical outcome of the reaction.^[205c] While this observation is in line with our finding that soluble acidic additives significantly decreased the enantiomeric ratio of the products, the solid supported acid did not influence the enantioselectivity of our reaction. Therefore, the ion exchange resin technology is expected to have a profound impact on future developments in enantioselective Brønsted acid catalysis.

6.3 The Catalytic Asymmetric 6 π Electrocyclization

Future work on the synthesis of 2-pyrazolines via a catalytic asymmetric 6 π electrocyclization may include detailed mechanistic studies supported by computational methods to unravel the true nature of the cyclization process.^[161] Moreover, the major limitation of this reaction so far is the substrate scope. Although the developed direct method enables the use of aliphatic enones, the obtained enantioselectivities in these cases

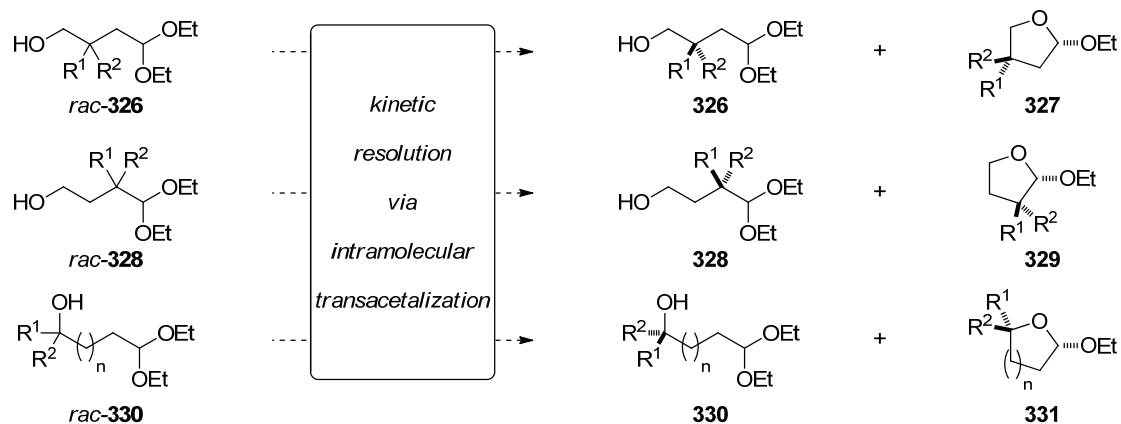
leave much to be desired. Since already a change of the catalyst from the phosphoric acid **33f** to the related *N*-triflyl phosphoramidate **44c** resulted in markedly increased enantioselectivities, the identification of more efficient catalysts for these substrates seems feasible. At the same time, the hydrazine component in our reaction is limited to arylhydrazines. In order to render the use of other substituted hydrazines or even the parent compound possible, the development of new catalysts is inevitably required. Especially the use of carbamate or benzyl protected hydrazines **324** would constitute a major improvement regarding the synthetic utility of the products. As potential new catalysts for these transformations, stronger Brønsted acids like new *N*-triflyl phosphoramidates, disulfonimides or disulfonic acids seem promising (Scheme 128).



Scheme 128. Proposed improved synthesis of 2-pyrazolines with different catalysts.

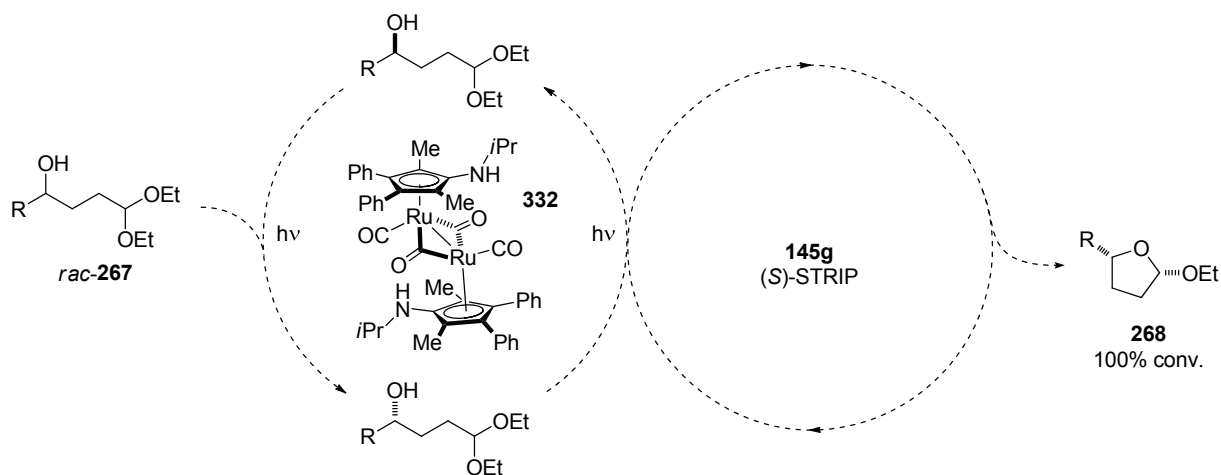
6.4 STRIP-Catalyzed Kinetic Resolution of Homoaldols

The performance of the new phosphoric acid STRIP (**145**) in the kinetic resolution of homoaldols is impressive, especially when compared to other catalysts tested. Possible future work in this field may include the resolution of other substrate classes. So far the stereocenter of the homoaldols was located at the carbon atom bearing the alcohol functional group. The resolution of substrates *rac*-**326** and *rac*-**328** with stereocenters in different positions along the aliphatic chain appears attractive due to the valuable compounds generated in such a process. Additionally, the use of substrates *rac*-**330** with different tether lengths can be envisioned (Scheme 129). However, a resolution of these is less attractive, since these products can also be accessed by other methods like (vinylogous) aldol reactions. One example in which the stereocenter was located in α -position to the acetal was already reported and the results obtained are highly encouraging. Thus an extension of this method to other substrates seems highly promising.



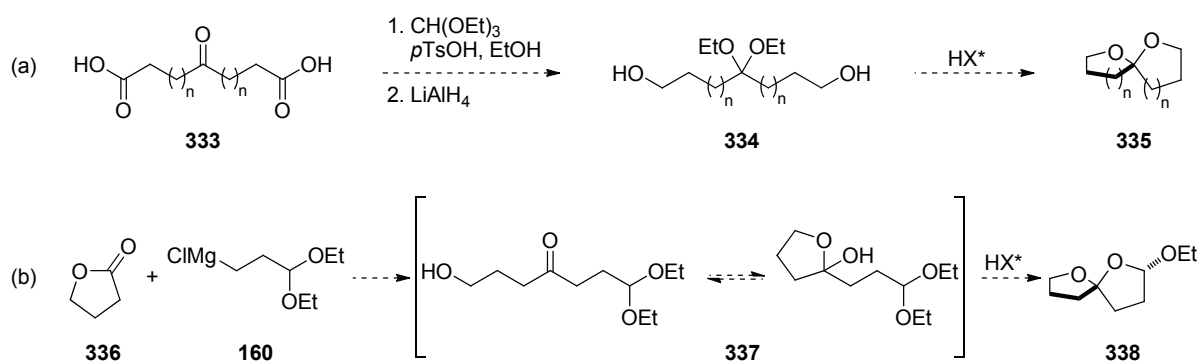
Scheme 129. Possible extension of the substrate scope of the kinetic resolution.

Another inherent drawback of the reported method is the fact that it is a kinetic resolution. Although the resolved starting material and the product are obtained in high enantioselectivities and can likewise well be utilized in further transformations, the yield of the desired stereoisomer is inevitably limited to 50 %. Therefore, the development of this methodology into a dynamic kinetic resolution constitutes an exciting opportunity. Such a process could, for instance, be achieved for the secondary homoaldols by combining the STRIP-catalyzed kinetic resolution with another catalyst system capable of continuously racemizing the starting material. In pioneering studies, the groups of Williamson^[206] and Bäckvall^[207] reported a related process, combining iridium, rhodium or ruthenium based metal catalysts with enzymes for the dynamic kinetic resolution of secondary alcohols. While the first generation of racemization catalysts required elevated temperatures^[207,208] or strong bases such as potassium *tert*-butoxide for their activation,^[209] more recently developed ruthenium complexes can simply be activated by light and efficiently racemize secondary alcohols at ambient temperature.^[210] Hence a combination of complex **332** with our STRIP-catalyzed transacetalization offers an appealing approach for the dynamic kinetic resolution of homoaldols (Scheme 130).



Scheme 130. Combined metal- and organo-catalyzed dynamic kinetic resolution of acetal protected secondary homoaldols *rac*-**267**.

The high stereocontrol of the newly formed acetal center provided by the catalyst also suggests further developments towards enantioselective acetal syntheses. A particularly intriguing class of targets in this respect are spiroacetals. Spiroacetals are widely distributed compounds in nature, ranging from small insect pheromones^[211] to complex macrolide natural products with interesting biological activities.^[212] Despite the importance of this chiral motif, catalytic enantioselective methods for the efficient construction of spiroacetals remain elusive. Accordingly, the utilization of the intramolecular transacetalization strategy to the spiroacetalization of readily available dihydroxy ketals **334** (Scheme 131a) or in the dynamic kinetic resolution of γ -hydroxy- γ' -acetal-tethered ketones **337** (Scheme 131b) appears to be promising towards this endeavor.



Scheme 131. Potential applications of the intramolecular transacetalization in the catalytic asymmetric synthesis of spiroketals from dihydroxy ketals **334** (a), and acetal-tethered lactols **337** (b).

7 Experimental Part

7.1 General Experimental Conditions

Solvents and Reagents

All air and moisture sensitive reactions were conducted in flame-dried glass ware under and inert Ar atmosphere using standard Schlenk techniques. Dry argon was purchased from Air Liquide with higher than 99.5% purity. All solvents employed in the reactions were dried using standard procedures^[213] or purchased from commercial suppliers unless otherwise stated. Dichloromethane and chloroform were distilled over CaH₂. THF was dried over Mg-anthracene. Chlorobenzene was distilled over P₂O₅. Ethanol and methanol were dried over magnesium. Diethyl ether, toluene and *n*-hexane were dried over sodium. Anhydrous acetone, acetonitrile, benzene, cyclohexane, DMF, DME, DMSO, NMP, trifluorotoluene, pyridine, di(*n*-butyl)ether and 1,4-dioxane were purchased from Sigma-Aldrich and used as received. All reagents were purchased from different commercial suppliers and used without further purification unless indicated. Phenylhydrazine (**100a**) was distilled and NEt₃ and TMEDA were purified by distillation over LiAlH₄. All dried solvents and purified reagents were distilled prior to use or stored under an inert Ar atmosphere.

Thin Layer Chromatography (TLC) and Preparative Thin Layer Chromatography (PTC)

Reactions were monitored by thin layer chromatography on silica gel pre-coated plastic sheets (0.2 mm, Machery-Nagel). Visualization was accomplished by irradiation with UV light at 254 nm and/or different staining reagents. Phosphomolybdic acid (PMA) stain: PMA (10 g) was dissolved in EtOH (100 mL). Anisaldehyde stain: Anisaldehyde (0.5 mL) and glacial acetic acid (10 mL) were dissolved in MeOH (85 mL) and conc. H₂SO₄ (5.0 mL) was added carefully to the mixture. KMnO₄ stain: KMnO₄ (1.5 g) and K₂CO₃ (10 g) were dissolved in H₂O (200 mL) prior to the addition of 10% NaOH (aq) (1.25 mL). Preparative thin layer chromatography was performed on silica gel pre-coated glass plates SIL G-25 UV₂₅₄ and SIL G-100 UV₂₅₄ with 0.25 mm and 1.0 mm SiO₂ layers (Machery-Nagel), respectively.

Column Chromatography (CC)

Column chromatography was performed on Merck silica gel (60, particle size 0.040-0.063 mm) as the stationary phase. Deactivated silica gel was obtained by thoroughly mixing an appropriate amount of SiO₂ and 7.5% (w/w) of concentrated aqueous ammonium hydroxide solution. The deactivated silica gel was allowed to stand over night before use. As the mobile phase solvent mixtures of *iso*-hexane, ethyl acetate, diethyl ether, *n*-pentane, CH₂Cl₂ and MeOH were used. The exact mixtures and ratios are specified in the individual experiment. The chromatography was either conducted in glass columns applying slightly elevated pressure or using the automatic column system Büchi Sepacore Flash (pump module C-605, UV-photometer C-635, fraction collector C-660).

High Performance Liquid Chromatography (HPLC)

Normal phase HPLC analyses were conducted on a Shimadzu LC 2010 C system and a Shimadzu system consisting of a DGC-20A₅ degasser unit, a LC-20AD pump, a CBM-20A communication bus module, a SIL-20AG auto sampler, a SPD-M20A diode array detector and a CTO-20AC column oven. Following stationary phases were used: Daicel Chiralcel OD-H (cellulose tris-(3,5-dimethylphenylcarbamate) on a silica support, 250 x 4.6mm, 5 µm particle size), Daicel Chiralcel OJ-H (cellulose tris-(4-methylbenzoate) on a silica support, 250 x 4.6 mm, 5 µm particle size), Daicel Chiralcel OB-H (cellulose tribenzoate on a silica support, 250 x 4.6 mm, 5 µm particle size), Daicel Chiralcel OD-3 (cellulose tris-(3,5-dimethylphenylcarbamate) on a silica support, 150 x 4.6 mm, 3 µm particle size), Daicel Chiralpak AD-3 (amylose tris-(3,5-dimethylphenylcarbamate) on a silica support, 150 x 4.6 mm, 3 µm particle size). For reversed phase HPLC a Shimadzu LC 2010 C system was employed. Stationary phases were as follows: Daicel Chiralcel OD-RH (cellulose tris-(3,5-dimethylphenylcarbamate) on a silica support, 250 x 4.6 mm, 5 µm particle size), Daicel Chiralcel OJ-RH (cellulose tris-(4-methylbenzoate) on a silica support, 250 x 4.6 mm, 5 µm particle size), Daicel Chiralcel OJ-3R (cellulose tris-(4-methylbenzoate) on a silica support, 150 x 4.6 mm, 3 µm particle size). As the mobile phase solvent mixture of *n*-heptane and *i*-PrOH were used for normal phase HPLC and aqueous mixtures of acetonitrile or MeOH were employed on the reversed phase system. Preparative HPLC was performed on a Shimadzu LC-8A system equipped with a FRC-10A fraction collector. As the stationary phase the Daicel Chiralpak QN-AX column (*O*-9-(*tert*-butylcarbamoyl) quinine immobilized on silica support,

150 x 21 mm, 5 μm particle size) was used. The mobile phases are specified in the individual experiment.

Gas Chromatography (GC)

Gas chromatography (GC) analysis was conducted on HP 6890 and 5890 series instruments equipped with a split-mode capillary injection system and a flame ionization detector (FID). Detailed conditions are given in the individual experiment.

Nuclear Magnetic Resonance Spectroscopy (NMR)

Proton, carbon and phosphorous NMR spectra were recorded on a Bruker AV-500, a Bruker AV-400 and a Bruker DPX 300 spectrometer in deuterated solvents. Proton chemical shifts (^1H) are reported in ppm (δ) relative to tetramethylsilane (TMS) with the solvent resonance employed as the internal standard (C_6D_6 , $\delta = 7.16$ ppm; CD_2Cl_2 , $\delta = 5.32$ ppm; CDCl_3 , $\delta = 7.26$; DMSO-d_6 , $\delta = 2.49$ ppm). Data are reported as follows: chemical shift, multiplicity (s = singlet, d = doublet, q = quartet, sept = septet, m = multiplet, br = broad), coupling constants (Hz) and integration. Carbon chemical shifts (^{13}C) are reported in ppm (δ) from tetramethylsilane (TMS) with the solvent resonance as the internal standard (C_6D_6 , $\delta = 128.06$ ppm; CD_2Cl_2 , $\delta = 53.8$ ppm; CDCl_3 , $\delta = 77.16$; DMSO-d_6 , $\delta = 39.5$ ppm). Phosphorous chemical shifts (^{31}P) are reported in ppm (δ) relative to H_3PO_4 as the external standard.

Mass Spectrometry (MS)

Electron impact (EI) mass spectrometry was conducted on a Finnigan MAT 8200 or a Finnigan MAT 8400 spectrometer. Electrospray ionisation (ESI) mass spectra were recorded on a Bruker ESQ 3000 spectrometer. High resolution mass spectroscopy (HRMS) was performed on Finnigan MAT 95 spectrometer in EI mode and on a Bruker APEX III FTMS (7 T magnet) in ESI mode.

Melting Points (mp)

Melting points (mp) were measured in open glass capillaries using a Büchi Melting Point B-540 apparatus and are uncorrected.

Optical Rotations (α_D)

Optical rotations were measured on a Autopol IV automatic polarimeter (Rudolph Research Analytical) using a 50 mm cell with temperature control. The optical rotations were measured at 25 °C at a wavelength of $\lambda = 598$ nm. Concentrations are given in $10 \text{ mg}\cdot\text{mL}^{-1}$.

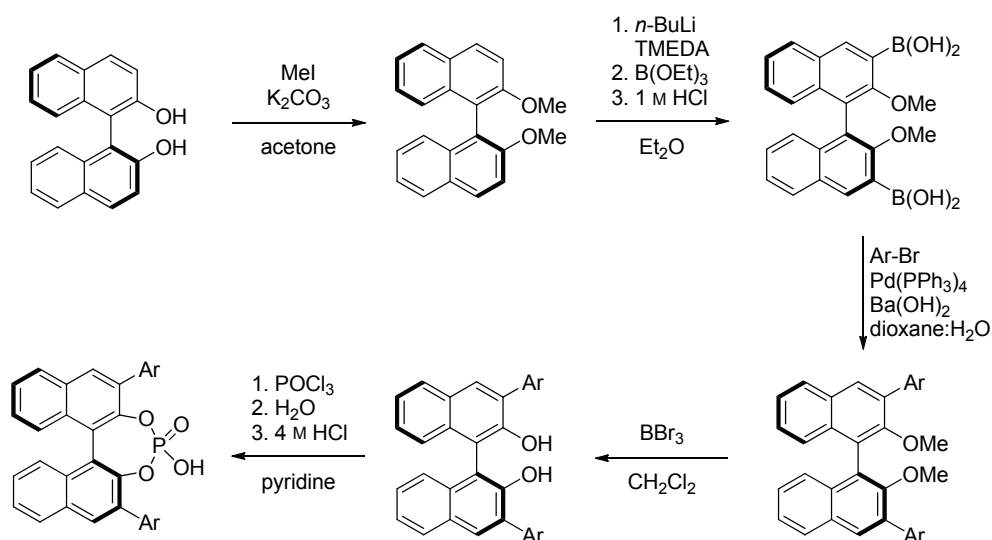
X-Ray Crystallography

X-Ray crystal structure analyses were performed on a AXS Enraf-Nonius KappaCCD (Mo- K_α radiation, $\lambda = 0.71073$ Å, graphite monochromator, X-ray source: $0.2 \times 2 \text{ mm}^2$ focus rotating anode, measurement method: CCD ϕ - and ω -scans), a Bruker-AXS Kappa Mach3 APEX-II (Mo- K_α radiation, $\lambda = 0.71073$ Å, Incoatec Helios mirror, X-ray source: $0.2 \times 2 \text{ mm}^2$ focus rotating anode, measurement method: CCD ϕ - and ω -scans) and a Bruker AXS X8 Proteum (Cu- K_α radiation, $\lambda = 1.54184$ Å, focussed multilayer optic, X-ray source: $0.2 \times 2 \text{ mm}^2$ focus rotating anode, measurement method: CCD ϕ - and ω -scans) diffractometer. The software package used for data collection and structure refinement consisted of DATCOL (Bruker AXS, 2006), DENZO (Bruker AXS, 2006), SAINT (Bruker AXS, 2004), SHELXS-97 (Sheldrick, 2008), SHELXL-97 (Sheldrick, 2008) and DIAMOND (Crystal Impact GbR, 2005). The X-ray crystal structure analyses were performed by the X-ray department of the Max-Planck-Institut für Kohlenforschung.

7.2 Synthesis of BINOL-, H₈-BINOL-, VAPOL- and TADDOL-Derived Catalysts

The BINOL-derived phosphoric acids **33** were synthesized from enantiomerically pure BINOL. Following the procedures reported by Jørgensen *et al.* and Wipf and co-workers BINOL was converted into the corresponding 3,3'-disubstituted diol by *O*-methylation, *ortho*-lithiation and diboronic acid synthesis, Suzuki-Miyaura cross coupling with arylbromides and subsequent deprotection (Scheme 132).^[214]

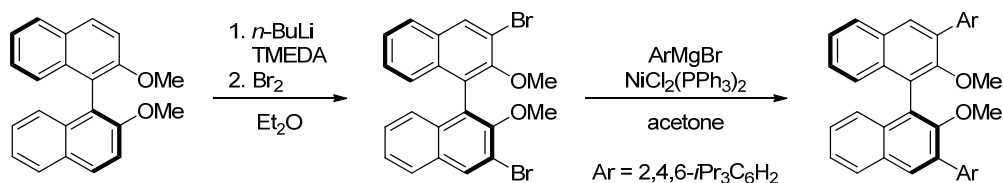
Further conversion to the desired phosphoric acids was achieved by treatment with POCl₃ in pyridine followed by hydrolysis of the intermediary phosphoric acid chloride and acidic work up as reported by the groups of Akiyama and Terada (Scheme 132).^[39,40]



Scheme 132. General route for the synthesis of BINOL-derived phosphoric acids.

The majority of BINOL-derived phosphoric acids were prepared using this protocol. The synthesis was accomplished mainly starting from advanced precursors kindly provided by H. van Thienen, S. Marcus and M. Hannappel, who also prepared some phosphoric acids.

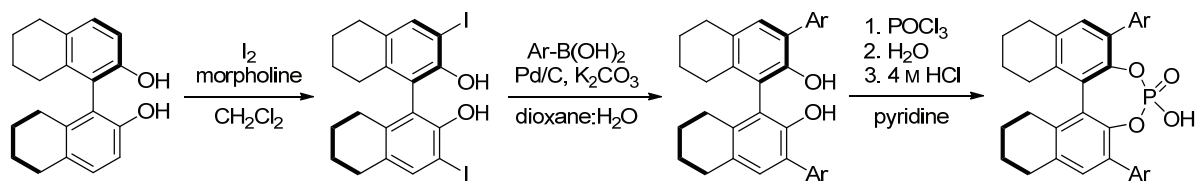
For the synthesis of TRIP (**33d**) the bulky 3,3'-substituents had to be introduced via a Kumada coupling, which was conducted according to a procedure reported by Schrock *et al.* (Scheme 133).^[215] The completion of the synthesis followed the procedure reported above with minor modifications.^[139]



Scheme 133. En-route to the BINOL-derived phosphoric acid TRIP (**33d**).

The BINOL-derived phosphoric acid **33o** and VAPOL phosphoric acid **39** were purchased from Sigma-Aldrich.

The general synthesis of 3,3'-disubstituted H₈-BINOLs was accomplished by iodination of H₈-BINOL followed by a palladium/charcoal-catalyzed Suzuki-Miyaura cross coupling with the corresponding boronic acids as reported by Blanchet *et al.* (Scheme 134).^[216] Further conversion to the desired phosphoric acids was achieved as described above by treatment with POCl₃ and subsequent hydrolysis.



Scheme 134. General route for the synthesis of H₈-BINOL-derived phosphoric acids.

The TADDOL-derived phosphoric acids **219** and **220** were synthesized according to the procedures reported by the groups of Akiyama and Charette.^[42]

N-Triflyl phosphoramides **44** were provided by D. Kampen and V. Wakchaure. The synthesis was accomplished by using a modification of the procedure reported by Nakashima and Yamamoto.^[49,217]

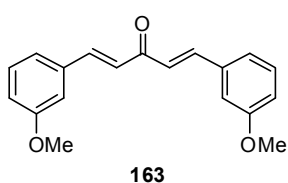
The disulfonimides **179** and disulfonic acids **212** were provided by H. van Thienen, S. Marcus, M. Hannappel, P. García García and F. Lay. These catalysts were synthesized according to a procedure reported by our group.^[127]

7.3 Synthesis of SPINOL-Derived Phosphoric Acids and Disulfonimides

7.3.1 SPINOL-Derived Phosphoric Acids

Racemic SPINOL (*rac*-**144**) was synthesized according to the protocol reported by Birman and co-workers with minor modifications.^[123] The resolution of diol *rac*-**144** was achieved following the protocol reported by the groups of Deng, Zhou and Ye.^[135]

(1*E*,4*E*)-1,5-Bis(3-methoxyphenyl)penta-1,4-dien-3-one (**163**)



A mixture of 3-methoxybenzaldehyde (**146**, 30.0 g, 220 mmol) and acetone (**13**, 6.40 g, 110 mmol) in EtOH (30 mL) was added dropwise to a solution of NaOH (22.9 g, 573 mmol) in EtOH:H₂O (400 mL, 1:1) while the reaction mixture was cooled in a water bath. After complete addition the mixture was allowed to stir for 2 h at room temperature. After addition of CH₂Cl₂ the layers were separated and the aqueous layer was extracted with CH₂Cl₂. The combined organic layers were washed with H₂O, dried over MgSO₄ and purified by column chromatography on silica gel with hexane:EtOAc (5:1) as the eluent. The title compound **163** (18.5 g, 62.9 mmol, 57%) was obtained as a yellow oil which solidified upon standing over night.

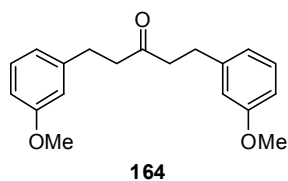
¹H NMR (500 MHz, CDCl₃) δ = 7.70 (d, *J* = 16.0 Hz, 2H), 7.33 (dd, *J* = 8.0 Hz, *J* = 7.9 Hz, 2H), 7.22 (d, *J* = 7.7 Hz, 2H), 7.14 (d, *J* = 1.8 Hz, 2H), 7.07 (d, *J* = 16.0 Hz, 2H), 6.97 (dd, *J* = 8.2 Hz, *J* = 2.4 Hz, 2H), 3.86 (s, 6H) ppm.

¹³C NMR (125 MHz, CDCl₃) δ = 189.0, 160.1, 143.4, 136.3, 130.1, 125.8, 121.3, 116.5, 113.4, 55.5 ppm.

MS (EI) *m/z* (%): 294 (100), 263 (33), 161 (24), 133 (17), 121 (35).

HRMS (ESI+) *m/z* calculated for C₁₉H₁₈O₃Na (M+Na⁺) 317.114810, found 317.115085.

1,5-Bis(3-methoxyphenyl)pentan-3-one (**164**)



A slurry of Raney-Ni in H₂O (Sigma Aldrich) was homogenized by vigorous shaking and 3 Pasteur pipets were transferred into a glass frit under argon. The water was removed and the solid was washed

first with MeOH and then with acetone before it was transferred into a round bottom flask containing a solution of dienone **163** (15.8 g, 53.7 mmol) in acetone (100 mL) under argon. The resulting mixture was stirred for 4 h under an atmosphere of H₂ until the starting material was completely consumed (TLC analysis, hexane:EtOAc 4:1). The catalyst was filtered over a pad of Celite, washed with acetone and the combined filtrates were concentrated under reduced pressure to afford the title compound **164** (15.7 g, 52.6 mmol, 98%) as a colorless oil which was used in the next step without further purification.

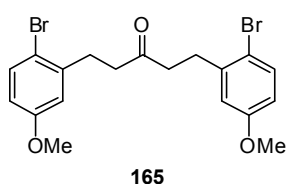
¹H NMR (500 MHz, CDCl₃) δ = 7.19 (dd, *J* = 7.9, 7.8 Hz, 2H), 6.75-6.73 (m, 4H), 6.71 (m, 2H), 3.79 (s, 6H), 2.86 (t, *J* = 7.6 Hz, 4H), 2.71 (t, *J* = 7.6 Hz, 4H) ppm.

¹³C NMR (125 MHz, CDCl₃) δ = 209.2, 159.8, 142.8, 129.6, 120.8, 114.2, 111.6, 55.3, 44.6, 29.9 ppm.

MS (EI) *m/z* (%): 298 (39), 163 (29), 135 (100), 121 (40).

HRMS (ESI+) *m/z* calculated for C₁₉H₂₂O₃Na (M+Na⁺) 321.146112, found 321.146158.

1,5-Bis(2-bromo-5-methoxyphenyl)pentan-3-one (**165**)



To a mixture of ketone **164** (15.7 g, 52.6 mmol) and pyridine (14.9 mL, 184 mmol) in CH₂Cl₂ (100 mL) was added a solution of Br₂ (21.0 g, 132 mmol) in CH₂Cl₂ (65 mL) dropwise at -10 °C over the course of 30 min. After complete addition the mixture was allowed to warm to 0

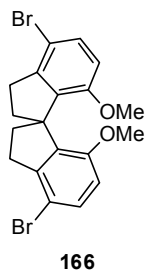
°C within 30 min before the cooling bath was completely removed. After stirring at room temperature for 2 h, a saturated aqueous solution of NaHSO₃ was added. The layers were separated and the aqueous layer was extracted with CH₂Cl₂ (3 x 80 mL). The combined organic layers were washed with 2 M HCl (100 mL) and H₂O (100 mL), dried over MgSO₄ and evaporated to dryness to afford the title compound **165** (23.1 g, 50.6 mmol, 96%) as a light yellow solid. The product was used in the next step without further purification.

¹H NMR (500 MHz, CDCl₃) δ = 7.39 (d, *J* = 8.8 Hz, 2H), 6.77 (d, *J* = 3.0 Hz, 2H), 6.63 (d, *J* = 8.8, 3.0 Hz, 2H), 3.77 (s, 6H), 2.96 (t, *J* = 7.7 Hz, 4H), 2.73 (t, *J* = 7.7 Hz, 4H) ppm.

¹³C NMR (125 MHz, CDCl₃) δ = 208.6, 159.1, 141.3, 133.5, 116.3, 114.8, 113.8, 55.6, 42.7, 30.7 ppm.

MS (EI) *m/z* (%): 458/456 (6/11), 454 (6), 377/375 (70/69), 296 (100), 215/213 (18/19), 201/199 (53/54), 160 (50), 134 (39).

HRMS (ESI+) *m/z* calculated for C₁₉H₂₀O₃Br₂Na (M+Na⁺) 476.967165, found 476.967310.

rac-4,4'-Dibromo-7,7'-dimethoxy-1,1'-spirobiindane (166)

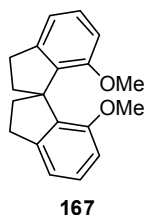
Ketone **165** (5.00 g, 11.0 mmol) was heated to 40 °C in MsOH (20 mL). After 1 h the mixture was cooled to room temperature and poured onto ice water. The aqueous phase was extracted with CH₂Cl₂ and the combined organic layers were dried over MgSO₄ and concentrated under reduced pressure to give a brown oil. Crystallization of this residue from CH₂Cl₂:hexane afforded a first fraction of the product **166** (1.89 g, 4.32 mmol, 39%) as colorless crystals. The mother liquor was concentrated and the residue was loaded on a pad of silica gel and eluted with hexane:EtOAc (9:1). The product containing fractions were combined and evaporated to dryness. Repeated crystallization of the residue afforded another fraction of the title compound **166** (1.34 g, 3.05 mmol, 28%) as colorless crystals, resulting in a total yield of 3.23 g (7.37 mmol, 67%).

¹H NMR (500 MHz, CDCl₃) δ = 7.26 (d, *J* = 8.6 Hz, 2H), 6.52 (d, *J* = 8.6 Hz, 2H), 3.52 (s, 6H), 3.07 (ddd, *J* = 16.3, 9.2, 3.7 Hz, 2H), 2.98-2.92 (m, 2H), 2.35-2.29 (m, 2H), 2.19-2.14 (m, 2H) ppm.

¹³C NMR (125 MHz, CDCl₃) δ = 155.7, 145.0, 138.2, 130.5, 110.9, 110.6, 62.0, 55.5, 38.1, 33.3 ppm.

MS (EI) *m/z* (%): 440/438/436 (50/100/51), 409/407/405 (7/13/6), 359/357 (90/91), 278 (78).

HRMS (ESI+) *m/z* calculated for C₁₉H₁₈O₂Br₂Na (M+Na⁺) 458.956601, found 458.956700.

rac-7,7'-Dimethoxy-1,1'-spirobiindane (167)

To a solution of dibromide **166** (4.99 g, 11.4 mmol) in THF (100 mL) was added *n*-BuLi (18.3 mL, 45.6 mmol, 2.5 M solution in hexanes) dropwise at -78 °C over 30 min. After stirring at this temperature for 2 h, EtOH (5.0 mL) was carefully added and the solution was allowed to warm to room temperature. The mixture was diluted with H₂O (40 mL) and extracted with CH₂Cl₂. The combined organic extracts were dried over MgSO₄ and evaporated to dryness to yield the product **167** (3.17 g, 11.3 mmol, 99%) as a colorless solid which was analytically pure and directly used in the next step.

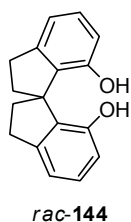
¹H NMR (500 MHz, CDCl₃) δ = 7.15 (dd, *J* = 8.1, 7.4 Hz, 2H), 6.87 (d, *J* = 7.4 Hz, 2H), 6.64 (d, *J* = 8.1 Hz, 2H), 3.54 (s, 6H), 3.11-3.05 (m, 2H), 3.03-2.97 (m, 2H), 2.39-2.33 (m, 2H), 2.21-2.16 (m, 2H) ppm.

^{13}C NMR (125 MHz, CDCl_3) δ = 156.7, 145.5, 137.0, 127.7, 116.9, 108.7, 59.3, 55.3, 38.9, 31.8 ppm.

MS (EI) m/z (%): 280 (100), 265 (38), 249 (61), 234 (21), 159 (35), 122 (26).

HRMS (ESI+) m/z calculated for $\text{C}_{19}\text{H}_{20}\text{O}_2\text{Na}$ ($\text{M}+\text{Na}^+$) 303.135552, found 303.135598.

rac-1,1'-Spirobiindane-7,7'-diol (*rac*-SPINOL, *rac*-144)



BBr_3 (24.4 mL, 24.4 mmol, 1 M solution in CH_2Cl_2) was added dropwise over 30 min to a solution of methylether **167** (2.98 g, 10.6 mmol) in CH_2Cl_2 (45 mL) at -78 °C. The reaction mixture was allowed to warm to room temperature over night and was carefully quenched by addition of H_2O . The layers were separated and the aqueous layer was extracted with CH_2Cl_2 . The combined organic layers were

dried over MgSO_4 and evaporated to dryness to afford racemic SPINOL (*rac*-**144**, 2.67 g, 10.6 mmol, quant. yield) as a colorless solid.

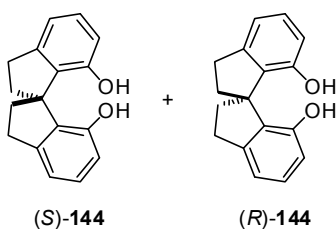
^1H NMR (500 MHz, CDCl_3) δ = 7.18 (dd, J = 8.0, 7.4 Hz, 2H), 6.90 (d, J = 7.4 Hz, 2H), 6.68 (d, J = 8.0 Hz, 2H), 4.61 (br, 2H), 3.09-2.98 (m, 4H), 2.31 (ddd, J = 12.9, 7.2, 1.6 Hz, 2H), 2.23-2.16 (m, 2H) ppm.

^{13}C NMR (125 MHz, CDCl_3) δ = 153.1, 146.0, 130.6, 130.1, 117.8, 114.5, 57.6, 37.6, 31.4 ppm.

MS (EI) m/z (%): 252 (100), 235 (57), 223 (25), 145 (31), 107 (17).

HRMS (ESI+) m/z calculated for $\text{C}_{17}\text{H}_{16}\text{O}_2\text{Na}$ ($\text{M}+\text{Na}^+$) 275.104249, found 275.104333.

Resolution of *rac*-1,1'-spirobiindane-7,7'-diol (*rac*-SPINOL, *rac*-144)



A solution of diol *rac*-**144** (3.62 g, 14.3 mmol) in toluene (112 mL) was treated with *N*-benzylcinchonidinium chloride (**168**, 3.32 g, 7.88 mmol) and the resulting mixture was heated to reflux for 90 min. After cooling to room temperature the precipitate consisting of a 1:1 complex of (*S*)-**144** and ammonium salt **168**

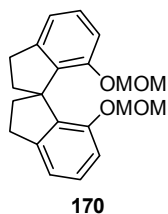
was filtered off and washed with toluene (20 mL). The solid was suspended in EtOAc (70 mL) and treated with 10% HCl until pH = 3 upon which a clear solution was obtained. The organic layer was washed with brine (2 x 40 mL), dried over MgSO_4 and evaporated to dryness. The residue was passed over a plug of silica (hexane:EtOAc 5:1) and the obtained product was recrystallized from hexane:EtOAc (10:1, 55 mL) to afford (*S*)-SPINOL ((*S*)-**144**, 0.91 g, 3.61 mmol, 25%) as colorless needles in enantiomerically pure form (er > 99.5:0.5).

The (*R*)-enantiomer-containing mother liquor was evaporated to dryness and the resulting solid was treated as described above for the (*S*)-enantiomer. Recrystallization from hexane:EtOAc (30:1, 160 mL) yielded (*R*)-SPINOL ((*R*)-**144**, 1.19 g, 4.72 mmol, 33%) as colorless needles in enantiomerically pure form (er > 99.5:0.5).

The analytical data of (*S*)-SPINOL ((*S*)-**144**) and (*R*)-SPINOL ((*R*)-**144**) (^1H NMR, ^{13}C NMR, MS) were in agreement with those obtained for *rac*-1,1'-spirobiindane-7,7'-diol (*rac*-SPINOL, *rac*-**144**).

The enantiomeric ratio was determined by HPLC analysis using Daicel Chiralpak AD-3 column: *n*-heptane:*i*-PrOH = 80:20, flow rate 1.0 mL/min, $\lambda = 220$ nm: $\tau_R = 4.68$ min, $\tau_S = 6.40$ min.

rac-7,7'-Bis(methoxymethoxy)-1,1'-spirobiindane (**170**)



A solution of diol *rac*-**144** (1.80 g, 7.11 mmol) in acetone (300 mL), was treated with Cs_2CO_3 (23.2 g, 71.1 mmol) and MOMCl (3.43 g, 42.6 mmol). The mixture was stirred at room temperature for 1 h and then quenched with sat. NaHCO_3 -solution. Approximately 80% of the acetone were removed under reduced pressure and the residual slurry was diluted with EtOAc (250 mL).

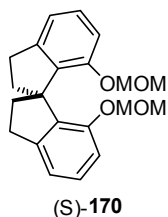
The layers were separated, the organic layer was washed with sat. NH_4Cl -solution and brine and dried over MgSO_4 . After evaporation of the solvent the residue was purified by column chromatography on silica gel (hexane:EtOAc 9:1) to afford the title compound **170** (2.40 g, 7.04 mmol, 99%) as a colorless solid.

^1H NMR (500 MHz, CDCl_3) $\delta = 7.08$ (dd, $J = 8.1, 7.5$ Hz, 2H), 6.89 (d, $J = 7.5$ Hz, 2H), 6.74 (d, $J = 8.1$ Hz, 2H), 4.88 (d, $J = 6.5$ Hz, 2H), 4.82 (d, $J = 6.5$ Hz, 2H), 3.13-3.08 (m, 2H), 3.06-3.00 (m, 2H), 3.04 (s, 6H), 2.47 (ddd, $J = 12.7, 9.1, 7.9$ Hz, 2H), 2.21 (ddd, $J = 12.8, 8.5, 4.2$ Hz, 2H) ppm.

^{13}C NMR (125 MHz, CDCl_3) $\delta = 153.6, 145.9, 137.8, 127.8, 117.9, 111.4, 93.6, 59.6, 55.6, 39.3, 31.9$ ppm.

MS (EI) m/z (%): 340 (57), 295 (10), 276 (14), 264 (100), 235 (34), 133 (28).

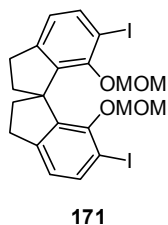
HRMS (EI) m/z calculated for $\text{C}_{21}\text{H}_{24}\text{O}_4$ 340.167460, found 340.167239.

(S)-7,7'-Bis(methoxymethoxy)-1,1'-spirobiindane ((S)-170)

For the synthesis of (S)-7,7'-bis(methoxymethoxy)-1,1'-spirobiindane ((S)-170) the method used for racemic compound **170** was slightly modified. A solution of diol (S)-**144** (1.34 g, 5.29 mmol) in acetone (90 mL), was treated with Cs₂CO₃ (14.4 g, 42.3 mmol) and MOMCl (2.13 g, 26.5 mmol). The mixture was stirred at room temperature for 4 h and then quenched with sat. NaHCO₃-solution. Approximately 80% of the acetone were removed under reduced pressure and the residual slurry was diluted with H₂O and extracted with CH₂Cl₂. The combined organic layers were dried over MgSO₄, concentrated under reduced pressure and the residue was purified by column chromatography on silica gel (hexane:EtOAc 9:1) to afford the title compound (S)-**170** (1.77 g, 5.19 mmol, 98%) as a colorless oil.

In analogous manner also (R)-7,7'-bis(methoxymethoxy)-1,1'-spirobiindane ((R)-**170**) was obtained from diol (R)-**144** as a colorless oil.

The analytical data for (S)-**170** and (R)-**170** (¹H NMR, ¹³C NMR, MS) were in agreement with those obtained for *rac*-7,7'-bis(methoxymethoxy)-1,1'-spirobiindane (**170**).

***rac*-6,6'-Diiodo-7,7'-bis(methoxymethoxy)-1,1'-spirobiindane (171)**

To a solution of MOM-protected SPINOL **170** (500 mg, 1.47 mmol) in Et₂O (5 mL) was added TMEDA (360 mg, 3.10 mmol) and the solution was cooled to -78 °C. Subsequently *n*-BuLi (1.76 mL, 4.41 mmol, 2.5 M solution in hexanes) was added dropwise. After complete addition the mixture was stirred at room temperature for 4 h before it was cooled to -78 °C again. A solution of I₂ (1.12 g, 4.41 mmol) in Et₂O (6 mL) was added over the course of 30 min and the resulting mixture was allowed to warm to room temperature over night. A saturated solution of NaHSO₃ was added, the layers were separated and the aqueous layer was extracted with Et₂O and CH₂Cl₂. The combined organic layers were dried over MgSO₄, evaporated to dryness and the residue was purified by column chromatography on silica gel (hexane:EtOAc 15:1). The product was found to be poorly soluble in the mobile phase was obtained as a mixture with another by-product. Recrystallization of this mixture from CH₂Cl₂:hexane eventually yielded the pure product **171** (394 mg, 0.665 mmol, 45%) as a colorless solid.

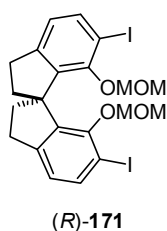
$^1\text{H NMR}$ (500 MHz, CDCl_3) δ = 7.62 (d, J = 7.9 Hz, 2H), 6.78 (d, J = 7.9 Hz, 2H), 4.85 (d, J = 5.1 Hz, 2H), 4.63 (d, J = 5.1 Hz, 2H), 3.04-2.98 (m, 4H), 2.96 (s, 6H), 2.49-2.43 (m, 2H), 2.18 (ddd, J = 12.5, 7.6, 3.0 Hz, 2H) ppm.

$^{13}\text{C NMR}$ (125 MHz, CDCl_3) δ = 154.3, 147.0, 143.7, 138.9, 122.8, 99.5, 89.2, 61.3, 57.2, 39.5, 31.2 ppm.

MS (EI) m/z (%): 516 (100), 433 (63), 401 (26), 259 (52), 45 (83).

HRMS (ESI+) m/z calculated for $\text{C}_{21}\text{H}_{22}\text{O}_4\text{I}_2\text{Na}$ ($\text{M}+\text{Na}^+$) 614.949976, found 614.950464.

(*R*)-6,6'-Diiodo-7,7'-bis(methoxymethoxy)-1,1'-spirobiindane ((*R*)-171)



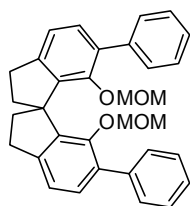
To a solution of MOM-protected SPINOL (*R*)-**170** (1.17 g, 3.44 mmol) in THF (30 mL) was added TMEDA (1.20 g, 10.3 mmol) and the solution was cooled to -78 °C. Subsequently *s*-BuLi (7.62 mL, 10.7 mmol, 1.4 M solution in hexanes) was added dropwise. After complete addition the mixture was stirred at -78 °C for 4 h before a solution of I_2 (3.50 g, 13.8 mmol) in THF (20 mL) was added

dropwise. The resulting mixture was allowed to warm to room temperature over night and a saturated solution of NaHSO_3 was added. The layers were separated, the aqueous layer was extracted with CH_2Cl_2 and the combined organic layers were dried over MgSO_4 and evaporated to dryness. Purification of the residue by column chromatography on SiO_2 (hexane:EtOAc 15:1) yielded the title compound (*R*)-**170** (1.22 g, 2.06 mmol, 60%) as a colorless solid.

In analogous manner also (*S*)-6,6'-diiodo-7,7'-bis(methoxymethoxy)-1,1'-spirobiindane ((*S*)-**171**) was obtained from (*S*)-**170** as a colorless solid.

The analytical data for (*S*)-**171** and (*R*)-**171** ($^1\text{H NMR}$, $^{13}\text{C NMR}$, MS) were in agreement with those obtained for *rac*-6,6'-diiodo-7,7'-bis(methoxymethoxy)-1,1'-spirobiindane (**171**).

After this step the optical purity was confirmed by HPLC analysis using Daicel Chiralpak AD-3 column: *n*-heptane:*i*-PrOH = 99:1, flow rate 1.0 mL/min, λ = 220 nm: τ_S = 4.26 min, τ_R = 8.95 min.

***rac*-7,7'-Bis(methoxymethoxy)-6,6'-diphenyl-1,1'-spirobiindane (173a)**

173a

A solution of diiodide **171** (500 mg, 0.844 mmol) and phenylboronic acid (**172a**, 412 mg, 3.38 mmol) in THF:MeOH (25:1, 26 mL) was degassed by passing a stream of Ar through the mixture. After 10 min Pd(PPh₃)₄ (146 mg, 0.127 mmol) and a solution of K₂CO₃ (2.66 mL, 5.32 mmol, 2 M in H₂O) were added and degassing was continued for further 5 min. The reaction mixture

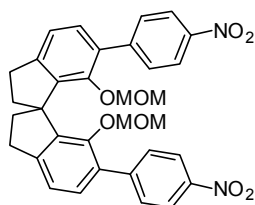
was refluxed over night, cooled to ambient temperature, diluted with H₂O (15 mL) and extracted with CH₂Cl₂. The combined organic layers were dried over MgSO₄, concentrated under reduced pressure and the residue was purified by column chromatography on SiO₂ (hexane:EtOAc 15:1) to yield the product **173a** (394 mg, 0.799 mmol, 95%) as a colorless solid.

¹H NMR (500 MHz, CDCl₃) δ = 7.52 (d, *J* = 7.7 Hz, 4H), 7.39 (dd, *J* = 7.7, 7.4 Hz, 4H), 7.29 (t, *J* = 7.4 Hz, 2H), 7.15 (d, *J* = 7.6 Hz, 2H), 7.05 (d, *J* = 7.6 Hz, 2H), 4.37 (d, *J* = 5.3 Hz, 2H), 4.23 (d, *J* = 5.3 Hz, 2H), 3.12-3.09 (m, 4H), 2.73 (s, 6H), 2.61-2.55 (m, 2H), 2.36-2.31 (m, 2H) ppm.

¹³C NMR (125 MHz, CDCl₃) δ = 151.8, 145.4, 142.6, 140.0, 133.1, 130.5, 129.3, 128.4, 126.9, 120.3, 98.6, 60.1, 56.4, 39.4, 31.3 ppm.

MS (EI) *m/z* (%): 492 (6), 416 (100), 401 (9), 233 (10), 209 (25).

HRMS (ESI+) *m/z* calculated for C₃₃H₃₂O₄Na (M+Na⁺) 515.219279, found 515.219561.

***rac*-7,7'-Bis(methoxymethoxy)-6,6'-bis(4-nitrophenyl)-1,1'-spirobiindane (173b)**

173b

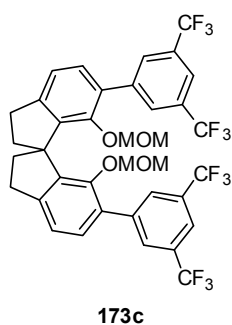
The coupling product **173b** was synthesized as reported for **173a** starting from diiodide **171** (100 mg, 0.169 mmol) and 4-nitrophenylboronic acid (**172b**, 113 mg, 0.676 mmol). Purification by column chromatography on SiO₂ (hexane:EtOAc 20:1) afforded the title compound **173b** (62.0 mg, 0.106 mmol, 63%) as a yellow solid.

¹H NMR (400 MHz, CDCl₃) δ = 8.27-8.24 (m, 4H), 7.70-7.67 (m, 4H), 7.17 (d, *J* = 7.7 Hz, 2H), 7.11 (d, *J* = 7.7 Hz, 2H), 4.31 (d, *J* = 5.5 Hz, 2H), 4.22 (d, *J* = 5.5 Hz, 2H), 3.13-3.10 (m, 4H), 2.72 (s, 6H), 2.59-2.51 (m, 2H), 2.38-2.32 (m, 2H) ppm.

¹³C NMR (100 MHz, CDCl₃) δ = 152.2, 147.2, 146.9, 146.8, 142.7, 131.1, 130.4, 130.1, 123.8, 121.0, 99.3, 60.1, 56.6, 39.5, 31.4 ppm.

MS (EI) *m/z* (%): 506 (98), 489 (12), 254 (32), 45 (100).

HRMS (ESI+) *m/z* calculated for C₃₃H₃₀N₂O₈Na (M+Na⁺) 605.189436, found 605.189619.

***rac*-6,6'-Bis(3,5-bis(trifluoromethyl)phenyl)-7,7'-bis(methoxymethoxy)-1,1'-spirobiindane**

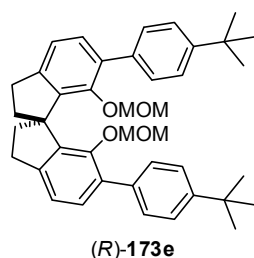
The coupling product **173c** was synthesized as reported for **173a** starting from diiodide **171** (300 mg, 0.507 mmol) and 3,5-bis(trifluoromethyl)phenylboronic acid (**172c**, 523 mg, 2.03 mmol). After purification by column chromatography on SiO₂ (hexane:EtOAc 50:1) the title compound **173c** (255 mg, 0.333 mmol, 66%) was obtained as a colorless solid.

¹H NMR (500 MHz, CDCl₃) δ = 7.99 (s, 4H), 7.80 (s, 2H), 7.18 (d, J = 7.7 Hz, 2H), 7.13 (d, J = 7.7 Hz, 2H), 4.20 (d, J = 5.5 Hz, 2H), 4.12 (d, J = 5.5 Hz, 2H), 3.21-3.09 (m, 4H), 2.74 (s, 6H), 2.63-2.56 (m, 2H), 2.38-2.33 (m, 2H) ppm.

¹³C NMR (125 MHz, CDCl₃) δ = 152.2, 147.3, 142.8, 141.9, 131.7 (q, J = 33.2 Hz), 130.5, 130.4, 129.5 (d, J = 2.2 Hz), 123.5 (q, J = 272.6 Hz), 121.2, 120.6 (quin, J = 2.4 Hz), 99.4, 60.1, 56.5, 40.0, 31.5 ppm.

MS (EI) m/z (%): 764 (1), 719 (2), 688 (91), 671 (9), 345 (48), 45 (100).

HRMS (ESI+) m/z calculated for C₃₇H₂₈O₄F₁₂Na (M+Na⁺) 787.168821, found 787.169332.

***(R)*-6,6'-Bis(4-(*tert*-butyl)phenyl)-7,7'-bis(methoxymethoxy)-1,1'-spirobiindane ((*R*)-173e)**

The coupling product (*R*)-**173e** was synthesized as reported for **173a** starting from diiodide (*R*)-**171** (200 mg, 0.338 mmol) and 4-(*tert*-butyl)phenylboronic acid (**172e**, 241 mg, 1.35 mmol). After purification by column chromatography on SiO₂ (hexane:EtOAc 20:1) the title compound (*R*)-**173e** (193 mg, 0.318 mmol, 94%) was obtained as a

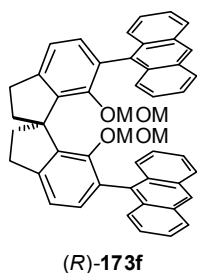
colorless solid.

¹H NMR (500 MHz, CDCl₃) δ = 7.44 (d, J = 8.3 Hz, 4H), 7.39 (d, J = 8.3 Hz, 4H), 7.14 (d, J = 7.6 Hz, 2H), 7.02 (d, J = 7.6 Hz, 2H), 4.36 (d, J = 5.3 Hz, 2H), 4.23 (d, J = 5.3 Hz, 2H), 3.08-3.06 (m, 4H), 2.69 (s, 6H), 2.57-2.51 (m, 2H), 2.33-2.29 (m, 2H), 1.33 (s, 18H) ppm.

¹³C NMR (125 MHz, CDCl₃) δ = 151.9, 149.8, 145.1, 142.6, 137.0, 133.0, 130.5, 128.9, 125.3, 120.3, 98.5, 60.1, 56.4, 39.3, 34.6, 31.5, 31.3 ppm.

MS (EI) m/z (%): 604 (9), 528 (100), 472 (74), 457 (7), 415 (5), 265 (18), 195 (21), 57 (38).

HRMS (ESI+) m/z calculated for C₄₁H₄₈O₄Na (M+Na⁺) 627.344479, found 627.344510.

(R)-6,6'-Bis(9-anthracenyl)-7,7'-bis(methoxymethoxy)-1,1'-spirobiindane ((R)-173f)

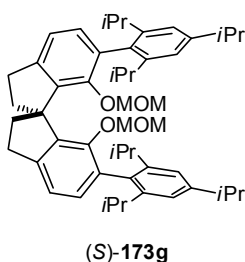
A Schlenk tube was charged with (*R*)-6,6'-diiodo-7,7'-bis(methoxymethoxy)-1,1'-spirobiindane ((*R*)-**171**, 400 mg, 0.675 mmol), 9-anthraceneboronic acid (**172f**, 600 mg, 2.70 mmol) and K_3PO_4 (1.15 g, 5.40 mmol). The solids were set under argon, taken up in DME (6 mL) and the resulting suspension was degassed. After 15 min $Pd(PPh_3)_4$ (78.0 mg, 0.068 mmol) was added and degassing was continued for further 5 min before the tube was sealed and heated to 80 °C for 48 h. After cooling to room temperature H_2O and CH_2Cl_2 were added and the layers were separated. The aqueous layer was extracted with CH_2Cl_2 , the combined extracts were dried over $MgSO_4$ and evaporated to dryness. Purification of the residue by column chromatography on SiO_2 (hexane: CH_2Cl_2 2:1) yielded the title compound (*R*)-**173f** (370 mg, 0.534 mmol, 79%) as a colorless solid.

1H NMR (400 MHz, CD_2Cl_2) δ = 8.52 (s, 2H), 8.07 (d, J = 8.1 Hz, 2H), 8.00 (d, J = 8.5 Hz, 2H), 7.95 (d, J = 8.9 Hz, 2H), 7.60 (dd, J = 8.8, 0.9 Hz, 2H), 7.51-7.42 (m, 4H), 7.23-7.19 (m, 2H), 7.15 (d, J = 7.5 Hz, 2H), 7.05 (d, J = 7.5 Hz, 2H), 6.30-6.26 (m, 2H), 4.32 (d, J = 5.7 Hz, 2H), 3.84 (d, J = 5.7 Hz, 2H), 3.33-3.25 (m, 2H), 3.14 (ddd, J = 15.8, 8.5, 1.2 Hz, 2H), 2.69-2.61 (m, 2H), 2.56 (ddd, J = 12.4, 7.9, 1.8 Hz, 2H), 2.47 (s, 6H).

^{13}C NMR (100 MHz, CD_2Cl_2) δ = 154.1, 146.0, 142.2, 134.8, 132.7, 131.9, 131.6, 130.9, 130.5, 128.9, 128.8, 127.9, 127.8, 127.2, 126.9, 126.3, 125.9, 125.8, 125.3, 120.2, 98.6, 60.5, 56.4, 39.4, 31.6 ppm.

MS (EI) m/z (%): 692 (100), 660 (29), 648 (12), 628 (32), 616 (86), 346 (11), 295 (27), 178 (13), 45 (8).

HRMS (ESI+) m/z calculated for $C_{49}H_{40}O_4Na$ ($M+Na^+$) 715.281878, found 715.282206.

(S)-7,7'-Bis(methoxymethoxy)-6,6'-bis(2,4,6-triisopropylphenyl)-1,1'-spirobiindane ((S)-173g)

In a flame-dried 50 mL three neck round bottom flask Mg (1.38 g, 56.8 mmol) was layered with a minimum amount of anhydrous Et_2O . After addition of 2,4,6-(triisopropyl)bromobenzene (\approx 0.1 mL) and a few drops of 1,2-dibromoethane the Grignard reaction was initiated by local heating (heat gun). After initiation, the remaining Et_2O (25 mL in total)

and 2,4,6-(triisopropyl)bromobenzene (9.06 g, 32.1 mmol in total) were added alternately to keep the reaction refluxing without the need for external heating. After complete addition the mixture was refluxed (oil bath heating) for 16 h. After cooling to ambient temperature one quarter of this Grignard solution (theoretically \approx 8 mmol of Grignard reagent) was added dropwise to a mixture of (*S*)-**171** (732 mg, 1.24 mmol) and Ni(PPh₃)₂Cl₂ (122 mg, 0.185 mmol) in anhydrous Et₂O (12 mL) upon which the mixture turned dark brown. The reaction mixture was refluxed for 24 h, cooled to ambient temperature, carefully quenched by slow addition of H₂O and saturated NH₄Cl-solution and diluted with CH₂Cl₂. The layers were separated and the aqueous layer extracted with CH₂Cl₂. The combined organic layers were dried over MgSO₄ and the solvent was removed under reduced pressure. The residue was purified by column chromatography on SiO₂ using hexane:CH₂Cl₂ (4:1) as the eluent yielding the title compound (*S*)-**173g** (697 mg, 0.935 mmol, 75%) as a colorless solid.

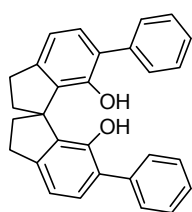
¹H NMR (500 MHz, CDCl₃) δ = 7.00 (m, 3H), 6.99-6.98 (m, 3H), 6.92-6.91 (m, 2H), 4.08 (d, *J* = 4.2 Hz, 2H), 3.88 (d, *J* = 4.2 Hz, 2H), 3.28-3.22 (m, 2H), 3.10-3.04 (m, 2H), 2.89 (sept, *J* = 6.9 Hz, 2H), 2.72-2.66 (m, 2H), 2.61 (sept, *J* = 6.9 Hz, 4H), 2.55 (s, 6H), 2.33-2.27 (m, 2H), 1.25 (d, *J* = 6.9 Hz, 12H), 1.22 (d, *J* = 6.9 Hz, 6H), 1.05-1.02 (m, 12H), 1.00 (d, *J* = 6.9 Hz, 6H) ppm.

¹³C NMR (125 MHz, CDCl₃) δ = 151.0, 148.2, 147.5, 146.8, 145.3, 143.5, 134.0, 131.6, 131.4, 120.7, 120.6, 119.8, 97.1, 60.8, 55.8, 41.5, 34.4, 31.7, 30.8, 30.7, 25.8, 25.5, 24.3, 24.3, 23.1, 23.0 ppm.

MS (EI) *m/z* (%): 744 (55), 699 (42), 668 (59), 626 (100), 595 (19), 279 (73).

HRMS (ESI+) *m/z* calculated for C₅₁H₆₈O₄Na (M+Na⁺) 767.500983, found 767.502066.

rac-6,6'-Diphenyl-1,1'-spirobiindane-7,7'-diol (**174a**)



174a

A solution of *rac*-7,7'-bis(methoxymethoxy)-6,6'-diphenyl-1,1'-spirobiindane (**173a**, 394 mg, 0.799 mmol) in MeOH:CHCl₃ (3:2, 14.5 mL) was treated with conc. HCl (5.8 mL) and the reaction mixture was refluxed for 3 h. After cooling to ambient temperature H₂O was added and the mixture was extracted with CH₂Cl₂. The combined organic layers were washed with saturated NaHCO₃-solution and brine, dried over MgSO₄ and evaporated to dryness. The residue was purified by column chromatography on silica gel using hexane:EtOAc (10:1) as the eluent to yield the diol **174a** (312 mg, 0.771 mmol, 98%) as a colorless solid.

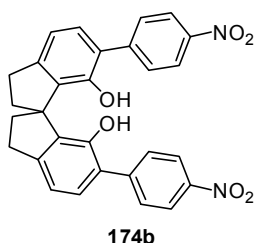
$^1\text{H NMR}$ (500 MHz, CDCl_3) δ = 7.48 (d, J = 7.6 Hz, 4H), 7.40 (dd, J = 7.6, 7.3 Hz, 4H), 7.31 (t, J = 7.3 Hz, 2H), 7.20 (d, J = 7.6 Hz, 2H), 6.94 (d, J = 7.6 Hz, 2H), 5.02 (s, 2H), 3.15-3.04 (m, 4H), 2.46-2.36 (m, 4H) ppm.

$^{13}\text{C NMR}$ (125 MHz, CDCl_3) δ = 149.6, 145.4, 137.6, 132.2, 130.7, 129.4, 128.7, 128.4, 127.4, 117.6, 58.6, 37.9, 31.3 ppm.

MS (EI) m/z (%): 404 (100), 387 (25), 327 (11), 221 (25), 208 (15), 183 (26).

HRMS (EI) m/z calculated for $\text{C}_{29}\text{H}_{24}\text{O}_2$ (M) 404.177626, found 404.177352.

***rac*-6,6'-Bis(4-nitrophenyl)-1,1'-spirobiindane-7,7'-diol (174b)**



Diol **174b** was synthesized as reported for **174a**, starting from *rac*-7,7'-bis(methoxymethoxy)-6,6'-bis(4-nitrophenyl)-1,1'-spirobiindane (**173b**, 62.0 mg, 0.106 mmol). After purification by column chromatography (hexane:EtOAc 9:1) the title compound **174b** (50.0 mg, 0.101 mmol, 95%) was obtained as a yellow solid.

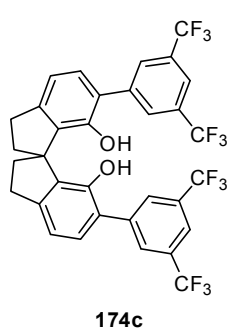
$^1\text{H NMR}$ (400 MHz, CDCl_3) δ = 8.26-8.22 (m, 4H), 7.71-7.64 (m, 4H), 7.28 (d, J = 7.7 Hz, 2H), 7.03 (d, J = 7.7 Hz, 2H), 4.96 (s, 2H), 3.20-3.07 (m, 4H), 2.47-2.42 (m, 2H), 2.39-2.31 (m, 2H) ppm.

$^{13}\text{C NMR}$ (125 MHz, CDCl_3) δ = 150.0, 147.1, 146.9, 144.6, 131.6, 131.2, 130.3, 125.3, 123.7, 118.5, 58.2, 37.8, 31.3 ppm.

MS (EI) m/z (%): 494 (100), 477 (19), 372 (7), 266 (19), 228 (23), 182 (6).

HRMS (ESI+) m/z calculated for $\text{C}_{29}\text{H}_{22}\text{N}_2\text{O}_6\text{Na}$ ($\text{M}+\text{Na}^+$) 517.137005, found 517.137249.

***rac*-6,6'-Bis(3,5-bis(trifluoromethyl)phenyl)-1,1'-spirobiindane-7,7'-diol (174c)**



Diol **174c** was synthesized according to the procedure reported for **174a**, starting from *rac*-6,6'-bis(3,5-bis(trifluoromethyl)phenyl)-7,7'-bis(methoxymethoxy)-1,1'-spirobiindane (**173c**, 190 mg, 0.248 mmol). Purification by column chromatography (hexane:EtOAc 50:1) afforded the title compound **174c** (146 mg, 0.215 mmol, 87%) as a colorless solid.

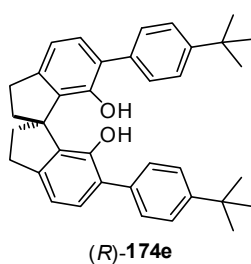
$^1\text{H NMR}$ (500 MHz, CDCl_3) δ = 8.00 (s, 4H), 7.81 (s, 2H), 7.31 (d, J = 7.7 Hz, 2H), 7.06 (d, J = 7.7 Hz, 2H), 4.95 (s, 2H), 3.21-3.11 (m, 4H), 2.48 (ddd, J = 13.2, 6.8, 1.9 Hz, 2H), 2.41-2.35 (m, 2H) ppm.

^{13}C NMR (125 MHz, CDCl_3) δ = 150.0, 147.2, 139.8, 131.8, 131.6 (q, J = 33.2 Hz), 130.8, 129.7 (d, J = 2.7 Hz), 124.8, 123.5 (q, J = 272.7 Hz), 120.9 (quin, J = 3.4 Hz), 118.7, 58.1, 37.8, 31.3 ppm.

MS (EI) m/z (%): 676 (100), 659 (19), 647 (16), 463 (9), 357 (19), 319 (23).

HRMS (ESI+) m/z calculated for $\text{C}_{33}\text{H}_{20}\text{O}_2\text{F}_{12}\text{Na}$ ($\text{M}+\text{Na}^+$) 699.116394, found 699.115990.

(*R*)-6,6'-Bis(4-(*tert*-butyl)phenyl)-1,1'-spirobiindane-7,7'-diol ((*R*)-174e)



Diol (*R*)-174e was synthesized according to the procedure reported for 174a, starting from (*R*)-6,6'-bis(4-(*tert*-butyl)phenyl)-7,7'-bis(methoxymethoxy)-1,1'-spirobiindane ((*R*)-173e, 146 mg, 0.241 mmol). After purification by column chromatography (hexane: CH_2Cl_2 4:1) the title compound (*R*)-174e (114 mg, 0.221 mmol, 91%) was

obtained as a colorless solid.

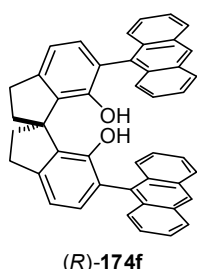
^1H NMR (500 MHz, CDCl_3) δ = 7.44-7.40 (m, 4H), 7.37-7.32 (m, 4H), 7.20 (d, J = 7.6 Hz, 2H), 6.93 (d, J = 7.6 Hz, 2H), 5.09 (br, 2H), 3.14-3.04 (m, 4H), 2.47-2.32 (m, 4H), 1.34 (s, 18H) ppm.

^{13}C NMR (125 MHz, CDCl_3) δ = 150.2, 149.7, 145.1, 134.6, 133.9, 132.2, 129.0, 129.0, 128.7, 128.6, 126.9, 125.7, 58.6, 38.0, 34.7, 31.5, 31.3 ppm.

MS (EI) m/z (%): 516 (100), 501 (26), 277 (9), 243 (28), 224 (7), 181 (6), 57 (12).

HRMS (ESI+) m/z calculated for $\text{C}_{37}\text{H}_{40}\text{O}_2\text{Na}$ ($\text{M}+\text{Na}^+$) 539.292049, found 539.292629.

(*R*)-6,6'-Bis(9-anthracenyl)-1,1'-spirobiindane-7,7'-diol ((*R*)-174f)



Diol (*R*)-174f was synthesized according to the procedure reported for 174a, starting from (*R*)-6,6'-bis(9-anthracenyl)-7,7'-bis(methoxymethoxy)-1,1'-spirobiindane ((*R*)-173f, 89.3 mg, 0.129 mmol). After purification by column chromatography (hexane: CH_2Cl_2 2:1) the title compound (*R*)-174f (114 mg, 0.221 mmol, 91%) was obtained as a colorless solid.

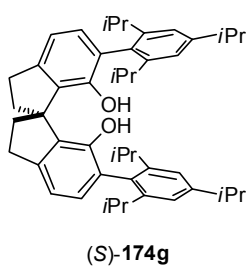
^1H NMR (500 MHz, CDCl_3) δ = 8.51 (s, 2H), 8.05 (d, J = 8.4 Hz, 2H), 8.00 (d, J = 8.4, 2H), 7.81 (d, J = 8.7 Hz, 2H), 7.48 (dd, J = 8.1, 6.7 Hz, 2H), 7.41 (dd, J = 8.0, 7.1 Hz, 2H), 7.34 (d, J = 8.8 Hz, 2H), 7.27 (dd, J = 7.3, 6.8 Hz, 2H), 7.08 (d, J = 7.5 Hz, 2H), 7.00 (d, J = 7.5 Hz, 2H), 6.48 (dd, J = 8.1, 7.2 Hz, 2H), 4.59 (s, 2H), 3.30-3.23 (m, 2H), 3.15 (dd, J = 14.7, 8.8 Hz, 2H), 2.64-2.53 (m, 4H) ppm.

^{13}C NMR (125 MHz, CDCl_3) δ = 150.8, 145.8, 133.5, 131.7, 131.7, 131.5, 131.1, 131.0, 130.8, 128.7, 128.2, 127.4, 126.6, 126.3, 126.3, 125.9, 125.5, 125.4, 122.8, 117.0, 59.0, 38.4, 31.8 ppm.

MS (EI) m/z (%): 604 (100), 575 (5), 321 (5), 302 (30), 283 (8).

HRMS (ESI+) m/z calculated for $\text{C}_{45}\text{H}_{32}\text{O}_2\text{Na}$ ($\text{M}+\text{Na}^+$) 627.229447, found 627.229264.

(S)-Bis(2,4,6-triisopropylphenyl)-1,1'-spirobiindane-7,7'-diol ((S)-174g)



Diol (S)-**174g** was synthesized according to the procedure reported for **174a**, starting from (S)-7,7'-bis(methoxymethoxy)-6,6'-bis(2,4,6-triisopropylphenyl)-1,1'-spirobiindane ((S)-**173g**, 697 mg, 0.935 mmol). Purification by column chromatography (hexane: CH_2Cl_2 4:1) afforded the title compound (S)-**174g** (557 mg, 0.848 mmol, 90%) as a colorless

solid.

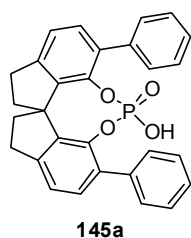
^1H NMR (500 MHz, CDCl_3) δ = 7.05 (s, 2H), 7.02 (s, 2H), 6.88 (d, J = 7.5 Hz, 2H), 6.84 (d, J = 7.5 Hz, 2H), 4.48 (s, 2H), 3.06-3.05 (m, 4H), 2.90 (sept, J = 6.9 Hz, 2H), 2.61-2.52 (m, 4H), 2.40-2.33 (m, 2H), 2.32-2.28 (m, 2H), 1.26 (d, J = 6.9 Hz, 12H), 1.11 (d, J = 6.9 Hz, 6H), 1.03-1.01 (m, 12H), 0.90 (d, J = 6.9 Hz, 6H) ppm.

^{13}C NMR (125 MHz, CDCl_3) δ = 150.1, 148.9, 148.4, 148.4, 144.7, 133.1, 130.3, 130.1, 124.5, 121.1, 121.1, 116.5, 59.0, 38.3, 34.5, 31.3, 30.5, 24.8, 24.7, 24.2, 24.1, 23.8 ppm.

MS (EI) m/z (%): 656 (100), 293 (9), 265 (21).

HRMS (ESI-) m/z calculated for $\text{C}_{47}\text{H}_{59}\text{O}_2$ ($\text{M}-\text{H}^+$) 655.452051, found 655.451876.

rac-6,6'-Diphenyl-1,1'-spirobiindane-7,7'-diyl hydrogenphosphate (145a)



A solution of diol **174a** (270 mg, 0.667 mmol) in pyridine (2.5 mL) was treated with POCl_3 (307 mg, 2.00 mmol) and heated to 80 °C for 16 h. After complete conversion of the starting material (monitored by TLC) the reaction was cooled to 0 °C, H_2O (1.5 mL) was carefully added and the mixture was again heated to 80 °C for 4 h. After cooling to ambient temperature 4 M HCl was added until pH = 1 and the mixture was extracted with CH_2Cl_2 . The solvent was removed under reduced pressure and the residue was taken up in MeOH and slowly concentrated again upon which a fraction of the product **145a** (254 mg, 0.544 mmol, 82%) precipitated as a colorless solid. The mother liquor was evaporated to dryness and the

remaining solid was purified by column chromatography on SiO₂ using CH₂Cl₂:MeOH (15:1) as the eluent. The obtained product was dissolved in CH₂Cl₂ and washed with 4 M HCl to fully protonate the phosphoric acid. Thus a second fraction of the product **145a** (20.2 mg, 0.043 mmol, 6%) was obtained, resulting in a total yield of phosphoric acid **145a** of 88%.

¹H NMR (500 MHz, CDCl₃) δ = 7.36-7.35 (m, 4H), 7.25 (d, *J* = 7.7 Hz, 2H), 7.16 (d, *J* = 7.7 Hz, 2H), 7.09-7.02 (m, 6H), 6.26 (br, 1H), 3.15-3.08 (m, 2H), 2.91 (dd, *J* = 16.2, 7.8 Hz, 2H), 2.33 (dd, *J* = 12.1, 6.4 Hz, 2H), 2.22-2.16 (m, 2H) ppm.

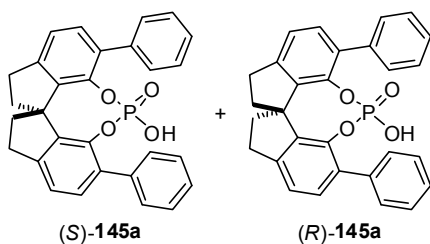
¹³C NMR (125 MHz, CDCl₃) δ = 145.4 (d, *J* = 1.8 Hz), 142.6 (d, *J* = 8.1 Hz), 140.8 (d, *J* = 3.5 Hz), 138.1, 134.5 (d, *J* = 3.8 Hz), 130.4, 129.6, 128.3, 127.0, 122.7, 60.2, 38.8, 30.4 ppm.

³¹P NMR (202 MHz, CDCl₃) δ = -11.1 ppm.

MS (EI) *m/z* (%): 446 (100), 437 (14), 386 (8), 357 (11).

HRMS (ESI-) *m/z* calculated for C₂₉H₂₂O₄P (M-H⁺) 465.126121, found 465.126312.

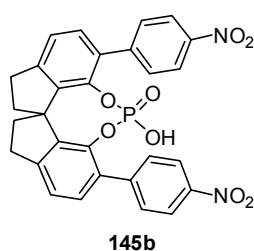
Resolution of *rac*-6,6'-diphenyl-1,1'-spirobiindane-7,7'-diyl hydrogenphosphate (**145a**) by preparative HPLC



A racemic sample of **145a** (49.2 mg, 0.105 mmol) was dissolved in CH₂Cl₂:MeOH:H₂O (15:8:1, 12 mL) and the two enantiomers (*S*)-**145a** and (*R*)-**145a** were separated by preparative HPLC using a Daicel Chiralpak QN-AX column: MeOH:0.1 M NH₄OAc (aq) = 90:10, flow rate 9.0

mL/min, column loading 1.50 mL (6.2 mg) per run, λ = 254 nm: τ₁ = 12.74 min, τ₂ = 16.88 min. The obtained fractions were evaporated to dryness, taken up in CH₂Cl₂ and washed with 4 M HCl to afford two fractions of the separated enantiomers. Fraction 1: 19.2 mg (0.041 mmol, 39%, er > 99.5:0.5). Fraction 2: 16.2 mg (0.035 mmol, 33%, er = 97.5:2.5). The absolute configuration of the products was not determined.

rac-6,6'-Bis(4-nitrophenyl)-1,1'-spirobiindane-7,7'-diyl hydrogenphosphate (**145b**)



A solution of diol **174b** (49.0 mg, 0.0991 mmol) in pyridine (1.0 mL) was treated with POCl₃ (46 mg, 0.297 mmol) and stirred at room temperature for 4 h. After complete conversion of the starting material (monitored by TLC) the reaction was carefully quenched with H₂O, then

4 M HCl was added until pH = 1 and the mixture was extracted with CH₂Cl₂. The solvent was removed under reduced pressure and the residue was taken up in THF (8 mL) and treated with 2% Na₂CO₃-solution at 70 °C for 20 h. After complete conversion of the intermediary acid chloride (monitored by TLC) the reaction was cooled to ambient temperature, acidified with 4 M HCl until pH = 1 and extracted with CH₂Cl₂. The combined organic layers were dried over MgSO₄, concentrated under reduced pressure and the residue was purified by column chromatography on SiO₂ using CH₂Cl₂:MeOH (15:1) as the eluent. The obtained product was dissolved in CH₂Cl₂ and washed with 4 M HCl to fully protonate the phosphoric acid and yield the desired product **145b** (31.0 mg, 0.056 mmol, 57%) as a yellow solid.

¹H NMR (400 MHz, CD₂Cl₂) δ = 8.11-8.08 (m, 4H), 7.66-7.63 (m, 4H), 7.32 (d, *J* = 7.7 Hz, 2H), 7.22 (d, *J* = 7.6 Hz, 2H), 3.17-3.10 (m, 2H), 2.88 (dd, *J* = 16.4, 7.8 Hz, 2H), 2.36 (dd, *J* = 12.1, 6.4 Hz, 2H), 2.20-2.13 (m, 2H) ppm.

¹³C NMR (100 MHz, CDCl₃) δ = 147.6, 147.0, 145.8, 143.7 (d, *J* = 8.0 Hz), 141.7, 132.9, 130.8, 130.6, 123.6, 122.9, 60.3, 39.1, 30.6 ppm.

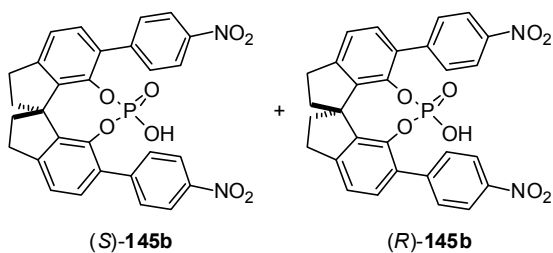
³¹P NMR (162 MHz, CD₂Cl₂) δ = -8.9 ppm.

MS (ESI-) *m/z*: 555 [M-H⁺].

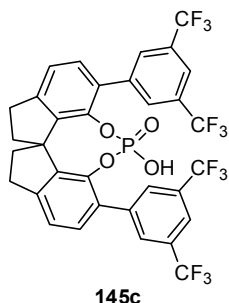
HRMS (ESI-) *m/z* calculated for C₂₉H₂₀N₂O₈P (M-H⁺) 555.096285, found 555.095743.

Resolution of *rac*-6,6'-bis(4-nitrophenyl)-1,1'-spirobiindane-7,7'-diyl hydrogenphosphate

(**145b**) by preparative HPLC



A racemic sample of **145b** (30.8 mg, 0.055 mmol) was dissolved in CH₂Cl₂:MeOH (1:1, 9 mL) and the two enantiomers (*S*)-**145b** and (*R*)-**145b** were separated by preparative HPLC using a Daicel Chiralpak QN-AX column: MeOH:AcOH = 98:2 + 5 g NH₄OAc per liter, flow rate 9.0 mL/min, column loading 1.50 mL (5.7 mg) per run, λ = 220 nm: τ₁ = 13.37 min, τ₂ = 19.77 min. The obtained fractions were evaporated to dryness, taken up in CH₂Cl₂ and washed with 4 M HCl to afford two fractions of the separated enantiomers. Fraction 1: 9.0 mg (0.016 mmol, 29%, er > 99.5:0.5). Fraction 2: 8.9 mg (0.016 mmol, 29%, er = 97.5:2.5). The absolute configuration of the products was not determined.

rac-6,6'-Bis(3,5-bis(trifluoromethyl)phenyl)-1,1'-spirobiindane-7,7'-diyl**hydrogenphosphate (145c)**

A solution of diol **174c** (300 mg, 0.443 mmol) in pyridine (1.5 mL) was treated with POCl₃ (202 mg, 1.32 mmol) and stirred at room temperature for 24 h. An additional aliquot of POCl₃ (202 mg, 1.32 mmol) was added and the reaction was stirred until complete conversion of the starting material (monitored by TLC). The reaction was carefully quenched with H₂O, then 4 M HCl was added until pH = 1 and the mixture was extracted

with CH₂Cl₂. The solvent was removed under reduced pressure and the residue was taken up in THF (30 mL) and treated with 2% Na₂CO₃-solution (2.2 mL) at 70 °C for 6 h. After complete conversion of the intermediary acid chloride (monitored by TLC) the reaction was cooled to ambient temperature, acidified with 4 M HCl until pH = 1 and extracted with CH₂Cl₂. The combined organic layers were dried over MgSO₄, concentrated under reduced pressure and the residue was purified by column chromatography on SiO₂ using hexane:EtOAc (2:1) as the eluent. The obtained product was dissolved in CH₂Cl₂ and washed with 4 M HCl to fully protonate the phosphoric acid and yield the desired product **145c** (324 mg, 0.439 mmol, 99%) as a colorless solid.

¹H NMR (500 MHz, CDCl₃) δ = 8.14 (br, 1H), 7.83 (s, 4H), 7.65 (s, 2H), 7.27 (s, 4H), 3.22-3.15 (m, 2H), 2.98 (dd, *J* = 16.3, 7.7 Hz, 2H), 2.40 (dd, *J* = 12.1, 6.4 Hz, 2H), 2.25 (dd, *J* = 19.4, 11.3 Hz, 2H) ppm.

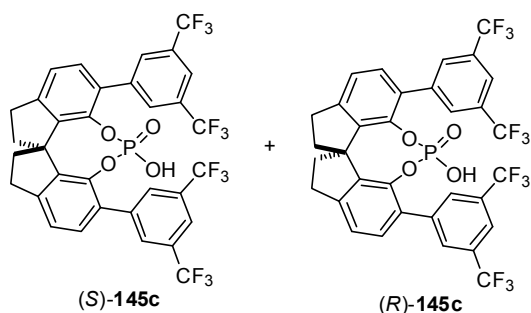
¹³C NMR (125 MHz, CDCl₃) δ = 147.6 (d, *J* = 1.9 Hz), 141.8 (d, *J* = 8.0 Hz), 140.7 (d, *J* = 3.7 Hz), 139.7, 132.1 (d, *J* = 3.7 Hz), 131.5 (q, *J* = 33.2 Hz), 130.5, 129.7, 123.6, 123.4 (q, *J* = 272.6 Hz), 120.8 (sept, *J* = 3.8 Hz), 60.1, 38.7, 30.6 ppm.

³¹P NMR (202 MHz, CD₂Cl₂) δ = -8.14 ppm.

MS (EI) *m/z* (%): 738 (37), 718 (100), 698 (6), 630 (5), 349 (17).

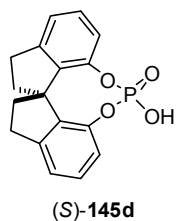
HRMS (ESI-) *m/z* calculated for C₃₃H₁₈O₄F₁₂P (M-H⁺) 737.075664, found 737.076412.

Resolution of *rac*-6,6'-bis(3,5-bis(trifluoromethyl)phenyl)-1,1'-spirobiindane-7,7'-diyl hydrogenphosphate (145c**) by preparative HPLC**



A racemic sample of **145c** (324 mg, 0.439 mmol) was dissolved in MeOH (16.5 mL) and the two enantiomers (*S*)-**145c** and (*R*)-**145c** were separated by preparative HPLC using a Daicel Chiralpak QN-AX column: MeOH:AcOH = 98:2 + 5 g NH₄OAc per liter, flow rate 9.0 mL/min, column loading 1.50 mL (30.0 mg) per run, $\lambda = 220$ nm: $\tau_1 = 3.12$ min, $\tau_2 = 4.91$ min. The obtained fractions were evaporated to dryness, taken up in CH₂Cl₂ and washed with 4 M HCl to afford two fractions of the separated enantiomers. Fraction 1: 146 mg (0.197 mmol, 45%, er > 99.5:0.5). Fraction 2: 134 mg (0.181 mmol, 41%, er > 99.5:0.5). The absolute configuration of the products was not determined.

(S)-1,1'-Spirobiindane-7,7'-diyl hydrogenphosphate (145d**)**



A solution of diol (*S*)-**144** (42.9 mg, 0.170 mmol) in pyridine (1.0 mL) was treated with POCl₃ (78.1 mg, 0.51 mmol) and stirred at room temperature for 1 h. The reaction was carefully quenched with H₂O, then 4 M HCl was added until pH = 1 and the mixture was extracted with CH₂Cl₂. The solvent was removed under reduced pressure and the residue was taken up in THF (5 mL) and treated with 2% Na₂CO₃-solution (1.0 mL) at 70 °C for 6 h. After complete conversion of the intermediary acid chloride (monitored by TLC) the reaction was cooled to ambient temperature, acidified with 4 M HCl until pH = 1 and extracted with CH₂Cl₂. The combined organic layers were dried over MgSO₄, concentrated under reduced pressure and the residue was purified by column chromatography on SiO₂ using CH₂Cl₂:MeOH (15:1) as the eluent. The obtained product was dissolved in CH₂Cl₂ and washed with 4 M HCl to fully protonate the phosphoric acid and yield the desired product **145d** (19.0 mg, 0.060 mmol, 36%) as a colorless solid.

¹H NMR (500 MHz, CDCl₃) $\delta = 10.70$ (br, 1H), 7.21-7.13 (m, 4H), 7.03 (d, $J = 7.5$ Hz, 2H), 3.13-3.06 (m, 2H), 2.83 (dd, $J = 15.9, 7.7$ Hz, 2H), 2.29-2.23 (m, 2H), 2.07-2.00 (m 2H) ppm.

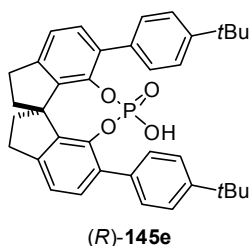
³¹P NMR (202 MHz, CD₂Cl₂) $\delta = -8.17$ ppm.

MS (EI) m/z (%): 314 (100), 299 (5), 285 (45), 233 (17), 215 (15), 189 (9).

HRMS (ESI-) m/z calculated for $C_{17}H_{14}O_4P$ ($M-H^+$) 313.063522, found 313.063659.

The obtained data are in agreement with those reported in the literature.^[218]

(R)-6,6'-Bis(4-(tert-butyl)phenyl)-1,1'-spirobiindane-7,7'-diyl hydrogenphosphate ((R)-145e)



A solution of diol (R)-**174e** (114 mg, 0.221 mmol) in pyridine (1.0 mL) was treated with $POCl_3$ (101 mg, 0.663 mmol) and heated to 80 °C for 2 h. After complete conversion of the starting material (monitored by TLC) the reaction was cooled to 0 °C, H_2O (1.0 mL) was carefully added and the mixture was again heated to 80 °C for 24 h. After cooling to

ambient temperature 4 M HCl was added until pH = 1 and the mixture was extracted with CH_2Cl_2 . The organic layers were dried over $MgSO_4$, evaporated to dryness and the remaining solid was purified by column chromatography on SiO_2 using $CH_2Cl_2:MeOH$ (100:1) as the eluent. The obtained product was dissolved in CH_2Cl_2 and washed with 4 M HCl to fully protonate the phosphoric acid yielding the title compound **145e** (114 mg, 0.198 mmol, 89%) as a colorless solid after evaporation of the solvent.

1H NMR (500 MHz, CD_2Cl_2) δ = 7.25-7.23 (m, 6H), 7.20-7.17 (m, 6H), 6.28 (br, 1H), 3.16- 3.09 (m, 2H), 2.90 (dd, J = 16.1, 7.8 Hz, 2H), 2.33 (dd, J = 12.0, 6.4 Hz, 2H), 2.16-2.10 (m, 2H), 1.14 (s, 18H) ppm.

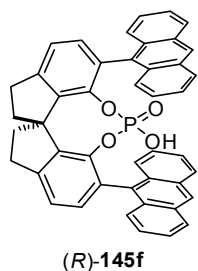
^{13}C NMR (125 MHz, CD_2Cl_2) δ = 150.0, 145.6 (d, J = 2.0 Hz), 142.6 (d, J = 8.1 Hz), 141.0, 135.1, 134.7 (d, J = 3.6 Hz), 130.5, 129.3, 125.5, 122.9, 60.3, 38.9, 34.6, 31.3, 30.5 ppm.

^{31}P NMR (202 MHz, CD_2Cl_2) δ = -9.29 ppm.

MS (EI) m/z (%): 578 (100), 563 (30), 507 (58), 466 (12), 274 (47), 57 (12).

HRMS (ESI-) m/z calculated for $C_{37}H_{38}O_4P$ ($M-H^+$) 577.251325, found 577.251752.

(R)-6,6'-Bis(9-anthracenyl)-1,1'-spirobiindane-7,7'-diyl hydrogenphosphate ((R)-145f)



At 0 °C $POCl_3$ (98.5 mg, 0.642 mmol) was added to a solution of diol (R)-**174f** (77.7 mg, 0.128 mmol) in anhydrous pyridine (1.5 mL) and the resulting mixture was heated to 80 °C in a stopper sealed flask. After 24 h a white precipitate had formed and the mixture was again cooled to 0 °C. 1,4-Dioxane (2 mL) and H_2O (0.6 mL) were added and the reaction was heated

to 100 °C for 48 h until the precipitate had completely dissolved. At ambient temperature the mixture was acidified with 4 M HCl and extracted with CH₂Cl₂. The combined organic layers were dried over MgSO₄, the solvent was removed under reduced pressure and the residue was purified by column chromatography on SiO₂ using CH₂Cl₂:MeOH (50:1 to 20:1) as the eluent. The obtained product was redissolved in CH₂Cl₂ (50 mL) and thoroughly washed with 4 M HCl to remove salt impurities and completely protonate the catalyst. The organic layer was separated and evaporated to dryness. The residue was dried *in vacuo* ($\approx 10^{-2}$ mbar) for 24 h to give the product (*R*)-**145f** (69.3 mg, 0.104 mmol, 81%) as a light yellow solid.

¹H NMR (500 MHz, CD₂Cl₂) δ = 8.25 (s, 2H), 7.92 (d, *J* = 7.6 Hz, 2H), 7.74 (d, *J* = 8.9 Hz, 2H), 7.65 (d, *J* = 8.2 Hz, 4H), 7.42-7.37 (m, 6H), 7.25 (d, *J* = 7.6 Hz, 2H), 7.22 (dd, *J* = 7.8, 7.0 Hz, 2H), 7.13 (dd, *J* = 8.4, 7.1 Hz, 2H), 3.98 (br, 1H), 3.40-3.33 (m, 2H), 3.13 (dd, *J* = 16.6, 7.9 Hz, 2H), 2.59 (dd, *J* = 12.1, 6.5 Hz, 2H), 2.49-2.43 (m, 2H) ppm.

¹³C NMR (125 MHz, CD₂Cl₂) δ = 146.8, 144.3 (d, *J* = 8.3 Hz), 140.7, 133.5, 132.4, 131.8, 131.2, 131.0, 130.4 (d, *J* = 3.9 Hz), 130.0, 128.8, 128.4, 128.1, 127.4, 126.5, 126.1, 125.2, 125.2, 124.9, 122.8, 60.5, 39.3, 30.7 ppm

³¹P NMR (202 MHz, CD₂Cl₂) δ = -12.7 ppm.

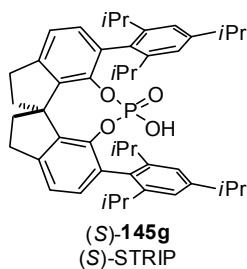
MS (EI) *m/z* (%): 666 (100), 333 (25), 265 (4).

HRMS (ESI-) *m/z* calculated for C₄₅H₃₀O₄P (M-H⁺) 665.188727, found 665.188513.

$[\alpha]_D^{25} = +445^\circ$ (c = 0.28, CH₂Cl₂).

(S)-Bis(2,4,6-triisopropylphenyl)-1,1'-spirobiindane-7,7'-diyl hydrogenphosphate ((S)-145g,

(S)-STRIP)



At 0 °C POCl₃ (543 mg, 330 μ L, 3.54 mmol) was added to a solution of (*S*)-**174g** (470 mg, 0.715 mmol) in anhydrous pyridine (13 mL) and the resulting mixture was heated to 100 °C in a stopper sealed flask. After 72 h the mixture was again cooled to 0 °C and an additional amount of POCl₃ (543 mg, 330 μ L, 3.54 mmol) was added before heating again to 100 °C for 48 h. The mixture was again cooled to 0 °C and H₂O (3.5 mL)

was carefully added dropwise. After complete addition the reaction was again heated to 100 °C for 48 h. At ambient temperature the mixture was acidified with 4 M HCl and extracted with CH₂Cl₂. The combined organic layers were dried over MgSO₄, the solvent was removed

under reduced pressure and the residue was purified by column chromatography on SiO₂ using hexane:EtOAc (2:1) as the eluent. The obtained product was redissolved in CH₂Cl₂ (150 mL) and thoroughly washed with 4 M HCl (two times) to remove salt impurities and completely protonate the catalyst. The organic layer was separated and concentrated under reduced pressure. The residue was taken up in toluene (15 mL), evaporated to dryness again and dried *in vacuo* ($\approx 10^{-2}$ mbar) for 24 h to give (*S*)-STRIP ((*S*)-**145g**, 375 mg, 0.522 mmol, 73%) as a colorless solid.

¹H NMR (500 MHz, CDCl₃) δ = 7.15 (d, *J* = 7.6 Hz, 2H), 7.10 (d, *J* = 7.6 Hz, 2H), 7.03 (d, *J* = 1.1 Hz, 2H), 6.97 (s, 2H), 3.29 (br, 1H), 3.19-3.12 (m, 2H), 2.95-2.80 (m, 6H), 2.65 (sept, *J* = 6.8 Hz, 2H), 2.31 (dd, *J* = 12.0, 6.4 Hz, 2H), 2.13-2.06 (m, 2H), 1.26 (d, *J* = 6.8 Hz, 12H), 1.21-1.19 (m, 12H), 1.12 (d, *J* = 6.7 Hz, 6H), 0.85 (d, *J* = 6.9 Hz, 6H) ppm.

¹³C NMR (125 MHz, CDCl₃) δ = 148.1 (d, *J* = 8.7 Hz), 147.5, 144.9, 143.3 (d, *J* = 8.3 Hz), 139.8, 139.8, 132.1, 132.0, 131.5 (d, *J* = 4.0 Hz), 122.0, 121.5, 120.5, 60.4, 38.6, 34.3, 30.9, 30.9, 30.2, 27.1, 25.2, 24.2, 24.1, 23.7, 23.6 ppm.

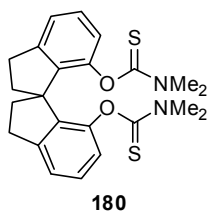
³¹P NMR (202 MHz, CDCl₃) δ = -10.45 ppm.

MS (EI) *m/z* (%): 718 (100), 675 (18), 633 (13), 591 (8), 507 (6).

HRMS (ESI-) *m/z* calculated for C₄₇H₅₈O₄P (M-H⁺) 717.407822, found 717.408188.

7.3.2 SPINOL-Derived Disulfonimides

rac-*O,O'*-(1,1'-Spirobiindane-7,7'-diyl) bis(dimethylcarbamothioate) (**180**)



NaH (1.39 g, 34.7 mmol, 60% in mineral oil) was added in several portions to a solution of *rac*-SPINOL (*rac*-**144**, 1.75 g, 6.94 mmol) in DMF (35 mL) at 0 °C. After complete addition the mixture was stirred for 20 min at 0 °C. Dimethylthiocarbamoyl chloride (3.86 g, 31.2 mmol) was added in one portion and the reaction was heated to 85 °C for 17 h. After cooling to ambient temperature the mixture was poured into 2% aqueous KOH-solution (150 mL) and CH₂Cl₂ was added. The layers were separated, the aqueous layer was extracted with CH₂Cl₂ and the combined organic layers were dried over MgSO₄. Evaporation of the solvent and

purification of the residue by column chromatography on SiO₂ (hexane:EtOAc 5:1) yielded the product **180** (1.91 g, 4.48 mmol, 65%) as a colorless solid.

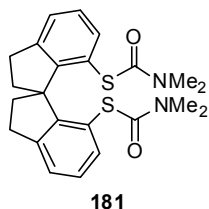
¹H NMR (500 MHz, CDCl₃) δ = 7.19 (dd, *J* = 7.8, 7.7 Hz, 2H), 7.11 (d, *J* = 7.3 Hz, 2H), 6.92 (d, *J* = 8.0 Hz, 2H), 3.22 (s, 6H), 3.10-3.03 (m, 2H), 2.95 (dd, *J* = 15.8, 8.7 Hz, 2H), 2.47 (s, 6H), 2.45-2.40 (m, 2H), 2.23 (ddd, *J* = 12.9, 8.0, 1.2 Hz, 2H) ppm.

¹³C NMR (125 MHz, CDCl₃) δ = 186.6, 150.3, 146.0, 140.4, 127.4, 122.8, 122.1, 59.1, 43.2, 38.3, 37.6, 31.3 ppm.

MS (EI) *m/z* (%): 410 (27), 338 (11), 88 (74), 72 (100).

HRMS (ESI+) *m/z* calculated for C₂₃H₂₆N₂O₂S₂Na (M+Na⁺) 449.132790, found 449.132531.

rac-*S,S'*-(1,1'-spirobiindane-7,7'-diyl) bis(dimethylcarbamothioate) (**181**)



O-Arylthiocarbamate **180** (600 mg, 1.41 mmol) was divided in two equal portions and heated two 285 °C for 45 min in a sealed vial under an Ar atmosphere. After cooling to ambient temperature the reaction mixture was directly submitted to column chromatography on silica gel (hexane:EtOAc 1:1) to afford the *S*-arylthiocarbamate **181** (485 mg, 1.14

mmol, 81%) as a colorless solid.

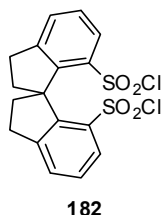
¹H NMR (500 MHz, CDCl₃) δ = 7.28 (d, *J* = 7.5 Hz, 2H), 7.24-7.20 (m, 4H), 3.10-2.98 (m, 4H), 2.85 (br, 6H), 2.66 (br, 6H), 2.36-2.29 (m, 2H), 2.27-2.22 (m, 2H) ppm.

¹³C NMR (125 MHz, CDCl₃) δ = 166.7, 153.0, 144.7, 136.7, 127.4, 125.4, 125.1, 63.3, 38.6, 36.9, 31.2 ppm.

MS (EI) *m/z* (%): 426 (16), 354 (8), 250 (7), 72 (100).

HRMS (EI) *m/z* calculated for C₂₃H₂₆N₂O₂S₂ (M) 426.143569, found 426.143447.

rac-1,1'-Spirobiindane-7,7'-disulfonyl dichloride (**182**)



A suspension of *S*-arylthiocarbamate **181** (55.0 mg, 0.129 mmol) in MeCN:2 M HCl (5:1, 1.8 mL) was cooled to 0 °C and treated with *N*-chlorosuccinimide (138 mg, 1.03 mmol). The reaction was allowed to warm to 10 °C within 30 min and was stirred at this temperature for further 15 min before being extracted with

Et₂O (3 x 10 mL). The combined organic layers were washed with brine, evaporated to dryness and the residue was submitted to column chromatography on silica gel

(hexane:CH₂Cl₂ 1:1) to afford the acid chloride **182** (45.0 mg, 0.108 mmol, 84%) as a colorless solid.

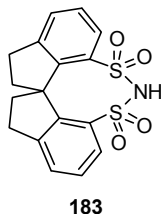
¹H NMR (500 MHz, CDCl₃) δ = 7.93 (d, *J* = 8.1 Hz, 2H), 7.63 (d, *J* = 7.4 Hz, 2H), 7.48 (dd, *J* = 8.1, 7.4 Hz, 2H), 3.28-3.23 (m, 2H), 3.19-3.12 (m, 2H), 2.69 (dd, *J* = 22.2, 10.0 Hz, 2H), 2.42 (ddd, *J* = 12.7, 8.6, 0.9 Hz, 2H) ppm.

¹³C NMR (125 MHz, CDCl₃) δ = 147.7, 146.7, 140.6, 131.8, 128.7, 128.3, 64.4, 39.0, 30.9 ppm.

MS (EI) *m/z* (%): 416 (5), 380 (35), 327 (34), 281 (100), 263 (77), 246 (35), 215 (94), 202 (96), 189 (44), 165 (11), 108 (45).

HRMS (EI) *m/z* calculated for C₁₇H₁₄O₄Cl₂S₂ 415.971061, found 415.970932.

rac-1,1'-Spirobiindane-7,7'-disulfonicacid imide (**183**)



A stream of NH₃ gas was passed through a solution of acid chloride **182** (295 mg, 0.707 mmol) in toluene (60 mL) at ambient temperature until the starting material was completely consumed (≈ 24 h, monitored by TLC). The solvent was removed *in vacuo*, the obtained solid was dissolved in CH₂Cl₂:MeOH, SiO₂ was added and the mixture evaporated to dryness. The residue was loaded onto a column packed with SiO₂ and the product was eluted with CH₂Cl₂:MeOH (15:1). After evaporation the residue was redissolved in CH₂Cl₂ and thoroughly washed with 6 M HCl to afford the disulfonimide **183** (244 mg, 0.675 mmol, 95%) as a colorless solid after removal of the solvent and drying *in vacuo* (≈ 10⁻² mbar).

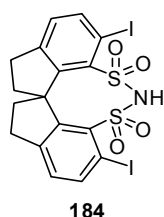
¹H NMR (500 MHz, CD₂Cl₂) δ = 7.78 (d, *J* = 7.9 Hz, 2H), 7.65 (dd, *J* = 7.5, 0.5 Hz, 2H), 7.46 (dd, *J* = 7.9, 7.5 Hz, 2H), 3.42 (s, 1H), 3.16-3.09 (m, 2H), 3.02-2.97 (m, 2H), 2.34-2.26 (m, 4H) ppm.

¹³C NMR (125 MHz, CD₂Cl₂) δ = 148.3, 146.5, 132.0, 130.5, 128.1, 126.8, 64.9, 37.5, 30.1 ppm.

MS (ESI-) *m/z*: 359.8 (M-H⁺).

HRMS (ESI-) *m/z* calculated for C₁₇H₁₄NO₄S₂ (M-H⁺) 360.036978, found 360.036543.

rac-6,6'-Diiodo-1,1'-spirobiindane-7,7'-disulfonicacid imide (**184**)



A solution of disulfonimide **183** (260 mg, 0.719 mmol) and TMEDA (376 mg, 3.24 mmol) in THF (7.5 mL) was cooled to -78 °C and *s*-BuLi (2.31 mL, 3.24 mmol, 1.4 M solution in hexane) was added dropwise. After complete addition the mixture was stirred at -78 °C for 4 h before a solution of I₂ (1.10 g, 4.32

mmol) in THF (5.0 mL) was added dropwise. The reaction was allowed to warm to ambient temperature over night and was quenched with saturated aqueous $\text{Na}_2\text{S}_2\text{O}_3$ -solution. The mixture was extracted with CH_2Cl_2 and evaporated to dryness. The residue was taken up in CH_2Cl_2 again and washed with 6 M HCl. After evaporation of the solvent the residue was purified by column chromatography on SiO_2 (CH_2Cl_2 :MeOH 15:1) to afford the product **184** (242 mg, 0.395 mmol, 95%) as a colorless solid.

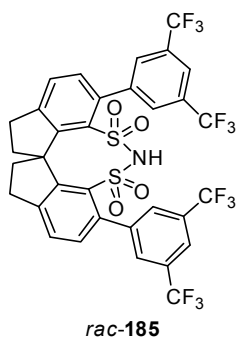
$^1\text{H NMR}$ (500 MHz, CD_2Cl_2 :MeOD) δ = 7.97 (d, J = 7.9 Hz, 2H), 7.00 (d, J = 8.0 Hz, 2H), 2.97-2.90 (m, 2H), 2.82-2.76 (m, 2H), 2.37-2.31 (m, 2H), 2.05-2.02 (m, 2H) ppm.

$^{13}\text{C NMR}$ (125 MHz, CD_2Cl_2 :MeOD) δ = 151.2, 145.5, 142.4, 135.2, 130.0, 87.0, 69.4, 36.7, 29.3 ppm

MS (EI) m/z (%): 613 (100), 532 (8), 470 (5), 341 (10), 214 (8), 101 (9).

HRMS (ESI-) m/z calculated for $\text{C}_{17}\text{H}_{12}\text{NO}_4\text{I}_2\text{S}_2$ ($\text{M}-\text{H}^+$) 611.830273, found 611.830677.

***rac*-6,6'-Bis(3,5-bis(trifluoromethyl)phenyl)-1,1'-spirobiindane-7,7'-disulfonicacid imide (*rac*-185)**



A Schlenk tube was charged with *rac*-6,6'-diiodo-1,1'-spirobiindane-7,7'-disulfonicacid imide (**184**, 103 mg, 0.168 mmol), 3,5-bis(trifluoromethyl)phenylboronic acid (**172c**, 217 mg, 0.840 mmol) and K_3PO_4 (357 mg, 1.68 mmol). The solids were set under argon, taken up in DME (3.5 mL) and the resulting suspension was degassed. After 10 min $\text{Pd}(\text{PPh}_3)_4$ (19.4 mg, 0.017 mmol) was added and degassing was continued for further 5 min before the tube was sealed and heated to 80 °C for 66 h. After cooling to room temperature H_2O and CH_2Cl_2 were added and the layers were separated. The aqueous layer was extracted with CH_2Cl_2 , the combined extracts were dried over MgSO_4 and evaporated to dryness. The residue was purified by column chromatography on SiO_2 (CH_2Cl_2 :MeOH 15:1) and the obtained product was redissolved in CH_2Cl_2 , washed with 4 M HCl and evaporated to dryness to yield the title compound *rac*-**185** (95.2 mg, 0.121 mmol, 72%) as a colorless solid.

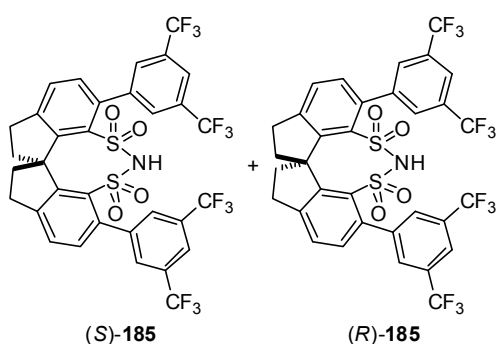
$^1\text{H NMR}$ (500 MHz, CD_2Cl_2) δ = 7.89 (s, 2H), 7.79 (s, 2H), 7.75 (s, 2H), 7.67 (d, J = 7.7 Hz, 2H), 7.21 (d, J = 7.7 Hz, 2H), 3.23-3.16 (m, 2H), 3.11-3.06 (m, 2H), 2.58-2.52 (m, 2H), 2.42-2.38 (m, 2H) ppm.

^{13}C NMR (125 MHz, CD_2Cl_2) δ = 150.6, 146.9, 142.6, 137.3, 132.0, 131.2, 131.0 (q, J = 33.1 Hz), 130.6 (q, J = 33.2 Hz), 130.6 (br), 128.8 (br), 128.5, 123.8 (q, J = 272.6 Hz), 123.7 (q, J = 272.9 Hz), 121.7 (sept, J = 1.9 Hz), 67.7, 37.6, 29.8 ppm.

MS (ESI-) m/z : 784 ($\text{M}-\text{H}^+$).

HRMS (ESI+) m/z calculated for $\text{C}_{33}\text{H}_{19}\text{F}_{12}\text{NO}_4\text{S}_2\text{Na}$ ($\text{M}+\text{Na}^+$) 808.045615, found 808.045554.

Resolution of *rac*-6,6'-bis(3,5-bis(trifluoromethyl)phenyl)-1,1'-spirobiindane-7,7'-disulfonicacid imide (*rac*-185) by preparative HPLC



A racemic sample of *rac*-185 (35.3 mg, 44.9 μmol) was dissolved in MeOH (1.0 mL) and the two enantiomers (*S*)-185 and (*R*)-185 were separated by preparative HPLC using a Daicel Chiralpak QN-AX column: MeOH:AcOH = 90:10 + 5 g NH_4OAc per liter, flow rate 9.0 mL/min, column loading 0.20 mL (7.8 mg) per run, λ = 254 nm: τ_1 = 3.30 min, τ_2 = 3.58 min.

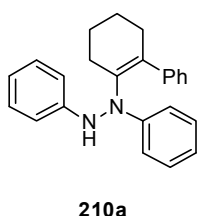
The obtained fractions were evaporated to dryness, taken up in CH_2Cl_2 and washed with 4 M HCl to afford two fractions of the separated enantiomers. Fraction 1: 8.9 mg (11.3 μmol , 25%, er > 99.5:0.5). Fraction 2: 7.3 mg (9.28 μmol , 21%, er = 98:2). The absolute configuration of the products was not determined.

7.4 The Catalytic Asymmetric Fischer Indolization

7.4.1 Indolenines and Indolines

7.4.1.1 Indolenines from Enehydrazines

1,2-Diphenyl-1-(3,4,5,6-tetrahydro-[1,1'-biphenyl]-2-yl)hydrazine (**210a**)



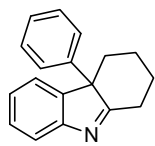
A mixture of 3,4,5,6-tetrahydro-[1,1'-biphenyl]-2-yl trifluoromethanesulfonate^[219] (**203**, 123 mg, 0.402 mmol), hydrazobenzene (**208**, 95.8 mg, 0.520 mmol), Pd₂(dba)₃ (10.9 mg, 0.012 mmol), Xantphos (20.8 mg, 0.036 mmol) and Cs₂CO₃ (182.5 mg, 0.560 mmol) in dioxane (2.5 mL) was degassed for 5 min and then heated to 50 °C for 24 h. After cooling to room temperature, the solids were filtered off, washed with CH₂Cl₂ and the combined filtrates were concentrated under reduced pressure. The residue was purified by column chromatography on deactivated silica gel (7.5% NH₃) using hexane:EtOAc (50:1) as the eluent to afford the product **210a** (92.6 mg, 0.272 mmol, 68%) as a light yellow solid.

¹H NMR (500 MHz, CD₂Cl₂) δ = 7.32-7.25 (m, 3H), 7.22 (dd, *J* = 8.6, 7.3 Hz, 2H), 7.18-7.16 (m, 2H), 7.09 (dd, *J* = 8.3, 7.4 Hz, 2H), 6.86 (d, *J* = 7.8 Hz, 2H), 6.81 (t, *J* = 7.3 Hz, 1H), 6.76 (t, *J* = 7.4 Hz, 1H), 6.46 (d, *J* = 7.7 Hz, 2H), 5.39 (s, 1H), 2.45-2.43 (m, 2H), 2.37 (m, 2H), 1.83-1.74 (m, 4H) ppm.

¹³C NMR (125 MHz, CD₂Cl₂) δ = 149.0, 148.4, 142.5, 137.9, 133.6, 129.3, 129.2, 128.9, 127.6, 127.5, 119.9, 119.3, 114.8, 113.2, 31.8, 28.2, 23.4, 23.3 ppm.

MS (EI) *m/z* (%): 340 (40), 248 (100), 206 (26), 170 (5), 145 (5), 115 (7), 91 (28), 77 (17).

HRMS (EI) *m/z* calculated for C₂₄H₂₄N₂ 340.193951, found 340.193615.

***rac*-4a-Phenyl-2,3,4,4a-tetrahydro-1H-carbazole (*rac*-211a)****211a**

A mixture of enehydrazine **210a** (26.0 mg, 0.076 mmol) and diphenylphosphate (3.75 mg, 0.015 mmol) in toluene (0.75 mL) was heated to 50 °C for 70 h. After cooling to ambient temperature, the mixture was directly

submitted to column chromatography on silica gel, eluting with hexane:EtOAc (4:1) to afford the product *rac*-**211a** (8.09 mg, 0.033 mmol, 43%) as a colorless solid.

¹H NMR (500 MHz, CD₂Cl₂) δ = 7.58 (d, J = 7.8 Hz, 1H), 7.31 (dd, J = 7.8, 7.5 Hz, 2H), 7.26 (ddd, J = 7.9, 5.9, 2.3 Hz, 1H), 7.23 (t, J = 7.3 Hz, 1H), 7.11-7.08 (m, 4H), 3.17-3.13 (m, 1H), 2.93-2.89 (m, 1H), 2.53 (ddd, J = 12.9, 12.9, 5.9 Hz, 1H), 2.13-2.09 (m, 1H), 1.73-1.70 (m, 1H), 1.67-1.56 (m, 1H), 1.56-1.47 (m, 1H), 1.27 (ddd, J = 13.7, 13.5, 3.4 Hz, 1H) ppm.

¹³C NMR (125 MHz, CD₂Cl₂) δ = 189.1, 154.7, 148.0, 139.1, 129.6, 127.8, 127.3, 126.4, 125.4, 122.5, 120.7, 63.2, 36.9, 30.9, 29.6, 22.2 ppm.

MS (EI) m/z (%): 247 (100), 218 (26), 204 (8), 170 (6), 109 (6), 89 (4).

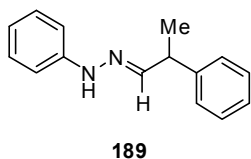
HRMS (EI) m/z calculated for C₁₈H₁₇N 247.136097, found 247.136273.

The enantiomeric ratio was determined by HPLC analysis using Daicel Chiralcel OD-H column: *n*-heptane:*i*-PrOH = 98:2, flow rate 0.5 mL/min, λ = 220 nm: τ_1 = 15.48 min, τ_2 = 17.09 min.

7.4.1.2 Fischer Indolizations of Phenylhydrazones from α -Branched Aldehydes.

General procedure for the synthesis of phenylhydrazones from α -branched aldehydes:

Phenylhydrazine (**100a**, 1 equiv) and the corresponding α -branched aldehyde (1.01 equiv) were stirred in toluene (0.3-0.4M) at room temperature until hydrazone formation was complete (monitored by TLC). The solvent was removed under reduced pressure and the residue was dried *in vacuo* to yield the crude hydrazones as yellow oils, which were immediately used without further purification.

Phenyl-2-(2-phenylpropylidene)hydrazine (189)

The reaction was conducted on a 4.62 mmol scale.

Yield: Yellow oil 1.03 g (4.59 mmol, 99%).

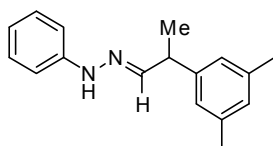
$^1\text{H NMR}$ (500 MHz, CDCl_3) δ = 7.33 (dd, J = 7.6, 7.5 Hz, 2H), 7.28-7.23 (m, 5H), 7.21-7.16 (m, 1H), 7.13 (d, J = 5.3 Hz, 1H), 7.02 (d, J = 7.9 Hz, 2H),

6.83 (t, J = 7.3 Hz, 1H), 3.77-3.72 (m, 1H), 1.52 (d, J = 7.1 Hz, 3H) ppm.

$^{13}\text{C NMR}$ (125 MHz, CDCl_3) δ = 145.5, 143.7, 143.5, 129.4, 128.8, 127.7, 126.8, 119.7, 112.7, 42.6, 19.2 ppm.

MS (EI) m/z (%): 224 (100), 209 (8), 182 (8), 130 (38), 119 (22), 105 (35), 93 (58).

HRMS (EI) m/z calculated for $\text{C}_{15}\text{H}_{16}\text{N}_2$ 224.131350, found 224.131442.

1-(2-(3,5-Dimethylphenyl)propylidene)-2-phenylhydrazine

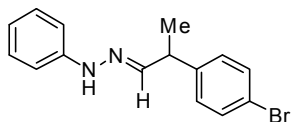
The reaction was conducted on a 0.378 mmol scale.

Yield: Yellow oil 93.8 mg (0.370 mmol, 98%).

$^1\text{H NMR}$ (500 MHz, CDCl_3) δ = 7.31 (dd, J = 8.4, 7.5 Hz, 2H), 7.25 (br, 1H), 7.15 (d, J = 5.2 Hz, 1H), 7.08 (dd, J = 8.5, 0.9 Hz, 1H), 6.98-6.94 (m, 3H), 6.89 (t, J = 7.4 Hz, 1H), 3.74-3.69 (m, 1H), 2.37 (s, 6H), 1.55 (d, J = 7.0 Hz, 3H) ppm.

$^{13}\text{C NMR}$ (125 MHz, CDCl_3) δ = 145.5, 144.0, 143.4, 138.3, 129.3, 128.4, 125.4, 119.6, 112.6, 42.5, 21.4, 19.2 ppm.

Mass spectra were not obtained due to decomposition of the material.

1-(2-(4-Bromophenyl)propylidene)-2-phenylhydrazine

The reaction was conducted on a 0.488 mmol scale.

Yield: Yellow oil 147 mg (0.484 mmol, 99%).

$^1\text{H NMR}$ (500 MHz, CDCl_3) δ = 7.47 (d, J = 8.4 Hz, 2H), 7.29-7.25 (m, 3H), 7.16 (d, J = 8.4 Hz, 2H), 7.06 (d, J = 5.2 Hz, 1H), 7.03 (d, J = 7.6 Hz, 2H), 6.87 (t, J = 7.3 Hz, 1H), 3.75-3.69 (m, 1H), 1.51 (d, J = 7.1 Hz, 3H) ppm.

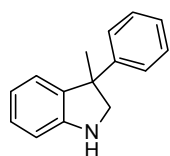
$^{13}\text{C NMR}$ (125 MHz, CDCl_3) δ = 145.3, 142.7, 142.5, 131.8, 129.4, 129.4, 120.5, 119.9, 112.7, 42.0, 19.1 ppm.

Mass spectra were not obtained due to decomposition of the material.

General procedure for the synthesis of indolines via the catalytic asymmetric Fischer indolization:

A Schlenk tube with an internal cooling finger was charged with the corresponding hydrazone (0.100 mmol) under argon. Benzene (2.0 mL) and phosphoric acid catalyst **33e** (6.01 mg, 0.010 mmol, 10 mol%) were added and the mixture was heated to 80 °C under a slight Ar stream. After complete conversion of the starting material, the mixture was cooled to room temperature, diluted with MeOH (1.0 mL) and NaCNBH₃ (62.8 mg, 1.00 mmol) was added. After stirring at room temperature for 30 min, silica gel (500 mg) was added and stirring was continued for another 30 min. The solvent was removed under reduced pressure and the residue was loaded onto a column packed with silica gel and eluted with hexane:EtOAc to afford the pure indoline product.

3-Methyl-3-phenylindoline (217)



217

Purification: CC on SiO₂ (hexane:EtOAc 9:1).

Yield: Colorless oil 15.1 mg (0.072 mmol, 72%).

¹H NMR (400 MHz, CD₂Cl₂) δ = 7.35-7.27 (m, 4H), 7.20 (tt, *J* = 7.0, 1.5 Hz, 1H), 7.07 (ddd, *J* = 7.6, 7.6, 1.3 Hz, 1H), 6.97-6.95 (m, 1H), 6.76-6.70 (m, 2H), 3.84

(br, 1H), 3.73 (d, *J* = 9.0 Hz, 1H), 3.58 (d, *J* = 9.0 Hz, 1H), 1.71 (s, 3H) ppm.

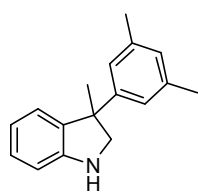
¹³C NMR (100 MHz, CD₂Cl₂) δ = 151.4, 148.4, 137.3, 128.5, 128.0, 126.8, 126.5, 124.3, 119.0, 110.1, 63.9, 49.9, 26.4 ppm.

MS (EI) *m/z* (%): 209 (40), 194 (100), 165 (9), 132 (7), 117 (6).

HRMS (EI) *m/z* calculated for C₁₅H₁₅N 209.120447, found 209.120287.

The enantiomeric ratio was determined by HPLC analysis using Daicel Chiralcel OD-3 column: *n*-heptane:*i*-PrOH = 90:10, flow rate 1.0 mL/min, λ = 220 nm: τ₁ = 4.23 min, τ₂ = 5.20 min.

3-(3,5-Dimethylphenyl)-3-methylindoline (221)^[220]



221

Purification: CC on SiO₂ (hexane:EtOAc 20:1).

Yield: Colorless oil 10.4 mg (0.044 mmol, 44%).

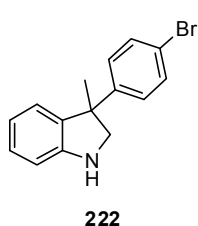
¹H NMR (500 MHz, CDCl₃) δ = 7.10 (ddd, *J* = 7.6, 7.6, 1.2 Hz, 1H), 6.98 (d, *J* = 7.3 Hz, 1H), 6.93 (s, 2H), 6.85 (s, 1H), 6.79 (ddd, *J* = 7.5, 7.4, 0.8 Hz, 1H), 6.76 (d, *J* = 7.8 Hz, 1H), 3.73 (d, *J* = 9.0 Hz, 1H), 3.55 (d, *J* = 9.0 Hz, 1H), 2.28 (s,

6H), 1.69 (s, 3H) ppm.

^{13}C NMR (125 MHz, CDCl_3) δ = 150.3, 147.6, 137.7, 137.6, 128.1, 127.7, 124.6, 124.4, 119.5, 110.4, 63.8, 49.7, 26.6, 21.6 ppm.

The enantiomeric ratio was determined by HPLC analysis using Daicel Chiralcel OD-3 column: *n*-heptane:*i*-PrOH = 98:2, flow rate 1.0 mL/min, λ = 220 nm: τ_1 = 4.79 min, τ_2 = 5.44 min.

3-(4-Bromophenyl)-3-methylindoline (222)^[220]



Purification: PTC on SiO_2 hexane:EtOAc (9:1).

Yield: Yellow oil (traces).

^1H NMR (500 MHz, CDCl_3) δ = 7.42-7.39 (m, 2H), 7.20-7.19 (m, 2H), 7.11 (ddd, J = 7.7, 7.6, 1.1 Hz, 1H), 6.95 (d, J = 6.9 Hz, 1H), 6.78 (ddd, J = 7.5, 7.3, 0.6 Hz, 1H), 6.74 (d, J = 7.9 Hz, 1H), 3.67 (d, J = 9.0 Hz, 1H), 3.57 (d, J = 9.0 Hz,

1H), 3.33 (br, 1H), 1.70 (s, 3H) ppm.

^{13}C NMR (125 MHz, CDCl_3) δ = 150.7, 146.9, 136.5, 131.4, 128.6, 128.1, 124.1, 120.3, 119.3, 110.2, 63.7, 49.5, 26.1 ppm.

The enantiomeric ratio was determined by HPLC analysis using Daicel Chiralcel OD-3 column: *n*-heptane:*i*-PrOH = 99:1, flow rate 1.0 mL/min, λ = 220 nm: τ_1 = 11.67 min, τ_2 = 12.23 min.

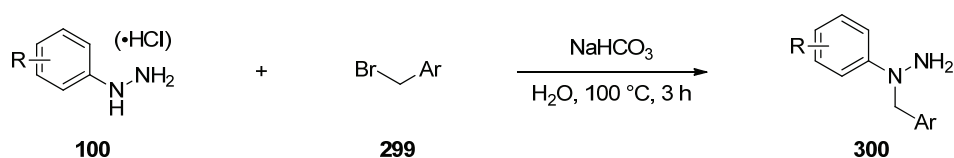
The obtained data match those reported in the literature.^[148]

7.4.2 Tetrahydrocarbazoles

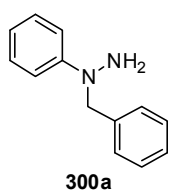
7.4.2.1 Synthesis of Hydrazines

General procedure for the *N*-benzylation of arylhydrazines:

The *N*-benzylation of arylhydrazines was accomplished following a literature reported protocol.^[193]



The hydrazine or its hydrochloride salt **100** (1 equiv), the corresponding benzyl bromide **299** (1 equiv) and NaHCO₃ (1 equiv for hydrazines, 2 equiv for hydrochloride salts) were mixed in H₂O (3-5 mL per 4 mmol of **100**) and heated to 100 °C under vigorous stirring. After 3 h the mixture was cooled to room temperature and diluted with Et₂O (30 mL). The layers were separated, the organic layer was dried over MgSO₄ and concentrated under reduced pressure. The residue was purified by column chromatography on silica gel.

1-Benzyl-1-phenylhydrazine (**300a**)

The reaction was conducted on a 8.00 mmol scale.

Purification: CC on SiO₂ (pentane:Et₂O 3:1).

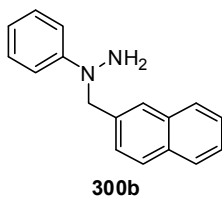
Yield: Orange solid 833 mg (4.20 mmol, 53%).

¹H NMR (500 MHz, CDCl₃) δ = 7.36-7.27 (m, 7H), 7.11 (d, *J* = 7.9 Hz, 2H), 6.84 (t, *J* = 7.3 Hz, 1H), 4.60 (s, 2H), 3.74 (br, 2H) ppm.

¹³C NMR (125 MHz, CD₂Cl₂) δ = 151.6, 137.5, 129.2, 128.8, 128.1, 127.6, 119.1, 114.1, 60.6 ppm.

MS (EI) *m/z* (%): 198 (36), 107 (100), 91 (24), 77 (34), 65 (7).

HRMS (EI) *m/z* calculated for C₁₃H₁₄N₂ 198.115696, found 198.115879.

1-(Naphthalen-2-ylmethyl)-1-phenylhydrazine (300b)

The reaction was conducted on a 4.00 mmol scale.

Purification: CC on SiO₂ (pentane:Et₂O 4:1).

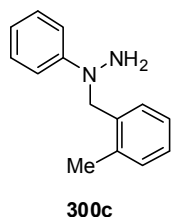
Yield: Yellow solid 411 mg (1.75 mmol, 44%).

¹H NMR (500 MHz, CD₂Cl₂) δ = 7.86-7.84 (m, 2H), 7.83-7.81 (m, 1H), 7.77 (s, 1H), 7.51-7.45 (m, 3H), 7.28-7.24 (m, 2H), 7.14-7.11 (m, 2H), 6.80 (tt, *J* = 7.3, 0.9 Hz, 1H), 4.75 (s, 2H), 3.62 (br, 2H) ppm.

¹³C NMR (125 MHz, CD₂Cl₂) δ = 152.3, 135.9, 133.8, 133.2, 129.3, 128.7, 128.0, 128.0, 126.8, 126.5, 126.3, 126.1, 118.7, 113.8, 60.9 ppm.

MS (EI) *m/z* (%): 248 (44), 141 (100), 115 (18), 107 (62), 77 (13).

HRMS (ESI+) *m/z* calculated for C₁₇H₁₆N₂Na (M+Na⁺) 271.120564, found 271.120526.

1-(2-Methylbenzyl)-1-phenylhydrazine (300c)

The reaction was conducted on a 4.00 mmol scale.

Purification: CC on SiO₂ (pentane:Et₂O 4:1).

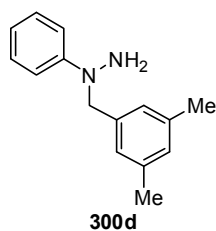
Yield: Yellow solid 495 mg (2.33 mmol, 58%).

¹H NMR (500 MHz, CD₂Cl₂) δ = 7.26-7.15 (m, 6H), 7.08-7.06 (m, 2H), 6.78 (tt, *J* = 7.3, 1.0 Hz, 1H), 4.55 (s, 2H), 3.57 (br, 2H), 2.36 (s, 3H) ppm.

¹³C NMR (125 MHz, CD₂Cl₂) δ = 152.3, 137.1, 135.9, 130.8, 129.3, 128.3, 127.5, 126.2, 118.4, 113.5, 58.7, 19.2 ppm.

MS (EI) *m/z* (%): 212 (38), 107 (100), 91 (4), 77 (31).

HRMS (EI) *m/z* calculated for C₁₄H₁₆N₂ 212.131344, found 212.131168.

1-(3,5-Dimethylbenzyl)-1-phenylhydrazine (300d)

The reaction was conducted on a 5.00 mmol scale.

Purification: CC on SiO₂ (hexane:EtOAc 9:1).

Yield: Yellow solid 490 mg (2.17 mmol, 43%).

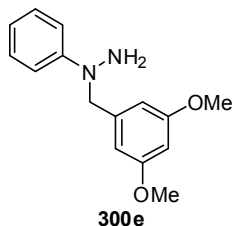
¹H NMR (500 MHz, CD₂Cl₂) δ = 7.23 (dd, *J* = 8.8, 7.3 Hz, 2H), 7.08-7.06 (m, 2H), 6.93 (s, 3H), 6.76 (tt, *J* = 7.3, 0.9 Hz, 1H), 4.49 (s, 2H), 3.56 (br, 2H), 2.29 (s, 6H) ppm.

^{13}C NMR (125 MHz, CD_2Cl_2) δ = 152.3, 138.6, 138.1, 129.2, 129.2, 126.0, 118.4, 113.7, 60.6, 21.4 ppm.

MS (EI) m/z (%): 226 (46), 211 (6), 119 (63), 107 (100).

HRMS (EI) m/z calculated for $\text{C}_{15}\text{H}_{18}\text{N}_2$ 226.146994, found 226.146925.

1-(3,5-Dimethoxybenzyl)-1-phenylhydrazine (300e)



The reaction was conducted on a 5.00 mmol scale.

Purification: CC on SiO_2 (pentane: Et_2O 3:1 to 1:1).

Yield: Colorless solid 792 mg (3.07 mmol, 61%).

^1H NMR (500 MHz, CD_2Cl_2) δ = 7.26-7.22 (m, 2H), 7.08-7.06 (m, 2H), 6.77 (tt, J = 7.2, 0.9 Hz, 1H), 6.46 (d, J = 2.3 Hz, 2H), 6.37 (t, J = 2.3 Hz, 1H),

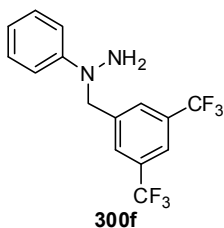
4.52 (s, 2H), 3.75 (s, 6H), 3.60 (br, 2H) ppm.

^{13}C NMR (125 MHz, CD_2Cl_2) δ = 161.5, 152.2, 140.8, 129.2, 118.6, 113.8, 105.9, 99.3, 60.8, 55.6 ppm.

MS (EI) m/z (%): 258 (64), 152 (69), 121 (8), 107 (100), 77 (30).

HRMS (ESI+) m/z calculated for $\text{C}_{15}\text{H}_{18}\text{N}_2\text{O}_2\text{Na}$ ($\text{M}+\text{Na}^+$) 281.126046, found 281.125871.

1-(3,5-Bis(trifluoromethyl)benzyl)-1-phenylhydrazine (300f)



The reaction was conducted on a 4.00 mmol scale.

Purification: CC on SiO_2 (pentane: Et_2O 4:1).

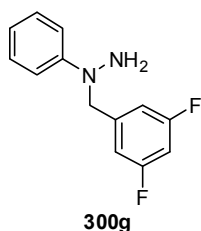
Yield: Yellow oil 976 mg (2.92 mmol, 73%).

^1H NMR (500 MHz, CD_2Cl_2) δ = 7.84 (s, 3H), 7.30-7.23 (m, 2H), 7.03-7.00 (m, 2H), 6.88-6.84 (m, 1H), 4.69 (s, 2H), 3.75 (br, 2H) ppm.

^{13}C NMR (125 MHz, CD_2Cl_2) δ = 152.0, 142.2, 131.9 (q, J = 33.5 Hz), 129.5, 128.3 (br), 123.9 (q, J = 272.6 Hz), 121.6 (sept, J = 4.0 Hz), 119.6, 113.7, 60.3 ppm.

MS (EI) m/z (%): 334 (13), 227 (5), 107 (100).

HRMS (EI) m/z calculated for $\text{C}_{15}\text{H}_{12}\text{N}_2\text{F}_6$ 334.090471, found 334.090074.

1-(3,5-Difluorobenzyl)-1-phenylhydrazine (300g)

The reaction was conducted on a 4.0 mmol scale.

Purification: CC on SiO₂ (pentane:Et₂O 5:1).

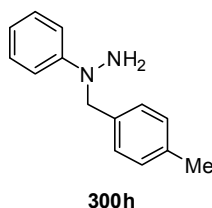
Yield: Colorless oil 582 mg (2.48 mmol, 62%).

¹H NMR (500 MHz, CD₂Cl₂) δ = 7.82-7.24 (m, 2H), 7.01-6.99 (m, 2H), 6.90-6.86 (m, 2H), 6.82 (tt, *J* = 7.3, 0.9 Hz, 1H), 6.75 (tt, *J* = 9.0, 2.3 Hz, 1H), 4.59 (s, 2H), 3.72 (br, 2H) ppm.

¹³C NMR (125 MHz, CD₂Cl₂) δ = 163.6 (dd, *J* = 248.2, 12.7 Hz), 151.8, 143.3 (t, *J* = 8.3 Hz), 129.4, 119.0, 113.4, 110.6 (dd, *J* = 19.6, 6.0 Hz), 102.7 (t, *J* = 25.7 Hz), 60.0 (t, *J* = 1.8 Hz) ppm.

MS (EI) *m/z* (%): 234 (35), 127 (13), 107 (100), 77 (43).

HRMS (EI) *m/z* calculated for C₁₃H₁₂N₂F₂ 234.096857, found 234.096643.

1-(4-Methylbenzyl)-1-phenylhydrazine (300h)

The reaction was conducted on a 4.00 mmol scale.

Purification: CC on SiO₂ pentane:Et₂O (4:1).

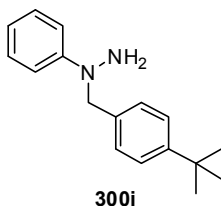
Yield: Yellow solid 371 mg (1.75 mmol, 44%).

¹H NMR (500 MHz, CD₂Cl₂) δ = 7.27-7.23 (m, 2H), 7.20 (d, *J* = 8.1 Hz, 2H), 7.17 (d, *J* = 8.1 Hz, 2H), 7.10-7.07 (m, 2H), 6.79 (tt, *J* = 7.3, 1.0 Hz, 1H), 4.55 (s, 2H), 3.53 (br, 2H), 2.35 (s, 3H) ppm.

¹³C NMR (125 MHz, CD₂Cl₂) δ = 152.2, 137.4, 134.9, 129.6, 129.2, 128.2, 118.5, 113.9, 60.2, 21.2 ppm.

MS (EI) *m/z* (%): 212 (52), 107 (100), 105 (76), 77 (35).

HRMS (EI) *m/z* calculated for C₁₄H₁₆N₂ 212.131351, found 212.131519.

1-(4-(*tert*-Butyl)benzyl)-1-phenylhydrazine (300i)

The reaction was conducted on a 4.00 mmol scale.

Purification: CC on SiO₂ (pentane:Et₂O 5:1).

Yield: Yellow solid 553 mg (2.18 mmol, 54%).

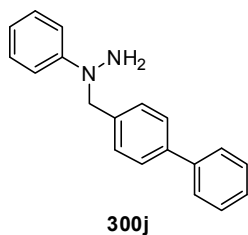
¹H NMR (500 MHz, CD₂Cl₂) δ = 7.39-7.36 (m, 2H), 7.25-7.22 (m, 4H), 7.10-7.07 (m, 2H), 6.77 (tt, *J* = 7.3, 0.9 Hz, 1H), 4.56 (s, 2H), 3.57 (br, 2H), 1.32 (s, 9H) ppm.

^{13}C NMR (125 MHz, CD_2Cl_2) δ = 152.3, 150.6, 135.0, 129.3, 128.0, 125.8, 118.4, 113.8, 60.0, 34.7, 31.5 ppm.

MS (EI) m/z (%): 254 (60), 147 (100), 132 (20), 117 (18), 107 (81).

HRMS (EI) m/z calculated for $\text{C}_{17}\text{H}_{22}\text{N}_2$ 254.178299, found 254.178383.

1-([1,1'-Biphenyl]-4-ylmethyl)-1-phenylhydrazine (300j)



The reaction was conducted on a 4.00 mmol scale.

Purification: CC on SiO_2 (pentane: Et_2O 3:1).

Yield: Yellow solid 549 mg (2.00 mmol, 50%).

^1H NMR (500 MHz, CD_2Cl_2) δ = 7.62-7.58 (m, 4H), 7.46-7.43 (m, 2H), 7.39 (d, J = 8.3 Hz, 2H), 7.35 (tt, J = 7.4, 1.2 Hz, 1H), 7.28-7.24 (m, 2H),

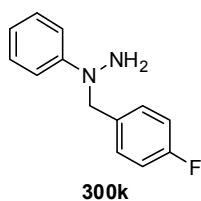
7.11-7.09 (m, 2H), 6.80 (tt, J = 7.3, 0.9 Hz, 1H), 4.65 (s, 2H), 3.64 (br, 2H) ppm.

^{13}C NMR (125 MHz, CD_2Cl_2) δ = 152.2, 141.1, 140.5, 137.4, 129.3, 129.1, 128.7, 127.6, 127.6, 127.3, 118.6, 113.8, 60.2 ppm.

MS (EI) m/z (%): 274 (30), 167 (100), 152 (9), 107 (30), 77 (9).

HRMS (EI) m/z calculated for $\text{C}_{19}\text{H}_{18}\text{N}_2$ 274.147000, found 274.147000.

1-(4-Fluorobenzyl)-1-phenylhydrazine (300k)



The reaction was conducted on a 4.00 mmol scale.

Purification: CC on SiO_2 (pentane: Et_2O 3:1).

Yield: Yellow solid 496 mg (2.29 mmol, 57%).

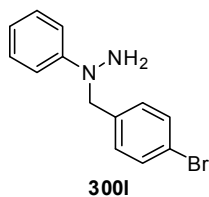
^1H NMR (500 MHz, CD_2Cl_2) δ = 7.32-7.28 (m, 2H), 7.28-7.24 (m, 2H), 7.08-

7.02 (m, 4H), 6.81 (tt, J = 7.3, 1.0 Hz, 1H), 4.56 (s, 2H), 3.57 (br, 2H) ppm.

^{13}C NMR (125 MHz, CD_2Cl_2) δ = 162.5 (d, J = 244.0 Hz), 152.1, 134.1 (d, J = 3.1.0 Hz), 129.9 (d, J = 7.6 Hz), 129.3, 118.8, 115.6 (d, J = 21.3 Hz), 113.8, 59.8 ppm.

MS (EI) m/z (%): 216 (29), 109 (31), 107 (100), 77 (39).

HRMS (EI) m/z calculated for $\text{C}_{13}\text{H}_{13}\text{N}_2\text{F}$ 216.106277, found 216.106170.

1-(4-Bromobenzyl)-1-phenylhydrazine (300l)

The reaction was conducted on a 5.00 mmol scale.

Purification: CC on SiO₂ (pentane:Et₂O 4:1 to 1:1).

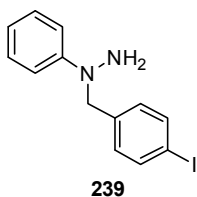
Yield: Yellow solid 895 mg (3.23 mmol, 65%).

¹H NMR (500 MHz, CD₂Cl₂) δ = 7.49-7.46 (m, 2H), 7.27-7.22 (m, 2H), 7.21 (d, *J* = 8.5 Hz, 2H), 7.04-7.02 (m, 2H), 6.79 (tt, *J* = 7.3, 1.0 Hz, 1H), 4.55 (s, 2H), 3.61 (br, 2H) ppm.

¹³C NMR (125 MHz, CD₂Cl₂) δ = 152.0, 137.6, 131.9, 130.0, 129.3, 121.2, 118.8, 113.7, 60.0 ppm.

MS (EI) *m/z* (%): 276/278 (10/10), 169/171 (7/7), 107 (100), 77 (24).

HRMS (EI) *m/z* calculated for C₁₃H₁₃N₂Br 276.026222, found 276.025986.

1-(4-Iodobenzyl)-1-phenylhydrazine (239)

The reaction was conducted on a 4.00 mmol scale.

Purification: CC on SiO₂ (pentane:Et₂O 3:1).

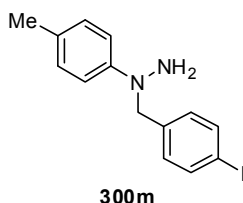
Yield: Orange solid 788 mg (2.43 mmol, 61%).

¹H NMR (500 MHz, CDCl₃) δ = 7.69-7.66 (m, 2H), 7.27-7.22 (m, 2H), 7.08 (d, *J* = 8.4 Hz, 2H), 7.04-7.02 (m, 2H), 6.80 (tt, *J* = 7.3, 1.0 Hz, 1H), 4.54 (s, 2H), 3.61 (br, 2H) ppm.

¹³C NMR (125 MHz, CDCl₃) δ = 152.0, 138.2, 137.9, 130.2, 129.3, 118.8, 113.7, 92.7, 60.0 ppm.

MS (EI) *m/z* (%): 324 (22), 217 (11), 107 (100), 90 (10), 77 (21).

HRMS (EI) *m/z* calculated for C₁₃H₁₃N₂I 324.012348, found 324.012027.

1-(4-Iodobenzyl)-1-(p-tolyl)hydrazine (300m)

The reaction was conducted on a 4.00 mmol scale.

Purification: CC on SiO₂ (hexane:EtOAc 7:1).

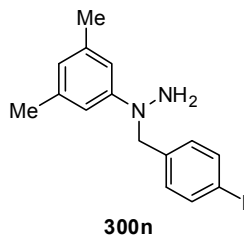
Yield: Yellow solid 839 mg (2.48 mmol, 62%).

¹H NMR (400 MHz, CD₂Cl₂) δ = 7.68-7.65 (m, 2H), 7.09-7.03 (m, 4H), 6.95-6.91 (m, 2H), 4.47 (s, 2H), 3.55 (br, 2H), 2.25 (s, 3H) ppm.

¹³C NMR (100 MHz, CD₂Cl₂) δ = 150.0, 138.4, 137.9, 130.4, 129.8, 128.4, 114.2, 92.6, 60.7, 20.4 ppm.

MS (EI) *m/z* (%): 338 (9), 217 (5), 121 (100), 91 (27), 77 (22).

HRMS (ESI+) *m/z* calculated for C₁₄H₁₅N₂I/Na (M+Na⁺) 361.017217, found 361.017179.

1-(3,5-Dimethylphenyl)-1-(4-iodobenzyl)hydrazine (300n)^[221]

The reaction was conducted on a 3.00 mmol scale.

Purification: CC on SiO₂ (pentane:Et₂O 4:1).

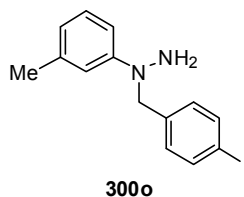
Yield: Pale brown solid 685 mg (1.94 mmol, 65%).

¹H NMR (500 MHz, CDCl₃) δ = 7.67 (d, J = 8.2 Hz, 2H), 7.07 (d, J = 8.2 Hz, 2H), 6.68 (s, 2H), 6.51 (s, 1H), 4.51 (s, 2H), 3.56 (br, 2H), 2.29 (s, 6H) ppm.

¹³C NMR (100 MHz, CDCl₃) δ = 152.1, 139.1, 138.1, 138.0, 130.1, 121.2, 111.7, 92.9, 60.2, 22.0 ppm.

MS (EI) m/z (%): 352 (24), 217 (9), 135 (100).

HRMS (EI) m/z calculated for C₁₅H₁₇N₂I 352.043646, found 352.043555.

1-(4-Iodobenzyl)-1-(m-tolyl)hydrazine (300o)^[221]

The reaction was conducted on a 3.00 mmol scale.

Purification: CC on SiO₂ (pentane:Et₂O 4:1).

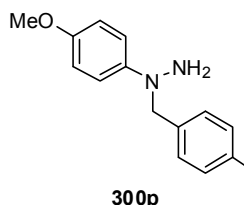
Yield: Pale brown solid 497 mg (1.47 mmol, 49%).

¹H NMR (500 MHz, CDCl₃) δ = 7.68-7.66 (m, 2H), 7.17 (d, J = 7.8, 7.8 Hz, 1H), 7.08-7.06 (m, 2H), 6.90 (s, 1H), 6.86-6.83 (m, 1H), 6.68 (d, J = 7.8 Hz, 1H), 4.53 (s, 2H), 3.67 (br, 2H), 2.34 (s, 3H) ppm.

¹³C NMR (100 MHz, CDCl₃) δ = 151.6, 138.9, 138.7, 137.6, 129.8, 128.9, 119.6, 113.4, 110.7, 92.5, 60.9, 21.8 ppm.

MS (EI) m/z (%): 338 (25), 217 (8), 121 (100), 91 (22), 77 (18).

HRMS (ESI+) m/z calculated for C₁₄H₁₅N₂INa (M+Na⁺) 361.017212, found 361.017037.

1-(4-Iodobenzyl)-1-(4-methoxyphenyl)hydrazine (300p)^[221]

The reaction was conducted on a 3.00 mmol scale.

Purification: CC on SiO₂ (pentane:Et₂O 4:1).

Yield: Pale yellow solid 468 mg (1.32 mmol, 44%).

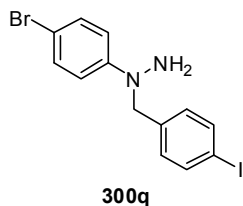
¹H NMR (500 MHz, CDCl₃) δ = 7.65-7.63 (m, 2H), 7.05 (d, J = 8.2 Hz, 2H), 7.01-7.00 (m, 2H), 6.83-6.82 (m, 2H), 4.37 (s, 2H), 3.76 (s, 3H), 3.48 (br, 2H) ppm.

^{13}C NMR (125 MHz, CDCl_3) δ = 153.6, 146.0, 137.7, 137.3, 130.3, 116.4, 114.5, 92.8, 61.8, 55.7 ppm.

MS (EI) m/z (%): 354 (15), 217 (7), 137 (100).

HRMS (EI) m/z calculated for $\text{C}_{14}\text{H}_{15}\text{N}_2\text{OI}$ 354.022909, found 354.023184.

1-(4-bromophenyl)-1-(4-iodobenzyl)hydrazine (**300q**)^[221]



The reaction was conducted on a 4.00 mmol scale.

Purification: CC on SiO_2 (pentane: Et_2O 4:1).

Yield: Pale brown solid 548 mg (1.83 mmol, 34%).

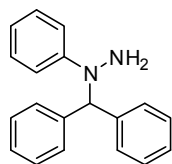
^1H NMR (500 MHz, CDCl_3) δ = 7.68-7.59 (m, 2H), 7.30 (d, J = 8.8 Hz, 2H), 7.00 (d, J = 8.1 Hz, 2H), 6.90 (d, J = 8.8 Hz, 2H), 4.49 (s, 2H), 3.54 (br, 2H) ppm.

^{13}C NMR (125 MHz, CDCl_3) δ = 150.6, 138.0, 136.9, 131.9, 129.8, 115.3, 110.9, 93.0, 59.8 ppm.

MS (EI) m/z (%): 404 (20), 402 (20), 217 (30), 187 (100), 185 (100), 90 (35), 77 (50).

HRMS (EI) m/z calculated for $\text{C}_{13}\text{H}_{12}\text{N}_2\text{BrI}$ 401.922871, found 401.922948.

1-Benzhydryl-1-phenylhydrazine



A solution of phenylhydrazine (**100a**, 2.16 g, 20.0) in THF (2 mL) was added dropwise to a suspension of NaNH_2 (4.34 g, 21.4 mmol) in THF (15 mL) at 0 °C.

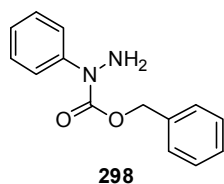
After complete addition the mixture was allowed to warm to room temperature and a stream of argon was passed through the solution for 1 h to remove the generated ammonia. After cooling to 0 °C again a solution of benzhydryl chloride (819 mg, 21.0 mmol) in THF (1 mL) was added dropwise over 30 min and the reaction was stirred at 0 °C for 90 min. Then H_2O (50 mL) was added, the aqueous layer was extracted with Et_2O and the combined organic layers were dried over MgSO_4 and concentrated *in vacuo*. Purification by column chromatography (pentane: Et_2O 4:1) afforded the title compound **100a** (99.6 mg, 0.363 mmol, 2%) as a yellow oil.

^1H NMR (500 MHz, CD_2Cl_2) δ = 7.39-7.26 (m, 10H), 7.21 (dd, J = 8.7, 7.3 Hz, 2H), 7.08 (d, J = 8.0 Hz, 2H), 6.76 (t, J = 7.3 Hz, 1H), 6.21 (s, 1H), 3.34 (br, 2H) ppm.

^{13}C NMR (125 MHz, CDCl_3) δ = 152.1, 139.9, 129.2, 129.2, 128.7, 127.7, 118.7, 114.4, 69.6 ppm.

MS (EI) m/z (%): 274 (6), 167 (100), 152 (12), 107 (5).

HRMS (EI) m/z calculated for $\text{C}_{19}\text{H}_{18}\text{N}_2$ 274.146998, found 274.146746.

Benzyl 1-phenylhydrazinecarboxylate (298)

A mixture of iodobenzene (**296**, 2.04 g, 10.0 mmol), benzyl hydrazinecarboxylate (**297**, 1.99 g, 12 mmol), CuI (190 mg, 1.0 mmol), 1,10-phenanthroline (360 mg, 2.0 mmol) and Cs₂CO₃ (4.56 g, 14 mmol) in DMF (10 mL) was degassed for 5 min and heated to 80 °C for 1 h. After cooling to room temperature the solids were filtered off, washed with Et₂O and the combined filtrates were concentrated under reduced pressure. Purification of the residue by column chromatography on silica gel (hexane:EtOAc 4:1) afforded the product **298** (1.89 g, 7.82 mmol, 78%) as a yellow oil.

¹H NMR (500 MHz, CD₂Cl₂) δ = 7.48 (d, *J* = 7.8 Hz, 2H), 7.39-7.30 (m, 7H), 7.15 (t, *J* = 7.4 Hz, 1H), 5.21 (s, 2H), 4.54 (br, 2H) ppm.

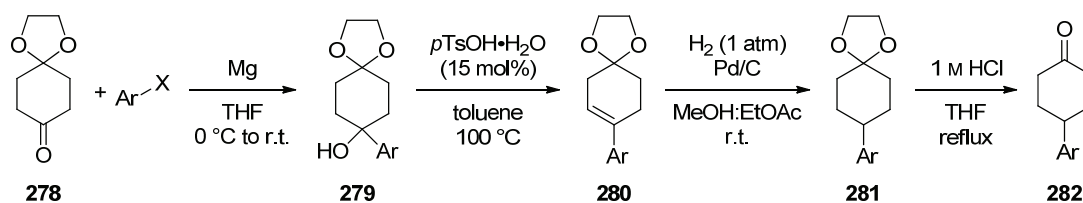
¹³C NMR (125 MHz, CDCl₃) δ = 156.3, 143.3, 136.7, 128.8, 128.6, 128.5, 128.3, 125.5, 124.0, 68.3 ppm.

MS (EI) *m/z* (%): 242 (4), 107 (55), 91 (100), 77 (11).

HRMS (EI) *m/z* calculated for C₁₄H₁₄N₂O₂ 242.10528, found 242.105299.

7.4.2.2 Synthesis of Ketones

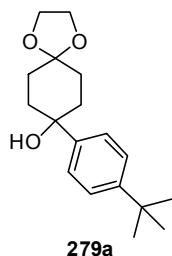
General procedure for the synthesis of 4-arylcyclohexanones:



All 4-aryl cyclohexanones **282** were prepared from 1,4-dioxaspiro[4.5]decan-8-one (**278**) by a sequence of Grignard-addition, alcohol elimination, double bond reduction and acetal deprotection. The intermediates **279**, **280** and **281** can be isolated and purified by column chromatography using appropriate conditions. However, during our work we found that the dehydration step yielded a mixture of the desired acetal and the corresponding ketone, resulting from partial hydrolysis of the product. Therefore we found it sufficient to only purify after the Grignard addition and from there on rely only on a short aqueous work up after each step to carry all the material through to the final product. Ultimately the hydrolyzed side product will lead to the same desired cyclohexanone. In the following

section these two methods are referred to as: Method A (Purification after each step) and method B (purification only after the first and the last step).

8-(4-(*tert*-Butyl)phenyl)-1,4-dioxaspiro[4.5]decan-8-ol (**279a**)



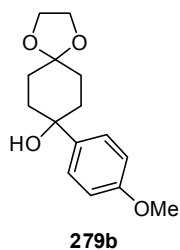
In a flame-dried 100 mL three neck round bottom flask Mg (467 mg, 19.2 mmol) was layered with a minimum amount of anhydrous THF. After addition of 4-*tert*-butylbromobenzene (ca. 0.1 mL) and a few drops of 1,2-dibromoethane the Grignard reaction was initiated by local heating (heat gun). After initiation the remaining THF (20 mL in total) and 4-*tert*-butylbromobenzene (4.09 g, 19.2 mmol in total) were added alternately to keep the reaction refluxing without the need for external heating. After complete addition the mixture was refluxed (oil bath heating) until the Mg was completely consumed. The Grignard solution was cooled to 0 °C and a solution of 1,4-dioxaspiro[4.5]decan-8-one (**278**, 1.50 g, 9.60 mmol) in anhydrous THF (15 mL) was added over 30 min. After complete addition, the cooling bath was removed and the mixture was stirred at ambient temperature until full conversion of ketone **278** was observed (monitored by TLC). The reaction was quenched with a saturated aqueous solution of NH₄Cl (5 mL), the layers were separated and the aqueous layer was extracted with CH₂Cl₂. The combined organic layers were dried over MgSO₄ and after evaporation of the solvent the residue was purified by column chromatography on SiO₂ eluting with hexane:EtOAc (2:1) to give the product **279a** (2.57 g, 8.85 mmol, 92%) as a colorless solid.

¹H NMR (500 MHz, CDCl₃) δ = 7.46-7.44 (m, 2H), 7.38-7.35 (m, 2H), 4.04-3.95 (m, 4H), 2.20-2.07 (m, 4H), 1.83-1.81 (m, 2H), 1.75-1.68 (m, 2H), 1.51 (br, 1H), 1.32 (s, 9H) ppm.

¹³C NMR (125 MHz, CDCl₃) δ = 149.9, 145.5, 125.3, 124.4, 108.6, 72.3, 64.5, 64.4, 36.7, 34.5, 31.5, 30.9 ppm.

MS (EI) *m/z* (%): 290 (1), 230 (7), 215 (13), 191 (9), 176 (15), 161 (73), 133 (16), 101 (100), 86 (26).

HRMS (ESI+) *m/z* calculated for C₁₈H₂₆O₃Na (M+Na⁺) 313.177418, found 313.177143.

8-(4-Methoxyphenyl)-1,4-dioxaspiro[4.5]decan-8-ol (279b)

The alcohol **279b** was synthesized as described for alcohol **279a**, starting from ketone **278** (500 mg, 3.20 mmol) and 4-methoxybromobenzene (1.20 g, 6.40 mmol).

Purification: CC on SiO₂ (hexane:EtOAc 2:1).

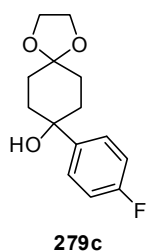
Yield: Colorless solid 765 mg (2.89 mmol, 90%).

¹H NMR (500 MHz, CD₂Cl₂) δ = 7.44-7.41 (m, 2H), 6.88-6.85 (m, 2H), 3.95-3.91 (m, 4H), 3.78 (s, 3H), 2.13-2.07 (m, 2H), 2.05-1.99 (m, 2H), 1.79-1.74 (m, 2H), 1.68 (s, 1H), 1.66-1.62 (m, 2H) ppm.

¹³C NMR (125 MHz, CD₂Cl₂) δ = 158.8, 141.3, 126.1, 113.7, 108.6, 72.1, 64.6, 64.5, 55.5, 37.0, 31.1 ppm.

MS (EI) *m/z* (%): 264 (7), 189 (6), 165 (9), 150 (33), 135 (25), 101 (100).

HRMS (ESI+) *m/z* calculated for C₁₅H₂₀O₄Na (M+Na⁺) 287.125382, found 287.125275.

8-(4-Fluorophenyl)-1,4-dioxaspiro[4.5]decan-8-ol (279c)

The alcohol **279c** was synthesized as described for alcohol **279a**, starting from ketone **278** (1.00 g, 6.40 mmol) and 4-fluorobromobenzene (2.24 g, 12.8 mmol).

Purification: CC on SiO₂ (hexane:EtOAc 3:1).

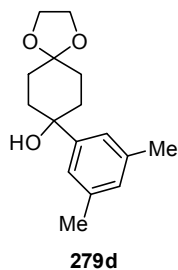
Yield: Colorless solid 1.37 g (5.43 mmol, 85%).

¹H NMR (500 MHz, CDCl₃) δ = 7.50-7.45 (m, 2H), 7.02-6.98 (m, 2H), 3.99-3.93 (m, 4H), 2.16-2.03 (m, 4H), 1.82-1.76 (m, 3H), 1.68-1.67 (m, 2H) ppm.

¹³C NMR (125 MHz, CDCl₃) δ = 161.9 (d, *J* = 245.5 Hz), 144.4 (d, *J* = 2.9 Hz), 126.4 (d, *J* = 7.9 Hz), 115.0 (d, *J* = 20.9 Hz) 108.4, 72.2, 64.4, 64.3, 36.8, 30.8 ppm.

MS (EI) *m/z* (%): 177 (3), 151 (4), 123 (15), 109 (5), 99 (100), 86 (43).

HRMS (ESI-) *m/z* calculated for C₁₄H₁₆O₃F (M-H⁺) 251.108900, found 251.108908.

8-(3,5-Dimethylphenyl)-1,4-dioxaspiro[4.5]decan-8-ol (279d)

The alcohol **279d** was synthesized as described for alcohol **279a** starting from ketone **278** (1.00 g, 6.40 mmol) and 3,5-dimethylbromobenzene (2.37 g, 12.8 mmol).

Purification: CC on SiO₂ (hexane:EtOAc 2:1).

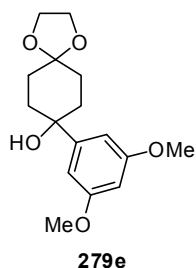
Yield: Colorless solid 1.61 g (6.12 mmol, 96%).

¹H NMR (500 MHz, CDCl₃) δ = 7.14 (s, 2H), 6.90 (s, 1H), 4.03-3.97 (m, 4H), 2.32 (s, 6H), 2.20-2.07 (m, 4H), 1.82-1.77 (m, 2H), 1.71-1.67 (m, 2H), 1.55 (s, 1H) ppm.

¹³C NMR (125 MHz, CDCl₃) δ = 148.7, 137.9, 128.6, 122.4, 108.6, 72.5, 64.5, 64.4, 36.8, 30.9, 21.6 ppm.

MS (EI) *m/z* (%): 262 (4), 202 (5), 163 (6), 148 (20), 133 (15), 101 (100).

HRMS (ESI+) *m/z* calculated for C₁₆H₂₂O₃Na (M+Na⁺) 285.146117, found 285.145934.

8-(3,5-dimethoxyphenyl)-1,4-dioxaspiro[4.5]decan-8-ol (279e)

The alcohol **279e** was synthesized as described for alcohol **279a**, starting from ketone **278** (1.56 g, 10.0 mmol) and 3,5-dimethoxybromobenzene (4.34 g, 20.0 mmol).

Purification: CC on SiO₂ (hexane:EtOAc 1:1).

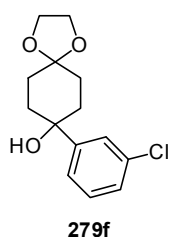
Yield: Colorless solid 2.60 g (8.82 mmol, 88%).

¹H NMR (500 MHz, CDCl₃) δ = 6.67 (d, *J* = 2.3 Hz, 2H), 6.35 (t, *J* = 2.3 Hz, 1H), 3.98-3.97 (m 4H), 3.79 (s, 6H), 2.17-2.05 (m, 4H), 1.81-1.76 (m, 2H), 1.75-1.66 (m, 3H) ppm.

¹³C NMR (125 MHz, CDCl₃) δ = 160.8, 151.4, 108.5, 103.0, 98.8, 72.7, 64.4, 64.3, 55.5, 36.6, 30.8 ppm.

MS (EI) *m/z* (%): 294 (58), 234 (9), 195 (9), 180 (66), 165 (17), 152 (23), 101 (100).

HRMS (ESI+) *m/z* calculated for C₁₆H₂₂O₅Na (M+Na⁺) 317.135941, found 317.136162.

8-(3-Chlorophenyl)-1,4-dioxaspiro[4.5]decan-8-ol (279f)

The alcohol **279f** was synthesized as described for alcohol **279a**, starting from ketone **278** (1.56 g, 10.0 mmol) and 1,3-dichlorobenzene (2.94 g, 20.0 mmol).

Purification: CC on SiO₂ (hexane:EtOAc 3:1).

Yield: Colorless solid 2.34 g (8.69 mmol, 87%).

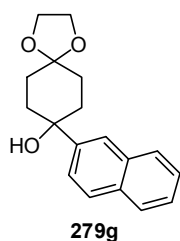
$^1\text{H NMR}$ (500 MHz, CDCl_3) δ = 7.52 (dd, J = 1.9, 1.9 Hz, 1H), 7.38 (ddd, J = 7.5, 1.5, 1.3 Hz, 1H), 7.26 (dd, J = 7.9, 6.9 Hz, 1H), 7.21 (ddd, J = 7.9, 2.0, 1.2 Hz, 1H), 4.00- 3.95 (m, 4H), 2.17-2.03 (m, 4H), 1.80-1.75 (m, 3H), 1.71-1.66 (m, 2H) ppm.

$^{13}\text{C NMR}$ (125 MHz, CDCl_3) δ = 150.9, 134.3, 129.7, 127.1, 125.2, 122.9, 108.4, 72.4, 64.5, 64.3, 36.6, 30.7 ppm.

MS (EI) m/z (%): 208 (2), 99 (100), 86 (44).

HRMS (ESI+) m/z calculated for $\text{C}_{14}\text{H}_{17}\text{O}_3\text{ClNa}$ ($\text{M}+\text{Na}^+$) 291.075842, found 291.075750.

8-(Naphthalen-2-yl)-1,4-dioxaspiro[4.5]decan-8-ol (**279g**)



The alcohol **279g** was synthesized as described for alcohol **279a**, starting from ketone **278** (1.56 g, 10.0 mmol) and 2-bromonaphthalene (4.14 g, 20.0 mmol).

Purification: CC on SiO_2 (hexane:EtOAc 2:1).

Yield: Colorless solid 2.57 g (9.04 mmol, 90%).

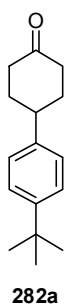
$^1\text{H NMR}$ (500 MHz, CDCl_3) δ = 7.97 (d, J = 1.5 Hz, 1H), 7.85-7.80 (m, 3H), 7.65 (dd, J = 8.7, 1.9 Hz, 1H), 7.49-7.44 (m, 2H), 4.04-3.98 (m, 4H), 2.30 (ddd, J = 13.6, 13.6, 4.1 Hz, 2H), 2.16 (ddd, J = 13.3, 13.3, 4.1 Hz, 2H), 1.92-1.86 (m, 2H), 1.76-1.70 (m, 3H) ppm.

$^{13}\text{C NMR}$ (125 MHz, CD_2Cl_2) δ = 146.0, 133.3, 132.5, 128.3, 128.1, 127.6, 126.2, 125.9, 123.6, 122.9, 108.6, 72.7, 64.5, 64.4, 36.7, 30.9 ppm.

MS (EI) m/z (%): 284 (25), 224 (7), 209 (6), 180 (12), 170 (52), 155 (21), 128 (16), 101 (100).

HRMS (ESI+) m/z calculated for $\text{C}_{18}\text{H}_{20}\text{O}_3\text{Na}$ ($\text{M}+\text{Na}^+$) 307.130464, found 307.130281.

4-(4-(*tert*-Butyl)phenyl)cyclohexanone (**282a**)



A mixture of 8-(4-(*tert*-butyl)phenyl)-1,4-dioxaspiro[4.5]decan-8-ol (**279a**, 2.54 g, 8.76 mmol) and *p*TsOH· H_2O (250 mg, 15 mol%) in toluene (30 mL) was heated to 100 °C until the starting material was fully converted (monitored by TLC). After cooling to room temperature, saturated aqueous NaHCO_3 solution (20 mL) was added. The layers were separated, the aqueous layer was extracted with CH_2Cl_2 and the combined organic layers were dried over MgSO_4 and evaporated to dryness.

The residue was taken up in a 1:1 mixture of MeOH and EtOAc (30 mL) and after addition of Pd/C (904 mg, 10 mol%, 10% Pd, dry) the mixture was stirred under an atmosphere of H_2

(balloon) until complete conversion was observed (monitored by TLC). The mixture was filtered over Celite, washed with EtOAc and evaporated to dryness.

The residue was dissolved in THF (30 mL) and heated to reflux together with 1 M HCl (10 mL). After full conversion (monitored by TLC), the solution was cooled to room temperature and basified by saturated aqueous NaHCO₃ solution. The layers were separated, the aqueous layer was extracted with CH₂Cl₂ and the combined organic layers were dried over MgSO₄ and evaporated to dryness. The residue was dissolved in a small amount of CH₂Cl₂ and filtered over a plug of SiO₂ eluting with hexane:EtOAc (9:1). After evaporation of the solvent the residue was recrystallized from hexane to yield the title compound **282a** (1.21 g, 5.23 mmol, 60% over 3 steps) as a colorless solid.

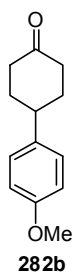
¹H NMR (500 MHz, CDCl₃) δ = 7.36-7.34 (m, 2H), 7.20-7.17 (m, 2H), 3.00 (tt, *J* = 6.0, 3.4 Hz, 1H), 2.55-2.47 (m, 4H), 2.26-2.20 (m, 2H), 1.98-1.90 (m, 2H), 1.32 (s, 9H) ppm.

¹³C NMR (125 MHz, CDCl₃) δ = 211.6, 149.5, 141.8, 126.5, 125.6, 42.3, 41.6, 34.5, 34.1 ppm.

MS (EI) *m/z* (%): 230 (22), 215 (100), 145 (8), 117 (7).

HRMS (EI) *m/z* calculated for C₁₆H₂₂O 230.167066, found 230.167280.

4-(4-Methoxyphenyl)cyclohexanone (**282b**)



Method A.

Purification: CC on SiO₂ (hexane:EtOAc 5:1).

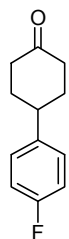
Yield: Colorless solid 433 mg (2.12 mmol, 71% over 3 steps).

¹H NMR (500 MHz, CD₂Cl₂) δ = 7.19-7.16 (m, 2H), 6.87-6.84 (m, 2H), 3.77 (s, 3H), 2.97 (tt, *J* = 6.1, 3.4 Hz, 1H), 2.50 (ddd, *J* = 14.1, 14.0, 6.0 Hz, 2H), 2.43-2.39 (m, 2H), 2.19-2.14 (m, 2H), 1.88 (ddd, *J* = 25.6, 13.2, 4.4 Hz, 2H) ppm.

¹³C NMR (125 MHz, CD₂Cl₂) δ = 210.9, 158.6, 137.6, 127.9, 114.1, 55.5, 42.2, 41.7, 34.6 ppm.

MS (EI) *m/z* (%): 204 (55), 147 (100), 134 (51), 121 (12), 103 (8), 91 (23).

HRMS (EI) *m/z* calculated for C₁₃H₁₆O₂ 204.115030, found 204.115038.

4-(4-fluorophenyl)cyclohexanone (282c)

Method A.

Purification: CC on SiO₂ (hexane:EtOAc 6:1).

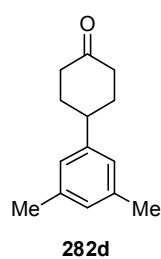
Yield: Colorless solid 489 mg (2.54 mmol, 49% over 3 steps).

¹H NMR (500 MHz, CDCl₃) δ = 7.23 (dd, J = 8.2, 5.6 Hz, 2H), 7.01 (dd, J = 8.7, 8.7 Hz, 2H), 3.06-3.00 (m 1H), 2.54-2.47 (m, 2H), 2.44-2.41 (m, 2H), 2.19-2.16 (m, 2H), 1.89 (dd, J = 25.8, 13.0, 4.1 Hz, 2H) ppm.

¹³C NMR (125 MHz, CDCl₃) δ = 210.6, 161.8 (d, J = 243.6 Hz), 141.3 (d, J = 3.1 Hz), 128.5 (d, J = 7.7 Hz), 115.5 (d, J = 21.2 Hz), 42.3, 41.6, 34.5 ppm.

MS (EI) m/z (%): 192 (96), 148 (12), 135 (60), 122 (100), 109 (68).

HRMS (EI) m/z calculated for C₁₂H₁₃FO 192.095044, found 192.094869.

4-(3,5-dimethylphenyl)cyclohexanone (282d)

Method A.

Purification: CC on SiO₂ (hexane:EtOAc 9:1).

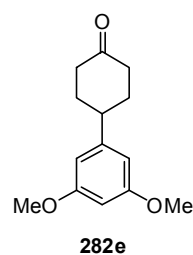
Yield: Colorless solid 336 mg (1.66 mmol, 27% over 3 steps).

¹H NMR (400 MHz, CD₂Cl₂) δ = 6.87-6.85 (m, 3H), 2.93 (tt, J = 6.1, 3.4 Hz, 1H), 2.50 (m, 2H), 2.44-2.39 (m, 2H), 2.29 (s, 6H), 2.20-2.12 (m, 2H), 1.90 (ddd, J = 25.4, 13.1, 4.7 Hz, 2H) ppm.

¹³C NMR (100 MHz, CD₂Cl₂) δ = 211.0, 145.5, 138.3, 128.3, 124.9, 43.0, 41.7, 34.4, 21.4 ppm.

MS (EI) m/z (%): 202 (79), 187 (5), 173 (22), 159 (9), 145 (54), 132 (100), 117 (32), 105 (14), 91 (29).

HRMS (EI) m/z calculated for C₁₄H₁₈O 202.135762, found 202.135792.

4-(3,5-Dimethoxyphenyl)cyclohexanone (282e)

Method B.

Purification: CC on SiO₂ (hexane:EtOAc 9:1).

Yield: Colorless solid 1.24 g (5.29 mmol, 60% over 3 steps).

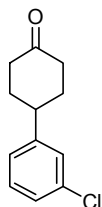
¹H NMR (500 MHz, CD₂Cl₂) δ = 6.40 (d, J = 2.3 Hz, 2H), 6.32 (t, J = 2.3 Hz, 1H), 3.77 (s, 6H), 2.95 (tt, J = 6.1, 3.4 Hz, 1H), 2.52-2.46 (m, 2H), 2.44-2.39 (m, 2H), 2.21- 2.15 (m, 2H), 1.90 (ddd, J = 25.6, 13.1, 4.5 Hz, 2H) ppm.

^{13}C NMR (125 MHz, CD_2Cl_2) δ = 210.8, 161.3, 148.0, 105.2, 98.3, 55.6, 43.4, 41.6, 34.2 ppm.

MS (EI) m/z (%): 234 (86), 191 (6), 177 (22), 164 (100), 152 (16).

HRMS (ESI+) m/z calculated for $\text{C}_{14}\text{H}_{18}\text{O}_3\text{Na}$ ($\text{M}+\text{Na}^+$) 257.114813, found 257.114721.

4-(3-Chlorophenyl)cyclohexanone (282f)



Method B.

Purification: CC on SiO_2 (hexane:EtOAc 15:1).

Yield: Colorless solid 466 mg (2.23 mmol, 26% over 3 steps).

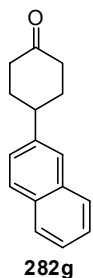
^1H NMR (500 MHz, CDCl_3) δ = 7.29-7.28 (m, 1H), 7.27-7.25 (m, 1H), 7.24-7.22 (m, 1H), 7.15 (d, J = 7.5 Hz, 1H), 3.02 (tt, J = 6.1, 3.4 Hz, 1H), 2.54-2.51 (m, 4H), 2.26-2.20 (m, 2H), 2.00-1.89 (m, 2H) ppm.

^{13}C NMR (125 MHz, CDCl_3) δ = 210.8, 146.9, 134.5, 130.0, 127.1, 126.9, 125.0, 42.6, 41.3, 33.9 ppm.

MS (EI) m/z (%): 208 (100), 179 (21), 164 (6), 153 (55), 138 (62), 125 (49), 115 (33), 103 (20).

HRMS (EI) m/z calculated for $\text{C}_{12}\text{H}_{13}\text{ClO}$ 208.065490, found 208.065299.

4-(Naphthalen-2-yl)cyclohexanone (282g)



Method B.

Purification: CC on SiO_2 (hexane:EtOAc 6:1).

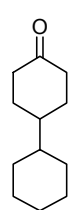
Yield: Colorless solid 1.43 g (6.38 mmol, 71% over 3 steps).

^1H NMR (500 MHz, CDCl_3) δ = 7.84-7.79 (m, 3H), 7.69 (s, 1H), 7.50-7.44 (m, 2H), 7.39 (dd, J = 8.5, 1.8 Hz, 1H), 3.18 (tt, J = 6.0-3.4 Hz, 1H), 2.61-2.52 (m, 4H), 2.35-2.29 (m, 2H), 2.10-2.01 (m, 2H) ppm.

^{13}C NMR (125 MHz, CDCl_3) δ = 211.3, 142.3, 133.7, 132.5, 128.3, 127.7, 127.7, 126.3, 125.7, 125.7, 124.9, 42.9, 41.5, 34.0 ppm.

MS (EI) m/z (%): 224 (100), 195 (6), 167 (64), 154 (72), 141 (12), 128 (10).

HRMS (EI) m/z calculated for $\text{C}_{16}\text{H}_{16}\text{O}$ 224.120115, found 224.119909.

4-Cyclohexyl-cyclohexanone (284)

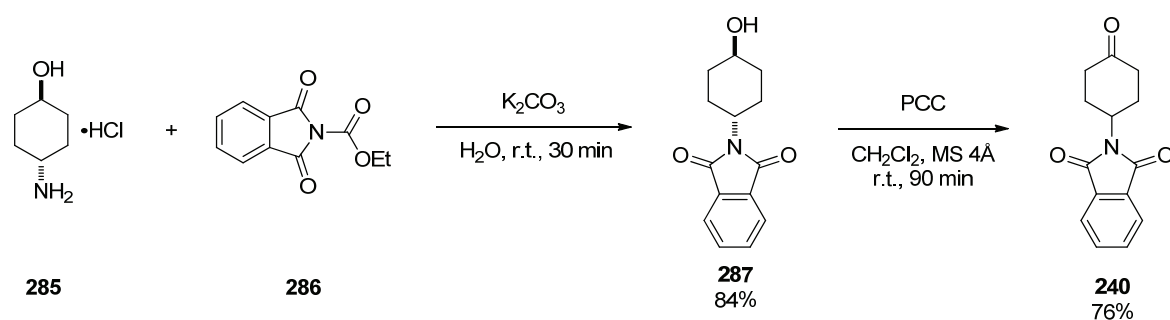
A mixture of 4-cyclohexyl-cyclohexanol (**283**, 729 mg, 4.00 mmol) and MS 4Å (2.80 g) in CH₂Cl₂ (20 mL) was treated with PCC (2.16 g, 10.0 mmol) and stirred at room temperature for 90 min. After complete consumption of the starting material (monitored by TLC), Florisil was added and stirring was continued for 10 min. The mixture was filtered over a pad of Florisil, the filter cake was washed with CH₂Cl₂ and the combined filtrates were evaporated to dryness and purified by column chromatography on silica gel (hexane:EtOAc 9:1) to yield ketone **284** (595 mg, 3.30 mmol, 83%) as a colorless solid.

¹H NMR (400 MHz, CDCl₃) δ = 2.40-2.25 (m, 4H), 2.03-1.99 (m, 2H), 1.77-1.61 (m, 5H), 1.57-1.41 (m, 3H), 1.28-1.07 (m, 4H), 1.07-0.95 (m, 2H) ppm.

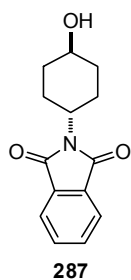
¹³C NMR (100 MHz, CDCl₃) δ = 212.8, 42.1, 41.9, 41.3, 30.5, 29.9, 26.8, 26.7 ppm.

MS (EI) *m/z* (%): 180 (25), 162 (11), 151 (45), 133 (11), 125 (37), 109 (20), 98 (28), 83 (59), 67 (34), 55 (100), 41 (69).

HRMS (EI) *m/z* calculated for C₁₂H₂₀O 180.151414, found 180.151590.

Synthesis of N-Phthalimido-4-aminocyclohexanone (240)

N-Phthalimido-4-aminocyclohexanone was prepared from *trans*-4-aminocyclohexanol hydrochloride (**285**) using a modified literature procedure.^[188]

***N*-Phthalimido-*trans*-4-aminocyclohexanol (287)**

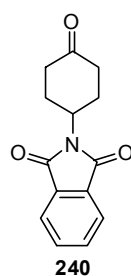
To a solution of *trans*-4-aminocyclohexanol hydrochloride (**285**, 2.27 g, 15 mmol) in H₂O (40 mL) was added K₂CO₃ (5.72 g, 41.4 mmol) and *N*-carbethoxy phthalimide (**286**, 3.69 g, 16.8 mmol). The mixture was stirred at room temperature for 30 min during which time the product precipitated. The solid was collected, washed with H₂O and dried *in vacuo* to yield the title compound **287** (3.07 g, 12.5 mmol, 84%) as a colorless solid.

¹H NMR (500 MHz, CDCl₃) δ = 7.83-7.79 (m, 2H), 7.71-7.68 (m, 2H), 4.12 (tt, *J* = 6.2, 4.0 Hz, 1H), 3.75 (tt, *J* = 5.5, 4.4 Hz, 1H), 2.34 (ddd, *J* = 25.9, 12.2, 3.5 Hz, 2H), 2.13-2.06 (m, 2H), 1.79-1.72 (m, 2H), 1.63 (br, 1H), 1.44 (ddd, *J* = 24.3, 13.2, 3.4 Hz, 2H) ppm.

¹³C NMR (125 MHz, CDCl₃) δ = 168.5, 134.0, 132.1, 123.2, 69.7, 49.8, 39.9, 34.9, 27.7 ppm.

MS (EI) *m/z* (%): 245 (75), 227 (12), 212 (25), 187 (25), 173 (17), 148 (100), 130 (64), 104 (38), 76 (48).

HRMS (ESI+) *m/z* calculated for C₁₄H₁₅NO₃Na (M+Na⁺) 268.094410, found 268.094135.

***N*-Phthalimido-4-aminocyclohexanone (240)**

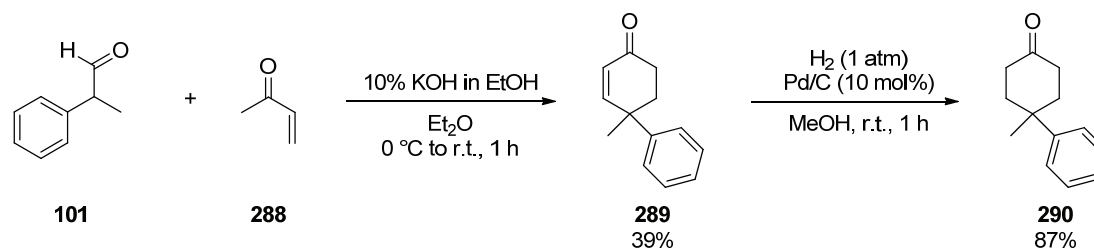
To a solution of *N*-phthalimido-*trans*-4-aminocyclohexanol (**287**, 1.00 g, 4.08 mmol) in CH₂Cl₂ (20 mL) were added MS 4Å (2.8 g) and PCC (2.22 g, 10.3 mmol). After stirring at room temperature for 90 min Florisil was added and stirring was continued for 10 min. The mixture was filtered over a pad of Florisil and washed with CH₂Cl₂. After removal of the solvent the residue was purified by column chromatography on SiO₂ eluting with hexane:EtOAc (2:1) to yield the title compound **240** (752 mg, 3.09 mmol, 76%) as colorless solid.

¹H NMR (500 MHz, CDCl₃) δ = 7.84-7.81 (m, 2H), 7.73-7.71 (m, 2H), 4.61 (tt, *J* = 6.0, 4.0 Hz, 1H), 2.71 (ddd, *J* = 24.8, 12.4, 5.9 Hz, 2H), 2.55-2.45 (m, 4H), 2.09-2.01 (m, 2H) ppm.

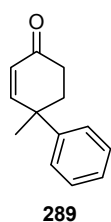
¹³C NMR (125 MHz, CDCl₃) δ = 209.0, 168.2, 134.2, 131.9, 123.4, 48.4, 40.0, 28.7 ppm.

MS (EI) *m/z* (%): 186 (8), 173 (8), 148 (13), 130 (11), 104 (12), 96 (100).

HRMS (ESI+) *m/z* calculated for C₁₄H₁₃NO₃Na (M+Na⁺) 266.078764, found 266.078360.

Synthesis of 4-methyl-4-phenylcyclohexanone (290)

4-Methyl-4-phenylcyclohexanone **290** was obtained from hydratropic aldehyde (**101**) and methyl vinyl ketone (**288**) in a procedure related to the one reported by Zimmerman *et al.*^[189]

4-Methyl-4-phenyl-cyclohexenone (289)

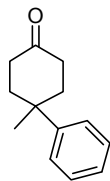
A solution of hydratropic aldehyde (**101**, 1.00 g, 7.54 mmol) and methyl vinyl ketone (**288**, 2.61 g, 37.3 mmol) in Et₂O (15 mL) was treated with a 10% (w/w) solution of KOH in ethanol (209 mg, 20.9 mg KOH, 0.373 mmol) at 0 °C. After 15 min the cooling bath was removed and the mixture was stirred at room temperature for 4 h. The reaction was diluted with H₂O (10 mL) and extracted with CH₂Cl₂. The combined organic layers were dried over MgSO₄, evaporated to dryness and the residue was purified by column chromatography on silica gel (hexane:EtOAc 8:1). The obtained 2-methyl-5-oxo-2-phenylhexanal was again dissolved in Et₂O (15 mL) and treated with a 10% (w/w) solution of KOH in ethanol (4.22 g, 422 mg KOH, 7.54 mmol) at room temperature. After 1 h the mixture was extracted with CH₂Cl₂, dried over MgSO₄ and evaporated to dryness to afford the title compound **289** (542 mg, 2.91 mmol, 39%) as a colorless oil.

¹H NMR (500 MHz, CD₂Cl₂) δ = 7.37-7.33 (m, 4H), 7.28-7.24 (m, 1H), 6.94 (dd, *J* = 10.2, 0.8 Hz, 1H), 6.08 (d, *J* = 10.2 Hz, 1H), 2.40-2.34 (m, 1H), 2.28-2.22 (m, 2H), 2.16-2.11 (m, 1H), 1.55 (s, 3H) ppm.

¹³C NMR (125 MHz, CD₂Cl₂) δ = 199.2, 157.2, 146.0, 128.8, 128.8, 126.9, 126.6, 40.9, 38.4, 35.0, 27.7 ppm.

MS (EI) *m/z* (%): 186 (100), 171 (25), 158 (47), 144 (90), 129 (88), 115 (31), 103 (6), 91 (8), 77 (11), 64 (16).

HRMS (EI) *m/z* calculated for C₁₃H₁₄O 186.104468, found 186.104247.

4-Methyl-4-phenylcyclohexanone (290)**290**

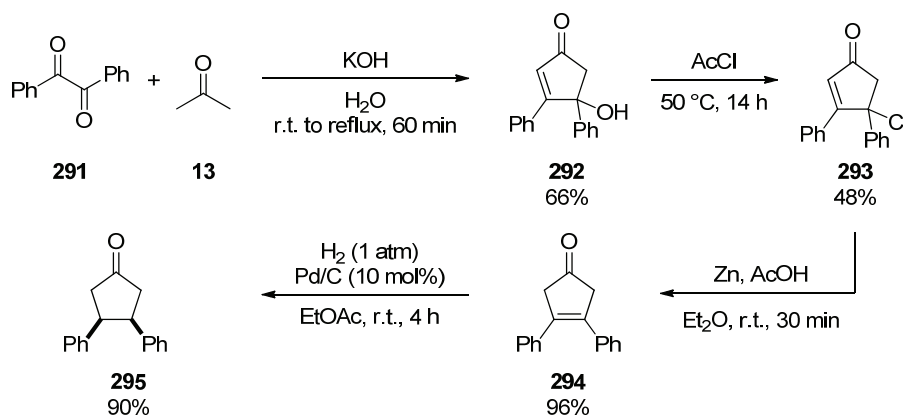
A mixture of cyclohexenone **289** (542 mg, 2.91 mmol) and Pd/C (310 mg, 10 mol%, 10% Pd, dry) in MeOH (15 mL) was stirred under an atmosphere of H₂ (balloon) for 1 h. The mixture was filtered over Celite, washed with ethyl acetate and evaporated to dryness. The residue was purified by column chromatography on silica gel eluting with hexane:EtOAc (6:1) to yield the title compound **290** (474 mg, 2.52 mmol, 87%) as a colorless oil.

¹H NMR (500 MHz, CDCl₃) δ = 7.45 (dd, *J* = 8.4, 1.1 Hz, 2H), 7.39 (dd, *J* = 8.3, 7.4 Hz, 2H), 7.25 (tt, *J* = 7.3, 1.2 Hz, 1H), 2.53-2.47 (m, 2H), 2.40-2.27 (m, 4H), 1.99-1.93 (m, 2H), 1.32 (s, 3H) ppm.

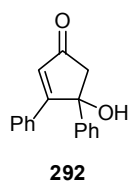
¹³C NMR (125 MHz, CDCl₃) δ = 212.0, 146.1, 129.0, 126.3, 125.8, 38.5, 37.9, 37.3, 31.3 ppm.

MS (EI) *m/z* (%): 188 (100), 173 (15), 159 (9), 144 (7), 131 (98), 117 (25), 103 (8), 91 (44).

HRMS (EI) *m/z* calculated for C₁₃H₁₆O 188.120118, found 188.120187.

Synthesis of *cis*-3,4-diphenyl-cyclopentanone (295)

The synthesis of *cis*-3,4-diphenyl-cyclopentanone was accomplished by using modifications of literature reported procedures.^[190,191]

4-Hydroxy-3,4-diphenylcyclopent-2-enone (292)**292**

To a mixture of benzil (**291**, 5.0 g, 23.8 mmol) and acetone (**13**, 3.2 g, 55 mmol) was added 0.1 mL of 32% aqueous solution of KOH. After stirring at room temperature for 5 min, another 2 mL of 32% solution of KOH was added and the mixture was heated to reflux for 1 h. The resulting brown oil was allowed to cool to room temperature and was then poured into H₂O and extracted with CH₂Cl₂. The

combined organic layers were dried over MgSO_4 , evaporated to dryness and the residue was crystallized from boiling toluene to yield the product **292** (3.94 g, 15.8 mmol, 66%) as a yellow solid.

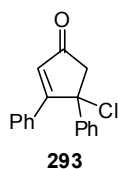
$^1\text{H NMR}$ (500 MHz, CDCl_3) δ = 7.53-7.51 (m, 2H), 7.46-7.44 (m, 2H), 7.37-7.34 (m, 3H), 7.31-7.27 (m, 3H), 6.70 (s, 1H), 3.02 (d, J = 18.5 Hz, 1H), 2.90 (d, J = 18.5 Hz, 1H), 2.70 (br, 1H) ppm.

$^{13}\text{C NMR}$ (125 MHz, CDCl_3) δ = 204.9, 174.0, 144.2, 131.4, 131.0, 129.3, 129.3, 129.0, 129.0, 127.7, 124.3, 81.8, 56.7 ppm.

MS (EI) m/z (%): 250 (100), 222 (13), 147 (12), 131 (35), 105 (48), 77 (24).

HRMS (ESI+) m/z calculated for $\text{C}_{17}\text{H}_{14}\text{O}_2\text{Na}$ ($\text{M}+\text{Na}^+$) 273.088597, found 273.088864.

4-Chloro-3,4-diphenylcyclopent-2-enone (**293**)



A solution of 4-hydroxy-3,4-diphenylcyclopent-2-enone (**292**, 1.06 g, 4.24 mmol) in AcCl (4 mL) was heated to 50 °C for 14 h. After cooling to room temperature the volatile components were removed under reduced pressure. The residue was taken up in toluene and the product was precipitated by adding hexane to this solution. The obtained solid was collected and washed with hexane to give the product **293** (546 mg, 2.03 mmol, 48%) as a colorless solid.

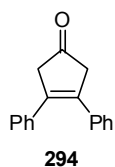
$^1\text{H NMR}$ (500 MHz, CD_2Cl_2) δ = 7.56-7.54 (m, 2H), 7.52-7.50 (m, 2H), 7.40-7.34 (m, 3H), 7.33-7.30 (m, 3H), 6.86 (s, 1H), 3.46 (d, J = 19.0 Hz, 1H), 3.07 (d, J = 19.0 Hz, 1H) ppm.

$^{13}\text{C NMR}$ (125 MHz, CD_2Cl_2) δ = 202.6, 172.6, 142.5, 131.3, 131.2, 130.2, 129.8, 129.2, 128.8, 128.4, 125.9, 74.2, 59.7 ppm.

MS (EI) m/z (%): 268 (28), 233 (100), 205 (26), 102 (16).

HRMS (EI) m/z calculated for $\text{C}_{17}\text{H}_{13}\text{ClO}$ 268.065495, found 268.065457.

3,4-Diphenylcyclopent-3-enone (**294**)



A solution of 4-chloro-3,4-diphenylcyclopent-2-enone (**293**, 540 mg, 2.01 mmol) in Et_2O (15 mL) was added to a vigorously stirred suspension of zinc dust (4.40 g, 67.3 mmol) in Et_2O (20 mL) and AcOH (1 mL). After complete addition the mixture was stirred for 30 min and then filtered over Celite and washed with Et_2O . The etheric layer was washed with H_2O and saturated NaHCO_3 -solution, dried over MgSO_4 and evaporated to dryness, to give the title compound **294** (451 mg, 1.92 mmol, 96%) as a colorless solid.

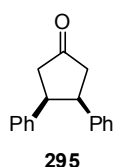
$^1\text{H NMR}$ (500 MHz, CD_2Cl_2) δ = 7.27-7.19 (m, 10H), 3.46 (s, 4H).

$^{13}\text{C NMR}$ (125 MHz, CD_2Cl_2) δ = 213.8, 137.0, 134.8, 128.6, 128.5, 127.8, 49.3 ppm.

MS (EI) m/z (%): 234 (100), 205 (58), 191 (24), 128 (16), 91 (41).

HRMS (EI) m/z calculated for $\text{C}_{17}\text{H}_{14}\text{O}$ 234.104465, found 234.104206.

cis-3,4-Diphenylcyclopentanone (**295**)



A mixture of 3,4-diphenylcyclopent-3-enone (**294**, 449 mg, 1.92 mmol) and Pd/C (204 mg, 10 mol%, 10% Pd, dry) in ethyl acetate (10 mL) was stirred under an atmosphere of H_2 (balloon) for 4 h. The mixture was filtered over Celite, washed with ethyl acetate and evaporated to dryness. The residue was purified by column chromatography on SiO_2 eluting with hexane:EtOAc (5:1) to yield the title compound **295** (410 mg, 1.74 mmol, 90%) as a colorless solid.

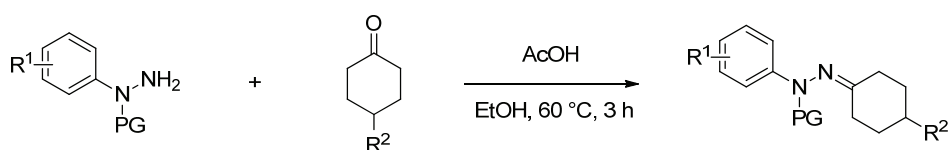
$^1\text{H NMR}$ (500 MHz, CD_2Cl_2) δ = 7.12-7.09 (m, 6H), 6.79-6.76 (m, 4H), 3.91-3.86 (m, 2H), 2.75 (dd, J = 18.9, 6.7 Hz, 2H), 2.67 (dd, J = 18.7, 8.2 Hz, 2H) ppm.

$^{13}\text{C NMR}$ (125 MHz, CD_2Cl_2) δ = 218.3, 140.2, 128.4, 128.2, 126.8, 47.6, 43.5 ppm.

MS (EI) m/z (%): 236 (36), 104 (100), 78 (8).

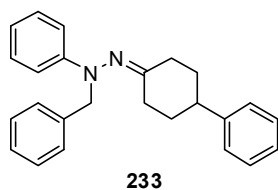
HRMS (EI) m/z calculated for $\text{C}_{17}\text{H}_{16}\text{O}$ 236.120118, found 236.120141.

7.4.2.3 Synthesis of Hydrazones



*General procedure for the synthesis of hydrazones **235** and **237**:*

A mixture of the protected arylhydrazine (1 equiv), the corresponding ketone (1 equiv) and one drop of AcOH in EtOH (1.0 mL per 0.50 mmol of ketone) was stirred at 60 °C for 3 h. After full conversion of the starting materials (monitored by TLC), the mixture was slowly cooled to -20 °C. The precipitate was filtered, washed with EtOH and dried *in vacuo* to yield the corresponding hydrazone. In cases where the desired product did not precipitate from the mixture, the solvent was removed under reduced pressure and the residue was purified by column chromatography on silica gel.

1-Benzyl-1-phenyl-2-(4-phenylcyclohexylidene)hydrazine (233)

233

The reaction was conducted on a 2.00 mmol scale.

Purification: Filtration.

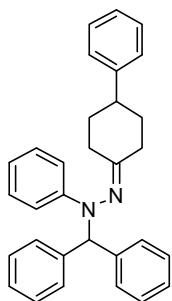
Yield: Colorless solid 612 mg (1.73 mmol, 86%).

¹H NMR (500 MHz, CD₂Cl₂) δ = 7.37 (d, J = 7.1 Hz, 2H), 7.33 (dd, J = 7.8, 7.3 Hz, 2H), 7.29-7.21 (m, 5H), 7.18 (tt, J = 7.2, 1.0 Hz, 1H), 7.13 (d, J = 7.2 Hz, 2H), 6.89- 6.87 (m, 2H), 6.84 (t, J = 7.3 Hz, 1H), 4.66 (d, J = 14.9 Hz, 1H), 4.53 (d, J = 14.9 Hz, 1H), 3.18-3.13 (m, 1H), 2.78-2.69 (m, 2H), 2.40 (ddd, J = 13.7, 13.7, 5.1 Hz, 1H), 2.09-2.04 (m, 1H), 1.82-1.78 (m, 1H), 1.71 (ddd, J = 13.8, 13.6, 6.6 Hz, 1H), 1.62 (ddd, J = 25.6, 13.1, 4.0 Hz, 1H), 1.15 (ddd, J = 25.6, 13.0, 4.1 Hz, 1H) ppm.

¹³C NMR (125 MHz, CD₂Cl₂) δ = 176.2, 150.9, 146.2, 139.4, 129.1, 129.0, 128.7, 128.6, 127.2, 127.0, 126.5, 120.0, 116.0, 60.5, 43.9, 35.3, 34.8, 33.5, 29.7 ppm.

MS (EI) m/z (%): 354 (100), 263 (100), 235 (8), 159 (14), 144 (41), 117 (15), 91 (37), 77 (36).

HRMS (EI) m/z calculated for C₂₅H₂₆N₂ 354.209599, found 354.209233.

1-Benzhydryl-1-phenyl-2-(4-phenylcyclohexylidene)hydrazine (235b)

235b

The reaction was conducted on a 0.338 mmol scale.

Purification: CC on SiO₂ (hexane:EtOAc 20:1).

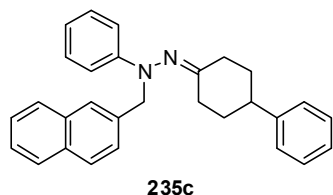
Yield: Colorless solid 105 mg (0.244 mmol, 72%).

¹H NMR (400 MHz, CD₂Cl₂) δ = 7.44-7.41 (m, 2H), 7.37-7.33 (m, 2H), 7.32-7.21 (m, 8H), 7.20-7.13 (m, 3H), 7.10-7.07 (m, 2H), 6.84-6.82 (m, 2H), 6.78 (tt, J = 7.3, 1.1 Hz, 1H), 6.17 (s, 1H), 3.19-3.14 (m, 1H), 2.70-2.58 (m, 2H), 2.30 (ddd, J = 13.7, 13.6, 5.0 Hz, 1H), 1.98-1.93 (m, 1H), 1.77-1.71 (m, 1H), 1.55 (ddd, J = 13.9, 13.7, 5.6 Hz, 1H), 1.41 (ddd, J = 25.5, 13.2, 4.0 Hz, 1H), 1.00 (ddd, J = 25.6, 13.2, 4.2 Hz, 1H) ppm.

¹³C NMR (100 MHz, CD₂Cl₂) δ = 177.5, 149.8, 146.3, 142.2, 141.5, 130.4, 130.1, 129.1, 128.7, 128.3, 128.2, 127.2, 127.1, 126.5, 120.3, 117.7, 71.1, 43.8, 35.3, 34.5, 33.4, 29.7 ppm.

MS (EI) m/z (%): 430 (18), 263 (89), 178 (21), 167 (100), 144 (17), 117 (6).

HRMS (EI) m/z calculated for C₃₁H₃₀N₂ 430.240896, found 430.240911.

1-(Naphthalen-2-ylmethyl)-1-phenyl-2-(4-phenylcyclohexylidene)hydrazine (235c)

The reaction was conducted on a 1.00 mmol scale.

Purification: Filtration.

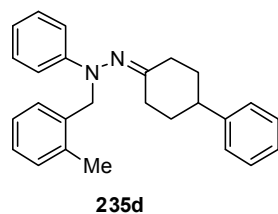
Yield: Colorless solid 362 mg (0.895 mmol, 90%).

¹H NMR (500 MHz, CD₂Cl₂) δ = 7.88-7.83 (m, 4H), 7.57 (dd, J = 8.4, 1.6 Hz, 1H), 7.54- 7.49 (m, 2H), 7.29-7.25 (m, 2H), 7.18-7.09 (m, 3H), 6.96 (d, J = 7.8 Hz, 2H), 6.88 (t, J = 7.3 Hz, 1H), 6.77-6.75 (m, 2H), 4.87 (d, J = 14.5 Hz, 1H), 4.61 (d, J = 14.5 Hz, 1H), 3.20-3.15 (m, 1H), 2.72-2.67 (m, 1H), 2.67-2.66 (m, 1H), 2.35 (ddd, J = 13.6, 13.6, 5.0 Hz, 1H), 1.99-1.93 (m, 1H), 1.70-1.61 (m, 2H), 1.41 (ddd, J = 25.7, 13.1, 4.0 Hz, 1H), 0.74 (ddd, J = 25.1, 12.6, 5.3 Hz, 1H) ppm.

¹³C NMR (125 MHz, CD₂Cl₂) δ = 177.0, 151.0, 146.0, 136.9, 133.7, 133.0, 129.2, 128.6, 128.2, 128.1, 128.1, 128.0, 127.7, 126.9, 126.5, 126.4, 126.0, 120.2, 116.1, 60.6, 43.8, 35.4, 35.0, 33.4, 29.6 ppm.

MS (EI) m/z (%): 404 (60), 387 (8), 283 (9), 263 (100), 235 (5), 159 (9), 141 (40), 115 (12).

HRMS (ESI+) m/z calculated for C₂₉H₂₈N₂Na (M+Na⁺) 427.214464, found 427.214678.

1-(2-Methylbenzyl)-1-phenyl-2-(4-phenylcyclohexylidene)hydrazine (235d)

The reaction was conducted on a 1.00 mmol scale.

Purification: CC on SiO₂ hexane:EtOAc (12:1).

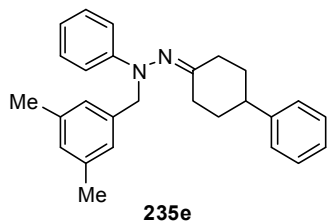
Yield: Yellow oil 340 mg (0.924 mmol, 92%).

¹H NMR (500 MHz, CD₂Cl₂) δ = 7.32 (d, J = 7.1 Hz, 1H), 7.29-7.24 (m, 4H), 7.23-7.17 (m, 4H), 7.11-7.09 (m, 2H), 6.93-6.91 (m, 2H), 6.88 (t, J = 7.3 Hz, 1H), 4.65 (d, J = 14.4 Hz, 1H), 4.56 (d, J = 14.4 Hz, 1H), 3.09-3.05 (m, 1H), 2.72-2.66 (m, 2H), 2.44 (s, 3H), 2.36 (ddd, J = 13.8, 13.5, 5.0 Hz, 1H), 2.06-2.00 (m, 1H), 1.73-1.68 (m, 1H), 1.60 (ddd, J = 13.8, 13.6, 5.4 Hz, 1H), 1.54 (ddd, J = 25.7, 13.1, 4.0 Hz, 1H), 0.89 (ddd, J = 25.8, 13.1, 4.1 Hz, 1H) ppm.

¹³C NMR (500 MHz, CD₂Cl₂) δ = 177.0, 151.1, 146.2, 137.4, 136.9, 130.5, 130.4, 129.2, 128.7, 127.5, 127.1, 126.5, 125.9, 120.2, 116.0, 58.1, 43.9, 35.3, 34.8, 33.4, 29.6, 19.4 ppm.

MS (EI) m/z (%): 368 (75), 263 (100), 159 (11), 144 (34), 117 (11), 92 (15), 77 (22).

HRMS (ESI+) m/z calculated for C₂₆H₂₈N₂Na (M+Na⁺) 391.214465, found 391.214604.

1-(3,5-Dimethylbenzyl)-1-phenyl-2-(4-phenylcyclohexylidene)hydrazine (235e)

The reaction was conducted on a 1.00 mmol scale.

Purification: CC on SiO₂ hexane:EtOAc (20:1).

Yield: Yellow oil 340 mg (0.996 mmol, >99%).

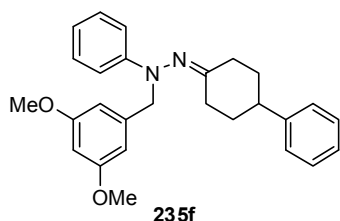
¹H NMR (500 MHz, CD₂Cl₂) δ = 7.30 (dd, J = 7.7, 7.5 Hz, 2H), 7.23 (dd, J = 8.6, 7.4 Hz, 2H), 7.18 (tt, J = 7.4, 1.1 Hz, 1H), 7.14-7.12 (m,

2H), 6.99 (s, 2H), 6.92 (s, 1H), 6.87 (d, J = 7.9 Hz, 2H), 6.84 (t, J = 7.3 Hz, 1H), 4.61 (d, J = 14.8 Hz, 1H), 4.43 (d, J = 14.8 Hz, 1H), 3.19-3.14 (m, 1H), 2.78-2.69 (m, 2H), 2.41 (ddd, J = 13.7, 13.6, 5.1 Hz, 1H), 2.30 (s, 6H), 2.10-2.05 (m, 1H), 1.82-1.77 (m, 1H), 1.71 (ddd, J = 13.8, 13.5, 5.5 Hz, 1H), 1.59 (ddd, J = 25.6, 13.1, 4.0 Hz, 1H), 1.13 (ddd, J = 25.6, 12.9, 4.1 Hz, 1H) ppm.

¹³C NMR (500 MHz, CD₂Cl₂) δ = 176.3, 151.0, 146.2, 139.3, 138.1, 129.1, 128.8, 128.7, 127.0, 126.7, 126.5, 119.9, 115.9, 60.6, 43.9, 35.4, 35.0, 33.4, 29.7, 21.4 ppm.

MS (EI) m/z (%): 382 (80), 263 (100), 235 (6), 159 (11), 144 (34), 119 (17).

HRMS (ESI+) m/z calculated for C₂₇H₃₀N₂Na (M+Na⁺) 405.230119, found 405.230226.

1-(3,5-Dimethoxybenzyl)-1-phenyl-2-(4-phenylcyclohexylidene)hydrazine (235f)

The reaction was conducted on a 1.00 mmol scale.

Purification: CC on SiO₂ hexane:EtOAc (15:1 to 1:1).

Yield: Yellow oil 392 mg (0.945 mmol, 95%).

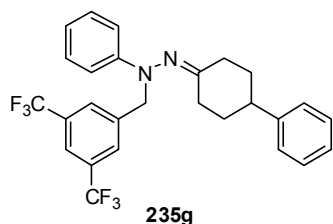
¹H NMR (500 MHz, CD₂Cl₂) δ = 7.30 (dd, J = 7.6, 7.5 Hz, 2H), 7.25 (dd, J = 8.7, 7.3 Hz, 2H), 7.20 (tt, J = 7.3, 1.2 Hz, 1H), 7.18-7.16 (m,

2H), 6.90-6.88 (m, 2H), 6.86 (tt, J = 7.3, 0.9 Hz, 1H), 6.56 (d, J = 2.3 Hz, 2H), 6.37 (d, J = 2.3 Hz, 1H), 4.62 (d, J = 15.1 Hz, 1H), 4.49 (d, J = 15.1 Hz, 1H), 3.77 (s, 6H), 3.23-3.18 (m, 1H), 2.82-2.72 (m, 2H), 2.43 (ddd, J = 13.7, 13.7, 5.0 Hz, 1H), 2.13-2.08 (m, 1H), 1.88-1.83 (m, 1H), 1.78 (ddd, J = 13.8, 13.4, 5.5 Hz, 1H), 1.67 (ddd, J = 25.6, 13.2, 4.1 Hz, 1H), 1.27 (ddd, J = 25.5, 12.9, 4.2 Hz, 1H) ppm.

¹³C NMR (125 MHz, CD₂Cl₂) δ = 175.9, 161.2, 151.0, 146.2, 142.0, 129.1, 128.7, 127.0, 126.6, 120.1, 116.0, 106.6, 99.0, 60.9, 55.6, 43.9, 35.4, 34.9, 33.6, 29.8 ppm.

MS (EI) m/z (%): 414 (83), 263 (100), 235 (5), 144 (32), 117 (10).

HRMS (ESI+) m/z calculated for C₂₇H₃₀N₂O₂Na (M+Na⁺) 437.219944, found 437.219723.

1-(3,5-bis(Trifluoromethyl)benzyl)-1-phenyl-2-(4-phenylcyclohexylidene)hydrazine (235g)

The reaction was conducted on a 1.00 mmol scale.

Purification: CC on SiO₂ hexane:EtOAc (15:1).

Yield: Colorless oil 445 mg (0.908 mmol, 91%).

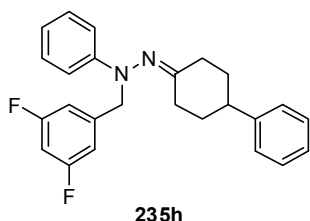
¹H NMR (500 MHz, CD₂Cl₂) δ = 7.88 (s, 2H), 7.83 (s, 1H), 7.30-7.25 (m, 4H), 7.18 (tt, J = 7.4, 1.4 Hz, 1H), 7.14-7.12 (m, 2H), 6.95-6.91

(m, 3H), 4.77 (d, J = 15.4 Hz, 1H), 4.73 (d, J = 15.4 Hz, 1H), 3.16-3.12 (m, 1H), 2.80-2.74 (m, 1H), 2.71-2.66 (m, 1H), 2.40 (ddd, J = 13.8, 13.7, 5.1 Hz, 1H), 2.11-2.06 (m, 1H), 1.90-1.84 (m, 1H), 1.72 (ddd, J = 14.1, 13.8, 5.5 Hz, 1H), 1.60 (ddd, J = 25.6, 13.2, 4.1 Hz, 1H), 1.27 (ddd, J = 25.7, 13.2, 4.2 Hz, 1H) ppm.

¹³C NMR (500 MHz, CD₂Cl₂) δ = 176.1, 151.0, 145.9, 142.8, 131.6 (q, J = 33.0 Hz), 129.5, 129.0 (q, J = 3.1 Hz), 128.8, 127.0, 126.6, 123.9 (q, J = 272.5 Hz), 121.2 (sept, J = 3.9 Hz), 117.3, 117.2, 61.4, 43.7, 35.3, 34.8, 33.4, 29.9 ppm.

MS (EI) m/z (%): 490 (100), 319 (5), 263 (60), 235 (5), 227 (4), 159 (10), 144 (29), 117 (11).

HRMS (ESI+) m/z calculated for C₂₇H₂₄N₂F₆Na (M+Na⁺) 513.173589, found 513.173978.

1-(3,5-Difluorobenzyl)-1-phenyl-2-(4-phenylcyclohexylidene)hydrazine (235h)

The reaction was conducted on a 1.00 mmol scale.

Purification: CC on SiO₂ hexane:EtOAc (13:1).

Yield: Colorless oil 313 mg (0.801 mmol, 80%).

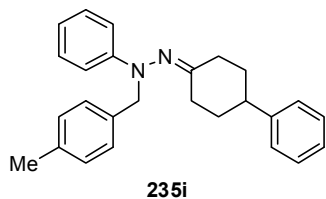
¹H NMR (500 MHz, CD₂Cl₂) δ = 7.33-7.28 (m, 2H), 7.27-7.24 (m, 2H), 7.21-7.17 (m, 3H), 6.98-6.93 (m, 2H), 6.91-6.86 (m, 3H), 6.73 (tt, J =

9.0, 2.4 Hz, 1H), 4.64 (d, J = 15.6 Hz, 1H), 4.58 (d, J = 15.6 Hz, 1H), 3.19-3.14 (m, 1H), 2.84-2.77 (m, 1H), 2.75-2.71 (m, 1H), 2.44 (ddd, J = 13.8, 13.7, 5.1 Hz, 1H), 2.15-2.10 (m, 1H), 1.94-1.87 (m, 1H), 1.80 (ddd, J = 14.0, 13.7, 5.5 Hz, 1H), 1.69 (ddd, J = 23.6, 13.2, 4.1 Hz, 1H), 1.36 (ddd, J = 25.6, 13.1, 4.2 Hz, 1H) ppm.

¹³C NMR (125 MHz, CD₂Cl₂) δ = 175.9, 163.3 (dd, J = 247.8, 12.4 Hz), 150.7, 146.0, 144.1, 129.3, 128.8, 127.0, 126.6, 120.7, 116.5, 111.3 (dd, J = 19.7, 5.8 Hz), 102.4 (t, J = 25.5 Hz), 60.7, 43.8, 35.3, 34.8, 33.6, 29.8 ppm.

MS (EI) m/z (%): 390 (100), 263 (52), 235 (4), 219 (4), 144 (26), 117 (11), 92 (18), 77 (30).

HRMS (ESI+) m/z calculated for C₂₅H₂₄N₂F₂Na (M+Na⁺) 413.179970, found 413.180191.

1-(4-Methylbenzyl)-1-phenyl-2-(4-phenylcyclohexylidene)hydrazine (235i)

The reaction was conducted on a 1.00 mmol scale.

Purification: Filtration.

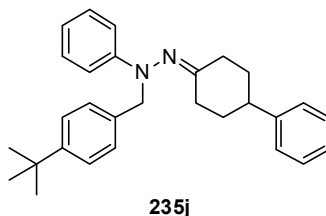
Yield: Colorless solid 295 mg (0.801 mmol, 80%).

¹H NMR (500 MHz, CD₂Cl₂) δ = 7.31-7.23 (m, 6H), 7.20 (tt, J = 7.4, 1.6 Hz, 1H), 7.17 (d, J = 7.9 Hz, 2H), 7.15-7.13 (m, 2H), 6.91-6.90 (m, 2H), 6.86 (t, J = 7.3 Hz, 1H), 4.66 (d, J = 14.6 Hz, 1H), 4.46 (d, J = 14.6 Hz, 1H), 3.19-3.14 (m, 1H), 2.78-2.70 (m, 2H), 2.41 (ddd, J = 13.7, 13.6, 5.1 Hz, 1H), 2.36 (s, 3H), 2.10-2.05 (m, 1H), 1.81- 1.75 (m, 1H), 1.71 (ddd, J = 13.8, 13.3, 5.5 Hz, 1H), 1.62 (ddd, J = 25.6, 13.1, 4.1 Hz, 1H), 1.06 (ddd, J = 25.4, 12.8, 4.2 Hz, 1H) ppm.

¹³C NMR (500 MHz, CD₂Cl₂) δ = 176.5, 150.9, 146.2, 136.9, 136.1, 129.2, 129.2, 129.1, 128.7, 127.0, 126.5, 120.0, 116.0, 59.9, 43.9, 35.4, 34.9, 33.5, 29.6, 21.2 ppm.

MS (EI) m/z (%): 368 (74), 263 (100), 235 (5), 159 (10), 144 (32), 117 (10), 105 (22), 92 (14), 77 (21).

HRMS (ESI+) m/z calculated for C₂₆H₂₈N₂Na (M+Na⁺) 391.214465, found 391.214526.

1-(4-(*tert*-Butyl)benzyl)-1-phenyl-2-(4-phenylcyclohexylidene)hydrazine (235j)

The reaction was conducted on a 1.00 mmol scale.

Purification: Filtration.

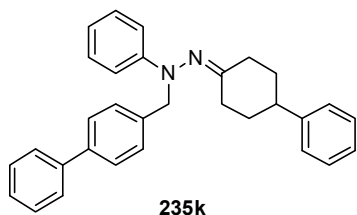
Yield: Colorless waxy solid 274 mg (0.668 mmol, 64%).

¹H NMR (500 MHz, CD₂Cl₂) δ = 7.36 (d, J = 8.3 Hz, 2H), 7.30-7.26 (m, 4H), 7.23 (dd, J = 8.4, 7.5 Hz, 2H), 7.18 (t, J = 7.4 Hz, 1H), 7.14 (d, J = 7.3 Hz, 2H), 6.88 (d, J = 8.0 Hz, 2H), 6.84 (t, J = 7.3 Hz, 1H), 4.65 (d, J = 15.0 Hz, 1H), 4.49 (d, J = 15.0 Hz, 1H), 3.18-3.15 (m, 1H), 2.79-2.70 (m, 2H), 2.41 (ddd, J = 13.7, 13.7, 5.0 Hz, 1H), 2.11-2.05 (m, 1H), 1.82-1.78 (m, 1H), 1.73 (ddd, J = 13.8, 13.4, 5.5 Hz, 1H), 1.64 (ddd, J = 25.7, 13.1, 4.0 Hz, 1H), 1.30 (s, 9H), 1.15 (ddd, J = 25.4, 12.7, 4.1 Hz, 1H) ppm.

¹³C NMR (125 MHz, CD₂Cl₂) δ = 176.2, 151.0, 150.2, 146.2, 136.3, 129.1, 128.7, 128.6, 127.0, 126.5, 125.4, 119.9, 115.9, 60.0, 43.8, 35.4, 34.7, 34.7, 33.6, 31.5, 29.7 ppm.

MS (EI) m/z (%): 410 (65), 263 (100), 235 (4), 159 (7), 144 (21), 117 (14), 92 (13), 77 (17).

HRMS (ESI+) m/z calculated for C₂₉H₃₄N₂Na (M+Na⁺) 433.261416, found 433.261294.

1-([1,1'-Biphenyl]-4-ylmethyl)-1-phenyl-2-(4-phenylcyclohexylidene)hydrazine (235k)

The reaction was conducted on a 1.00 mmol scale.

Purification: Filtration.

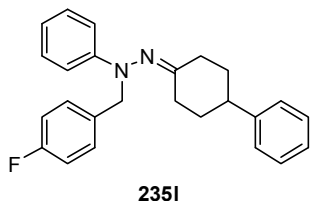
Yield: Colorless solid 397 mg (0.922 mmol, 92%).

¹H NMR (500 MHz, CD₂Cl₂) δ = 7.65-7.62 (m, 4H), 7.49-7.45 (m, 4H), 7.38 (t, J = 7.4 Hz, 1H), 7.30-7.26 (m, 2H), 7.18-7.12 (m, 3H), 7.08-7.06 (m, 2H), 6.94 (d, J = 7.8 Hz, 2H), 6.89 (t, J = 7.3 Hz, 1H), 4.76 (d, J = 14.6 Hz, 1H), 4.54 (d, J = 14.6 Hz, 1H), 3.24-3.19 (m, 1H), 2.77-2.71 (m, 2H), 2.42 (ddd, J = 13.7, 13.7, 5.0 Hz, 1H), 2.09-2.04 (m, 1H), 1.82-1.71 (m, 2H), 1.60 (ddd, J = 25.7, 13.1, 5.0 Hz, 1H), 1.10 (ddd, J = 25.7, 12.4, 4.5 Hz, 1H) ppm.

¹³C NMR (125 MHz, CD₂Cl₂) δ = 176.7, 150.9, 146.1, 141.0, 140.0, 138.5, 129.8, 129.2, 129.1, 128.7, 127.6, 127.3, 127.1, 127.0, 126.5, 120.1, 116.1, 60.0, 43.9, 35.4, 35.0, 33.5, 29.7 ppm.

MS (EI) m/z (%): 430 (66), 263 (100), 235 (4), 167 (48), 144 (22), 117 (9).

HRMS (EI) m/z calculated for C₃₁H₃₀N₂ 453.230113, found 453.230525.

1-(4-Fluorobenzyl)-1-phenyl-2-(4-phenylcyclohexylidene)hydrazine (235l)

The reaction was conducted on a 1.00 mmol scale.

Purification: Filtration.

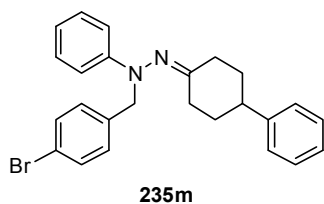
Yield: Colorless solid 239 mg (0.642 mmol, 64%).

¹H NMR (500 MHz, CD₂Cl₂) δ = 7.36 (dd, J = 8.5, 5.6 Hz, 2H), 7.29 (dd, J = 7.7, 7.5 Hz, 2H), 7.24 (dd, J = 8.6, 7.3 Hz, 2H), 7.19 (t, J = 7.4 Hz, 1H), 7.14 (d, J = 7.1 Hz, 2H), 7.06-7.01 (m, 2H), 6.89 (d, J = 7.9 Hz, 2H), 6.87 (t, J = 7.4 Hz, 1H), 4.62 (d, J = 14.7 Hz, 1H), 4.51 (d, J = 14.7 Hz, 1H), 3.16-3.12 (m, 1H), 2.79-2.69 (m, 2H), 2.40 (ddd, J = 13.7, 13.7, 5.1 Hz, 1H), 2.11-2.06 (m, 1H), 1.85-1.79 (m, 1H), 1.70 (ddd, J = 13.9, 13.7, 5.5 Hz, 1H), 1.63 (ddd, J = 26.6, 13.2, 4.0 Hz, 1H), 1.17 (ddd, J = 25.8, 13.1, 4.2 Hz, 1H) ppm.

¹³C NMR (125 MHz, CD₂Cl₂) δ = 176.4, 162.3 (d, J = 244.6 Hz), 150.8, 146.1, 135.2 (d, J = 3.1 Hz), 130.8 (d, J = 8.2 Hz), 129.2, 128.7, 127.0, 126.6, 120.3, 116.3, 115.2 (d, J = 21.3 Hz), 59.8, 43.8, 35.3, 34.8, 33.6, 29.7 ppm.

MS (EI) m/z (%): 372 (96), 263 (100), 235 (6), 159 (12), 144 (39), 109 (18), 92 (18), 77 (26).

HRMS (ESI+) m/z calculated for C₂₅H₂₅N₂FNa (M+Na⁺) 395.189394, found 395.189501.

1-(4-Bromobenzyl)-1-phenyl-2-(4-phenylcyclohexylidene)hydrazine (235m)

The reaction was conducted on a 1.00 mmol scale.

Purification: Filtration.

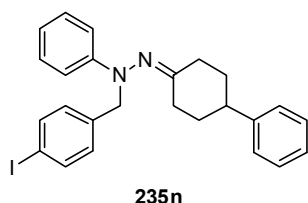
Yield: Colorless solid 405 mg (0.934 mmol, 93%).

$^1\text{H NMR}$ (500 MHz, CD_2Cl_2) δ = 7.50-7.46 (m, 2H), 7.32-7.28 (m, 4H), 7.27-7.24 (m, 2H), 7.20 (tt, J = 7.4, 1.2 Hz, 1H), 7.16-7.14 (m, 2H), 6.90-6.87 (m, 3H), 4.63 (d, J = 14.8 Hz, 1H), 4.48 (d, J = 14.8 Hz, 1H), 3.17-3.12 (m, 1H), 2.79-2.68 (m, 2H), 2.41 (ddd, J = 13.7, 13.7, 5.0 Hz, 1H), 2.11-2.05 (m, 1H), 1.85-1.79 (m, 1H), 1.72 (ddd, J = 13.8, 13.6, 5.5 Hz, 1H), 1.60 (ddd, J = 25.6, 13.2, 4.1 Hz, 1H), 1.13 (ddd, J = 25.6, 13.0, 4.1 Hz, 1H) ppm.

$^{13}\text{C NMR}$ (125 MHz, CD_2Cl_2) δ = 176.5, 150.8, 146.1, 138.5, 131.6, 131.1, 129.2, 128.8, 127.1, 126.6, 121.0, 120.4, 116.2, 59.9, 43.8, 35.4, 34.9, 33.6, 29.7 ppm.

MS (EI) m/z (%): 432/434 (41/42), 263 (100), 235 (5), 159 (11), 144 (33), 117 (11).

HRMS (ESI+) m/z calculated for $\text{C}_{25}\text{H}_{25}\text{N}_2\text{BrNa}$ ($\text{M}+\text{Na}^+$) 455.109342, found 455.109769.

1-(4-Iodobenzyl)-1-phenyl-2-(4-phenylcyclohexylidene)hydrazine (235n)

The reaction was conducted on a 1.00 mmol scale.

Purification: Filtration.

Yield: Colorless solid 410 mg (0.853 mmol, 85%).

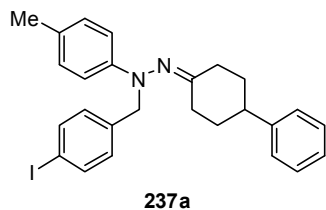
$^1\text{H NMR}$ (500 MHz, CD_2Cl_2) δ = 7.71-7.68 (m, 2H), 7.34-7.31 (m, 2H), 7.28-7.24 (m, 2H), 7.23-7.19 (m, 1H), 7.18-7.15 (m, 4H), 6.90-6.87 (m, 3H), 4.63 (d, J = 14.8 Hz, 1H), 4.46 (d, J = 14.8 Hz, 1H), 3.17-3.13 (m, 1H), 2.80-2.69 (m, 2H), 2.41 (ddd, J = 13.7, 13.7, 5.1 Hz, 1H), 2.11-2.06 (m, 1H), 1.84-1.80 (m, 1H), 1.71-1.70 (m, 1H), 1.60 (ddd, J = 25.6, 13.2, 4.1 Hz, 1H), 1.23 (ddd, J = 25.6, 13.0, 4.1 Hz, 1H) ppm.

$^{13}\text{C NMR}$ (125 MHz, CD_2Cl_2) δ = 176.5, 150.7, 146.1, 139.2, 137.6, 131.3, 129.2, 128.8, 127.1, 126.5, 120.4, 116.2, 92.5, 60.0, 43.8, 35.4, 34.9, 33.5, 29.6 ppm.

MS (EI) m/z (%): 480 (88), 263 (100), 217 (10), 159 (10), 144 (31), 117 (10).

HRMS (ESI+) m/z calculated for $\text{C}_{25}\text{H}_{25}\text{N}_2\text{INa}$ ($\text{M}+\text{Na}^+$) 503.095463, found 503.095951.

mp = 135-136 °C (EtOH).

1-(4-Iodobenzyl)-2-(4-phenylcyclohexylidene)-1-(p-tolyl)hydrazine (237a)

The reaction was conducted on a 0.500 mmol scale.

Purification: Filtration.

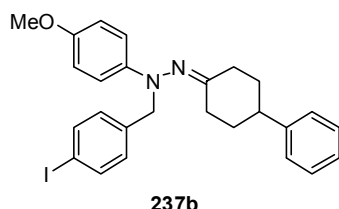
Yield: Colorless solid 206 mg (0.416 mmol, 83%).

¹H NMR (400 MHz, CD₂Cl₂) δ = 7.67 (d, J = 8.2 Hz, 2H), 7.31 (dd, J = 7.6, 7.4 Hz, 2H), 7.19 (t, J = 7.4 Hz, 1H), 7.17-7.14 (m, 4H), 7.06 (d, J = 8.2 Hz, 2H), 6.80 (d, J = 8.5 Hz, 2H), 4.55 (d, J = 14.6 Hz, 1H), 4.40 (d, J = 14.6 Hz, 1H), 3.17-3.13 (m, 1H), 2.77-2.71 (m, 1H), 2.71-2.65 (m, 1H), 2.38 (ddd, J = 13.7, 13.6, 5.0 Hz, 1H), 2.27 (s, 3H), 2.08-2.04 (m, 1H), 1.82-1.78 (m, 1H), 1.70 (ddd, J = 13.8, 13.5, 5.4 Hz, 1H), 1.58 (ddd, J = 25.7, 13.1, 4.0 Hz, 1H), 1.11 (ddd, J = 25.6, 12.9, 4.1 Hz, 1H) ppm.

¹³C NMR (100 MHz, CD₂Cl₂) δ = 175.7, 148.9, 146.2, 139.5, 137.6, 131.4, 130.2, 129.7, 128.8, 127.1, 126.5, 116.8, 92.5, 60.7, 43.9, 35.4, 35.0, 33.6, 29.7, 20.6 ppm.

MS (EI) m/z (%): 494 (100), 477 (23), 373 (22), 277 (97), 217 (40), 144 (41).

HRMS (ESI+) m/z calculated for C₂₆H₂₇N₂INa (M+Na⁺) 517.111115, found 517.110718.

1-(4-Iodobenzyl)-1-(4-methoxyphenyl)-2-(4-phenylcyclohexylidene)hydrazine (237b)^[221]

The reaction was conducted on a 0.500 mmol scale.

Purification: Filtration.

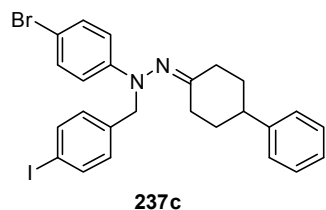
Yield: Colorless solid 184 mg (0.360 mmol, 72%).

¹H NMR (500 MHz, CDCl₃) δ = 7.65 (d, J = 8.0 Hz, 2H), 7.31-7.28 (m, 2H), 7.19-7.17 (m, 1H), 7.12-7.09 (m, 4H), 6.89-6.88 (m, 2H), 6.83-6.80 (m, 2H), 4.45 (d, J = 14.1 Hz, 1H), 4.36 (d, J = 14.1 Hz, 1H), 3.76 (s, 3H), 3.23-3.20 (m, 1H), 2.72-2.63 (m, 2H), 2.32 (ddd, J = 13.5, 13.5, 4.8 Hz, 1H), 2.05-2.03 (m, 1H), 1.80-1.78 (m, 1H), 1.67-1.60 (m, 1H), 1.54 (ddd, J = 25.8, 13.2, 4.1 Hz, 1H), 1.07 (ddd, J = 25.8, 13.1, 4.1 Hz, 1H) ppm.

¹³C NMR (125 MHz, CDCl₃) δ = 174.9, 154.7, 145.6, 145.4, 138.9, 137.4, 131.3, 128.7, 126.9, 126.4, 119.3, 114.4, 92.5, 61.9, 55.7, 43.7, 35.3, 34.7, 33.2, 29.5 ppm.

MS (EI) m/z (%): 493 (100), 389 (95), 262 (15), 217 (15), 172 (45).

HRMS (ESI+) m/z calculated for C₂₆H₂₇N₂OINa (M+Na⁺) 533.106032, found 533.106085.

1-(4-Bromophenyl)-1-(4-iodobenzyl)-2-(4-phenylcyclohexylidene)hydrazine (237c)^[221]

The reaction was conducted on a 0.300 mmol scale.

Purification: Filtration.

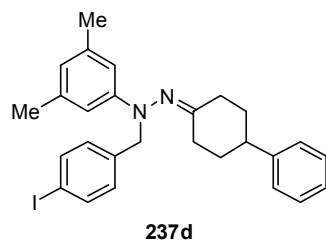
Yield: Colorless solid 107 mg (0.191 mmol, 64%).

¹H NMR (500 MHz, CDCl₃) δ = 7.66-7.64 (m, 2H), 7.32-7.48 (m, 4H), 7.20-7.17 (m, 1H), 7.10-7.07 (m, 4H), 6.74-6.70 (m, 2H), 4.54 (d, J = 14.7 Hz, 1H), 4.40 (d, J = 14.7 Hz, 1H), 3.10-3.06 (m, 1H), 2.74-2.68 (m, 2H), 2.36 (ddd, J = 13.7, 13.7, 5.0 Hz, 1H), 2.10-2.05 (m, 1H), 1.84-1.79 (m, 1H), 1.68 (ddd, J = 13.7, 13.7, 5.5 Hz, 1H), 1.60-1.51 (m, 1H), 1.07 (ddd, J = 25.8, 13.3, 4.2 Hz, 1H) ppm.

¹³C NMR (125 MHz, CDCl₃) δ = 177.4, 149.4, 145.3, 138.0, 137.6, 131.9, 131.0, 128.7, 126.8, 126.5, 117.6, 112.7, 92.8, 59.9, 43.6, 35.2, 34.7, 33.3, 29.6 ppm.

MS (EI) m/z (%): 560 (100), 558 (100), 343 (70), 341 (70), 262 (15), 217 (30), 172 (20), 170 (20), 144 (35), 117 (20), 93 (30), 91 (30).

HRMS (EI) m/z calculated for C₂₅H₂₄BrI 558.016774, found 558.016667.

1-(3,5-Dimethylphenyl)-1-(4-iodobenzyl)-2-(4-phenylcyclohexylidene)hydrazine (235d)^[221]

The reaction was conducted on a 0.500 mmol scale.

Purification: Filtration.

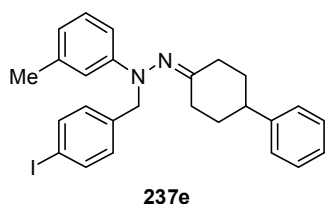
Colorless solid 113 mg (0.222 mmol, 44%).

¹H NMR (500 MHz, CDCl₃) δ = 7.69-7.67 (m, 2H), 7.34-7.31 (m, 2H), 7.23-7.20 (m, 1H), 7.15-7.12 (m, 4H), 6.57-6.53 (m, 3H), 4.60 (d, J = 14.6 Hz, 1H), 4.44 (d, J = 14.6 Hz, 1H), 3.17-3.14 (m, 1H), 2.76-2.70 (m, 2H), 2.39 (td, J = 13.7, 5.0 Hz, 1H), 2.29 (s, 6H), 2.10-2.06 (m, 1H), 1.83-1.78 (m, 1H), 1.68 (dt, J = 13.7, 5.4 Hz, 1H), 1.62-1.53 (m, 1H), 1.12-1.03 (m, 1H) ppm.

¹³C NMR (125 MHz, CDCl₃) δ = 176.3, 150.7, 145.5, 138.9, 138.6, 137.3, 131.0, 128.6, 126.7, 126.3, 122.5, 114.0, 92.4, 60.5, 43.6, 35.2, 34.7, 33.1, 29.5, 21.7 ppm.

MS (EI) m/z (%): 508 (90), 291 (100), 217 (10), 144 (27).

HRMS (ESI+) m/z calculated for C₂₇H₂₉N₂INa (M+Na⁺) 531.126763, found 531.126824.

1-(4-Iodobenzyl)-2-(4-phenylcyclohexylidene)-1-(m-tolyl)hydrazine (237e)

The reaction was conducted on a 0.300 mmol scale.

Purification: CC on SiO₂ eluting (hexane:EtOAc 9:1).

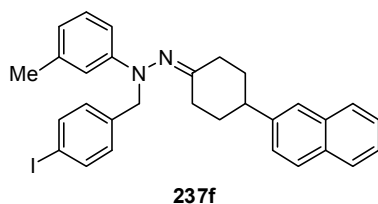
Yield: Pale yellow solid 73.0 mg (0.147 mmol, 49%).

¹H NMR (400 MHz, CDCl₃) δ = 7.72-7.68 (m, 2H), 7.36-7.33 (m, 2H), 7.25-7.21 (m, 1H), 7.19-7.14 (m, 5H), 6.76-6.70 (m, 3H), 4.63 (d, J = 14.6 Hz, 1H), 4.48 (d, J = 14.6 Hz, 1H), 3.21-3.16 (m, 1H), 2.79-2.71 (m, 2H), 2.42 (ddd, J = 18.6, 13.7, 5.0 Hz, 1H), 2.35 (s, 3H), 2.15-2.09 (m, 1H), 1.87-1.80 (m, 1H), 1.75-1.56 (m, 2H), 1.18-1.07 (m, 1H) ppm.

¹³C NMR (100 MHz, CDCl₃) 176.3, 150.6, 145.4, 138.8, 138.8, 137.3, 131.0, 128.9, 128.6, 126.7, 126.3, 121.4, 116.8, 113.2, 92.4, 60.3, 43.6, 35.1, 34.6, 33.1, 29.5, 21.8 ppm.

MS (EI) m/z (%): 494 (75), 277 (100), 217 (10), 144 (35).

HRMS (ESI+) m/z calculated for C₂₆H₂₈N₂I (M⁺) 495.128899, found 495.129166.

1-(4-Iodobenzyl)-2-(4-(naphthalen-2-yl)cyclohexylidene)-1-(m-tolyl)hydrazine (237f)

The reaction was conducted on a 0.300 mmol scale.

Purification: CC on SiO₂ (hexane:EtOAc 9:1).

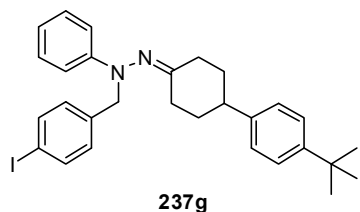
Yield: Pale yellow solid 135 mg (0.247 mmol, 82%).

¹H NMR (400 MHz, CD₂Cl₂) δ = 7.84-7.80 (m, 3H), 7.71-7.68 (m, 2H), 7.59 (d, J = 0.8 Hz, 1H), 7.49-7.41 (m, 2H), 7.30 (dd, J = 8.5, 1.7 Hz, 1H), 7.18-7.11 (m, 3H), 6.73- 6.67 (m, 3H), 4.61 (d, J = 14.8 Hz, 1H), 4.46 (d, J = 14.8 Hz, 1H), 3.20-3.14 (m, 1H), 2.97-2.89 (m, 1H), 2.76-2.71 (m, 1H), 2.45 (ddd, J = 13.7, 13.6, 5.0 Hz, 1H), 2.32 (s, 3H), 2.19-2.14 (m, 1H), 1.93-1.88 (m, 1H), 1.81-1.65 (m, 2H), 1.25 (ddd, J = 25.5, 13.1, 4.2 Hz, 1H) ppm.

¹³C NMR (100 MHz, CD₂Cl₂) δ = 176.2, 150.9, 143.6, 139.4, 139.1, 137.6, 134.0, 132.7, 131.3, 129.1, 128.4, 128.0, 127.8, 126.3, 126.1, 125.6, 125.0, 121.4, 117.1, 113.5, 92.5, 60.3, 44.0, 35.4, 34.8, 33.5, 29.7, 21.8 ppm.

MS (EI) m/z (%): 544 (87), 327 (100), 194 (21), 167 (21), 91 (25).

HRMS (ESI+) m/z calculated for C₃₀H₂₉N₂I/Na (M+Na⁺) 567.126763, found 567.127244.

2-(4-(4-(*tert*-Butyl)phenyl)cyclohexylidene)-1-(4-iodobenzyl)-1-phenylhydrazine (237g)

The reaction was conducted on a 0.500 mmol scale.

Purification: Filtration.

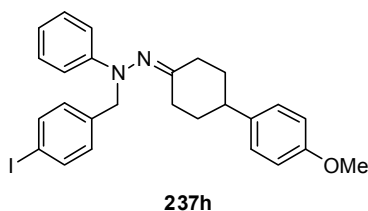
Yield: Colorless solid 222 mg (0.414 mmol, 83%).

¹H NMR (500 MHz, CD₂Cl₂) δ = 7.67 (d, J = 8.2 Hz, 2H), 7.33 (d, J = 8.3 Hz, 2H), 7.23 (dd, J = 8.1, 7.8 Hz, 2H), 7.15 (d, J = 8.2 Hz, 2H), 7.07 (d, J = 8.3 Hz, 2H), 6.87-6.84 (m, 3H), 4.60 (d, J = 14.9 Hz, 1H), 4.45 (d, J = 14.9 Hz, 1H), 3.14-3.08 (m, 1H), 2.75-2.65 (m, 2H), 2.42-2.34 (m, 1H), 2.08-2.02 (m, 1H), 1.82-1.77 (m, 1H), 1.71 (ddd, J = 13.8, 13.6, 5.5 Hz, 1H), 1.62-1.53 (m, 1H), 1.30 (s, 9H), 1.11 (ddd, J = 25.6, 12.9, 4.1 Hz, 1H) ppm.

¹³C NMR (125 MHz, CD₂Cl₂) δ = 176.6, 150.8, 149.4, 143.0, 139.2, 137.6, 131.3, 129.2, 126.7, 125.7, 120.3, 116.2, 92.5, 60.0, 43.3, 35.4, 35.0, 34.6, 33.6, 31.5, 29.7 ppm.

MS (EI) m/z (%): 536 (82), 359 (7), 319 (31), 263 (100), 217 (9).

HRMS (ESI+) m/z calculated for C₂₉H₃₃N₂I (M+Na⁺) 559.158063, found 559.157849.

1-(4-Iodobenzyl)-2-(4-(4-methoxyphenyl)cyclohexylidene)-1-phenylhydrazine (237h)

The reaction was conducted on a 0.500 mmol scale.

Purification: Filtration.

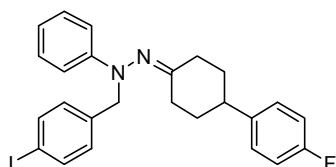
Yield: Colorless solid 154 mg (0.302 mmol, 60%).

¹H NMR (500 MHz, CD₂Cl₂) δ = 7.67 (d, J = 8.2 Hz, 2H), 7.23 (dd, J = 8.1, 7.8 Hz, 2H), 7.15 (d, J = 8.2 Hz, 2H), 7.05 (d, J = 8.6 Hz, 2H), 6.87-6.83 (m, 5H), 4.61 (d, J = 14.8 Hz, 1H), 4.44 (d, J = 14.8 Hz, 1H), 3.76 (s, 3H), 3.12-3.09 (m, 1H), 2.72-2.66 (m, 2H), 2.38 (ddd, J = 13.7, 13.6, 5.0 Hz, 1H), 2.05-2.02 (m, 1H), 1.79-1.75 (m, 1H), 1.70 (ddd, J = 13.8, 13.3, 5.4 Hz, 1H), 1.54 (ddd, J = 25.8, 13.1, 4.0 Hz, 1H), 1.06 (ddd, J = 25.5, 12.8, 4.1 Hz, 1H) ppm.

¹³C NMR (125 MHz, CD₂Cl₂) δ = 176.7, 158.4, 150.7, 139.2, 138.1, 137.6, 131.3, 129.2, 127.9, 120.3, 116.2, 114.1, 92.5, 60.0, 55.5, 43.0, 35.4, 35.2, 33.8, 29.7 ppm.

MS (EI) m/z (%): 510 (90), 293 (100), 265 (11), 217 (9), 147 (24).

HRMS (ESI+) m/z calculated for C₂₆H₂₇N₂O (M+Na⁺) 533.106026, found 533.106125.

2-(4-(4-Fluorophenyl)cyclohexylidene)-1-(4-iodobenzyl)-1-phenylhydrazine (237i)**237i**

The reaction was conducted on a 0.500 mmol scale.

Purification: Filtration.

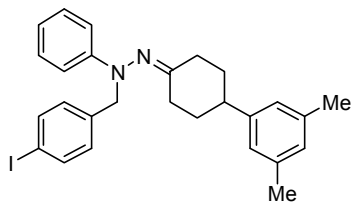
Yield: Colorless solid 202 mg (0.405 mmol, 81%).

¹H NMR (500 MHz, CD₂Cl₂) δ = 7.69-7.67 (m, 2H), 7.26-7.22 (m, 2H), 7.15 (d, J = 8.2 Hz, 2H), 7.12-7.09 (m, 2H), 7.03-6.98 (m, 2H), 6.88-6.86 (m, 3H), 4.62 (d, J = 14.7 Hz, 1H), 4.43 (d, J = 14.7 Hz, 1H), 3.15-3.10 (m, 1H), 2.77-2.66 (m, 2H), 2.39 (ddd, J = 13.7, 13.7, 5.0 Hz, 1H), 2.07-2.02 (m, 1H), 1.81-1.75 (m, 1H), 1.70 (ddd, J = 13.8, 13.8, 5.5 Hz, 1H), 1.53 (ddd, J = 25.7, 13.1, 4.1 Hz, 1H), 1.02 (ddd, J = 25.6, 12.9, 4.1 Hz, 1H) ppm.

¹³C NMR (125 MHz, CD₂Cl₂) δ = 176.4, 161.7 (d, J = 243.3 Hz), 150.7, 141.8 (d, J = 3.1 Hz), 139.2, 137.6, 131.4, 129.2, 128.5 (d, J = 7.6 Hz), 120.4, 116.2, 115.4 (d, J = 21.1 Hz), 92.5, 60.0, 43.1, 35.3, 35.1, 33.7, 29.6 ppm.

MS (EI) m/z (%): 498 (93), 281 (100), 217 (11), 162 (41), 135 (11).

HRMS (ESI+) m/z calculated for C₂₅H₂₄N₂FINa (M+Na⁺) 521.086043, found 521.085570.

2-(4-(3,5-Dimethylphenyl)cyclohexylidene)-1-(4-iodobenzyl)-1-phenylhydrazine (237j)**237j**

The reaction was conducted on a 0.500 mmol scale.

Purification: Filtration.

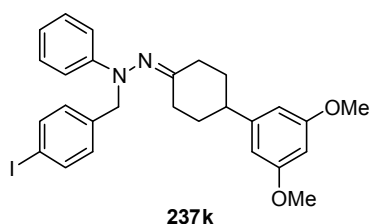
Yield: Colorless solid 106 mg (0.209 mmol, 42%).

¹H NMR (500 MHz, CD₂Cl₂) δ = 7.67-7.65 (m, 2H), 7.25-7.21 (m, 2H), 7.14 (d, J = 8.3 Hz, 2H), 6.87-6.83 (m, 4H), 6.76 (s, 2H), 4.59 (d, J = 15.1 Hz, 1H), 4.47 (d, J = 15.1 Hz, 1H), 3.14-3.09 (m, 1H), 2.71-2.65 (m, 2H), 2.38 (ddd, J = 13.7, 13.7, 5.1 Hz, 1H), 2.29 (s, 6H), 2.07-2.01 (m, 1H), 1.82-1.77 (m, 1H), 1.71 (ddd, J = 13.9, 13.6, 5.5 Hz, 1H), 1.64-1.55 (m, 1H), 1.17 (ddd, J = 25.6, 12.9, 4.1 Hz, 1H) ppm.

¹³C NMR (125 MHz, CD₂Cl₂) δ = 176.4, 150.8, 145.9, 139.2, 138.2, 137.6, 131.1, 129.2, 128.2, 124.8, 120.3, 116.2, 92.3, 60.1, 43.8, 35.4, 34.8, 33.6, 29.8, 21.5 ppm.

MS (EI) m/z (%): 508 (100), 291 (94), 217 (9), 198 (21), 145 (15).

HRMS (ESI+) m/z calculated for C₂₇H₂₉N₂INa (M+Na⁺) 531.126763, found 531.127213.

2-(4-(3,5-Dimethoxyphenyl)cyclohexylidene)-1-(4-iodobenzyl)-1-phenylhydrazine (237k)

The reaction was conducted on a 0.500 mmol scale.

Purification: Filtration.

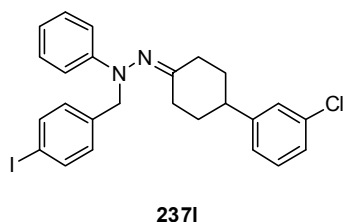
Yield: Colorless solid 220 mg (0.407 mmol, 81%).

¹H NMR (400 MHz, CDCl₃) δ = 7.65 (d, J = 8.2 Hz, 2H), 7.26 (dd, J = 7.9, 7.9 Hz, 2H), 7.12 (d, J = 8.2 Hz, 2H), 6.92-9.87 (m, 3H), 6.32 (s, 3H), 4.56 (s, 2H), 3.79 (s, 6H), 3.18-3.14 (m, 1H), 2.78-2.67 (m, 2H), 2.42-2.34 (m, 1H), 2.16-2.06 (m, 1H), 1.92-1.82 (m, 1H), 1.74-1.60 (m, 2H), 1.32-1.22 (m, 1H) ppm.

¹³C NMR (100 MHz, CDCl₃) δ = 175.4, 161.0, 150.6, 148.0, 138.8, 137.5, 130.6, 129.1, 120.7, 116.3, 105.1, 98.1, 92.4, 60.6, 55.4, 43.9, 35.1, 34.3, 33.2, 29.6 ppm.

MS (EI) m/z (%): 540 (96), 359 (6), 323 (100), 217 (21), 177 (10).

HRMS (ESI+) m/z calculated for C₂₇H₂₉N₂O₂INa (M+Na⁺) 563.116592, found 563.116729.

2-(4-(3-Chlorophenyl)cyclohexylidene)-1-(4-iodobenzyl)-1-phenylhydrazine (237l)

The reaction was conducted on a 0.500 mmol scale.

Purification: Filtration.

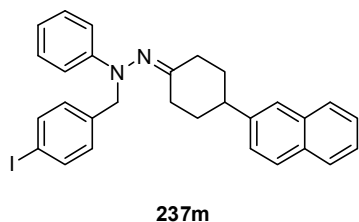
Yield: Colorless solid 192 mg (0.373 mmol, 75%).

¹H NMR (400 MHz, CD₂Cl₂) δ = 7.72-7.70 (m, 2H), 7.32-7.26 (m, 3H), 7.23-7.17 (m, 4H), 7.08 (d, J = 7.6 Hz, 1H), 6.92-6.90 (m, 3H), 4.63 (d, J = 14.9 Hz, 1H), 4.51 (d, J = 14.9 Hz, 1H), 3.19-3.15 (m, 1H), 2.80-2.73 (m, 2H), 2.42 (ddd, J = 18.6, 13.6, 5.0 Hz, 1H), 2.12-2.08 (m, 1H), 1.86-1.70 (m, 2H), 1.62 (ddd, J = 25.6, 13.1, 4.1 Hz, 1H), 1.15 (ddd, J = 25.6, 13.1, 4.1 Hz, 1H) ppm.

¹³C NMR (100 MHz, CD₂Cl₂) δ = 175.8, 150.9, 148.2, 139.2, 137.7, 134.4, 131.3, 130.3, 129.3, 127.4, 126.7, 125.4, 120.6, 116.4, 92.6, 60.3, 43.6, 35.3, 34.6, 33.4, 29.6 ppm.

MS (EI) m/z (%): 514/516 (76/28), 297/299 (100/35), 217 (16), 178 (23), 159 (12).

HRMS (ESI+) m/z calculated for C₂₅H₂₄N₂ClINa (M+Na⁺) 537.056494, found 537.056326.

1-(4-Iodobenzyl)-2-(4-(naphthalen-2-yl)cyclohexylidene)-1-phenylhydrazine (237m)

The reaction was conducted on a 0.500 mmol scale.

Purification: Filtration.

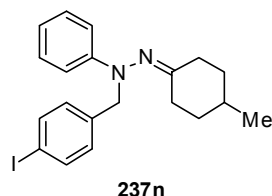
Yield: Colorless solid 203 mg (0.382 mmol, 76%).

¹H NMR (400 MHz, CD₂Cl₂) δ = 7.88-7.84 (m, 3H), 7.74-7.72 (m, 2H), 7.64 (s, 1H), 7.52- 7.45 (m, 2H), 7.35-7.27 (m, 3H), 7.21 (d, J = 8.3 Hz, 2H), 6.94-6.90 (m, 3H), 4.67 (d, J = 14.9 Hz, 1H), 4.52 (d, J = 14.9 Hz, 1H), 3.25-3.19 (m, 1H), 3.00-2.93 (m, 1H), 2.81-2.76 (m, 1H), 2.49 (ddd, J = 18.8, 13.7, 5.1 Hz, 1H), 2.25-2.18 (m, 1H), 1.99-1.93 (m, 1H), 1.86-1.70 (m, 2H), 1.30 (ddd, J = 25.5, 13.2, 4.3 Hz, 1H) ppm.

¹³C NMR (100 MHz, CD₂Cl₂) δ = 176.4, 150.9, 143.6, 139.3, 137.7, 134.0, 132.7, 131.3, 129.3, 128.4, 128.0, 127.9, 126.3, 126.2, 125.7, 125.0, 120.5, 116.3, 92.5, 60.2, 44.0, 35.4, 34.8, 33.5, 29.7 ppm.

MS (EI) m/z (%): 530 (100), 313 (83), 217 (17), 194 (12), 167 (28), 77 (38).

HRMS (ESI+) m/z calculated for C₂₉H₂₇N₂INa (M+Na⁺) 553.111113, found 553.110976.

1-(4-Iodobenzyl)-2-(4-methylcyclohexylidene)-1-phenylhydrazine (237n)^[221]

The reaction was conducted on a 0.500 mmol scale.

Purification: Filtration.

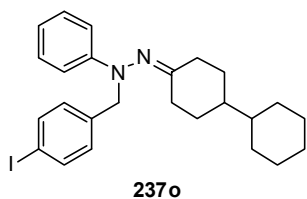
Yield: Colorless solid 72.0 mg (0.172 mmol, 34%).

¹H NMR (400 MHz, CDCl₃) δ = 7.62-7.59 (m, 2H), 7.24-7.18 (m, 2H), 7.08-7.06 (m, 2H), 6.87-6.78 (m, 3H), 4.52 (d, J = 15.2 Hz, 1H), 4.47 (d, J = 15.1 Hz, 1H), 2.95-2.90 (m, 1H), 2.59-2.53 (m, 1H), 2.22 (ddd, J = 13.2, 13.2, 5.1 Hz, 1H), 1.90-1.83 (m, 1H), 1.64-1.55 (m, 3H), 1.18-1.07 (m, 1H), 0.88 (d, J = 6.5 Hz, 3H), 0.76-0.66 (m, 1H) ppm.

¹³C NMR (100 MHz, CDCl₃) δ = 177.2, 150.5, 138.9, 137.4, 130.6, 129.1, 120.3, 116.0, 92.3, 60.3, 35.4, 34.7, 34.2, 31.9, 29.2, 21.5 ppm.

MS (EI) m/z (%): 418 (50), 217 (10), 201 (100), 77 (15).

HRMS (ESI+) m/z calculated for C₂₀H₂₃N₂INa (M+Na⁺) 441.079813, found 411.079454.

2-([1,1'-Bi(cyclohexan)]-4-ylidene)-1-(4-iodobenzyl)-1-phenylhydrazine (237o)

The reaction was conducted on a 0.500 mmol scale.

Purification: Filtration.

Yield: Colorless solid 67.6 mg (0.139 mmol, 28%).

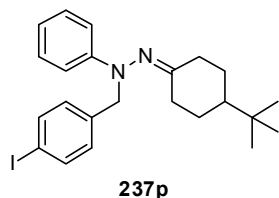
¹H NMR (400 MHz, CD₂Cl₂) δ = 7.65-7.61 (m, 2H), 7.23-7.18 (m, 2H), 7.10 (d, J = 8.3 Hz, 2H), 6.85-6.79 (m, 3H), 4.55 (d, J = 15.0 Hz, 1H), 4.42 (d, J = 15.0 Hz, 1H), 2.97- 2.92 (m, 1H), 2.59-2.53 (m, 1H), 2.17 (td, J = 6.8, 5.0 Hz, 1H), 1.92-1.87 (m, 1H), 1.74-1.71 (m, 2H), 1.65-1.61 (m, 3H), 1.58-1.53 (m, 2H), 1.33-1.07 (m, 6H), 0.98-0.89 (m, 2H), 0.72 (ddd, J = 23.9, 12.2, 4.1 Hz, 1H) ppm.

¹³C NMR (100 MHz, CD₂Cl₂) δ = 177.8, 150.8, 139.3, 137.6, 131.1, 129.2, 120.1, 116.0, 92.4, 59.9, 54.3, 53.3, 42.8, 42.7, 35.2, 30.7, 30.6, 29.6, 29.4, 27.2, 27.1 ppm.

MS (EI) m/z (%): 486 (87), 469 (9), 269 (100), 217 (13), 176 (7).

HRMS (ESI+) m/z calculated for C₂₅H₃₁N₂INa (M+Na⁺) 509.142412, found 509.142420.

mp = 78.2-78.6 °C (EtOH).

2-(4-(*tert*-Butyl)cyclohexylidene)-1-(4-iodobenzyl)-1-phenylhydrazine (237p)^[221]

The reaction was conducted on a 0.500 mmol scale.

Purification: Filtration.

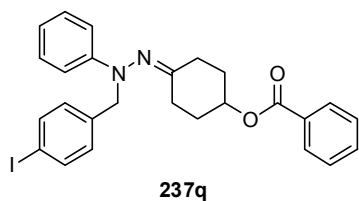
Yield: Colorless solid 113 mg (0.246 mmol, 49%).

¹H NMR (400 MHz, CDCl₃) δ = 7.66-7.62 (m, 2H), 7.26-7.22 (m, 2H), 7.11 (d, J = 8.3 Hz, 2H), 6.89-6.83 (m, 3H), 4.57 (d, J = 14.9 Hz, 1H), 4.47 (d, J = 14.9 Hz, 1H), 3.09- 3.03 (m, 1H), 2.67-2.61 (m, 1H), 2.20 (td, J = 13.4, 4.8 Hz, 1H), 2.01-1.96 (m, 1H), 1.74-1.69 (m, 1H), 1.51 (ddd, J = 19.4, 13.9, 5.5 Hz, 1H), 1.25-1.09 (m, 2H), 0.84 (s, 9H), 0.76-0.65 (m, 1H) ppm.

¹³C NMR (100 MHz, CDCl₃) δ = 177.2, 150.1, 138.3, 136.9, 133.3, 128.6, 119.8, 115.5, 91.9, 59.6, 47.0, 34.7, 32.0, 29.2, 27.7, 27.2, 26.5 ppm.

MS (EI) m/z (%): 460 (47), 243 (100), 217 (13), 187 (5).

HRMS (ESI+) m/z calculated for C₂₃H₂₉N₂INa (M+Na⁺) 483.126767, found 483.126607.

4-(2-(4-iodobenzyl)-2-phenylhydrazono)cyclohexyl benzoate (237q)^[221]

The reaction was conducted on a 0.250 mmol scale.

Purification: Filtration.

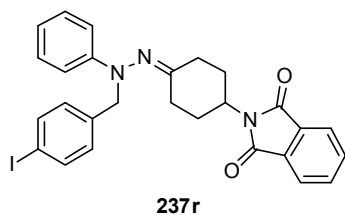
Yield: Colorless solid 70.6 mg (0.135 mmol, 54%).

¹H NMR (500 MHz, CDCl₃) δ = 8.01-8.00 (m, 2H), 7.63 (d, J = 8.4 Hz, 2H), 7.56-7.53 (m, 1H), 7.43 (dd, J = 7.8, 7.8 Hz, 2H), 7.25-7.22 (m, 2H), 7.09 (d, J = 8.2 Hz, 2H), 6.90-6.84 (m, 3H), 5.22-5.18 (m, 1H), 4.52 (s, 2H), 2.70-2.64 (m, 1H), 2.52-2.45 (m, 2H), 2.40-2.34 (m, 1H), 2.05-1.93 (m, 2H), 1.70-1.60 (m, 2H),

¹³C NMR (125 MHz, CDCl₃) δ = 174.5, 165.9, 150.6, 138.7, 137.5, 133.2, 130.7, 130.5, 129.7, 129.2, 128.5, 120.9, 116.4, 92.4, 70.3, 60.7, 31.3, 31.2, 30.1, 25.8 ppm.

MS (EI) m/z (%): 524 (70), 217 (12), 185 (100).

HRMS (ESI+) m/z calculated for C₂₆H₂₅N₂O₂INa (M+Na⁺) 547.085296, found 547.085746.

2-(4-(2-(4-iodobenzyl)-2-phenylhydrazono)cyclohexyl)isoindoline-1,3-dione (237r)

The reaction was conducted on a 0.500 mmol scale.

Purification: Filtration.

Yield: Colorless solid 217 mg (0.395 mmol, 79%).

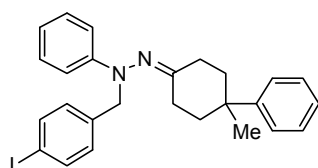
¹H NMR (500 MHz, CD₂Cl₂) δ = 7.81-7.71 (m, 4H), 7.66 (d, J = 8.0 Hz, 2H), 7.26-7.23 (m, 2H), 7.12 (d, J = 7.9 Hz, 2H), 6.90-6.84 (m, 3H), 4.58 (d, J = 15.6 Hz, 1H), 4.54 (d, J = 15.6 Hz, 1H), 4.39-4.34 (m, 1H), 3.16 (d, J = 14.9 Hz, 1H), 2.75 (d, J = 13.0 Hz, 1H), 2.54-2.45 (m, 1H), 2.43-2.37 (m, 1H), 2.17-2.08 (m, 1H), 1.99-1.98 (m, 1H), 1.76-1.69 (m, 2H) ppm.

¹³C NMR (125 MHz, CDCl₃) δ = 173.4, 168.3, 150.8, 139.1, 137.7, 134.3, 132.3, 130.6, 129.2, 123.3, 120.6, 116.5, 92.5, 60.6, 49.6, 34.2, 29.7, 28.5, 28.5 ppm.

MS (EI) m/z (%): 549 (100), 385 (6), 332 (62), 217 (18), 185 (67), 168 (15).

HRMS (ESI+) m/z calculated for C₂₇H₂₄N₃O₂INa (M+Na⁺) 572.080541, found 572.080076.

mp = 150-152 °C (EtOH).

1-(4-Iodobenzyl)-2-(4-methyl-4-phenylcyclohexylidene)-1-phenylhydrazine (237s)

237s

The reaction was conducted on a 0.500 mmol scale.

Purification: Filtration.

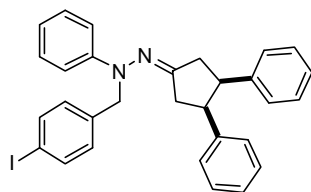
Yield: Colorless solid 208 mg (0.421 mmol, 84%).

$^1\text{H NMR}$ (500 MHz, CD_2Cl_2) δ = 7.64 (d, J = 8.2 Hz, 2H), 7.37-7.33 (m, 4H), 7.24-7.17 (m, 3H), 7.11 (d, J = 8.1 Hz, 2H), 6.83 (t, J = 7.3 Hz, 1H), 6.79 (d, J = 8.1 Hz, 2H), 4.53 (d, J = 15.2 Hz, 1H), 4.47 (d, J = 15.2 Hz, 1H), 2.60-2.55 (m, 1H), 2.52-2.48 (m, 1H), 2.36-2.29 (m, 2H), 2.69-1.98 (m, 2H), 1.77-1.71 (m, 1H), 1.40-1.34 (m, 1H), 1.21 (s, 3H) ppm.

$^{13}\text{C NMR}$ (125 MHz, CD_2Cl_2) δ = 176.5, 150.7, 147.4, 139.2, 137.6, 130.9, 129.2, 128.9, 126.1, 126.1, 120.2, 116.1, 92.3, 60.0, 38.3, 38.2, 36.8, 31.8, 30.6, 26.6 ppm.

MS (EI) m/z (%): 494 (100), 277 (90), 249 (21), 217 (11), 171 (21), 131 (11), 77 (23).

HRMS (EI) m/z calculated for $\text{C}_{26}\text{H}_{27}\text{N}_2\text{I}$ 494.121893, found 494.121489.

2-((*cis*)-3,4-Diphenylcyclopentylidene)-1-(4-iodobenzyl)-1-phenylhydrazine (237t)

237t

The reaction was conducted on a 0.500 mmol scale.

Purification: CC on SiO_2 (hexane:EtOAc 4:1).

Yield: Pale yellow solid 215 mg (0.397 mmol, 79%).

$^1\text{H NMR}$ (500 MHz, CD_2Cl_2) δ = 7.71 (d, J = 8.3 Hz, 2H), 7.30 (dd, J = 8.4, 7.5 Hz, 2H), 7.25 (d, J = 8.2 Hz, 2H), 7.13-7.01 (m, 8H), 6.96 (t, J = 7.3 Hz, 1H), 6.66 (d, J = 6.9 Hz, 2H), 6.57 (d, J = 6.9 Hz, 2H), 4.68 (d, J = 15.1 Hz, 1H), 4.61 (d, J = 15.1 Hz, 1H), 3.65-3.60 (m, 1H), 3.59-3.54 (m, 1H), 2.98-2.97 (m, 2H), 2.68 (dd, J = 18.7, 6.8 Hz, 1H), 2.59 (dd, J = 18.7, 7.9 Hz, 1H).

$^{13}\text{C NMR}$ (125 MHz, CD_2Cl_2) δ = 179.6, 151.1, 140.6, 140.5, 139.7, 137.7, 130.8, 129.4, 128.4, 128.0, 128.0, 126.5, 121.6, 118.1, 92.6, 62.3, 49.0, 48.4, 38.0, 36.8 ppm

MS (EI) m/z (%): 542 (100), 325 (53), 221 (66).

HRMS (ESI+) m/z calculated for $\text{C}_{30}\text{H}_{27}\text{N}_2\text{I}^+\text{Na}^+$ 565.111116, found 565.110673.

7.4.2.4 Synthesis of Tetrahydrocarbazoles with Different Protecting Groups

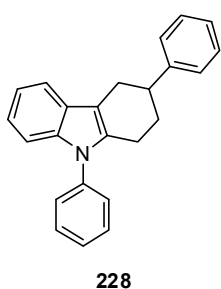
General procedure for the screening of different nitrogen protecting groups:

A solution of the protected hydrazone (0.050 mmol) in benzene (0.5 mL) was allowed to react in a sealed vial in the presence of catalysts **33d** (10 mol%) or **33f** (10 mol%), respectively. The reactions were conducted at 80 °C and stopped after a significant amount of product had formed (determined by TLC). A sample of the reaction mixture was submitted to preparative TLC or column chromatography on silica gel and the enantiomeric ratio of the obtained product was analyzed by HPLC analysis on a chiral stationary phase by comparison with the authentic racemic sample.

General procedure for the synthesis of racemic tetrahydrocarbazoles:

The racemates were prepared by heating a 1:1 mixture of the corresponding hydrazone (usually 0.10 mmol) and diphenyl phosphate to 80 °C in toluene (0.1 M) for 1 h. The crude reaction mixture was directly submitted to column chromatography on silica gel.

***rac*-3,9-Diphenyl-2,3,4,9-tetrahydro-1H-carbazole (228)**



The reaction was conducted on a 1.00 mmol scale.

Purification: CC on SiO₂ (hexane:EtOAc 5:1).

Yield: Colorless solid 309 mg (0.807 mmol, 81%).

¹H NMR (500 MHz, CD₂Cl₂) δ = 7.45 (dd, *J* = 7.9, 7.7 Hz, 2H), 7.41-7.38 (m, 1H), 7.33 (t, *J* = 7.5 Hz, 1H), 7.32-7.30 (m, 2H), 7.29-7.24 (m, 4H), 7.18-7.11 (m, 2H), 7.03- 6.98 (m, 2H), 3.08-3.03 (m, 2H), 2.81-2.73 (m, 2H),

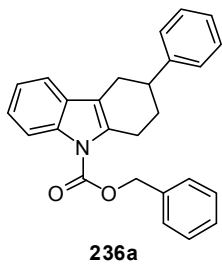
2.60-2.55 (m, 1H), 2.12- 2.09 (m, 1H), 2.04-1.96 (m, 1H) ppm.

¹³C NMR (125 MHz, CD₂Cl₂) δ = 147.2, 138.3, 137.8, 135.8, 129.7, 128.8, 127.9, 127.4, 127.4, 127.4, 126.5, 121.6, 119.9, 118.0, 111.2, 110.1, 41.4, 30.9, 29.8, 23.7 ppm.

MS (EI) *m/z* (%): 323 (80), 219 (100).

HRMS (EI) *m/z* calculated for C₂₄H₂₁N 323.167399, found 323.167437.

The enantiomeric ratio was determined by HPLC analysis using Daicel Chiralcel OD-3 column: *n*-heptane:*i*-PrOH = 98:2, flow rate 1.0 mL/min, λ = 220 nm: τ₁ = 4.21 min, τ₂ = 4.56 min.

***rac*-Benzyl 3-phenyl-3,4-dihydro-1H-carbazole-9(2H)-carboxylate (236a)**

The reaction was conducted on a 0.200 mmol scale.

Purification: CC on SiO₂ (hexane:EtOAc 10:1).

Yield: Colorless solid 24.6 mg (0.064 mmol, 32%).

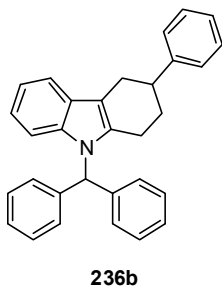
¹H NMR (500 MHz, CD₂Cl₂) δ = 7.51 (d, *J* = 8.3 Hz, 2H), 7.43 (dd, *J* = 8.2, 7.0 Hz, 2H), 7.41-7.38 (m, 2H), 7.37-7.32 (m, 4H), 7.26-7.20 (m, 4H), 5.47 (d, *J* = 12.3 Hz, 1H), 5.44 (d, *J* = 12.3 Hz, 1H), 3.25-3.20 (m, 1H), 3.09-2.98 (m, 3H), 2.76-2.71 (m, 1H), 2.22-2.19 (m, 1H), 2.08-2.00 (m, 1H) ppm.

¹³C NMR (100 MHz, CD₂Cl₂) δ = 152.2, 146.7, 136.4, 135.9, 135.7, 130.1, 129.0, 128.9, 128.8, 128.8, 127.3, 126.6, 124.0, 123.1, 117.9, 117.4, 115.8, 68.7, 40.3, 31.2, 29.5, 26.3 ppm.

MS (EI) *m/z* (%): 381 (49), 337 (5), 290 (10), 233 (60), 218 (5), 91 (100).

HRMS (EI) *m/z* calculated for C₂₆H₂₃NO₂ 381.172882, found 381.172645.

The enantiomeric ratio was determined by HPLC analysis using Daicel Chiralpak AD-3 column: *n*-heptane:*i*-PrOH = 99:1, flow rate 1.0 mL/min, λ = 220 nm: τ₁ = 15.21 min, τ₂ = 17.50 min.

***rac*-9-Benzhydryl-3-phenyl-2,3,4,9-tetrahydro-1H-carbazole (236b)**

The reaction was conducted on a 0.055 mmol scale.

Purification: CC on SiO₂ (hexane:EtOAc 20:1).

Yield: Colorless solid 14.8 mg (0.036 mmol, 66%).

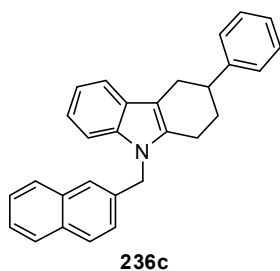
¹H NMR (500 MHz, CD₂Cl₂) δ = 7.45 (d, *J* = 7.8 Hz, 1H), 7.36-7.30 (m, 10H), 7.25-7.20 (m, 1H), 7.19-7.17 (m, 2H), 7.16-7.14 (m, 2H), 7.00 (t, *J* = 7.4 Hz, 1H), 6.92 (s, 1H), 6.90 (t, *J* = 7.2 Hz, 1H), 6.83 (d, *J* = 8.3 Hz, 1H), 3.12-3.08 (m, 1H), 3.06-3.01 (m, 1H), 2.87-2.82 (m, 1H), 2.68-2.65 (m, 1H), 2.60-2.53 (m, 1H), 2.14-2.12 (m, 1H), 2.09-2.02 (m, 1H) ppm.

¹³C NMR (125 MHz, CD₂Cl₂) δ = 147.2, 140.2, 139.9, 137.1, 136.3, 128.9, 128.8, 128.8, 128.7, 128.6, 128.0, 127.4, 126.5, 121.0, 119.1, 118.0, 111.4, 110.8, 62.4, 41.1, 31.0, 29.7, 24.1 ppm.

MS (EI) *m/z* (%): 413 (34), 309 (3), 167 (100), 152 (10).

HRMS (EI) *m/z* calculated for C₃₁H₂₇N 413.213347, found 413.214080.

The enantiomeric ratio was determined by HPLC analysis using Daicel Chiralcel OD-3 column: *n*-heptane:*i*-PrOH = 99.5:0.5, flow rate 1.0 mL/min, λ = 220 nm: τ₁ = 8.19 min, τ₂ = 11.33 min.

***rac*-9-(Naphthalen-2-ylmethyl)-3-phenyl-2,3,4,9-tetrahydro-1H-carbazole (236c)**

The reaction was conducted on a 0.100 mmol scale.

Purification: CC on SiO₂ (hexane:EtOAc 20:1).

Yield: Colorless solid 32.0 mg (0.083 mmol, 83%).

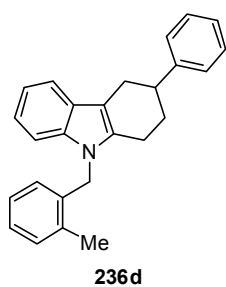
¹H NMR (500 MHz, CD₂Cl₂) δ = 7.83-7.81 (m, 1H), 7.79 (d, J = 8.5 Hz, 1H), 7.76-7.74 (m, 1H), 7.53-7.52 (m, 1H), 7.49-7.46 (m, 3H), 7.37-7.35 (m, 4H), 7.29 (dd, J = 7.1, 1.3 Hz, 1H), 7.27-7.24 (m, 1H), 7.22 (dd, J = 8.5, 1.7 Hz, 1H), 7.13-7.07 (m, 2H), 5.47 (d, J = 16.9 Hz, 1H), 5.42 (d, J = 16.9 Hz, 1H), 3.17-3.08 (m, 2H), 2.92-2.87 (m, 1H), 2.85-2.81 (m, 2H), 2.24-2.21 (m, 1H), 2.18-2.09 (m, 1H) ppm.

¹³C NMR (125 MHz, CD₂Cl₂) δ = 147.2, 137.3, 136.3, 135.7, 133.7, 133.0, 128.8, 128.7, 128.0, 128.0, 127.7, 127.4, 126.6, 126.5, 126.2, 125.1, 124.8, 121.1, 119.2, 118.1, 110.1, 109.4, 46.9, 41.3, 30.8, 29.7, 22.7 ppm.

MS (EI) m/z (%): 387 (89), 283 (99), 268 (19), 141 (100), 115 (15).

HRMS (ESI+) m/z calculated for C₂₉H₂₅NNa (M+Na⁺) 410.187916, found 410.188343.

The enantiomeric ratio was determined by reversed phase HPLC analysis using Daicel Chiralcel OJ-RH column: MeCN:H₂O = 90:10, flow rate 1.0 mL/min, λ = 220 nm: τ_1 = 11.00 min, τ_2 = 20.31 min.

***rac*-9-(2-Methylbenzyl)-3-phenyl-2,3,4,9-tetrahydro-1H-carbazole (236d)**

The reaction was conducted on a 0.100 mmol scale.

Purification: CC on SiO₂ (hexane:EtOAc 30:1).

Yield: Colorless solid 26.8 mg, (0.076 mmol, 76%).

¹H NMR (500 MHz, CD₂Cl₂) δ = 7.52-7.50 (m, 1H), 7.37-7.33 (m, 4H), 7.26-7.21 (m, 2H), 7.15-7.13 (m, 2H), 7.11-7.05 (m, 2H), 6.99 (t, J = 7.6 Hz, 1H), 6.26 (d, J = 7.7 Hz, 1H), 5.24 (s, 2H), 3.17-3.08 (m, 2H), 2.92-2.87 (m, 1H), 2.79-2.70 (m, 2H), 2.44 (s, 3H), 2.24-2.20 (m, 1H), 2.17-2.09 (m, 1H) ppm.

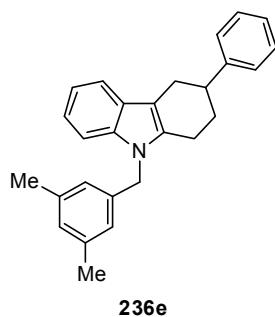
¹³C NMR (125 MHz, CD₂Cl₂) δ = 147.2, 137.2, 136.6, 135.9, 135.2, 130.4, 128.7, 127.7, 127.4, 127.3, 126.6, 126.5, 125.4, 121.1, 119.2, 118.1, 110.0, 109.3, 44.5, 41.3, 30.7, 29.7, 22.4, 19.2 ppm

MS (EI) m/z (%): 351 (73), 247 (27), 232 (100), 105 (28).

HRMS (ESI+) m/z calculated for C₂₆H₂₅NNa (M+Na⁺) 374.187920, found 374.187996.

The enantiomeric ratio was determined by HPLC analysis using Daicel Chiralcel OJ-H column: *n*-heptane:*i*-PrOH = 60:40, flow rate 1.0 mL/min, λ = 220 nm: τ_1 = 26.13 min, τ_2 = 30.29 min.

***rac*-9-(3,5-Dimethylbenzyl)-3-phenyl-2,3,4,9-tetrahydro-1H-carbazole (236e)**



The reaction was conducted on a 0.100 mmol scale.

Purification: CC on SiO₂ (hexane:EtOAc 20:1).

Yield: Yellow oil 34.9 mg (0.095 mmol, 95%).

¹H NMR (500 MHz, CD₂Cl₂) δ = 7.49 (d, *J* = 7.5 Hz, 1H), 7.38-7.34 (m, 4H), 7.27-7.23 (m, 2H), 7.11 (ddd, *J* = 8.2, 7.3, 1.2 Hz, 1H), 7.08-7.05 (m, 1H), 6.90 (s, 1H), 6.70 (s, 2H), 5.23 (d, *J* = 16.7 Hz, 1H), 5.18 (d, *J* = 16.7 Hz, 1H), 3.15-3.08 (m, 2H), 2.91- 2.85 (m, 1H), 2.83-2.81 (m, 2H), 2.26 (s, 6H), 2.24-2.22 (m, 1H), 2.17-2.12 (m, 1H) ppm.

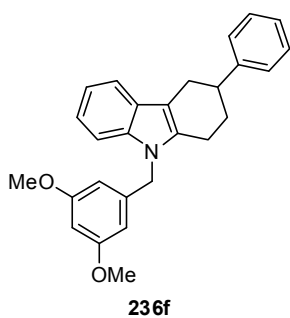
¹³C NMR (125 MHz, CD₂Cl₂) δ = 147.2, 138.7, 137.2, 135.7, 129.3, 129.2, 128.7, 128.5, 127.4, 126.5, 124.4, 121.0, 119.1, 118.0, 109.8, 109.4, 46.7, 41.3, 30.8, 29.7, 22.7, 21.4 ppm.

MS (EI) *m/z* (%): 365 (88), 261 (100), 246 (31), 231 (5), 119 (43).

HRMS (EI) *m/z* calculated for C₂₇H₂₇N 365.214351, found 365.214114.

The enantiomeric ratio was determined by HPLC analysis using Daicel Chiralcel OD-3 column: *n*-heptane:*i*-PrOH = 95:5, flow rate 1.0 mL/min, λ = 220 nm: τ_1 = 4.74 min, τ_2 = 5.44 min.

***rac*-9-(3,5-Dimethoxybenzyl)-3-phenyl-2,3,4,9-tetrahydro-1H-carbazole (236f)**



The reaction was conducted on a 0.100 mmol scale.

Purification: CC on SiO₂ (hexane:EtOAc 20:1 to 10:1).

Yield: Colorless solid 36.5 mg (0.092 mmol, 92%).

¹H NMR (500 MHz, CD₂Cl₂) δ = 7.49 (d, *J* = 7.5 Hz, 1H), 7.37-7.33 (m, 4H), 7.26-7.23 (m, 2H), 7.11 (ddd, *J* = 7.9, 7.1, 1.1 Hz, 1H), 7.07 (ddd, *J* = 7.8, 6.9, 0.9 Hz, 1H), 6.34 (t, *J* = 2.2 Hz, 1H), 6.17 (d, *J* = 2.2 Hz, 2H), 5.23 (d, *J* = 16.9 Hz, 1H), 5.19 (d, *J* = 16.9 Hz, 1H), 3.71 (s, 6H), 3.14-3.07 (m, 2H), 2.90-2.81 (m, 3H), 2.25-2.22 (m, 1H), 2.17-2.09 (m, 1H) ppm.

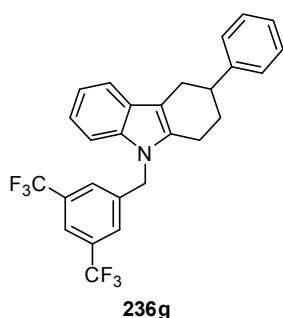
¹³C NMR (125 MHz, CD₂Cl₂) δ = 161.6, 147.2, 141.3, 137.3, 135.6, 128.7, 127.7, 127.4, 126.5, 121.1, 119.2, 118.1, 110.0, 109.3, 104.7, 98.7, 55.5, 46.7, 41.3, 30.8, 29.7, 22.6 ppm.

MS (EI) *m/z* (%): 397 (100), 292 (88), 278 (19), 262 (19), 247 (5), 151 (26), 143 (6).

HRMS (ESI+) *m/z* calculated for C₂₇H₂₇NO₂Na (M+Na⁺) 420.193396, found 420.193732.

The enantiomeric ratio was determined by reversed phase HPLC analysis using Daicel Chiralcel OJ-3R column: MeCN:H₂O = 85:15, flow rate 1.0 mL/min, λ = 220 nm: τ_1 = 6.14 min, τ_2 = 6.83 min.

***rac*-9-(3,5-bis(Trifluoromethyl)benzyl)-3-phenyl-2,3,4,9-tetrahydro-1H-carbazole (236g)**



The reaction was conducted on a 0.100 mmol scale.

Purification: CC on SiO₂ (hexane:EtOAc 15:1).

Yield: Colorless solid 37.8 mg (0.080 mmol, 80%).

¹H NMR (500 MHz, CD₂Cl₂) δ = 7.83 (s, 1H), 7.53 (d, J = 7.1 Hz, 1H), 7.51 (s, 2H), 7.37- 7.33 (m, 4H), 7.28-7.22 (m, 1H), 7.20-7.09 (m, 3H), 5.41 (d, J = 17.5 Hz, 1H), 5.37 (d, J = 17.5 Hz, 1H), 3.17-3.09 (m, 2H),

2.92-2.87 (m, 1H), 2.82-2.73 (m, 2H), 2.26-2.23 (m, 1H), 2.19-2.11 (m, 1H) ppm.

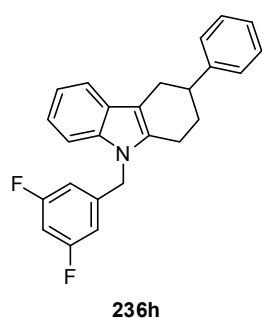
¹³C NMR (125 MHz, CD₂Cl₂) δ = 147.0, 141.8, 137.1, 135.2, 132.3 (q, J = 33.3 Hz), 128.8, 128.0, 127.4, 126.8 (q, J = 2.7 Hz), 126.6, 123.6 (q, J = 272.5 Hz), 121.9 (sept, J = 3.7 Hz), 121.7, 119.8, 118.5, 111.1, 108.9, 46.1, 41.2, 30.7, 29.5, 22.5 ppm.

MS (EI) m/z (%): 473 (68), 369 (100), 300 (10), 142 (15), 115 (9).

HRMS (EI) m/z calculated for C₂₇H₂₁NF₆ 473.157820, found 473.157751.

The enantiomeric ratio was determined by HPLC analysis using Daicel Chiralcel OD-3 column: *n*-heptane:*i*-PrOH = 98:2, flow rate 1.0 mL/min, λ = 220 nm: τ_1 = 19.34 min, τ_2 = 21.61 min.

***rac*-9-(3,5-Difluorobenzyl)-3-phenyl-2,3,4,9-tetrahydro-1H-carbazole (236h)**



The reaction was conducted on a 0.100 mmol scale.

Purification: CC on SiO₂ (hexane:EtOAc 30:1).

Yield: Colorless oil 33.0 mg (0.088 mmol, 88%).

¹H NMR (500 MHz, CD₂Cl₂) δ = 7.50 (d, J = 7.4 Hz, 1H), 7.36-7.33 (m, 4H), 7.27-7.21 (m, 1H), 7.19 (d, J = 7.8 Hz, 1H), 7.13 (ddd, J = 8.0, 7.0, 1.1 Hz, 1H), 7.09 (ddd, J = 7.5, 7.1, 1.1 Hz, 1H), 6.71 (tt, J = 9.0, 2.3 Hz,

1H), 6.56-6.52 (m, 2H), 5.28 (d, J = 17.4 Hz, 1H), 5.24 (d, J = 17.4 Hz, 1H), 3.14-3.08 (m, 2H), 2.90-2.84 (m, 1H), 2.81-2.73 (m, 2H), 2.25-2.22 (m, 1H), 2.18-2.10 (m, 1H) ppm.

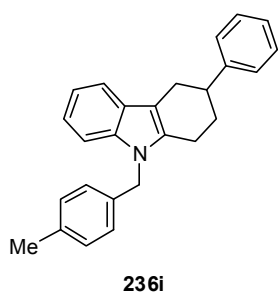
¹³C NMR (125 MHz, CD₂Cl₂) δ = 163.7 (dd, J = 248.9, 12.7 Hz), 147.0, 143.2 (t, J = 8.5 Hz), 137.0, 135.3, 128.8, 127.8, 127.4, 126.5, 121.4, 119.6, 118.3, 110.6, 109.4 (dd, J = 19.8, 6.1 Hz), 109.1, 102.9 (t, J = 25.5 Hz), 46.0, 41.2, 30.7, 29.6, 22.5 ppm.

MS (EI) m/z (%): 373 (73), 269 (100), 254 (5), 142 (12), 115 (10).

HRMS (ESI+) m/z calculated for $C_{25}H_{21}F_2NNa$ ($M+Na^+$) 396.153428, found 396.153260.

The enantiomeric ratio was determined by reversed phase HPLC analysis using Daicel Chiralcel OJ-RH column: MeCN:H₂O = 80:20, flow rate 1.0 mL/min, λ = 220 nm: τ_1 = 6.98 min, τ_2 = 8.23 min.

***rac*-9-(4-Methylbenzyl)-3-phenyl-2,3,4,9-tetrahydro-1H-carbazole (236i)**



The reaction was conducted on a 0.100 mmol scale.

Purification: CC on SiO₂ (hexane:EtOAc 30:1).

Yield: Colorless solid 28.6 mg (0.081 mmol, 81%).

¹H NMR (500 MHz, CD₂Cl₂) δ = 7.48 (d, J = 7.4 Hz, 1H), 7.36-7.33 (m, 4H), 7.27-7.23 (m, 2H), 7.11-7.08 (m, 3H), 7.06 (ddd, J = 7.7, 7.1, 1.1 Hz, 1H), 6.93 (d, J = 8.0 Hz, 2H), 5.27 (d, J = 16.7 Hz, 1H), 5.22 (d, J = 16.7 Hz, 1H), 3.14-3.06 (m, 2H), 2.89- 2.80 (m, 3H), 2.31 (s, 3H), 2.24-2.21 (m, 1H), 2.17-2.09 (m, 1H) ppm.

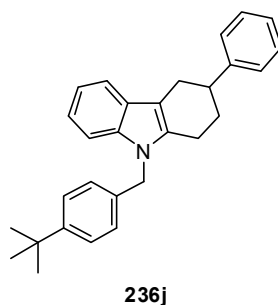
¹³C NMR (125 MHz, CD₂Cl₂) δ = 147.2, 137.3, 137.2, 135.7, 135.7, 129.6, 128.7, 127.6, 127.4, 126.5, 126.5, 121.0, 119.1, 118.0, 109.9, 109.4, 46.5, 41.3, 30.1, 29.7, 22.7, 21.1 ppm.

MS (EI) m/z (%): 351 (81), 247 (100), 232 (20), 115 (5), 105 (51).

HRMS (ESI+) m/z calculated for $C_{26}H_{25}NNa$ ($M+Na^+$) 374.187918 found 374.187834.

The enantiomeric ratio was determined by HPLC analysis using Daicel Chiralpak AD-3 column: *n*-heptane:*i*-PrOH = 99.5:0.5, flow rate 1.0 mL/min, λ = 220 nm: τ_1 = 7.67 min, τ_2 = 8.16 min.

***rac*-9-(4-(*tert*-Butyl)benzyl)-3-phenyl-2,3,4,9-tetrahydro-1H-carbazole (236j)**



The reaction was conducted on a 0.373 mmol scale.

Purification: CC on SiO₂ (hexane:EtOAc 30:1).

Yield: Pale yellow solid 133 mg (0.337 mmol, 90%).

¹H NMR (500 MHz, CD₂Cl₂) δ = 7.51 (d, J = 7.4 Hz, 1H), 7.38-7.36 (m, 4H), 7.35-7.32 (m, 2H), 7.28-7.25 (m, 2H), 7.13 (ddd, J = 8.0, 7.0, 1.3 Hz, 1H), 7.08 (ddd, J = 7.7, 7.1, 1.1 Hz, 1H), 6.99 (d, J = 8.4 Hz, 2H), 5.29 (d, J = 16.8 Hz, 1H), 5.24 (d, J = 16.8 Hz, 1H), 3.16-3.08 (m, 2H), 2.92-2.83 (m, 3H), 2.27-2.23 (m, 1H), 2.19- 2.11 (m, 1H), 1.31 (s, 9H) ppm.

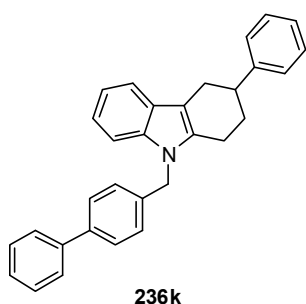
^{13}C NMR (125 MHz, CD_2Cl_2) δ = 150.6, 147.2, 137.2, 135.7, 135.7, 128.8, 127.7, 127.4, 126.5, 126.3, 125.9, 121.1, 119.2, 118.1, 109.9, 109.4, 46.3, 41.4, 34.7, 31.4, 30.8, 29.7, 22.7 ppm.

MS (EI) m/z (%): 393 (98), 289 (100), 274 (13), 232 (16), 189 (8), 147 (37), 129 (26), 115 (15).

HRMS (ESI+) m/z calculated for $\text{C}_{29}\text{H}_{31}\text{NNa}$ ($\text{M}+\text{Na}^+$) 416.234866, found 416.235186.

The enantiomeric ratio was determined by reversed phase HPLC analysis using Daicel Chiralcel OJ-RH column: MeCN:H₂O = 90:10, flow rate 1.0 mL/min, λ = 220 nm: τ_1 = 8.39 min, τ_2 = 9.26 min.

***rac*-9-([1,1'-Biphenyl]-4-ylmethyl)-3-phenyl-2,3,4,9-tetrahydro-1H-carbazole (236k)**



The reaction was conducted on a 0.100 mmol scale.

Purification: CC on SiO_2 (hexane:EtOAc 25:1).

Yield: Colorless solid 39.3 mg (0.095 mmol, 95%).

^1H NMR (500 MHz, CD_2Cl_2) δ = 7.58-7.56 (m, 2H), 7.54-7.52 (m, 2H), 7.51 (d, J = 7.6 Hz, 1H), 7.45-7.42 (m, 2H), 7.38-7.33 (m, 5H), 7.28 (d, J = 8.0 Hz, 1H), 7.26-7.23 (m, 1H), 7.14-7.07 (m, 4H), 5.36 (d, J =

16.9 Hz, 1H), 5.31 (d, J = 16.9 Hz, 1H), 3.16- 3.08 (m, 2H), 2.91-2.83 (m, 3H), 2.26-2.22 (m, 1H), 2.19-2.11 (m, 1H) ppm.

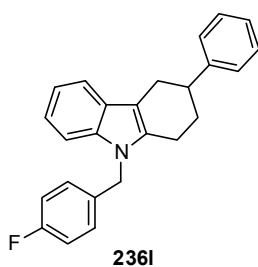
^{13}C NMR (125 MHz, CD_2Cl_2) δ = 147.2, 140.9, 140.4, 137.9, 137.2, 135.7, 129.3, 129.1, 128.7, 127.7, 127.7, 127.4, 127.3, 127.0, 126.5, 121.1, 119.3, 118.1, 110.1, 109.4, 46.4, 41.3, 30.8, 29.7, 22.7 ppm.

MS (EI) m/z (%): 413 (78), 309 (79), 167 (100).

HRMS (ESI+) m/z calculated for $\text{C}_{31}\text{H}_{27}\text{NNa}$ ($\text{M}+\text{Na}^+$) 436.203566, found 436.203841.

The enantiomeric ratio was determined by reversed phase HPLC analysis using Daicel Chiralcel OJ-RH column: MeCN:H₂O = 90:10, flow rate 1.0 mL/min, λ = 220 nm: τ_1 = 24.92 min, τ_2 = 29.64 min.

***rac*-9-(4-Fluorobenzyl)-3-phenyl-2,3,4,9-tetrahydro-1H-carbazole (236l)**



The reaction was conducted on a 0.100 mmol scale.

Purification: CC on SiO_2 (hexane:EtOAc 30:1).

Yield: Colorless solid 28.2 mg (0.079 mmol, 79%).

^1H NMR (500 MHz, CD_2Cl_2) δ = 7.49 (d, J = 7.4 Hz, 1H), 7.36-7.32 (m,

4H), 7.27-7.21 (m, 2H), 7.11 (ddd, $J = 7.9, 7.1, 1.3$ Hz, 1H), 7.07 (ddd, $J = 7.7, 7.1, 1.1$ Hz, 1H), 7.02-6.96 (m, 4H), 5.28 (d, $J = 16.8$ Hz, 1H), 5.24 (d, $J = 16.8$ Hz, 1H), 3.14-3.06 (m, 2H), 2.89-2.83 (m, 1H), 2.80-2.78 (m, 2H), 2.26-2.21 (m, 1H), 2.17-2.10 (m, 1H) ppm.

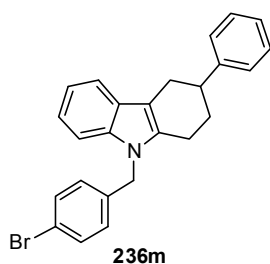
^{13}C NMR (125 MHz, CD_2Cl_2) $\delta = 162.3$ (d, $J = 244.2$ Hz), 147.1, 137.1, 135.5, 134.6 (d, $J = 3.1$ Hz), 128.7, 128.2 (d, $J = 7.7$ Hz), 127.7, 127.4, 126.5, 121.2, 119.3, 118.1, 115.8 (d, $J = 22.0$ Hz), 110.2, 109.3, 46.0, 41.3, 30.7, 29.6, 22.6 ppm

MS (EI) m/z (%): 355 (72), 251 (100), 236 (10), 142 (5), 115 (5), 109 (37).

HRMS (ESI+) m/z calculated for $\text{C}_{25}\text{H}_{22}\text{NFNa}$ ($\text{M}+\text{Na}^+$) 378.162844 found 378.162676.

The enantiomeric ratio was determined by HPLC analysis using Daicel Chiralpak AD-3 column: *n*-heptane:*i*-PrOH = 99.5:0.5, flow rate 1.0 mL/min, $\lambda = 220$ nm: $\tau_1 = 10.04$ min, $\tau_2 = 10.60$ min.

***rac*-9-(4-Bromobenzyl)-3-phenyl-2,3,4,9-tetrahydro-1H-carbazole (236m)**



The reaction was conducted on a 0.100 mmol scale.

Purification: CC on SiO_2 (hexane:EtOAc 20:1).

Yield: Colorless solid 39.9 mg (0.096 mmol, 96%).

^1H NMR (500 MHz, CD_2Cl_2) $\delta = 7.49$ (d, $J = 7.2$ Hz, 1H), 7.43-7.40 (m, 2H), 7.36-7.31 (m, 4H), 7.27-7.23 (m, 1H), 7.20 (d, $J = 7.8$ Hz, 1H), 7.11 (ddd, $J = 8.0, 7.1, 1.3$ Hz, 1H), 7.07 (ddd, $J = 7.5, 7.1, 1.1$ Hz, 1H), 6.89 (d, $J = 8.4$ Hz, 2H), 5.25 (d, $J = 17.1$ Hz, 1H), 5.21 (d, $J = 17.1$ Hz, 1H), 3.14-3.06 (m, 2H), 2.89-2.84 (m, 1H), 2.78-2.76 (m, 2H), 2.24-2.21 (m, 1H), 2.16-2.08 (m, 1H) ppm.

^{13}C NMR (125 MHz, CD_2Cl_2) $\delta = 147.1, 137.9, 137.1, 135.5, 132.1, 128.7, 128.3, 127.7, 127.4, 126.5, 121.2, 121.2, 119.4, 118.2, 110.3, 109.2, 46.1, 41.3, 30.7, 29.6, 22.6$ ppm.

MS (EI) m/z (%): 415/417 (77/77), 311/313 (100/98), 232 (29), 169/171 (32/31), 142 (13), 115 (17).

HRMS (ESI+) m/z calculated for $\text{C}_{25}\text{H}_{22}\text{NBrNa}$ ($\text{M}+\text{Na}^+$) 438.082795 found 438.082398.

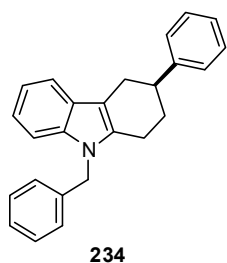
The enantiomeric ratio was determined by HPLC analysis using Daicel Chiralpak AD-3 column: *n*-heptane:*i*-PrOH = 98:2, flow rate 1.0 mL/min, $\lambda = 220$ nm: $\tau_1 = 5.21$ min, $\tau_2 = 5.52$ min.

7.4.2.5 Enantioselective Synthesis of 3-Substituted Tetrahydrocarbazoles

General procedure for the catalytic asymmetric Fischer indolization:

A reaction vial was charged with catalyst (*R*)-**145f** (3.33 mg, 0.005 mmol), Amberlite CG50 (200 mg), the corresponding hydrazone (0.100 mmol) and 4Å molecular sieves (50 mg). Under an atmosphere of argon, benzene (1.0 mL) was added and the resulting mixture was stirred in the sealed vial at 30 °C until complete conversion was indicated by TLC. The crude reaction mixture was directly submitted to column chromatography on silica gel.

(*S*)-9-Benzyl-3-phenyl-2,3,4,9-tetrahydro-1H-carbazole (**234**)



234

Purification: CC on SiO₂ (hexane:EtOAc 9:1).

Yield: Colorless solid 31.8 mg (0.094 mmol, 94%).

¹H NMR (500 MHz, CDCl₃) δ = 7.43 (d, *J* = 7.2 Hz, 1H), 7.29-7.25 (m, 4H), 7.22-7.14 (m, 5H), 7.08-7.04 (m, 1H), 7.04-7.01 (m, 1H), 6.95 (d, *J* = 7.1 Hz, 2H), 5.23 (d, *J* = 16.9 Hz, 1H), 5.19 (d, *J* = 16.9 Hz, 1H), 3.09-3.05 (m, 1H),

3.04-2.98 (m, 1H), 2.84-2.79 (m, 1H), 2.73-2.68 (m, 2H), 2.18-2.12 (m, 1H), 2.08-1.98 (m, 1H) ppm.

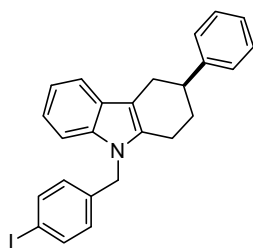
¹³C NMR (125 MHz, CDCl₃) δ = 146.8, 138.3, 137.0, 135.3, 128.9, 128.6, 127.4, 127.3, 127.2, 126.4, 126.3, 121.1, 119.2, 117.9, 109.9, 109.2, 46.5, 41.1, 30.5, 29.5, 22.5 ppm.

MS (EI) *m/z* (%): 337 (70), 233 (100), 218 (14), 142 (5), 115 (7), 91 (34).

HRMS (EI) *m/z* calculated for C₂₅H₂₃N 337.183049, found 337.183072.

The enantiomeric ratio was determined by reversed phase HPLC analysis using Daicel Chiralcel OJ-RH column: MeCN:H₂O = 90:10, flow rate 1.0 mL/min, λ = 220 nm: τ₁ = 5.10 min, τ₂ = 7.87 min.

(*S*)-9-(4-iodobenzyl)-3-phenyl-2,3,4,9-tetrahydro-1H-carbazole (**236n**)



236n

Purification: CC on SiO₂ (hexane:EtOAc 9:1).

Yield: Colorless solid 45.8 mg (0.099 mmol, 99%).

¹H NMR (500 MHz, CD₂Cl₂) δ = 7.62-7.60 (m, 2H), 7.48 (d, *J* = 7.3 Hz, 1H), 7.35-7.34 (m, 4H), 7.26-7.22 (m, 1H), 7.19 (d, *J* = 7.8 Hz, 1H), 7.10 (ddd, *J* = 8.0, 7.0, 1.2 Hz, 1H), 7.07 (ddd, *J* = 7.5, 7.2, 1.1 Hz, 1H), 6.76 (d, *J* =

8.4 Hz, 2H), 5.25 (d, $J = 17.1$ Hz, 1H), 5.20 (d, $J = 17.1$ Hz, 1H), 3.13-3.05 (m, 2H), 2.89-2.83 (m, 1H), 2.78- 2.75 (m, 2H), 2.26-2.20 (m, 1H), 2.16-2.08 (m, 1H) ppm.

^{13}C NMR (125 MHz, CD_2Cl_2) $\delta = 147.1, 138.6, 138.1, 137.1, 135.5, 128.7, 128.6, 127.7, 127.4, 126.5, 121.2, 119.4, 118.2, 110.3, 109.2, 92.7, 46.2, 41.3, 30.7, 29.6, 22.6$ ppm.

MS (EI) m/z (%): 463 (100), 359 (97), 344 (5), 232 (16), 217 (37).

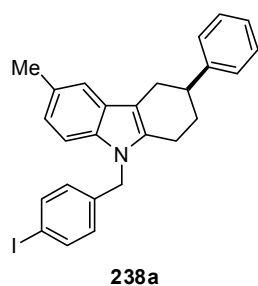
HRMS (ESI+) m/z calculated for $\text{C}_{25}\text{H}_{22}\text{NINa}$ ($\text{M}+\text{Na}^+$) 486.068919, found 486.068606.

mp = 123-125 °C (CH_2Cl_2).

$[\alpha]_{\text{D}}^{25} = -4.10$ ° ($c = 0.34, \text{CHCl}_3, \text{er} = 95:5$).

The enantiomeric ratio was determined by reversed phase HPLC analysis using Daicel Chiralcel OJ-RH column: MeCN:H₂O = 90:10, flow rate 1.0 mL/min, $\lambda = 220$ nm: $\tau_1 = 11.07$ min, $\tau_2 = 13.23$ min.

(S)-9-(4-Iodobenzyl)-6-methyl-3-phenyl-2,3,4,9-tetrahydro-1H-carbazole (238a)



Purification: CC on SiO_2 (hexane:EtOAc 15:1).

Yield: Colorless solid 47.2 mg (0.099 mmol, 99%).

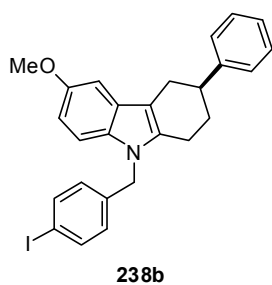
^1H NMR (400 MHz, CD_2Cl_2) $\delta = 7.50-7.47$ (m, 2H), 7.23-7.22 (m, 4H), 7.16 (s, 1H), 7.14- 7.11 (m, 1H), 6.95 (d, $J = 8.2$ Hz, 1H), 6.82 (dd, $J = 8.2, 1.4$ Hz, 1H), 6.64-6.62 (m, 2H), 5.09 (d, $J = 17.0$ Hz, 1H), 5.04 (d, $J = 17.0$ Hz, 1H), 3.00-2.92 (m, 2H), 2.75-2.68 (m, 1H), 2.64-2.61 (m, 2H), 2.31 (s, 3H), 2.11-2.07 (m, 1H), 2.03-1.95 (m, 1H) ppm.

^{13}C NMR (100 MHz, CDCl_3) $\delta = 147.2, 138.8, 138.1, 135.6, 135.5, 128.8, 128.7, 128.6, 128.0, 127.4, 126.5, 122.8, 118.1, 109.9, 109.0, 92.6, 46.3, 41.3, 30.8, 29.6, 22.6, 21.6$ ppm.

MS (EI) m/z (%): 477 (100), 373 (96), 246 (18), 217 (15), 156 (20).

HRMS (ESI+) m/z calculated for $\text{C}_{26}\text{H}_{24}\text{NINa}$ ($\text{M}+\text{Na}^+$) 500.084567, found 500.084895.

The enantiomeric ratio was determined by reversed phase HPLC analysis using Daicel Chiralcel OD-RH column: MeCN:H₂O = 80:20, flow rate 1.0 mL/min, $\lambda = 220$ nm: $\tau_1 = 13.76$ min, $\tau_2 = 14.86$ min.

(S)-9-(4-iodobenzyl)-6-methoxy-3-phenyl-2,3,4,9-tetrahydro-1H-carbazole (238b)^[221]

Purification: CC on SiO₂ (hexane:EtOAc 9:1).

Yield: Colorless solid 47.1 mg (0.096 mmol, 96%).

¹H NMR (500 MHz, CDCl₃) δ = 7.49 (d, *J* = 8.2 Hz, 2H), 7.25-7.23 (m, 4H), 7.17-7.14 (m, 1H), 6.97 (d, *J* = 8.8 Hz, 1H), 6.87 (d, *J* = 2.2 Hz, 1H), 6.69 (dd, *J* = 8.8, 2.2 Hz, 1H), 6.63 (d, *J* = 8.1 Hz, 2H), 5.10 (d, *J* = 17.0 Hz, 1H), 5.05 (d, *J* = 17.0 Hz, 1H), 3.75 (s, 3H), 3.02-2.95 (m, 2H), 2.78-

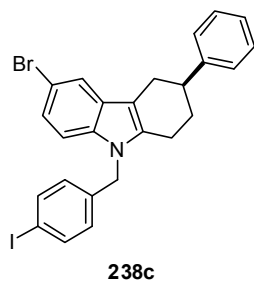
2.73 (m, 1H), 2.64-2.62 (m, 2H), 2.14-2.11 (m, 1H), 2.05-1.99 (m, 1H) ppm.

¹³C NMR (100 MHz, CDCl₃) δ = 154.1, 146.6, 138.1, 137.9, 135.8, 132.0, 128.6, 128.2, 127.6, 127.1, 126.4, 110.8, 109.9, 109.7, 100.4, 92.6, 56.0, 46.1, 41.1, 30.4, 29.5, 22.5 ppm.

MS (EI) *m/z* (%): 493 (100), 389 (95), 262 (15), 172 (45).

HRMS (ESI+) *m/z* calculated for C₂₆H₂₄NOiNa (M+Na⁺) 516.079478, found 516.079951.

The enantiomeric ratio was determined by reversed phase HPLC analysis using Daicel Chiralcel OJ-RH column: MeCN:H₂O = 90:10, flow rate 1.0 mL/min, λ = 220 nm: τ_1 = 8.73 min, τ_2 = 10.12 min.

(S)-6-Bromo-9-(4-iodobenzyl)-3-phenyl-2,3,4,9-tetrahydro-1H-carbazole (238c)^[221]

Purification: CC on SiO₂ (hexane:EtOAc 9:1).

Yield: Colorless solid 44.2 mg (0.075 mmol, 75%).

¹H NMR (500 MHz, CDCl₃) δ = 7.58-7.57 (m, 3H), 7.34-7.27 (m, 4H), 7.24-7.22 (m, 1H), 7.17 (dd, *J* = 8.6, 1.4 Hz, 1H), 7.02 (d, *J* = 8.6 Hz, 1H), 6.68 (d, *J* = 8.0 Hz, 2H), 5.18 (d, *J* = 17.2 Hz, 1H), 5.14 (d, *J* = 17.2 Hz, 1H),

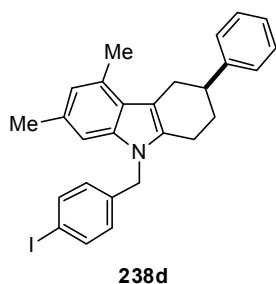
3.06-3.02 (m, 2H), 2.83-2.78 (m, 1H), 2.70-2.69 (m, 2H), 2.21-2.19 (m, 1H), 2.11-2.05 (m, 1H) ppm.

¹³C NMR (100 MHz, CDCl₃) δ = 146.2, 138.0, 137.5, 136.5, 135.5, 129.1, 128.6, 128.1, 127.1, 126.5, 123.9, 120.8, 112.6, 110.5, 110.0, 92.9, 46.1, 40.8, 30.3, 29.1, 22.3 ppm.

MS (EI) *m/z* (%): 543 (100), 541 (100), 437 (95), 435 (95), 358 (10), 310 (15), 231 (25), 217 (70), 167 (10), 141 (15), 90 (30).

HRMS (EI) *m/z* calculated for C₂₅H₂₁NBrI 540.990224, found 540.989881.

The enantiomeric ratio was determined by reversed phase HPLC analysis using Daicel Chiralcel OJ-RH column: MeCN:H₂O = 90:10, flow rate 1.0 mL/min, λ = 220 nm: τ_1 = 11.36 min, τ_2 = 14.02 min.

(S)-9-(4-iodobenzyl)-5,7-dimethyl-3-phenyl-2,3,4,9-tetrahydro-1H-carbazole (238d)

Purification: CC on SiO₂ (hexane:EtOAc 9:1).

Yield: Colorless solid 44.1 mg (0.090 mmol, 90%).

¹H NMR (400 MHz, CD₂Cl₂) δ = 7.51-7.48 (m, 2H), 7.22 (d, *J* = 1.4 Hz, 4H), 7.14-7.11 (m, 1H), 6.69 (s, 1H), 6.65-6.62 (m, 2H), 6.52 (s, 1H), 5.07 (d, *J* = 17.1 Hz, 1H), 5.02 (d, *J* = 17.1 Hz, 1H), 3.32-3.24 (m, 1H), 3.00-2.90 (m, 2H), 2.63-2.59 (m, 2H), 2.48 (s, 3H), 2.24 (s, 3H), 2.09-

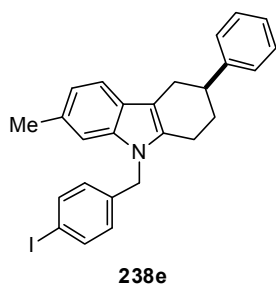
2.02 (m, 1H), 2.00-1.92 (m, 1H) ppm.

¹³C NMR (100 MHz, CD₂Cl₂) δ = 147.4, 138.9, 138.1, 137.6, 134.1, 131.0, 130.3, 128.8, 128.6, 127.5, 126.5, 124.5, 122.6, 110.7, 107.1, 92.6, 46.1, 41.9, 32.5, 30.3, 22.7, 21.7, 20.0 ppm.

MS (EI) *m/z* (%): 460 (47), 243 (100), 217 (13), 187 (5).

HRMS (ESI+) *m/z* calculated for C₂₇H₂₆NINa (M+Na⁺) 514.100212, found 514.100342.

The enantiomeric ratio was determined by reversed phase HPLC analysis using Daicel Chiralcel OJ-RH column: MeCN:H₂O = 90:10, flow rate 1.0 mL/min, λ = 220 nm: τ₁ = 14.84 min, τ₂ = 19.55 min.

(S)-9-(4-iodobenzyl)-7-methyl-3-phenyl-2,3,4,9-tetrahydro-1H-carbazole (238e)

Purification: CC on SiO₂ (hexane:EtOAc 9:1).

Yield: Colorless solid 43.5 mg (0.091 mmol, 91%).

The product was obtained as a 6:1 mixture with its regioisomer 9-(4-iodobenzyl)-5-methyl-3-phenyl-2,3,4,9-tetrahydro-1H-carbazole (determined by ¹H NMR).

¹H NMR (400 MHz, CD₂Cl₂) δ = 7.63-7.60 (m, 2H), 7.38-7.31 (m, 5H), 7.27-7.22 (m, 1H), 7.00 (s, 1H), 6.93-6.90 (m, 1H), 6.78-6.74 (m, 2H), 5.21 (d, *J* = 17.2 Hz, 1H), 5.16 (d, *J* = 17.2 Hz, 1H), 3.11-3.03 (m, 2H), 2.88-2.80 (m, 1H), 2.77-2.72 (m, 2H), 2.42 (s, 3H), 2.23-2.15 (m, 1H), 2.14-2.05 (m, 1H) ppm.

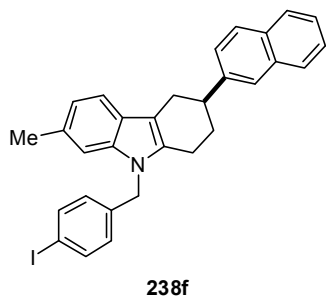
¹³C NMR (100 MHz, CD₂Cl₂) δ = 147.2, 138.8, 138.1, 137.5, 134.8, 131.1, 128.7, 128.6, 127.4, 126.5, 125.6, 121.0, 117.9, 110.1, 109.3, 92.6, 46.1, 41.3, 30.8, 29.7, 22.6, 22.0 ppm.

MS (EI) *m/z* (%): 477 (100), 373 (75), 246 (15), 217 (20).

HRMS (ESI+) *m/z* calculated for C₂₆H₂₄NINa (M+Na⁺) 500.084567, found 500.084895.

The enantiomeric ratio was determined by reversed phase HPLC analysis using Daicel Chiralcel OJ-RH column: MeCN:H₂O = 80:20, flow rate 1.0 mL/min, λ = 220 nm: τ_1 = 25.05 min, τ_2 = 30.18 min.

(S)-9-(4-iodobenzyl)-7-methyl-3-(naphthalen-2-yl)-2,3,4,9-tetrahydro-1H-carbazole (238f)



Purification: CC on SiO₂ (hexane:EtOAc 9:1).

Yield: Colorless solid 47.7 mg (0.090 mmol, 90%).

The product was obtained as a 6:1 mixture with its regioisomer 9-(4-iodobenzyl)-5-methyl-3-(naphthalen-2-yl)-2,3,4,9-tetrahydro-1H-carbazole (determined by ¹H NMR).

¹H NMR (400 MHz, CD₂Cl₂) δ = 7.85-7.80 (m, 3H), 7.77 (d, J = 0.5 Hz, 1H), 7.62-7.59 (m, 2H), 7.53-7.43 (m, 3H), 7.38 (d, J = 7.9 Hz, 1H), 7.01 (s, 1H), 6.93-6.91 (m, 1H), 6.78-6.75 (m, 2H), 5.22 (d, J = 7.9 Hz, 1H), 5.18 (d, J = 7.9 Hz, 1H), 3.28-3.21 (m, 1H), 3.17 (dd, J = 15.3, 5.0 Hz, 1H), 2.99-2.92 (m, 1H), 2.83-2.76 (m, 2H), 2.43 (s, 3H), 2.33-2.27 (m, 1H), 2.24-2.15 (m, 1H) ppm.

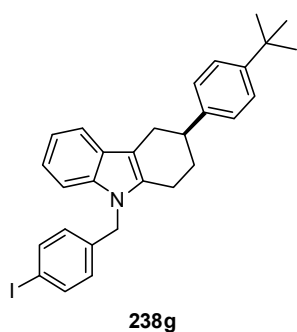
¹³C NMR (100 MHz, CD₂Cl₂) δ = 144.6, 138.8, 138.1, 137.5, 134.8, 134.1, 132.7, 131.1, 130.7, 128.5, 128.2, 127.9, 127.9, 126.5, 126.2, 125.7, 125.6, 125.3, 121.1, 117.9, 109.3, 92.6, 46.1, 41.4, 30.8, 29.5, 22.6, 21.9 ppm.

MS (EI) m/z (%): 527 (96), 373 (100), 358 (7), 246 (14), 217 (20), 156 (10).

HRMS (ESI+) m/z calculated for C₃₀H₂₆NINa (M+Na⁺) 550.100216, found 550.100582.

The enantiomeric ratio was determined by HPLC analysis using Daicel Chiralpak AD-3 column: *n*-heptane:*i*-PrOH = 99:1, flow rate 1.0 mL/min, λ = 220 nm: τ_1 = 10.43 min, τ_2 = 11.49 min.

(S)-3-(4-(*tert*-Butyl)phenyl)-9-(4-iodobenzyl)-2,3,4,9-tetrahydro-1H-carbazole (238g)



Purification: CC on SiO₂ (hexane:EtOAc 9:1).

Yield: Colorless solid 49.6 mg (0.095 mmol, 95%).

¹H NMR (500 MHz, CD₂Cl₂) δ = 7.62-7.60 (m, 2H), 7.48 (d, J = 7.3 Hz, 1H), 7.38-7.36 (m, 2H), 7.28-7.27 (m, 2H), 7.19 (d, J = 7.8 Hz, 1H), 7.10 (ddd, J = 8.0, 7.0, 1.0 Hz, 1H), 7.06 (ddd, J = 7.5, 7.1, 1.0 Hz, 1H), 6.76 (d, J = 8.3 Hz, 2H), 5.24 (d, J = 17.1 Hz, 1H), 5.20 (d, J = 17.0 Hz, 1H), 3.11-3.03 (m, 2H), 2.87-2.82 (m, 1H), 2.77-2.75 (m, 2H), 2.22-2.19 (m, 1H), 2.14-2.06 (m, 1H), 1.34 (s, 9H) ppm.

^{13}C NMR (125 MHz, CD_2Cl_2) δ = 149.4, 144.0, 138.6, 138.1, 137.1, 135.5, 128.6, 127.7, 127.0, 125.6, 121.2, 119.4, 118.2, 110.4, 109.2, 92.6, 46.2, 40.7, 34.6, 31.5, 30.8, 29.7, 22.6 ppm.

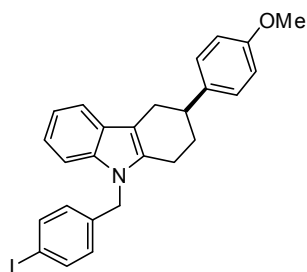
MS (EI) m/z (%): 519 (84), 359 (100), 232 (12), 217 (26).

HRMS (ESI+) m/z calculated for $\text{C}_{29}\text{H}_{30}\text{NINa}$ ($\text{M}+\text{Na}^+$) 542.131518, found 542.131503.

mp = 170-171 °C (MeOH).

The enantiomeric ratio was determined by reversed phase HPLC analysis using Daicel Chiralcel OJ-RH column: MeCN:H₂O = 90:10, flow rate 1.0 mL/min, λ = 220 nm: τ_1 = 8.52 min, τ_2 = 9.58 min.

(S)-9-(4-iodobenzyl)-3-(4-methoxyphenyl)-2,3,4,9-tetrahydro-1H-carbazole (238h)



238h

Purification: CC on SiO_2 (hexane:EtOAc 9:1).

Yield: Colorless solid 46.2 mg (0.094 mmol, 94%).

^1H NMR (500 MHz, CD_2Cl_2) δ = 7.61 (d, J = 8.3 Hz, 2H), 7.49 (d, 7.3 Hz, 1H), 7.26 (d, J = 8.6 Hz, 2H), 7.19 (d, J = 7.9 Hz, 1H), 7.11 (dd, J = 7.6, 6.3 Hz, 1H), 7.07 (dd, J = 7.0, 6.7 Hz, 1H), 6.88 (d, J = 8.6 Hz, 2H), 6.76 (d, J = 8.3 Hz, 2H), 5.23 (d, J = 17.1 Hz, 1H), 5.19 (d, J = 17.1 Hz,

1H), 3.80 (s, 3H), 3.10-3.01 (m, 2H), 2.84-2.79 (m, 1H), 2.77-2.73 (m, 2H), 2.20-2.17 (m, 1H), 2.11-2.04 (m, 1H) ppm.

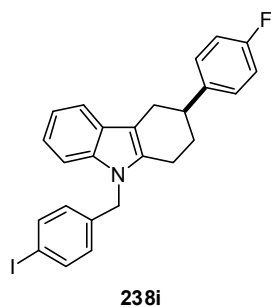
^{13}C NMR (125 MHz, CD_2Cl_2) δ = 158.4, 139.1, 138.6, 138.0, 137.1, 135.5, 128.6, 128.2, 127.7, 121.2, 119.3, 118.2, 114.0, 110.4, 109.2, 92.7, 55.5, 46.2, 40.4, 30.9, 29.8, 22.6 ppm.

MS (EI) m/z (%): 493 (72), 359 (100), 344 (5), 232 (14), 217 (31).

HRMS (ESI+) m/z calculated for $\text{C}_{26}\text{H}_{24}\text{NOINa}$ ($\text{M}+\text{Na}^+$) 516.079477, found 516.079157.

mp = 148-150 °C (CH_2Cl_2).

The enantiomeric ratio was determined by HPLC analysis using Daicel Chiralcel OD-3 column: *n*-heptane:*i*-PrOH = 99.5:0.5, flow rate 1.0 mL/min, λ = 220 nm: τ_1 = 41.52 min, τ_2 = 47.12 min and by reversed phase HPLC analysis using Daicel Chiralcel OD-RH column: MeCN:H₂O = 65:35, flow rate 1.0 mL/min, λ = 220 nm: τ_1 = 37.18 min, τ_2 = 40.01 min.

(S)-3-(4-Fluorophenyl)-9-(4-iodobenzyl)-2,3,4,9-tetrahydro-1H-carbazole (238i)

Purification: CC on SiO₂ (hexane:EtOAc 9:1).

Yield: Colorless solid 47.8 mg (0.099 mmol, 99%).

¹H NMR (400 MHz, CD₂Cl₂) δ = 7.62-7.60 (m, 2H), 7.49-7.47 (m, 1H), 7.32-7.29 (m, 2H), 7.21-7.18 (m, 1H), 7.13-7.10 (m, 1H), 7.08-7.06 (m, 1H), 7.06-7.01 (m, 2H), 6.77-6.75 (m, 2H), 5.24 (d, *J* = 17.1 Hz, 1H), 5.20 (d, *J* = 17.1 Hz, 1H), 3.13-3.05 (m, 2H), 2.86-2.81 (m, 1H), 2.79-

2.74 (m, 2H), 2.23-2.17 (m, 1H), 2.11-2.03 (m, 1H) ppm.

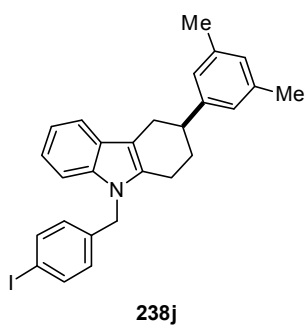
¹³C NMR (100 MHz, CD₂Cl₂) δ = 161.7 (d, *J* = 242.7 Hz), 142.8 (d, *J* = 3.1 Hz), 138.6, 138.1, 137.1, 135.4, 128.8 (d, *J* = 7.6 Hz), 128.6, 127.6, 121.3, 119.4, 118.1, 115.3 (d, *J* = 21.1 Hz), 110.1, 109.3, 92.7, 46.2, 40.5, 30.8, 29.7, 22.5 ppm.

MS (EI) *m/z* (%): 481 (100), 359 (95), 344 (5), 232 (17), 217 (39).

HRMS (ESI+) *m/z* calculated for C₂₅H₂₁NFINa (M+Na⁺) 504.059492, found 504.059141.

mp = 132-133 °C (CH₂Cl₂).

The enantiomeric ratio was determined by HPLC analysis using Daicel Chiralcel OD-3 column: *n*-heptane:*i*-PrOH = 98:2, flow rate 1.0 mL/min, λ = 220 nm: τ₁ = 12.67 min, τ₂ = 14.70 min.

(S)-3-(3,5-Dimethylphenyl)-9-(4-iodobenzyl)-2,3,4,9-tetrahydro-1H-carbazole (238j)

Purification: CC on SiO₂ (hexane:EtOAc 9:1).

Yield: Colorless solid 43.7 mg (0.089 mmol, 89%).

¹H NMR (400 MHz, CD₂Cl₂) δ = 7.63-7.60 (m, 2H), 7.49-7.47 (m, 1H), 7.20-7.18 (m, 1H), 7.10 (ddd, *J* = 7.9, 7.0, 1.2 Hz, 1H), 7.06 (ddd, *J* = 7.4, 7.1, 1.2 Hz, 1H), 6.96 (s, 2H), 6.89 (s, 1H), 6.79-6.76 (m, 2H), 5.25 (d, *J* = 17.1 Hz, 1H), 5.20 (d, *J* = 17.1 Hz, 1H), 3.07 (dd, *J* = 14.8,

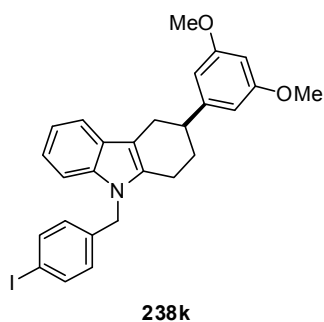
5.1 Hz, 1H), 3.02-2.95 (m, 1H), 2.86-2.81 (m, 1H), 2.79-2.76 (m, 2H), 2.32 (s, 6H), 2.21-2.15 (m, 1H), 2.12-2.05 (m, 1H) ppm.

¹³C NMR (100 MHz, CD₂Cl₂) δ = 147.0, 138.7, 138.2, 138.1, 137.1, 135.5, 128.6, 128.1, 127.8, 125.2, 121.2, 119.3, 118.2, 110.5, 109.2, 92.7, 46.2, 41.3, 30.8, 29.8, 22.8, 21.5 ppm.

MS (EI) *m/z* (%): 491 (82), 359 (100), 344 (5), 232 (14), 217 (32).

HRMS (ESI+) *m/z* calculated for C₂₇H₂₆NINa (M+Na⁺) 514.100212, found 514.100059.

The enantiomeric ratio was determined by HPLC analysis using Daicel Chiralcel OD-H column: *n*-heptane:*i*-PrOH = 98:2, flow rate 0.5 mL/min, λ = 220 nm: τ₁ = 19.07 min, τ₂ = 21.31 min.

(S)-3-(3,5-Dimethoxyphenyl)-9-(4-iodobenzyl)-2,3,4,9-tetrahydro-1H-carbazole (238k)

Purification: CC on SiO₂ (hexane:EtOAc 6:1).

Yield: Colorless solid 51.2 mg (0.098 mmol, 98%).

¹H NMR (400 MHz, CD₂Cl₂) δ = 7.62-7.59 (m, 2H), 7.49-7.47 (m, 1H), 7.20-7.17 (m, 1H), 7.12-7.04 (m, 2H), 6.77-6.74 (m, 2H), 6.50 (d, *J* = 2.2 Hz, 2H), 6.35 (t, *J* = 2.3 Hz, 1H), 5.25 (d, *J* = 17.1 Hz, 1H), 5.20 (d, *J* = 17.0 Hz, 1H), 3.78 (s, 6H), 3.12-2.98 (m, 2H), 2.88-2.80

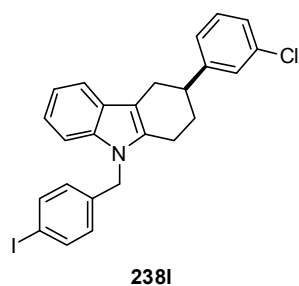
(m, 1H), 2.78-2.75 (m, 2H), 2.23-2.19 (m, 1H), 2.13-2.03 (m, 1H) ppm.

¹³C NMR (100 MHz, CD₂Cl₂) δ = 161.3, 149.6, 138.6, 138.1, 137.1, 135.5, 128.6, 127.7, 121.3, 119.4, 118.2, 110.2, 109.2, 105.5, 98.1, 92.7, 55.6, 46.2, 41.7, 30.7, 29.5, 22.6 ppm.

MS (EI) *m/z* (%): 523 (96), 359 (100), 344 (4), 232 (14), 217 (43).

HRMS (ESI+) *m/z* calculated for C₂₇H₂₆NO₂INa (M+Na⁺) 546.090047, found 546.089902.

The enantiomeric ratio was determined by reversed phase HPLC analysis using Daicel Chiralcel OJ-RH column: MeCN:H₂O = 70:30, flow rate 1.0 mL/min, λ = 220 nm: τ₁ = 17.26 min, τ₂ = 19.42 min.

(S)-3-(3-Chlorophenyl)-9-(4-iodobenzyl)-2,3,4,9-tetrahydro-1H-carbazole (238l)

Purification: CC on SiO₂ (hexane:EtOAc 9:1).

Yield: Colorless solid 48.2 mg (0.097 mmol, 97%).

¹H NMR (400 MHz, CD₂Cl₂) δ = 7.62-7.59 (m, 2H), 7.48-7.46 (m, 1H), 7.33 (dd, *J* = 1.9, 1.8 Hz, 1H), 7.28 (dd, *J* = 7.8, 7.3 Hz, 1H), 7.25-7.21 (m, 2H), 7.19 (ddd, *J* = 8.2, 1.2, 1.0 Hz, 1H), 7.12-7.04 (m, 2H), 6.77-6.74 (m, 2H), 5.25 (d, *J* = 17.0 Hz, 1H), 5.20 (d, *J* = 17.1 Hz, 1H), 3.13-

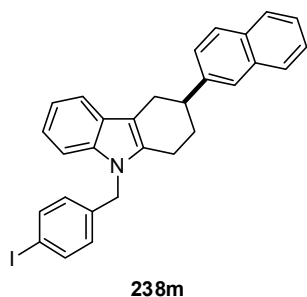
3.04 (m, 2H), 2.87-2.74 (m, 3H), 2.24-2.18 (m, 1H), 2.14-2.03 (m, 1H) ppm.

¹³C NMR (100 MHz, CD₂Cl₂) δ = 149.2, 138.6, 138.1, 137.1, 135.4, 134.4, 130.1, 128.6, 127.7, 127.6, 126.6, 125.8, 121.4, 119.5, 118.2, 110.0, 109.3, 92.7, 46.3, 41.0, 30.5, 29.4, 22.4 ppm.

MS (EI) *m/z* (%): 497 (80), 359 (100), 232 (18), 217 (54), 142 (9), 115 (9), 90 (21).

HRMS (ESI+) *m/z* calculated for C₂₅H₂₁NClINa (M+Na⁺) 520.029946, found 520.029908.

The enantiomeric ratio was determined by reversed phase HPLC analysis using Daicel Chiralcel OD-RH column: MeCN:H₂O = 70:30, flow rate 1.0 mL/min, λ = 220 nm: τ₁ = 36.86 min, τ₂ = 39.63 min.

(S)-9-(4-iodobenzyl)-3-(naphthalen-2-yl)-2,3,4,9-tetrahydro-1H-carbazole (238m)

Purification: CC on SiO₂ (hexane:EtOAc 9:1).

Yield: Colorless solid 51.0 mg (0.099 mmol, 99%).

¹H NMR (400 MHz, CD₂Cl₂) δ = 7.89-7.81 (m, 3H), 7.78-7.77 (m, 1H), 7.62-7.59 (m, 2H), 7.53-7.50 (m, 2H), 7.49-7.44 (m, 2H), 7.22-7.19 (m, 1H), 7.15-7.07 (m, 2H), 6.79-6.76 (m, 2H), 5.25 (d, *J* = 17.1 Hz, 1H), 5.20 (d, *J* = 17.1 Hz, 1H), 3.30-3.18 (m, 2H), 3.02-2.95 (m, 1H),

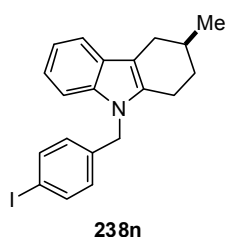
2.86-2.79 (m, 2H), 2.36-2.29 (m, 1H), 2.27-2.17 (m, 1H) ppm.

¹³C NMR (100 MHz, CD₂Cl₂) δ = 144.5, 138.6, 138.1, 137.1, 135.6, 134.1, 132.7, 128.6, 128.2, 127.9, 127.9, 127.8, 126.5, 126.3, 125.6, 125.3, 121.3, 119.4, 118.2, 110.3, 109.3, 92.7, 46.2, 41.4, 30.7, 29.5, 22.6 ppm.

MS (EI) *m/z* (%): 513 (100), 359 (94), 232 (12), 217 (31), 154 (9).

HRMS (ESI+) *m/z* calculated for C₂₉H₂₄NINa (M+Na⁺) 536.085466, found 536.084749.

The enantiomeric ratio was determined by reversed phase HPLC analysis using Daicel Chiralcel OD-RH column: MeCN:H₂O = 90:10, flow rate 1.0 mL/min, λ = 220 nm: τ₁ = 9.39 min, τ₂ = 10.50 min.

(S)-9-(4-iodobenzyl)-3-methyl-2,3,4,9-tetrahydro-1H-carbazole (238n)^[221]

Purification: CC on SiO₂ (hexane:EtOAc 19:1).

Yield: Colorless solid 28.1 mg (0.070 mmol, 70%).

¹H NMR (500 MHz, CDCl₃) δ = 7.56 (d, *J* = 8.3 Hz, 2H), 7.50-7.48 (m, 1H), 7.15-7.13 (m, 1H), 7.11-7.07 (m, 2H), 6.71 (d, *J* = 8.3 Hz, 2H), 5.18 (d, *J* = 17.3 Hz, 1H), 5.14 (d, *J* = 17.3 Hz, 1H), 2.88 (dd, *J* = 15.5, 4.7 Hz, 1H), 2.66-

2.56 (m, 2H), 2.35-2.30 (m, 1H), 1.96-1.94 (m, 2H), 1.59-1.50 (m, 1H), 1.13 (d, *J* = 6.5 Hz, 3H) ppm.

¹³C NMR (100 MHz, CDCl₃) δ = 138.1, 137.9, 136.8, 135.3, 128.2, 127.5, 121.0, 119.1, 118.0, 110.2, 108.9, 92.6, 45.9, 31.4, 29.6, 29.6, 21.9, 21.7 ppm.

MS (EI) *m/z* (%): 401 (100), 359 (35), 274 (5), 232 (10), 217 (25).

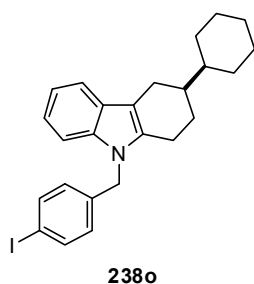
HRMS (ESI+): *m/z* calculated for C₂₀H₂₁NI (M+H⁺) 402.071318, found 402.071822.

mp = 121-122 °C (MeOH).

[α]_D²⁵ = -27.0° (c = 0.23, CH₂Cl₂, er = 95.5).

The enantiomeric ratio was determined by HPLC analysis using Daicel Chiralpak AD-3 column: *n*-heptane:*i*-PrOH = 99:1, flow rate 1.0 mL/min, $\lambda = 220$ nm: $\tau_1 = 4.243$ min, $\tau_2 = 4.60$ min

(S)-3-Cyclohexyl-9-(4-iodobenzyl)-2,3,4,9-tetrahydro-1H-carbazole (238o)



Purification: CC on SiO₂ (hexane:EtOAc 9:1).

Yield: Colorless solid 46.0 mg (0.098 mmol, 98%).

¹H NMR (400 MHz, CD₂Cl₂) $\delta = 7.60$ -7.57 (m, 2H), 7.47-7.44 (m, 1H), 7.15-7.12 (m, 1H), 7.08-7.01 (m, 2H), 6.75-6.72 (m, 2H), 5.21 (d, $J = 17.0$ Hz, 1H), 5.16 (d, $J = 17.0$ Hz, 1H), 2.86-2.81 (m, 1H), 2.73-2.68 (m, 1H), 2.62-2.55 (m, 1H), 2.48-2.42 (m, 1H), 2.08-2.04 (m, 1H), 1.86-1.77 (m,

4H), 1.71-1.65 (m, 1H), 1.64-1.51 (m, 2H), 1.40-1.06 (m, 6H) ppm.

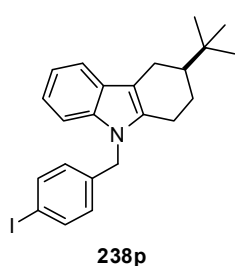
¹³C NMR (100 MHz, CD₂Cl₂) $\delta = 138.8, 138.0, 136.0, 128.6, 128.6, 128.1, 121.0, 119.2, 118.1, 110.6, 109.1, 92.6, 46.2, 42.8, 40.7, 31.1, 30.6, 27.2, 27.2, 24.8, 22.8$ ppm.

MS (EI) m/z (%): 469 (100), 359 (41), 232 (6), 217 (19).

HRMS (ESI+) m/z calculated for C₂₅H₂₈NINa (M+Na⁺) 492.115866, found 492.116240.

The enantiomeric ratio was determined by reversed phase HPLC analysis using Daicel Chiralcel OD-RH column: MeCN:H₂O = 70:30, flow rate 1.0 mL/min, $\lambda = 220$ nm: $\tau_1 = 38.30$ min, $\tau_2 = 41.46$ min.

(S)-3-(*tert*-Butyl)-9-(4-iodobenzyl)-2,3,4,9-tetrahydro-1H-carbazole (238p)



Purification: CC on SiO₂ (hexane:EtOAc 9:1).

Yield: Colorless solid 39.9 mg (0.090 mmol, 90%).

¹H NMR (400 MHz, CDCl₃) $\delta = 7.60$ -7.57 (m, 2H), 7.56-7.52 (m, 1H), 7.19-7.15 (m, 1H), 7.14-7.09 (m, 1H), 6.74 (d, $J = 8.4$ Hz, 2H), 5.21 (d, $J = 17.0$ Hz, 1H), 5.15 (d, $J = 17.0$ Hz, 1H), 2.93-2.88 (m, 1H), 2.76-2.71 (m, 1H),

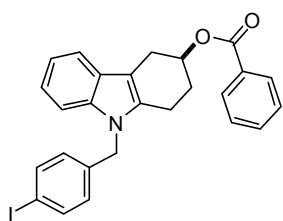
2.60-2.45 (m, 2H), 2.15-2.11 (m, 1H), 2.93-2.88 (m, 1H), 1.59-1.49 (m, 2H), 1.03 (s, 9H) ppm.

¹³C NMR (100 MHz, CDCl₃) $\delta = 138.2, 137.9, 136.9, 135.6, 128.3, 127.8, 121.0, 119.2, 117.9, 110.7, 109.0, 92.6, 46.0, 45.4, 32.7, 27.7, 24.9, 23.2, 22.5$ ppm.

MS (EI) m/z (%): 460 (47), 243 (100), 217 (13), 187 (5).

HRMS (ESI+) m/z calculated for C₂₃H₂₆NINa (M+Na⁺) 466.100217, found 466.100293.

The enantiomeric ratio was determined by HPLC analysis using Daicel Chiralpak OD-3 column: *n*-heptane:*i*-PrOH = 99:1, flow rate 1.0 mL/min, $\lambda = 220$ nm: $\tau_1 = 4.93$ min, $\tau_2 = 5.52$ min.

(S)-9-(4-Iodobenzyl)-2,3,4,9-tetrahydro-1H-carbazol-3-yl benzoate (238q)^[221]

238q

Purification: CC on SiO₂ (hexane:EtOAc 9:1).

Yield: Colorless solid 50.6 mg (0.087 mmol, 87%).

¹H NMR (500 MHz, CDCl₃) δ = 7.99 (d, *J* = 7.8 Hz, 2H), 7.58-7.50 (m, 4H), 7.41 (dd, *J* = 7.8, 7.8 Hz, 2H), 7.19 (d, *J* = 7.9 Hz, 1H), 7.16-7.10 (m, 2H), 6.70 (d, *J* = 8.1 Hz, 2H), 5.61-5.57 (m, 1H), 5.24 (d, *J* = 17.1 Hz,

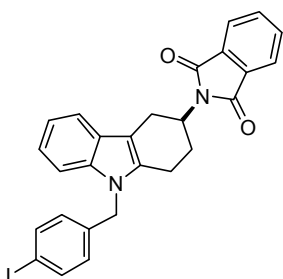
1H), 5.19 (d, *J* = 17.1 Hz, 1H), 3.26 (dd, *J* = 15.9, 4.2 Hz, 1H), 3.06 (dd, *J* = 15.9, 5.8 Hz, 1H), 2.85-2.74 (m, 2H), 2.31-2.19 (m, 2H) ppm.

¹³C NMR (100 MHz, CDCl₃) δ = 166.3, 137.9, 137.9, 137.0, 134.0, 133.0, 130.7, 129.7, 128.4, 128.1, 127.4, 121.5, 119.5, 118.1, 109.1, 107.1, 92.7, 70.3, 46.0, 27.8, 27.3, 19.4 ppm.

MS (EI) *m/z* (%): 507 (60), 385 (100), 258 (10), 217 (30), 168 (25), 90 (10).

HRMS (ESI+) *m/z* calculated for C₂₆H₂₂NO₂INa (M+Na⁺) 530.058747, found 530.058533.

The enantiomeric ratio was determined by HPLC analysis using Daicel Chiralpak OD-3 column: *n*-heptane:*i*-PrOH = 80:20, flow rate 1.0 mL/min, λ = 220 nm: τ₁ = 8.35 min, τ₂ = 14.14 min.

(S)-2-(9-(4-Iodobenzyl)-2,3,4,9-tetrahydro-1H-carbazol-3-yl)isoindoline-1,3-dione (238r)

238r

Purification: CC on SiO₂ (hexane:EtOAc 1:1 then CH₂Cl₂:EtOAc 1:1).

Yield: Colorless solid 52.5 mg (0.099 mmol, 99%).

¹H NMR (500 MHz, CD₂Cl₂) δ = 7.87-7.83 (m, 2H), 7.77-7.73 (m, 2H), 7.62 (d, *J* = 8.4 Hz, 2H), 7.44 (d, *J* = 7.7 Hz, 1H), 7.18 (d, *J* = 8.1 Hz, 1H), 7.09 (ddd, *J* = 8.0, 7.1, 1.0 Hz, 1H), 7.05 (ddd, *J* = 7.4, 7.4, 0.9 Hz, 1H), 6.76 (d, *J* = 8.4 Hz, 2H), 5.25 (d, *J* = 17.1 Hz, 1H), 5.20 (d, *J* = 17.1 Hz,

1H), 4.69-4.58 (m, 1H), 3.50 (dd, *J* = 14.1, 11.7 Hz, 1H), 2.98 (dd, *J* = 14.6, 5.5 Hz, 1H), 2.91-2.79 (m, 3H), 2.12-2.05 (m, 1H) ppm.

¹³C NMR (125 MHz, CD₂Cl₂) δ = 168.7, 138.4, 138.1, 137.3, 134.5, 134.3, 132.5, 128.5, 127.5, 123.3, 121.5, 119.5, 118.2, 109.3, 108.8, 92.7, 48.4, 46.3, 27.1, 25.1, 22.4 ppm.

MS (EI) *m/z* (%): 532 (54), 385 (100), 359 (10), 258 (12), 217 (29), 168 (35).

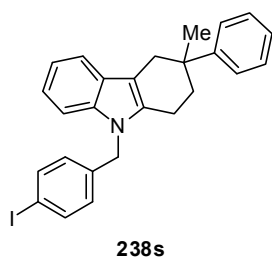
HRMS (ESI+) *m/z* calculated for C₂₇H₂₁N₂O₂INa (M+Na⁺) 555.053992, found 555.054480.

mp = 256-257 °C (CH₂Cl₂).

[α]_D²⁵ = -2.80° (c = 0.50, CH₂Cl₂, er = 93.5:6.5).

The enantiomeric ratio was determined by HPLC analysis using Daicel Chiralpak AD-3 column: *n*-heptane:*i*-PrOH = 80:20, flow rate 1.0 mL/min, $\lambda = 220$ nm: $\tau_1 = 9.69$ min, $\tau_2 = 14.32$ min. (The sample was dissolved in CH₂Cl₂)

9-(4-iodobenzyl)-3-methyl-3-phenyl-2,3,4,9-tetrahydro-1H-carbazole (238s)



Purification: CC on SiO₂ (hexane:EtOAc 20:1).

Yield: Colorless solid 5.2 mg (0.011 mmol, 11%).

Starting material **237s** recovered (38.0 mg, 77%).

¹H NMR (500 MHz, CD₂Cl₂) $\delta = 7.59$ -7.57 (m, 1H), 7.49-7.47 (m, 2H), 7.36-7.34 (m, 2H), 7.25-7.22 (m, 2H), 7.17-7.14 (m, 1H), 7.13-7.10 (m, 1H), 7.10-7.07 (m, 2H), 6.50 (d, $J = 8.4$ Hz, 2H), 5.11 (s, 2H), 3.22 (d, $J = 15.8$ Hz, 1H), 2.86 (d, $J = 15.8$ Hz, 1H), 2.60 (ddd, $J = 16.2, 5.2, 4.8$ Hz, 1H), 2.33-2.28 (m, 1H), 2.26-2.20 (m, 1H), 2.08-2.01 (m, 1H), 1.43 (s, 3H) ppm.

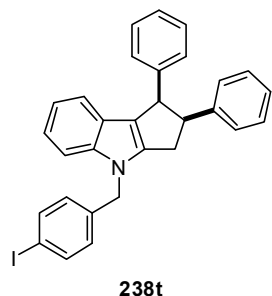
¹³C NMR (125 MHz, CD₂Cl₂) $\delta = 148.2, 138.5, 137.9, 137.1, 135.3, 128.3, 128.2, 127.8, 126.4, 125.9, 121.1, 119.3, 118.1, 109.9, 109.2, 92.4, 46.0, 38.1, 36.2, 33.5, 29.8, 20.2$ ppm.

MS (EI) m/z (%): 477 (63), 359 (100), 344 (4), 232 (15), 217 (31).

HRMS (EI) m/z calculated for C₂₆H₂₄NI 477.095347, found 477.095027.

The enantiomeric ratio was determined by reversed phase HPLC analysis using Daicel Chiralcel OJ-RH column: MeCN:H₂O = 90:10, flow rate 1.0 mL/min, $\lambda = 220$ nm: $\tau_1 = 6.97$ min, $\tau_2 = 15.27$ min.

(1R,2S)-4-(4-iodobenzyl)-1,2-diphenyl-1,2,3,4-tetrahydrocyclopenta[b]indole (238t)



Purification: CC on SiO₂ (hexane:EtOAc 15:1).

Yield: Yellow solid 32.6 mg (0.062 mmol, 62%).

¹H NMR (400 MHz, CD₂Cl₂) $\delta = 7.71$ -7.67 (m, 2H), 7.29-7.27 (m, 1H), 7.19 (d, $J = 7.8$ Hz, 1H), 7.10 (ddd, $J = 7.1, 7.1, 1.2$ Hz, 1H), 7.05-6.98 (m, 7H), 6.96 (d, $J = 8.4$ Hz, 2H), 6.91-6.89 (m, 2H), 6.75-6.72 (m, 2H), 5.36 (d, $J = 16.5$ Hz, 1H), 5.31 (d, $J = 16.5$ Hz, 1H), 4.79 (d, $J = 8.0$ Hz, 1H), 4.54 (dd, $J = 16.0, 8.0$ Hz, 1H), 3.27-3.16 (m, 2H) ppm.

¹³C NMR (100 MHz, CD₂Cl₂) $\delta = 145.8, 141.7, 141.7, 141.3, 138.2, 138.2, 129.1, 129.0, 128.8, 127.8, 127.8, 126.2, 126.1, 124.9, 121.0, 120.1, 119.9, 119.1, 110.3, 93.0, 55.9, 50.6, 48.2, 31.2$ ppm

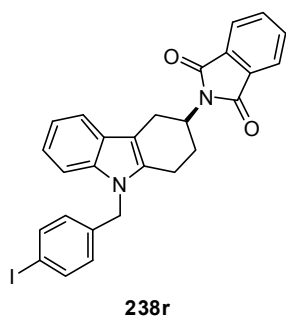
MS (EI) m/z (%): 525 (100), 434 (19), 306 (14), 230 (16), 217 (38).

HRMS (ESI+) m/z calculated for $C_{30}H_{24}NINa$ ($M+Na^+$) 548.084563, found 548.084784.

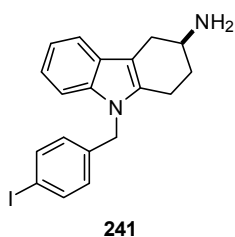
The enantiomeric ratio was determined by reversed phase HPLC analysis using Daicel Chiralcel OJ-RH column: MeCN:H₂O = 70:30, flow rate 1.0 mL/min, λ = 220 nm: τ_1 = 31.81 min, τ_2 = 43.74 min.

7.4.2.6 Large Scale Indolization and Formal Synthesis of (*S*)-Ramatroban

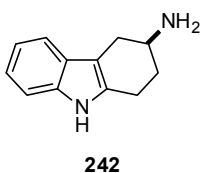
(*S*)-2-(9-(4-Iodobenzyl)-2,3,4,9-tetrahydro-1H-carbazol-3-yl)isoindoline-1,3-dione (**238r**)



A round-bottomed flask was charged with catalyst (*R*)-**145f** (66.6 mg, 0.010 mmol), Amberlite CG50 (4.00 g), hydrazone **237r** (1.10 g, 2.00 mmol) and 4Å molecular sieves (1.00 g). Under an atmosphere of argon, benzene (20.0 mL) was added and the resulting mixture was stirred at 30 °C for 6 days. The reaction mixture was then filtered and the residue washed thoroughly with CH₂Cl₂. The filtrate was concentrated *in vacuo* to give the crude product as a mixture of **238r** (93.5:6.5 er) and catalyst (*R*)-**145f**. Recrystallization of this solid from boiling toluene (27 mL) gave the pure product **238r** as a fine colorless solid (856 mg, 1.61 mmol, 80.4%) with 94:6 er. The mother liquor was evaporated and subsequently subjected to column chromatography on silica gel eluting with hexane:EtOAc (1:1) then CH₂Cl₂:EtOAc (1:1) then CH₂Cl₂:MeOH (19:1). From this a further yield of **238r** (109 mg, 0.205 mmol, 10.2%) was obtained with 93.5:6.5 er, resulting in an overall yield of 91% of **238r**. Spectroscopic data was in accordance with that reported above. Additionally recovery of catalyst (*R*)-**145f** (36.7 mg, 0.055 mmol, 55%) was achieved after acidification of the relevant fractions as described previously.

(S)-9-(4-iodobenzyl)-2,3,4,9-tetrahydro-1H-carbazol-3-amine (241)

In a Schlenk tube under argon, NEt_3 (50 μL , 0.361 mmol) and hydrazine hydrate (26 μL , 0.542 mmol) were added to a suspension of phthalimide **238r** (96.4 mg, 0.181 mmol) in CH_2Cl_2 (2 mL) and *i*-PrOH (0.5 mL). The mixture was stirred at 40 °C for 48 h before the solvent was evaporated *in vacuo*. The resulting solid was used directly in the next step without purification.

(S)-2,3,4,9-Tetrahydro-1H-carbazol-3-amine (242)^[221]

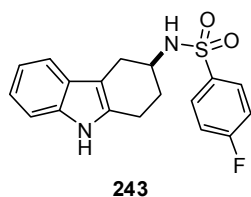
A suspension of (*S*)-9-(4-iodobenzyl)-2,3,4,9-tetrahydro-1H-carbazol-3-amine (**241**, 0.181 mmol; assumed quantitative from **238r**) in THF (1.5 mL) was cooled to -78 °C in a Schlenk tube. Ammonia (3 mL) was condensed into the flask and lithium powder (12.6 mg, 1.81 mmol) was then added.

The resulting deep blue solution was stirred at -78 °C for 3 h. The reaction was quenched by the addition of EtOH (500 μL) at -78 °C. The reaction was then allowed to warm to room temperature, allowing the ammonia to evaporate. The mixture was diluted with 10% aqueous HCl (5 mL) and subsequently washed with Et_2O (2 x 5 mL). The aqueous layer was then cooled in ice and basified to pH = 10 with NaOH. This basic aqueous mixture was then extracted with CH_2Cl_2 (3 x 5 mL). The combined CH_2Cl_2 extracts were then dried over MgSO_4 and concentrated *in vacuo* to yield crude **242** (42.0 mg) as a colorless solid which was used directly in the next step without purification.

$^1\text{H NMR}$ (300 MHz, CD_2Cl_2) δ = 8.13 (s, broad, 1H), 7.42 (d, J = 7.3 Hz, 1H), 7.28-7.26 (m, 1H), 7.11-7.00 (m, 2H), 3.29-3.22 (m, 1H), 3.03-2.96 (m, 1H), 2.84-2.79 (m, 2H), 2.46-2.38 (m, 1H), 2.10-2.01 (m, 1H), 1.85-1.75 (m, 1H) ppm.

MS (EI) m/z (%): 186 (30), 168 (15), 143 (100).

HRMS (EI) m/z calculated for $\text{C}_{12}\text{H}_{14}\text{N}_2$ 186.115685, found 186.115542.

(S)-4-Fluoro-N-(2,3,4,9-tetrahydro-1H-carbazol-3-yl)benzenesulfonamide (243)

To a suspension of (S)-2,3,4,9-tetrahydro-1H-carbazol-3-amine (**242**, 0.181 mmol; assumed quantitative from **238r**) in CH₂Cl₂ (2 mL) was added NEt₃ (50.4 μL, 0.362 mmol) and 4-fluorobenzenesulfonyl chloride (70.4 mg, 0.362 mmol). The reaction was stirred at room temperature for 2 h before saturated aqueous NaHCO₃ (4 mL) was added. The organic phase was separated and the aqueous phase extracted with CH₂Cl₂ (2 x 4 mL). The combined organic extracts were dried over MgSO₄ and concentrated *in vacuo*. The crude material was purified by flash chromatography on SiO₂ eluting with hexane:EtOAc (90:10 to 70:30) to give sulfonamide **243** (45.4 mg, 0.132 mmol, 73% over 3 steps from **238r**; 93:7 er) as a colorless solid.

¹H NMR (400 MHz, CD₂Cl₂) δ = 7.83-7.79 (m, 3H), 7.19-7.18 (m, 2H), 7.16-7.11 (m, 2H), 7.03-6.99 (m, 1H), 6.95-6.91 (m, 1H), 4.73 (d, *J* = 8.0 Hz, 1H), 3.71-3.66 (m, 1H), 2.82-2.77 (m, 1H), 2.73-2.70 (m, 2H), 2.45-2.39 (m, 1H), 1.97-1.84 (m, 2H) ppm.

¹³C NMR (100 MHz, CD₂Cl₂) δ = 165.5 (d, *J* = 252 Hz), 137.7, 136.6, 133.0, 130.1 (d, *J* = 9.4 Hz), 127.8, 121.8, 119.6, 117.8, 116.7 (d, *J* = 22.6 Hz), 110.8, 106.9, 50.0, 29.6, 28.8, 20.7 ppm.

MS (EI) *m/z* (%): 344 (90), 185 (90), 169 (100), 156 (25), 143 (90).

HRMS (ESI+) *m/z* calculated for C₁₈H₁₇N₂O₂FSNa (M+Na⁺) 367.088700, found 367.088723.

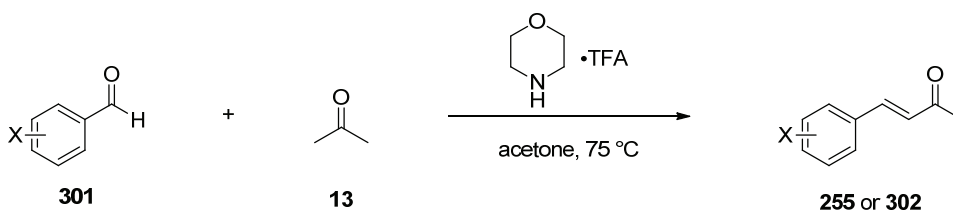
[α]_D²⁵ = -35.2° (c = 0.25, CHCl₃).

The enantiomeric ratio was determined by reversed phase HPLC analysis using Daicel Chiralcel OJ-RH column: MeCN:H₂O = 50:50, flow rate 1.0 mL/min, λ = 220 nm: τ₁ = 7.52 min, τ₂ = 9.28 min.

7.5 Catalytic Asymmetric 6π Electrocyclization

7.5.1 Synthesis of α,β -Unsaturated Ketones

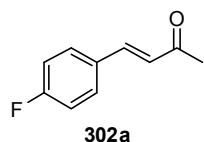
The α,β -unsaturated ketones were synthesized using a morpholinium trifluoroacetate-catalyzed aldol condensation between acetone (**13**) and benzaldehydes (**301**) as reported by our group.^[195]



General procedure for the aldol condensation of benzaldehydes with acetone:

To a solution of aldehyde **301** in acetone (0.4 M) was added morpholinium trifluoroacetate (20 mol%) and the resulting mixture was heated to 70 °C in a sealed vial for 48 h. After cooling to room temperature the mixture was poured into ice water (20 mL) and stirred for 5 min. In cases where the product precipitated the solid was filtered off and dried *in vacuo*. In cases where no precipitate was formed the mixture was extracted with CH_2Cl_2 , the combined organic layers were dried over MgSO_4 , concentrated under reduced pressure and purified by column chromatography on silica gel.

(*E*)-4-(4-Fluorophenyl)but-3-en-2-one (**302a**)



The reaction was conducted on a 5.00 mmol scale.

Purification: CC on SiO_2 (hexane:EtOAc 9:1).

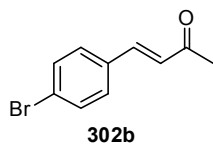
Yield: Yellow oil 610 mg (3.71 mmol, 74%).

$^1\text{H NMR}$ (500 MHz, CDCl_3) δ = 7.53 (dd, J = 8.6, 5.4 Hz, 2H), 7.48 (d, J = 16.3 Hz, 1H), 7.09 (dd, J = 8.6, 8.6 Hz, 2H), 6.65 (d, J = 16.3 Hz, 1H), 2.37 (s, 3H) ppm.

$^{13}\text{C NMR}$ (125 MHz, CDCl_3) δ = 198.3, 164.2 (d, J = 251.9 Hz), 142.2, 130.8 (d, J = 3.5 Hz), 130.3 (d, J = 8.8 Hz), 127.0 (d, J = 2.3 Hz), 116.3 (d, J = 22.0 Hz), 27.8 ppm.

MS (EI) m/z (%): 164 (63), 149 (100), 121 (44), 101 (33), 95 (7), 75 (13).

HRMS (EI) m/z calculated for $\text{C}_{10}\text{H}_9\text{OF}$ 164.063747, found 164.063679.

(E)-4-(4-Bromophenyl)but-3-en-2-one (302b)

The reaction was conducted on a 4.43 mmol scale.

Purification: Filtration.

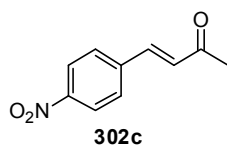
Yield: Pale yellow solid 830 mg (3.69 mmol, 83%).

$^1\text{H NMR}$ (500 MHz, CDCl_3) δ = 7.53 (d, J = 8.5 Hz, 2H), 7.44 (d, 16.3 Hz, 1H), 7.40 (d, 8.5 Hz, 2H), 6.70 (d, 16.3 Hz, 1H), 2.38 (s, 3H) ppm.

$^{13}\text{C NMR}$ (125 MHz, CDCl_3) δ = 198.2, 142.1, 133.5, 132.4, 129.7, 127.7, 124.9, 27.8 ppm.

MS (EI) m/z (%): 224/226 (30/29), 209/211 (63/61), 181/183 (20/19), 145 (57), 130 (13), 115 (7), 102 (100), 75 (26), 63 (9), 51 (31), 43 (41).

HRMS (EI) m/z calculated for $\text{C}_{10}\text{H}_9\text{OBr}$ 223.983691, found 223.983875.

(E)-4-(4-Nitrophenyl)but-3-en-2-one (302c)

The reaction was conducted on a 5.00 mmol scale.

Purification: Filtration.

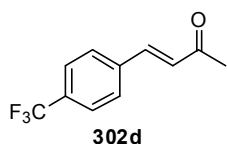
Yield: Colorless solid 850 mg (4.45 mmol, 89%).

$^1\text{H NMR}$ (500 MHz, CDCl_3) δ = 8.25 (d, J = 8.8 Hz, 2H), 7.69 (d, J = 8.7 Hz, 2H), 7.53 (d, J = 16.3 Hz, 1H), 6.81 (d, J = 16.3 Hz, 1H), 2.42 (s, 3H) ppm.

$^{13}\text{C NMR}$ (125 MHz, CDCl_3) δ = 197.7, 148.7, 140.8, 140.2, 130.5, 128.9, 124.4, 28.2 ppm.

MS (EI) m/z (%): 191 (20), 176 (100), 43 (32).

HRMS (EI) m/z calculated for $\text{C}_{10}\text{H}_9\text{NO}_3$ 191.058247, found 191.058171.

(E)-4-(4-(Trifluoromethyl)phenyl)but-3-en-2-one (302d)

The reaction was conducted on a 5.00 mmol scale.

Purification: CC on SiO_2 (hexane:EtOAc 9:1).

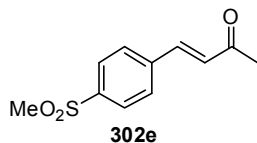
Yield: Yellow oil 704 mg (3.28 mmol, 66%).

$^1\text{H NMR}$ (500 MHz, CDCl_3) δ = 7.67-7.63 (m, 4H), 7.52 (d, J = 16.3 Hz, 1H), 6.78 (d, J = 16.3 Hz, 1H), 2.41 (s, 3H) ppm.

$^{13}\text{C NMR}$ (125 MHz, CDCl_3) δ = 198.0, 141.4, 138.0, 132.1 (q, J = 32.7 Hz), 129.2, 128.5, 126.1 (q, J = 3.8 Hz), 123.9 (q, J = 272.3 Hz), 28.0 ppm.

MS (EI) m/z (%): 214 (41), 199 (100), 171 (52), 151 (39), 145 (28), 102 (10), 43 (22).

HRMS (EI) m/z calculated for $\text{C}_{11}\text{H}_9\text{OF}_3$ 214.060550, found 214.060344.

(E)-4-(4-(Methylsulfonyl)phenyl)but-3-en-2-one (302e)

The reaction was conducted on a 2.00 mmol scale.

Purification: Filtration.

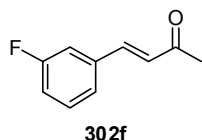
Yield: Pale yellow solid 395 mg (1.76 mmol, 88%).

$^1\text{H NMR}$ (500 MHz, CDCl_3) δ = 7.97 (d, J = 8.4 Hz, 2H), 7.72 (d, J = 8.4 Hz, 2H), 7.53 (d, J = 16.3 Hz, 1H), 6.81 (d, J = 16.3 Hz, 1H), 3.08 (s, 3H), 2.42 (s, 3H) ppm.

$^{13}\text{C NMR}$ (125 MHz, CDCl_3) δ = 197.8, 141.7, 140.6, 139.9, 130.2, 129.0, 128.2, 44.6, 28.1 ppm.

MS (EI) m/z (%): 224 (40), 209 (100), 144 (96), 131 (72), 119 (23), 102 (34), 91 (13), 76 (16), 43 (38).

HRMS (ESI+) m/z calculated for $\text{C}_{11}\text{H}_{12}\text{O}_3\text{SNa}$ ($\text{M}+\text{Na}^+$) 247.039934, found 247.039690.

(E)-4-(3-Fluorophenyl)but-3-en-2-one (302f)

The reaction was conducted on a 5.00 mmol scale.

Purification: CC on SiO_2 (hexane:EtOAc 9:1).

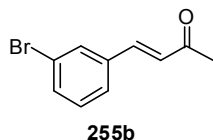
Yield: Yellow oil 654 mg (3.98 mmol, 80%).

$^1\text{H NMR}$ (500 MHz, CDCl_3) δ = 7.46 (d, J = 16.3 Hz, 1H), 7.39-7.35 (m, 1H), 7.31 (d, J = 7.8, 1H), 7.25-7.22 (m, 1H), 7.11-7.08 (m, 1H), 6.70 (d, J = 16.3 Hz, 1H), 2.39 (s, 3H) ppm.

$^{13}\text{C NMR}$ (125 MHz, CDCl_3) δ = 198.2, 163.2 (d, J = 247.2), 142.0 (d, J = 2.8), 136.9 (d, J = 7.7), 130.7 (d, J = 8.2), 128.3, 124.4, (d, J = 2.7), 117.5 (d, J = 21.7), 114.6 (d, J = 22.0), 27.9 ppm.

MS (EI) m/z (%): 164 (66), 149 (100), 121 (43), 101 (31), 95 (6), 75 (11), 43 (13).

HRMS (EI) m/z calculated for $\text{C}_{10}\text{H}_9\text{OF}$ 164.063741, found 164.063657.

(E)-4-(3-Bromophenyl)but-3-en-2-one (255b)

The reaction was conducted on a 5.25 mmol scale.

Purification: Filtration.

Yield: Colorless solid 1.00 g (4.46 mmol, 85%).

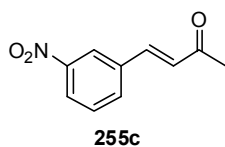
$^1\text{H NMR}$ (500 MHz, CDCl_3) δ = 7.69-7.68 (m, 1H), 7.52 (d, J = 8.0 Hz, 1H), 7.46 (d, J = 7.8 Hz, 1H), 7.43 (d, J = 16.3 Hz, 1H), 7.27 (dd, J = 7.9, 7.4 Hz, 1H), 6.70 (d, J = 16.3 Hz, 1H), 2.38 (s, 3H) ppm.

^{13}C NMR (125 MHz, CDCl_3) δ = 198.1, 141.7, 136.7, 133.4, 131.1, 130.6, 128.3, 127.0, 123.2, 27.9 ppm.

MS (EI) m/z (%): 224/226 (42/41), 209/211 (74/72), 181/183 (24/23), 145 (67), 130 (13), 115 (7), 102 (100), 75 (23), 51 (28), 43 (38).

HRMS (ESI+) m/z calculated for $\text{C}_{10}\text{H}_9\text{OBrNa}$ ($\text{M}+\text{Na}^+$) 246.972909, found 246.972619.

(E)-4-(3-Nitrophenyl)but-3-en-2-one (255c)



The reaction was conducted on a 5.00 mmol scale.

Purification: Filtration.

Yield: Colorless solid 843 mg (4.40 mmol, 88%).

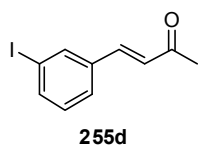
^1H NMR (500 MHz, CDCl_3) δ = 8.40 (s, 1H), 8.24 (dd, J = 8.2, 1.2 Hz, 1H), 7.85 (d, J = 7.8 Hz, 1H), 7.60 (dd, J = 8.0, 8.0 Hz, 1H), 7.55 (d, J = 16.3 Hz, 1H), 6.83 (d, J = 16.3 Hz, 1H), 2.42 (s, 3H) ppm.

^{13}C NMR (125 MHz, CDCl_3) δ = 197.7, 148.9, 140.3, 136.4, 133.9, 130.2, 129.5, 124.8, 122.7, 28.2 ppm.

MS (EI) m/z (%): 191 (33), 176 (100), 148 (9), 129 (25), 118 (16), 102 (58), 76 (20), 63 (10), 51 (15), 43 (72).

HRMS (EI) m/z calculated for $\text{C}_{10}\text{H}_9\text{NO}_3$ 191.058240, found 191.058072.

(E)-4-(3-Iodophenyl)but-3-en-2-one (255d)



The reaction was conducted on a 4.00 mmol scale.

Purification: Filtration.

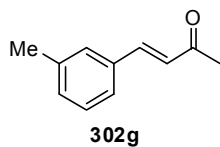
Yield: Colorless solid 867 mg (3.18 mmol, 81%).

^1H NMR (500 MHz, CDCl_3) δ = 7.89 (s, 1H), 7.71 (d, J = 7.9 Hz, 1H), 7.49 (d, J = 7.8 Hz, 1H), 7.39 (d, J = 16.3 Hz, 1H), 7.13 (dd, J = 7.8, 7.8 Hz, 1H), 6.68 (d, J = 16.3 Hz, 1H), 2.37 (s, 3H) ppm.

^{13}C NMR (125 MHz, CDCl_3) δ = 198.1, 141.6, 139.3, 137.1, 136.8, 130.7, 128.2, 127.5, 94.9, 27.9 ppm

MS (EI) m/z (%): 272 (30), 257 (21), 145 (96), 130 (100), 115 (11), 102 (89), 76 (33), 43 (64).

HRMS (EI) m/z calculated for $\text{C}_{10}\text{H}_9\text{OI}$ 271.969811, found 271.969605.

(E)-4-(m-Tolyl)but-3-en-2-one (302g)

The reaction was conducted on a 5.00 mmol scale.

Purification: CC on SiO₂ (hexane:EtOAc 9:1).

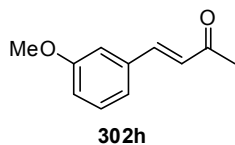
Yield: Colorless oil 768 mg (4.79 mmol, 96%).

¹H NMR (500 MHz, CDCl₃) δ = 7.49 (d, *J* = 16.3 Hz, 1H), 7.36-7.34 (m, 2H), 7.29 (dd, *J* = 7.8, 7.4 Hz, 1H), 7.22 (d, *J* = 7.5 Hz, 1H), 6.71 (d, *J* = 16.3 Hz, 1H), 2.38 (s, 6H) ppm.

¹³C NMR (125 MHz, CDCl₃) δ = 198.6, 143.8, 138.8, 134.5, 131.5, 129.1, 129.0, 127.1, 125.6, 27.6, 21.5 ppm.

MS (EI) *m/z* (%): 160 (40), 145 (100), 115 (35), 91 (18), 65 (10), 43 (16).

HRMS (EI) *m/z* calculated for C₁₁H₁₂O 160.088813, found 160.088767.

(E)-4-(3-Methoxyphenyl)but-3-en-2-one (302h)

The reaction was conducted on a 5.00 mmol scale.

Purification: CC on SiO₂ (hexane:EtOAc 9:1).

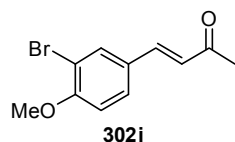
Yield: Colorless oil 791 mg (4.49 mmol, 90%).

¹H NMR (500 MHz, CDCl₃) δ = 7.48 (d, *J* = 16.3 Hz, 1H), 7.31 (dd, *J* = 8.0, 7.9 Hz, 1H), 7.14 (d, *J* = 7.6 Hz, 1H), 7.06 (s, 1H), 6.95 (dd, *J* = 8.2, 2.2 Hz, 1H), 6.70 (d, *J* = 16.3 Hz, 1H), 3.84 (s, 3H), 2.38 (s, 3H) ppm.

¹³C NMR (125 MHz, CDCl₃) δ = 198.6, 160.1, 143.5, 135.9, 130.1, 127.6, 121.1, 116.6, 113.2, 55.5, 27.6 ppm.

MS (EI) *m/z* (%): 176 (83), 161 (100), 145 (38), 133 (24), 118 (18), 103 (5).

HRMS (EI) *m/z* calculated for C₁₁H₁₂O₂ 176.083727, found 176.083705.

(E)-4-(3-Bromo-4-methoxyphenyl)but-3-en-2-one (302i)

The reaction was conducted on a 5.00 mmol scale.

Purification: Filtration.

Yield: Colorless solid 1.21 g (4.73 mmol, 95%).

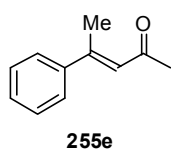
¹H NMR (500 MHz, CDCl₃) δ = 7.76 (d, *J* = 2.1 Hz, 1H), 7.46 (dd, *J* = 8.5, 2.1 Hz, 1H), 7.40 (d, *J* = 16.2 Hz, 1H), 6.91 (d, *J* = 8.6 Hz, 1H), 6.60 (d, *J* = 16.2 Hz, 1H), 3.93 (s, 3H), 2.35 (s, 3H) ppm.

^{13}C NMR (125 MHz, CDCl_3) δ = 198.2, 157.7, 141.7, 133.0, 129.3, 128.6, 126.1, 112.5, 112.0, 56.5, 27.8 ppm.

MS (EI) m/z (%): 254/256 (38/37), 239/241 (47/47), 175 (11), 160 (100), 145 (9), 132 (29), 117 (14), 102 (15), 89 (44), 75 (9), 63 (28), 43 (44).

HRMS (ESI+) m/z calculated for $\text{C}_{11}\text{H}_{11}\text{O}_2\text{BrNa}$ ($\text{M}+\text{Na}^+$) 276.983477, found 276.983370.

(*E*)-4-Phenylpent-3-en-2-one (255e)



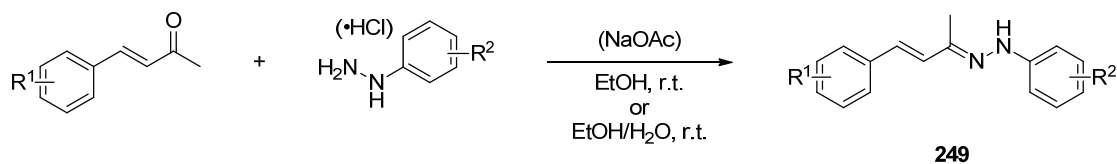
Iodobenzene (**296**, 306 mg, 1.50 mmol), TBACl (438 mg, 1.57 mmol) and NaOAc (148 mg, 1.80 mmol) were suspended in NMP (12 mL) and ethylidene acetone (**303**, 252 mg, 3.00 mmol) and $\text{Pd}(\text{OAc})_2$ (6.8 mg, 0.03 mmol) were subsequently added. The mixture was heated to 90 °C in a sealed flask under argon. After 12 h the reaction was cooled to room temperature and poured into half concentrated aqueous NaHCO_3 solution (80 mL). The mixture was extracted with CH_2Cl_2 (3 x 40 mL) and the combined organic layers were washed with brine, dried over MgSO_4 and concentrated under reduced pressure. The remaining NMP solution was loaded onto a column packed with silica gel and the product was eluted with hexane:EtOAc (25:1) to afford the title compound **255e** (128 mg, 0.799 mmol, 53%) as a pale yellow oil.

^1H NMR (400 MHz, CDCl_3) δ = 7.50-7.46 (m, 2H), 7.41-7.35 (m, 3H), 6.51 (d, J = 1.1 Hz, 1H), 2.54 (d, J = 1.2 Hz, 3H), 2.30 (s, 3H) ppm.

MS (EI) m/z (%): 159 (100), 145 (94), 115 (62), 91 (27), 43 (23).

HRMS (EI) m/z calculated for $\text{C}_{11}\text{H}_{12}\text{O}$ 160.088814, found 160.088845.

The obtained data were in accordance with literature reported data.^[222]

7.5.2 Synthesis of α,β -Unsaturated Arylhydrazones

General procedure for the synthesis of α,β -unsaturated arylhydrazones:

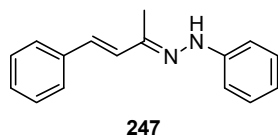
The α,β -unsaturated hydrazones **249** were synthesized by condensation of the corresponding enone and the arylhydrazine, using modifications of reported procedures.^[197]

Method A: The pure arylhydrazine (1 equiv) was added to a solution of the corresponding enone (1 equiv) in EtOH (0.5-0.6 M) and the mixture was stirred at 60 °C until the starting material was consumed (monitored by TLC), then the reaction was cooled to room temperature again. In cases where the product precipitated, the solid was filtered off and dried *in vacuo*. In cases where no precipitate was formed the mixture was concentrated under reduced pressure and the residue was crystallized from an appropriate solvent or solvent mixture to afford the pure hydrazone.

Method B: The arylhydrazine hydrochloride (1.4 equiv) was added to an aqueous solution of NaOAc (2.5 equiv) and EtOH was added until the solids had completely dissolved. This mixture was then added dropwise to a solution of the corresponding enone (1 equiv) in EtOH and the mixture was stirred vigorously at room temperature. The precipitate was filtered off and recrystallized from an appropriate solvent or solvent mixture to afford the pure hydrazone.

(E)-1-Phenyl-2-((E)-4-phenylbut-3-en-2-ylidene)hydrazine (247)

Method A.



The reaction was conducted on a 18.5 mmol scale.

Purification: Filtration and recrystallization from CH₂Cl₂:hexane.

Yield: Yellow needles 3.58 g (15.1 mmol, 82%).

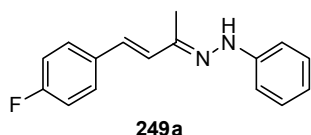
¹H NMR (500 MHz, CD₂Cl₂) δ = 7.51 (d, *J* = 7.3 Hz, 2H), 7.47 (br, 1H), 7.36 (dd, *J* = 8.0, 7.5 Hz, 2H), 7.30-7.24 (m, 3H), 7.15-7.13 (m, 2H), 7.04 (d, *J* = 16.5 Hz, 1H), 6.88 (tt, *J* = 7.3, 1.1 Hz, 1H), 6.78 (d, *J* = 16.5 Hz, 1H), 2.09 (s, 3H) ppm.

^{13}C NMR (125 MHz, CD_2Cl_2) δ = 145.2, 143.4, 137.6, 130.3, 129.6, 129.4, 129.0, 127.9, 126.8, 120.5, 113.3, 10.2 ppm.

MS (EI) m/z (%): 236 (100), 159 (36), 144 (23), 128 (5), 118 (5), 103 (24).

HRMS (ESI+) m/z calculated for $\text{C}_{16}\text{H}_{16}\text{N}_2\text{Na}$ ($\text{M}+\text{Na}^+$) 259.120570, found 259.120341.

(E)-1-((E)-4-(4-Fluorophenyl)but-3-en-2-ylidene)-2-phenylhydrazine (249a)



Method A.

The reaction was conducted on a 1.50 mmol scale.

Purification: Crystallization from CH_2Cl_2 :hexane.

Yield: Yellow solid 281 mg (1.11 mmol, 74%).

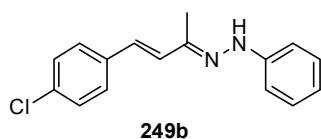
^1H NMR (500 MHz, CDCl_3) δ = 7.44 (dd, J = 8.6, 5.5 Hz, 2H), 7.41 (br, 1H), 7.29 (dd, J = 7.6, 7.4 Hz, 2H), 7.14 (d, J = 8.4 Hz, 2H), 7.04 (dd, J = 8.7, 8.6 Hz, 2H), 6.96 (d, J = 16.4 Hz, 1H), 6.90 (t, J = 7.4 Hz, 1H), 6.70 (d, J = 16.4 Hz, 1H), 2.08 (s, 3H) ppm.

^{13}C NMR (125 MHz, CDCl_3) δ = 162.5 (d, J = 247.7 Hz), 144.6, 143.4, 133.4 (d, J = 3.0 Hz), 129.7, 129.4, 128.3, 128.2 (d, J = 8.0 Hz), 120.6, 115.8 (d, J = 21.8 Hz), 113.3, 10.3 ppm.

MS (EI) m/z (%): 254 (100), 159 (34), 146 (5), 132 (7), 121 (22), 109 (8), 91 (33).

HRMS (EI) m/z calculated for $\text{C}_{16}\text{H}_{15}\text{N}_2\text{F}$ 254.121922, found 254.122029.

(E)-1-((E)-4-(4-Chlorophenyl)but-3-en-2-ylidene)-2-phenylhydrazine (249b)



Method A.

The reaction was conducted on a 3.00 mmol scale.

Purification: Crystallization from CH_2Cl_2 :hexane.

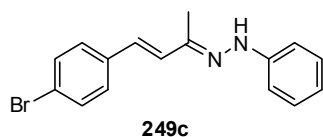
Yield: Yellow needles 512 mg (1.89 mmol, 63%).

^1H NMR (500 MHz, CDCl_3) δ = 7.41-7.39 (m, 3H), 7.31 (d, J = 8.4 Hz, 2H), 7.28 (dd, J = 7.6, 7.5 Hz, 2H), 7.13 (d, J = 8.4 Hz, 2H), 7.01 (d, J = 16.5 Hz, 1H), 6.89 (t, J = 7.3 Hz, 1H), 6.68 (d, J = 16.5 Hz, 1H), 2.08 (s, 3H) ppm.

^{13}C NMR (125 MHz, CDCl_3) δ = 148.6, 146.0, 141.6, 133.2, 129.5, 129.4, 129.1, 127.9, 127.5, 113.5, 113.3, 16.0 ppm.

MS (EI) m/z (%): 270 (100), 193 (5), 178 (17), 159 (52), 101 (23).

HRMS (EI) m/z calculated for $\text{C}_{16}\text{H}_{15}\text{N}_2\text{Cl}$ 270.092373, found 270.092045.

(E)-1-((E)-4-(4-Bromophenyl)but-3-en-2-ylidene)-2-phenylhydrazine (249c)

Method A.

The reaction was conducted on a 2.00 mmol scale.

Purification: Filtration and crystallization from MeOH.

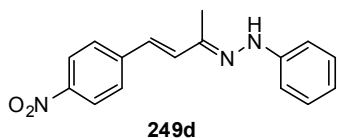
Yield: Yellow solid 325 mg (1.03 mmol, 52%).

$^1\text{H NMR}$ (500 MHz, CD_2Cl_2) δ = 7.49 (br, 1H), 7.48 (d, J = 8.6 Hz, 2H), 7.38 (d, J = 8.5 Hz, 2H), 7.27 (dd, J = 8.3, 7.5 Hz, 2H), 7.13 (d, J = 7.7 Hz, 2H), 7.02 (d, J = 16.5 Hz, 1H), 6.87 (t, J = 7.3 Hz, 1H), 6.70 (d, J = 16.5 Hz, 1H), 2.07 (s, 3H) ppm.

$^{13}\text{C NMR}$ (125 MHz, CD_2Cl_2) δ = 145.0, 143.0, 136.7, 132.1, 131.1, 129.6, 128.3, 127.9, 121.4, 120.7, 113.4, 10.2 ppm.

MS (EI) m/z (%): 316/314 (100/98), 224/222 (11/11), 181/183 (13/13), 159 (86), 143 (27), 128 (25), 102 (85), 91 (78), 77 (48), 65 (42).

HRMS (EI) m/z calculated for $\text{C}_{16}\text{H}_{15}\text{N}_2\text{Br}$ 314.041872, found 314.041949.

(E)-1-((E)-4-(4-Nitrophenyl)but-3-en-2-ylidene)-2-phenylhydrazine (249d)

Method A.

The reaction was conducted on a 2.00 mmol scale.

Purification: Filtration.

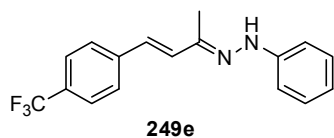
Yield: Red solid 213 mg (0.756 mmol, 38%).

$^1\text{H NMR}$ (500 MHz, CD_2Cl_2) δ = 8.18 (d, J = 8.5 Hz, 2H), 7.63-7.61 (m, 3H), 7.31-7.26 (m, 2H), 7.19 (d, J = 16.4 Hz, 1H), 7.16 (d, J = 8.3 Hz, 2H), 6.91 (t, J = 7.3 Hz, 1H), 6.79 (d, J = 16.4 Hz, 1H), 2.10 (s, 3H) ppm.

$^{13}\text{C NMR}$ (125 MHz, CD_2Cl_2) δ = 146.9, 144.6, 144.4, 142.3, 134.8, 129.7, 127.1, 126.5, 124.4, 121.1, 113.5, 10.2 ppm.

MS (EI) m/z (%): 281 (100), 234 (6), 189 (4), 159 (31), 143 (12), 128 (5), 92 (34), 77 (31), 65 (19).

HRMS (ESI+) m/z calculated for $\text{C}_{16}\text{H}_{15}\text{N}_3\text{O}_2\text{Na}$ ($\text{M}+\text{Na}^+$) 304.105645, found 304.105576.

(E)-1-Phenyl-2-((E)-4-(4-(trifluoromethyl)phenyl)but-3-en-2-ylidene)hydrazine (249e)

Method A.

The reaction was conducted on a 1.50 mmol scale.

Purification: Filtration.

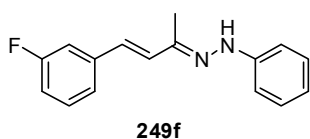
Yield: Yellow solid 289 mg (0.950 mmol, 63%).

¹H NMR (500 MHz, CDCl₃) δ = 7.59 (d, *J* = 8.4 Hz, 2H), 7.56 (d, *J* = 8.4 Hz, 2H), 7.48 (br, 1H), 7.31 (dd, *J* = 8.1, 7.7 Hz, 2H), 7.16 (d, *J* = 7.8 Hz, 2H), 7.12 (d, *J* = 16.5 Hz, 1H), 6.92 (t, *J* = 7.3 Hz, 1H), 6.73 (d, *J* = 16.5 Hz, 1H), 2.09 (s, 3H) ppm.

¹³C NMR (125 MHz, CDCl₃) δ = 144.4, 142.6, 140.8, 132.4, 129.5, 129.3 (q, *J* = 31.4 Hz), 127.6, 126.7, 125.8 (q, *J* = 3.8 Hz), 124.4 (q, *J* = 271.8 Hz), 120.9, 113.4, 10.2 ppm.

MS (EI) *m/z* (%): 304 (100), 212 (21), 171 (12), 159 (31), 151 (16), 92 (25), 77 (26).

HRMS (EI) *m/z* calculated for C₁₇H₁₄N₂F₃ 303.111459, found 303.111230.

(E)-1-((E)-4-(3-Fluorophenyl)but-3-en-2-ylidene)-2-phenylhydrazine (249f)

Method A.

The reaction was conducted on a 2.00 mmol scale.

Purification: Filtration and recrystallization from MeOH.

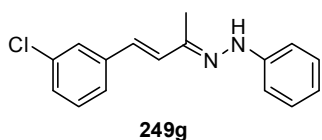
Yield: Yellow solid 190 mg (0.748 mmol, 37%).

¹H NMR (500 MHz, CD₂Cl₂) δ = 7.50 (br, 1H), 7.35-7.29 (m, 1H), 7.29-7.26 (m, 3H), 7.21 (d, *J* = 10.4 Hz, 1H), 7.14 (d, *J* = 7.8 Hz, 2H), 7.03 (d, *J* = 16.5 Hz, 1H), 6.95 (ddd, *J* = 8.1, 8.1, 1.5 Hz, 1H), 6.88 (t, *J* = 7.3 Hz, 1H), 6.73 (d, *J* = 16.5 Hz, 1H), 2.08 (s, 3H) ppm.

¹³C NMR (125 MHz, CD₂Cl₂) δ = 163.6 (d, *J* = 244.2), 145.0, 142.9, 140.1 (d, *J* = 7.6), 131.7, 130.5 (d, *J* = 8.3), 129.6, 128.0 (d, *J* = 2.3), 122.8 (d, *J* = 2.6), 120.7, 114.5 (d, *J* = 21.4), 113.4, 113.0 (d, *J* = 22.0), 10.2 ppm.

MS (EI) *m/z* (%): 254 (100), 159 (45), 146 (26), 109 (13), 101 (36), 91 (32), 77 (34), 65 (31).

HRMS (EI) *m/z* calculated for C₁₆H₁₅N₂F 254.121928, found 254.121805.

(E)-1-((E)-4-(3-Chlorophenyl)but-3-en-2-ylidene)-2-phenylhydrazine (249g)

Method A.

The reaction was conducted on a 3.00 mmol scale.

Purification: Crystallization from CH₂Cl₂:hexane.

Yield: Yellow needles 498 mg (1.83 mmol, 61%).

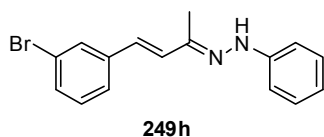
$^1\text{H NMR}$ (500 MHz, CDCl_3) δ = 7.59 (br, 1H), 7.57 (s, 1H), 7.45 (d, J = 7.7 Hz, 1H), 7.41- 7.36 (m, 3H), 7.32 (d, J = 8.3 Hz, 1H), 7.25 (d, J = 8.1 Hz, 2H), 7.16 (d, J = 16.5 Hz, 1H), 7.01 (t, J = 7.3 Hz, 1H), 6.77 (d, J = 16.5 Hz, 1H), 2.19 (s, 3H) ppm.

$^{13}\text{C NMR}$ (125 MHz, CDCl_3) δ = 148.6, 144.4, 139.1, 134.8, 131.2, 130.0, 129.5, 129.1, 127.7, 126.6, 124.8, 120.8, 113.4, 10.3 ppm.

MS (EI) m/z (%): 270 (100), 178 (19), 159 (59), 137 (13), 91 (29), 77 (27), 65 (18) ppm.

HRMS (ESI+) m/z calculated for $\text{C}_{16}\text{H}_{15}\text{N}_2\text{ClNa}$ ($\text{M}+\text{Na}^+$) 293.081597, found 293.081757.

(*E*)-1-((*E*)-4-(3-Bromophenyl)but-3-en-2-ylidene)-2-phenylhydrazine (249h)



Method A.

The reaction was conducted on a 2.00 mmol scale.

Purification: Crystallization from $\text{MeOH}:\text{H}_2\text{O}$.

Yield: Yellow solid 260 mg (0.825 mmol, 41%).

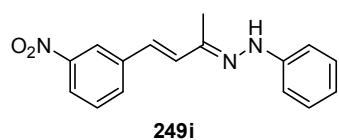
$^1\text{H NMR}$ (500 MHz, CD_2Cl_2) δ = 7.66 (s, 1H), 7.51 (s, 1H), 7.43 (d, J = 7.7 Hz, 1H), 7.37 (dd, J = 8.0, 0.7 Hz, 1H), 7.28 (dd, J = 8.3, 7.5 Hz, 2H), 7.23 (dd, J = 7.9, 7.8 Hz, 1H), 7.14 (d, J = 7.7 Hz, 2H), 7.03 (d, J = 16.5 Hz, 1H), 6.88 (t, J = 7.3 Hz, 1H), 6.69 (d, J = 16.5 Hz, 1H), 2.07 (s, 3H) ppm.

$^{13}\text{C NMR}$ (125 MHz, CD_2Cl_2) δ = 145.0, 142.8, 140.0, 131.8, 130.6, 130.6, 129.6, 129.5, 127.5, 125.5, 123.1, 120.7, 113.4, 10.2 ppm.

MS (EI) m/z (%): 314/316 (100/98), 222/224 (12/11), 181/183 (8/8), 159 (89), 143 (27), 128 (21), 102 (73), 91 (47), 77 (48), 65 (38).

HRMS (ESI+) m/z calculated for $\text{C}_{16}\text{H}_{16}\text{N}_2\text{Br}$ ($\text{M}+\text{H}^+$) 315.049150, found 315.048646.

(*E*)-1-((*E*)-4-(3-Nitrophenyl)but-3-en-2-ylidene)-2-phenylhydrazine (249i)



Method A.

The reaction was conducted on a 2.00 mmol scale.

Purification: Crystallization from MeOH .

Yield: Red solid 159 mg (0.564 mmol, 28%).

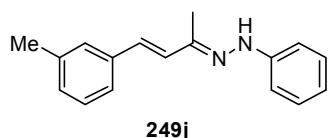
$^1\text{H NMR}$ (500 MHz, CD_2Cl_2) δ = 8.32 (s, 1H), 8.06 (dd, J = 8.2, 1.4 Hz, 1H), 7.81 (d, J = 7.8 Hz, 1H), 7.57 (br, 1H), 7.52 (dd, J = 8.0, 8.0 Hz, 1H), 7.29 (dd, J = 8.2, 7.6 Hz, 2H), 7.17-7.14 (m, 3H), 6.90 (t, J = 7.3 Hz, 1H), 6.80 (d, J = 16.5 Hz, 1H), 2.10 (s, 3H) ppm.

^{13}C NMR (125 MHz, CD_2Cl_2) δ = 149.1, 144.8, 142.3, 139.5, 133.2, 132.4, 130.0, 129.6, 126.5, 122.1, 121.2, 120.9, 113.5, 10.2 ppm.

MS (EI) m/z (%): 281 (100), 234 (26), 159 (32), 148 (9), 128 (9), 92 (31), 77 (45), 65 (33).

HRMS (EI) m/z calculated for $\text{C}_{16}\text{H}_{16}\text{N}_3\text{O}_2$ 282.123699, found 282.123668.

(E)-1-Phenyl-2-((E)-4-(m-tolyl)but-3-en-2-ylidene)hydrazine (249j)



Method A.

The reaction was conducted on a 2.00 mmol scale.

Purification: Crystallization from MeOH.

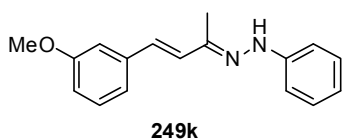
Yield: Orange solid 193 mg (0.770 mmol, 39%).

^1H NMR (500 MHz, CDCl_3) δ = 7.55 (br, 1H), 7.31-7.23 (m, 5H), 7.13 (d, J = 7.7 Hz, 2H), 7.10-7.07 (m, 2H), 6.88 (t, J = 7.3 Hz, 1H), 6.74 (d, J = 16.4 Hz, 1H), 2.37 (s, 3H), 2.12 (s, 3H) ppm.

^{13}C NMR (125 MHz, CDCl_3) δ = 148.7, 144.3, 143.3, 138.9, 138.5, 129.4, 129.2, 128.8, 127.7, 124.3, 123.1, 120.9, 113.6, 21.6, 10.8 ppm.

MS (EI) m/z (%): 250 (100), 159 (56), 91 (55), 77 (27).

(E)-1-((E)-4-(3-Methoxyphenyl)but-3-en-2-ylidene)-2-phenylhydrazine (249k)



Method A.

The reaction was conducted on a 2.00 mmol scale.

Purification: Filtration and recrystallization from MeOH.

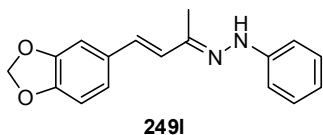
Yield: Yellow solid 128 mg (0.480 mmol, 24%).

^1H NMR (500 MHz, CD_2Cl_2) δ = 7.47 (s, 1H), 7.29-7.25 (m, 3H), 7.13 (d, J = 7.8 Hz, 2H), 7.08 (d, J = 7.6 Hz, 1H), 7.04-7.01 (m, 2H), 6.87 (t, J = 7.3 Hz, 1H), 6.81 (dd, J = 8.1, 1.9 Hz, 1H), 6.75 (d, J = 16.5 Hz, 1H), 3.83 (s, 3H), 2.08 (s, 3H) ppm.

^{13}C NMR (125 MHz, CD_2Cl_2) δ = 160.4, 145.1, 143.4, 139.0, 130.5, 130.0, 129.6, 129.4, 120.6, 119.6, 113.9, 113.4, 111.6, 55.6, 10.3 ppm.

MS (EI) m/z (%): 266 (84), 174 (49), 159 (100), 131 (19), 118 (19), 102 (11), 91 (50), 77 (44), 65 (36).

HRMS (ESI+) m/z calculated for $\text{C}_{17}\text{H}_{18}\text{N}_2\text{O}_2\text{Na}$ ($\text{M}+\text{Na}^+$) 289.131129, found 289.130877.

(E)-1-((E)-4-(Benzo[d][1,3]dioxol-5-yl)but-3-en-2-ylidene)-2-phenylhydrazine (249l)

Method A.

The reaction was conducted on a 3.00 mmol scale.

Purification: Crystallization from CH₂Cl₂:hexane.

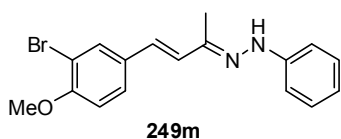
Yield: Orange solid 569 mg (2.03 mmol, 68%).

¹H NMR (500 MHz, CDCl₃) δ = 7.40 (br, 1H), 7.28 (dd, *J* = 8.4, 7.5 Hz, 2H), 7.13 (d, *J* = 7.6 Hz, 2H), 7.04 (d, *J* = 1.5 Hz, 1H), 6.92-6.86 (m, 3H), 6.79 (d, *J* = 8.1 Hz, 1H), 6.67 (d, *J* = 16.4 Hz, 1H), 5.97 (s, 2H), 2.07 (s, 3H) ppm.

¹³C NMR (125 MHz, CDCl₃) δ = 148.4, 147.6, 144.7, 131.8, 129.4, 129.0, 128.2, 128.2, 121.8, 120.5, 113.3, 108.6, 105.8, 101.3, 10.4 ppm.

MS (EI) *m/z* (%): 280 (100), 188 (21), 159 (40), 147 (9), 132 (9), 115 (8), 91 (43).

HRMS (ESI+) *m/z* calculated for C₁₇H₁₆N₂O₂Na (M+Na⁺) 303.110397, found 303.110000.

(E)-1-((E)-4-(3-Bromo-4-methoxyphenyl)but-3-en-2-ylidene)-2-phenylhydrazine (249m)

Method A.

The reaction was conducted on a 2.00 mmol scale.

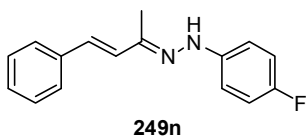
Purification: Crystallization from CH₂Cl₂:hexane.

Yield: Yellow needles 558 mg (1.62 mmol, 81%).

¹H NMR (500 MHz, CD₂Cl₂) δ = 7.71 (d, *J* = 2.1 Hz, 1H), 7.46 (br, 1H), 7.42 (dd, *J* = 8.5, 2.0 Hz, 1H), 7.27 (dd, *J* = 8.6, 7.3 Hz, 2H), 7.12 (dd, *J* = 8.5, 0.5 Hz, 2H), 6.92 (d, *J* = 1.9 Hz, 1H), 6.89 (d, *J* = 9.9 Hz, 1H), 6.86 (t, *J* = 7.3 Hz, 1H), 6.66 (d, *J* = 16.5 Hz, 1H), 3.90 (s, 3H), 2.06 (s, 3H) ppm.

¹³C NMR (125 MHz, CD₂Cl₂) δ = 155.8, 145.2, 143.4, 131.8, 131.4, 129.6, 129.5, 127.6, 127.1, 120.5, 113.3, 112.4, 112.2, 56.6, 10.3 ppm.

HRMS (ESI+) *m/z* calculated for C₁₇H₁₇N₂OBrNa (M+Na⁺) 367.041657, found 367.041774.

(E)-1-(4-Fluorophenyl)-2-((E)-4-phenylbut-3-en-2-ylidene)hydrazine (249n)

Method B.

The reaction was conducted on a 2.50 mmol scale.

Purification: Recrystallization from MeOH.

Yield: Yellow solid 327 mg (0.515 mmol, 21%).

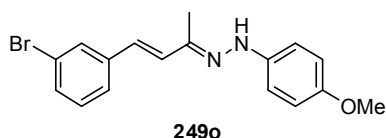
^1H NMR (500 MHz, CD_2Cl_2) δ = 7.50 (d, J = 7.6 Hz, 2H), 7.40 (br, 1H), 7.36 (dd, J = 7.7, 7.5 Hz, 2H), 7.26 (t, J = 7.4 Hz, 1H), 7.12-7.09 (m, 2H), 7.03-6.98 (m, 3H), 6.78 (d, J = 16.5 Hz, 1H), 2.07 (s, 3H) ppm.

^{13}C NMR (125 MHz, CD_2Cl_2) δ = 157.7 (d, J = 237.3 Hz), 143.8, 141.7 (d, J = 1.8 Hz), 137.5, 130.1, 129.6, 129.1, 128.0, 126.8, 116.0 (d, J = 22.4 Hz), 114.4 (d, J = 7.3 Hz), 10.3 ppm.

MS (EI) m/z (%): 254 (100), 177 (38), 144 (24), 128 (7), 109 (35), 103 (42), 77 (28).

HRMS (EI) m/z calculated for $\text{C}_{16}\text{H}_{15}\text{N}_2\text{F}$ 254.121927, found 254.121675.

(E)-1-((E)-4-(3-Bromophenyl)but-3-en-2-ylidene)-2-(4-methoxyphenyl)hydrazine (249o)



Method B.

The reaction was conducted on a 1.00 mmol scale.

Purification: Recrystallization from MeOH.

Yield: Yellow needles 179 mg (0.518 mmol, 52%).

^1H NMR (500 MHz, CD_2Cl_2) δ = 7.65 (s, 1H), 7.42 (d, J = 7.7 Hz, 1H), 7.37 (br, 1H), 7.36 (d, J = 7.9 Hz, 1H), 7.22 (dd, J = 7.9, 7.9 Hz, 1H), 7.08 (d, J = 9.0 Hz, 2H), 7.01 (d, J = 16.5 Hz, 1H), 6.85 (d, J = 9.0 Hz, 2H), 6.65 (d, J = 16.5 Hz, 1H), 3.77 (s, 3H), 2.05 (s, 3H) ppm.

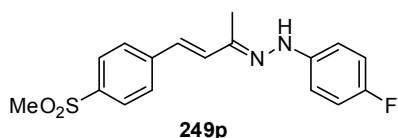
^{13}C NMR (125 MHz, CD_2Cl_2) δ = 151.9, 144.0, 140.0, 139.0, 131.7, 130.6, 130.5, 129.5, 127.2, 125.4, 123.1, 115.0, 114.6, 55.9, 10.2 ppm.

MS (EI) m/z (%): 344/346 (45/45), 189 (10), 122 (100), 102 (16).

HRMS (ESI+) m/z calculated for $\text{C}_{17}\text{H}_{17}\text{N}_2\text{OBrNa}$ ($\text{M}+\text{Na}^+$) 367.041657, found 367.041894.

(E)-1-(4-Fluorophenyl)-2-((E)-4-(4-(methylsulfonyl)phenyl)but-3-en-2-ylidene)hydrazine

(249p)



Method B.

The reaction was conducted on a 1.00 mmol scale.

Purification: Recrystallization from MeOH.

Yield: Yellow solid 179 mg (0.514 mmol, 51%).

^1H NMR (500 MHz, CD_2Cl_2) δ = 7.87 (d, J = 8.4 Hz, 2H), 7.66 (d, J = 8.4 Hz, 2H), 7.57 (br, 1H), 7.15 (d, J = 16.4 Hz, 1H), 7.14-7.10 (m, 2H), 7.03-6.98 (m, 2H), 6.78 (d, J = 16.4 Hz, 1H), 3.04 (s, 3H), 2.08 (s, 3H) ppm.

^{13}C NMR (125 MHz, CD_2Cl_2) δ = 157.9 (d, J = 237.6 Hz), 143.0, 142.6, 141.3 (d, J = 1.9 Hz), 139.2, 133.9, 128.1, 127.3, 127.0, 116.1 (d, J = 22.9 Hz), 114.5 (d, J = 7.5 Hz), 44.8, 10.3 ppm.

MS (EI) m/z (%): 332 (100), 252 (8), 177 (33), 143 (16), 119 (12), 110 (41), 95 (13), 83 (15).

HRMS (ESI+) m/z calculated for $\text{C}_{17}\text{H}_{17}\text{N}_2\text{O}_2\text{FSNa}$ ($\text{M}+\text{Na}^+$) 355.088700, found 355.088502.

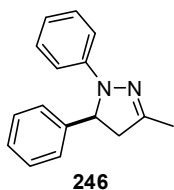
7.5.3 Synthesis of 2-Pyrazolines

General procedure for the electrocyclization of α,β -unsaturated hydrazones (Method A):

The corresponding hydrazone **249** (0.100 mmol) and catalyst (*S*)-**33f** (7.00 mg, 0.010 mmol) were placed in a reaction vial under Ar and dissolved in dry chlorobenzene (1.0 mL). The mixture was stirred at 30 °C until the starting material was completely consumed (monitored by TLC). After cooling to ambient temperature the mixture was directly submitted to flash chromatography on silica gel to obtain the pure 2-pyrazolines.

General procedure for the reaction of α,β -unsaturated ketones and phenylhydrazine (Method B):

The corresponding enone (0.105 mmol in the case of aromatic enones; 0.110 mmol in the case of aliphatic enones) and 4Å molecular sieves (30 mg) were placed in a reaction vial under argon and suspended in 0.5 mL of a stock solution of phenylhydrazine (**100a**, 0.10 mmol, 0.2 M in chlorobenzene). After stirring for 4 h at 50 °C, the cold mixture was filtered into a reaction vial containing catalyst (*S*)-**33f** (7.00 mg, 0.010 mmol). The solid was washed with additional 0.5 mL of chlorobenzene into the reaction vial and the resulting mixture was stirred at 30 °C until complete conversion (monitored by TLC). After cooling to ambient temperature the mixture was directly submitted to flash chromatography on silica gel to obtain the pure 2-pyrazolines.

(S)-3-Methyl-1,5-diphenyl-4,5-dihydro-1H-pyrazole (246)

Method A.

Purification: CC on SiO₂ (hexane:EtOAc 9:1).

Yield: Colorless solid 21.7 mg (0.092 mmol, 92%).

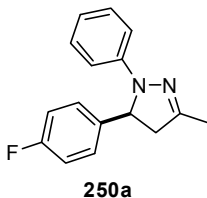
¹H NMR (500 MHz, CDCl₃) δ = 7.35-7.30 (m, 4H), 7.27 (m, 1H), 7.14 (dd, *J* = 7.9, 7.3 Hz, 2H), 6.92 (d, *J* = 7.9 Hz, 2H), 6.74 (t, *J* = 7.3 Hz, 1H), 5.01 (dd, *J* = 11.9, 8.1 Hz, 1H), 3.42 (dd, *J* = 17.5, 11.9 Hz, 1H), 2.73 (dd, *J* = 17.5, 8.1 Hz, 1H), 2.07 (s, 3H) ppm.

¹³C NMR (100 MHz, CDCl₃) δ = 148.7, 146.2, 143.1, 129.2, 129.0, 127.5, 126.0, 118.8, 113.2, 64.9, 48.0, 16.1 ppm.

MS (EI) *m/z* (%): 236 (100), 159 (67).

HRMS (EI) *m/z* calculated for C₁₆H₁₆N₂ 236.131348, found 236.131539.

The enantiomeric ratio was determined by HPLC analysis using Daicel Chiralcel OD-H column: *n*-heptane:*i*-PrOH = 90:10, flow rate 0.5 mL/min, λ = 254 nm: τ₁ = 10.68 min, τ₂ = 13.68 min.

(S)-5-(4-Fluorophenyl)-3-methyl-1-phenyl-4,5-dihydro-1H-pyrazole (250a)

Method A.

Purification: CC on SiO₂ (hexane:EtOAc 9:1).

Yield: Colorless solid 23.8 mg (0.094 mmol, 94%).

¹H NMR (500 MHz, CDCl₃) δ = 7.27 (m, 2H), 7.15 (m, 2H), 7.02 (m, 2H), 6.90 (d, *J* = 8.3 Hz, 2H), 6.75 (t, *J* = 7.3 Hz, 1H), 5.00 (dd, *J* = 11.9, 8.0 Hz, 1H), 3.40 (dd, *J* = 17.5, 11.9 Hz, 1H), 2.68 (dd, *J* = 17.5, 8.0 Hz, 1H), 2.07 (s, 3H) ppm.

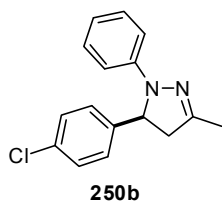
¹³C NMR (125 MHz, CDCl₃) δ = 162.2 (d, *J* = 245.7 Hz), 148.6, 146.1, 138.8 (d, *J* = 2.9 Hz), 129.0, 127.7 (d, *J* = 8.1 Hz), 119.0, 116.0 (d, *J* = 21.8 Hz), 113.3, 64.3, 48.0, 16.0 ppm.

MS (EI) *m/z* (%): 254 (100), 159 (46).

HRMS (EI) *m/z* calculated for C₁₆H₁₅N₂F 254.121923 found 254.122174.

The enantiomeric ratio was determined by HPLC analysis using Daicel Chiralcel OD-H column: *n*-heptane:*i*-PrOH = 90:10, flow rate 0.5 mL/min, λ = 254 nm: τ₁ = 10.43 min, τ₂ = 12.29 min.

[α]_D²⁵ = -445.2° (c = 1.00, CH₂Cl₂, er = 94.5:5.5).

(S)-5-(4-Chlorophenyl)-3-methyl-1-phenyl-4,5-dihydro-1H-pyrazole (250b)

Method A.

Purification: CC on SiO₂ (hexane:EtOAc 6:1).

Yield: Colorless solid 26.0 mg (0.096 mmol, 96%).

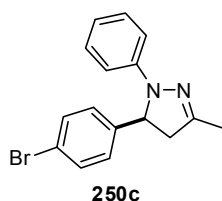
¹H NMR (500 MHz, CDCl₃) δ = 7.30 (d, *J* = 8.5 Hz, 2H), 7.24 (d, *J* = 8.5 Hz, 2H), 7.15 (dd, *J* = 8.5, 7.3 Hz, 2H), 6.89 (m, 2H), 6.76 (t, *J* = 7.3 Hz, 1H), 4.99 (dd, *J* = 11.9, 8.0 Hz, 1H), 3.41 (dd, *J* = 17.3, 11.9 Hz, 1H), 2.68 (dd, *J* = 17.3, 8.0 Hz, 1H), 2.07 (s, 3H) ppm.

¹³C NMR (125 MHz, CDCl₃) δ = 148.6, 146.0, 141.6, 133.2, 129.4, 129.0, 127.5, 119.0, 113.3, 64.3, 47.9, 16.0 ppm.

MS (EI) *m/z* (%): 272/270 (34/99), 159 (66), 91 (100).

HRMS (EI) *m/z* calculated for C₁₆H₁₅N₂Cl 270.092375, found 270.092047.

The enantiomeric ratio was determined by HPLC analysis using Daicel Chiralcel OD-H column: *n*-heptane:*i*-PrOH = 90:10, flow rate 0.5 mL/min, λ = 254 nm: τ₁ = 12.28 min, τ₂ = 16.29 min.

(S)-5-(4-Bromophenyl)-3-methyl-1-phenyl-4,5-dihydro-1H-pyrazole (250c)

Method A.

Purification: CC on SiO₂ (hexane:EtOAc 6:1).

Yield: Yellow solid 30.0 mg (0.095 mmol, 95%).

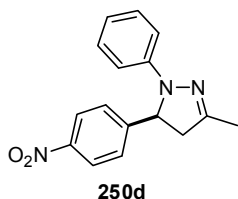
¹H NMR (500 MHz, CD₂Cl₂) δ = 7.47 (d, *J* = 8.4 Hz, 2H), 7.19 (d, *J* = 8.4 Hz, 2H), 7.11 (dd, *J* = 8.1, 7.3 Hz, 2H), 6.86 (d, *J* = 8.1 Hz, 2H), 6.72 (t, *J* = 7.3 Hz, 1H), 4.99 (dd, *J* = 12.0, 7.9 Hz, 1H), 3.43 (dd, *J* = 17.4, 12.0 Hz, 1H), 2.67 (dd, *J* = 17.4, 7.9 Hz, 1H), 2.05 (s, 3H) ppm.

¹³C NMR (125 MHz, CD₂Cl₂) δ = 149.0, 146.3, 142.7, 132.4, 129.2, 128.2, 121.3, 118.9, 113.3, 64.4, 47.9, 15.9 ppm.

MS (EI) *m/z* (%): 316/314 (69/74), 159 (68), 91 (100).

HRMS (EI) *m/z* calculated for C₁₆H₁₅N₂Br 314.041875, found 314.041608.

The enantiomeric ratio was determined by HPLC analysis using Daicel Chiralcel OD-H column: *n*-heptane:*i*-PrOH = 90:10, flow rate 0.5 mL/min, λ = 254 nm: τ₁ = 10.83 min, τ₂ = 13.31 min.

(S)-3-Methyl-5-(4-nitrophenyl)-1-phenyl-4,5-dihydro-1H-pyrazole (250d)

Method A.

Purification: CC on SiO₂ (hexane:EtOAc 6:1).

Yield: Orange solid 26.1 mg (0.093 mmol, 93%).

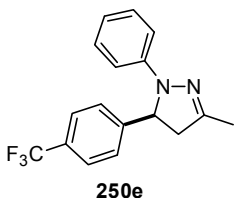
¹H NMR (500 MHz, CDCl₃) δ = 8.20 (d, *J* = 8.7 Hz, 2H), 7.49 (d, *J* = 8.7 Hz, 2H), 7.16 (dd, *J* = 7.9, 7.3 Hz, 2H), 6.86 (d, *J* = 7.9 Hz, 2H), 6.78 (t, *J* = 7.3 Hz, 1H), 5.11 (dd, *J* = 12.1, 8.1 Hz, 1H), 3.48 (dd, *J* = 17.5, 12.1 Hz, 1H), 2.70 (dd, *J* = 17.5, 8.1 Hz, 1H), 2.09 (s, 3H) ppm.

¹³C NMR (125 MHz, CDCl₃) δ = 150.5, 148.6, 147.5, 145.7, 129.2, 127.1, 124.6, 119.5, 113.3, 64.3, 47.6, 15.9 ppm.

MS (EI) *m/z* (%): 281 (100), 159 (55).

HRMS (EI) *m/z* calculated for C₁₆H₁₅N₃O₂ 281.116424, found 281.116172.

The enantiomeric ratio was determined by HPLC analysis using Daicel Chiralcel OD-H column: *n*-heptane:*i*-PrOH = 90:10, flow rate 0.5 mL/min, λ = 254 nm: τ₁ = 20.42 min, τ₂ = 28.63 min.

(S)-3-Methyl-1-phenyl-5-(4-(trifluoromethyl)phenyl)-4,5-dihydro-1H-pyrazole (250e)

Method A.

Purification: CC on SiO₂ (hexane:EtOAc 6:1).

Yield: Colorless solid 26.9 mg (0.088 mmol, 88%).

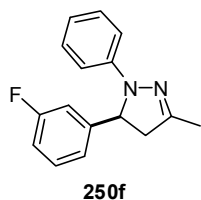
¹H NMR (500 MHz, CDCl₃) δ = 7.60 (d, *J* = 8.1 Hz, 2H), 7.43 (d, *J* = 8.1 Hz, 2H), 7.16 (dd, *J* = 8.4, 7.3 Hz, 2H), 6.89 (d, *J* = 8.4 Hz, 2H), 6.77 (t, *J* = 7.3 Hz, 1H), 5.07 (dd, *J* = 12.0, 8.0 Hz, 1H), 3.45 (dd, *J* = 17.5, 12.0 Hz, 1H), 2.70 (dd, *J* = 17.5, 8.0 Hz, 1H), 2.08 (s, 3H) ppm.

¹³C NMR (125 MHz, CDCl₃) δ = 148.6, 147.1, 145.9, 129.9 (q, *J* = 32.1 Hz), 129.1, 126.5, 126.2 (q, *J* = 3.8 Hz), 124.2 (q, *J* = 270.6 Hz), 119.2, 113.2, 64.5, 47.7, 16.0 ppm.

MS (EI) *m/z* (%): 304 (100), 159 (64).

HRMS (ESI+) *m/z* calculated for C₁₇H₁₆N₂F₃ (M+H⁺) 305.126011, found 305.126003.

The enantiomeric ratio was determined by HPLC analysis using Daicel Chiralcel OD-H column: *n*-heptane:*i*-PrOH = 90:10, flow rate 0.5 mL/min, λ = 254 nm: τ₁ = 9.62 min, τ₂ = 13.18 min.

(S)-5-(3-Fluorophenyl)-3-methyl-1-phenyl-4,5-dihydro-1H-pyrazole (250f)

Method A.

Purification: CC on SiO₂ (hexane:EtOAc 9:1).

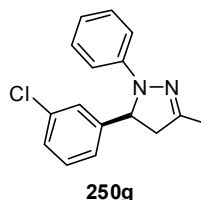
Yield: Yellow solid 23.1 mg (0.091 mmol, 91%).

¹H NMR (500 MHz, CD₂Cl₂) δ = 7.35-7.31 (m, 1H), 7.14-7.10 (m, 3H), 7.03-7.01 (m, 1H), 6.99-6.95 (m, 1H), 6.88 (d, *J* = 8.4 Hz, 2H), 6.73 (t, *J* = 7.3 Hz, 1H), 5.01 (dd, *J* = 11.9, 7.8 Hz, 1H), 3.44 (dd, *J* = 17.6, 11.9 Hz, 1H), 2.70 (dd, *J* = 17.6, 7.8 Hz, 1H), 2.05 (s, 3H) ppm.

¹³C NMR (125 MHz, CD₂Cl₂) δ = 163.7 (d, *J* = 245.8 Hz), 149.0, 146.4 (d, *J* = 6.6 Hz), 146.3, 131.0 (d, *J* = 8.2 Hz), 129.2, 122.0 (d, *J* = 2.7 Hz), 118.9, 114.5 (d, *J* = 21.2 Hz), 113.3, 113.1 (d, *J* = 22.4 Hz), 64.5 (d, *J* = 1.4 Hz), 47.9, 15.9 ppm.

MS (EI) *m/z* (%): 254 (100), 159 (66).HRMS (EI) *m/z* calculated for C₁₆H₁₅N₂F 254.121928, found 254.121714.

The enantiomeric ratio was determined by HPLC analysis using Daicel Chiralcel OD-H column: *n*-heptane:*i*-PrOH = 90:10, flow rate 0.5 mL/min, λ = 254 nm: τ₁ = 10.34 min, τ₂ = 13.83 min.

(S)-5-(3-Chlorophenyl)-3-methyl-1-phenyl-4,5-dihydro-1H-pyrazole (250g)

Method A.

Purification: CC on SiO₂ (hexane:EtOAc 9:1).

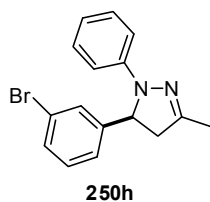
Yield: Colorless solid 25.9 mg (0.096 mmol, 96%).

¹H NMR (500 MHz, CDCl₃) δ = 7.30 (br s, 1H), 7.24-7.21 (m, 2H), 7.18-7.16 (m, 1H), 7.14 (dd, *J* = 8.6, 7.3 Hz, 2H), 6.88 (d, *J* = 8.6 Hz, 2H), 6.75 (t, *J* = 7.3 Hz, 1H), 4.94 (dd, *J* = 12.0, 8.1 Hz, 1H), 3.39 (dd, *J* = 17.6, 12.0 Hz, 1H), 2.68 (dd, *J* = 17.6, 8.1 Hz, 1H), 2.05 (s, 3H) ppm.

¹³C NMR (125 MHz, CDCl₃) δ = 148.6, 146.0, 145.4, 135.1, 130.5, 129.1, 127.8, 126.2, 124.2, 119.1, 133.3, 64.5, 47.8, 16.0 ppm.

MS (EI) *m/z* (%): 272/270 (30/92), 159 (100).HRMS (EI) *m/z* calculated for C₁₆H₁₅N₂Cl 270.092376, found 270.092155.

The enantiomeric ratio was determined by HPLC analysis using Daicel Chiralcel OD-H column: *n*-heptane:*i*-PrOH = 90:10, flow rate 0.5 mL/min, λ = 254 nm: τ₁ = 12.31 min, τ₂ = 17.96 min.

(S)-5-(3-Bromophenyl)-3-methyl-1-phenyl-4,5-dihydro-1H-pyrazole (250h)

Method A.

Purification: CC on SiO₂ (hexane:EtOAc 9:1).

Yield: Yellow solid 30.0 mg (0.095 mmol, 95%).

¹H NMR (500 MHz, CD₂Cl₂) δ = 7.48 (br s, 1H), 7.42-7.40 (m, 1H), 7.26-7.21 (m, 2H), 7.13 (dd, J = 8.2, 7.3 Hz, 2H), 6.88 (d, J = 8.2 Hz, 2H), 6.73 (t, J = 7.3 Hz, 1H), 4.98 (dd, J = 12.0, 7.9 Hz, 1H), 3.43 (dd, J = 17.6, 12.0 Hz, 1H), 2.69 (dd, J = 17.6, 7.9 Hz, 1H), 2.05 (s, 3H) ppm.

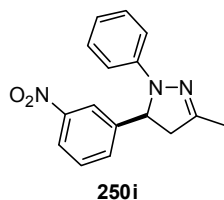
¹³C NMR (125 MHz, CD₂Cl₂) δ = 149.0, 146.3, 146.1, 131.0, 130.8, 129.3, 129.2, 125.1, 123.3, 119.0, 113.3, 64.5, 48.0, 15.9 ppm.

MS (EI) m/z (%): 316/314 (56/58), 159 (100).

HRMS (ESI+) calculated for C₁₆H₁₅N₂BrNa (M+Na⁺) 337.031089, found 337.031150.

The enantiomeric ratio was determined by HPLC analysis using Daicel Chiralcel OD-H column: *n*-heptane:*i*-PrOH = 90:10, flow rate 0.5 mL/min, λ = 254 nm: τ_1 = 10.90 min, τ_2 = 14.52 min.

$[\alpha]_D^{25}$ = -350.2° (c = 1.00, CH₂Cl₂, er = 96:4).

(S)-3-Methyl-5-(3-nitrophenyl)-1-phenyl-4,5-dihydro-1H-pyrazole (250i)

Method A.

Purification: CC on SiO₂ (hexane:EtOAc 4:1).

Yield: Orange oil 28.0 mg (0.099 mmol, 99%).

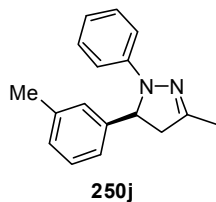
¹H NMR (500 MHz, CDCl₃) δ = 8.20 (dd, J = 1.7, 1.7 Hz, 1H), 8.13 (dd, J = 8.1, 1.7 Hz, 1H), 7.65 (d, J = 7.7 Hz, 1H), 7.51 (dd, J = 8.1, 7.7 Hz, 1H), 7.16 (dd, J = 7.9, 7.3 Hz, 2H), 6.88 (d, J = 7.9 Hz, 2H), 6.78 (t, J = 7.3 Hz, 1H), 5.12 (dd, J = 12.0, 8.0 Hz, 1H), 3.49 (dd, J = 17.5, 12.0, 1H), 2.72 (dd, J = 17.5, 8.0, 1H), 2.09 (s, 3H) ppm.

¹³C NMR (125 MHz, CDCl₃) δ = 149.0, 148.6, 145.7, 145.4, 132.3, 130.4, 129.2, 122.8, 121.3, 119.5, 113.3, 64.3, 47.8, 16.0 ppm.

MS (EI) m/z (%): 281 (100), 159 (67).

HRMS (EI) m/z calculated for C₁₆H₁₅N₃O₂ 281.116430, found 281.116163.

The enantiomeric ratio was determined by HPLC analysis using Daicel Chiralcel OD-H column: *n*-heptane:*i*-PrOH = 90:10, flow rate 0.5 mL/min, λ = 254 nm: τ_1 = 27.20 min, τ_2 = 31.92 min.

(S)-3-Methyl-1-phenyl-5-(m-tolyl)-4,5-dihydro-1H-pyrazole (250j)

Method A.

Purification: CC on SiO₂ (hexane:EtOAc 6:1).

Yield: Yellow oil 21.1 mg (0.084 mmol, 84%).

¹H NMR (500 MHz, CDCl₃) δ = 7.24 (dd, *J* = 7.6, 7.6 Hz, 1H), 7.17-7.11 (m, 4H), 7.08 (d, *J* = 7.5 Hz, 1H), 6.94 (dd, *J* = 8.5, 0.7 Hz, 2H), 6.75 (t, *J* = 7.3 Hz,

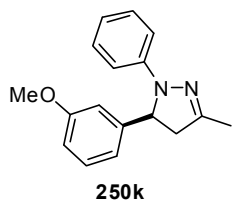
1H), 4.96 (dd, *J* = 11.9, 8.3 Hz, 1H), 3.40 (ddd, *J* = 17.5, 12.0, 1.0 Hz, 1H), 2.72 (ddd, *J* = 17.6, 8.2 Hz, 1H), 2.34 (s, 3H), 2.08 (s, 3H) ppm.

¹³C NMR (125 MHz, CDCl₃) δ = 148.7, 146.4, 143.2, 138.9, 129.0, 129.0, 128.3, 126.6, 123.1, 118.7, 113.2, 65.0, 48.0, 21.6, 16.1 ppm.

MS (EI) *m/z* (%): 250 (100), 159 (63), 117 (9), 91 (69), 77 (18).

HRMS (EI) *m/z* calculated for C₁₇H₁₈N₂ 250.146996, found 250.146813.

The enantiomeric ratio was determined by HPLC analysis using Daicel Chiralcel OD-H column: *n*-heptane:*i*-PrOH = 90:10, flow rate 0.5 mL/min, λ = 254 nm: τ₁ = 9.10 min, τ₂ = 10.76 min.

(S)-5-(3-Methoxyphenyl)-3-methyl-1-phenyl-4,5-dihydro-1H-pyrazole (250k)

Method A.

Purification: CC on SiO₂ (hexane:EtOAc 6:1).

Yield: Yellow oil 24.6 mg (0.092 mmol, 92%).

¹H NMR (400 MHz, CDCl₃) δ = 7.25 (dd, *J* = 7.9, 7.8 Hz, 1H), 7.17-7.12 (m, 2H), 6.95-6.94 (m, 1H), 6.93-6.92 (m, 1H), 6.92-6.90 (m, 1H), 6.87-6.86 (m,

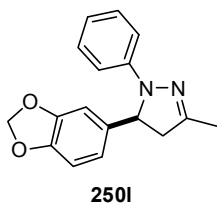
1H), 6.80 (ddd, *J* = 8.2, 2.6, 1.0 Hz, 1H), 6.75 (tt, *J* = 7.3, 1.1 Hz, 1H), 4.96 (dd, *J* = 11.9, 8.3 Hz, 1H), 3.77 (s, 3H), 3.40 (ddq, *J* = 17.5, 12.0, 1.2 Hz, 1H), 2.72 (ddq, *J* = 17.6, 8.3, 1.2 Hz, 1H), 2.07 (dd, *J* = 1.2, 1.1 Hz, 3H) ppm.

¹³C NMR (100 MHz, CDCl₃) δ = 160.3, 148.7, 146.3, 145.0, 130.2, 129.0, 118.8, 118.3, 113.3, 112.9, 111.5, 65.1, 55.4, 48.0, 16.0 ppm.

MS (EI) *m/z* (%): 266 (100), 159 (65), 91 (53), 77 (14).

HRMS (EI) *m/z* calculated for C₁₇H₁₈N₂O 266.141913, found 266.141913.

The enantiomeric ratio was determined by HPLC analysis using Daicel Chiralcel OD-H column: *n*-heptane:*i*-PrOH = 90:10, flow rate 0.5 mL/min, λ = 254 nm: τ₁ = 12.21 min, τ₂ = 15.68 min.

(S)-5-(Benzo[d][1,3]dioxol-5-yl)-3-methyl-1-phenyl-4,5-dihydro-1H-pyrazole (250l)

Method A.

Purification: CC on SiO₂ (hexane:EtOAc 6:1).

Yield: Colorless solid 23.9 mg (0.085 mmol, 85%).

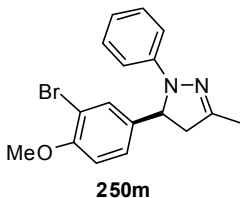
¹H NMR (500 MHz, CDCl₃) δ = 7.15 (dd, *J* = 8.5, 7.4 Hz, 2H), 6.94 (d, *J* = 8.5 Hz, 2H), 6.79-6.73 (m, 4H), 5.94-5.92 (m, 2H), 4.92 (dd, *J* = 11.9, 8.1 Hz, 1H), 3.67 (dd, *J* = 17.5, 11.9 Hz, 1H), 2.69 (dd, *J* = 17.5, 8.1 Hz, 1H), 2.06 (s, 3H) ppm.

¹³C NMR (125 MHz, CDCl₃) δ = 148.6, 148.4, 147.0, 146.1, 137.2, 129.0, 119.2, 118.8, 113.2, 108.7, 106.4, 101.2, 64.7, 48.0, 16.1 ppm

MS (EI) *m/z* (%): 280 (100), 159 (38).

HRMS (EI) *m/z* calculated for C₁₇H₁₆N₂O₂ 280.121178, found 280.120995.

The enantiomeric ratio was determined by HPLC analysis using Daicel Chiralcel OD-H column: *n*-heptane:*i*-PrOH = 95:05, flow rate 0.5 mL/min, λ = 254 nm: τ₁ = 21.34 min, τ₂ = 22.84 min.

(S)-5-(3-Bromo-4-methoxyphenyl)-3-methyl-1-phenyl-4,5-dihydro-1H-pyrazole (250m)

Method A.

Purification: CC on SiO₂ (hexane:EtOAc 6:1).

Yield: Colorless solid 32.0 mg (0.093 mmol, 93%).

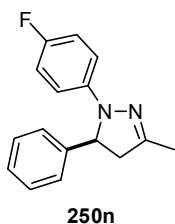
¹H NMR (500 MHz, CD₂Cl₂) δ = 7.49 (d, *J* = 1.6 Hz, 1H), 7.21 (dd, *J* = 8.5, 1.6 Hz, 1H), 7.13 (dd, *J* = 7.8, 7.9 Hz, 2H), 6.88 (m, 3H), 6.72 (t, *J* = 7.3 Hz, 1H), 4.94 (dd, *J* = 11.8, 7.9 Hz, 1H), 3.86 (s, 3H), 3.40 (dd, *J* = 17.5, 11.9 Hz, 1H), 2.67 (dd, *J* = 17.5, 7.9 Hz, 1H), 2.05 (s, 3H) ppm.

¹³C NMR (125 MHz, CD₂Cl₂) δ = 157.5, 151.1, 148.4, 139.2, 133.1, 131.1, 128.5, 120.9, 115.3, 114.7, 114.3, 66.0, 58.6, 50.1, 18.0 ppm.

MS (EI) *m/z* (%): 346/344 (88/86), 159 (59), 91 (100).

HRMS (ESI+) *m/z* calculated for C₁₇H₁₇N₂OBrNa (M+Na⁺) 367.041653, found 367.041661.

The enantiomeric ratio was determined by HPLC analysis using Daicel Chiralcel OD-H column: *n*-heptane:*i*-PrOH = 90:10, flow rate 0.5 mL/min, λ = 254 nm: τ₁ = 14.10 min, τ₂ = 15.29 min.

(S)-1-(4-Fluorophenyl)-3-methyl-5-phenyl-4,5-dihydro-1H-pyrazole (250n)

Method A.

Purification: CC on SiO₂ (hexane:EtOAc 6:1).

Yield: Colorless solid 23.0 mg (0.090 mmol, 90%).

¹H NMR (500 MHz, CD₂Cl₂) δ = 7.36-7.33 (m, 2H), 7.31-7.30 (m, 2H), 7.26 (tt, *J* = 7.1, 1.7 Hz, 1H), 6.86-6.81 (m, 4H), 4.94 (dd, *J* = 11.8, 8.5 Hz, 1H), 3.42 (ddd,

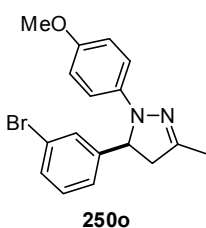
J = 17.5, 11.8, 1.0 Hz, 1H), 2.71 (ddd, *J* = 17.6, 8.5, 1.1 Hz, 1H), 2.04 (s, 3H) ppm.

¹³C NMR (125 MHz, CD₂Cl₂) δ = 156.7 (d, *J* = 235.4), 149.3, 143.4 (d, *J* = 2.1), 143.3, 129.3, 127.8, 126.4, 115.4 (d, *J* = 22.2), 114.4 (d, *J* = 7.4), 65.7, 48.3, 15.9 ppm.

MS (EI) *m/z* (%): 254 (100), 177 (54), 109 (80), 95 (13).

HRMS (EI) *m/z* calculated for C₁₆H₁₅N₂F 254.121926, found 254.121896.

The enantiomeric ratio was determined by HPLC analysis using Daicel Chiralcel OD-H column: *n*-heptane:*i*-PrOH = 90:10, flow rate 0.5 mL/min, λ = 254 nm: τ₁ = 9.95 min, τ₂ = 12.25 min.

(S)-5-(3-Bromophenyl)-1-(4-methoxyphenyl)-3-methyl-4,5-dihydro-1H-pyrazole (250o)

Method A.

Purification: CC on SiO₂ (hexane:EtOAc 6:1).

Yield: Colorless solid 31.4 mg (0.091 mmol, 91%).

¹H NMR (500 MHz, CD₂Cl₂) δ = 7.50 (br s, 1H), 7.41 (d, *J* = 7.7 Hz, 1H), 7.28 (d, *J* = 7.6 Hz, 1H), 7.23 (dd, *J* = 7.7, 7.5 Hz, 1H), 6.83 (d, *J* = 8.3 Hz, 2H), 6.71

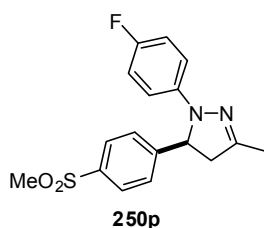
(d, *J* = 9.0, 2H), 4.85 (br s, 1H), 3.69 (s, 3H), 3.37 (m, 1H), 2.68 (dd, *J* = 17.2, 9.1 Hz, 1H), 2.03 (s, 3H) ppm.

¹³C NMR (125 MHz, CD₂Cl₂) δ = 153.6, 148.8, 146.3, 141.2, 131.0, 130.8, 129.6, 125.3, 123.3, 115.0, 114.6, 65.9, 55.8, 48.2, 15.9 ppm.

MS (EI) *m/z* (%): 346/344 (94/96), 331/329 (23/23), 189 (60).

HRMS (ESI+) *m/z* calculated for C₁₇H₁₇N₂OBrNa (M+Na⁺) 367.041654, found 367.041570.

The enantiomeric ratio was determined by HPLC analysis using Daicel Chiralcel OD-H column: *n*-heptane:*i*-PrOH = 90:10, flow rate 0.5 mL/min, λ = 254 nm: τ₁ = 13.13 min, τ₂ = 16.70 min.

(S)-1-(4-Fluorophenyl)-3-methyl-5-(4-(methylsulfonyl)phenyl)-4,5-dihydro-1H-pyrazole**(250p)**

Method A.

Purification: CC on SiO₂ (hexane:EtOAc 1:1).

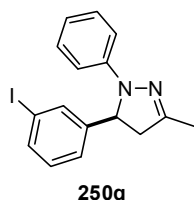
Yield: Yellow solid 29.3 mg (0.088 mmol, 88%).

¹H NMR (500 MHz, CD₂Cl₂) δ = 7.89 (d, *J* = 8.0 Hz, 2H), 7.52 (d, *J* = 8.0 Hz, 2H), 6.87-6.80 (m, 4H), 5.03 (dd, *J* = 11.8, 8.7 Hz, 1H), 3.47 (dd, *J* =17.5, 11.8, 8.5 Hz, 1H), 3.03 (s, 3H), 2.70 (dd, *J* = 17.5, 8.5 Hz, 1H), 2.05 (s, 3H) ppm.¹³C NMR (125 MHz, CDCl₃) δ = 157.0 (d, *J* = 236.6 Hz), 149.5, 149.4, 143.1, 140.3, 128.5, 127.5, 115.6 (d, *J* = 22.4 Hz), 114.6 (d, *J* = 7.4 Hz), 65.3, 48.1, 44.7, 15.8 ppm.**MS** (EI) *m/z* (%): 332 (100), 177 (49).**HRMS** (ESI+) *m/z* calculated for C₁₇H₁₇N₂O₂FSNa (M+Na⁺) 355.088698, found 355.088461.The enantiomeric ratio was determined by HPLC analysis using Daicel Chiralcel OD-3 column: *n*-heptane:*i*-PrOH = 70:30, flow rate 0.5 mL/min, λ = 254 nm: τ₁ = 15.67 min, τ₂ = 16.69 min.**(S)-5-(3-Iodophenyl)-3-methyl-1-phenyl-4,5-dihydro-1H-pyrazole (250q)**

Method B.

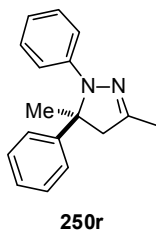
Purification: CC on SiO₂ (hexane:EtOAc 9:1).

Yield: Yellow solid 32.3 mg (0.089 mmol, 89%).

¹H NMR (500 MHz, CDCl₃) δ = 7.68 (s, 1H), 7.60 (d, *J* = 7.8 Hz, 1H), 7.27 (d, *J* = 7.8 Hz, 1H), 7.16 (dd, *J* = 8.1, 7.6 Hz, 2H), 7.06 (dd, *J* = 7.8, 7.8 Hz, 1H), 6.90 (d, *J* = 8.1 Hz, 2H), 6.77 (t, *J* = 7.3 Hz, 1H), 4.92 (dd, *J* = 11.9, 8.2 Hz, 1H), 3.41(dd, *J* = 17.6, 11.9 Hz, 1H), 2.70 (dd, *J* = 17.6, 8.2 Hz, 1H), 2.07 (s, 3H) ppm.¹³C NMR (125 MHz, CDCl₃) δ = 148.6, 146.1, 145.7, 136.7, 135.0, 131.0, 129.1, 125.3, 119.1, 113.3, 95.1, 64.4, 47.9, 16.0 ppm.**MS** (EI) *m/z* (%): 362 (100), 159 (68).**HRMS** (ESI+) *m/z* calculated for C₁₆H₁₅N₂INa (M+Na⁺) 385.017217, found 385.017255.The enantiomeric ratio was determined by HPLC analysis using Daicel Chiralcel OD-H column: *n*-heptane:*i*-PrOH = 90:10, flow rate 0.5 mL/min, λ = 254 nm: τ₁ = 11.23 min, τ₂ = 14.39 min.

(S)-3,5-Dimethyl-1,5-diphenyl-4,5-dihydro-1H-pyrazole (250r)

Method B.

Purification: CC on SiO₂ (hexane:EtOAc 9:1).

Yield: Yellow oil 22.1 mg (0.088 mmol, 88%).

¹H NMR (400 MHz, CDCl₃) δ = 7.48-7.45 (m, 2H), 7.37-7.33 (m, 2H), 7.25 (tt, J = 7.4, 1.3 Hz, 1H), 7.07-7.02 (m, 2H), 6.83 (dd, J = 8.8, 1.0 Hz, 2H), 6.70 (tt, J = 7.3, 1.0 Hz, 1H), 3.01 (d, J = 17.3 Hz, 1H), 2.94 (d, J = 17.3 Hz, 1H), 2.06 (s, 3H), 1.65

(s, 3H) ppm.

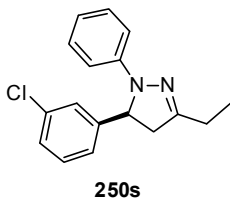
¹³C NMR (100 MHz, CDCl₃) δ = 147.0, 146.4, 144.6, 129.0, 128.6, 127.1, 125.8, 118.9, 115.1, 69.5, 57.8, 21.8, 16.2 ppm.

MS (EI) m/z (%): 250 (76), 235 (100), 173 (28), 91 (37), 77 (16).**HRMS** (EI) m/z calculated for C₁₇H₁₈N₂ 250.146999, found 250.146778.

The enantiomeric ratio was determined by HPLC analysis using Daicel Chiralcel OD-H column: *n*-heptane:*i*-PrOH = 90:10, flow rate 0.5 mL/min, λ = 254 nm: τ_1 = 9.34 min, τ_2 = 10.94 min.

(S)-5-(3-Chlorophenyl)-3-ethyl-1-phenyl-4,5-dihydro-1H-pyrazole (250s)

Method B.

Purification: CC on SiO₂ (hexane:EtOAc 9:1).

Yield: Colorless oil 19.0 mg (0.067 mmol, 67%).

¹H NMR (500 MHz, CD₂Cl₂) δ = 7.32 (br, 1H), 7.29-7.24 (m, 2H), 7.20 (d, J = 7.4 Hz, 1H), 7.14 (d, J = 8.5 Hz, 1H), 7.12 (d, J = 7.4 Hz, 1H), 6.89 (d, J =

7.9 Hz, 2H), 6.73 (t, J = 7.3 Hz, 1H), 4.98 (dd, J = 12.0, 7.9 Hz, 1H), 3.44 (dd, J = 17.5, 12.0 Hz, 1H), 2.69 (dd, J = 17.5, 7.9 Hz, 1H), 2.40 (q, J = 7.5 Hz, 2H), 1.20 (t, J = 7.5 Hz, 3H) ppm.

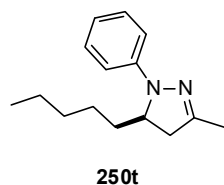
¹³C NMR (125 MHz, CD₂Cl₂) δ = 153.7, 146.4, 145.9, 135.1, 130.8, 129.2, 127.9, 126.4, 124.6, 119.0, 113.4, 64.3, 46.2, 23.9, 11.2 ppm.

MS (EI) m/z (%): 284/286 (100/33), 173 (90), 91 (89), 77 (34).**HRMS** (ESI+) m/z calculated for C₁₇H₁₇N₂ClNa (M+Na⁺) 307.097245, found 307.097230.

The enantiomeric ratio was determined by HPLC analysis using Daicel Chiralcel OD-H column: *n*-heptane:*i*-PrOH = 90:10, flow rate 0.5 mL/min, λ = 254 nm: τ_1 = 9.01 min, τ_2 = 11.77 min.

(R)-3-Methyl-5-pentyl-1-phenyl-4,5-dihydro-1H-pyrazole (250t)

Method B.

Purification: CC on deactivated SiO₂ (hexane:EtOAc 30:1).

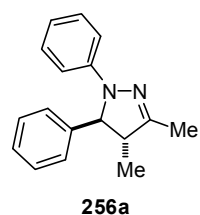
Yield: Colorless oil 9.1 mg (0.040 mmol, 40%).

¹H NMR (500 MHz, CD₂Cl₂) δ = 7.20 (dd, *J* = 7.7, 7.6 Hz, 2H), 6.96 (d, *J* = 8.3 Hz, 2H), 6.73 (t, *J* = 7.2 Hz, 1H), 4.10-4.06 (m, 1H), 3.03 (dd, *J* = 17.3, 11.0 Hz, 1H), 2.54 (dd, *J* = 17.3, 5.6 Hz, 1H), 2.02 (s, 3H), 1.81-1.74 (m, 1H), 1.47-1.40 (m, 1H), 1.31 (br m, 6H), 0.89 (t, *J* = 6.1 Hz, 3H) ppm.

¹³C NMR (125 MHz, CD₂Cl₂) δ = 149.8, 146.2, 129.3, 118.2, 113.1, 60.3, 42.9, 33.1, 32.1, 25.2, 23.0, 16.1, 14.1 ppm.

MS (EI) *m/z* (%): 230 (23), 159 (100).HRMS (ESI+) *m/z* calculated for C₁₅H₂₂N₂Na (M+Na⁺) 253.167519, found 253.167351.

The enantiomeric ratio was determined by HPLC analysis using Daicel Chiralcel OD-H column: *n*-heptane:*i*-PrOH = 95:5, flow rate 0.5 mL/min, λ = 254 nm: τ₁ = 10.69 min, τ₂ = 12.82 min.

7.5.4 Derivatizations of 2-Pyrazolines**(4R,5S)-3,4-Dimethyl-1,5-diphenyl-4,5-dihydro-1H-pyrazole (256a)**

A solution of (*S*)-**246** (100 mg, 0.423 mmol, er = 88:12) in THF (1.0 mL) was added dropwise to a solution of LDA [freshly prepared from *n*-BuLi (300 μL, 0.750 mmol, 2.5 M in hexanes) and diisopropylamine (100 μL, 0.712 mmol) in THF (4.0 mL)] at -78 °C. The resulting red solution was stirred at -78 °C for 1 h before MeI (40 μL, 0.635 mmol) was added. After stirring at -78 °C for 3 h, the mixture was quenched by addition of brine (2 mL) and extracted with CH₂Cl₂ (3 × 20 mL). The combined organic layers were dried over MgSO₄ and, after evaporation of the solvent, the residue was purified by column chromatography on silica gel (hexane:EtOAc 50:1) to give the product **256a** (67.7 mg, 0.270 mmol, 64%) as a colorless solid.

¹H NMR (500 MHz, CD₂Cl₂) δ = 7.39-7.34 (m, 4H), 7.31-7.28 (m, 1H), 7.13-7.09 (m, 2H), 6.91 (dd, *J* = 8.7, 0.9 Hz, 2H), 6.72 (t, *J* = 7.3 Hz, 1H), 4.43 (d, *J* = 8.9 Hz, 1H), 2.91 (m, 1H), 2.03 (d, *J* = 1.0 Hz, 3H), 1.32 (d, *J* = 7.2 Hz, 3H) ppm.

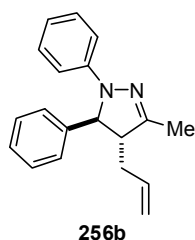
^{13}C NMR (125 MHz, CD_2Cl_2) δ = 153.0, 146.9, 143.1, 129.4, 129.0, 127.8, 126.2, 119.0, 113.7, 73.3, 55.2, 16.6, 13.9 ppm.

MS (EI) m/z (%): 250 (100), 235 (13), 173 (53).

HRMS (ESI+) m/z calculated for $\text{C}_{17}\text{H}_{18}\text{N}_2\text{Na}$ ($\text{M}+\text{Na}^+$) 273.136220, found 273.136182.

The enantiomeric ratio was determined by HPLC analysis using a Daicel Chiralcel OD-H column: *n*-heptane:*i*-PrOH, 90:10; flow rate: 0.5 mL/min; λ = 254 nm: τ_1 = 9.31 min, τ_2 = 10.02 min.

4,5-*trans*-4-Allyl-3-methyl-1,5-diphenyl-4,5-dihydro-1H-pyrazole (256b)



Following the procedure described for the synthesis of **256a** with allylbromide as the alkylating agent and starting from *rac*-**246** (100 mg, 0.423 mmol), the title compound **256b** (70.9 mg, 0.258 mmol, 61%) was obtained after column chromatography on silica gel (hexane:EtOAc 50:1) as a colorless solid.

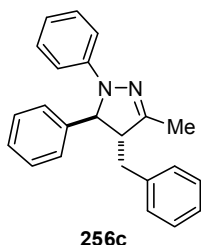
^1H NMR (500 MHz, CD_2Cl_2) δ = 7.36-7.33 (m, 2H), 7.28-7.27 (m, 3H), 7.12 (dd, J = 8.1, 7.2 Hz, 2H), 6.89 (d, J = 8.1 Hz, 2H), 6.70 (t, J = 7.2 Hz, 1H), 5.79-5.74 (m, 1H), 5.25-5.19 (m, 2H), 4.72 (d, J = 6.6 Hz, 1H), 3.02-2.99 (m, 1H), 2.57-2.52 (m, 1H), 2.42-2.36 (m, 1H), 2.06 (s, 3H) ppm.

^{13}C NMR (125 MHz, CD_2Cl_2) δ = 150.5, 145.9, 143.0, 134.9, 129.3, 129.1, 127.7, 126.3, 118.5, 118.4, 113.0, 68.9, 59.7, 35.8, 14.5 ppm.

MS (EI) m/z (%): 276 (40), 235 (100).

HRMS (ESI+) m/z calculated for $\text{C}_{19}\text{H}_{20}\text{N}_2\text{Na}$ ($\text{M}+\text{Na}^+$) 299.151865, found: 299.151789.

4,5-*trans*-4-Benzyl-3-methyl-1,5-diphenyl-4,5-dihydro-1H-pyrazole (256c)



A solution of *rac*-**246** (100 mg, 0.423 mmol) in THF (1.0 mL) was added dropwise to a solution of LDA [freshly prepared from *n*-BuLi (200 μL , 0.50 mmol, 2.5 M in hexanes) and diisopropylamine (72 μL , 0.50 mmol) in THF (1.0 mL)] at -78 $^\circ\text{C}$. The resulting red solution was stirred at -78 $^\circ\text{C}$ for 1 h before a solution of benzylbromide (100 μL , 0.846 mmol) in THF (1.0 mL) was added over a period of 30 min. After stirring at -78 $^\circ\text{C}$ for 8 h, the mixture was quenched by addition of brine (2 mL) and extracted with CH_2Cl_2 (3×20 mL). The combined organic layers were dried over MgSO_4 and, after evaporation of the solvent, the

residue was purified by column chromatography on silica gel (hexane:EtOAc 50:1) to give the product **256c** (83.4 mg, 0.254mmol, 60%) as a yellow oil.

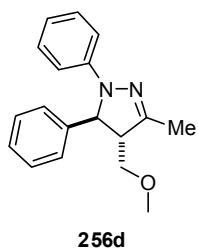
$^1\text{H NMR}$ (500 MHz, CD_2Cl_2) δ = 7.38-7.35 (m, 2H), 7.32-7.29 (m, 1H), 7.23 (d, J = 7.1 Hz, 2H), 7.20-7.17 (m, 3H), 7.13-7.09 (m, 2H), 6.85 (d, J = 8.0 Hz, 2H), 6.82-6.80 (m, 2H), 6.69 (t, J = 7.3 Hz, 1H), 4.75 (d, J = 5.2 Hz, 1H), 3.23-3.19 (m, 2H), 2.74 (dd, J = 14.9, 11.4 Hz, 1H), 2.08 (s, 3H) ppm.

$^{13}\text{C NMR}$ (125 MHz, CD_2Cl_2) δ = 150.5, 145.6, 142.6, 138.6, 129.7, 129.1, 129.1, 129.0, 127.5, 127.1, 126.0, 118.3, 112.7, 68.7, 61.9, 38.2, 14.7 ppm.

MS (EI) m/z (%): 326 (35), 235 (100).

HRMS (ESI+) m/z calculated for $\text{C}_{23}\text{H}_{22}\text{N}_2\text{Na}$ ($\text{M}+\text{Na}^+$) 349.167520, found 349.167337.

4,5-*trans*-4-(Methoxymethyl)-3-methyl-1,5-diphenyl-4,5-dihydro-1H-pyrazole (**256d**)



The procedure for the synthesis of **256c** was followed. After complete addition of the chloromethyl methyl ether solution, the mixture was stirred for 2 h at -78 °C and then worked up as described to give pyrazoline **256d** (71.4 mg, 0.254 mmol, 60%) after column chromatography on silica gel (hexane:EtOAc 20:1) as a colorless solid.

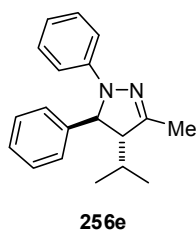
$^1\text{H NMR}$ (500 MHz, CD_2Cl_2) δ = 7.37-7.31 (m, 4H), 7.29-7.26 (m, 1H), 7.11 (dd, J = 8.0, 7.3 Hz, 2H), 6.88 (d, J = 8.0 Hz, 2H), 6.70 (t, J = 7.3 Hz, 1H), 4.82 (d, J = 8.0 Hz, 1H), 3.58 (d, J = 5.1 Hz, 2H), 3.38 (s, 3H), 3.08-3.06 (m, 1H), 2.04 (s, 3H) ppm.

$^{13}\text{C NMR}$ (125 MHz, CD_2Cl_2) δ = 149.1, 146.3, 143.2, 129.3, 129.1, 127.8, 126.3, 118.8, 113.3, 71.3, 67.9, 61.0, 59.3, 14.5 ppm.

MS (EI) m/z (%): 280 (59), 235 (100).

HRMS (ESI+) m/z calculated for $\text{C}_{18}\text{H}_{20}\text{N}_2\text{ONa}$ ($\text{M}+\text{Na}^+$) 303.146778, found 303.146534.

4,5-*trans*-4-Isopropyl-3-methyl-1,5-diphenyl-4,5-dihydro-1H-pyrazole (**256e**)



The procedure for the synthesis of **256c** was followed. After complete addition of the isopropyl iodide solution, the mixture was stirred for 8 h at -78 °C, then warmed up to -35 °C within 12 h and worked up as described to give the product **256e** (51.7 mg, 0.182 mmol, 43%) after column chromatography on silica gel (hexane:EtOAc 50:1) as a pale yellow oil.

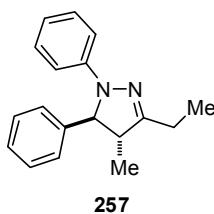
^1H NMR (400 MHz, CD_2Cl_2) δ = 7.35-7.32 (m, 2H), 7.27-7.24 (m, 3H), 7.15-7.10 (m, 2H), 6.90-6.87 (m, 2H), 6.70-6.66 (m, 1H), 4.78 (d, J = 5.2 Hz, 1H), 2.91-2.89 (m, 1H), 2.16-2.10 (m, 1H), 2.06 (d, J = 0.8 Hz, 3H), 1.11 (d, J = 6.9 Hz, 3H), 0.84 (d, J = 6.9 Hz, 3H) ppm.

^{13}C NMR (100 MHz, CD_2Cl_2) δ = 150.3, 145.3, 144.1, 129.3, 129.2, 127.5, 126.2, 118.1, 112.5, 66.8, 64.9, 28.6, 20.3, 17.2, 14.9 ppm.

MS (EI) m/z (%): 278 (47), 235 (100).

HRMS (ESI+) m/z calculated for $\text{C}_{19}\text{H}_{22}\text{N}_2\text{Na}$ ($\text{M}+\text{Na}^+$) 301.167514, found 301.167422.

4,5-*trans*-3-Ethyl-4-methyl-1,5-diphenyl-4,5-dihydro-1H-pyrazole (257)



A solution of pyrazoline *rac*-**246** (100 mg, 0.423 mmol) in THF (1.0 mL) was added dropwise to solution of LDA [freshly prepared from *n*-BuLi (415 μL , 1.04 mmol, 2.5 M in hexanes) and diisopropylamine (143 μL , 1.02 mmol) in THF (4.0 mL)] at -78°C . The resulting red solution was stirred at -78°C for 1 h before MeI (35 μL , 0.55 mmol) was added. After stirring at -78°C for 2 h, a second portion of MeI (35 μL , 0.55 mmol) was added. After stirring for an additional 5 h at -78°C , the mixture was quenched by addition of brine (2 mL) and extracted with CH_2Cl_2 (3 \times 20 mL). The combined organic layers were dried over MgSO_4 and, after evaporation of the solvent, the residue was purified by column chromatography on silica gel (hexane:EtOAc 50:1) to afford pyrazoline **257** (99.4 mg, 0.376 mmol, 89%) as a colorless solid.

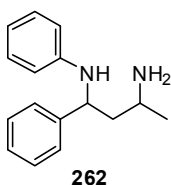
^1H NMR (500 MHz, CD_2Cl_2) δ = 7.37-7.33 (m, 4H), 7.30-7.27 (m, 1H), 7.10 (dd, J = 8.0, 7.3 Hz, 2H), 6.91 (d, J = 8.0 Hz, 2H), 6.71 (t, J = 7.3 Hz, 1H), 4.42 (d, J = 8.7 Hz, 1H), 2.98-2.92 (m, 1H), 2.49-2.40 (m, 1H), 2.34-2.26 (m, 1H), 1.30 (d, J = 7.2 Hz, 3H), 1.21 (t, J = 7.2 Hz, 3H) ppm.

^{13}C NMR (125 MHz, CD_2Cl_2) δ = 157.3, 147.0, 143.1, 129.3, 129.0, 127.8, 126.2, 118.9, 113.7, 73.3, 54.0, 21.8, 16.7, 11.1 ppm.

MS (EI) m/z (%): 264 (100), 249 (17), 187 (45).

HRMS (ESI+) m/z calculated for $\text{C}_{18}\text{H}_{20}\text{N}_2\text{Na}$ ($\text{M}+\text{Na}^+$) 287.151864, found 287.151826.

cis/trans- N^1 ,1-Diphenylbutane-1,3-diamine (262)



A mixture of pyrazoline **246** (200 mg, 0.846 mmol) and Raney-Ni (approx. 3 mL, slurry in H_2O) in MeOH (16 mL) was stirred under an atmosphere of H_2 (balloon) for 24 h. After complete consumption of the starting material

(monitored by TLC) the mixture was filtered over Celite and the solvent was removed under reduced pressure to afford diamine **262** (178 mg, 0.741 mmol, 89%, dr = 1:1) as a colorless oil. The diastereoisomers were not separable by column chromatography.

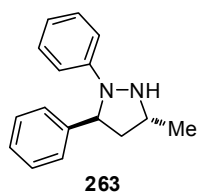
¹H NMR (500 MHz, CDCl₃) δ = 7.42-7.39 (m, 4H), 7.36-7.35 (m, 4H), 7.27-7.25 (m, 2H), 7.13-7.10 (m, 4H), 6.68-6.66 (m, 2H), 6.56-6.55 (m, 4H), 4.57 (dd, J = 7.6, 5.3 Hz, 1H), 4.44 (dd, J = 8.5, 5.6 Hz, 1H), 3.10 (m, 1H), 3.06 (m, 1H), 1.89-1.69 (m, 4H), 1.16 (d, J = 6.0 Hz, 6H) ppm. (exchanging *NH*-protons were not detectable).

¹³C NMR (125 MHz, CDCl₃) δ = 147.9, 147.6, 144.8, 144.3, 129.1, 129.1, 128.7, 128.6, 127.0, 126.9, 126.4, 126.2, 117.1, 117.0, 113.6, 113.3, 58.2, 55.8, 48.4, 47.7, 46.2, 44.1, 26.3, 24.9 ppm.

MS (EI) m/z (%): 240 (25), 222 (41), 208 (19), 196 (9), 182 (100), 147 (60), 132 (14), 104 (30), 93 (26), 77 (36).

HRMS (EI) m/z calculated for C₁₆H₂₀N₂ 240.162647, found 240.162570.

3,5-*trans*-3-Methyl-1,5-diphenylpyrazolidine (**263**)



To a solution of pyrazoline *rac*-**246** (100 mg, 0.423 mmol) in THF (5.0 mL) were added AlMe₃ (1.5 mL, 2.96 mmol, 2 M solution on hexane) and LiAlH₄ (112 mg, 2.96 mmol) at -78 °C. The reaction was allowed to warm to room temperature over night and was quenched at 0 °C by dropwise addition of

H₂O. The mixture was extracted with CH₂Cl₂, the combined organic layers were dried over MgSO₄ and solvent was evaporated. Purification of the residue by column chromatography on silica gel (hexane:EtOAc 30:1) afforded pyrazolidine **263** (89.3 mg, 0.375 mmol, 89%) as a colorless solid.

¹H NMR (500 MHz, CD₂Cl₂) δ = 7.47-7.42 (m, 2H), 7.42-7.38 (m, 2H), 7.30 (tt, J = 7.1, 1.7 Hz, 1H), 7.18 (dd, J = 8.8, 7.3 Hz, 2H), 7.03-6.99 (m, 2H), 6.76 (tt, J = 7.2, 1.1 Hz, 1H), 4.69 (dd, J = 9.6, 7.5 Hz, 1H), 3.82 (br, 1H), 3.25-3.18 (m, 1H), 2.90 (ddd, J = 12.1, 7.4, 4.8 Hz, 1H), 1.66 (ddd, J = 12.1, 11.0, 9.6 Hz, 1H), 1.29 (d, J = 6.2 Hz, 3H) ppm.

¹³C NMR (125 MHz, CD₂Cl₂) δ = 152.9, 145.0, 129.1, 128.9, 127.2, 126.1, 118.5, 113.8, 70.2, 55.2, 50.3, 16.7 ppm.

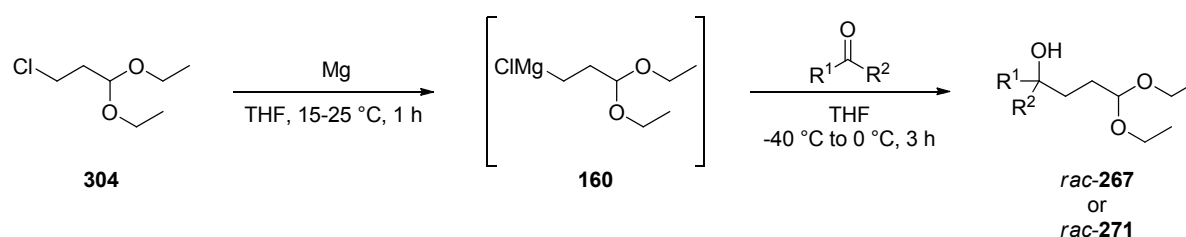
MS (EI) m/z (%): 238 (100), 134 (83), 118 (23), 91 (49).

HRMS (ESI+) m/z calculated for C₁₆H₁₈N₂Na (M+Na⁺) 261.137318, found 261.135891.

7.6 STRIP-Catalyzed Kinetic Resolution of Homoaldols

7.6.1 Synthesis of Racemic Homoaldols

General procedure for the synthesis of homoaldols *rac-268a-i* and *rac-271a-g*:

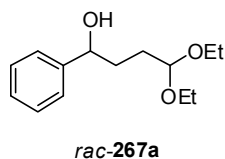


Preparation of the Grignard reagent:

A solution of freshly distilled 3-chloropropionaldehyde diethylacetal (**304**, 8.00 g, 48.0 mmol) in THF (10 mL) was added to activated magnesium turnings (1.46 g, 60.0 mmol). If there was no exothermic reaction at this point, initiation was performed by adding 1,2-dibromoethane and fast short heating to reflux (with a heat gun) before cooling again to 25 °C (repeated until reaction becomes exothermic after cooling). The temperature of the exothermic reaction mixture was kept between 15-25 °C by cooling with an ice bath. Depending on the purity of the starting materials and the activity of the magnesium sometimes a dry ice/acetone bath is necessary for sufficient cooling. After heat development had ceased, the mixture was diluted with THF (15 mL) and the resulting solution was used immediately.

Addition to aldehydes and ketones:

One quarter of the solution of the Grignard reagent prepared above (\approx 8 mL, 12.0 mmol) was added dropwise to a solution of the corresponding aldehyde or ketone (3.00 mmol) in THF (4 mL) at -40 °C. The mixture was stirred at -40 °C for 30 min and then allowed to warm to 0 °C within 2 h. It was then quenched at 0 °C with saturated aqueous NaHCO_3 (5 mL) and H_2O (5 mL), and extracted with Et_2O (3 x 10 mL). The combined organic extracts were dried over Na_2CO_3 , filtered, and concentrated directly prior to purification. Flash chromatography on silica gel yielded pure products. The products were stored as 0.1-0.2 M solutions in EtOAc or Et_2O , or used immediately in the transacetalization reaction.

4,4-Diethoxy-1-phenylbutan-1-ol (*rac*-267a)

Purification: CC on SiO₂ (pentane:Et₂O 2:1).

Yield: Colorless oil 657 mg (2.76 mmol, 92%).

¹H NMR (500 MHz, C₆D₆) δ = 7.29 (d, *J* = 7.3 Hz, 2H), 7.19-7.16 (m, 2H), 7.10-7.07 (m, 1H), 4.51-4.48 (m, 1H), 4.40-4.38 (m, 1H), 3.51-3.44 (m, 2H),

3.32-3.24 (m, 2H), 2.06 (br, 1H), 1.88-1.80 (m, 3H), 1.75-1.71 (m, 1H), 1.69-1.05 (m, 6H) ppm.

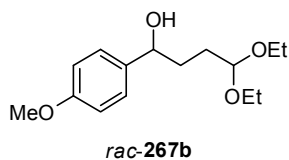
¹³C NMR (125 MHz, C₆D₆) δ = 145.9, 128.5, 127.4, 126.2, 103.1, 74.1, 61.1, 60.9, 34.9, 30.4, 15.5 ppm.

MS (EI) *m/z* (%): 192 (31), 147 (86), 129 (44), 120 (65), 103 (100).

HRMS (ESI+) *m/z* calculated for C₁₄H₂₂O₃Na (M+Na⁺) 261.146115, found 261.145833.

The enantiomeric ratio was determined by HPLC analysis using Daicel Chiralcel OJ-H column: *n*-heptane:*i*-PrOH = 90:10, flow rate 0.5 mL/min, λ = 220 nm: τ₁ = 13.17 min, τ₂ = 14.95 min.

[α]_D²⁵ = -31.2° (c = 0.50, CH₂Cl₂, er = 96.5:3.5).

4,4-Diethoxy-1-(4-methoxyphenyl)butan-1-ol (*rac*-267b)

Purification: CC on SiO₂ (pentane:Et₂O 2:1).

Yield: Colorless oil 764 mg (2.85 mmol, 95%).

¹H NMR (500 MHz, C₆D₆) δ = 7.23 (d, *J* = 8.6 Hz, 2H), 6.80 (d, *J* = 8.6 Hz, 2H), 4.55-4.52 (m, 1H), 4.43 (t, *J* = 5.2 Hz, 1H), 3.51-3.45 (m, 2H),

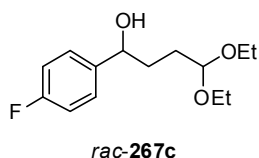
3.34 (s, 3H), 3.33-3.28 (m, 2H), 2.46 (br, 1H), 1.93-1.83 (m, 3H), 1.77-1.72 (m, 1H), 1.09 (m, 6H) ppm.

¹³C NMR (125 MHz, C₆D₆) δ = 159.4, 138.0, 127.4, 114.0, 103.1, 73.8, 61.0, 60.9, 54.8, 35.0, 30.5, 15.6 ppm.

MS (EI) *m/z* (%): 222 (5), 177 (25), 150 (100), 137 (43).

HRMS (ESI+) *m/z* calculated for C₁₅H₂₄O₄Na (M+Na⁺) 291.156679, found 291.156687.

The enantiomeric ratio was determined by HPLC analysis using Daicel Chiralcel OJ-H column: *n*-heptane:*i*-PrOH = 80:20, flow rate 0.5 mL/min, λ = 220 nm: τ₁ = 12.93 min, τ₂ = 14.13 min.

4,4-Diethoxy-1-(4-fluorophenyl)butan-1-ol (*rac*-267c)

Purification: CC on SiO₂ (pentane:Et₂O 2:1).

Yield: Colorless oil 689 mg (2.69 mmol, 90%).

¹H NMR (500 MHz, C₆D₆) δ = 7.07-7.04 (m, 2H), 6.84-6.80 (m, 2H), 4.40-4.36 (m, 2H), 3.51-3.44 (m, 2H), 3.32-3.24 (m, 2H), 2.18 (d, br, *J* = 3.5 Hz, 1H), 1.80-1.65 (m, 4H), 1.10-1.05 (m, 6H) ppm.

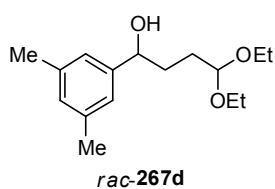
¹³C NMR (125 MHz, C₆D₆) δ = 162.4 (d, *J* = 244.5 Hz), 141.6 (d, *J* = 2.9 Hz), 127.7 (d, *J* = 7.6 Hz), 115.2 (d, *J* = 21.2 Hz), 103.0, 73.4, 61.2, 61.1, 34.9, 30.4, 15.5 ppm.

MS (EI) *m/z* (%): 210 (20), 165 (99), 147 (37), 138 (100), 125 (38), 103 (98), 86 (90), 75 (80), 58 (79), 47 (95).

HRMS (ESI+) *m/z* calculated for C₁₄H₂₁FO₃Na (M+Na⁺) 279.136689, found 279.136498.

The enantiomeric ratio was determined by HPLC analysis using Daicel Chiralcel OJ-H column: *n*-heptane:*i*-PrOH = 95:5, flow rate 0.5 mL/min, λ = 220 nm: τ₁ = 16.99 min, τ₂ = 22.95 min.

[α]_D²⁵ = -28.8° (c = 0.50, CH₂Cl₂, er = 97.5:2.5).

1-(3,5-Dimethylphenyl)-4,4-diethoxybutan-1-ol (*rac*-267d)

Purification: CC on SiO₂ (pentane:Et₂O 2:1).

Yield: Colorless oil 771 mg (2.90 mmol, 97%).

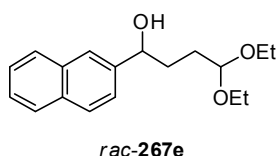
¹H NMR (500 MHz, C₆D₆) δ = 7.00 (s, 2H), 6.76 (s, 1H), 4.54-4.53 (m, 1H), 4.44-4.42 (m, 1H), 3.51-3.47 (m, 2H), 3.33-3.27 (m, 2H), 2.34 (br, 1H), 2.17 (s, 6H), 1.95-1.87 (m, 3H), 1.80-1.78 (m, 1H), 1.10-1.06 (m, 6H) ppm.

¹³C NMR (125 MHz, C₆D₆) δ = 146.0, 137.8, 129.1, 124.1, 103.1, 74.3, 61.0, 60.9, 35.0, 30.6, 21.4, 15.6 ppm.

MS (EI) *m/z* (%): 220 (27), 175 (41), 148 (100), 135 (17), 103 (41).

HRMS (ESI+) *m/z* calculated for C₁₆H₂₆O₃Na (M+Na⁺) 289.177416, found 289.177500.

The enantiomeric ratio was determined by HPLC analysis using Daicel Chiralpak AD-3 column: *n*-heptane:*i*-PrOH = 99:1, flow rate 1.0 mL/min, λ = 220 nm: τ₁ = 17.74 min, τ₂ = 20.90 min.

4,4-Diethoxy-1-(naphthalen-2-yl)butan-1-ol (*rac*-267e)

Purification: CC on SiO₂ (pentane:Et₂O 1:1).

Yield: Colorless oil 817 mg (2.83 mmol, 94%).

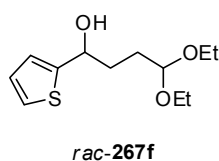
¹H NMR (500 MHz, C₆D₆) δ = 7.74 (s, 1H), 7.68-7.63 (m, 3H), 7.42 (dd, *J* = 8.5, 1.6 Hz, 1H), 7.30-7.25 (m, 2H), 4.67-4.65 (m, 1H), 4.43-4.41 (m, 1H), 3.50-3.45 (m, 2H), 3.31-3.26 (m, 2H), 2.37 (d, *J* = 3.5 Hz, 1H), 1.95-1.87 (m, 3H), 1.80-1.77 (m, 1H), 1.11-1.06 (m, 6H) ppm.

¹³C NMR (125 MHz, C₆D₆) δ = 143.4, 134.0, 133.5, 128.4, 128.3, 128.0, 126.3, 125.8, 124.8, 124.7, 103.1, 74.3, 61.1, 61.0, 34.7, 30.5, 15.6 ppm.

MS (EI) *m/z* (%): 242 (16), 197 (23), 170 (100), 129 (35).

HRMS (ESI+) *m/z* calculated for C₁₈H₂₄O₃Na (M+Na⁺) 311.161768, found 311.161760.

The enantiomeric ratio was determined by HPLC analysis using Daicel Chiralcel OJ-H column: *n*-heptane:*i*-PrOH = 80:20, flow rate 0.5 mL/min, λ = 220 nm: τ₁ = 14.13 min, τ₂ = 18.58 min.

4,4-Diethoxy-1-(thiophen-2-yl)butan-1-ol (*rac*-267f)

Purification: CC on SiO₂ (pentane:Et₂O 2:1).

Yield: Yellowish oil 714 mg (2.93 mmol, 97%).

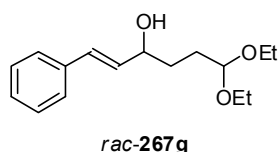
¹H NMR (500 MHz, C₆D₆) δ = 6.87 (dd, *J* = 5.0, 1.2 Hz, 1H), 6.78-6.77 (m, 1H), 6.73 (dd, *J* = 5.0, 3.5 Hz, 1H), 4.77-4.74 (m, 1H), 4.37 (t, *J* = 5.5 Hz, 1H), 3.49-3.43 (m, 2H), 3.30-3.23 (m, 2H), 2.67 (d, *J* = 4.3 Hz, 1H), 1.96-1.90 (m, 2H), 1.86-1.80 (m, 1H), 1.76-1.72 (m, 1H), 1.08-1.05 (m, 6H) ppm.

¹³C NMR (125 MHz, C₆D₆) δ = 150.2, 126.7, 124.2, 123.4, 102.9, 70.2, 61.1, 61.1, 35.1, 30.3, 15.5 ppm.

MS (EI) *m/z* (%): 198 (22), 153 (40), 126 (100).

HRMS (ESI+) *m/z* calculated for C₁₂H₂₁O₃S (M+H⁺) 267.102536, found 267.102704.

The enantiomeric ratio was determined by HPLC analysis using Daicel Chiralcel OJ-H column: *n*-heptane:*i*-PrOH = 90:10, flow rate 0.5 mL/min, λ = 220 nm: τ₁ = 14.34 min, τ₂ = 15.48 min.

(E)-6,6-Diethoxy-1-phenylhex-1-en-3-ol (rac-267g)

Purification: CC on SiO₂ (pentane:Et₂O 2:1).

Yield: Colorless oil 641 mg (2.43 mmol, 81%).

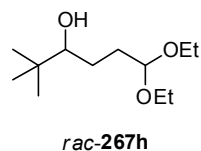
¹H NMR (500 MHz, C₆D₆) δ = 7.25 (d, *J* = 7.3 Hz, 2H), 7.13 (dd, *J* = 7.3, 7.3 Hz, 2H), 7.05 (t, *J* = 7.3 Hz, 1H), 6.54 (d, *J* = 15.9 Hz, 1H), 6.15 (dd, *J* = 15.9, 6.2 Hz, 1H), 4.46 (t, *J* = 5.5 Hz, 1H), 4.15-4.14 (m, 1H), 3.55-3.49 (m, 2H), 3.37-3.30 (m, 2H), 2.11 (d, *J* = 3.0 Hz, 1H), 1.89-1.81 (m, 2H), 1.74-1.70 (m, 2H), 1.12-1.09 (m, 6H) ppm.

¹³C NMR (125 MHz, C₆D₆) δ = 137.5, 133.5, 129.9, 128.8, 127.6, 126.9, 103.1, 72.5, 61.1, 61.0, 32.9, 30.1, 15.6 ppm.

MS (EI) *m/z* (%): 218 (26), 173 (19), 146 (100), 129 (40), 103 (41).

HRMS (ESI+) *m/z* calculated for C₁₆H₂₄O₃Na (M+Na⁺) 287.161765, found 287.161872.

The enantiomeric ratio was determined by HPLC analysis using Daicel Chiralpak AD-3 column: *n*-heptane:*i*-PrOH = 95:5, flow rate 1.0 mL/min, λ = 220 nm: τ₁ = 8.85 min, τ₂ = 9.58 min.

6,6-Diethoxy-2,2-dimethylhexan-3-ol (rac-267h)

Purification: CC on SiO₂ (pentane:Et₂O 2:1).

Yield: Colorless oil 504 mg (2.31 mmol, 77%).

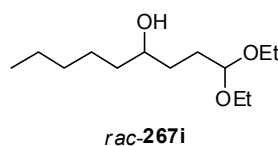
¹H NMR (500 MHz, C₆D₆) δ = 4.46 (t, *J* = 5.5 Hz, 1H), 3.58-3.50 (m, 2H), 3.38-3.32 (m, 2H), 3.11-3.09 (m, 1H), 2.07 (d, *J* = 3.9 Hz, 1H), 1.99-1.92 (m, 1H), 1.77-1.70 (m, 1H), 1.65-1.58 (m, 1H), 1.40-1.32 (m, 1H), 1.11 (t, *J* = 7.1 Hz, 6H), 0.90 (s, 9H) ppm.

¹³C NMR (125 MHz, C₆D₆) δ = 103.4, 79.5, 61.1, 61.0, 35.2, 31.7, 27.0, 26.0, 15.6, 15.6 ppm.

MS (EI) *m/z* (%): 173 (5), 127 (13), 115 (100), 109 (27), 87 (64).

HRMS (ESI+) *m/z* calculated for C₁₂H₂₆O₃Na (M+Na⁺) 241.177415, found 241.177430.

The enantiomeric ratio was determined by GC analysis using BGB-176 column (30 m, 2,3-dimethyl-6-*tert*-butyldimethylsilyl-β-cyclodextrin), Detector: FID; Temperature: injector 220 °C, detector 320 °C, oven 110 °C; gas: 0.5 bar H₂. τ₁ = 17.23 min, τ₂ = 18.80 min.

1,1-Diethoxynonan-4-ol (rac-267i)

Purification: CC on SiO₂ (pentane:Et₂O 2:1).

Yield: Colorless oil 555 mg (2.39 mmol, 80%).

^1H NMR (500 MHz, C_6D_6) δ = 4.47 (t, J = 5.4 Hz, 1H), 3.57-3.51 (m, 2H), 3.50-3.48 (m, 1H), 3.39-3.32 (m, 2H), 2.00 (br, 1H), 1.90-1.84 (m, 1H), 1.79-1.75 (m, 1H), 1.60-1.53 (m, 1H), 1.51-1.10 (m, 9H), 1.14-1.10 (m, 6H), 0.89 (t, J = 7.1 Hz, 3H) ppm.

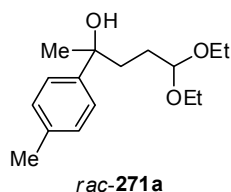
^{13}C NMR (125 MHz, C_6D_6) δ = 103.3, 71.4, 61.1, 60.9, 38.2, 33.0, 32.4, 30.5, 25.9, 23.1, 15.6, 15.6, 14.3 ppm.

MS (EI) m/z (%): 187 (6), 169 (10), 141 (14), 115 (26), 103 (100).

HRMS (ESI+) m/z calculated for $\text{C}_{13}\text{H}_{28}\text{O}_3\text{Na}$ ($\text{M}+\text{Na}^+$) 255.193064, found 255.192881.

The enantiomeric ratio was determined by GC analysis using BGB-176 column (30 m, 2,3-dimethyl-6-*tert*-butyldimethylsilyl- β -cyclodextrin), Detector: FID; Temperature: injector 220 °C, detector 320 °C, oven: 105 °C, 0.25 °C/min until 125 °C; gas: 0.4 bar H_2 . τ_1 = 65.99 min, τ_2 = 66.77 min.

5,5-Diethoxy-2-(*p*-tolyl)pentan-2-ol (*rac*-271a)



Purification: CC on SiO_2 (pentane: Et_2O 2:1).

Yield: Colorless oil 656 mg (2.46 mmol, 82%).

^1H NMR (500 MHz, C_6D_6) δ = 7.37 (d, J = 8.2 Hz, 2H), 7.04 (d, J = 8.0 Hz, 2H), 4.37 (t, J = 5.4 Hz, 1H), 3.48-3.45 (m, 1H), 3.43-3.39 (m, 1H), 3.28-3.23 (m, 2H), 2.30 (s, 1H), 2.15 (s, 3H), 1.96-1.90 (m, 2H), 1.79-1.75 (m, 1H), 1.65-1.62 (m, 1H), 1.43 (s, 3H), 1.09-1.04 (m, 6H) ppm.

^{13}C NMR (125 MHz, C_6D_6) δ = 145.9, 135.7, 129.0, 125.4, 103.3, 73.9, 61.1, 60.7, 39.2, 31.3, 28.8, 21.0, 15.5, 15.5 ppm.

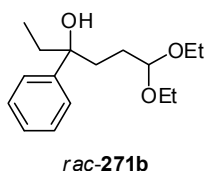
MS (EI) m/z (%): 205 (40), 175 (37), 157 (32), 135 (99), 103 (44), 86 (100).

HRMS (ESI+) m/z calculated for $\text{C}_{16}\text{H}_{26}\text{O}_3\text{Na}$ ($\text{M}+\text{Na}^+$) 289.177412, found 289.177404.

The enantiomeric ratio was determined by HPLC analysis using Daicel Chiralcel OD-3 column: *n*-heptane:*i*-PrOH = 99:1, flow rate 1.0 mL/min, λ = 220 nm: τ_1 = 8.53 min, τ_2 = 9.34 min.

$[\alpha]_{\text{D}}^{25}$ = -9.1° (c = 0.837, CH_2Cl_2 , er = 96:4).

6,6-Diethoxy-3-phenylhexan-3-ol (*rac*-271b)



Purification: CC on SiO_2 (pentane: Et_2O 2:1).

Yield: Colorless oil 773 mg (2.90 mmol, 97%).

^1H NMR (500 MHz, C_6D_6) δ = 7.41 (dd, J = 8.3, 1.0 Hz, 2H), 7.21 (dd, J = 8.3,

7.4 Hz, 2H), 7.08 (t, $J = 7.4$ Hz, 1H), 4.33 (t, $J = 5.3$ Hz, 1H), 3.48-3.42 (m, 1H), 3.40-3.34 (m, 1H), 3.27-3.19 (m, 2H), 2.55 (s br, 1H), 1.96-1.89 (m, 2H), 1.77-1.68 (m, 3H), 1.57-1.51 (m, 1H), 1.07 (t, $J = 7.0$ Hz, 3H), 1.04 (t, $J = 7.0$ Hz, 3H), 0.78 (t, $J = 7.4$ Hz, 3H) ppm.

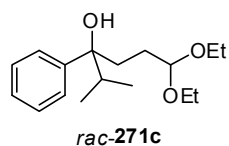
^{13}C NMR (125 MHz, C_6D_6) $\delta = 146.8, 128.26, 126.4, 126.0, 103.3, 76.5, 61.3, 60.7, 37.6, 36.8, 28.3, 15.5, 15.5, 8.1$ ppm.

MS (EI) m/z (%): 237 (3), 203 (3), 191 (100), 175 (13), 157 (15), 145 (9), 135 (20), 117 (26), 130 (27).

HRMS (ESI+) m/z calculated for $\text{C}_{16}\text{H}_{26}\text{O}_3\text{Na}$ ($\text{M}+\text{Na}^+$) 289.177412, found 289.177328.

The enantiomeric ratio was determined by HPLC analysis using Daicel Chiralcel OJ-H column: *n*-heptane:*i*-PrOH = 80:20, flow rate 0.5 mL/min, $\lambda = 220$ nm: $\tau_1 = 7.38$ min, $\tau_2 = 12.83$ min.

6,6-Diethoxy-2-methyl-3-phenylhexan-3-ol (*rac*-271c)



Purification: CC on SiO_2 (pentane: Et_2O 5:1).

Yield: Colorless oil 812 mg (2.89 mmol, 96%).

^1H NMR (500 MHz, C_6D_6) $\delta = 7.42$ (dd, $J = 8.3, 1.0$ Hz, 2H), 7.21 (dd, $J = 8.3, 7.3$ Hz, 2H), 7.08 (t, $J = 7.3$ Hz, 1H), 4.31 (t, $J = 5.3$ Hz, 1H), 3.46-3.40 (m, 1H), 3.37-3.31 (m, 1H), 3.24-3.16 (m, 2H), 2.66 (s br, 1H), 2.04-1.98 (m, 1H), 1.96-1.91 (m, 1H), 1.90-1.86 (m, 1H), 1.67-1.61 (m, 1H), 1.49-1.44 (m, 1H), 1.07-1.01 (m, 6H), 1.00 (d, $J = 6.8$ Hz, 3H), 0.77 (d, $J = 6.8$ Hz, 3H) ppm.

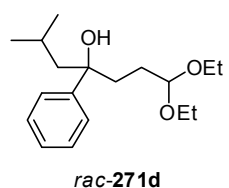
^{13}C NMR (125 MHz, C_6D_6) $\delta = 146.6, 128.1, 126.4, 126.3, 103.3, 78.4, 61.6, 60.7, 39.0, 34.5, 28.6, 17.9, 17.0, 15.5, 15.4$ ppm.

MS (EI) m/z (%): 217 (3), 191 (100), 163 (8), 145 (11), 117 (22), 103 (12).

HRMS (ESI+) m/z calculated for $\text{C}_{17}\text{H}_{28}\text{O}_3\text{Na}$ ($\text{M}+\text{Na}^+$) 303.193065, found 303.192836.

The enantiomeric ratio was determined by HPLC analysis using Daicel Chiralcel OJ-H column: *n*-heptane:*i*-PrOH = 90:10, flow rate 0.5 mL/min, $\lambda = 220$ nm: $\tau_1 = 8.25$ min, $\tau_2 = 10.46$ min.

1,1-Diethoxy-6-methyl-4-phenylheptan-4-ol (*rac*-271d)



Purification: CC on SiO_2 (hexane: EtOAc 9:1).

Yield: Colorless oil 838 mg (2.85 mmol, 95%).

^1H NMR (500 MHz, C_6D_6) $\delta = 7.42$ (dd, $J = 8.4, 1.2$ Hz, 2H), 7.21 (t, $J = 7.7$ Hz, 2H), 7.07 (dt, $J = 7.4, 1.1$ Hz, 1H), 4.32 (t, $J = 5.3$ Hz, 1H), 3.48-3.42 (m,

1H), 3.38-3.32 (m, 1H), 3.26-3.18 (m, 2H), 2.45 (s, 1H), 1.96-1.86 (m, 2H), 1.74-1.67 (m, 3H), 1.63-1.58 (m, 1H), 1.53-1.46 (m, 1H), 1.08 (t, $J = 7.0$ Hz, 3H), 1.04 (t, $J = 7.0$ Hz, 3H), 0.99 (d, $J = 6.5$ Hz, 3H), 0.69 (d, $J = 6.4$ Hz, 3H) ppm.

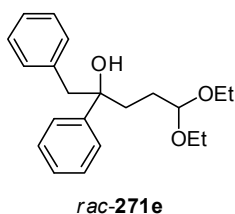
^{13}C NMR (125 MHz, C_6D_6) $\delta = 147.3, 126.3, 126.0, 103.3, 76.9, 61.5, 60.7, 52.9, 39.1, 28.2, 24.8, 24.7, 24.5, 15.47, 15.45$ ppm.

MS (EI) m/z (%): 163 (29), 191 (100), 203 (4), 237 (2).

HRMS (ESI+) m/z calculated for $\text{C}_{18}\text{H}_{30}\text{O}_3\text{Na}$ ($\text{M}+\text{Na}^+$) 317.2087, found 317.2083.

The enantiomeric ratio was determined by HPLC analysis using Daicel Chiralpak AD-3 column: *n*-heptane:*i*-PrOH = 99.5:0.5, flow rate 1.0 mL/min, $\lambda = 210$ nm: $\tau_1 = 14.74$ min, $\tau_2 = 16.58$ min.

5,5-Diethoxy-1,2-diphenylpentan-2-ol (*rac*-271e)



Purification: CC on SiO_2 (pentane: Et_2O 4:1).

Yield: Colorless oil 673 mg (2.05 mmol, 68%).

^1H NMR (500 MHz, C_6D_6) $\delta = 7.31$ (dd, $J = 8.3, 1.1$ Hz, 2H), 7.16-7.13 (m, 2H), 7.07-7.00 (m, 4H), 6.99-6.96 (m, 2H), 4.30 (t, $J = 5.4$ Hz, 1H), 3.45-3.39 (m, 1H), 3.37-3.31 (m, 1H), 3.22-3.16 (m, 2H), 3.03 (d, $J = 13.3$ Hz, 1H), 2.95 (d, $J = 13.3$ Hz, 1H), 2.55 (s, 1H), 2.10-2.04 (m, 1H), 1.97-1.91 (m, 1H), 1.81-1.74 (m, 1H), 1.58-1.51 (m, 1H), 1.06-1.01 (m, 6H) ppm.

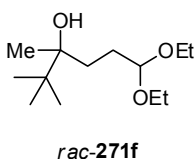
^{13}C NMR (125 MHz, C_6D_6) $\delta = 146.7, 137.3, 131.2, 128.2, 128.1, 126.7, 126.5, 126.1, 103.2, 76.5, 61.3, 60.6, 50.8, 36.8, 28.3, 15.5, 15.4$ ppm.

MS (EI) m/z (%): 237 (9), 191 (100), 163 (9), 145 (11), 17 (26).

HRMS (ESI+) m/z calculated for $\text{C}_{21}\text{H}_{28}\text{O}_3\text{Na}$ ($\text{M}+\text{Na}^+$) 351.193062, found 351.193062.

The enantiomeric ratio was determined by HPLC analysis using Daicel Chiralcel OJ-H column: *n*-heptane:*i*-PrOH = 90:10, flow rate 0.5 mL/min, $\lambda = 220$ nm: $\tau_1 = 10.07$ min, $\tau_2 = 11.72$ min.

6,6-Diethoxy-2,2,3-trimethylhexan-3-ol (*rac*-271f)



Purification: CC on SiO_2 (hexane: EtOAc 7:1).

Yield: Colorless oil 453 mg (1.95 mmol, 65%).

^1H NMR (500 MHz, C_6D_6) $\delta = 4.46$ -4.43 (m, 1H), 3.60-3.50 (m, 2H), 3.41-3.31 (m, 2H), 2.00-1.91 (m, 1H), 1.77-1.68 (m, 2H), 1.53-1.45 (m, 2H), 1.12 (t, $J = 7.0$ Hz, 3H, overlapped), 1.12 (t, $J = 7.0$ Hz, 3H, overlapped), 0.99 (s, 3H), 0.93 (s, 9H) ppm.

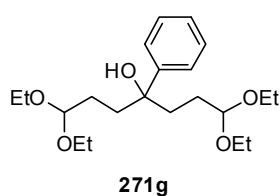
^{13}C NMR (125 MHz, C_6D_6) δ = 103.9, 75.3, 61.2, 60.8, 38.4, 30.9, 28.5, 25.5, 21.4, 15.7, 15.6 ppm.

MS (ESI+) m/z (%): 255.1 (M+Na).

HRMS (ESI+) m/z calculated for $\text{C}_{13}\text{H}_{28}\text{O}_3\text{Na}$ (M+Na⁺) 255.1931, found 255.1930.

The enantiomeric ratio was determined by GC analysis using BGB-176 column SE/SE52 (30 m, 2,3-dimethyl-6-*tert*-butyldimethylsilyl- β -cyclodextrin, i.D. 0.25 mm, df. 0.25 μm), Detector: FID; Temperature: injector 220 $^\circ\text{C}$, detector 350 $^\circ\text{C}$, oven: 125 $^\circ\text{C}$; gas: 0.5 bar H_2 . τ_1 = 25.11 min, τ_2 = 26.26 min.

1,1,7,7-Tetraethoxy-4-phenylheptan-4-ol (*rac*-271f)



Purification: CC on SiO_2 (pentane:Et₂O 2:1).

Yield: Colorless oil 643 mg (1.74 mmol, 58%).

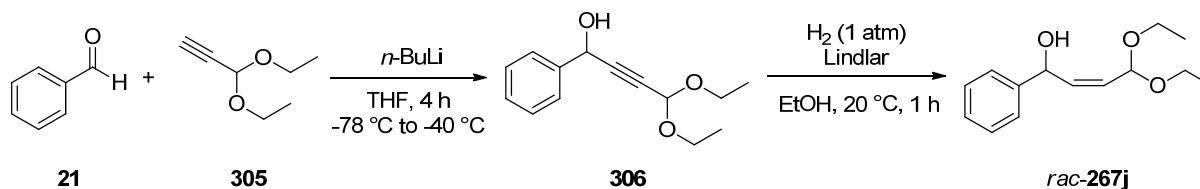
^1H NMR (500 MHz, C_6D_6) δ = 7.47 (dd, J = 8.3, 1.0 Hz, 2H), 7.20 (dd, J = 8.0, 7.6 Hz, 2H), 7.07 (t, J = 7.4 Hz, 1H), 4.35 (t, J = 5.6 Hz, 2H), 3.49-3.43 (m, 2H), 3.41-3.36 (m, 2H), 3.35 (s, 1H), 3.27-3.19 (m, 4H), 2.00-1.97 (m, 4H), 1.87-1.81 (m, 2H), 1.61-1.55 (m, 2H), 1.07 (t, J = 7.0 Hz, 6H), 1.04 (t, J = 7.0 Hz, 6H) ppm.

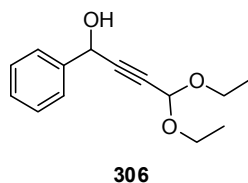
^{13}C NMR (125 MHz, C_6D_6) δ = 147.3, 126.4, 126.1, 103.3, 76.0, 61.2, 60.7, 38.6, 28.3, 15.5, 15.5 ppm.

MS (EI) m/z (%): 231 (15), 191 (100), 117 (12), 103 (24).

HRMS (ESI+) m/z calculated for $\text{C}_{21}\text{H}_{36}\text{O}_5\text{Na}$ (M+Na⁺) 391.245495, found 391.245495.

Synthesis of racemic homoaldol *rac*-267j



4,4-Diethoxy-1-phenylbut-2-yn-1-ol (306)

n-BuLi (1.32 mL, 3.30 mmol, 2.5 M solution in hexanes) was added dropwise to a solution of 3,3-diethoxyprop-1-yne (**305**, 385 mg, 3.00 mmol) in THF (10 mL) at -78 °C. The mixture was stirred at -78 °C for 30 min, before benzaldehyde (**21**, 350 mg, 3.30 mmol) was added. After

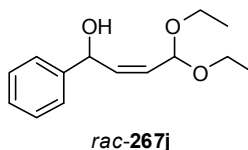
being stirred at -78 °C for 2 h the mixture was warmed up to -40 °C within 1 h and was then quenched with saturated NaHCO₃-solution (10 mL) and water (10 mL). The layers were separated, the aqueous layer was extracted with Et₂O (3 x 30 mL) and the combined organic layers were dried over MgSO₄. The solvent was removed under reduced pressure and the residue was purified by silica gel chromatography with pentane:Et₂O (3:1) as the eluent to give the title compound **306** (663 mg, 2.83 mmol, 94%) as a colorless oil.

¹H NMR (500 MHz, CDCl₃) δ = 7.52 (d, *J* = 7.2 Hz, 2H), 7.39-7.37 (m, 2H), 7.34-7.31 (m, 1H), 5.52 (s, 1H), 5.34 (d, *J* = 1.2 Hz, 1H), 3.77-3.71 (m, 2H), 3.63-3.56 (m, 2H), 2.62 (s br, 1H), 1.24-1.21 (m, 6H) ppm.

¹³C NMR (125 MHz, CDCl₃) δ = 140.1, 128.7, 128.6, 126.8, 91.4, 85.2, 82.0, 64.5, 61.1, 61.1, 15.2 ppm.

MS (EI) *m/z* (%): 189 (90), 159 (18), 143 (17), 133 (74), 115 (100), 105 (64).

HRMS (ESI+) *m/z* calculated for C₁₄H₁₈O₃Na (M+Na⁺) 257.114813, found 257.114561.

(Z)-4,4-Diethoxy-1-phenylbut-2-en-1-ol (rac-267j)

A mixture of 4,4-diethoxy-1-phenylbut-2-yn-1-ol (**306**, 442 mg, 1.89 mmol) and Lindlar catalyst (19 mg) in EtOH (7 mL) was stirred under 1 atm of H₂ at 20 °C for 1 h. After complete conversion of the starting

material (indicated by TLC), the mixture was filtered over Celite, concentrated and purified by silica gel chromatography with pentane:Et₂O (2:1) as the eluent to give *rac*-**267j** (389 mg, 1.64 mmol, 87%) as a colorless oil.

¹H NMR (500 MHz, C₆D₆) δ = 7.49 (d, *J* = 7.3 Hz, 2H), 7.20 (dd, *J* = 7.3, 7.3 Hz, 2H), 7.09 (t, *J* = 7.3 Hz, 1H), 5.73 (ddd, *J* = 11.3, 8.3, 1.3 Hz, 1H), 5.62 (ddd, *J* = 11.3, 8.3, 1.0 Hz, 1H), 5.59 (dd, *J* = 8.3, 3.3 Hz, 1H), 5.38 (d, *J* = 5.5, 1.2 Hz, 1H), 3.60-3.54 (m, 1H), 3.47-3.42 (m, 1H), 3.41-3.31 (m, 2H), 2.56 (d, *J* = 3.7 Hz, 1H), 1.10 (t, *J* = 7.1 Hz, 3H), 1.05 (t, *J* = 7.1 Hz, 3H) ppm.

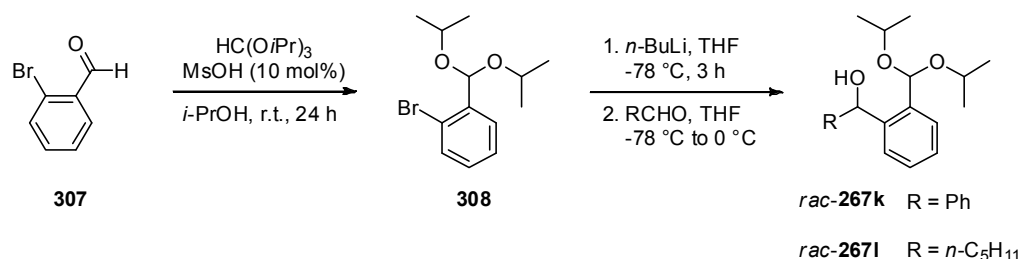
¹³C NMR (125 MHz, C₆D₆) δ = 143.9, 137.1, 129.1, 128.6, 127.6, 126.5, 98.0, 70.2, 60.6, 60.0, 15.5, 15.4 ppm.

MS (EI) m/z (%): 190 (100), 161 (27), 145 (49), 133 (51), 117 (69), 105 (43), 91 (25).

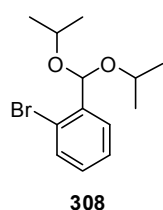
HRMS (ESI+) m/z calculated for $C_{14}H_{20}O_3Na$ ($M+Na^+$) 259.130461, found 259.130377.

The enantiomeric ratio was determined by HPLC analysis using Daicel Chiralcel OJ-H column: *n*-heptane:*i*-PrOH = 98:2, flow rate 0.5 mL/min, $\lambda = 220$ nm: $\tau_1 = 29.00$ min, $\tau_2 = 31.35$ min.

Synthesis of Racemic Homoaldols *rac*-267k-l^[223]



1-Bromo-2-(diisopropoxymethyl)benzene (308)



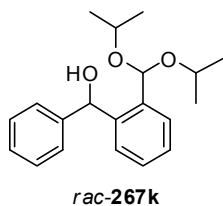
A solution of 2-bromobenzaldehyde (**307**, 2.78 g, 15.0 mmol), triisopropyl orthoformate (5 mL), and methanesulfonic acid (97 μ l, 144 mg, 1.50 mmol, 10 mol%) in *i*-PrOH (20 mL) was stirred at room temperature. After 24 h, Na_2CO_3 (2 g) was added, the mixture was stirred for 5 min and then filtered and concentrated. Purification of the residue by silica gel chromatography with hexane:EtOAc (20:1) as the eluent afforded the title compound **308** (3.89 g, 13.5 mmol, 90%) as a colorless oil.

¹H NMR (500 MHz, DMSO- d_6) $\delta = 7.57$ (dd, $J = 7.8, 1.4$ Hz, 2H), 7.39 (td, $J = 6.5, 0.9$ Hz, 1H), 7.26 (td, $J = 7.7, 1.8$ Hz, 1H), 5.67 (s, 1H), 3.82 (sept, $J = 6.1$ Hz, 2H), 1.13 (d, $J = 6.2$ Hz, 6H), 1.08 (d, $J = 6.2$ Hz, 6H) ppm.

¹³C NMR (125 MHz, DMSO- d_6) $\delta = 139.1, 132.4, 130.2, 128.5, 127.6, 122.0, 98.1, 68.3, 22.8, 22.3$ ppm.

MS (EI) m/z (%): 185 (100), 187 (91), 227 (53), 229 (51), 286 (4), 288 (4).

HRMS (ESI+) m/z calculated for $C_{13}H_{19}BrO_2Na$ ($M+Na^+$) 309.0461, found 309.0457.

(2-(Diisopropoxymethyl)phenyl)(phenyl)methanol (*rac*-267k)

n-BuLi (1.32 mL, 3.30 mmol, 2.5 M solution in hexane) was added dropwise to the solution of 1-bromo-2-(diisopropoxymethyl)benzene (**308**, 1.03 g, 3.59 mmol) in THF (5.0 mL) at -78°C. After 2.5 h a solution of benzaldehyde (**21**, 303 μ L, 318 mg, 3.00 mmol) in THF (1.0 mL) was added dropwise to this mixture at -78°C. The reaction was stirred at -78 °C for 3

h and then allowed to warm to 0 °C. Water (10 mL) was added and mixture was extracted with diethyl ether (20 mL, 2 x 10 mL). The combined organic extracts were washed with concentrated aqueous Na₂CO₃-solution (10 mL), dried (MgSO₄) and concentrated. The product was purified by silica gel chromatography with hexane:EtOAc (9:1) as the eluent to afford the title compound *rac*-**267k** as a colorless oil (821 mg, 2.61 mmol, 87%).

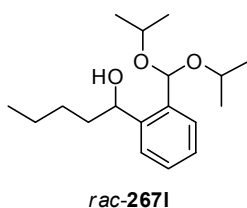
¹H NMR (500 MHz, C₆D₆) δ = 7.61 (d, *J* = 7.9 Hz, 2H), 7.54 (dd, *J* = 7.4, 1.3 Hz, 1H), 7.25 (dd, *J* = 7.4, 1.3 Hz, 1H), 7.20 (t, *J* = 7.8 Hz, 2H), 7.10 (t, *J* = 7.30 Hz, 1H), 7.08 (td, *J* = 7.5, 1.5 Hz, 1H), 7.03 (td, *J* = 7.3, 1.5 Hz, 1H), 6.58 (d, *J* = 4.5 Hz, 1H), 5.63 (s, 1H), 3.82 (sept, *J* = 6.1 Hz, 1H), 3.76 (d, *J* = 4.6 Hz, 1H), 3.69 (sept, *J* = 6.3 Hz, 1H), 1.05 (d, *J* = 6.2 Hz, 3H), 1.03 (d, *J* = 6.2 Hz, 3H), 0.97 (d, *J* = 6.1 Hz, 3H), 0.93 (d, *J* = 6.1 Hz, 3H) ppm.

¹³C NMR (125 MHz, C₆D₆) δ = 144.3, 143.5, 138.5, 129.8, 128.9, 128.4, 127.5, 127.2, 127.1, 99.2, 72.7, 68.6, 68.3, 23.2, 22.8, 22.4 ppm.

MS (EI) *m/z* (%): 133 (32), 165 (20), 195 (100), 211 (98), 254 (21), 314 (<0.1).

HRMS (ESI+) *m/z* calculated for C₂₀H₂₆O₃Na (M+Na⁺) 337.1774, found 337.1773.

The enantiomeric ratio was determined by HPLC analysis using Daicel Chiralcel OJ-H column: *n*-heptane:*i*-PrOH = 98:2, flow rate 0.5 mL/min, λ = 210 nm: τ_1 = 12.40 min, τ_2 = 16.19 min.

1-(2-(Diisopropoxymethyl)phenyl)pentan-1-ol (*rac*-267l)

Homoaldol (*rac*-**267l**) was prepared using the procedure described for compound *rac*-**267k**, starting from 3.0 mmol of pentanal. Purification: CC on SiO₂ (hexane:EtOAc 9:1).

Yield: Colorless oil 671 mg (2.28 mmol, 76%).

¹H NMR (500 MHz, C₆D₆) δ = 7.56 (t, *J* = 8.6 Hz, 2H), 7.19 (td, *J* = 7.5, 1.4 Hz, 1H), 7.12 (td, *J* = 7.5, 1.3 Hz, 1H), 5.71 (s, 1H), 5.41-5.38 (m, 1H), 3.80 (sept d, *J* = 6.2, 1.6 Hz, 2H), 2.52 (d, *J* = 3.1 Hz, 1H), 2.03-1.96 (m, 1H), 1.93-1.86 (m, 1H), 1.72-1.63 (m, 1H), 1.52-

1.43 (m, 1H), 1.42-1.34 (m, 2H), 1.12 (d, $J = 6.1$ Hz, 3H), 1.10 (d, $J = 6.1$ Hz, 3H), 1.05 (d, $J = 6.2$ Hz, 3H), 1.00 (d, $J = 6.1$ Hz, 3H), 0.90 (t, $J = 7.3$ Hz, 3H) ppm.

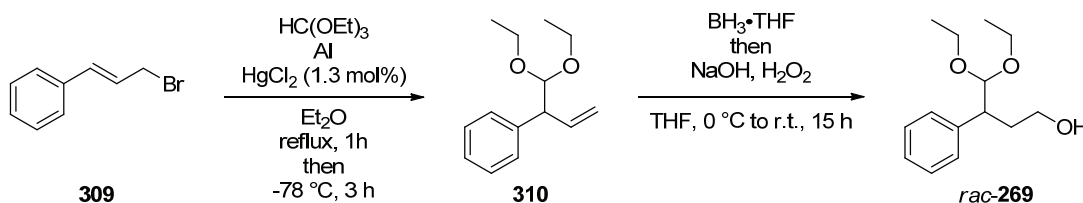
^{13}C NMR (125 MHz, C_6D_6) $\delta = 144.1, 137.9, 128.9, 127.7, 127.0, 126.9, 99.5, 69.6, 68.7, 68.2, 37.4, 29.2, 23.22, 23.15, 22.6, 22.4, 14.4$ ppm.

MS (EI) m/z (%): 135 (100), 175 (68), 177 (33), 191 (74), 234 (13), 235 (15), 276 (3).

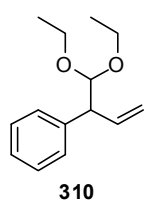
HRMS (ESI+) m/z calculated for $\text{C}_{18}\text{H}_{30}\text{O}_3\text{Na}$ ($\text{M}+\text{Na}^+$) 317.2087, found 317.2085.

The enantiomeric ratio was determined by HPLC analysis using Daicel Chiralpak AD-3 column: n -heptane: i -PrOH = 99:1, flow rate 1.0 mL/min, $\lambda = 210$ nm: $\tau_1 = 7.28$ min, $\tau_2 = 9.54$ min.

Synthesis of Racemic Homoaldol *rac*-269



(1,1-Diethoxybut-3-en-2-yl)benzene (310)



A mixture of Al (621 mg, 23.0 mmol) and HgCl_2 (35.3 mg, 0.130 mmol) in Et_2O (5.0 mL) was refluxed for 15 min, before a solution of cinnamyl bromide (**309**, 296 mg, 15.0 mmol) in Et_2O (10 mL) was added dropwise over 30 min at room temperature. After complete addition, the mixture was refluxed for 1 h and then cooled to -78 °C. A solution of triethylorthoformate (1.48 g, 1.66 mL, 10.0 mmol) in Et_2O (2.0 mL) was added dropwise over 30 min and the mixture was allowed to stir at -78 °C for 3 h before H_2O (20 mL) and 2 M NaOH (5.0 mL) were added. After warming to room temperature, Celite was added to the mixture and stirring was continued for 10 min. The mixture was filtered over a pad of Celite, washed with Et_2O (3 x 50 mL) and concentrated under reduced pressure. Purification of the residue by column chromatography on silica gel (penate: Et_2O 30:1) afforded the title compound **310** (909 mg, 4.13 mmol, 41%) as a colorless oil.

^1H NMR (500 MHz, CD_2Cl_2) $\delta = 7.32$ - 7.29 (m, 2H), 7.26 - 7.25 (m, 2H), 7.24 - 7.20 (m, 1H), 6.16 (ddd, $J = 17.6, 9.9, 7.4$ Hz, 1H), 5.13- 5.10 (m, 1H), 5.04- 5.00 (m, 1H), 4.64 (d, $J = 6.3$ Hz, 1H),

3.73-3.67 (m, 1H), 3.62-3.56 (m, 2H), 3.54-3.47 (m, 1H), 3.45-3.36 (m, 1H), 1.19 (t, $J = 7.1$ Hz, 3H), 1.05 (t, $J = 7.1$ Hz, 3H) ppm.

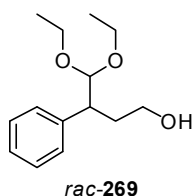
^{13}C NMR (125 MHz, CD_2Cl_2) $\delta = 141.1, 138.4, 129.2, 128.5, 126.7, 116.5, 105.4, 62.9, 62.8, 54.4, 15.4, 15.3$ ppm.

MS (EI) m/z (%): 129 (17), 117 (19), 103 (100), 91 (16).

HRMS (ESI+) m/z calculated for $\text{C}_{14}\text{H}_{20}\text{O}_2\text{Na}$ ($\text{M}+\text{Na}^+$) 243.135547, found 243.135272.

$[\alpha]_{\text{D}}^{25} = +15.2^\circ$ ($c = 0.475, \text{CH}_2\text{Cl}_2, \text{er} = 97.5:2.5$).

4,4-Diethoxy-3-phenylbutan-1-ol (*rac*-269)



To a solution of olefin **310** (364 mg, 1.65 mmol) in THF (7.0 mL) was added $\text{BH}_3\cdot\text{THF}$ (1.65 mL, 1.65 mmol, 1 M solution in THF) at 0°C . After stirring for 12 h at room temperature, the reaction was cooled again to 0°C and 2 M NaOH-solution (1.1 mL) was added. The mixture was stirred for 30 min at 0°C , then 30% aqueous H_2O_2 -solution (0.73 mL) was added and stirring was continued for 2 h at 0°C . The mixture was diluted with H_2O , extracted with Et_2O , dried over MgSO_4 and concentrated under reduced pressure. The residue was purified by column chromatography on silica gel (pentane: Et_2O 2:1) to yield the title compound *rac*-**269** (301 mg, 1.26 mmol, 76%) as a colorless oil.

^1H NMR (500 MHz, C_6D_6) $\delta = 7.22$ (d, $J = 7.2$ Hz, 2H), 7.18 (dd, $J = 7.7, 7.4$ Hz, 2H), 7.08 (t, $J = 7.2$ Hz, 1H), 4.44 (d, $J = 6.0$ Hz, 1H), 3.60-3.54 (m, 1H), 3.53-3.49 (m, 1H), 3.42-3.34 (m, 2H), 3.27-3.22 (m, 1H), 3.21-3.13 (m, 2H), 2.33-2.24 (m, 1H), 2.17 (br, 1H), 1.87-1.80 (m, 1H), 1.09 (t, $J = 7.1$ Hz, 3H), 0.92 (t, $J = 7.0$ Hz, 3H) ppm.

^{13}C NMR (125 MHz, CD_2Cl_2) $\delta = 142.1, 129.2, 128.5, 126.7, 106.5, 62.9, 62.6, 60.8, 47.0, 34.3, 15.4, 15.3$ ppm.

MS (EI) m/z (%): 193 (3), 147 (7), 117 (6), 103 (100).

HRMS (ESI+) m/z calculated for $\text{C}_{14}\text{H}_{22}\text{O}_3\text{Na}$ ($\text{M}+\text{Na}^+$) 261.146115, found 261.146283.

The enantiomeric ratio was determined by HPLC analysis using Daicel Chiralcel OJ-H column: *n*-heptane:*i*-PrOH = 90:10, flow rate 0.5 mL/min, $\lambda = 220$ nm: $\tau_1 = 11.88$ min, $\tau_2 = 15.18$ min.

7.6.2 Kinetic Resolution of Racemic Homoaldols

General procedure for STRIP-catalyzed kinetic resolution of homoaldols via asymmetric transacetalization:

4Å molecular sieves (50 mg) and a solution of (*S*)-STRIP (**145g**, 0.72 mg, 0.0010 mmol) in dry dichloromethane (1.0 mL), were added to the solution of the racemic homoaldol (0.10 mmol) in dry CH₂Cl₂ (3.0 mL) and the mixture was stirred at 20 °C. Samples (ca. 300 µL) were removed from the reaction mixture and quenched by a few drops of Et₃N. Subsequently, the product and remaining starting material were isolated by silica gel chromatography using pentane:Et₂O as the eluent. All product containing fractions were combined (important for the correct dr determination) and the solvent was carefully evaporated to prevent loss of volatile products. The samples were analyzed by HPLC or GC on a chiral stationary phase. The conversions were calculated from the enantiomeric excesses of products and starting material.

Preparation of the racemates:

Diphenyl phosphate (10.0 mg, 0.040 mmol) was added to the solution of the racemic homoaldol (0.200 mmol) in CH₂Cl₂ (2.0 mL). After 15 min at room temperature, the reaction was quenched with Et₃N (ca. 50 µL). The mixture was concentrated and the products were isolated by silica gel chromatography using Et₂O:pentane or EtOAc:hexane as the eluents.

Determination of conversion and dr:

Conversions were calculated from ee and dr values. The corresponding formula was derived from two simple and reasonable assumptions:

a) Since the reactions are very clean and no significant by-products are formed, the conversion can be represented by eq 1.

b) The preformed alcohol stereocenter is not racemizing under the reaction conditions. The absolute configuration of this stereocenter in the major product was found to be opposite to the configuration of the minor diastereoisomer and the starting material (this finding is

further supported by the significant formation of the minor diastereoisomer at higher levels of conversion). The sum of ee-values with respect to this stereocenter has to be zero at every time (eq 4). Consequently the conversion can easily be calculated by using eq 5, derived from eq 1, eq 2 and eq 4.

$$\text{conversion} = 1 - y_{\text{SM}} = y_{\text{maj}} + y_{\text{min}} \quad (\text{eq 1})$$

$$\text{dr} = \frac{y_{\text{maj}}}{y_{\text{min}}} = F \times \frac{\text{Area}_{\text{maj}}}{\text{Area}_{\text{min}}} \quad (\text{eq 2})$$

$$F = \frac{\text{dr}_{\text{NMR}}(\text{racemate})}{\text{dr}_{\text{HPLC}}(\text{racemate})} \quad (\text{eq 3})$$

$$y_{\text{SM}} \times \text{ee}_{\text{SM}} - y_{\text{maj}} \times \text{ee}_{\text{maj}} + y_{\text{min}} \times \text{ee}_{\text{min}} = 0 \quad (\text{eq 4})$$

$$\text{conversion} = \frac{1}{1 + \frac{\text{ee}_{\text{maj}} - \text{ee}_{\text{min}}/\text{dr}}{\text{ee}_{\text{SM}} \times (1 + 1/\text{dr})}} \quad (\text{eq 5})$$

y_{SM} = yield of the starting material

y_{maj} = yield of the major diastereoisomer

y_{min} = yield of the minor diastereoisomer

Area_{maj} = HPLC or GC area of major diastereomer peaks

Area_{min} = HPLC or GC area of minor diastereomer peaks

ee = enantiomeric excess

dr = diastereomeric ratio

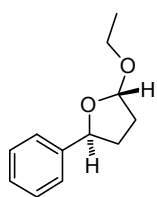
F = correction factor for different responses of the HPLC detector for two diastereomers

As the diastereomeric ratio determined by HPLC depends on detector responses for two diastereomers, the correction factor (F) must be added to calculate the real dr value (eq 2). This factor F was determined by comparing NMR (real dr) and HPLC diastereomeric ratios of prepared mixtures of both diastereoisomers (eq 3). In cases where it was not possible to determine the response factor, it was assumed to be $F = 1$ (small variations of F value have little influence on calculated conversion). For GC traces with FID detection F factor is taken as 1.

Product	268a	268b	268c	268d	268e	268f	268g	268h
F	0.79	1	0.71	1	1.05	1.06	1	1

Product	268i	268j	268k	268l	272a	272b	272c	272d
F	1	n.d. (1)	0.96	1.05	n.d. (1)	n.d. (1)	1	1

Product	272e	272f
F	0.80	1

trans-2-Ethoxy-5-phenyltetrahydrofuran (rac-5-epi-268a)*rac-5-epi-268a*

Purification: CC on SiO₂ (pentane:Et₂O 9:1). Colorless oil.

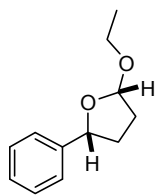
¹H NMR (500 MHz, C₆D₆) δ = 7.30 (d, J = 7.4 Hz, 2H), 7.18 (dd, J = 7.4, 7.3 Hz, 2H), 7.09 (t, J = 7.3 Hz, 1H), 5.22 (dd, J = 4.8, 2.6 Hz, 1H), 5.10 (t, J = 7.2 Hz, 1H), 3.88-3.82 (m, 1H), 3.41-3.35 (m, 1H), 2.18-2.13 (m, 1H), 1.87-1.82 (m, 2H), 1.52-1.44 (m, 1H), 1.15 (t, J = 7.1 Hz, 3H) ppm.

¹³C NMR (125 MHz, C₆D₆) δ = 143.6, 128.5, 127.4, 126.1, 104.5, 79.4, 63.1, 33.4, 32.7, 15.6 ppm.

MS (EI) m/z (%): 192 (9), 147 (52), 129 (19), 117 (56), 91 (44), 86 (100).

HRMS (EI) m/z calculated for C₁₂H₁₆O₂ 192.115034, found 192.115255.

The enantiomeric ratio was determined by HPLC analysis using Daicel Chiralcel OJ-H column: *n*-heptane:*i*-PrOH = 90:10, flow rate 0.5 mL/min, λ = 220 nm: τ_1 = 23.49 min, τ_2 = 27.89 min.

cis-2-Ethoxy-5-phenyltetrahydrofuran (rac-268a)*rac-268a*

Purification: CC on SiO₂ (pentane:Et₂O 9:1). Colorless oil.

¹H NMR (500 MHz, C₆D₆) δ = 7.44 (d, J = 7.3 Hz, 2H), 7.23 (dd, J = 7.4, 7.3 Hz, 2H), 7.11 (t, J = 7.4 Hz, 1H), 5.09 (d, J = 5.1 Hz, 1H), 4.87 (dd, J = 9.1, 6.4 Hz, 1H), 3.94-3.88 (m, 1H), 3.38-3.32 (m, 1H), 2.00-1.92 (m, 2H), 1.88-1.83 (m, 1H), 1.67-1.63 (m, 1H), 1.15 (t, J = 7.1 Hz, 3H) ppm.

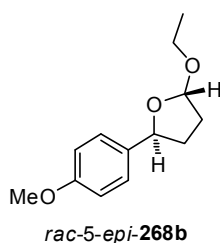
¹³C NMR (125 MHz, C₆D₆) δ = 144.5, 128.6, 127.5, 126.7, 104.3, 82.8, 62.9, 34.2, 33.5, 15.5 ppm.

MS (EI) m/z (%): 192 (10), 147 (69), 129 (28), 117 (85), 104 (15), 91 (56), 86 (100).

HRMS (EI) m/z calculated for C₁₂H₁₆O₂ 192.115033, found 192.115079.

The enantiomeric ratio was determined by HPLC analysis using Daicel Chiralcel OJ-H column: *n*-heptane:*i*-PrOH = 90:10, flow rate 0.5 mL/min, λ = 220 nm: τ_1 = 12.24 min, τ_2 = 19.58 min.

$[\alpha]_D^{25}$ = +148.7° (c = 0.39, CH₂Cl₂, er = 97.5:2.5).

trans-2-Ethoxy-5-(4-methoxyphenyl)tetrahydrofuran (*rac*-5-*epi*-268b)

Purification: CC on SiO₂ (pentane:Et₂O 3:1). Colorless oil.

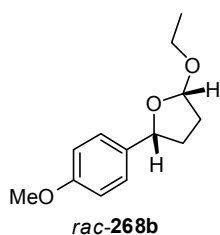
¹H NMR (500 MHz, C₆D₆) δ = 7.25 (d, *J* = 8.6 Hz, 2H), 6.82 (d, *J* = 8.6 Hz, 2H), 5.25 (t, *J* = 3.7 Hz, 1H), 5.11 (t, *J* = 7.2 Hz, 1H), 3.90-3.85 (m, 1H), 3.42-3.38 (m, 1H), 3.31 (s, 3H), 2.19-2.15 (m, 1H), 1.92-1.88 (m, 2H), 1.56-1.50 (m, 1H), 1.16 (t, *J* = 7.1 Hz, 3H) ppm.

¹³C NMR (125 MHz, C₆D₆) δ = 159.5, 135.4, 127.4, 114.0, 104.4, 79.2, 63.1, 54.8, 33.6, 32.9, 15.6 ppm.

MS (EI) *m/z* (%): 222 (30), 177 (43), 148 (22), 137 (53), 121 (29), 108 (13), 86 (85), 58 (100).

HRMS (EI) *m/z* calculated for C₁₃H₁₈O₃ 222.125593, found 222.125441.

The enantiomeric ratio was determined by HPLC analysis using Daicel Chiralcel OJ-H column: *n*-heptane:*i*-PrOH = 80:20, flow rate 0.5 mL/min, λ = 220 nm: τ₁ = 31.16 min, τ₂ = 37.79 min.

***cis*-2-Ethoxy-5-(4-methoxyphenyl)tetrahydrofuran (*rac*-268b)**

Purification: CC on SiO₂ (pentane:Et₂O 3:1). Colorless oil.

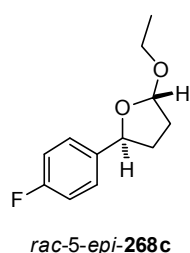
¹H NMR (500 MHz, C₆D₆) δ = 7.38 (d, *J* = 8.6 Hz, 2H), 6.86 (d, *J* = 8.6 Hz, 2H), 5.10 (d, *J* = 5.0 Hz, 1H), 4.89 (dd, *J* = 9.5, 6.3 Hz, 1H), 3.95-3.89 (m, 1H), 3.40-3.33 (m, 1H), 3.32 (s, 3H), 2.05-1.96 (m, 2H), 1.90-1.85 (m, 1H), 1.71-1.65 (m, 1H), 1.17 (t, *J* = 7.1 Hz, 3H) ppm.

¹³C NMR (125 MHz, C₆D₆) δ = 159.6, 136.4, 114.1, 104.1, 82.6, 62.8, 54.8, 34.3, 33.4, 30.5, 15.5 ppm.

MS (EI) *m/z* (%): 222 (32), 177 (36), 147 (24), 137 (53), 121 (29), 108 (17), 86 (87), 58 (100).

HRMS (EI) *m/z* calculated for C₁₃H₁₈O₃ 222.125593, found 222.125385.

The enantiomeric ratio was determined by HPLC analysis using Daicel Chiralcel OJ-H column: *n*-heptane:*i*-PrOH = 80:20, flow rate 0.5 mL/min, λ = 220 nm: τ₁ = 17.51 min, τ₂ = 25.17 min.

trans-2-Ethoxy-5-(4-fluorophenyl)tetrahydrofuran (*rac*-5-*epi*-268c)

Purification: CC on SiO₂ (pentane:Et₂O 4:1). Colorless oil.

¹H NMR (500 MHz, C₆D₆) δ = 7.06-7.03 (m, 2H), 6.84-6.80 (m, 2H), 5.17 (dd, *J* = 5.2, 2.2 Hz, 1H), 5.00 (t, *J* = 7.2 Hz, 1H), 3.86-3.80 (m, 1H), 3.40-3.33 (m, 1H), 2.10-2.05 (m, 1H), 1.85-1.78 (m, 2H), 1.37-1.31 (m, 1H), 1.15 (t, *J* = 7.1

Hz, 3H) ppm.

^{13}C NMR (125 MHz, C_6D_6) δ = 162.5 (d, J = 244.5 Hz), 139.2 (d, J = 2.9 Hz), 127.7 (d, J = 7.7 Hz), 115.2 (d, J = 21.2 Hz), 104.5, 78.7, 63.1, 33.4, 32.7, 15.6 ppm.

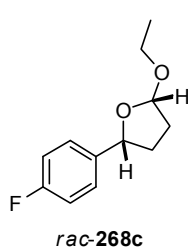
MS (EI) m/z (%): 210 (7), 165 (42), 135 (41), 109 (47), 86 (100).

HRMS (EI) m/z calculated for $\text{C}_{12}\text{H}_{15}\text{O}_2\text{F}$ 210.105606, found 210.105423.

The enantiomeric ratio was determined by HPLC analysis using Daicel Chiralcel OJ-H column: *n*-heptane:*i*-PrOH = 95:5, flow rate 0.5 mL/min, λ = 220 nm: τ_1 = 18.69 min, τ_2 = 23.85 min.

$[\alpha]_{\text{D}}^{25}$ = +59.1° (c = 0.45, CH_2Cl_2 , er = 99.5:0.5).

cis-2-Ethoxy-5-(4-fluorophenyl)tetrahydrofuran (*rac*-268c)



Purification: CC on SiO_2 (pentane:Et₂O 4:1). Colorless oil.

^1H NMR (500 MHz, C_6D_6) δ = 7.23-7.20 (m, 2H), 6.88-6.84 (m, 2H), 5.04 (d, J = 5.0 Hz, 1H), 4.74 (dd, J = 9.1, 6.6 Hz, 1H), 3.86-3.79 (m, 1H), 3.35-3.29 (m, 1H), 1.93-1.76 (m, 3H), 1.65-1.59 (m, 1H), 1.12 (t, J = 7.1 Hz, 3H) ppm.

^{13}C NMR (125 MHz, C_6D_6) δ = 162.6 (d, J = 244.6 Hz), 140.2 (d, J = 2.7 Hz), 128.4 (d, J = 7.7 Hz), 115.3 (d, J = 21.2 Hz), 104.3, 82.0, 62.9, 34.1, 33.4, 15.4 ppm.

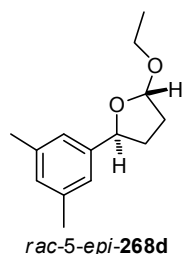
MS (EI) m/z (%): 210 (9), 165 (43), 136 (51), 109 (56), 86 (100).

HRMS (EI) m/z calculated for $\text{C}_{12}\text{H}_{15}\text{O}_2\text{F}$ 210.105611, found 210.105474.

The enantiomeric ratio was determined by HPLC analysis using Daicel Chiralcel OJ-H column: *n*-heptane:*i*-PrOH = 95:5, flow rate 0.5 mL/min, λ = 220 nm: τ_1 = 12.50 min, τ_2 = 13.49 min.

$[\alpha]_{\text{D}}^{25}$ = +137.1° (c = 0.75, CH_2Cl_2 , er = 97.5:2.5).

trans-5-(3,5-Dimethylphenyl)-2-ethoxytetrahydrofuran (*rac*-5-*epi*-268d)



Purification: CC on SiO_2 (pentane:Et₂O 9:1). Colorless oil.

^1H NMR (500 MHz, C_6D_6) δ = 7.03 (s, 2H), 6.77 (s, 1H), 5.27 (t, J = 3.7 Hz, 1H), 5.13 (t, J = 7.2 Hz, 1H), 3.93-3.86 (m, 1H), 3.44-3.38 (m, 1H), 2.24-2.19 (m, 1H), 2.17 (s, 6H), 1.93-1.89 (m, 2H), 1.60-1.53 (m, 1H), 1.17 (t, J = 7.1 Hz, 3H) ppm.

^{13}C NMR (125 MHz, C_6D_6) δ = 143.5, 137.7, 129.1, 124.0, 104.5, 79.5, 63.1, 33.6, 32.9, 21.4, 15.6 ppm.

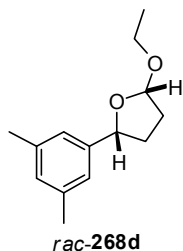
MS (EI) m/z (%): 220 (19), 175 (42), 157 (13), 146 (16), 131 (52), 119 (22), 105 (16), 91 (24), 86 (100).

HRMS (ESI+) m/z calculated for $C_{14}H_{20}O_2Na$ ($M+Na^+$) 243.135551, found 243.135330.

The enantiomeric ratio was determined by HPLC analysis using Daicel Chiralcel OJ-RH column:

MeOH:H₂O = 80:20, flow rate 1.0 mL/min, λ = 220 nm: τ_1 = 11.20 min, τ_2 = 12.34 min.

***cis*-5-(3,5-Dimethylphenyl)-2-ethoxytetrahydrofuran (*rac*-268d)**



Purification: CC on SiO₂ (pentane:Et₂O 9:1). Colorless oil.

¹H NMR (500 MHz, C₆D₆) δ = 7.13 (s, 2H), 6.79 (s, 1H), 5.11 (d, J = 5.0 Hz, 1H), 4.91 (dd, J = 9.5, 6.4 Hz, 1H), 4.00-3.94 (m, 1H), 3.41-3.35 (m, 1H), 2.21 (s, 6H), 2.09-1.89 (m, 3H), 1.72-1.64 (m, 1H), 1.20 (t, J = 7.1 Hz, 3H) ppm.

¹³C NMR (125 MHz, C₆D₆) δ = 144.5, 137.7, 129.1, 124.8, 104.3, 83.0, 62.7, 34.3, 33.5, 21.5, 15.5 ppm.

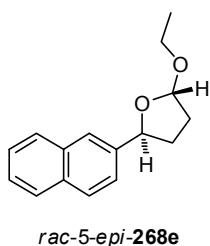
MS (EI) m/z (%): 220 (11), 176 (45), 157 (14), 146 (18), 131 (57), 119 (26), 106 (19), 91 (25), 86 (100).

HRMS (ESI+) m/z calculated for $C_{14}H_{20}O_2Na$ ($M+Na^+$) 243.135548, found 243.135342.

The enantiomeric ratio was determined by HPLC analysis using Daicel Chiralcel OJ-RH column:

MeOH:H₂O = 80:20, flow rate 1.0 mL/min, λ = 220 nm: τ_1 = 5.68 min, τ_2 = 9.96 min.

***trans*-2-Ethoxy-5-(naphthalen-2-yl)tetrahydrofuran (*rac*-5-*epi*-268e)**



Purification: CC on SiO₂ (pentane:Et₂O 4:1). Colorless oil.

¹H NMR (500 MHz, C₆D₆) δ = 7.81 (s, 1H), 7.70-7.64 (m, 3H), 7.38 (dd, J = 8.5, 1.6 Hz, 1H), 7.29-7.24 (m, 2H), 5.30 (dd, J = 4.9, 2.3 Hz, 1H), 5.26 (t, J = 7.2 Hz, 1H), 3.94-3.88 (m, 1H), 3.46-3.39 (m, 1H), 2.28-2.21 (m, 1H), 1.95-1.85 (m, 2H), 1.60-1.53 (m, 1H), 1.19 (t, J = 7.1 Hz, 3H) ppm.

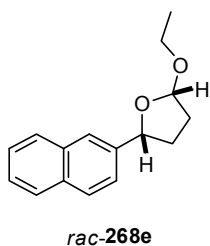
¹³C NMR (125 MHz, C₆D₆) δ = 141.0, 133.9, 133.4, 128.4, 128.3, 128.1, 126.3, 125.9, 124.7, 124.5, 104.7, 79.5, 63.2, 33.3, 32.8, 15.6 ppm.

MS (EI) m/z (%): 242 (61), 197 (43), 167 (38), 154 (37), 141 (34), 128 (63), 86 (100).

HRMS (ESI+) m/z calculated for $C_{16}H_{18}O_2Na$ ($M+Na^+$) 265.119896, found 265.119713.

The enantiomeric ratio was determined by HPLC analysis using Daicel Chiralpak AD-3 column:

n-heptane:*i*-PrOH = 99:1, flow rate 1.0 mL/min, λ = 220 nm: τ_1 = 3.60 min, τ_2 = 4.12 min.

cis-2-Ethoxy-5-(naphthalen-2-yl)tetrahydrofuran (*rac*-268e)

Purification: CC on SiO₂ (pentane:Et₂O 4:1). Colorless solid.

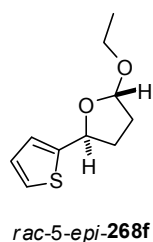
¹H NMR (500 MHz, C₆D₆) δ = 7.80 (s, 1H), 7.71-7.70 (m, 2H), 7.66-7.63 (m, 2H), 7.31-7.25 (m, 2H), 5.14 (d, *J* = 5.0 Hz, 1H), 5.03 (dd, *J* = 9.6, 6.5 Hz, 1H), 4.01-3.95 (m, 1H), 3.43-3.37 (m, 1H), 2.10-2.04 (m, 1H), 2.02-1.98 (m, 1H), 1.95-1.89 (m, 1H), 1.74-1.67 (m, 1H), 1.20 (t, *J* = 7.1 Hz, 3H) ppm.

¹³C NMR (125 MHz, C₆D₆) δ = 141.8, 133.9, 133.5, 128.6, 128.3, 128.1, 126.3, 125.9, 125.6, 125.1, 104.4, 83.0, 62.9, 34.3, 33.3, 15.5 ppm.

MS (EI) *m/z* (%): 242 (58), 197 (38), 167 (45), 154 (49), 141 (37), 128 (76), 86 (96), 58 (100).

HRMS (ESI+) *m/z* calculated for C₁₆H₁₈O₂Na (M+Na⁺) 265.119901, found 265.119634.

The enantiomeric ratio was determined by HPLC analysis using Daicel Chiralpak AD-3 column: *n*-heptane:*i*-PrOH = 99:1, flow rate 1.0 mL/min, λ = 220 nm: τ₁ = 6.79 min, τ₂ = 7.46 min.

trans-2-Ethoxy-5-(thiophen-2-yl)tetrahydrofuran (*rac*-5-*epi*-268f)

Purification: CC on SiO₂ (pentane:Et₂O 15:1). Colorless oil.

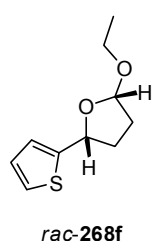
¹H NMR (500 MHz, C₆D₆) δ = 6.86 (dd, *J* = 5.0, 1.2 Hz, 1H), 6.77-6.76 (m, 1H), 6.72 (dd, *J* = 5.0, 3.5 Hz, 1H), 5.29 (t, *J* = 6.9 Hz, 1H), 5.14 (dd, *J* = 5.2, 2.0 Hz, 1H), 3.83-3.77 (m, 1H), 3.34-3.28 (m, 1H), 2.16-2.11 (m, 1H), 1.88-1.79 (m, 2H), 1.68-1.61 (m, 1H), 1.11 (t, *J* = 7.1 Hz, 3H) ppm.

¹³C NMR (125 MHz, C₆D₆) δ = 147.3, 126.7, 124.5, 123.8, 104.3, 75.9, 63.2, 33.7, 32.7, 15.5 ppm.

MS (EI) *m/z* (%): 198 (41), 153 (52), 123 (32), 97 (49), 86 (88), 58 (100).

HRMS (EI) *m/z* calculated for C₁₀H₁₄O₂S 198.071450, found 198.071412.

The enantiomeric ratio was determined by HPLC analysis using Daicel Chiralcel OJ-H column: *n*-heptane:*i*-PrOH = 50:50, flow rate 0.5 mL/min, λ = 220 nm: τ₁ = 15.58 min, τ₂ = 21.64 min.

cis-2-Ethoxy-5-(thiophen-2-yl)tetrahydrofuran (*rac*-268f)

Purification: CC on SiO₂ (pentane:Et₂O 15:1). Colorless oil.

¹H NMR (500 MHz, C₆D₆) δ = 6.91 (dd, *J* = 5.1, 1.1 Hz, 1H), 6.84-6.83 (m, 1H), 6.73 (dd, *J* = 5.1, 3.5 Hz, 1H), 5.07 (dd, *J* = 9.3, 6.6 Hz, 1H), 5.01 (d, *J* = 4.9 Hz, 1H), 3.96-3.90 (m, 1H), 3.34-3.28 (m, 1H), 2.17-2.10 (m, 1H), 1.95-1.91 (m, 1H),

1.89-1.83 (m, 1H), 1.61-1.53 (m, 1H), 1.16 (t, $J = 7.1$ Hz, 3H) ppm.

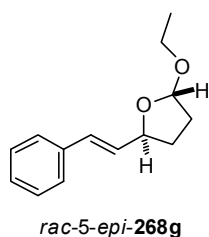
^{13}C NMR (125 MHz, C_6D_6) $\delta = 148.7, 126.6, 125.0, 124.4, 104.0, 78.0, 62.8, 34.2, 33.6, 15.4$ ppm.

MS (EI) m/z (%): 198 (40), 153 (48), 123 (34), 97 (51), 86 (85), 58 (100).

HRMS (EI) m/z calculated for $\text{C}_{10}\text{H}_{14}\text{O}_2\text{S}$ 198.071450, found 198.071343.

The enantiomeric ratio was determined by HPLC analysis using Daicel Chiralcel OJ-H column: n -heptane: i -PrOH = 50:50, flow rate 0.5 mL/min, $\lambda = 220$ nm: $\tau_1 = 12.43$ min, $\tau_2 = 18.87$ min.

***trans*-2-Ethoxy-5-((*E*-styryl)tetrahydrofuran (*rac*-5-*epi*-268g)**



Purification: CC on SiO_2 (pentane: Et_2O 6:1). Colorless oil.

^1H NMR (500 MHz, C_6D_6) $\delta = 7.25$ (d, $J = 7.3$ Hz, 2H), 7.11 (dd, $J = 7.3, 7.3$ Hz, 2H), 7.04 (t, $J = 7.3$ Hz, 1H), 6.60 (d, $J = 15.8$ Hz, 1H), 6.16 (d, $J = 15.8, 6.4$ Hz, 1H), 5.16 (dd, $J = 5.1, 2.1$ Hz, 1H), 4.71-4.67 (m, 1H), 3.91-3.85 (m, 1H), 3.41-3.35 (m, 1H), 2.04-1.98 (m, 1H), 1.89-1.81 (m, 2H), 1.43-1.36 (m, 1H), 1.16 (t, $J = 7.1$ Hz, 3H) ppm.

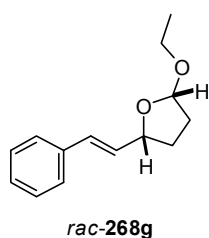
^{13}C NMR (125 MHz, C_6D_6) $\delta = 137.5, 130.8, 130.4, 128.8, 127.7, 126.9, 104.4, 78.5, 63.0, 32.7, 31.0, 15.6$ ppm.

MS (EI) m/z (%): 218 (39), 173 (20), 146 (19), 129 (59), 115 (30), 105 (32), 91 (42), 85 (100).

HRMS (ESI+) m/z calculated for $\text{C}_{14}\text{H}_{18}\text{O}_2\text{Na}$ ($\text{M}+\text{Na}^+$) 241.119900, found 241.119709.

The enantiomeric ratio was determined by HPLC analysis using Daicel Chiralcel OJ-H column: n -heptane: i -PrOH = 95:5, flow rate 0.5 mL/min, $\lambda = 220$ nm: $\tau_1 = 18.93$ min, $\tau_2 = 21.46$ min.

***cis*-2-Ethoxy-5-((*E*-styryl)tetrahydrofuran (*rac*-268g)**



Purification: CC on SiO_2 (pentane: Et_2O 6:1). Colorless oil.

^1H NMR (500 MHz, C_6D_6) $\delta = 7.27$ (d, $J = 7.3$ Hz, 2H), 7.11 (dd, $J = 7.3, 7.3$ Hz, 2H), 7.04 (t, $J = 7.3$ Hz, 1H), 6.53 (d, $J = 15.9$ Hz, 1H), 6.35 (d, $J = 15.8, 7.4$ Hz, 1H), 5.07 (d, $J = 4.9$ Hz, 1H), 4.54-4.50 (m, 1H), 3.92-3.86 (m, 1H), 3.39-3.33 (m, 1H), 1.96-1.93 (m, 1H), 1.91-1.83 (m, 1H), 1.77-1.71 (m, 1H), 1.66-1.61 (m, 1H), 1.15 (t, $J = 7.1$ Hz, 3H) ppm.

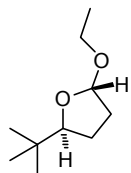
^{13}C NMR (125 MHz, C_6D_6) $\delta = 137.5, 132.9, 130.8, 128.8, 127.7, 126.9, 104.1, 81.3, 62.7, 33.8, 30.7, 15.6$ ppm.

MS (EI) m/z (%): 218 (43), 173 (18), 146 (19), 129 (61), 115 (32), 105 (33), 91 (45), 85 (100).

HRMS (ESI+) m/z calculated for $C_{14}H_{18}O_2Na$ ($M+Na^+$) 241.119900, found 241.120167.

The enantiomeric ratio was determined by HPLC analysis using Daicel Chiralcel OJ-H column: n -heptane: i -PrOH = 95:5, flow rate 0.5 mL/min, λ = 220 nm: τ_1 = 11.25 min, τ_2 = 13.75 min.

***trans*-5-(*tert*-Butyl)-2-ethoxytetrahydrofuran (*rac*-5-*epi*-268h)**



Purification: CC on SiO_2 (pentane:Et₂O 15:1). Colorless oil.

¹H NMR (500 MHz, C₆D₆) δ = 5.06 (dd, J = 4.9, 1.6 Hz, 1H), 3.82-3.76 (m, 2H), 3.38-3.33 (m, 1H), 1.86-1.82 (m, 1H), 1.73-1.67 (m, 2H), 1.34-1.32 (m, 1H), 1.15 (t, J = 7.1 Hz, 3H), 0.91 (s, 9H) ppm.

rac-5-*epi*-268h

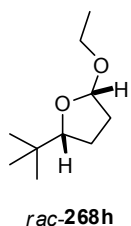
¹³C NMR (125 MHz, C₆D₆) δ = 104.1, 85.5, 62.6, 33.5, 33.0, 25.9, 24.7, 15.7 ppm.

MS (EI) m/z (%): 127 (17), 115 (100), 109 (29), 87 (76).

HRMS (CI) m/z calculated for $C_{10}H_{21}O_2$ ($M+H^+$) 173.1542, found 173.1540.

The enantiomeric ratio was determined by GC analysis using BGB-176 column (30 m, 2,3-dimethyl-6-*tert*-butyldimethylsilyl- β -cyclodextrin), Detector: FID; Temperature: injector 220 °C, detector 350 °C, oven: 60 °C, 1 °C/min until 85 °C, 8 °C/min until 220 °C; gas: 0.4 bar H₂. τ_1 = 13.89 min, τ_2 = 15.86 min.

***cis*-5-(*tert*-Butyl)-2-ethoxytetrahydrofuran (*rac*-268g)**



Purification: CC on SiO_2 (pentane:Et₂O 15:1). Colorless oil.

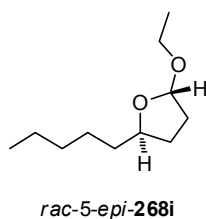
¹H NMR (500 MHz, C₆D₆) δ = 4.95 (d, J = 5.0 Hz, 1H), 3.83-3.78 (m, 1H), 3.60 (dd, J = 10.6, 5.8 Hz, 1H), 3.30-3.24 (m, 1H), 1.88 (dd, J = 12.1, 7.0 Hz, 1H), 1.74-1.67 (m, 1H), 1.62-1.57 (m, 1H), 1.38-1.33 (m, 1H), 1.12 (t, J = 7.1 Hz, 3H), 0.96 (s, 9H) ppm.

¹³C NMR (125 MHz, C₆D₆) δ = 103.4, 89.3, 62.3, 33.9, 33.6, 26.2, 24.7, 15.4 ppm.

MS (EI) m/z (%): 127 (9), 115 (100), 109 (30), 87 (84).

HRMS (CI) m/z calculated for $C_{10}H_{21}O_2$ ($M+H^+$) 173.154153, found 173.153985.

The enantiomeric ratio was determined by GC analysis using BGB-176 column (30 m, 2,3-dimethyl-6-*tert*-butyldimethylsilyl- β -cyclodextrin), Detector: FID; Temperature: injector 220 °C, detector 350 °C, oven: 60 °C, 1 °C/min until 85 °C, 8 °C/min until 220 °C; gas: 0.4 bar H₂. τ_1 = 14.39 min, τ_2 = 16.69 min.

trans-2-ethoxy-5-pentyltetrahydrofuran (*rac*-5-*epi*-268i)

Purification: CC on SiO₂ (pentane:Et₂O 20:1). Colorless oil.

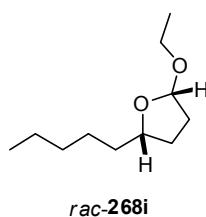
¹H NMR (500 MHz, C₆D₆) δ = 5.10 (dd, *J* = 5.1, 1.5 Hz, 1H), 4.11-4.06 (m, 1H), 3.87-3.81 (m, 1H), 3.39-3.33 (m, 1H), 1.93-1.77 (m, 3H), 1.63-1.57 (m, 1H), 1.47-1.17 (m, 8H), 1.15 (t, *J* = 7.1 Hz, 3H), 0.87 (t, *J* = 7.0 Hz, 3H) ppm.

¹³C NMR (125 MHz, C₆D₆) δ = 104.0, 77.9, 62.8, 36.1, 32.7, 32.3, 30.0, 26.3, 23.1, 15.6, 14.3 ppm.

MS (EI) *m/z* (%): 141 (15), 123 (11), 115 (100), 87 (55).

HRMS (CI) *m/z* calculated for C₁₁H₂₃O₂ (M+H⁺) 187.169801, found 187.169618.

The enantiomeric ratio was determined by GC analysis using BGB-176/SE column (30 m, 2,3-dimethyl-6-*tert*-butyldimethylsilyl-β-cyclodextrin), Detector: FID; Temperature: injector 220 °C, detector 320 °C, oven: 90 °C; gas: 0.4 bar H₂. τ₁ = 25.85 min, τ₂ = 27.73 min.

cis-2-Ethoxy-5-pentyltetrahydrofuran (*rac*-268i)

Purification: CC on SiO₂ (pentane:Et₂O 20:1). Colorless oil.

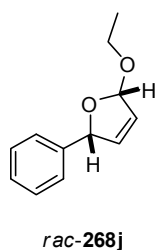
¹H NMR (500 MHz, C₆D₆) δ = 5.02 (d, *J* = 4.3, 1H), 3.97-3.91 (m, 1H), 3.87-3.81 (m, 1H), 3.36-3.30 (m, 1H), 1.94-1.91 (m, 1H), 1.76-1.70 (m, 1H), 1.67-1.62 (m, 3H), 1.51-1.44 (m, 2H), 1.38-1.23 (m, 5H), 1.14 (t, *J* = 7.1 Hz, 3H), 0.89 (t, *J* = 6.9 Hz, 3H) ppm.

¹³C NMR (125 MHz, C₆D₆) δ = 103.7, 80.6, 62.3, 38.2, 33.7, 32.3, 29.8, 26.6, 23.1, 15.6, 14.3 ppm.

MS (EI) *m/z* (%): 141 (11), 123 (8), 115 (100), 87 (57).

HRMS (CI) *m/z* calculated for C₁₁H₂₃O₂ (M+H⁺) 187.169803, found 187.169651.

The enantiomeric ratio was determined by GC analysis using BGB-176/SE column (30 m, 2,3-dimethyl-6-*tert*-butyldimethylsilyl-β-cyclodextrin), Detector: FID; Temperature: injector 220 °C, detector 320 °C, oven: 90 °C; gas: 0.4 bar H₂. τ₁ = 26.53 min, τ₂ = 27.13 min.

cis-2-Ethoxy-5-phenyl-2,5-dihydrofuran (*rac*-268i)

Prepared with 1 mol% of diphenyl phosphate.

Purification: CC on SiO₂ (pentane:Et₂O 20:1). Colorless solid.

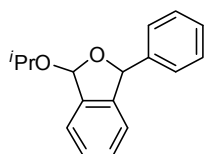
¹H NMR (500 MHz, C₆D₆) δ = 7.41 (d, *J* = 7.1 Hz, 2H), 7.18 (dd, *J* = 7.4, 7.1 Hz, 2H), 7.07 (d, *J* = 7.4 Hz, 1H), 5.81 (m, 1H), 5.73-5.71 (m, 1H), 5.62-5.60 (m, 1H), 5.57 (br, 1H), 3.89-3.82 (m, 1H), 3.46-3.40 (m, 1H), 1.13 (t, *J* = 7.1 Hz, 3H) ppm.

¹³C NMR (125 MHz, C₆D₆) δ = 141.6, 135.4, 128.6, 128.0, 127.4, 126.3, 109.2, 88.1, 63.9, 15.7 ppm.

MS (EI) *m/z* (%): 190 (9), 161 (10), 145 (100), 127 (20), 117 (51), 112 (64), 105 (29).

HRMS (ESI+) *m/z* calculated for C₁₂H₁₄O₂Na (M+Na⁺) 213.088601, found 213.088364.

The enantiomeric ratio was determined by HPLC analysis using Daicel Chiralcel OJ-H column: *n*-heptane:*i*-PrOH = 98:2, flow rate 0.5 mL/min, λ = 220 nm: τ₁ = 19.43 min, τ₂ = 22.95 min.

1-Isopropoxy-3-phenyl-1,3-dihydroisobenzofuran (*rac*-268k)^[223]

Purification: CC on SiO₂ (hexane:EtOAc 9:1). Diastereomers were not separated. Colorless oil. Diastereomeric ratio *cis/trans* 2.59:1 determined by ¹H NMR. Relative configuration determined by NOESY.

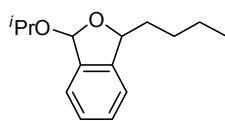
cis-268k/*trans*-268k
dr = 2.59:1 ¹H NMR (500 MHz, C₆D₆) δ = 7.46-7.45 (m, 2H_{maj}), 7.30 (d, *J* = 7.5 Hz, 1H_{maj} + 1H_{min}), 7.24-7.22 (m, 2H_{min}), 7.15-7.12 (m, 2H_{maj} + 2H_{min}), 7.09-7.03 (m, 2H_{maj} + 2H_{min}), 7.00-6.97 (m, 1H_{maj} + 1H_{min}), 6.83-6.78 (m, 1H_{maj} + 1H_{min}), 6.49 (d, *J* = 1.9 Hz, 1H_{min}), 6.38 (s, 1H_{maj}), 6.27 (s, 1H_{min}), 6.05 (s, 1H_{maj}), 4.10 (sept, *J* = 6.2 Hz, 1H_{maj} + 1H_{min}), 1.31 (d, *J* = 6.2 Hz, 3H_{min}), 1.26 (d, *J* = 6.2 Hz, 3H_{maj}), 1.20 (d, *J* = 6.2 Hz, 3H_{min}), 1.17 (d, *J* = 6.2 Hz, 3H_{maj}) ppm.

¹³C NMR (125 MHz, C₆D₆) δ = 144.2, 143.8, 143.1, 142.0, 139.5, 138.8, 129.3, 129.2, 128.7, 128.6, 127.6, 123.4, 123.2, 122.5, 122.4, 105.8, 105.6, 86.3, 84.9, 71.1, 70.6, 24.1, 24.0, 22.6, 22.5 ppm.

MS (EI) *m/z* (%): 134 (9), 165 (20), 167 (13), 195 (100), 196 (20), 211 (16), 253 (8).

HRMS (ESI+) *m/z* calculated for C₁₇H₁₈O₂Na (M+Na⁺) 277.1199, found 277.1196.

The enantiomeric ratio was determined by HPLC analysis using Daicel Chiralcel OJ-H column: *n*-heptane:*i*-PrOH = 60:40, flow rate 0.5 mL/min, λ = 210 nm: τ_{1(cis)} = 10.05 min, τ_{1(trans)} = 12.89 min, τ_{2(cis)} = 12.12 min, τ_{2(trans)} = 20.05 min.

1-Butyl-3-isopropoxy-1,3-dihydroisobenzofuran (*rac*-268k)^[223]

cis-268/*trans*-268
dr = 1:1.14

Purification: CC on SiO₂ (hexane:EtOAc 20:1). Diastereomers were not separated. Colorless oil. Diastereomeric ratio *cis/trans* 1:1.14 determined by ¹H NMR. Relative configuration determined by NOESY.

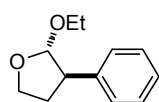
¹H NMR (500 MHz, C₆D₆) δ = 7.29-7.26 (m, 1H_{maj} + 1H_{min}), 7.13-7.07 (m, 2H_{maj} + 2H_{min}), 6.93-6.89 (m, 1H_{maj} + 1H_{min}), 6.33 (s, 1H_{maj}), 6.26 (s, 1H_{min}), 5.34 (t, *J* = 3.4 Hz, 1H_{maj}), 5.10 (dd, *J* = 7.4, 4.8 Hz, 1H_{min}), 4.07 (sept, *J* = 6.2 Hz, 1H_{maj} + 1H_{min}), 1.83-1.71 (m, 3H), 1.63-1.52 (m, 3H), 1.50-1.40 (m, 2H), 1.36-1.23 (m, 10H), 1.17 (t, *J* = 5.7 Hz, 6H), 0.89-0.84 (m, 6H) ppm.

¹³C NMR (125 MHz, C₆D₆) δ = 144.1, 144.0, 140.0, 128.9, 128.8, 127.68, 127.66, 123.5, 123.4, 121.4, 121.1, 105.2, 104.9, 83.7, 82.4, 70.4, 70.1, 38.0, 35.8, 28.3, 27.7, 24.2, 24.1, 23.2, 23.1, 22.64, 22.59, 14.3 ppm.

MS (EI) *m/z* (%): 135 (100), 175 (34), 177 (49), 191 (7), 233 (4).

HRMS (ESI+) *m/z* calculated for C₁₅H₂₂O₂Na (M+Na⁺) 257.1512, found 257.1511.

The enantiomeric ratio was determined by HPLC analysis using Daicel Chiralpak AD-3 column: *n*-heptane:*i*-PrOH = 99.9:0.1, flow rate 1.0 mL/min, λ = 210 nm: τ_{1(trans)} = 3.11 min, τ_{2(trans)} = 3.72 min, τ_{1(cis)} = 5.60 min, τ_{2(cis)} = 6.55 min. The *cis*-diastereomer is the major product in the asymmetric reaction, opposite to the racemic reaction.

***trans*-2-Ethoxy-3-phenyltetrahydrofuran (*rac*-2-*epi*-270)**

2-*epi*-*rac*-270

Purification: CC on SiO₂ (hexane:EtOAc 15:1). Colorless oil.

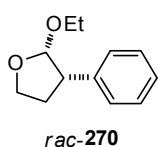
¹H NMR (500 MHz, C₆D₆) δ = 7.18-7.13 (m, 4H), 7.06 (tt, *J* = 7.0, 1.7 Hz, 1H), 5.10 (d, *J* = 1.8 Hz, 1H), 3.94-3.88 (m, 2H), 3.81-3.74 (m, 1H), 3.38-3.35 (m, 1H), 3.30-3.24 (m, 1H), 2.20-2.14 (m, 1H), 1.70-1.64 (m, 1H), 1.10 (t, *J* = 7.1 Hz, 3H) ppm.

¹³C NMR (125 MHz, C₆D₆) δ = 143.4, 128.9, 128.5, 126.7, 109.8, 67.1, 63.0, 52.0, 33.6, 15.5 ppm.

MS (EI) *m/z* (%): 147 (16), 118 (100), 91 (23).

HRMS (EI) *m/z* calculated for C₁₂H₁₆O₂ 192.115029, found 192.114922.

The enantiomeric ratio was determined by HPLC analysis using Daicel Chiralcel OJ-H column: *n*-heptane:*i*-PrOH = 98:2, flow rate 0.5 mL/min, λ = 220 nm: τ₁ = 12.27 min, τ₂ = 17.86 min.

cis-2-Ethoxy-3-phenyltetrahydrofuran (*rac*-270)

Purification: CC on SiO₂ (hexane:EtOAc 15:1). Colorless oil.

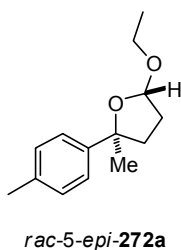
¹H NMR (500 MHz, C₆D₆) δ = 7.29 (d, J = 7.4 Hz, 2H), 7.20 (dd, J = 7.8, 7.5 Hz, 2H), 7.10 (t, J = 7.3 Hz, 1H), 5.01 (d, J = 4.5 Hz, 1H), 4.03-3.99 (m, 1H), 3.77-3.68 (m, 2H), 3.20-3.14 (m, 1H), 3.01-2.97 (m, 1H), 2.31-2.22 (m, 1H), 1.84-1.78 (m, 1H), 0.96 (t, J = 7.1 Hz, 3H) ppm.

¹³C NMR (125 MHz, C₆D₆) δ = 138.7, 129.6, 128.2, 126.8, 104.0, 66.7, 62.8, 50.3, 29.8, 15.3 ppm.

MS (EI) m/z (%): 147 (12), 118 (100), 91 (25).

HRMS (EI) m/z calculated for C₁₂H₁₆O₂ 192.115032, found 192.115078.

The enantiomeric ratio was determined by HPLC analysis using Daicel Chiralcel OJ-H column: *n*-heptane:*i*-PrOH = 98:2, flow rate 0.5 mL/min, λ = 220 nm: τ_1 = 12.65 min, τ_2 = 13.18 min.

trans-2-Ethoxy-5-methyl-5-(*p*-tolyl)tetrahydrofuran (*rac*-5-*epi*-272a)

Purification: CC on SiO₂ (pentane:Et₂O 20:1). Colorless oil.

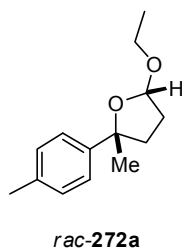
¹H NMR (500 MHz, C₆D₆) δ = 7.34 (d, J = 8.2 Hz, 2H), 7.05 (d, J = 7.9 Hz, 2H), 5.16 (d, J = 5.2 Hz, 1H), 3.95-3.89 (m, 1H), 3.44-3.38 (m, 1H), 2.20-2.14 (m, 1H), 2.16 (s, 3H), 1.95-1.86 (m, 2H), 1.73-1.66 (m, 1H), 1.67 (s, 3H), 1.18 (t, J = 7.1 Hz, 3H) ppm.

¹³C NMR (125 MHz, C₆D₆) δ = 146.2, 135.8, 129.0, 125.1, 104.4, 85.7, 62.7, 38.6, 32.9, 31.6, 21.0, 15.6 ppm.

MS (EI) m/z (%): 220 (6), 205 (100), 175 (27), 157 (13), 131 (68).

HRMS (ESI+) m/z calculated for C₁₄H₂₀O₂Na (M+Na⁺) 243.135547, found 243.135715.

The enantiomeric ratio was determined by HPLC analysis using Daicel Chiralcel OJ-H column: *n*-heptane:*i*-PrOH = 90:10, flow rate 0.5 mL/min, λ = 220 nm: τ_1 = 16.35 min, τ_2 = 29.00 min.

cis-2-Ethoxy-5-methyl-5-(*p*-tolyl)tetrahydrofuran (*rac*-272a)

Purification: CC on SiO₂ (pentane:Et₂O 20:1). Colorless oil.

¹H NMR (500 MHz, C₆D₆) δ = 7.45 (d, *J* = 8.2 Hz, 2H), 7.07 (d, *J* = 7.9 Hz, 2H), 5.15 (dd, *J* = 4.8; 1.5 Hz, 1H), 3.94-3.88 (m, 1H), 3.40-3.34 (m, 1H), 2.31-2.22 (m, 1H), 2.16 (s, 3H), 1.93-1.88 (m, 1H), 1.87-1.81 (m, 1H), 1.80-1.75 (m, 1H), 1.42 (s, 3H), 1.08 (t, *J* = 7.1 Hz, 3H) ppm.

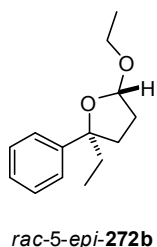
¹³C NMR (125 MHz, C₆D₆) δ = 146.9, 135.7, 128.9, 125.3, 104.5, 85.7, 62.9, 37.7, 33.1, 30.7, 21.0, 15.4 ppm.

MS (EI) *m/z* (%): 220 (9), 205 (100), 175 (23), 159 (13), 131 (70).

HRMS (ESI+) *m/z* calculated for C₁₄H₂₀O₂Na (M+Na⁺) 243.135546, found 243.135668.

The enantiomeric ratio was determined by HPLC analysis using Daicel Chiralcel OJ-H column: *n*-heptane:*i*-PrOH = 90:10, flow rate 0.5 mL/min, λ = 220 nm: τ₁ = 7.39 min, τ₂ = 9.95 min.

[α]_D²⁵ = +102.8° (c = 0.876, CH₂Cl₂, er = 98.5:1.5).

trans-2-Ethoxy-5-ethyl-5-phenyltetrahydrofuran (*rac*-5-*epi*-272b)

Purification: CC on SiO₂ (pentane:Et₂O 20:1). Colorless oil.

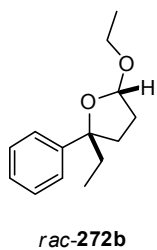
¹H NMR (500 MHz, C₆D₆) δ = 7.37 (dd, *J* = 8.1, 1.0 Hz, 2H), 7.21 (dd, *J* = 8.1, 7.4 Hz, 2H), 7.10 (t, *J* = 7.4 Hz, 1H), 5.12 (d, *J* = 5.1 Hz, 1H), 3.93-3.87 (m, 1H), 3.42-3.36 (m, 1H), 2.21-2.15 (m, 1H), 1.99-1.90 (m, 2H), 1.89-1.81 (m, 2H), 1.64-1.57 (m, 1H), 1.17 (t, *J* = 7.1 Hz, 3H), 0.90 (t, *J* = 7.4 Hz, 3H) ppm.

¹³C NMR (125 MHz, C₆D₆) δ = 147.3, 128.2, 126.5, 125.7, 104.1, 88.7, 62.7, 37.0, 36.6, 32.4, 15.6, 9.2 ppm.

MS (EI) *m/z* (%): 191 (100), 175 (10), 163 (9), 145 (11), 131 (5), 117 (39).

HRMS (ESI+) *m/z* calculated for C₁₄H₂₀O₂Na (M+Na⁺) 243.135553, found 243.135812.

The enantiomeric ratio was determined by HPLC analysis using Daicel Chiralcel OJ-H column: *n*-heptane:*i*-PrOH = 90:10, flow rate 0.5 mL/min, λ = 220 nm: τ₁ = 21.42 min, τ₂ = 26.68 min.

cis-2-Ethoxy-5-ethyl-5-phenyltetrahydrofuran (*rac*-272a)

Purification: CC on SiO₂ (pentane:Et₂O 20:1). Colorless oil.

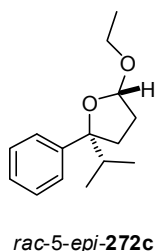
¹H NMR (500 MHz, C₆D₆) δ = 7.45 (dd, *J* = 8.3, 1.1 Hz, 2H), 7.23 (dd, *J* = 8.3, 7.4 Hz, 2H), 7.11 (t, *J* = 7.4 Hz, 1H), 5.13-5.12 (m, 1H), 3.91-3.85 (m, 1H), 3.40-3.33 (m, 1H), 2.27-2.21 (m, 1H), 1.90-1.75 (m, 3H), 1.69-1.61 (m, 2H), 1.03 (t, *J* = 7.1 Hz, 3H), 0.82 (t, *J* = 7.4 Hz, 3H) ppm.

¹³C NMR (125 MHz, C₆D₆) δ = 148.3, 128.0, 126.4, 125.8, 104.5, 88.4, 63.0, 36.5, 36.2, 33.1, 15.4, 8.9 ppm.

MS (EI) *m/z* (%): 191 (100), 175 (8), 163 (9), 145 (12), 131 (4), 117 (40).

HRMS (ESI+) *m/z* calculated for C₁₄H₂₀O₂Na (M+Na⁺) 243.135546, found 243.135714.

The enantiomeric ratio was determined by HPLC analysis using Daicel Chiralcel OJ-H column: *n*-heptane:*i*-PrOH = 90:10, flow rate 0.5 mL/min, λ = 220 nm: τ₁ = 8.29 min, τ₂ = 9.57 min.

trans-2-Ethoxy-5-isopropyl-5-phenyltetrahydrofuran (*rac*-5-*epi*-272c)

Purification: CC on SiO₂ (pentane:Et₂O 50:1). Colorless oil.

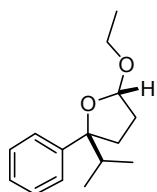
¹H NMR (500 MHz, C₆D₆) δ = 7.38 (dd, *J* = 8.3, 1.1 Hz, 2H), 7.20 (dd, *J* = 8.3, 7.4 Hz, 2H), 7.10 (t, *J* = 7.4 Hz, 1H), 5.04 (d, *J* = 5.1 Hz, 1H), 3.93-3.87 (m, 1H), 3.39-3.33 (m, 1H), 2.28-2.22 (m, 1H), 2.11-2.05 (m, 1H), 1.88 (ddd, *J* = 11.9, 7.6, 1.5 Hz, 1H), 1.79 (dd, *J* = 12.4, 7.1 Hz, 1H), 1.55-1.48 (m, 1H), 1.17 (t, *J* = 7.1 Hz, 3H), 1.02 (d, *J* = 6.7 Hz, 3H), 0.87 (d, *J* = 6.7 Hz, 3H) ppm.

¹³C NMR (125 MHz, C₆D₆) δ = 145.7, 127.8, 126.6, 126.6, 103.5, 91.4, 62.7, 38.6, 33.8, 32.6, 18.8, 17.9, 15.5 ppm.

MS (EI) *m/z* (%): 191 (100), 163 (9), 145 (12), 117 (29).

HRMS (ESI+) *m/z* calculated for C₁₅H₂₂O₂Na (M+Na⁺) 257.151196, found 257.151410.

The enantiomeric ratio was determined by HPLC analysis using Daicel Chiralcel OJ-H column: *n*-heptane:*i*-PrOH = 95:5, flow rate 0.5 mL/min, λ = 220 nm: τ₁ = 12.57 min, τ₂ = 48.83 min.

cis-2-Ethoxy-5-isopropyl-5-phenyltetrahydrofuran (*rac*-272c)*rac*-272c

Purification: CC on SiO₂ (pentane:Et₂O 50:1). Colorless oil.

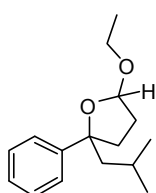
¹H NMR (500 MHz, C₆D₆) δ = 7.41 (dd, *J* = 8.2, 1.1 Hz, 2H), 7.22 (dd, *J* = 8.2, 7.4 Hz, 2H), 7.11 (t, *J* = 7.4 Hz, 1H), 5.12 (dd, *J* = 5.0, 2.0 Hz, 1H), 3.85-3.79 (m, 1H), 3.36-3.30 (m, 1H), 2.27-2.21 (m, 1H), 1.96-1.91 (m, 1H), 1.86-1.73 (m, 3H), 0.97 (t, *J* = 7.1 Hz, 3H), 0.87 (d, *J* = 6.7 Hz, 3H), 0.80 (d, *J* = 6.9 Hz, 3H) ppm.

¹³C NMR (125 MHz, C₆D₆) δ = 147.5, 127.5, 126.6, 126.4, 104.7, 90.6, 62.9, 39.2, 33.8, 33.5, 18.4, 17.6, 15.3 ppm.

MS (EI) *m/z* (%): 191 (100), 163 (9), 145 (13), 117 (31).

HRMS (ESI+) *m/z* calculated for C₁₅H₂₂O₂Na (M+Na⁺) 257.151198, found 257.151435.

The enantiomeric ratio was determined by HPLC analysis using Daicel Chiralcel OJ-H column: *n*-heptane:*i*-PrOH = 95:5, flow rate 0.5 mL/min, λ = 220 nm: τ₁ = 7.33 min, τ₂ = 8.47 min.

5-Ethoxy-2-isobutyl-2-phenyltetrahydrofuran (*rac*-272d)^[223]*cis*-272d/*trans*-272d
dr = 3.3:1

Purification: CC on SiO₂ (hexane:EtOAc 50:1). Diastereomers were not separated. Colorless oil. Diastereomeric ratio *cis/trans* 3.3:1 determined by ¹H NMR.

¹H NMR (500 MHz, C₆D₆) δ = 7.47-7.45 (m, 2H_{maj}), 7.35-7.33 (m, 2H_{min}), 7.25-7.19 (m, 2H_{maj} + 2H_{min}), 7.11-7.07 (m, 1H_{maj} + 1H_{min}), 5.13-5.12 (m, 1H_{maj} + 1H_{min}), 3.96-3.87 (m, 1H_{maj} + 1H_{min}), 3.42-3.35 (m, 1H_{maj} + 1H_{min}), 2.25-2.16 (m, 1H_{maj} + 1H_{min}), 1.95 (dd, *J* = 14.0, 4.6 Hz, 1H_{min}), 1.88 (ddd, *J* = 11.8, 7.8, 1.9 Hz, 1H_{min}), 1.85-1.76 (m, 3H_{maj} + 2H_{min}), 1.69-1.51 (m, 3H_{maj} + 2H_{min}), 1.19 (t, *J* = 7.1 Hz, 3H_{min}), 1.07 (t, *J* = 7.1 Hz, 3H_{maj}, overlapped), 1.07 (d, *J* = 6.6 Hz, 3H_{min}, overlapped), 1.01 (d, *J* = 6.4 Hz, 3H_{maj}), 0.75 (d, *J* = 6.7 Hz, 3H_{min}), 0.73 (d, *J* = 6.3 Hz, 3H_{maj}) ppm.

¹³C NMR (125 MHz, C₆D₆) δ (major *cis* diastereomer) = 148.5, 126.4, 125.8, 104.9, 88.5, 63.3, 52.3, 38.4, 32.7, 24.9, 24.7, 24.4, 15.4 ppm; δ (minor *trans* diastereomer) = 147.5, 126.5, 125.7, 104.4, 88.8, 62.7, 52.5, 39.3, 31.8, 25.3, 24.7, 23.9, 15.6 ppm.

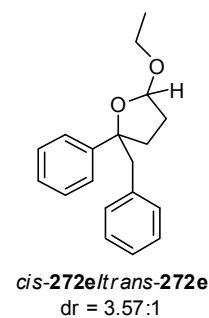
MS (EI) *m/z* (%): 117(21), 145 (8), 163 (7), 191 (100), 203 (3).

HRMS (ESI+) *m/z* calculated for C₁₆H₂₄O₂Na (M+Na⁺) 271.1668, found 271.1664.

The enantiomeric ratio was determined by GC analysis using Astek G-DA column (30 m, dialkyl-γ-cyclodextrin, i.D. 0.25 mm), Detector: FID; Temperature: injector 220 °C, detector

320 °C, oven: 130 °C; gas: 0.5 bar H₂. $\tau_{1(cis)} = 37.36$ min, $\tau_{2(cis)} = 38.38$ min, $\tau_{1(trans)} = 40.37$ min, $\tau_{2(trans)} = 42.03$ min.

5-Benzyl-2-ethoxy-5-phenyltetrahydrofuran (*rac*-272e)^[223]



Purification: CC on SiO₂ (pentane:Et₂O 15:1). Colorless oil. Diastereoisomers were not separated. Diastereomeric ratio *cis/trans* = 3.57:1 determined by ¹H NMR.

¹H NMR (500 MHz, C₆D₆) $\delta = 7.38$ (dd, $J = 8.2, 1.1$ Hz, 2H_{maj}), 7.22-7.17 (m, 2H_{maj} + 2H_{min}), 7.13-7.01 (m, 6H_{maj} + 8H_{min}), 5.07-5.05 (m, 1H_{maj} + 1H_{min}), 3.98-3.92 (m, 1H_{min}), 3.83-3.77 (m, 1H_{maj}), 3.41-3.36 (m, 1H_{min}), 3.34-3.28 (m, 1H_{maj}), 3.18 (d, $J = 13.6$ Hz, 1H_{min}), 3.16 (d, $J = 13.6$ Hz, 1H_{min}), 2.97 (d, $J = 13.4$ Hz, 1H_{maj}), 2.81 (d, $J = 13.4$ Hz, 1H_{maj}), 2.29-2.23 (m, 1H_{maj} + 1H_{min}), 2.04-1.99 (m, 1H_{maj}), 1.94-1.90 (m, 1H_{min}), 1.83-1.78 (m, 1H_{min}), 1.73-1.69 (m, 1H_{maj}), 1.60-1.53 (m, 1H_{min}), 1.33-1.28 (m, 1H_{maj}), 1.16 (t, $J = 7.1$ Hz, 3H_{min}), 0.97 (t, $J = 7.1$ Hz, 3H_{maj}) ppm.

¹³C NMR (125 MHz, C₆D₆) $\delta = 149.0, 146.6, 138.1, 138.0, 131.1, 131.0, 128.3, 128.0, 127.9, 127.8, 126.7, 126.6, 126.5, 126.4, 126.1, 125.8, 104.7, 104.2, 88.7, 88.4, 63.1, 62.9, 50.4, 50.0, 36.5, 35.0, 33.0, 32.2, 15.5, 15.3$ ppm.

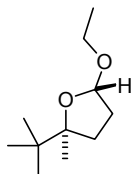
MS (EI) m/z (%): 237 (6), 191 (100), 163 (10), 145 (12), 117 (33).

HRMS (ESI+) m/z calculated for C₁₉H₂₂O₂Na (M+Na⁺) 305.151203, found 305.150760.

The enantiomeric ratio was determined by HPLC analysis. The diastereoisomers were separated on a Zorbax Eclipse Plus C18 column (50 mm, 1.8 μ m particle size): MeOH:H₂O = 70:30, flow rate 1.0 mL/min, $\lambda = 220$ nm: $\tau_{maj} = 9.69$ min, $\tau_{min} = 10.09$ min. The enantiomeric ratio of the major diastereoisomer was determined by using a column-switching technique, switching to a Kromasil AmyCoat RP column (150 mm) while the separated diastereoisomer is being eluted: MeCN:H₂O = 65:35, flow rate 1.0 mL/min, $\lambda = 220$ nm: $\tau_1 = 13.48$ min, $\tau_2 = 14.23$ min.

***trans*-2-(*tert*-Butyl)-5-ethoxy-2-methyltetrahydrofuran (*rac*-5-*epi*-272f)^[223]**

Purification: CC on SiO₂ (hexane:EtOAc 50:1). Colorless oil.



¹H NMR (500 MHz, C₆D₆) δ = 5.03 (d, J = 5.2 Hz, 1H), 3.85-3.79 (m, 1H), 3.34-3.28 (m, 1H), 1.97-1.92 (m, 1H), 1.79-1.66 (m, 2H), 1.61-1.56 (m, 1H), 1.37 (s, 3H), 1.14 (t, J = 7.0 Hz, 3H), 0.93 (s, 9H) ppm.

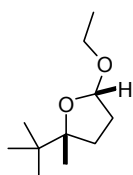
rac-5-*epi*-272f

¹³C NMR (125 MHz, C₆D₆) δ = 104.7, 89.0, 62.2, 37.6, 34.3, 31.9, 25.7, 25.1, 15.6 ppm.

MS (EI) m/z (%): 83 (85), 101 (42), 123 (42), 129 (100), 141 (25), 171 (9).

HRMS (CI (FE) *i*-butane) m/z calculated for C₁₁H₂₃O₂ (M+H⁺) 187.1698, found 187.1696.

The enantiomeric ratio was determined by GC analysis using BGB-176 column SE/SE52 (30 m, 2,3-dimethyl-6-*tert*-butyldimethylsilyl- β -cyclodextrin, i.D. 0.25 mm, df. 0.25 μ m), Detector: FID; Temperature: injector 220 °C, detector 350 °C, oven: 105 °C; gas: 0.5 bar H₂. τ_1 = 8.41 min, τ_2 = 8.76 min.

***cis*-2-(*tert*-Butyl)-5-ethoxy-2-methyltetrahydrofuran (*rac*-272f)^[223]**

Purification: CC on SiO₂ (hexane:EtOAc 50:1). Colorless oil.

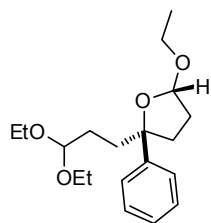
¹H NMR (500 MHz, C₆D₆) δ = 4.96 (d, J = 5.1 Hz, 1H), 3.83-3.76 (m, 1H), 3.28-3.22 (m, 1H), 2.08-2.02 (m, 1H), 1.87-1.80 (m, 2H), 1.16-1.10 (m, 1H, overlapped), 1.12 (t, J = 7.1 Hz, 3H, overlapped), 1.05 (s, 3H), 1.03 (s, 9H) ppm.

¹³C NMR (125 MHz, C₆D₆) δ = 103.7, 90.0, 62.4, 36.8, 32.9, 30.3, 26.3, 22.6, 15.3 ppm.

MS (EI) m/z (%): 83 (80), 101 (39), 123 (34), 129 (100), 141 (19), 171 (9).

HRMS (CI (FE) *i*-butane) m/z calculated for C₁₁H₂₃O₂ (M+H⁺) 187.1698, found 187.1697.

The enantiomeric ratio was determined by GC analysis using BGB-176 column SE/SE52 (30 m, 2,3-dimethyl-6-*tert*-butyldimethylsilyl- β -cyclodextrin, i.D. 0.25 mm, df. 0.25 μ m), Detector: FID; Temperature: injector 220 °C, detector 350 °C, oven: 105 °C; gas: 0.5 bar H₂. τ_1 = 9.26 min, τ_2 = 10.64 min.

***trans*-2-(3,3-diethoxypropyl)-5-ethoxy-2-phenyltetrahydrofuran (*rac*-5-*epi*-272g)***rac*-5-*epi*-272g

Purification: CC on SiO₂ (pentane:Et₂O 9:1). Colorless oil.

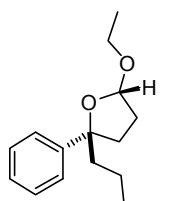
¹H NMR (500 MHz, C₆D₆) δ = 7.37 (d, *J* = 7.2 Hz, 2H), 7.19 (dd, *J* = 8.0, 7.5 Hz, 2H), 7.07 (t, *J* = 7.4 Hz, 1H), 5.11 (d, *J* = 5.0 Hz, 1H), 4.45 (t, *J* = 5.7 Hz, 1H), 3.96-3.90 (m, 1H), 3.54-3.44 (m, 2H), 3.42-3.36 (m, 1H), 3.33-3.27 (m, 2H), 2.27-2.21 (m, 1H), 2.15 (dd, *J* = 9.1, 7.3 Hz, 2H), 2.06-1.99 (m, 1H), 1.90-1.80 (m, 2H), 1.69-1.55 (m, 2H), 1.20 (t, *J* = 7.1 Hz, 3H), 1.09 (t, *J* = 7.0 Hz, 3H), 1.07 (t, *J* = 7.0 Hz, 3H) ppm.

¹³C NMR (125 MHz, C₆D₆) δ = 147.4, 126.6, 125.6, 104.2, 103.1, 88.1, 62.8, 60.5, 60.4, 38.9, 37.7, 32.4, 29.3, 15.6, 15.6 ppm.

MS (EI) *m/z* (%): 231 (12), 191 (100), 163 (5), 141 (6), 117 (14), 103 (14).

HRMS (ESI+) *m/z* calculated for C₁₉H₃₀O₄Na (M+Na⁺) 345.203629, found 345.203629.

The enantiomeric ratio was determined by HPLC analysis using Daicel Chiralcel OJ-H column: *n*-heptane:*i*-PrOH = 98:2, flow rate 0.5 mL/min, λ = 220 nm: τ_1 = 8.04 min, τ_2 = 61.84 min.

***cis*-2-(3,3-Diethoxypropyl)-5-ethoxy-2-phenyltetrahydrofuran (*rac*-272g)***rac*-272g

Purification: CC on SiO₂ (pentane:Et₂O 9:1). Colorless oil.

¹H NMR (500 MHz, C₆D₆) δ = 7.47 (dd, *J* = 8.3, 1.1 Hz, 2H), 7.21 (dd, *J* = 8.0, 7.5 Hz, 2H), 7.08 (t, *J* = 7.4 Hz, 1H), 5.11 (dd, *J* = 4.5, 2.0 Hz, 1H), 4.38 (t, *J* = 5.3 Hz, 1H), 3.89-3.84 (m, 1H), 3.52-3.42 (m, 2H), 3.38-3.32 (m, 1H), 3.31-3.25 (m, 2H), 2.28-2.22 (m, 1H), 1.98-1.78 (m, 6H), 1.67-1.61 (m, 1H), 1.08 (t, *J* = 7.0 Hz, 3H), 1.07 (t, *J* = 7.0 Hz, 3H), 1.03 (t, *J* = 7.1 Hz, 3H) ppm.

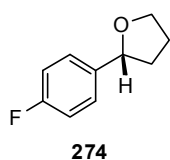
¹³C NMR (125 MHz, C₆D₆) δ = 148.4, 126.5, 125.7, 104.7, 103.1, 87.8, 63.1, 60.7, 60.4, 38.8, 37.0, 33.0, 28.9, 15.6, 15.4 ppm.

MS (EI) *m/z* (%): 231 (11), 191 (100), 163 (5), 141 (5), 117 (14), 103 (11).

HRMS (ESI+) *m/z* calculated for C₁₉H₃₀O₄Na (M+Na⁺) 345.203633, found 345.203831.

The enantiomeric ratio was determined by HPLC analysis using Daicel Chiralcel OJ-H column: *n*-heptane:*i*-PrOH = 98:2, flow rate 0.5 mL/min, λ = 220 nm: τ_1 = 8.83 min, τ_2 = 12.45 min.

7.6.3 Transformations of Resolved Homoaldols

(R)-2-(4-fluorophenyl)tetrahydrofuran (274)^[223]

$\text{BF}_3 \cdot \text{OEt}_2$ (38 μL , 0.30 mmol) was added dropwise to the solution of *cis*-2-ethoxy-5-(4-fluorophenyl)tetrahydrofuran (**268c**, 21.0 mg, 0.100 mmol, er = 97.5:2.5) and Et_3SiH (162 μL , 116 mg, 1.00 mmol,) in dry CH_2Cl_2 (1.0 mL) at -30°C under argon atmosphere. The mixture was allowed to warm to -10°C during 1.5 h. Then saturated aqueous NaHCO_3 -solution (1 mL) was added and the mixture was extracted with Et_2O (10 mL) and dried (MgSO_4). The product was purified by silica gel chromatography with pentane: Et_2O (9:1) as the eluent to afford tetrahydrofuran **274** (15.3 mg, 0.092 mmol, 92%) as a colorless oil.

$^1\text{H NMR}$ (500 MHz, CDCl_3) δ = 7.10-7.06 (m, 2H), 6.86-6.81 (m, 2H), 4.59 (t, J = 7.1 Hz, 1H), 3.81 (td, J = 7.7, 6.2 Hz, 1H), 3.64 (td, J = 7.9, 6.3 Hz, 1H), 1.84-1.77 (m, 1H), 1.56-1.42 (m, 2H), 1.40-1.33 (m, 1H) ppm.

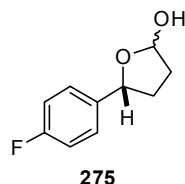
$^{13}\text{C NMR}$ (125 MHz, CDCl_3) δ = 162.4 (d, J = 244 Hz), 140.0 (d, J = 3.1 Hz), 127.5 (d, J = 7.5 Hz), 115.2 (d, J = 21.2 Hz), 80.0, 68.4, 34.9, 26.0 ppm.

MS (EI) m/z (%): 109 (19), 123 (92), 135 (16), 165 (99), 166 (100).

HRMS (EI) m/z calculated for $\text{C}_{10}\text{H}_{11}\text{O}_1\text{F}_1$ 166.0794, found 166.0793.

The enantiomeric ratio was determined by HPLC analysis using Daicel Chiralcel OJ-H column: *n*-heptane:*i*-PrOH = 80:20, flow rate 0.5 mL/min, λ = 210 nm: τ_1 = 12.15 min, τ_2 = 13.90 min.

$[\alpha]_{\text{D}}^{25}$ = $+37.9^\circ$ (c = 0.75, CH_2Cl_2 , er = 98:2).

(5R)-5-(4-Fluorophenyl)tetrahydrofuran-2-ol (275)

A solution of (**268c**, 21.0 mg, 0.100 mmol, er = 97.5:2.5) in MeCN (3.0 mL) was treated with 1 M HCl (1.0 mL). After being stirred at room temperature for 90 min the mixture was diluted with H_2O and extracted with CH_2Cl_2 (3 x 10 mL). The combined organic layers were dried over MgSO_4 , concentrated under reduced pressure and the residue was purified by column chromatography on silica gel using hexane: EtOAc (2:1) as the eluent to give the title compound **275** (16.6 mg, 0.091 mmol, 91%, 1.2:1 mixture of anomers) as a colorless oil.

Major diastereoisomer:

$^1\text{H NMR}$ (500 MHz, C_6D_6) δ = 7.01-6.98 (m, 2H), 6.84-6.78 (m, 2H), 5.42 (dd, J = 6.9, 3.4 Hz, 1H), 5.02 (dd, J = 7.1, 7.1 Hz, 1H), 2.74 (d, J = 3.1 Hz, 1H), 2.09-2.02 (m, 1H), 1.83-1.75 (m, 1H), 1.74-1.67 (m, 1H), 1.35-1.28 (m, 1H) ppm.

Minor diastereoisomer:

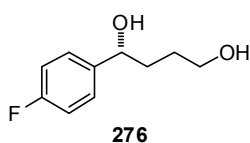
$^1\text{H NMR}$ (500 MHz, C_6D_6) δ = 7.23-7.19 (m, 2H), 6.89-6.84 (m, 2H), 5.31 (dd, J = 4.6, 3.5 Hz, 1H), 4.65 (dd, J = 9.2, 6.4 Hz, 1H), 2.83 (dd, J = 3.2, 1.5 Hz, 1H), 1.83-1.75 (m, 1H), 1.74-1.67 (m, 2H), 1.56-1.49 (m, 1H) ppm.

$^{13}\text{C NMR}$ (125 MHz, C_6D_6) δ = 162.6 (d, J = 244.7 Hz), 162.5 (d, J = 244.6 Hz), 139.7 (d, J = 3.1 Hz), 139.0 (d, J = 3.0 Hz), 128.4 (d, J = 8.0 Hz), 127.6 (d, J = 8.2 Hz), 115.4, 115.2, 99.1, 98.8, 82.2, 78.9, 34.7, 33.2, 33.2 ppm.

MS (EI) m/z (%): 182 (15), 135 (31), 125 (100), 115 (9), 109 (22), 97 (29).

HRMS (EI) m/z calculated for $\text{C}_{10}\text{H}_{11}\text{O}_2\text{F}_1$ 182.0743, found 182.0744.

(*R*)-1-(4-Fluorophenyl)butane-1,4-diol (**276**)



At 0 °C NaBH_4 (18.7 mg, 0.494 mmol) was added to a solution of lactol **275** (15.0 mg, 0.082 mmol, er = 97.5:2.5) in MeOH (2.0 mL). The mixture was stirred at 0 °C for 30 min, then SiO_2 (500 mg) was added and the solvent was removed *in vacuo*. The residue was loaded onto a pad of silica gel and eluted with hexane:EtOAc:MeOH (1:3:0.2) to give the title compound **276** (13.6 mg, 0.0738 mmol, 90%) as a colorless solid.

$^1\text{H NMR}$ (500 MHz, CDCl_3) δ = 7.33-7.30 (m, 2H), 7.04-7.00 (m, 2H), 4.71 (t, J = 6.3 Hz, 1H), 3.73-3.64 (m, 2H), 2.53 (s, 2H), 1.85-1.81 (m, 2H), 1.70-1.63 (m, 2H) ppm.

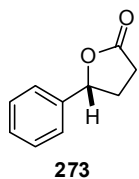
$^{13}\text{C NMR}$ (125 MHz, CDCl_3) δ = 162.2 (d, J = 245.6 Hz), 140.5 (d, J = 3.0 Hz), 127.5 (d, J = 7.7 Hz), 115.4 (d, J = 21.4 Hz), 73.9, 63.0, 36.6, 29.2 ppm.

MS (EI) m/z (%): 184 (13), 138 (5), 125 (100), 97 (36).

HRMS (EI) m/z calculated for $\text{C}_{10}\text{H}_{13}\text{O}_2\text{F}_1$ 184.0900, found 182.0898.

The enantiomeric ratio was determined by HPLC analysis using Daicel Chiralcel OB-H column: *n*-heptane:*i*-PrOH = 90:10, flow rate 0.5 mL/min, λ = 220 nm: τ_1 = 21.66 min, τ_2 = 23.29 min.

$[\alpha]_{\text{D}}^{25}$ = +44.1 (c = 0.200, CH_2Cl_2 , er = 97.5:2.5).

(R)-5-Phenyldihydrofuran-2(3H)-one (273)

A small sample of **268a** (er = 96.5:3.5) was oxidized as described below for **272a** to give the title compound **273** as a colorless oil.

$^1\text{H NMR}$ (500 MHz, C_6D_6) δ = 7.10-7.02 (m, 3H), 7.01-6.99 (m, 2H), 4.72 (t, J = 7.5 Hz, 1H), 1.97-1.91 (m, 1H), 1.86-1.79 (m, 1H), 1.61-1.54 (m, 1H), 1.39-1.28 (m,

1H) ppm.

$^{13}\text{C NMR}$ (125 MHz, C_6D_6) δ = 175.6, 140.4, 128.8, 128.3, 125.5, 80.4, 30.9, 28.6 ppm.

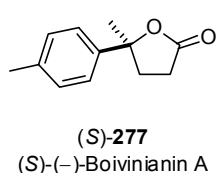
MS (EI) m/z (%): 162 (100), 117 (30), 107 (70), 91 (14), 77 (30).

HRMS (EI) m/z calculated for $\text{C}_{10}\text{H}_{10}\text{O}_2$ 162.068082, found 162.068013.

The enantiomeric ratio was determined by HPLC analysis using Daicel Chiralcel OB-H column: *n*-heptane:*i*-PrOH = 60:40, flow rate 1.0 mL/min, λ = 220 nm: τ_1 = 12.94 min, τ_2 = 16.89 min.

$[\alpha]_{\text{D}}^{25}$ = +31.1° (c = 0.135, CHCl_3 , er = 96.5:3.5)

The absolute configuration was assigned as (*R*) by comparison of the optical rotation with a literature reported value.^[177]

(S)-5-Methyl-5-(*p*-tolyl)dihydrofuran-2(3H)-one ((S)-Boivinianin A, (S)-277)

CrO_3 (60.0 mg, 0.600 mmol) and conc. H_2SO_4 (2 drops) were subsequently added to a vigorously stirred solution of (*S*)-5,5-diethoxy-2-(*p*-tolyl)pentan-2-ol ((*S*)-**271a**, 26.6 mg, 0.100 mmol, er = 96:4) in acetone: H_2O (3:1, 2.0 mL) at ambient temperature. The mixture was

stirred for 24 h before the reaction was quenched with *i*-PrOH (0.5 mL) and diluted with H_2O (5 mL) and CH_2Cl_2 (10 mL). The layers were separated and the green aqueous layer was extracted with CH_2Cl_2 (3 x 10 mL). The combined organic layers were dried over MgSO_4 and concentrated under reduced pressure. Purification of the residue by column chromatography on silica gel using pentane: Et_2O (1:1) as the eluent afforded the title compound (**S**)-**277** (17.0 mg, 0.089 mmol, 89%) as a colorless oil.

$^1\text{H NMR}$ (500 MHz, C_6D_6) δ = 7.09 (d, J = 8.2 Hz, 2H), 6.92 (d, J = 8.0 Hz, 2H), 2.07 (s, 3H), 2.02-1.88 (m, 2H), 1.76-1.70 (m, 1H), 1.57-1.51 (m, 1H), 1.28 (s, 3H) ppm.

$^{13}\text{C NMR}$ (125 MHz, C_6D_6) δ = 175.3, 142.4, 137.1, 129.4, 124.4, 85.8, 36.0, 29.2, 28.8, 20.9 ppm.

MS (EI) m/z (%): 190 (25), 175 (100), 147 (8), 135 (37), 119 (35), 91 (21).

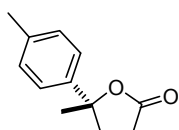
HRMS (EI) m/z calculated for $\text{C}_{12}\text{H}_{14}\text{O}_2$ 190.099378, found 190.099233.

The enantiomeric ratio was determined by HPLC analysis using Daicel Chiralcel OJ-H column: *n*-heptane:*i*-PrOH = 70:30, flow rate 0.5 mL/min, $\lambda = 220$ nm: $\tau_1 = 12.34$ min, $\tau_2 = 15.30$ min.

$[\alpha]_D^{25} = -49.0^\circ$ ($c = 0.204$, CHCl_3 , er = 96:4)

The absolute configuration was assigned as (*S*) by comparison of the optical rotation with a literature reported value.^[179]

(*R*)-5-Methyl-5-(*p*-tolyl)dihydrofuran-2(3H)-one ((*R*)-Boivinianin A, (*R*)-277)



(*R*)-277
(*R*)-(+)-Boivinianin A

Following the same procedure as described for homoaldol **271a** and using 30.0 mg (0.300 mmol) of CrO_3 the title compound was obtained from (2*R*,5*S*)-2-ethoxy-5-methyl-5-(*p*-tolyl)tetrahydrofuran (**272a**, 22.0 mg, 0.100 mmol, er = 98.5:1.5) as a colorless oil (18.2 mg, 0.096 mmol, 96%).

The enantiomeric ratio was determined by HPLC analysis using Daicel Chiralcel OJ-H column: *n*-heptane:*i*-PrOH = 70:30, flow rate 0.5 mL/min, $\lambda = 220$ nm: $\tau_1 = 12.34$ min, $\tau_2 = 15.30$ min.

$[\alpha]_D^{25} = +50.8^\circ$ ($c = 0.370$, CHCl_3 , er = 98:2)

The absolute configuration was assigned as (*R*) by comparison of the optical rotation with a literature reported value.^[179]

When a sample of (5-*epi*-**272a**) was oxidized under identical conditions, (*S*)-(–)-Boivinianin A (*S*)-**277** was obtained (absolute configuration assigned by comparison of the previously obtained HPLC retention time).

7.7 X-Ray Crystal Structure Data

Compound 145a

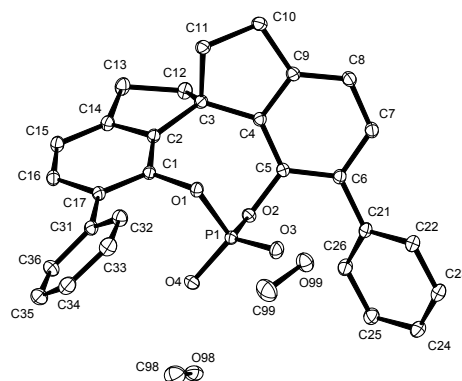
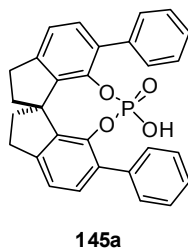


Table 1. Crystal data and structure refinement.

Identification code	6515	
Empirical formula	C ₃₁ H ₃₁ O ₆ P	
Color	colorless	
Formula weight	530.53 g·mol ⁻¹	
Temperature	100 K	
Wavelength	0.71073 Å	
Crystal system	Triclinic	
Space group	P1, (no. 2)	
Unit cell dimensions	a = 9.4417(2) Å b = 12.6075(3) Å c = 12.9731(3) Å	α = 99.2400(10)°. β = 110.8050(10)°. γ = 107.5480(10)°.
Volume	1312.87(5) Å ³	
Z	2	
Density (calculated)	1.342 Mg·m ⁻³	
Absorption coefficient	0.149 mm ⁻¹	
F(000)	560 e	
Crystal size	0.50 x 0.50 x 0.30 mm ³	
θ range for data collection	3.31 to 37.91°.	
Index ranges	-16 ≤ h ≤ 16, -21 ≤ k ≤ 19, -22 ≤ l ≤ 22	
Reflections collected	36822	
Independent reflections	13943 [R _{int} = 0.0268]	
Reflections with I > 2σ(I)	12478	
Completeness to θ = 37.91°	98.1%	
Absorption correction	Empirical	
Max. and min. transmission	0.96 and 0.56	
Refinement method	Full-matrix least-squares on F ²	
Data / restraints / parameters	13943 / 0 / 346	
Goodness-of-fit on F ²	1.265	
Final R indices [I > 2σ(I)]	R ₁ = 0.0701	wR ² = 0.1669
R indices (all data)	R ₁ = 0.0746	wR ² = 0.1729
Extinction coefficient	0.71(2)	
Largest diff. peak and hole	1.293 and -1.423 e·Å ⁻³	

Table 2. Atomic coordinates and equivalent isotropic displacement parameters (\AA^2).

U_{eq} is defined as one third of the trace of the orthogonalized U_{ij} tensor.

	x	y	z	U_{eq}
C(1)	0.8970(1)	0.8530(1)	0.2882(1)	0.011(1)
C(2)	0.7954(1)	0.9139(1)	0.2611(1)	0.012(1)
C(3)	0.7580(1)	0.9733(1)	0.1677(1)	0.012(1)
C(4)	0.7544(1)	0.9305(1)	0.0503(1)	0.012(1)
C(5)	0.7084(1)	0.8184(1)	-0.0177(1)	0.012(1)
C(6)	0.6899(1)	0.7960(1)	-0.1323(1)	0.012(1)
C(7)	0.7299(1)	0.8924(1)	-0.1734(1)	0.014(1)
C(8)	0.7896(1)	1.0065(1)	-0.1032(1)	0.014(1)
C(9)	0.8004(1)	1.0247(1)	0.0083(1)	0.013(1)
C(10)	0.8593(1)	1.1384(1)	0.0995(1)	0.015(1)
C(11)	0.8875(1)	1.1008(1)	0.2101(1)	0.014(1)
C(12)	0.5892(1)	0.9753(1)	0.1565(1)	0.015(1)
C(13)	0.6025(1)	0.9930(1)	0.2806(1)	0.016(1)
C(14)	0.7173(1)	0.9348(1)	0.3314(1)	0.013(1)
C(15)	0.7503(1)	0.9023(1)	0.4320(1)	0.014(1)
C(16)	0.8618(1)	0.8488(1)	0.4621(1)	0.014(1)
C(17)	0.9366(1)	0.8217(1)	0.3910(1)	0.012(1)
C(21)	0.6292(1)	0.6761(1)	-0.2100(1)	0.013(1)
C(22)	0.7005(1)	0.6526(1)	-0.2844(1)	0.015(1)
C(23)	0.6403(1)	0.5418(1)	-0.3606(1)	0.017(1)
C(24)	0.5071(1)	0.4523(1)	-0.3645(1)	0.017(1)
C(25)	0.4341(1)	0.4744(1)	-0.2917(1)	0.018(1)
C(26)	0.4955(1)	0.5854(1)	-0.2145(1)	0.016(1)
C(31)	1.0588(1)	0.7685(1)	0.4304(1)	0.013(1)
C(32)	1.2045(1)	0.8042(1)	0.4159(1)	0.016(1)
C(33)	1.3264(1)	0.7632(1)	0.4647(1)	0.018(1)
C(34)	1.3064(1)	0.6860(1)	0.5290(1)	0.019(1)
C(35)	1.1611(1)	0.6480(1)	0.5420(1)	0.019(1)
C(36)	1.0379(1)	0.6881(1)	0.4925(1)	0.017(1)
C(98)	0.9849(1)	0.4494(1)	0.2180(1)	0.025(1)
C(99)	1.3211(2)	0.6554(1)	0.1492(1)	0.030(1)
O(1)	0.9587(1)	0.8212(1)	0.2096(1)	0.012(1)
O(2)	0.6847(1)	0.7266(1)	0.0314(1)	0.013(1)
O(3)	0.9397(1)	0.6864(1)	0.0382(1)	0.017(1)
O(4)	0.7733(1)	0.6086(1)	0.1498(1)	0.017(1)
O(98)	0.8218(1)	0.4296(1)	0.1388(1)	0.019(1)
O(99)	1.2367(1)	0.6971(1)	0.0597(1)	0.021(1)
P(1)	0.8440(1)	0.7044(1)	0.1028(1)	0.012(1)

Compound 183

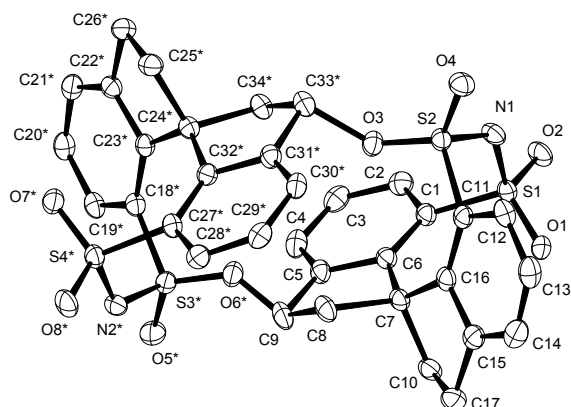
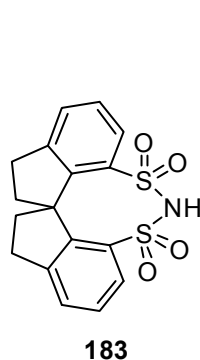


Table 1. Crystal data and structure refinement.

Identification code	6820	
Empirical formula	$C_{17}H_{15}NO_4S_2$	
Color	colourless	
Formula weight	$361.42 \text{ g}\cdot\text{mol}^{-1}$	
Temperature	100(2) K	
Wavelength	0.71073 \AA	
Crystal system	monoclinic	
Space group	$P2_1/n$, (no. 14)	
Unit cell dimensions	$a = 9.9771(2) \text{ \AA}$	$\alpha = 90^\circ$.
	$b = 14.2047(3) \text{ \AA}$	$\beta = 94.0600(10)^\circ$.
	$c = 21.9197(4) \text{ \AA}$	$\gamma = 90^\circ$.
Volume	$3098.70(11) \text{ \AA}^3$	
Z	8	
Density (calculated)	$1.549 \text{ Mg}\cdot\text{m}^{-3}$	
Absorption coefficient	0.366 mm^{-1}	
F(000)	1504 e	
Crystal size	$0.22 \times 0.16 \times 0.05 \text{ mm}^3$	
θ range for data collection	3.02 to 33.29° .	
Index ranges	$-15 \leq h \leq 15$, $-21 \leq k \leq 21$, $-33 \leq l \leq 33$	
Reflections collected	85682	
Independent reflections	11835 [$R_{\text{int}} = 0.1117$]	
Reflections with $I > 2\sigma(I)$	7293	
Completeness to $\theta = 33.29^\circ$	99.0 %	
Absorption correction	Gaussian	
Max. and min. transmission	0.98 and 0.94	
Refinement method	Full-matrix least-squares on F^2	
Data / restraints / parameters	11835 / 0 / 433	
Goodness-of-fit on F^2	1.024	
Final R indices [$I > 2\sigma(I)$]	$R_1 = 0.0637$	$wR^2 = 0.1434$
R indices (all data)	$R_1 = 0.1214$	$wR^2 = 0.1707$
Largest diff. peak and hole	0.620 and $-0.880 \text{ e}\cdot\text{\AA}^{-3}$	

Table 2. Atomic coordinates and equivalent isotropic displacement parameters (\AA^2).

U_{eq} is defined as one third of the trace of the orthogonalized U_{ij} tensor.

	x	y	z	U_{eq}
C(1)	0.5730(2)	0.3291(2)	0.1245(1)	0.020(1)
C(2)	0.4400(2)	0.3306(2)	0.1410(1)	0.023(1)
C(3)	0.4081(3)	0.2925(2)	0.1964(1)	0.026(1)
C(4)	0.5105(3)	0.2558(2)	0.2363(1)	0.025(1)
C(5)	0.6423(2)	0.2587(2)	0.2209(1)	0.021(1)
C(6)	0.6767(2)	0.2947(2)	0.1641(1)	0.019(1)
C(7)	0.8273(2)	0.2826(2)	0.1588(1)	0.020(1)
C(8)	0.8775(3)	0.2817(2)	0.2279(1)	0.024(1)
C(9)	0.7663(3)	0.2307(2)	0.2599(1)	0.026(1)
C(10)	0.8566(2)	0.1855(2)	0.1294(1)	0.024(1)
C(11)	0.9152(2)	0.4444(2)	0.1108(1)	0.020(1)
C(12)	1.0172(2)	0.4870(2)	0.0795(1)	0.025(1)
C(13)	1.1202(3)	0.4318(2)	0.0597(1)	0.028(1)
C(14)	1.1208(2)	0.3357(2)	0.0690(1)	0.028(1)
C(15)	1.0206(2)	0.2940(2)	0.1011(1)	0.023(1)
C(16)	0.9165(2)	0.3475(2)	0.1230(1)	0.020(1)
C(17)	1.0041(3)	0.1910(2)	0.1152(1)	0.027(1)
C(18)	0.4557(2)	0.8203(2)	0.1142(1)	0.020(1)
C(19)	0.5609(2)	0.7813(2)	0.0836(1)	0.022(1)
C(20)	0.6547(2)	0.8398(2)	0.0587(1)	0.023(1)
C(21)	0.6402(2)	0.9370(2)	0.0619(1)	0.023(1)
C(22)	0.5337(2)	0.9754(2)	0.0912(1)	0.020(1)
C(23)	0.4410(2)	0.9181(2)	0.1192(1)	0.018(1)
C(24)	0.3449(2)	0.9806(2)	0.1523(1)	0.019(1)
C(25)	0.3528(2)	1.0737(2)	0.1150(1)	0.023(1)
C(26)	0.4984(2)	1.0780(2)	0.0971(1)	0.024(1)
C(27)	0.0972(2)	0.9120(2)	0.1278(1)	0.021(1)
C(28)	-0.0347(2)	0.9101(2)	0.1454(1)	0.022(1)
C(29)	-0.0675(2)	0.9574(2)	0.1980(1)	0.023(1)
C(30)	0.0332(2)	1.0021(2)	0.2343(1)	0.022(1)
C(31)	0.1642(2)	1.0016(2)	0.2171(1)	0.021(1)
C(32)	0.1985(2)	0.9588(2)	0.1627(1)	0.019(1)
C(33)	0.2864(2)	1.0431(2)	0.2517(1)	0.023(1)
C(34)	0.4021(2)	0.9973(2)	0.2199(1)	0.023(1)
N(1)	0.6595(2)	0.4871(1)	0.0728(1)	0.022(1)
N(2)	0.2033(2)	0.7495(1)	0.0873(1)	0.021(1)
O(1)	0.7065(2)	0.3290(1)	0.0267(1)	0.023(1)
O(2)	0.4783(2)	0.3965(1)	0.0191(1)	0.025(1)
O(3)	0.7364(2)	0.4927(1)	0.1858(1)	0.023(1)
O(4)	0.8063(2)	0.6132(1)	0.1126(1)	0.025(1)
O(5)	0.3807(2)	0.6472(1)	0.1323(1)	0.027(1)
O(6)	0.2912(2)	0.7734(1)	0.1963(1)	0.023(1)
O(7)	0.2191(2)	0.9023(1)	0.0263(1)	0.024(1)
O(8)	0.0042(2)	0.8178(1)	0.0311(1)	0.028(1)
S(1)	0.6032(1)	0.3804(1)	0.0544(1)	0.019(1)
S(2)	0.7795(1)	0.5170(1)	0.1268(1)	0.019(1)
S(3)	0.3350(1)	0.7419(1)	0.1389(1)	0.020(1)
S(4)	0.1279(1)	0.8499(1)	0.0611(1)	0.021(1)

Table 3. Bond lengths [Å] and angles [°].

C(1)-C(6)	1.391(3)	C(1)-C(2)	1.400(3)
C(1)-S(1)	1.746(2)	C(2)-C(3)	1.386(4)
C(3)-C(4)	1.397(4)	C(4)-C(5)	1.382(3)
C(5)-C(6)	1.411(3)	C(5)-C(9)	1.506(3)
C(6)-C(7)	1.525(3)	C(7)-C(16)	1.535(3)
C(7)-C(10)	1.559(3)	C(7)-C(8)	1.563(3)
C(8)-C(9)	1.535(3)	C(10)-C(17)	1.527(4)
C(11)-C(16)	1.403(3)	C(11)-C(12)	1.404(3)
C(11)-S(2)	1.756(2)	C(12)-C(13)	1.387(4)
C(13)-C(14)	1.380(4)	C(14)-C(15)	1.394(4)
C(15)-C(16)	1.399(3)	C(15)-C(17)	1.507(4)
C(18)-C(19)	1.399(3)	C(18)-C(23)	1.402(3)
C(18)-S(3)	1.754(2)	C(19)-C(20)	1.392(3)
C(20)-C(21)	1.391(4)	C(21)-C(22)	1.391(3)
C(22)-C(23)	1.404(3)	C(22)-C(26)	1.508(3)
C(23)-C(24)	1.527(3)	C(24)-C(32)	1.526(3)
C(24)-C(25)	1.559(3)	C(24)-C(34)	1.568(3)
C(25)-C(26)	1.532(3)	C(27)-C(32)	1.392(3)
C(27)-C(28)	1.397(3)	C(27)-S(4)	1.754(2)
C(28)-C(29)	1.394(3)	C(29)-C(30)	1.390(4)
C(30)-C(31)	1.386(3)	C(31)-C(32)	1.402(3)
C(31)-C(33)	1.509(3)	C(33)-C(34)	1.535(3)
N(1)-S(1)	1.657(2)	N(1)-S(2)	1.678(2)
N(2)-S(3)	1.675(2)	N(2)-S(4)	1.694(2)
O(1)-S(1)	1.4327(18)	O(2)-S(1)	1.4376(17)
O(3)-S(2)	1.4329(17)	O(4)-S(2)	1.4306(18)
O(5)-S(3)	1.4312(18)	O(6)-S(3)	1.4318(17)
O(7)-S(4)	1.4356(18)	O(8)-S(4)	1.4316(18)
C(6)-C(1)-C(2)	121.4(2)	C(6)-C(1)-S(1)	121.89(18)
C(2)-C(1)-S(1)	116.56(18)	C(3)-C(2)-C(1)	120.1(2)
C(2)-C(3)-C(4)	119.4(2)	C(5)-C(4)-C(3)	120.2(2)
C(4)-C(5)-C(6)	121.4(2)	C(4)-C(5)-C(9)	127.7(2)
C(6)-C(5)-C(9)	110.8(2)	C(1)-C(6)-C(5)	117.4(2)
C(1)-C(6)-C(7)	133.3(2)	C(5)-C(6)-C(7)	109.2(2)
C(6)-C(7)-C(16)	125.53(19)	C(6)-C(7)-C(10)	110.25(19)
C(16)-C(7)-C(10)	100.84(19)	C(6)-C(7)-C(8)	100.19(19)
C(16)-C(7)-C(8)	110.04(19)	C(10)-C(7)-C(8)	109.69(19)
C(9)-C(8)-C(7)	104.70(19)	C(5)-C(9)-C(8)	102.01(19)
C(17)-C(10)-C(7)	104.5(2)	C(16)-C(11)-C(12)	121.2(2)
C(16)-C(11)-S(2)	122.35(18)	C(12)-C(11)-S(2)	116.12(19)
C(13)-C(12)-C(11)	119.2(2)	C(14)-C(13)-C(12)	120.6(2)
C(13)-C(14)-C(15)	120.0(2)	C(14)-C(15)-C(16)	121.2(2)
C(14)-C(15)-C(17)	127.5(2)	C(16)-C(15)-C(17)	111.2(2)
C(15)-C(16)-C(11)	117.7(2)	C(15)-C(16)-C(7)	108.7(2)
C(11)-C(16)-C(7)	133.6(2)	C(15)-C(17)-C(10)	102.27(19)
C(19)-C(18)-C(23)	121.0(2)	C(19)-C(18)-S(3)	116.81(18)
C(23)-C(18)-S(3)	121.84(18)	C(20)-C(19)-C(18)	120.0(2)
C(21)-C(20)-C(19)	119.9(2)	C(20)-C(21)-C(22)	119.9(2)
C(21)-C(22)-C(23)	121.5(2)	C(21)-C(22)-C(26)	127.6(2)
C(23)-C(22)-C(26)	110.9(2)	C(18)-C(23)-C(22)	117.6(2)
C(18)-C(23)-C(24)	133.2(2)	C(22)-C(23)-C(24)	109.05(19)
C(32)-C(24)-C(23)	126.38(19)	C(32)-C(24)-C(25)	109.54(19)
C(23)-C(24)-C(25)	100.76(18)	C(32)-C(24)-C(34)	100.25(18)
C(23)-C(24)-C(34)	109.79(18)	C(25)-C(24)-C(34)	109.77(19)
C(26)-C(25)-C(24)	104.60(19)	C(22)-C(26)-C(25)	102.43(19)

C(32)-C(27)-C(28)	121.3(2)	C(32)-C(27)-S(4)	122.34(18)
C(28)-C(27)-S(4)	116.34(18)	C(29)-C(28)-C(27)	120.0(2)
C(30)-C(29)-C(28)	119.4(2)	C(31)-C(30)-C(29)	119.9(2)
C(30)-C(31)-C(32)	121.7(2)	C(30)-C(31)-C(33)	127.2(2)
C(32)-C(31)-C(33)	111.1(2)	C(27)-C(32)-C(31)	117.6(2)
C(27)-C(32)-C(24)	132.9(2)	C(31)-C(32)-C(24)	109.44(19)
C(31)-C(33)-C(34)	102.27(19)	C(33)-C(34)-C(24)	104.99(19)
S(1)-N(1)-S(2)	128.01(13)	S(3)-N(2)-S(4)	126.22(12)
O(1)-S(1)-O(2)	118.43(11)	O(1)-S(1)-N(1)	109.14(11)
O(2)-S(1)-N(1)	104.53(10)	O(1)-S(1)-C(1)	109.51(11)
O(2)-S(1)-C(1)	110.05(11)	N(1)-S(1)-C(1)	104.13(11)
O(4)-S(2)-O(3)	119.90(11)	O(4)-S(2)-N(1)	102.90(10)
O(3)-S(2)-N(1)	109.34(10)	O(4)-S(2)-C(11)	111.01(11)
O(3)-S(2)-C(11)	108.86(11)	N(1)-S(2)-C(11)	103.45(11)
O(5)-S(3)-O(6)	120.01(11)	O(5)-S(3)-N(2)	103.47(11)
O(6)-S(3)-N(2)	107.43(10)	O(5)-S(3)-C(18)	109.58(11)
O(6)-S(3)-C(18)	109.38(11)	N(2)-S(3)-C(18)	105.94(10)
O(8)-S(4)-O(7)	118.65(11)	O(8)-S(4)-N(2)	103.62(11)
O(7)-S(4)-N(2)	109.53(10)	O(8)-S(4)-C(27)	110.30(11)
O(7)-S(4)-C(27)	109.70(11)	N(2)-S(4)-C(27)	103.87(11)

Table 4. Anisotropic displacement parameters (\AA^2).

The anisotropic displacement factor exponent takes the form:

$$-2\pi^2 [h^2 a^{*2} U_{11} + \dots + 2 h k a^* b^* U_{12}].$$

	U_{11}	U_{22}	U_{33}	U_{23}	U_{13}	U_{12}
C(1)	0.023(1)	0.019(1)	0.016(1)	-0.001(1)	-0.001(1)	-0.001(1)
C(2)	0.023(1)	0.023(1)	0.024(1)	-0.003(1)	-0.001(1)	0.000(1)
C(3)	0.024(1)	0.026(1)	0.027(1)	-0.007(1)	0.005(1)	-0.005(1)
C(4)	0.034(1)	0.024(1)	0.019(1)	-0.002(1)	0.005(1)	-0.009(1)
C(5)	0.028(1)	0.019(1)	0.016(1)	-0.001(1)	-0.001(1)	-0.004(1)
C(6)	0.024(1)	0.017(1)	0.017(1)	-0.001(1)	-0.001(1)	-0.001(1)
C(7)	0.022(1)	0.020(1)	0.016(1)	0.001(1)	-0.004(1)	0.001(1)
C(8)	0.026(1)	0.027(1)	0.018(1)	0.003(1)	-0.007(1)	-0.001(1)
C(9)	0.035(1)	0.026(1)	0.017(1)	0.005(1)	-0.005(1)	-0.004(1)
C(10)	0.028(1)	0.021(1)	0.022(1)	0.002(1)	-0.004(1)	0.004(1)
C(11)	0.019(1)	0.023(1)	0.015(1)	-0.002(1)	-0.002(1)	0.000(1)
C(12)	0.023(1)	0.031(1)	0.019(1)	0.005(1)	-0.002(1)	-0.003(1)
C(13)	0.020(1)	0.044(2)	0.021(1)	0.003(1)	0.002(1)	-0.004(1)
C(14)	0.019(1)	0.041(2)	0.023(1)	-0.006(1)	-0.002(1)	0.004(1)
C(15)	0.021(1)	0.029(1)	0.018(1)	-0.002(1)	-0.004(1)	0.003(1)
C(16)	0.019(1)	0.026(1)	0.014(1)	0.000(1)	-0.003(1)	0.001(1)
C(17)	0.028(1)	0.027(1)	0.025(1)	0.000(1)	-0.003(1)	0.009(1)
C(18)	0.022(1)	0.021(1)	0.016(1)	-0.001(1)	0.000(1)	0.001(1)
C(19)	0.024(1)	0.024(1)	0.017(1)	-0.002(1)	-0.002(1)	0.004(1)
C(20)	0.018(1)	0.033(1)	0.019(1)	-0.002(1)	0.002(1)	0.003(1)
C(21)	0.019(1)	0.031(1)	0.018(1)	0.001(1)	0.001(1)	-0.002(1)
C(22)	0.019(1)	0.023(1)	0.018(1)	-0.001(1)	-0.002(1)	-0.002(1)
C(23)	0.017(1)	0.022(1)	0.015(1)	0.000(1)	-0.001(1)	0.001(1)
C(24)	0.020(1)	0.020(1)	0.018(1)	-0.001(1)	-0.001(1)	0.001(1)
C(25)	0.024(1)	0.019(1)	0.025(1)	0.000(1)	-0.001(1)	-0.001(1)
C(26)	0.025(1)	0.022(1)	0.024(1)	0.001(1)	0.000(1)	-0.004(1)
C(27)	0.022(1)	0.023(1)	0.015(1)	0.000(1)	-0.001(1)	0.001(1)
C(28)	0.020(1)	0.025(1)	0.022(1)	0.002(1)	-0.002(1)	0.000(1)

C(29)	0.021(1)	0.026(1)	0.023(1)	0.005(1)	0.004(1)	0.004(1)
C(30)	0.027(1)	0.023(1)	0.017(1)	0.001(1)	0.003(1)	0.005(1)
C(31)	0.024(1)	0.020(1)	0.018(1)	0.001(1)	0.000(1)	0.003(1)
C(32)	0.020(1)	0.019(1)	0.017(1)	0.002(1)	0.000(1)	0.001(1)
C(33)	0.027(1)	0.024(1)	0.020(1)	-0.004(1)	-0.001(1)	0.002(1)
C(34)	0.022(1)	0.025(1)	0.020(1)	-0.004(1)	-0.002(1)	0.001(1)
N(1)	0.024(1)	0.020(1)	0.022(1)	0.003(1)	-0.006(1)	0.002(1)
N(2)	0.022(1)	0.021(1)	0.022(1)	-0.003(1)	0.002(1)	-0.004(1)
O(1)	0.028(1)	0.026(1)	0.015(1)	-0.002(1)	-0.001(1)	0.004(1)
O(2)	0.025(1)	0.027(1)	0.022(1)	0.003(1)	-0.010(1)	0.003(1)
O(3)	0.027(1)	0.024(1)	0.017(1)	-0.002(1)	0.002(1)	-0.002(1)
O(4)	0.030(1)	0.020(1)	0.027(1)	0.002(1)	0.001(1)	-0.002(1)
O(5)	0.034(1)	0.020(1)	0.027(1)	0.002(1)	0.004(1)	0.002(1)
O(6)	0.028(1)	0.025(1)	0.017(1)	0.002(1)	0.004(1)	0.001(1)
O(7)	0.025(1)	0.029(1)	0.018(1)	0.002(1)	0.001(1)	-0.003(1)
O(8)	0.024(1)	0.039(1)	0.021(1)	-0.006(1)	-0.004(1)	-0.006(1)
S(1)	0.022(1)	0.021(1)	0.015(1)	0.001(1)	-0.004(1)	0.002(1)
S(2)	0.022(1)	0.019(1)	0.016(1)	0.000(1)	0.000(1)	-0.001(1)
S(3)	0.024(1)	0.020(1)	0.017(1)	0.000(1)	0.003(1)	0.000(1)
S(4)	0.022(1)	0.025(1)	0.016(1)	-0.002(1)	-0.001(1)	-0.002(1)

Compound 185

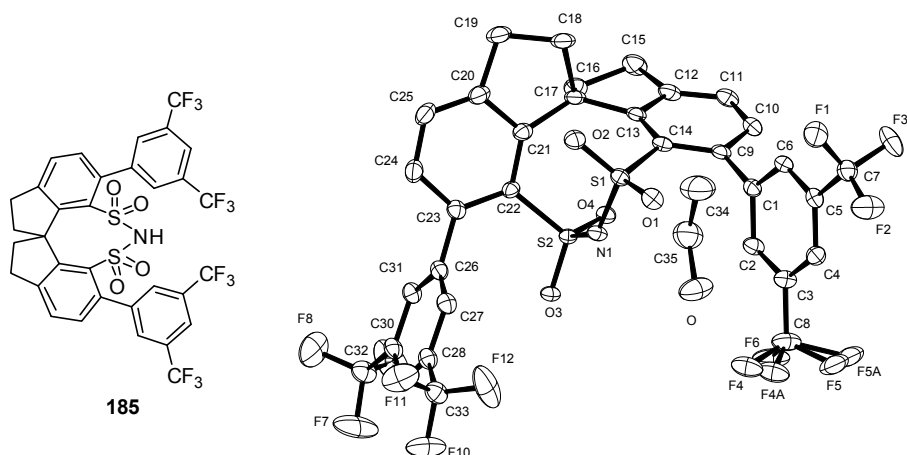


Table 1. Crystal data and structure refinement.

Identification code	KappaCCD	
Empirical formula	$C_{35}H_{25}F_{12}NO_5S_2$	
Color	colourless	
Formula weight	$831.68 \text{ g}\cdot\text{mol}^{-1}$	
Temperature	100 K	
Wavelength	0.71073 \AA	
Crystal system	MONOCLINIC	
Space group	$P2_1/c$, (no. 14)	
Unit cell dimensions	$a = 13.701(2) \text{ \AA}$	$\alpha = 90^\circ$.
	$b = 15.7984(19) \text{ \AA}$	$\beta = 111.365(14)^\circ$.
	$c = 16.969(3) \text{ \AA}$	$\gamma = 90^\circ$.
Volume	$3420.6(9) \text{ \AA}^3$	
Z	4	
Density (calculated)	$1.615 \text{ Mg}\cdot\text{m}^{-3}$	
Absorption coefficient	0.267 mm^{-1}	
F(000)	1688 e	
Crystal size	$0.20 \times 0.19 \times 0.08 \text{ mm}^3$	
θ range for data collection	2.71 to 27.50° .	
Index ranges	$-17 \leq h \leq 17$, $-20 \leq k \leq 20$, $-22 \leq l \leq 22$	
Reflections collected	52651	
Independent reflections	7837 [$R_{\text{int}} = 0.0677$]	
Reflections with $I > 2\sigma(I)$	5897	
Completeness to $\theta = 27.50^\circ$	99.9 %	
Absorption correction	Gaussian	
Max. and min. transmission	0.98 and 0.94	
Refinement method	Full-matrix least-squares on F^2	
Data / restraints / parameters	7837 / 0 / 505	
Goodness-of-fit on F^2	1.069	
Final R indices [$I > 2\sigma(I)$]	$R_1 = 0.0498$	$wR^2 = 0.1122$
R indices (all data)	$R_1 = 0.0745$	$wR^2 = 0.1288$
Largest diff. peak and hole	0.908 and $-0.454 \text{ e}\cdot\text{\AA}^{-3}$	

Table 2. Atomic coordinates and equivalent isotropic displacement parameters (\AA^2). U_{eq} is defined as one third of the trace of the orthogonalized U_{ij} tensor.

	x	y	z	U_{eq}
S(1)	0.1243(1)	0.0661(1)	0.4791(1)	0.019(1)
S(2)	-0.0024(1)	0.2218(1)	0.4227(1)	0.017(1)
O(3)	-0.1066(1)	0.2320(1)	0.3614(1)	0.021(1)
O(1)	0.1186(1)	-0.0129(1)	0.4362(1)	0.024(1)
O(2)	0.1274(1)	0.0638(1)	0.5645(1)	0.025(1)
N(1)	0.0217(2)	0.1195(1)	0.4178(1)	0.019(1)
F(1)	0.3756(1)	-0.2098(1)	0.4150(1)	0.037(1)
F(6)	0.0294(2)	0.0671(1)	0.1230(1)	0.044(1)
C(14)	0.2311(2)	0.1283(2)	0.4788(2)	0.019(1)
C(22)	0.0030(2)	0.2340(2)	0.5277(2)	0.018(1)
C(30)	-0.3575(2)	0.3159(2)	0.4061(2)	0.023(1)
C(1)	0.2569(2)	0.0363(2)	0.3622(2)	0.020(1)
F(3)	0.4582(1)	-0.1641(1)	0.3381(1)	0.045(1)
F(2)	0.3223(2)	-0.2419(1)	0.2835(1)	0.048(1)
C(23)	-0.0896(2)	0.2348(2)	0.5458(2)	0.021(1)
C(17)	0.2146(2)	0.2391(2)	0.5938(2)	0.023(1)
C(26)	-0.1993(2)	0.2375(2)	0.4809(2)	0.021(1)
C(13)	0.2553(2)	0.2025(2)	0.5279(2)	0.020(1)
C(4)	0.2114(2)	-0.0941(2)	0.2419(2)	0.023(1)
C(6)	0.3184(2)	-0.0360(2)	0.3778(2)	0.022(1)
C(21)	0.1022(2)	0.2318(2)	0.5930(2)	0.021(1)
F(10)	-0.4964(2)	0.0965(1)	0.2839(1)	0.054(1)
C(20)	0.1063(2)	0.2282(2)	0.6765(2)	0.027(1)
C(5)	0.2946(2)	-0.1011(2)	0.3183(2)	0.022(1)
C(2)	0.1725(2)	0.0438(2)	0.2849(2)	0.023(1)
C(3)	0.1509(2)	-0.0204(2)	0.2256(2)	0.024(1)
C(29)	-0.4080(2)	0.2423(2)	0.3675(2)	0.023(1)
C(9)	0.2840(2)	0.1087(2)	0.4237(2)	0.020(1)
C(11)	0.3890(2)	0.2354(2)	0.4704(2)	0.026(1)
C(12)	0.3334(2)	0.2559(2)	0.5212(2)	0.024(1)
C(27)	-0.2500(2)	0.1637(2)	0.4429(2)	0.023(1)
C(31)	-0.2537(2)	0.3138(2)	0.4630(2)	0.022(1)
C(10)	0.3651(2)	0.1616(2)	0.4232(2)	0.024(1)
C(25)	0.0162(2)	0.2285(2)	0.6954(2)	0.030(1)
F(11)	-0.4306(2)	0.0373(1)	0.4026(1)	0.055(1)
C(24)	-0.0810(2)	0.2336(2)	0.6303(2)	0.027(1)
F(4)	-0.0276(3)	-0.0532(2)	0.1483(3)	0.041(1)
C(28)	-0.3533(2)	0.1663(2)	0.3864(2)	0.023(1)
C(18)	0.2795(2)	0.2004(2)	0.6823(2)	0.030(1)
F(8)	-0.4357(2)	0.4271(1)	0.4537(1)	0.066(1)
F(7)	-0.5062(2)	0.3951(1)	0.3246(2)	0.071(1)
C(16)	0.2427(2)	0.3347(2)	0.5924(2)	0.029(1)
C(7)	0.3622(2)	-0.1790(2)	0.3383(2)	0.027(1)
F(12)	-0.3450(2)	0.0364(1)	0.3212(2)	0.073(1)
C(33)	-0.4053(2)	0.0848(2)	0.3473(2)	0.029(1)
C(15)	0.3447(2)	0.3352(2)	0.5737(2)	0.032(1)
F(5)	0.0764(4)	-0.0493(3)	0.0802(2)	0.053(1)
C(8)	0.0604(2)	-0.0131(2)	0.1432(2)	0.034(1)
C(19)	0.2180(2)	0.2242(2)	0.7387(2)	0.035(1)
C(32)	-0.4148(2)	0.3991(2)	0.3880(2)	0.031(1)
O	0.1082(2)	0.5271(2)	0.2073(1)	0.049(1)
C(35)	0.1851(3)	0.5687(2)	0.2775(2)	0.053(1)

C(34)	0.2576(3)	0.5059(3)	0.3392(3)	0.064(1)
O(4)	0.0802(1)	0.2713(1)	0.4127(1)	0.020(1)
F(9)	-0.3606(2)	0.4596(1)	0.3691(2)	0.074(1)
F(5A)	0.1097(12)	-0.0197(10)	0.0739(8)	0.053(1)
F(4A)	-0.0063(9)	-0.0618(8)	0.1213(8)	0.041(1)

Table 3. Bond lengths [Å] and angles [°].

S(1)-O(1)	1.4312(19)	S(1)-O(2)	1.4354(19)		
S(1)-N(1)	1.645(2)	S(1)-C(14)	1.765(3)		
S(2)-O(4)	1.4338(18)	S(2)-O(3)	1.4365(17)		
S(2)-N(1)	1.658(2)	S(2)-C(22)	1.767(2)		
F(1)-C(7)	1.337(3)	F(6)-C(8)	1.340(3)		
C(14)-C(13)	1.406(3)	C(14)-C(9)	1.409(4)		
C(22)-C(21)	1.406(3)	C(22)-C(23)	1.410(3)		
C(30)-C(29)	1.389(4)	C(30)-C(31)	1.398(4)		
C(30)-C(32)	1.504(4)	C(1)-C(6)	1.387(4)		
C(1)-C(2)	1.402(3)	C(1)-C(9)	1.501(3)		
F(3)-C(7)	1.337(3)	F(2)-C(7)	1.335(3)		
C(23)-C(24)	1.395(4)	C(23)-C(26)	1.506(3)		
C(17)-C(13)	1.533(4)	C(17)-C(21)	1.540(4)		
C(17)-C(16)	1.560(4)	C(17)-C(18)	1.564(4)		
C(26)-C(27)	1.390(4)	C(26)-C(31)	1.391(3)		
C(13)-C(12)	1.399(4)	C(4)-C(5)	1.383(4)		
C(4)-C(3)	1.397(4)	C(6)-C(5)	1.394(4)		
C(21)-C(20)	1.399(4)	F(10)-C(33)	1.330(3)		
C(20)-C(25)	1.384(4)	C(20)-C(19)	1.511(4)		
C(5)-C(7)	1.504(4)	C(2)-C(3)	1.382(4)		
C(3)-C(8)	1.499(4)	C(29)-C(28)	1.391(4)		
C(9)-C(10)	1.393(4)	C(11)-C(12)	1.381(4)		
C(11)-C(10)	1.384(4)	C(12)-C(15)	1.511(4)		
C(27)-C(28)	1.391(4)	C(25)-C(24)	1.389(4)		
F(11)-C(33)	1.342(3)	F(4)-C(8)	1.392(5)		
C(28)-C(33)	1.503(4)	C(18)-C(19)	1.535(4)		
F(8)-C(32)	1.325(4)	F(7)-C(32)	1.322(3)		
C(16)-C(15)	1.541(4)	F(12)-C(33)	1.317(3)		
F(5)-C(8)	1.299(5)	C(8)-F(4A)	1.147(12)		
C(8)-F(5A)	1.558(15)	C(32)-F(9)	1.320(4)		
O-C(35)	1.431(4)	C(35)-C(34)	1.520(5)		
O(1)-S(1)-O(2)	117.87(11)	O(1)-S(1)-N(1)	104.45(11)	O(2)-S(1)-N(1)	110.83(11)
O(1)-S(1)-C(14)	112.09(11)	O(2)-S(1)-C(14)	107.31(11)	N(1)-S(1)-C(14)	103.36(11)
O(4)-S(2)-O(3)	118.20(10)	O(4)-S(2)-N(1)	110.24(11)	O(3)-S(2)-N(1)	103.65(11)
O(4)-S(2)-C(22)	108.34(11)	O(3)-S(2)-C(22)	112.51(11)	N(1)-S(2)-C(22)	102.69(11)
S(1)-N(1)-S(2)	127.46(13)	C(13)-C(14)-C(9)	120.6(2)	C(13)-C(14)-S(1)	118.67(19)
C(9)-C(14)-S(1)	120.42(19)	C(21)-C(22)-C(23)	121.0(2)	C(21)-C(22)-S(2)	117.76(19)
C(23)-C(22)-S(2)	120.72(18)	C(29)-C(30)-C(31)	120.9(2)	C(29)-C(30)-C(32)	120.1(2)
C(31)-C(30)-C(32)	119.0(2)	C(6)-C(1)-C(2)	119.0(2)	C(6)-C(1)-C(9)	121.1(2)
C(2)-C(1)-C(9)	119.8(2)	C(24)-C(23)-C(22)	118.6(2)	C(24)-C(23)-C(26)	116.1(2)
C(22)-C(23)-C(26)	125.3(2)	C(13)-C(17)-C(21)	126.4(2)	C(13)-C(17)-C(16)	101.3(2)
C(21)-C(17)-C(16)	108.9(2)	C(13)-C(17)-C(18)	108.8(2)	C(21)-C(17)-C(18)	101.3(2)
C(16)-C(17)-C(18)	109.7(2)	C(27)-C(26)-C(31)	119.2(2)	C(27)-C(26)-C(23)	120.8(2)
C(31)-C(26)-C(23)	119.8(2)	C(12)-C(13)-C(14)	118.5(2)	C(12)-C(13)-C(17)	108.9(2)
C(14)-C(13)-C(17)	132.6(2)	C(5)-C(4)-C(3)	118.6(2)	C(1)-C(6)-C(5)	120.3(2)
C(20)-C(21)-C(22)	118.1(2)	C(20)-C(21)-C(17)	108.8(2)	C(22)-C(21)-C(17)	132.9(2)

C(25)-C(20)-C(21)	121.6(2)	C(25)-C(20)-C(19)	126.9(2)	C(21)-C(20)-C(19)	111.5(2)
C(4)-C(5)-C(6)	121.0(2)	C(4)-C(5)-C(7)	120.5(2)	C(6)-C(5)-C(7)	118.5(2)
C(3)-C(2)-C(1)	120.3(2)	C(2)-C(3)-C(4)	120.9(2)	C(2)-C(3)-C(8)	120.5(2)
C(4)-C(3)-C(8)	118.6(2)	C(30)-C(29)-C(28)	118.7(2)	C(10)-C(9)-C(14)	118.4(2)
C(10)-C(9)-C(1)	116.6(2)	C(14)-C(9)-C(1)	124.9(2)	C(12)-C(11)-C(10)	119.4(2)
C(11)-C(12)-C(13)	121.4(2)	C(11)-C(12)-C(15)	126.9(3)	C(13)-C(12)-C(15)	111.7(2)
C(26)-C(27)-C(28)	120.4(2)	C(26)-C(31)-C(30)	120.0(2)	C(11)-C(10)-C(9)	121.5(2)
C(20)-C(25)-C(24)	119.6(2)	C(25)-C(24)-C(23)	121.1(3)	C(29)-C(28)-C(27)	120.8(2)
C(29)-C(28)-C(33)	120.5(2)	C(27)-C(28)-C(33)	118.7(2)	C(19)-C(18)-C(17)	104.7(2)
C(15)-C(16)-C(17)	104.8(2)	F(2)-C(7)-F(3)	106.4(2)	F(2)-C(7)-F(1)	106.5(2)
F(3)-C(7)-F(1)	106.4(2)	F(2)-C(7)-C(5)	112.9(2)	F(3)-C(7)-C(5)	112.3(2)
F(1)-C(7)-C(5)	111.9(2)	F(12)-C(33)-F(10)	109.1(3)	F(12)-C(33)-F(11)	105.3(3)
F(10)-C(33)-F(11)	103.7(2)	F(12)-C(33)-C(28)	113.0(2)	F(10)-C(33)-C(28)	113.2(2)
F(11)-C(33)-C(28)	111.8(2)	C(12)-C(15)-C(16)	102.2(2)	F(4A)-C(8)-F(5)	78.0(6)
F(4A)-C(8)-F(6)	114.2(7)	F(5)-C(8)-F(6)	109.8(3)	F(4A)-C(8)-F(4)	27.1(7)
F(5)-C(8)-F(4)	105.1(3)	F(6)-C(8)-F(4)	104.2(3)	F(4A)-C(8)-C(3)	122.8(7)
F(5)-C(8)-C(3)	113.8(3)	F(6)-C(8)-C(3)	112.9(2)	F(4)-C(8)-C(3)	110.4(3)
F(4A)-C(8)-F(5A)	102.9(7)	F(5)-C(8)-F(5A)	25.9(5)	F(6)-C(8)-F(5A)	93.2(6)
F(4)-C(8)-F(5A)	129.8(6)	C(3)-C(8)-F(5A)	105.1(6)	C(20)-C(19)-C(18)	102.7(2)
F(9)-C(32)-F(7)	106.7(3)	F(9)-C(32)-F(8)	105.9(3)	F(7)-C(32)-F(8)	105.7(3)
F(9)-C(32)-C(30)	112.7(2)	F(7)-C(32)-C(30)	113.2(2)	F(8)-C(32)-C(30)	112.1(2)
O-C(35)-C(34)	111.8(3)				

Symmetry transformations used to generate equivalent atoms:

Table 4. Anisotropic displacement parameters (\AA^2).

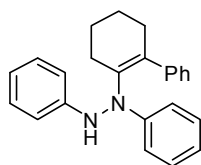
The anisotropic displacement factor exponent takes the form:

$$-2 \pi^2 [h^2 a^{*2} U_{11} + \dots + 2 h k a^* b^* U_{12}].$$

	U_{11}	U_{22}	U_{33}	U_{23}	U_{13}	U_{12}
S(1)	0.017(1)	0.017(1)	0.021(1)	0.002(1)	0.005(1)	0.002(1)
S(2)	0.015(1)	0.018(1)	0.015(1)	0.002(1)	0.003(1)	0.002(1)
O(3)	0.016(1)	0.028(1)	0.016(1)	0.003(1)	0.001(1)	0.003(1)
O(1)	0.024(1)	0.017(1)	0.031(1)	0.000(1)	0.009(1)	-0.001(1)
O(2)	0.024(1)	0.026(1)	0.022(1)	0.006(1)	0.007(1)	0.004(1)
N(1)	0.015(1)	0.018(1)	0.020(1)	-0.002(1)	0.001(1)	0.000(1)
F(1)	0.041(1)	0.036(1)	0.036(1)	0.011(1)	0.015(1)	0.016(1)
F(6)	0.045(1)	0.025(1)	0.038(1)	0.001(1)	-0.014(1)	0.003(1)
C(14)	0.014(1)	0.019(1)	0.019(1)	0.003(1)	0.001(1)	0.002(1)
C(22)	0.021(1)	0.019(1)	0.014(1)	0.002(1)	0.005(1)	0.004(1)
C(30)	0.021(1)	0.022(1)	0.028(1)	0.004(1)	0.010(1)	0.007(1)
C(1)	0.016(1)	0.022(1)	0.022(1)	-0.001(1)	0.007(1)	-0.002(1)
F(3)	0.026(1)	0.047(1)	0.066(1)	0.010(1)	0.023(1)	0.013(1)
F(2)	0.049(1)	0.031(1)	0.046(1)	-0.014(1)	-0.003(1)	0.017(1)
C(23)	0.021(1)	0.018(1)	0.023(1)	0.002(1)	0.008(1)	0.004(1)
C(17)	0.017(1)	0.025(1)	0.018(1)	-0.005(1)	-0.002(1)	0.003(1)
C(26)	0.019(1)	0.022(1)	0.022(1)	0.005(1)	0.009(1)	0.003(1)
C(13)	0.013(1)	0.024(1)	0.019(1)	-0.002(1)	-0.001(1)	0.004(1)
C(4)	0.022(1)	0.022(1)	0.023(1)	-0.005(1)	0.008(1)	-0.001(1)
C(6)	0.015(1)	0.027(1)	0.020(1)	0.000(1)	0.004(1)	0.003(1)
C(21)	0.023(1)	0.021(1)	0.018(1)	-0.001(1)	0.004(1)	0.006(1)
F(10)	0.053(1)	0.037(1)	0.043(1)	-0.006(1)	-0.015(1)	-0.001(1)
C(20)	0.030(1)	0.029(1)	0.018(1)	-0.002(1)	0.004(1)	0.009(1)
C(5)	0.018(1)	0.023(1)	0.025(1)	0.000(1)	0.009(1)	0.003(1)

C(2)	0.018(1)	0.022(1)	0.024(1)	0.000(1)	0.003(1)	0.003(1)
C(3)	0.021(1)	0.023(1)	0.023(1)	0.000(1)	0.002(1)	-0.001(1)
C(29)	0.019(1)	0.026(1)	0.024(1)	0.002(1)	0.007(1)	0.003(1)
C(9)	0.014(1)	0.022(1)	0.018(1)	0.001(1)	0.000(1)	0.004(1)
C(11)	0.015(1)	0.030(1)	0.029(1)	-0.003(1)	0.004(1)	-0.006(1)
C(12)	0.016(1)	0.023(1)	0.027(1)	-0.005(1)	0.000(1)	-0.001(1)
C(27)	0.023(1)	0.019(1)	0.026(1)	0.004(1)	0.010(1)	0.004(1)
C(31)	0.022(1)	0.020(1)	0.026(1)	0.000(1)	0.010(1)	0.000(1)
C(10)	0.016(1)	0.030(1)	0.025(1)	-0.002(1)	0.006(1)	0.002(1)
C(25)	0.039(2)	0.034(2)	0.018(1)	0.000(1)	0.012(1)	0.009(1)
F(11)	0.067(1)	0.043(1)	0.046(1)	0.001(1)	0.011(1)	-0.029(1)
C(24)	0.030(1)	0.031(2)	0.027(1)	0.000(1)	0.015(1)	0.005(1)
F(4)	0.026(2)	0.043(1)	0.043(2)	-0.002(1)	-0.002(1)	-0.010(1)
C(28)	0.022(1)	0.021(1)	0.026(1)	0.002(1)	0.010(1)	0.003(1)
C(18)	0.024(1)	0.037(2)	0.020(1)	-0.004(1)	-0.004(1)	0.007(1)
F(8)	0.090(2)	0.057(1)	0.053(1)	0.001(1)	0.028(1)	0.047(1)
F(7)	0.053(1)	0.040(1)	0.077(2)	-0.014(1)	-0.026(1)	0.026(1)
C(16)	0.025(1)	0.026(1)	0.029(1)	-0.012(1)	0.004(1)	-0.001(1)
C(7)	0.025(1)	0.027(1)	0.028(1)	-0.004(1)	0.009(1)	0.005(1)
F(12)	0.048(1)	0.049(1)	0.136(2)	-0.054(1)	0.051(2)	-0.015(1)
C(33)	0.026(1)	0.025(1)	0.034(2)	-0.001(1)	0.009(1)	0.002(1)
C(15)	0.023(1)	0.030(2)	0.038(2)	-0.012(1)	0.005(1)	-0.006(1)
F(5)	0.052(3)	0.075(3)	0.020(1)	-0.008(2)	-0.001(1)	0.023(2)
C(8)	0.032(2)	0.025(1)	0.030(2)	-0.007(1)	-0.005(1)	0.003(1)
C(19)	0.032(2)	0.046(2)	0.018(1)	-0.004(1)	-0.002(1)	0.012(1)
C(32)	0.028(2)	0.024(1)	0.037(2)	0.000(1)	0.007(1)	0.006(1)
O	0.061(2)	0.038(1)	0.033(1)	-0.005(1)	-0.002(1)	0.016(1)
C(35)	0.045(2)	0.053(2)	0.053(2)	-0.012(2)	0.010(2)	0.007(2)
C(34)	0.052(2)	0.080(3)	0.046(2)	0.000(2)	-0.001(2)	0.013(2)
O(4)	0.018(1)	0.020(1)	0.020(1)	0.002(1)	0.005(1)	0.000(1)
F(9)	0.063(2)	0.028(1)	0.146(2)	0.033(1)	0.056(2)	0.018(1)
F(5A)	0.052(3)	0.075(3)	0.020(1)	-0.008(2)	-0.001(1)	0.023(2)
F(4A)	0.026(2)	0.043(1)	0.043(2)	-0.002(1)	-0.002(1)	-0.010(1)

Compound 210a



210a

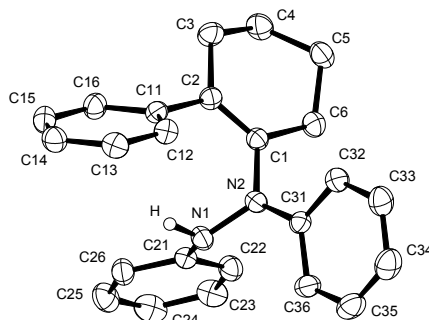


Table 1. Crystal data and structure refinement.

Identification code	6784	
Empirical formula	C ₂₄ H ₂₄ N ₂	
Color	colorless	
Formula weight	340.45 g·mol ⁻¹	
Temperature	200 K	
Wavelength	0.71073 Å	
Crystal system	Triclinic	
Space group	P1, (no. 2)	
Unit cell dimensions	a = 9.5272(5) Å	α = 119.211(2)°.
	b = 10.6681(5) Å	β = 91.387(2)°.
	c = 10.7108(5) Å	γ = 97.801(2)°.
Volume	936.22(8) Å ³	
Z	2	
Density (calculated)	1.208 Mg·m ⁻³	
Absorption coefficient	0.071 mm ⁻¹	
F(000)	364 e	
Crystal size	0.7 x 0.6 x 0.5 mm ³	
θ range for data collection	3.86 to 34.98°.	
Index ranges	-15 ≤ h ≤ 15, -16 ≤ k ≤ 17, -17 ≤ l ≤ 17	
Reflections collected	30384	
Independent reflections	8131 [R _{int} = 0.0298]	
Reflections with I > 2σ(I)	6851	
Completeness to θ = 34.98°	98.5 %	
Absorption correction	Empirical	
Max. and min. transmission	0.97 and 0.52	
Refinement method	Full-matrix least-squares on F ²	
Data / restraints / parameters	8131 / 0 / 239	
Goodness-of-fit on F ²	1.040	
Final R indices [I > 2σ(I)]	R ₁ = 0.0468	wR ² = 0.1284
R indices (all data)	R ₁ = 0.0567	wR ² = 0.1377
Largest diff. peak and hole	0.369 and -0.223 e·Å ⁻³	

Table 2. Atomic coordinates and equivalent isotropic displacement parameters (\AA^2).

U_{eq} is defined as one third of the trace of the orthogonalized U_{ij} tensor.

	x	y	z	U_{eq}
C(1)	0.1483(1)	0.4397(1)	0.7278(1)	0.024(1)
C(2)	0.2257(1)	0.4324(1)	0.6218(1)	0.024(1)
C(3)	0.3461(1)	0.5540(1)	0.6484(1)	0.032(1)
C(4)	0.3882(1)	0.6648(1)	0.8072(1)	0.033(1)
C(5)	0.2565(1)	0.7043(1)	0.8858(1)	0.033(1)
C(6)	0.1709(1)	0.5691(1)	0.8786(1)	0.031(1)
C(11)	0.1982(1)	0.3074(1)	0.4719(1)	0.024(1)
C(12)	0.0628(1)	0.2621(1)	0.3955(1)	0.027(1)
C(13)	0.0371(1)	0.1434(1)	0.2562(1)	0.031(1)
C(14)	0.1466(1)	0.0694(1)	0.1902(1)	0.033(1)
C(15)	0.2819(1)	0.1138(1)	0.2642(1)	0.034(1)
C(16)	0.3077(1)	0.2316(1)	0.4035(1)	0.030(1)
C(21)	0.1697(1)	0.1465(1)	0.7199(1)	0.024(1)
C(22)	0.1884(1)	0.2184(1)	0.8700(1)	0.030(1)
C(23)	0.2773(1)	0.1726(1)	0.9390(1)	0.037(1)
C(24)	0.3474(1)	0.0564(1)	0.8615(1)	0.040(1)
C(25)	0.3300(1)	-0.0137(1)	0.7125(1)	0.039(1)
C(26)	0.2433(1)	0.0316(1)	0.6416(1)	0.031(1)
C(31)	-0.1015(1)	0.3355(1)	0.7198(1)	0.024(1)
C(32)	-0.1507(1)	0.4503(1)	0.7137(1)	0.030(1)
C(33)	-0.2942(1)	0.4633(1)	0.7236(1)	0.036(1)
C(34)	-0.3903(1)	0.3623(1)	0.7378(1)	0.040(1)
C(35)	-0.3414(1)	0.2478(1)	0.7428(1)	0.038(1)
C(36)	-0.1986(1)	0.2340(1)	0.7348(1)	0.030(1)
N(1)	0.0721(1)	0.1792(1)	0.6445(1)	0.026(1)
N(2)	0.0431(1)	0.3217(1)	0.7110(1)	0.026(1)

Table 3. Bond lengths [\AA] and angles [$^\circ$].

C(1)-C(2)	1.3456(10)	C(1)-N(2)	1.4315(9)
C(1)-C(6)	1.5117(10)	C(2)-C(11)	1.4902(10)
C(2)-C(3)	1.5158(10)	C(3)-C(4)	1.5253(12)
C(4)-C(5)	1.5201(12)	C(5)-C(6)	1.5231(12)
C(11)-C(12)	1.4002(10)	C(11)-C(16)	1.4025(10)
C(12)-C(13)	1.3939(11)	C(13)-C(14)	1.3874(12)
C(14)-C(15)	1.3901(13)	C(15)-C(16)	1.3907(12)
C(21)-C(22)	1.3966(10)	C(21)-C(26)	1.3986(10)
C(21)-N(1)	1.4016(9)	C(22)-C(23)	1.3913(12)
C(23)-C(24)	1.3852(14)	C(24)-C(25)	1.3867(15)
C(25)-C(26)	1.3883(13)	C(31)-C(32)	1.3991(10)
C(31)-C(36)	1.3993(10)	C(31)-N(2)	1.4056(9)
C(32)-C(33)	1.3933(11)	C(33)-C(34)	1.3857(14)
C(34)-C(35)	1.3895(15)	C(35)-C(36)	1.3885(12)
N(1)-N(2)	1.4008(9)		
C(2)-C(1)-N(2)	123.06(6)	C(2)-C(1)-C(6)	123.24(7)
N(2)-C(1)-C(6)	113.58(6)	C(1)-C(2)-C(11)	122.78(6)
C(1)-C(2)-C(3)	121.29(7)	C(11)-C(2)-C(3)	115.93(6)
C(2)-C(3)-C(4)	113.80(7)	C(5)-C(4)-C(3)	110.51(7)

C(4)-C(5)-C(6)	109.52(7)	C(1)-C(6)-C(5)	112.34(7)
C(12)-C(11)-C(16)	118.18(7)	C(12)-C(11)-C(2)	121.13(6)
C(16)-C(11)-C(2)	120.69(6)	C(13)-C(12)-C(11)	120.86(7)
C(14)-C(13)-C(12)	120.26(7)	C(13)-C(14)-C(15)	119.55(7)
C(14)-C(15)-C(16)	120.38(8)	C(15)-C(16)-C(11)	120.76(7)
C(22)-C(21)-C(26)	119.26(7)	C(22)-C(21)-N(1)	122.07(7)
C(26)-C(21)-N(1)	118.52(7)	C(23)-C(22)-C(21)	119.52(8)
C(24)-C(23)-C(22)	121.24(8)	C(23)-C(24)-C(25)	119.13(8)
C(24)-C(25)-C(26)	120.53(8)	C(25)-C(26)-C(21)	120.28(8)
C(32)-C(31)-C(36)	118.93(7)	C(32)-C(31)-N(2)	120.79(6)
C(36)-C(31)-N(2)	120.28(7)	C(33)-C(32)-C(31)	120.18(7)
C(34)-C(33)-C(32)	120.82(8)	C(33)-C(34)-C(35)	118.94(8)
C(36)-C(35)-C(34)	121.06(8)	C(35)-C(36)-C(31)	120.07(8)
N(2)-N(1)-C(21)	117.45(6)	N(1)-N(2)-C(31)	116.05(6)
N(1)-N(2)-C(1)	120.51(6)	C(31)-N(2)-C(1)	120.80(6)

Table 4. Anisotropic displacement parameters (\AA^2).

The anisotropic displacement factor exponent takes the form:

$$-2\pi^2 [h^2 a^2 U_{11} + \dots + 2 h k a^* b^* U_{12}].$$

	U_{11}	U_{22}	U_{33}	U_{23}	U_{13}	U_{12}
C(1)	0.023(1)	0.022(1)	0.025(1)	0.010(1)	0.003(1)	0.004(1)
C(2)	0.021(1)	0.025(1)	0.025(1)	0.011(1)	0.002(1)	0.003(1)
C(3)	0.027(1)	0.031(1)	0.032(1)	0.014(1)	0.003(1)	-0.002(1)
C(4)	0.027(1)	0.028(1)	0.036(1)	0.010(1)	-0.001(1)	-0.002(1)
C(5)	0.035(1)	0.023(1)	0.035(1)	0.010(1)	0.003(1)	0.005(1)
C(6)	0.034(1)	0.026(1)	0.026(1)	0.008(1)	0.005(1)	0.003(1)
C(11)	0.023(1)	0.025(1)	0.024(1)	0.013(1)	0.004(1)	0.003(1)
C(12)	0.026(1)	0.030(1)	0.026(1)	0.014(1)	0.001(1)	0.006(1)
C(13)	0.032(1)	0.031(1)	0.027(1)	0.014(1)	-0.002(1)	0.003(1)
C(14)	0.042(1)	0.027(1)	0.026(1)	0.010(1)	0.004(1)	0.004(1)
C(15)	0.034(1)	0.030(1)	0.033(1)	0.012(1)	0.011(1)	0.008(1)
C(16)	0.025(1)	0.031(1)	0.032(1)	0.013(1)	0.005(1)	0.005(1)
C(21)	0.025(1)	0.022(1)	0.025(1)	0.011(1)	0.004(1)	0.003(1)
C(22)	0.037(1)	0.027(1)	0.025(1)	0.012(1)	0.003(1)	0.006(1)
C(23)	0.041(1)	0.035(1)	0.032(1)	0.018(1)	-0.005(1)	0.001(1)
C(24)	0.032(1)	0.041(1)	0.051(1)	0.027(1)	-0.006(1)	0.004(1)
C(25)	0.030(1)	0.034(1)	0.052(1)	0.019(1)	0.005(1)	0.011(1)
C(26)	0.030(1)	0.028(1)	0.032(1)	0.011(1)	0.006(1)	0.008(1)
C(31)	0.025(1)	0.024(1)	0.021(1)	0.010(1)	0.004(1)	0.003(1)
C(32)	0.029(1)	0.028(1)	0.034(1)	0.016(1)	0.007(1)	0.007(1)
C(33)	0.032(1)	0.037(1)	0.040(1)	0.016(1)	0.005(1)	0.012(1)
C(34)	0.025(1)	0.046(1)	0.042(1)	0.017(1)	0.005(1)	0.006(1)
C(35)	0.030(1)	0.041(1)	0.039(1)	0.019(1)	0.005(1)	-0.003(1)
C(36)	0.031(1)	0.029(1)	0.029(1)	0.016(1)	0.004(1)	0.000(1)
N(1)	0.033(1)	0.022(1)	0.023(1)	0.010(1)	0.003(1)	0.007(1)
N(2)	0.026(1)	0.021(1)	0.032(1)	0.013(1)	0.006(1)	0.005(1)

Compound 236n

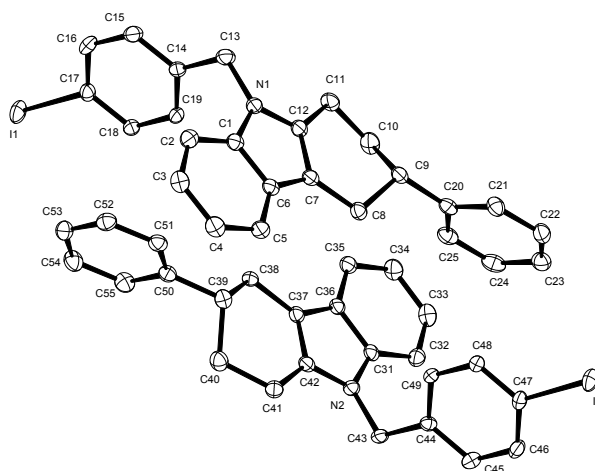
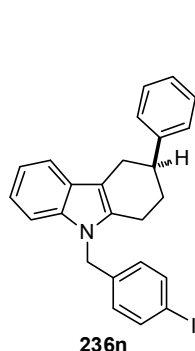


Table 1. Crystal data and structure refinement.

Identification code	7395	
Empirical formula	C ₂₅ H ₂₂ IN	
Color	colourless	
Formula weight	463.34 g·mol ⁻¹	
Temperature	100 K	
Wavelength	0.71073 Å	
Crystal system	ORTHORHOMBIC	
Space group	P2 ₁ 2 ₁ 2 ₁ , (no. 19)	
Unit cell dimensions	a = 9.3325(9) Å	α = 90°.
	b = 13.9742(14) Å	β = 90°.
	c = 30.898(3) Å	γ = 90°.
Volume	4029.5(7) Å ³	
Z	8	
Density (calculated)	1.528 Mg·m ⁻³	
Absorption coefficient	1.598 mm ⁻¹	
F(000)	1856 e	
Crystal size	0.64 x 0.05 x 0.04 mm ³	
θ range for data collection	1.32 to 31.03°.	
Index ranges	-13 ≤ h ≤ 13, -20 ≤ k ≤ 20, -44 ≤ l ≤ 44	
Reflections collected	147552	
Independent reflections	12832 [R _{int} = 0.0567]	
Reflections with I > 2σ(I)	11149	
Completeness to θ = 27.50°	100.0 %	
Absorption correction	Gaussian	
Max. and min. transmission	0.94 and 0.58	
Refinement method	Full-matrix least-squares on F ²	
Data / restraints / parameters	12832 / 0 / 487	
Goodness-of-fit on F ²	1.072	
Final R indices [I > 2σ(I)]	R ₁ = 0.0298	wR ² = 0.0743
R indices (all data)	R ₁ = 0.0398	wR ² = 0.0832
Absolute structure parameter	-0.002(14)	
Largest diff. peak and hole	0.625 and -1.222 e·Å ⁻³	

Table 2. Atomic coordinates and equivalent isotropic displacement parameters (\AA^2).

U_{eq} is defined as one third of the trace of the orthogonalized U_{ij} tensor.

	x	y	z	U_{eq}
I(1)	1.0763(1)	0.7526(1)	0.4893(1)	0.027(1)
I(2)	0.5710(1)	0.2432(1)	0.4930(1)	0.025(1)
N(1)	0.5651(3)	0.5698(1)	0.3417(1)	0.019(1)
N(2)	0.0692(2)	0.4306(1)	0.3439(1)	0.017(1)
C(1)	0.4692(3)	0.6451(2)	0.3464(1)	0.018(1)
C(2)	0.3991(3)	0.6778(2)	0.3834(1)	0.021(1)
C(3)	0.3090(3)	0.7556(2)	0.3785(1)	0.023(1)
C(4)	0.2879(3)	0.7994(2)	0.3378(1)	0.023(1)
C(5)	0.3578(3)	0.7665(2)	0.3013(1)	0.020(1)
C(6)	0.4525(3)	0.6887(2)	0.3052(1)	0.017(1)
C(7)	0.5465(3)	0.6399(2)	0.2762(1)	0.017(1)
C(8)	0.5716(3)	0.6542(2)	0.2285(1)	0.019(1)
C(9)	0.6379(3)	0.5632(2)	0.2091(1)	0.019(1)
C(10)	0.7675(3)	0.5328(2)	0.2367(1)	0.025(1)
C(11)	0.7215(3)	0.5001(2)	0.2821(1)	0.024(1)
C(12)	0.6134(3)	0.5693(2)	0.2992(1)	0.019(1)
C(13)	0.6234(3)	0.5141(2)	0.3774(1)	0.022(1)
C(14)	0.7360(3)	0.5685(2)	0.4031(1)	0.018(1)
C(15)	0.7565(3)	0.5470(2)	0.4469(1)	0.021(1)
C(16)	0.8565(3)	0.5976(2)	0.4714(1)	0.022(1)
C(17)	0.9342(3)	0.6705(2)	0.4518(1)	0.019(1)
C(18)	0.9169(3)	0.6919(2)	0.4084(1)	0.018(1)
C(19)	0.8174(3)	0.6401(2)	0.3843(1)	0.018(1)
C(20)	0.6724(3)	0.5741(2)	0.1615(1)	0.019(1)
C(21)	0.5760(3)	0.5390(2)	0.1311(1)	0.022(1)
C(22)	0.6042(3)	0.5444(2)	0.0872(1)	0.024(1)
C(23)	0.7297(3)	0.5860(2)	0.0725(1)	0.025(1)
C(24)	0.8263(3)	0.6237(2)	0.1024(1)	0.025(1)
C(25)	0.7970(3)	0.6173(2)	0.1465(1)	0.023(1)
C(31)	-0.0267(3)	0.3565(2)	0.3495(1)	0.016(1)
C(32)	-0.0984(3)	0.3264(2)	0.3868(1)	0.020(1)
C(33)	-0.1902(3)	0.2488(2)	0.3831(1)	0.024(1)
C(34)	-0.2110(3)	0.2028(2)	0.3432(1)	0.023(1)
C(35)	-0.1404(3)	0.2327(2)	0.3061(1)	0.019(1)
C(36)	-0.0444(3)	0.3101(2)	0.3090(1)	0.017(1)
C(37)	0.0489(3)	0.3571(2)	0.2790(1)	0.016(1)
C(38)	0.0726(3)	0.3378(2)	0.2318(1)	0.017(1)
C(39)	0.2012(3)	0.3943(2)	0.2143(1)	0.021(1)
C(40)	0.2054(3)	0.4958(2)	0.2332(1)	0.023(1)
C(41)	0.2210(3)	0.4975(2)	0.2824(1)	0.022(1)
C(42)	0.1155(3)	0.4291(2)	0.3011(1)	0.017(1)
C(43)	0.1303(3)	0.4862(2)	0.3790(1)	0.019(1)
C(44)	0.2393(3)	0.4310(2)	0.4052(1)	0.015(1)
C(45)	0.2654(3)	0.4559(2)	0.4483(1)	0.021(1)
C(46)	0.3627(3)	0.4045(2)	0.4731(1)	0.021(1)
C(47)	0.4347(3)	0.3271(2)	0.4548(1)	0.018(1)
C(48)	0.4129(3)	0.3026(2)	0.4117(1)	0.018(1)
C(49)	0.3154(3)	0.3547(2)	0.3871(1)	0.016(1)
C(50)	0.2031(3)	0.3982(2)	0.1650(1)	0.019(1)
C(51)	0.3184(3)	0.3605(2)	0.1425(1)	0.020(1)
C(52)	0.3245(3)	0.3675(2)	0.0976(1)	0.022(1)
C(53)	0.2175(3)	0.4116(2)	0.0746(1)	0.023(1)

C(54)	0.1007(3)	0.4494(2)	0.0966(1)	0.025(1)
C(55)	0.0941(3)	0.4430(2)	0.1416(1)	0.023(1)

Table 3. Bond lengths [Å] and angles [°].

I(1)-C(17)	2.101(2)	I(2)-C(47)	2.094(2)
N(1)-C(1)	1.388(3)	N(1)-C(12)	1.388(3)
N(1)-C(13)	1.456(3)	N(2)-C(31)	1.379(3)
N(2)-C(42)	1.389(3)	N(2)-C(43)	1.452(3)
C(1)-C(2)	1.396(4)	C(1)-C(6)	1.417(3)
C(2)-C(3)	1.383(4)	C(3)-C(4)	1.412(3)
C(4)-C(5)	1.383(4)	C(5)-C(6)	1.407(3)
C(6)-C(7)	1.428(3)	C(7)-C(8)	1.504(3)
C(7)-C(12)	1.369(3)	C(8)-C(9)	1.535(3)
C(9)-C(10)	1.538(4)	C(9)-C(20)	1.515(3)
C(10)-C(11)	1.536(4)	C(11)-C(12)	1.495(4)
C(13)-C(14)	1.522(4)	C(14)-C(15)	1.397(3)
C(14)-C(19)	1.384(3)	C(15)-C(16)	1.394(4)
C(16)-C(17)	1.388(4)	C(17)-C(18)	1.385(3)
C(18)-C(19)	1.394(3)	C(20)-C(21)	1.390(3)
C(20)-C(25)	1.390(4)	C(21)-C(22)	1.385(3)
C(22)-C(23)	1.384(4)	C(23)-C(24)	1.394(4)
C(24)-C(25)	1.392(4)	C(31)-C(32)	1.397(3)
C(31)-C(36)	1.419(3)	C(32)-C(33)	1.386(4)
C(33)-C(34)	1.405(4)	C(34)-C(35)	1.386(3)
C(35)-C(36)	1.406(3)	C(36)-C(37)	1.433(3)
C(37)-C(38)	1.500(3)	C(37)-C(42)	1.367(3)
C(38)-C(39)	1.535(3)	C(39)-C(40)	1.534(3)
C(39)-C(50)	1.525(3)	C(40)-C(41)	1.528(4)
C(41)-C(42)	1.489(4)	C(43)-C(44)	1.511(3)
C(44)-C(45)	1.398(3)	C(44)-C(49)	1.397(3)
C(45)-C(46)	1.390(4)	C(46)-C(47)	1.393(3)
C(47)-C(48)	1.389(3)	C(48)-C(49)	1.392(3)
C(50)-C(51)	1.385(4)	C(50)-C(55)	1.397(4)
C(51)-C(52)	1.391(3)	C(52)-C(53)	1.372(4)
C(53)-C(54)	1.389(4)	C(54)-C(55)	1.393(4)
C(1)-N(1)-C(13)	124.6(2)	C(12)-N(1)-C(1)	108.16(19)
C(12)-N(1)-C(13)	126.3(2)	C(31)-N(2)-C(42)	108.12(19)
C(31)-N(2)-C(43)	124.2(2)	C(42)-N(2)-C(43)	126.6(2)
N(1)-C(1)-C(2)	129.4(2)	N(1)-C(1)-C(6)	107.7(2)
C(2)-C(1)-C(6)	122.9(2)	C(3)-C(2)-C(1)	116.9(2)
C(2)-C(3)-C(4)	121.6(2)	C(5)-C(4)-C(3)	121.1(2)
C(4)-C(5)-C(6)	118.8(2)	C(1)-C(6)-C(7)	106.9(2)
C(5)-C(6)-C(1)	118.7(2)	C(5)-C(6)-C(7)	134.4(2)
C(6)-C(7)-C(8)	130.4(2)	C(12)-C(7)-C(6)	107.3(2)
C(12)-C(7)-C(8)	122.3(2)	C(7)-C(8)-C(9)	109.57(19)
C(8)-C(9)-C(10)	109.3(2)	C(20)-C(9)-C(8)	112.44(19)
C(20)-C(9)-C(10)	113.4(2)	C(11)-C(10)-C(9)	111.6(2)
C(12)-C(11)-C(10)	108.6(2)	N(1)-C(12)-C(11)	124.0(2)
C(7)-C(12)-N(1)	109.9(2)	C(7)-C(12)-C(11)	126.2(2)
N(1)-C(13)-C(14)	112.74(19)	C(15)-C(14)-C(13)	119.5(2)
C(19)-C(14)-C(13)	121.3(2)	C(19)-C(14)-C(15)	119.2(2)
C(16)-C(15)-C(14)	120.5(2)	C(17)-C(16)-C(15)	119.1(2)
C(16)-C(17)-I(1)	119.43(17)	C(18)-C(17)-I(1)	119.27(19)

C(18)-C(17)-C(16)	121.3(2)	C(17)-C(18)-C(19)	118.9(2)
C(14)-C(19)-C(18)	121.1(2)	C(21)-C(20)-C(9)	118.9(2)
C(21)-C(20)-C(25)	118.0(2)	C(25)-C(20)-C(9)	123.1(2)
C(22)-C(21)-C(20)	121.3(3)	C(23)-C(22)-C(21)	120.3(3)
C(22)-C(23)-C(24)	119.4(3)	C(25)-C(24)-C(23)	119.7(3)
C(20)-C(25)-C(24)	121.3(3)	N(2)-C(31)-C(32)	129.9(2)
N(2)-C(31)-C(36)	107.9(2)	C(32)-C(31)-C(36)	122.2(2)
C(33)-C(32)-C(31)	117.7(2)	C(32)-C(33)-C(34)	121.0(2)
C(35)-C(34)-C(33)	121.5(2)	C(34)-C(35)-C(36)	118.8(2)
C(31)-C(36)-C(37)	106.9(2)	C(35)-C(36)-C(31)	118.9(2)
C(35)-C(36)-C(37)	134.2(2)	C(36)-C(37)-C(38)	129.6(2)
C(42)-C(37)-C(36)	106.8(2)	C(42)-C(37)-C(38)	123.5(2)
C(37)-C(38)-C(39)	111.4(2)	C(40)-C(39)-C(38)	111.2(2)
C(50)-C(39)-C(38)	112.2(2)	C(50)-C(39)-C(40)	110.3(2)
C(41)-C(40)-C(39)	113.3(2)	C(42)-C(41)-C(40)	108.3(2)
N(2)-C(42)-C(41)	124.4(2)	C(37)-C(42)-N(2)	110.2(2)
C(37)-C(42)-C(41)	125.3(2)	N(2)-C(43)-C(44)	113.02(19)
C(45)-C(44)-C(43)	120.0(2)	C(49)-C(44)-C(43)	121.2(2)
C(49)-C(44)-C(45)	118.8(2)	C(46)-C(45)-C(44)	120.7(2)
C(45)-C(46)-C(47)	119.5(2)	C(46)-C(47)-I(2)	119.88(16)
C(48)-C(47)-I(2)	119.37(18)	C(48)-C(47)-C(46)	120.7(2)
C(47)-C(48)-C(49)	119.3(2)	C(48)-C(49)-C(44)	120.9(2)
C(51)-C(50)-C(39)	119.8(2)	C(51)-C(50)-C(55)	118.4(2)
C(55)-C(50)-C(39)	121.7(2)	C(50)-C(51)-C(52)	120.4(3)
C(53)-C(52)-C(51)	121.2(3)	C(52)-C(53)-C(54)	119.2(2)
C(53)-C(54)-C(55)	119.9(3)	C(54)-C(55)-C(50)	120.9(3)

Table 4. Anisotropic displacement parameters (\AA^2).

The anisotropic displacement factor exponent takes the form:

$$-2 \pi^2 [h^2 a^{*2} U_{11} + \dots + 2 h k a^* b^* U_{12}].$$

	U_{11}	U_{22}	U_{33}	U_{23}	U_{13}	U_{12}
I(1)	0.027(1)	0.036(1)	0.017(1)	-0.002(1)	-0.007(1)	-0.005(1)
I(2)	0.025(1)	0.033(1)	0.017(1)	0.003(1)	-0.006(1)	0.003(1)
N(1)	0.022(1)	0.015(1)	0.019(1)	0.000(1)	-0.007(1)	0.003(1)
N(2)	0.018(1)	0.015(1)	0.018(1)	-0.001(1)	-0.004(1)	-0.001(1)
C(1)	0.016(1)	0.016(1)	0.022(1)	0.000(1)	-0.005(1)	-0.001(1)
C(2)	0.018(1)	0.023(1)	0.022(1)	0.001(1)	-0.003(1)	-0.005(1)
C(3)	0.017(1)	0.027(1)	0.025(1)	-0.005(1)	0.001(1)	0.000(1)
C(4)	0.018(1)	0.024(1)	0.029(1)	-0.003(1)	-0.004(1)	0.004(1)
C(5)	0.018(1)	0.019(1)	0.024(1)	0.000(1)	-0.006(1)	0.005(1)
C(6)	0.014(1)	0.015(1)	0.022(1)	-0.001(1)	-0.006(1)	-0.002(1)
C(7)	0.017(1)	0.014(1)	0.021(1)	-0.001(1)	-0.006(1)	0.001(1)
C(8)	0.019(1)	0.018(1)	0.020(1)	-0.002(1)	-0.003(1)	0.000(1)
C(9)	0.020(1)	0.014(1)	0.021(1)	-0.002(1)	-0.001(1)	0.000(1)
C(10)	0.022(1)	0.026(1)	0.028(1)	-0.006(1)	-0.005(1)	0.011(1)
C(11)	0.028(2)	0.018(1)	0.027(1)	-0.002(1)	-0.009(1)	0.009(1)
C(12)	0.021(1)	0.016(1)	0.021(1)	-0.002(1)	-0.007(1)	0.002(1)
C(13)	0.024(1)	0.017(1)	0.024(1)	0.003(1)	-0.007(1)	0.000(1)
C(14)	0.019(1)	0.015(1)	0.019(1)	0.001(1)	-0.005(1)	0.006(1)
C(15)	0.023(1)	0.019(1)	0.022(1)	0.004(1)	-0.002(1)	-0.001(1)
C(16)	0.025(1)	0.027(1)	0.014(1)	0.004(1)	-0.002(1)	0.002(1)
C(17)	0.019(1)	0.019(1)	0.017(1)	-0.002(1)	-0.004(1)	0.003(1)

C(18)	0.019(1)	0.017(1)	0.017(1)	0.001(1)	-0.002(1)	0.002(1)
C(19)	0.022(1)	0.017(1)	0.014(1)	0.000(1)	-0.003(1)	0.003(1)
C(20)	0.019(1)	0.014(1)	0.025(1)	-0.002(1)	0.000(1)	0.003(1)
C(21)	0.022(1)	0.020(1)	0.024(1)	-0.003(1)	0.002(1)	-0.004(1)
C(22)	0.028(1)	0.023(1)	0.022(1)	-0.004(1)	-0.001(1)	-0.004(1)
C(23)	0.031(2)	0.020(1)	0.024(1)	-0.001(1)	0.006(1)	0.001(1)
C(24)	0.018(1)	0.018(1)	0.038(1)	0.002(1)	0.003(1)	0.000(1)
C(25)	0.019(1)	0.017(1)	0.032(1)	0.000(1)	-0.005(1)	-0.001(1)
C(31)	0.015(1)	0.014(1)	0.018(1)	0.002(1)	-0.004(1)	0.002(1)
C(32)	0.021(1)	0.022(1)	0.017(1)	0.000(1)	-0.001(1)	0.003(1)
C(33)	0.021(1)	0.029(1)	0.024(1)	0.006(1)	0.001(1)	0.002(1)
C(34)	0.019(1)	0.025(1)	0.025(1)	0.004(1)	-0.001(1)	-0.007(1)
C(35)	0.020(1)	0.017(1)	0.021(1)	0.001(1)	-0.005(1)	-0.001(1)
C(36)	0.018(1)	0.014(1)	0.018(1)	0.001(1)	-0.003(1)	0.001(1)
C(37)	0.017(1)	0.015(1)	0.017(1)	0.002(1)	-0.003(1)	-0.001(1)
C(38)	0.021(1)	0.013(1)	0.017(1)	0.000(1)	-0.002(1)	-0.004(1)
C(39)	0.020(1)	0.021(1)	0.021(1)	0.003(1)	0.000(1)	0.000(1)
C(40)	0.023(1)	0.023(1)	0.024(1)	0.004(1)	-0.001(1)	-0.004(1)
C(41)	0.027(2)	0.018(1)	0.021(1)	0.001(1)	-0.004(1)	-0.008(1)
C(42)	0.018(1)	0.013(1)	0.020(1)	0.002(1)	-0.004(1)	0.000(1)
C(43)	0.025(1)	0.014(1)	0.018(1)	-0.004(1)	-0.007(1)	0.001(1)
C(44)	0.014(1)	0.014(1)	0.018(1)	-0.002(1)	-0.002(1)	0.000(1)
C(45)	0.022(1)	0.022(1)	0.018(1)	-0.005(1)	0.000(1)	0.000(1)
C(46)	0.025(1)	0.025(1)	0.012(1)	-0.002(1)	-0.002(1)	-0.002(1)
C(47)	0.017(1)	0.023(1)	0.014(1)	0.002(1)	-0.002(1)	-0.003(1)
C(48)	0.021(1)	0.017(1)	0.014(1)	0.000(1)	-0.001(1)	0.001(1)
C(49)	0.020(1)	0.015(1)	0.013(1)	-0.002(1)	-0.003(1)	0.000(1)
C(50)	0.021(1)	0.016(1)	0.021(1)	0.001(1)	0.000(1)	-0.004(1)
C(51)	0.020(1)	0.017(1)	0.024(1)	-0.001(1)	-0.004(1)	-0.002(1)
C(52)	0.022(1)	0.022(1)	0.024(1)	-0.003(1)	0.001(1)	-0.003(1)
C(53)	0.027(1)	0.023(1)	0.019(1)	0.002(1)	0.003(1)	-0.001(1)
C(54)	0.025(1)	0.025(1)	0.027(1)	0.004(1)	0.001(1)	0.007(1)
C(55)	0.021(1)	0.024(1)	0.026(1)	0.001(1)	0.004(1)	0.003(1)

Compound 247

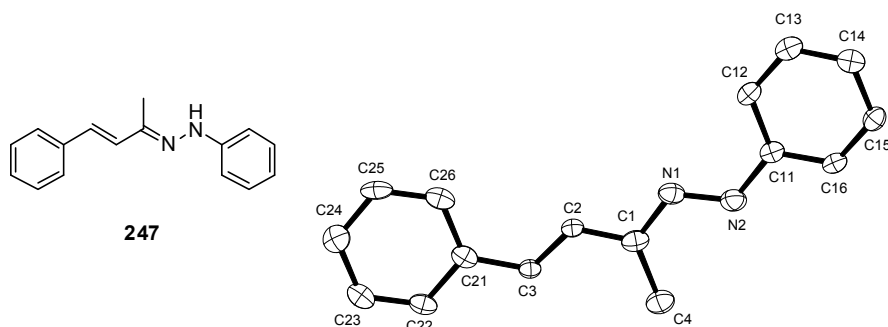


Table 1. Crystal data and structure refinement.

Identification code	6561	
Empirical formula	C ₁₆ H ₁₆ N ₂	
Color	colorless	
Formula weight	236.31 g·mol ⁻¹	
Temperature	100 K	
Wavelength	0.71073 Å	
Crystal system	Orthorhombic	
Space group	P2₁2₁2₁, (no. 19)	
Unit cell dimensions	a = 5.652(2) Å	α = 90°.
	b = 7.628(3) Å	β = 90°.
	c = 29.933(11) Å	γ = 90°.
Volume	1290.5(8) Å ³	
Z	4	
Density (calculated)	1.216 Mg·m ⁻³	
Absorption coefficient	0.072 mm ⁻¹	
F(000)	504 e	
Crystal size	0.18 x 0.14 x 0.02 mm ³	
θ range for data collection	4.08 to 26.37°.	
Index ranges	-7 ≤ h ≤ 7, -9 ≤ k ≤ 9, -37 ≤ l ≤ 37	
Reflections collected	21980	
Independent reflections	2621 [R _{int} = 0.0579]	
Reflections with I > 2σ(I)	2524	
Completeness to θ = 26.37°	99.3 %	
Absorption correction	Empirical	
Max. and min. transmission	0.75 and 0.57	
Refinement method	Full-matrix least-squares on F ²	
Data / restraints / parameters	2621 / 0 / 168	
Goodness-of-fit on F ²	1.190	
Final R indices [I > 2σ(I)]	R ₁ = 0.0779	wR ² = 0.1922
R indices (all data)	R ₁ = 0.0807	wR ² = 0.1936
Absolute structure parameter	-2(7)	
Largest diff. peak and hole	0.366 and -0.324 e·Å ⁻³	

Table 2. Atomic coordinates and equivalent isotropic displacement parameters (\AA^2).

U_{eq} is defined as one third of the trace of the orthogonalized U_{ij} tensor.

	x	y	z	U_{eq}
C(1)	0.5468(7)	0.8244(5)	0.1553(1)	0.025(1)
C(2)	0.6840(6)	0.8456(4)	0.1933(1)	0.017(1)
C(3)	0.6181(6)	0.7882(4)	0.2338(1)	0.019(1)
C(4)	0.3130(8)	0.7348(5)	0.1567(2)	0.032(1)
C(11)	0.6301(6)	0.9423(4)	0.0371(1)	0.020(1)
C(12)	0.8462(7)	1.0328(5)	0.0359(1)	0.023(1)
C(13)	0.9387(6)	1.0902(5)	-0.0048(1)	0.026(1)
C(14)	0.8207(7)	1.0567(5)	-0.0442(1)	0.025(1)
C(15)	0.6037(7)	0.9692(5)	-0.0433(1)	0.025(1)
C(16)	0.5109(6)	0.9152(4)	-0.0025(1)	0.021(1)
C(21)	0.7678(7)	0.8000(5)	0.2725(1)	0.023(1)
C(22)	0.6993(7)	0.7176(5)	0.3119(1)	0.025(1)
C(23)	0.8373(7)	0.7191(5)	0.3490(1)	0.030(1)
C(24)	1.0533(7)	0.8072(6)	0.3490(2)	0.032(1)
C(25)	1.1230(7)	0.8942(5)	0.3106(1)	0.031(1)
C(26)	0.9839(7)	0.8912(5)	0.2725(1)	0.028(1)
N(1)	0.6435(6)	0.8914(4)	0.1172(1)	0.027(1)
N(2)	0.5286(7)	0.8784(4)	0.0778(1)	0.031(1)

Table 3. Bond lengths [\AA] and angles [$^\circ$].

C(1)-N(1)	1.366(5)	C(1)-C(2)	1.384(5)
C(1)-C(4)	1.488(5)	C(2)-C(3)	1.342(5)
C(3)-C(21)	1.438(5)	C(11)-C(16)	1.380(5)
C(11)-C(12)	1.404(5)	C(11)-N(2)	1.432(5)
C(12)-C(13)	1.396(5)	C(13)-C(14)	1.379(5)
C(14)-C(15)	1.397(5)	C(15)-C(16)	1.390(5)
C(21)-C(22)	1.390(5)	C(21)-C(26)	1.405(5)
C(22)-C(23)	1.359(6)	C(23)-C(24)	1.393(6)
C(24)-C(25)	1.384(6)	C(25)-C(26)	1.384(6)
N(1)-N(2)	1.348(5)	N(2)-H(2A)	1.12(6)
N(1)-C(1)-C(2)	114.7(3)	N(1)-C(1)-C(4)	123.3(4)
C(2)-C(1)-C(4)	121.9(4)	C(3)-C(2)-C(1)	123.2(3)
C(2)-C(3)-C(21)	123.0(3)	C(16)-C(11)-C(12)	118.4(3)
C(16)-C(11)-N(2)	119.0(3)	C(12)-C(11)-N(2)	122.6(3)
C(13)-C(12)-C(11)	120.2(3)	C(14)-C(13)-C(12)	120.5(3)
C(13)-C(14)-C(15)	119.7(4)	C(16)-C(15)-C(14)	119.4(3)
C(11)-C(16)-C(15)	121.8(3)	C(22)-C(21)-C(26)	117.7(4)
C(22)-C(21)-C(3)	119.4(4)	C(26)-C(21)-C(3)	122.9(3)
C(23)-C(22)-C(21)	122.0(4)	C(22)-C(23)-C(24)	120.4(4)
C(25)-C(24)-C(23)	118.8(4)	C(26)-C(25)-C(24)	120.9(4)
C(25)-C(26)-C(21)	120.2(3)	N(2)-N(1)-C(1)	120.7(3)
N(1)-N(2)-C(11)	121.7(3)	N(1)-N(2)-H(2A)	119(3)
C(11)-N(2)-H(2A)	118(3)		

Table 4. Anisotropic displacement parameters (\AA^2).

The anisotropic displacement factor exponent takes the form:

$$-2\pi^2 [h^2 a^{*2} U_{11} + \dots + 2 h k a^* b^* U_{12}].$$

	U_{11}	U_{22}	U_{33}	U_{23}	U_{13}	U_{12}
C(1)	0.026(2)	0.015(2)	0.034(2)	-0.006(2)	0.005(2)	0.000(1)
C(2)	0.011(2)	0.018(2)	0.023(2)	-0.001(1)	0.005(1)	0.002(1)
C(3)	0.018(2)	0.018(2)	0.022(2)	-0.001(1)	0.004(1)	-0.001(1)
C(4)	0.032(2)	0.024(2)	0.040(2)	-0.003(2)	0.001(2)	-0.002(2)
C(11)	0.016(2)	0.014(2)	0.030(2)	-0.003(1)	0.002(2)	0.006(1)
C(12)	0.019(2)	0.018(2)	0.032(2)	-0.005(1)	-0.003(2)	0.003(1)
C(13)	0.017(2)	0.019(2)	0.043(2)	-0.003(2)	-0.001(2)	0.005(1)
C(14)	0.023(2)	0.020(2)	0.032(2)	-0.003(2)	0.009(2)	0.007(2)
C(15)	0.022(2)	0.025(2)	0.029(2)	-0.004(2)	-0.003(2)	0.002(2)
C(16)	0.014(2)	0.016(1)	0.033(2)	-0.003(1)	0.001(2)	0.003(1)
C(21)	0.030(2)	0.013(2)	0.027(2)	-0.001(1)	0.007(2)	0.006(2)
C(22)	0.028(2)	0.015(2)	0.032(2)	0.002(2)	0.008(2)	0.003(2)
C(23)	0.034(2)	0.027(2)	0.030(2)	0.006(2)	0.008(2)	0.005(2)
C(24)	0.026(2)	0.030(2)	0.041(2)	0.000(2)	-0.002(2)	0.008(2)
C(25)	0.025(2)	0.016(2)	0.052(2)	0.004(2)	0.007(2)	-0.003(2)
C(26)	0.028(2)	0.022(2)	0.034(2)	0.003(2)	0.012(2)	0.004(2)
N(1)	0.032(2)	0.020(2)	0.031(2)	-0.001(1)	0.004(1)	-0.003(2)
N(2)	0.036(2)	0.024(2)	0.032(2)	0.000(1)	0.001(2)	-0.006(2)

Compound 246

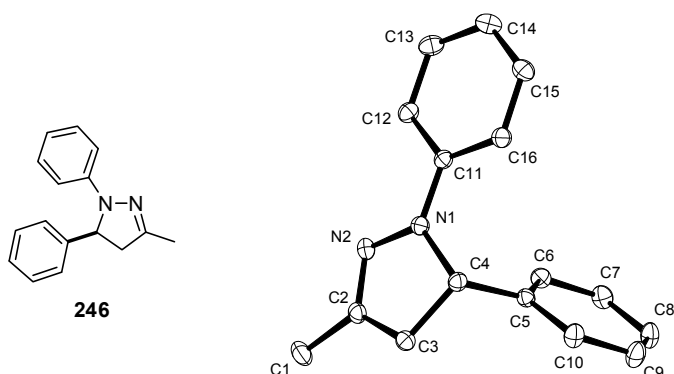


Table 1. Crystal data and structure refinement.

Identification code	6697	
Empirical formula	$C_{16}H_{16}N_2$	
Color	colourless	
Formula weight	$236.31 \text{ g}\cdot\text{mol}^{-1}$	
Temperature	100 K	
Wavelength	0.71073 \AA	
Crystal system	Triclinic	
Space group	P1, (no. 2)	
Unit cell dimensions	$a = 6.2589(12) \text{ \AA}$ $b = 8.1229(16) \text{ \AA}$ $c = 12.366(2) \text{ \AA}$	$\alpha = 89.027(4)^\circ$ $\beta = 81.308(4)^\circ$ $\gamma = 89.676(4)^\circ$
Volume	$621.4(2) \text{ \AA}^3$	
Z	2	
Density (calculated)	$1.263 \text{ Mg}\cdot\text{m}^{-3}$	
Absorption coefficient	0.075 mm^{-1}	
F(000)	252 e	
Crystal size	$0.03 \times 0.02 \times 0.02 \text{ mm}^3$	
θ range for data collection	1.67 to 34.36°	
Index ranges	$-9 \leq h \leq 9$, $-12 \leq k \leq 12$, $-19 \leq l \leq 19$	
Reflections collected	20890	
Independent reflections	5084 [$R_{\text{int}} = 0.0368$]	
Reflections with $I > 2\sigma(I)$	3788	
Completeness to $\theta = 34.36^\circ$	97.6 %	
Absorption correction	Gaussian	
Max. and min. transmission	0.61 and 0.39	
Refinement method	Full-matrix least-squares on F^2	
Data / restraints / parameters	5084 / 0 / 164	
Goodness-of-fit on F^2	1.443	
Final R indices [$I > 2\sigma(I)$]	$R_1 = 0.0518$	$wR^2 = 0.1874$
R indices (all data)	$R_1 = 0.0775$	$wR^2 = 0.2053$
Largest diff. peak and hole	0.540 and $-0.400 \text{ e}\cdot\text{\AA}^{-3}$	

Table 2. Atomic coordinates and equivalent isotropic displacement parameters (\AA^2).

U_{eq} is defined as one third of the trace of the orthogonalized U_{ij} tensor.

	x	y	z	U_{eq}
N(1)	0.4922(2)	-1.9795(1)	-1.1568(1)	0.016(1)
N(2)	0.3161(2)	-2.0745(1)	-1.1097(1)	0.016(1)
C(1)	0.2457(2)	-2.3401(2)	-1.0185(1)	0.023(1)
C(2)	0.3899(2)	-2.2118(1)	-1.0770(1)	0.016(1)
C(3)	0.6318(2)	-2.2248(1)	-1.0985(1)	0.017(1)
C(4)	0.6947(2)	-2.0744(1)	-1.1742(1)	0.014(1)
C(5)	0.7648(2)	-2.1228(1)	-1.2922(1)	0.013(1)
C(6)	0.6208(2)	-2.1256(1)	-1.3678(1)	0.015(1)
C(7)	0.6884(2)	-2.1797(1)	-1.4733(1)	0.018(1)
C(8)	0.9002(2)	-2.2294(2)	-1.5045(1)	0.020(1)
C(9)	1.0458(2)	-2.2245(2)	-1.4303(1)	0.022(1)
C(10)	0.9783(2)	-2.1713(2)	-1.3247(1)	0.018(1)
C(11)	0.4570(2)	-1.8297(1)	-1.2057(1)	0.014(1)
C(12)	0.2486(2)	-1.7616(1)	-1.1971(1)	0.016(1)
C(13)	0.2188(2)	-1.6079(1)	-1.2431(1)	0.020(1)
C(14)	0.3921(2)	-1.5194(1)	-1.2982(1)	0.021(1)
C(15)	0.5981(2)	-1.5869(1)	-1.3074(1)	0.019(1)
C(16)	0.6319(2)	-1.7407(1)	-1.2621(1)	0.016(1)

Table 3. Bond lengths [\AA] and angles [$^\circ$].

N(1)-C(11)	1.3811(14)	N(1)-N(2)	1.3963(13)
N(1)-C(4)	1.4689(15)	N(2)-C(2)	1.2873(15)
C(1)-C(2)	1.4864(16)	C(2)-C(3)	1.5010(18)
C(3)-C(4)	1.5425(16)	C(4)-C(5)	1.5171(16)
C(5)-C(10)	1.3925(17)	C(5)-C(6)	1.3934(16)
C(6)-C(7)	1.3868(17)	C(7)-C(8)	1.3834(19)
C(8)-C(9)	1.3885(18)	C(9)-C(10)	1.3860(17)
C(11)-C(16)	1.4027(16)	C(11)-C(12)	1.4037(17)
C(12)-C(13)	1.3866(16)	C(13)-C(14)	1.3883(18)
C(14)-C(15)	1.3874(19)	C(15)-C(16)	1.3889(16)
C(11)-N(1)-N(2)	119.62(10)	C(11)-N(1)-C(4)	125.67(10)
N(2)-N(1)-C(4)	112.52(9)	C(2)-N(2)-N(1)	107.80(10)
N(2)-C(2)-C(1)	122.05(12)	N(2)-C(2)-C(3)	113.73(10)
C(1)-C(2)-C(3)	124.14(11)	C(2)-C(3)-C(4)	102.26(9)
N(1)-C(4)-C(5)	113.66(9)	N(1)-C(4)-C(3)	100.67(9)
C(5)-C(4)-C(3)	112.33(9)	C(10)-C(5)-C(6)	119.17(11)
C(10)-C(5)-C(4)	118.71(10)	C(6)-C(5)-C(4)	122.08(10)
C(7)-C(6)-C(5)	120.31(11)	C(8)-C(7)-C(6)	120.12(11)
C(7)-C(8)-C(9)	120.01(12)	C(10)-C(9)-C(8)	119.94(12)
C(9)-C(10)-C(5)	120.43(11)	N(1)-C(11)-C(16)	119.94(11)
N(1)-C(11)-C(12)	121.01(10)	C(16)-C(11)-C(12)	119.02(10)
C(13)-C(12)-C(11)	119.88(11)	C(12)-C(13)-C(14)	121.07(12)
C(15)-C(14)-C(13)	119.14(11)	C(14)-C(15)-C(16)	120.82(11)
C(15)-C(16)-C(11)	120.07(11)		

Table 4. Anisotropic displacement parameters (\AA^2).

The anisotropic displacement factor exponent takes the form:

$$-2\pi^2 [h^2 a^{*2} U_{11} + \dots + 2 h k a^* b^* U_{12}].$$

	U ₁₁	U ₂₂	U ₃₃	U ₂₃	U ₁₃	U ₁₂
N(1)	0.012(1)	0.015(1)	0.019(1)	0.003(1)	0.002(1)	0.001(1)
N(2)	0.015(1)	0.018(1)	0.014(1)	0.001(1)	0.000(1)	-0.002(1)
C(1)	0.028(1)	0.021(1)	0.018(1)	0.005(1)	0.000(1)	-0.005(1)
C(2)	0.018(1)	0.017(1)	0.012(1)	0.000(1)	-0.002(1)	-0.001(1)
C(3)	0.020(1)	0.018(1)	0.014(1)	0.002(1)	-0.002(1)	0.003(1)
C(4)	0.013(1)	0.016(1)	0.014(1)	0.000(1)	-0.002(1)	0.002(1)
C(5)	0.012(1)	0.014(1)	0.014(1)	0.002(1)	-0.002(1)	0.000(1)
C(6)	0.012(1)	0.017(1)	0.017(1)	0.001(1)	-0.003(1)	0.000(1)
C(7)	0.017(1)	0.022(1)	0.015(1)	0.001(1)	-0.005(1)	-0.001(1)
C(8)	0.020(1)	0.027(1)	0.013(1)	-0.001(1)	0.000(1)	0.000(1)
C(9)	0.014(1)	0.032(1)	0.019(1)	-0.001(1)	0.000(1)	0.004(1)
C(10)	0.013(1)	0.026(1)	0.016(1)	0.000(1)	-0.004(1)	0.002(1)
C(11)	0.014(1)	0.014(1)	0.013(1)	-0.002(1)	-0.002(1)	0.000(1)
C(12)	0.014(1)	0.016(1)	0.018(1)	-0.002(1)	-0.002(1)	0.000(1)
C(13)	0.017(1)	0.018(1)	0.024(1)	-0.002(1)	-0.007(1)	0.003(1)
C(14)	0.024(1)	0.016(1)	0.025(1)	0.002(1)	-0.008(1)	0.000(1)
C(15)	0.020(1)	0.017(1)	0.020(1)	0.002(1)	-0.003(1)	-0.003(1)
C(16)	0.015(1)	0.016(1)	0.017(1)	0.000(1)	-0.002(1)	0.000(1)

Compound 250h

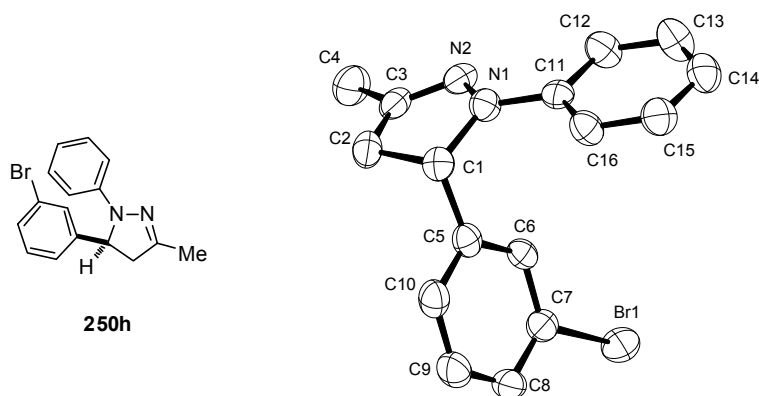


Table 1. Crystal data and structure refinement.

Identification code	6593	
Empirical formula	C ₁₆ H ₁₅ Br N ₂	
Color	colourless	
Formula weight	315.21 g·mol ⁻¹	
Temperature	200 K	
Wavelength	1.54178 Å	
Crystal system	Triclinic	
Space group	P 1, (no. 1)	
Unit cell dimensions	a = 6.3869(2) Å b = 13.0600(4) Å c = 13.2188(5) Å	α = 100.876(1)°. β = 92.7320(10)°. γ = 101.600(1)°.
Volume	1056.49(6) Å ³	
Z	3	
Density (calculated)	1.486 Mg·m ⁻³	
Absorption coefficient F(000)	3.860 mm ⁻¹ 480 e	
Crystal size	0.40 x 0.30 x 0.10 mm ³	
θ range for data collection	3.42 to 66.95°.	
Index ranges	-7 ≤ h ≤ 7, -12 ≤ k ≤ 14, -15 ≤ l ≤ 15	
Reflections collected	24198	
Independent reflections	6017 [R _{int} = 0.0319]	
Reflections with I > 2σ(I)	5931	
Completeness to θ = 66.95°	95.7 %	
Absorption correction	Gaussian	
Max. and min. transmission	0.72464 and 0.19898	
Refinement method	Full-matrix least-squares on F ²	
Data / restraints / parameters	6017 / 3 / 518	
Goodness-of-fit on F ²	1.059	
Final R indices [I > 2σ(I)]	R ₁ = 0.0237	wR ² = 0.0594
R indices (all data)	R ₁ = 0.0240	wR ² = 0.0595
Absolute structure parameter	-0.004(10)	
Extinction coefficient	0.00044(17)	
Largest diff. peak and hole	0.297 and -0.266 e·Å ⁻³	

Table 2. Atomic coordinates and equivalent isotropic displacement parameters (\AA^2).

U_{eq} is defined as one third of the trace of the orthogonalized U_{ij} tensor.

	x	y	z	U_{eq}
C(1)	-0.0613(4)	0.8632(2)	0.3650(2)	0.035(1)
C(2)	-0.0224(4)	0.8105(2)	0.4581(2)	0.041(1)
C(3)	0.2068(4)	0.8032(2)	0.4517(2)	0.038(1)
C(4)	0.3374(6)	0.7766(3)	0.5354(3)	0.054(1)
C(5)	-0.0569(4)	0.9810(2)	0.4015(2)	0.035(1)
C(6)	0.1226(4)	1.0601(2)	0.4004(2)	0.033(1)
C(7)	0.1160(4)	1.1650(2)	0.4406(2)	0.037(1)
C(8)	-0.0616(5)	1.1944(3)	0.4829(2)	0.045(1)
C(9)	-0.2398(5)	1.1146(3)	0.4836(3)	0.050(1)
C(10)	-0.2387(4)	1.0096(3)	0.4424(2)	0.043(1)
C(11)	0.1663(4)	0.8762(2)	0.2139(2)	0.034(1)
C(12)	0.3659(5)	0.8759(3)	0.1758(2)	0.045(1)
C(13)	0.4090(5)	0.9107(3)	0.0849(2)	0.055(1)
C(14)	0.2592(5)	0.9459(3)	0.0300(2)	0.049(1)
C(15)	0.0616(5)	0.9453(3)	0.0670(2)	0.047(1)
C(16)	0.0137(5)	0.9116(3)	0.1582(2)	0.041(1)
C(17)	0.5390(4)	0.4908(2)	0.6493(2)	0.037(1)
C(18)	0.5805(5)	0.4210(2)	0.7275(2)	0.043(1)
C(19)	0.8073(5)	0.4132(2)	0.7125(2)	0.042(1)
C(20)	0.9411(6)	0.3702(3)	0.7820(3)	0.064(1)
C(21)	0.5437(4)	0.6047(2)	0.7032(2)	0.033(1)
C(22)	0.7209(4)	0.6869(2)	0.7068(2)	0.033(1)
C(23)	0.7195(4)	0.7877(2)	0.7608(2)	0.034(1)
C(24)	0.5453(5)	0.8109(2)	0.8120(2)	0.040(1)
C(25)	0.3680(5)	0.7288(3)	0.8075(2)	0.043(1)
C(26)	0.3658(4)	0.6274(3)	0.7529(2)	0.039(1)
C(27)	0.7350(4)	0.5066(2)	0.4880(2)	0.036(1)
C(28)	0.9157(5)	0.4938(3)	0.4346(2)	0.045(1)
C(29)	0.9288(6)	0.5192(3)	0.3381(2)	0.055(1)
C(30)	0.7687(6)	0.5567(3)	0.2922(2)	0.058(1)
C(31)	0.5902(5)	0.5685(3)	0.3436(2)	0.053(1)
C(32)	0.5732(4)	0.5440(2)	0.4414(2)	0.042(1)
C(33)	0.3832(5)	0.2562(3)	1.0529(2)	0.044(1)
C(34)	0.4790(6)	0.2463(3)	1.1591(2)	0.055(1)
C(35)	0.6716(5)	0.2028(3)	1.1328(2)	0.047(1)
C(36)	0.8246(7)	0.1823(4)	1.2120(3)	0.067(1)
C(37)	0.3674(5)	0.3690(3)	1.0488(2)	0.040(1)
C(38)	0.5364(5)	0.4407(2)	1.0218(2)	0.042(1)
C(39)	0.5197(5)	0.5451(3)	1.0249(2)	0.050(1)
C(40)	0.3384(7)	0.5809(3)	1.0544(3)	0.062(1)
C(41)	0.1706(7)	0.5091(4)	1.0804(3)	0.065(1)
C(42)	0.1831(6)	0.4047(3)	1.0779(3)	0.056(1)
C(43)	0.4760(4)	0.1694(2)	0.8800(2)	0.033(1)
C(44)	0.6039(4)	0.1095(2)	0.8228(2)	0.040(1)
C(45)	0.5449(6)	0.0651(3)	0.7196(3)	0.049(1)
C(46)	0.3611(5)	0.0797(3)	0.6710(2)	0.047(1)
C(47)	0.2342(5)	0.1393(3)	0.7269(2)	0.044(1)
C(48)	0.2898(5)	0.1840(2)	0.8305(2)	0.041(1)
Br(1)	0.3587(1)	1.2747(1)	0.4349(1)	0.052(1)
Br(2)	0.9603(1)	0.9006(1)	0.7616(1)	0.044(1)
Br(3)	0.7543(1)	0.6439(1)	0.9912(1)	0.077(1)
N(1)	0.1182(3)	0.8413(2)	0.3051(2)	0.036(1)

N(2)	0.2816(4)	0.8195(2)	0.3662(2)	0.038(1)
N(3)	0.7161(3)	0.4812(2)	0.5844(2)	0.038(1)
N(4)	0.8764(3)	0.4440(2)	0.6316(2)	0.038(1)
N(5)	0.5349(4)	0.2170(2)	0.9837(2)	0.041(1)
N(6)	0.6969(4)	0.1848(2)	1.0364(2)	0.043(1)

Table 3. Bond lengths [Å] and angles [°].

C(1)-N(1)	1.469(3)	C(1)-C(5)	1.518(4)
C(1)-C(2)	1.552(4)	C(2)-C(3)	1.491(4)
C(3)-N(2)	1.285(4)	C(3)-C(4)	1.488(4)
C(5)-C(6)	1.383(4)	C(5)-C(10)	1.393(4)
C(6)-C(7)	1.382(4)	C(7)-C(8)	1.379(4)
C(7)-Br(1)	1.903(3)	C(8)-C(9)	1.382(5)
C(9)-C(10)	1.377(5)	C(11)-N(1)	1.392(3)
C(11)-C(12)	1.394(4)	C(11)-C(16)	1.395(4)
C(12)-C(13)	1.383(4)	C(13)-C(14)	1.375(5)
C(14)-C(15)	1.374(4)	C(15)-C(16)	1.387(4)
C(17)-N(3)	1.463(3)	C(17)-C(21)	1.518(4)
C(17)-C(18)	1.548(4)	C(18)-C(19)	1.493(4)
C(19)-N(4)	1.279(4)	C(19)-C(20)	1.484(4)
C(21)-C(22)	1.386(4)	C(21)-C(26)	1.394(4)
C(22)-C(23)	1.376(4)	C(23)-C(24)	1.385(4)
C(23)-Br(2)	1.902(3)	C(24)-C(25)	1.385(4)
C(25)-C(26)	1.380(4)	C(27)-N(3)	1.382(4)
C(27)-C(32)	1.393(4)	C(27)-C(28)	1.402(4)
C(28)-C(29)	1.380(5)	C(29)-C(30)	1.382(5)
C(30)-C(31)	1.375(5)	C(31)-C(32)	1.392(4)
C(33)-N(5)	1.465(4)	C(33)-C(37)	1.507(5)
C(33)-C(34)	1.543(4)	C(34)-C(35)	1.485(5)
C(35)-N(6)	1.276(4)	C(35)-C(36)	1.494(4)
C(37)-C(38)	1.387(4)	C(37)-C(42)	1.395(4)
C(38)-C(39)	1.382(5)	C(39)-C(40)	1.379(5)
C(39)-Br(3)	1.900(4)	C(40)-C(41)	1.378(6)
C(41)-C(42)	1.376(6)	C(43)-N(5)	1.393(3)
C(43)-C(48)	1.393(4)	C(43)-C(44)	1.394(4)
C(44)-C(45)	1.379(5)	C(45)-C(46)	1.376(5)
C(46)-C(47)	1.379(5)	C(47)-C(48)	1.383(4)
N(1)-N(2)	1.396(3)	N(3)-N(4)	1.388(3)
N(5)-N(6)	1.396(3)		
N(1)-C(1)-C(5)	114.2(2)	N(1)-C(1)-C(2)	100.5(2)
C(5)-C(1)-C(2)	110.7(2)	C(3)-C(2)-C(1)	101.4(2)
N(2)-C(3)-C(4)	122.4(3)	N(2)-C(3)-C(2)	114.2(2)
C(4)-C(3)-C(2)	123.3(2)	C(6)-C(5)-C(10)	119.0(3)
C(6)-C(5)-C(1)	122.9(2)	C(10)-C(5)-C(1)	118.1(3)
C(7)-C(6)-C(5)	118.9(2)	C(8)-C(7)-C(6)	122.9(3)
C(8)-C(7)-Br(1)	118.0(2)	C(6)-C(7)-Br(1)	119.1(2)
C(7)-C(8)-C(9)	117.7(3)	C(10)-C(9)-C(8)	120.6(3)
C(9)-C(10)-C(5)	121.0(3)	N(1)-C(11)-C(12)	121.1(2)
N(1)-C(11)-C(16)	120.4(2)	C(12)-C(11)-C(16)	118.5(2)
C(13)-C(12)-C(11)	119.9(3)	C(14)-C(13)-C(12)	121.8(3)
C(15)-C(14)-C(13)	118.5(3)	C(14)-C(15)-C(16)	121.2(3)
C(15)-C(16)-C(11)	120.2(3)	N(3)-C(17)-C(21)	113.4(2)
N(3)-C(17)-C(18)	100.9(2)	C(21)-C(17)-C(18)	111.6(2)

C(19)-C(18)-C(17)	101.5(2)	N(4)-C(19)-C(20)	122.2(3)
N(4)-C(19)-C(18)	114.0(3)	C(20)-C(19)-C(18)	123.9(3)
C(22)-C(21)-C(26)	118.7(3)	C(22)-C(21)-C(17)	122.3(2)
C(26)-C(21)-C(17)	119.0(3)	C(23)-C(22)-C(21)	119.7(2)
C(22)-C(23)-C(24)	122.2(3)	C(22)-C(23)-Br(2)	119.2(2)
C(24)-C(23)-Br(2)	118.5(2)	C(23)-C(24)-C(25)	117.9(3)
C(26)-C(25)-C(24)	120.7(3)	C(25)-C(26)-C(21)	120.8(3)
N(3)-C(27)-C(32)	120.5(2)	N(3)-C(27)-C(28)	120.6(3)
C(32)-C(27)-C(28)	118.9(3)	C(29)-C(28)-C(27)	119.2(3)
C(28)-C(29)-C(30)	121.9(3)	C(31)-C(30)-C(29)	119.2(3)
C(30)-C(31)-C(32)	120.1(3)	C(31)-C(32)-C(27)	120.7(3)
N(5)-C(33)-C(37)	112.7(2)	N(5)-C(33)-C(34)	101.7(2)
C(37)-C(33)-C(34)	112.7(3)	C(35)-C(34)-C(33)	102.9(2)
N(6)-C(35)-C(34)	114.2(3)	N(6)-C(35)-C(36)	122.5(3)
C(34)-C(35)-C(36)	123.3(3)	C(38)-C(37)-C(42)	118.6(3)
C(38)-C(37)-C(33)	121.7(3)	C(42)-C(37)-C(33)	119.6(3)
C(39)-C(38)-C(37)	119.7(3)	C(40)-C(39)-C(38)	121.8(3)
C(40)-C(39)-Br(3)	118.6(3)	C(38)-C(39)-Br(3)	119.6(2)
C(41)-C(40)-C(39)	118.2(3)	C(42)-C(41)-C(40)	121.2(3)
C(41)-C(42)-C(37)	120.5(3)	N(5)-C(43)-C(48)	120.1(3)
N(5)-C(43)-C(44)	121.2(2)	C(48)-C(43)-C(44)	118.6(2)
C(45)-C(44)-C(43)	120.3(3)	C(46)-C(45)-C(44)	121.0(3)
C(45)-C(46)-C(47)	119.1(3)	C(46)-C(47)-C(48)	120.8(3)
C(47)-C(48)-C(43)	120.2(3)	C(11)-N(1)-N(2)	119.2(2)
C(11)-N(1)-C(1)	124.9(2)	N(2)-N(1)-C(1)	111.76(19)
C(3)-N(2)-N(1)	107.8(2)	C(27)-N(3)-N(4)	121.0(2)
C(27)-N(3)-C(17)	126.9(2)	N(4)-N(3)-C(17)	112.1(2)
C(19)-N(4)-N(3)	108.3(2)	C(43)-N(5)-N(6)	118.7(2)
C(43)-N(5)-C(33)	122.5(2)	N(6)-N(5)-C(33)	112.3(2)
C(35)-N(6)-N(5)	108.8(2)		

Table 4. Anisotropic displacement parameters (\AA^2).

The anisotropic displacement factor exponent takes the form:

$$-2\pi^2 [h^2 a^{*2} U_{11} + \dots + 2 h k a^* b^* U_{12}].$$

	U_{11}	U_{22}	U_{33}	U_{23}	U_{13}	U_{12}
C(1)	0.030(1)	0.036(2)	0.036(1)	0.006(1)	-0.001(1)	0.002(1)
C(2)	0.046(2)	0.039(2)	0.038(1)	0.013(1)	0.005(1)	0.002(1)
C(3)	0.048(1)	0.026(2)	0.038(1)	0.008(1)	0.000(1)	0.007(1)
C(4)	0.064(2)	0.056(2)	0.048(2)	0.020(2)	0.000(1)	0.021(2)
C(5)	0.037(1)	0.042(2)	0.029(1)	0.011(1)	0.002(1)	0.009(1)
C(6)	0.034(1)	0.037(2)	0.026(1)	0.004(1)	0.003(1)	0.009(1)
C(7)	0.046(1)	0.035(2)	0.029(1)	0.005(1)	0.001(1)	0.007(1)
C(8)	0.063(2)	0.043(2)	0.035(1)	0.009(1)	0.012(1)	0.024(1)
C(9)	0.048(2)	0.060(2)	0.053(2)	0.022(2)	0.018(1)	0.026(2)
C(10)	0.036(1)	0.050(2)	0.049(2)	0.020(1)	0.010(1)	0.009(1)
C(11)	0.040(1)	0.027(1)	0.030(1)	-0.001(1)	0.000(1)	0.004(1)
C(12)	0.042(1)	0.058(2)	0.036(1)	0.009(1)	0.002(1)	0.018(1)
C(13)	0.047(2)	0.076(3)	0.043(2)	0.014(2)	0.010(1)	0.014(2)
C(14)	0.055(2)	0.056(2)	0.035(1)	0.011(1)	0.005(1)	0.010(2)
C(15)	0.053(2)	0.052(2)	0.036(1)	0.009(1)	-0.001(1)	0.013(1)
C(16)	0.041(2)	0.051(2)	0.032(1)	0.008(1)	0.004(1)	0.013(1)
C(17)	0.034(1)	0.035(2)	0.041(1)	0.004(1)	0.007(1)	0.004(1)

C(18)	0.050(2)	0.031(2)	0.050(2)	0.010(1)	0.016(1)	0.009(1)
C(19)	0.050(2)	0.026(2)	0.049(2)	0.010(1)	0.007(1)	0.006(1)
C(20)	0.062(2)	0.061(3)	0.084(2)	0.044(2)	0.010(2)	0.018(2)
C(21)	0.034(1)	0.034(2)	0.031(1)	0.008(1)	0.003(1)	0.008(1)
C(22)	0.034(1)	0.033(2)	0.033(1)	0.008(1)	0.005(1)	0.010(1)
C(23)	0.038(1)	0.031(2)	0.031(1)	0.010(1)	-0.001(1)	0.004(1)
C(24)	0.052(2)	0.035(2)	0.037(1)	0.009(1)	0.009(1)	0.016(1)
C(25)	0.044(2)	0.042(2)	0.046(2)	0.010(1)	0.013(1)	0.018(1)
C(26)	0.036(1)	0.038(2)	0.047(2)	0.012(1)	0.008(1)	0.009(1)
C(27)	0.038(1)	0.026(2)	0.037(1)	0.000(1)	0.005(1)	-0.001(1)
C(28)	0.047(2)	0.042(2)	0.042(2)	0.003(1)	0.010(1)	0.008(1)
C(29)	0.061(2)	0.061(2)	0.043(2)	0.008(2)	0.017(2)	0.011(2)
C(30)	0.065(2)	0.066(2)	0.037(2)	0.008(2)	0.006(1)	0.002(2)
C(31)	0.051(2)	0.052(2)	0.049(2)	0.010(1)	-0.011(1)	0.000(1)
C(32)	0.040(1)	0.038(2)	0.044(2)	0.004(1)	0.003(1)	0.003(1)
C(33)	0.053(2)	0.042(2)	0.040(2)	0.011(1)	0.006(1)	0.013(1)
C(34)	0.082(2)	0.055(2)	0.034(1)	0.015(1)	0.009(1)	0.024(2)
C(35)	0.063(2)	0.041(2)	0.038(2)	0.012(1)	-0.005(1)	0.008(1)
C(36)	0.087(3)	0.070(3)	0.046(2)	0.017(2)	-0.012(2)	0.018(2)
C(37)	0.052(2)	0.041(2)	0.029(1)	0.003(1)	0.000(1)	0.017(1)
C(38)	0.051(2)	0.037(2)	0.039(1)	0.007(1)	-0.002(1)	0.013(1)
C(39)	0.067(2)	0.041(2)	0.042(2)	0.008(1)	-0.006(1)	0.014(1)
C(40)	0.097(3)	0.048(2)	0.049(2)	0.006(2)	-0.005(2)	0.037(2)
C(41)	0.076(2)	0.073(3)	0.062(2)	0.018(2)	0.017(2)	0.046(2)
C(42)	0.058(2)	0.069(3)	0.052(2)	0.019(2)	0.014(2)	0.027(2)
C(43)	0.043(1)	0.025(1)	0.032(1)	0.010(1)	0.002(1)	0.003(1)
C(44)	0.045(1)	0.035(2)	0.039(1)	0.009(1)	0.003(1)	0.008(1)
C(45)	0.062(2)	0.044(2)	0.042(2)	0.006(2)	0.010(2)	0.012(2)
C(46)	0.060(2)	0.045(2)	0.031(1)	0.007(1)	-0.004(1)	0.000(1)
C(47)	0.044(2)	0.041(2)	0.046(2)	0.018(1)	-0.006(1)	-0.002(1)
C(48)	0.047(2)	0.038(2)	0.039(2)	0.011(1)	0.004(1)	0.009(1)
Br(1)	0.061(1)	0.032(1)	0.055(1)	-0.002(1)	0.008(1)	-0.001(1)
Br(2)	0.046(1)	0.033(1)	0.048(1)	0.006(1)	0.002(1)	0.001(1)
Br(3)	0.078(1)	0.050(1)	0.101(1)	0.036(1)	-0.021(1)	-0.002(1)
N(1)	0.038(1)	0.039(1)	0.033(1)	0.009(1)	0.002(1)	0.010(1)
N(2)	0.044(1)	0.030(1)	0.040(1)	0.007(1)	0.000(1)	0.010(1)
N(3)	0.039(1)	0.040(1)	0.036(1)	0.006(1)	0.008(1)	0.011(1)
N(4)	0.039(1)	0.027(1)	0.047(1)	0.005(1)	0.005(1)	0.007(1)
N(5)	0.054(1)	0.039(1)	0.034(1)	0.007(1)	-0.003(1)	0.017(1)
N(6)	0.051(1)	0.037(1)	0.042(1)	0.011(1)	-0.002(1)	0.009(1)

Compound 256d

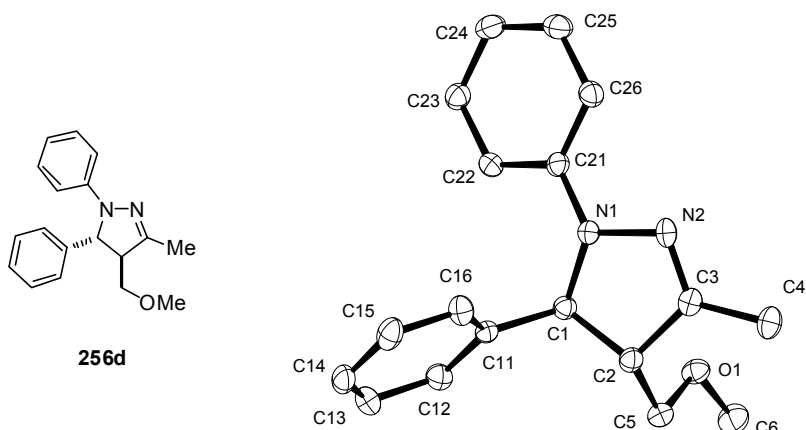


Table 1. Crystal data and structure refinement.

Identification code	6952	
Empirical formula	$C_{18}H_{20}N_2O$	
Color	colourless	
Formula weight	$280.36 \text{ g}\cdot\text{mol}^{-1}$	
Temperature	100 K	
Wavelength	0.71073 \AA	
Crystal system	ORTHORHOMBIC	
Space group	$Pna2_1$, (no. 33)	
Unit cell dimensions	$a = 10.9384(13) \text{ \AA}$	$\alpha = 90^\circ$.
	$b = 16.1053(19) \text{ \AA}$	$\beta = 90^\circ$.
	$c = 8.7343(9) \text{ \AA}$	$\gamma = 90^\circ$.
Volume	$1538.7(3) \text{ \AA}^3$	
Z	4	
Density (calculated)	$1.210 \text{ Mg}\cdot\text{m}^{-3}$	
Absorption coefficient	0.076 mm^{-1}	
F(000)	600 e	
Crystal size	$0.28 \times 0.09 \times 0.04 \text{ mm}^3$	
θ range for data collection	2.65 to 31.80° .	
Index ranges	$-16 \leq h \leq 16$, $-23 \leq k \leq 23$, $-12 \leq l \leq 12$	
Reflections collected	38794	
Independent reflections	2775 [$R_{\text{int}} = 0.0764$]	
Reflections with $I > 2\sigma(I)$	2250	
Completeness to $\theta = 27.50^\circ$	99.9 %	
Absorption correction	Gaussian	
Max. and min. transmission	0.99 and 0.98	
Refinement method	Full-matrix least-squares on F^2	
Data / restraints / parameters	2775 / 1 / 192	
Goodness-of-fit on F^2	1.074	
Final R indices [$I > 2\sigma(I)$]	$R_1 = 0.0418$	$wR^2 = 0.0804$
R indices (all data)	$R_1 = 0.0639$	$wR^2 = 0.0896$
Absolute structure parameter	-0.4(15)	
Largest diff. peak and hole	0.199 and $-0.214 \text{ e}\cdot\text{\AA}^{-3}$	

Table 2. Atomic coordinates and equivalent isotropic displacement parameters (\AA^2).

U_{eq} is defined as one third of the trace of the orthogonalized U_{ij} tensor.

	x	y	z	U_{eq}
O(1)	0.3374(1)	0.4422(1)	0.3796(2)	0.022(1)
N(1)	0.6680(1)	0.4097(1)	0.4677(2)	0.021(1)
N(2)	0.6436(1)	0.4957(1)	0.4622(2)	0.020(1)
C(1)	0.5597(1)	0.3624(1)	0.5190(2)	0.018(1)
C(2)	0.4778(2)	0.4320(1)	0.5869(2)	0.019(1)
C(3)	0.5407(2)	0.5090(1)	0.5283(2)	0.019(1)
C(4)	0.4893(2)	0.5941(1)	0.5464(2)	0.025(1)
C(5)	0.3446(2)	0.4267(1)	0.5402(2)	0.023(1)
C(6)	0.2146(2)	0.4487(1)	0.3293(3)	0.030(1)
C(11)	0.5917(2)	0.2944(1)	0.6323(2)	0.018(1)
C(12)	0.5231(2)	0.2214(1)	0.6368(2)	0.024(1)
C(13)	0.5504(2)	0.1597(1)	0.7440(3)	0.030(1)
C(14)	0.6464(2)	0.1700(1)	0.8451(2)	0.028(1)
C(15)	0.7159(2)	0.2421(1)	0.8401(2)	0.028(1)
C(16)	0.6885(2)	0.3040(1)	0.7348(2)	0.024(1)
C(21)	0.7527(2)	0.3778(1)	0.3646(2)	0.018(1)
C(22)	0.7536(2)	0.2926(1)	0.3307(2)	0.020(1)
C(23)	0.8422(2)	0.2597(1)	0.2335(2)	0.022(1)
C(24)	0.9301(2)	0.3102(1)	0.1670(2)	0.025(1)
C(25)	0.9269(2)	0.3950(1)	0.1979(2)	0.025(1)
C(26)	0.8409(2)	0.4288(1)	0.2962(2)	0.022(1)

Table 3. Bond lengths [\AA] and angles [$^\circ$].

O(1)-C(5)	1.427(2)	O(1)-C(6)	1.417(2)
N(1)-N(2)	1.4110(19)	N(1)-C(21)	1.390(2)
N(1)-C(1)	1.479(2)	N(2)-C(3)	1.282(2)
C(21)-C(26)	1.401(2)	C(21)-C(22)	1.403(2)
C(26)-C(25)	1.385(3)	C(15)-C(14)	1.388(3)
C(15)-C(16)	1.390(3)	C(5)-C(2)	1.516(2)
C(14)-C(13)	1.382(3)	C(2)-C(1)	1.552(2)
C(2)-C(3)	1.509(2)	C(24)-C(25)	1.392(3)
C(24)-C(23)	1.386(3)	C(1)-C(11)	1.517(2)
C(3)-C(4)	1.490(2)	C(23)-C(22)	1.393(2)
C(13)-C(12)	1.398(3)	C(12)-C(11)	1.396(2)
C(16)-C(11)	1.395(2)		
O(1)-C(5)-C(2)	107.92(14)	N(1)-C(21)-C(26)	121.21(16)
N(1)-C(21)-C(22)	120.23(15)	N(1)-C(1)-C(2)	101.90(13)
N(1)-C(1)-C(11)	112.62(13)	N(2)-N(1)-C(1)	111.35(13)
N(2)-C(3)-C(2)	114.53(15)	N(2)-C(3)-C(4)	122.21(16)
C(21)-N(1)-N(2)	117.87(15)	C(21)-N(1)-C(1)	122.65(15)
C(26)-C(21)-C(22)	118.53(16)	C(26)-C(25)-C(24)	121.51(17)
C(15)-C(16)-C(11)	120.56(17)	C(5)-C(2)-C(1)	114.30(14)
C(14)-C(15)-C(16)	120.22(19)	C(14)-C(13)-C(12)	120.29(18)
C(24)-C(23)-C(22)	121.00(17)	C(25)-C(26)-C(21)	120.12(17)
C(3)-N(2)-N(1)	108.38(14)	C(3)-C(2)-C(5)	113.15(15)
C(3)-C(2)-C(1)	101.60(14)	C(4)-C(3)-C(2)	123.26(16)
C(23)-C(24)-C(25)	118.46(17)	C(23)-C(22)-C(21)	120.36(16)

C(6)-O(1)-C(5)	111.71(15)	C(13)-C(14)-C(15)	119.79(18)
C(12)-C(11)-C(1)	120.13(16)	C(16)-C(11)-C(1)	120.93(15)
C(16)-C(11)-C(12)	118.94(16)	C(11)-C(1)-C(2)	113.89(14)
C(11)-C(12)-C(13)	120.20(18)		

Table 4. Anisotropic displacement parameters (\AA^2).

The anisotropic displacement factor exponent takes the form:

$$-2\pi^2 [h^2 a^{*2} U_{11} + \dots + 2 h k a^* b^* U_{12}].$$

	U_{11}	U_{22}	U_{33}	U_{23}	U_{13}	U_{12}
O(1)	0.017(1)	0.028(1)	0.021(1)	-0.001(1)	-0.001(1)	0.001(1)
N(1)	0.023(1)	0.015(1)	0.025(1)	0.002(1)	0.006(1)	0.002(1)
N(2)	0.025(1)	0.014(1)	0.022(1)	0.000(1)	-0.004(1)	0.001(1)
C(1)	0.018(1)	0.018(1)	0.017(1)	0.000(1)	0.000(1)	0.001(1)
C(2)	0.022(1)	0.020(1)	0.016(1)	0.000(1)	0.002(1)	0.004(1)
C(3)	0.022(1)	0.019(1)	0.017(1)	-0.002(1)	-0.004(1)	0.002(1)
C(4)	0.028(1)	0.018(1)	0.028(1)	-0.004(1)	-0.005(1)	0.004(1)
C(5)	0.021(1)	0.023(1)	0.024(1)	0.001(1)	0.005(1)	0.003(1)
C(6)	0.020(1)	0.033(1)	0.036(1)	0.002(1)	-0.005(1)	0.001(1)
C(11)	0.019(1)	0.019(1)	0.018(1)	0.001(1)	0.003(1)	0.003(1)
C(12)	0.021(1)	0.023(1)	0.029(1)	0.004(1)	0.001(1)	-0.001(1)
C(13)	0.031(1)	0.021(1)	0.038(1)	0.008(1)	0.007(1)	0.000(1)
C(14)	0.036(1)	0.026(1)	0.022(1)	0.007(1)	0.006(1)	0.012(1)
C(15)	0.033(1)	0.029(1)	0.021(1)	0.000(1)	-0.004(1)	0.010(1)
C(16)	0.029(1)	0.020(1)	0.023(1)	0.000(1)	-0.002(1)	0.001(1)
C(21)	0.017(1)	0.020(1)	0.017(1)	0.003(1)	-0.001(1)	0.003(1)
C(22)	0.022(1)	0.020(1)	0.018(1)	0.003(1)	0.002(1)	0.001(1)
C(23)	0.024(1)	0.021(1)	0.021(1)	-0.001(1)	0.002(1)	0.003(1)
C(24)	0.019(1)	0.032(1)	0.023(1)	0.000(1)	0.004(1)	0.003(1)
C(25)	0.020(1)	0.030(1)	0.024(1)	0.004(1)	0.002(1)	-0.002(1)
C(26)	0.020(1)	0.021(1)	0.024(1)	0.004(1)	-0.001(1)	-0.001(1)

8 Bibliography

- [1] M. Klussmann, D. G. Blackmond, in *Chemical Evolution II: From the Origins of Life to Modern Society*, L. Zaikowski, J. M. Friedrich, S. R. Seidel (Eds.), ACS Symposium Series, **2009**, vol. 1025, chapter 7, pp. 133-145.
- [2] A. Burger, in *Drugs and People: Medications, Their History and Origins, and the Way They Act*, University Press of Virginia, USA, **1980**, pp. 4-5.
- [3] L. Pasteur, *Compt. Rend. Acad. Sci.* **1848**, *34*, 535.
- [4] J. H. van't Hoff, *Arch. Neerl. Sci. Exactes Nat.* **1874**, *9*, 445.
- [5] J. A. Le Bel, *Bull. Soc. Chim. France* **1874**, *22*, 331.
- [6] For a review on the origin of biomolecular handedness, see: S. F. Mason, *Nature* **1984**, *311*, 19.
- [7] (a) E. Fischer, *Ber. Dtsch. Chem. Ges.* **1894**, *27*, 2985. (b) E. Fischer, *Ber. Dtsch. Chem. Ges.* **1894**, *27*, 3479. (c) E. Fischer, *J. Chem. Soc., Trans.* **1907**, *91*, 1749.
- [8] J. Gal, in *Chirality in Drug Research*, E. Francotte, W. Lindner (Eds.), Wiley-VCH: Weinheim, **2006**.
- [9] FDA's Policy Statement for the Development of New Stereoisomeric Drugs, *Chirality* **1992**, *4*, 338.
- [10] Data are based on market studies by the market research firm Frost & Sullivan and were reported in: (a) S. S. Stinson, *Chem. Eng. News* **2001**, *79* (43), 45. (b) A. M. Rouhi, *Chem. Eng. News* **2004**, *82* (24), 47.
- [11] J. Halpern, B. M. Trost, *Proc. Natl. Acad. Sci. U.S.A.* **2004**, *101*, 5347.
- [12] "The Nobel Prize in Chemistry 2001". Nobelprize.org. 20 Oct 2011 http://www.nobelprize.org/nobel_prizes/chemistry/laureates/2001/
- [13] K. C. Nicolaou, E. J. Sorensen, *Classics in Total Synthesis*, Wiley-VCH: Weinheim, Germany, **1996**.
- [14] B. List, Y. W. Yang, *Science* **2006**, *313*, 1584.
- [15] W. S. Knowles, M. J. Sabacky, B. D. Vineyard, D. J. Weinkauff, *J. Am. Chem. Soc.* **1975**, *97*, 2567.
- [16] M. Kitamura, T. Ohkuma, S. Inoue, N. Sayo, H. Kumabayashi, S. Akutagawa, T. Ohta, H. Takaya, R. Noyori, *J. Am. Chem. Soc.* **1988**, *110*, 629.

- [17] T. Katsuki, K. B. Sharpless, *J. Am. Chem. Soc.* **1980**, *102*, 5976.
- [18] For recent reviews on asymmetric catalysis, see: (a) E. M. Carreira, L. Kvaerno, *Classics in Stereoselective Synthesis*; Wiley-VCH: Weinheim, Germany, **2009**. (b) E. J. Corey, L. Kürti, *Enantioselective Chemical Synthesis*; Direct Book Publishing, LLC: Dallas, USA, **2010**.
- [19] B. List, R. A. Lerner, C. F. Barbas III, *J. Am. Chem. Soc.* **2000**, *122*, 2395.
- [20] K. A. Ahrendt, C. J. Borths, D. W. C. MacMillan, *J. Am. Chem. Soc.* **2000**, *122*, 4243.
- [21] B. List, *Angew. Chem.* **2010**, *122*, 1774; *Angew. Chem. Int. Ed.* **2010**, *49*, 1730.
- [22] F. Wöhler, J. von Liebig, *Ann. Pharm.* **1832**, *3*, 249.
- [23] G. Breiding, P. S. Fiske, *Biochem. Z.* **1912**, *46*, 7.
- [24] For a reinvestigation of this reaction and first mechanistic studies, see: V. Prelog, M. Wilhelm, *Helv. Chim. Acta* **1954**, *37*, 1634.
- [25] H. Pracejus, *Liebigs Ann. Chem.* **1960**, *634*, 9.
- [26] (a) Z. G. Hajos, D. R. Parrish, *J. Org. Chem.* **1974**, *39*, 1615. (b) U. Eder, G. Sauer, R. Wiechert, *Angew. Chem.* **1971**, *83*, 492; *Angew. Chem. Int. Ed.* **1971**, *10*, 496.
- [27] For comprehensive reviews about asymmetric organocatalysis, see: (a) A. Berkessel, H. Gröger (Eds.), *Asymmetric Organocatalysis*, Wiley-VCH: Weinheim, **2005**. (b) P. I. Dalko (Ed.), *Enantioselective Organocatalysis: Reactions and Experimental Procedures*, Wiley-VCH: Weinheim, **2007**.
- [28] Data are based on a SciFinder® search of publications containing the concept 'organocatalysis'. The search was performed on November 20th, 2011. Although not all publications dealing with purely organic catalysts may be included, we consider this chart representative to illustrate the development of the field in recent years.
- [29] J. Seayad, B. List, *Org. Biomol. Chem.* **2005**, *3*, 719.
- [30] J. N. Brønsted, *Recl. Trav. Chim. Pays-Bas* **1923**, *42*, 718.
- [31] T. M. Lowry, *Chem. and Ind.* **1923**, *42*, 43.
- [32] M. S. Taylor, E. N. Jacobsen, *Angew. Chem.* **2006**, *118*, 1550; *Angew. Chem. Int. Ed.* **2006**, *45*, 1520.
- [33] For a related discussion concerning phosphoric acids, see: M. Fleischmann, D. Drettwan, E. Sugiono, M. Rueping, R. M. Gschwind, *Angew. Chem.* **2011**, *123*, 6488; *Angew. Chem. Int. Ed.* **2011**, *50*, 6364.
- [34] M. S. Sigman, E. N. Jacobsen, *J. Am. Chem. Soc.* **1998**, *120*, 4901.

- [35] Y. Hang, V. H. Rawal, *J. Am. Chem. Soc.* **2002**, *124*, 9662.
- [36] Y. Huang, A. K. Unni, A. N. Thadani, V. H. Rawal, *Nature* **2003**, *424*, 146.
- [37] For reviews on enantioselective catalysis by chiral hydrogen bond donors, see: (a) A. G. Doyle, E. N. Jacobsen, *Chem. Rev.* **2007**, *107*, 5713. (b) J. Alemán, A. Parra, H. Jiang, K. A. Jørgensen, *Chem. Eur. J.* **2011**, *17*, 6890.
- [38] For a study on the pK_a values of chiral Brønsted acids, see: P. Christ, A. G. Lindsay, S. S. Vormittag, J.-M. Neudörfl, A. Berkessel, A. C. O'Donoghue, *Chem. Eur. J.* **2011**, *17*, 8524.
- [39] T. Akiyama, J. Itoh, K. Yokota, K. Fuchibe, *Angew. Chem.* **2004**, *116*, 1592; *Angew. Chem. Int. Ed.* **2004**, *43*, 1566.
- [40] D. Uraguchi, M. Terada, *J. Am. Chem. Soc.* **2004**, *126*, 5356.
- [41] M. Hatano, K. Moriyama, T. Maki, K. Ishihara, *Angew. Chem.* **2010**, *122*, 3783; *Angew. Chem. Int. Ed.* **2010**, *49*, 3823.
- [42] (a) T. Akiyama, Y. Saitoh, H. Morita, K. Fuchibe, *Adv. Synth. Catal.* **2005**, *347*, 1523. See also: (b) A. Voiturez, A. B. Charette, *Adv. Synth. Catal.* **2006**, *348*, 2363.
- [43] G. B. Rowland, H. Zhang, E. B. Rowland, S. Chennamadhavuni, Y. Wang, J. C. Antilla, *J. Am. Chem. Soc.* **2005**, *127*, 15696.
- [44] X.-H. Chen, X.-Y. Xu, H. Liu, L.-F. Cun, L.-Z. Gong, *J. Am. Chem. Soc.* **2006**, *128*, 14802.
- [45] Q.-S. Guo, D.-M. Du, J. Xu, *Angew. Chem.* **2008**, *120*, 771; *Angew. Chem. Int. Ed.* **2008**, *47*, 759.
- [46] X.-H. Chen, W.-Q. Zhang, L.-Z. Gong, *J. Am. Chem. Soc.* **2008**, *130*, 5652.
- [47] M. Terada, K. Sorimachi, D. Uraguchi, *Synlett* **2006**, 133.
- [48] (a) P. Burk, I. A. Koppel, I. Koppel, L. M. Yagupolskii, R. W. Taft, *J. Comput. Chem.* **1996**, *17*, 30. (b) I. Leito, I. Kaljurand, I. A. Koppel, L. M. Yagupolskii, V. M. Vlasov, *J. Org. Chem.* **1998**, *63*, 7868. (c) I. A. Koppel, J. Koppel, I. Leito, I. Koppel, M. Mishima, L. M. Yagupolskii, *J. Chem. Soc., Perkin Trans. 2* **2001**, 229. (d) L. M. Yagupolskii, V. N. Petrik, N. V. Kondratenko, L. Sooväli, I. Kaljurand, I. Leito, I. A. Koppel, *J. Chem. Soc., Perkin Trans. 2* **2002**, 1950.
- [49] D. Nakashima, H. Yamamoto, *J. Am. Chem. Soc.* **2006**, *128*, 9626.
- [50] T. Hashimoto, K. Maruoka, *J. Am. Chem. Soc.* **2007**, *129*, 10054.
- [51] D. Uraguchi, K. Sorimachi, M. Terada, *J. Am. Chem. Soc.* **2004**, *126*, 11804.
- [52] J. Seayad, A. M. Seayad, B. List, *J. Am. Chem. Soc.* **2006**, *128*, 1086.

- [53] M. Terada, K. Machioka, K. Sorimachi, *Angew. Chem.* **2006**, *118*, 2312; *Angew. Chem. Int. Ed.* **2006**, *45*, 2254.
- [54] M. Rueping, E. Sugiono, C. Azap, *Angew. Chem.* **2006**, *118*, 2679; *Angew. Chem. Int. Ed.* **2006**, *45*, 2617.
- [55] S. Xu, Z. Wang, X. Zhang, X. Zhang, K. Ding, *Angew. Chem.* **2008**, *120*, 2882; *Angew. Chem. Int. Ed.* **2008**, *47*, 2840.
- [56] X. Cheng, R. Goddard, B. List, *Angew. Chem.* **2008**, *120*, 5157; *Angew. Chem.* **2008**, *47*, 5079.
- [57] For reviews on strong chiral Brønsted acid catalysis, see: (a) M. Terada, *Synthesis* **2010**, 1929. (b) D. Kampen, C. M. Reisinger, B. List, *Top. Curr. Chem.* **2009**, *291*, 395. (c) T. Akiyama, *Chem. Rev.* **2007**, *107*, 5744.
- [58] I. Fleming, *Pericyclic Reactions (Oxford Chemistry Primers)*, Oxford University Press, **1998**.
- [59] (a) A. Wohl, *Ber. Dtsch. Chem. Ges.* **1919**, *52*, 51. (b) A. Wohl, K. Jaschinowski, *Ber. Dtsch. Chem. Ges.* **1921**, *54*, 476. (c) K. Ziegler, G. Schenk, E. W. Krockow, A. Siebert, A. Wenz, H. Weber, *Liebigs Ann. Chem.* **1942**, *551*, 1. (d) K. Ziegler, A. Spath, E. Schaaf, W. Schumann, E. Winkelmann, *Liebigs Ann. Chem.* **1942**, *551*, 80.
- [60] A. Williamson, *Liebigs Ann. Chem.* **1851**, *77*, 37.
- [61] I. Fleming, *Molecular Orbitals and Organic Chemical Reactions*, John Wiley & Sons Ltd: Chichester, West Sussex, United Kingdom, **2002**.
- [62] O. Diels, K. Alder, *Liebigs Ann. Chem.* **1928**, *460*, 98
- [63] For reviews on the asymmetric catalysis of cycloadditions, see: (a) H. B. Kagan, O. Riant, *Chem. Rev.* **1992**, *92*, 1007. (b) K. V. Gothelf, K. A. Jørgensen, *Chem. Rev.* **1998**, *98*, 863. (c) K. A. Jørgensen, *Angew. Chem.* **2000**, *112*, 3702; *Angew. Chem. Int. Ed.* **2000**, *39*, 3558. (d) E. J. Corey, *Angew. Chem.* **2002**, *114*, 1724; *Angew. Chem. Int. Ed.* **2002**, *41*, 1650. (e) L. M. Stanley, M. P. Sibi, *Chem. Rev.* **2008**, *108*, 2887. f) S. Kobayashi, K. A. Jørgensen (Eds.), *Cycloaddition Reactions in Organic Synthesis*, Wiley-VCH: Weinheim, **2002**.
- [64] L. Claisen, *Ber. Dtsch. Chem. Ges.* **1912**, *45*, 3157.
- [65] A. C. Cope, E. M. Hardy, *J. Am. Chem. Soc.* **1940**, *62*, 441.
- [66] For reviews, see: (a) M. Hiersemann, U. Nubbemeyer (Eds.), *The Claisen Rearrangement*, Wiley-VCH: Weinheim, **2007**; (b) M. Hiersemann, L. Abraham, *Eur. J.*

- Org. Chem.* **2002**, 1461. (c) U. Nubbemeyer, *Synthesis* **2003**, 961. (d) A. M. Martín Castro, *Chem. Rev.* **2004**, *104*, 2939.
- [67] A. McNally, B. Evans, M. J. Gaunt, *Angew. Chem.* **2006**, *118*, 2170; *Angew. Chem. Int. Ed.* **2006**, *45*, 2116.
- [68] S. Kobbelgaard, S. Brandes, K. A. Jørgensen, *Chem. Eur. J.* **2008**, *14*, 1464.
- [69] C. Uyeda, E. N. Jacobsen, *J. Am. Chem. Soc.* **2008**, *130*, 9228.
- [70] M. Rueping, A. P. Antonchick, *Angew. Chem.* **2008**, *120*, 10244; *Angew. Chem. Int. Ed.* **2008**, *47*, 10090.
- [71] For a review on biosynthetic and biomimetic electrocyclizations, see: C. M. Beaudry, J. P. Malerich, D. Trauner, *Chem. Rev.* **2005**, *105*, 4757.
- [72] T. Nakatsuka, Y. Hirose, *Bull. Agric. Chem. Soc. Jpn.* **1956**, *20*, 215.
- [73] A. G. Hortmann, *Tetrahedron Lett.* **1968**, *9*, 5785.
- [74] For a review, see: A. J. Frontiera, C. Collison, *Tetrahedron* **2005**, *61*, 7577.
- [75] (a) G. Liang, S. N. Gradl, D. Trauner, *Org. Lett.* **2003**, *5*, 4931. (b) G. Liang, D. Trauner, *J. Am. Chem. Soc.* **2004**, *126*, 9544.
- [76] V. K. Aggarwal, A. J. Belfield, *Org. Lett.* **2003**, *5*, 5075.
- [77] (a) M. Rueping, W. leawsuwan, A. P. Antonchick, B. J. Nachtsheim, *Angew. Chem.* **2007**, *119*, 2143; *Angew. Chem. Int. Ed.* **2007**, *46*, 2097. (b) M. Rueping, W. leawsuwan, *Adv. Synth. Catal.* **2009**, *351*, 78.
- [78] For a review including organocatalytic and metall-catalyzed versions, see: N. Shimada, C. Stewart, M. A. Tius, *Tetrahedron* **2011**, *67*, 5851.
- [79] L. M. Bishop, J. E. Barbarow, R. G. Bergman, D. Trauner, *Angew. Chem.* **2008**, *120*, 8220; *Angew. Chem. Int. Ed.* **2008**, *47*, 8100.
- [80] K. Alder, F. Pascher, A. Schmitz, *Ber. Dtsch. Chem. Ges.* **1943**, *76*, 27.
- [81] M. Terada, in *Science of Synthesis 3: Stereoselective Percyclic Reactions, Cross Coupling, and C-H and C-X Activation*, P. A. Evans (Ed.), Thieme, Stuttgart, **2011**, pp. 309-346.
- [82] W. von E. Doering, W. R. Roth, *Tetrahedron* **1962**, *18*, 67.
- [83] R. B. Woodward, R. Hoffmann, *Angew. Chem.* **1969**, *81*, 797; *Angew. Chem. Int. Ed.* **1969**, *8*, 781.
- [84] R. E. K. Winter, *Tetrahedron Lett.* **1965**, *6*, 1207.
- [85] K. Fukui, T. Yonezawa, H. Shingu, *J. Chem. Phys.* **1952**, *20*, 722.

- [86] C. W. Jefford, G. Bernardinelli, Y. Wang, D. C. Spellmeyer, A. Buda, K. N. Houk, *J. Am. Chem. Soc.* **1992**, *114*, 1157.
- [87] E. Fischer, F. Jourdan, *Ber. Dtsch. Chem. Ges.* **1883**, *16*, 2241.
- [88] E. Fischer, O. Hess, *Ber. Dtsch. Chem. Ges.* **1884**, *17*, 559.
- [89] G. M. Robinson, R. Robsinon, *J. Chem. Soc., Trans.* **1924**, *125*, 827.
- [90] For reviews, see: (a) B. Robinson, *Chem. Rev.* **1963**, *63*, 373. (b) B. Robinson, *Chem. Rev.* **1969**, *69*, 227. (c) B. Robinson, *The Fischer Indole Synthesis*; Wiley-Interscience: New York, USA, **1982**.
- [91] (a) G. W. Gribble, *Contemp. Org. Synth.* **1994**, *1*, 145. (b) G. W. Gribble, *J. Chem. Soc., Perkin Trans. 1* **2000**, 1045. (c) G. R. Humphrey, J. T. Kuethe, *Chem. Rev.* **2006**, *106*, 2875.
- [92] (a) S. Wagaw, B. H. Yang, S. L. Buchwald, *J. Am. Chem. Soc.*, **1998**, *120*, 6621. (b) S. Wagaw, B. H. Yang, S. L. Buchwald, *J. Am. Chem. Soc.* **1999**, *121*, 10251.
- [93] (a) O. Miyata, Y. Kimura, K. Muroya, H. Hiramatsu, T. Naito, *Tetrahedron Lett.* **1999**, *40*, 3601. (b) O. Miyata, Y. Kimura, T. Naito, *Synthesis* **2001**, 1635. (c) O. Miyata, N. Takeda, Y. Kimura, Y. Takemoto, N. Tohnai, M. Miyatac, T. Naito, *Tetrahedron* **2006**, *62*, 3629.
- [94] G. Stork, J. E. Dolfini, *J. Am. Chem. Soc.* **1963**, *85*, 2872.
- [95] K. G. Liu, A. J. Robichaud, *Tetrahedron Lett.* **2007**, *48*, 461.
- [96] K. G. Liu, A. J. Robichaud, J. R. Lo, J. F. Mattes, Y. Cai, *Org. Lett.* **2006**, *8*, 5769.
- [97] I. I. Grandberg, T. I. Zuyanova, N. I. Afonina, T. A. Ivanova, *Dokl. Akad. Nauk SSSR* **1967**, *176*, 583.
- [98] R. Tsuji, M. Nakagawa, A. Nishida, *Heterocycles* **2002**, *58*, 587.
- [99] A. Nishida, S. Ushigome, A. Sugimoto, S. Arai, *Heterocycles* **2005**, *66*, 181.
- [100] P. Rosenmund, E. Sadri, *Liebigs Ann. Chem.* **1979**, 927.
- [101] B. W. Boal, A. W. Schammel, N. K. Garg, *Org. Lett.* **2009**, *11*, 3458.
- [102] A. W. Schammel, B. W. Boal, L. Zu, T. Mesganaw, N. K. Garg, *Tetrahedron* **2010**, *66*, 4687.
- [103] For a review, see: H.-J. Knölker, K. R. Reddy, in *The Alkaloids: Chemistry and Biology*; G. A. Cordell (Ed.); Academic Press: San Diego, **2008**; Vol. 65, pp 181-193.

- [104] I. Brackenridge, C. Spray, S. McIntyre, J. Knight, D. Hartley, *Process for the Production of (R)-(+)-6-Carboxamido-3-N-methylamino-1,2,3,4-tetrahydrocyrbazole*, WO 9954302, **1998**.
- [105] (a) E. Palaska, D. Erol, R. Demirdamar, *Eur. J. Med. Chem.* **1996**, *31*, 43. (b) J. H. M. Lange, H. K. A. C. Coolen, H. H. van Stuivenberg, J. A. R. Dijksman, A. H. J. Herremans, E. Ronken, H. G. Keizer, K. Tipker, A. C. McCreary, W. Veerman, H. C. Wals, B. Stork, P. C. Verveer, A. P. den Hartog, N. M. J. de Jong, T. J. P. Adolfs, J. Hoogendoorn, C. G. Kruse, *J. Med. Chem.* **2004**, *47*, 627. (c) F. Chimenti, A. Bolasco, F. Manna, D. Secci, P. Chimenti, O. Befani, P. Turini, V. Giovannini, B. Mondovì, R. Cirilli, F. La Torre, *J. Med. Chem.* **2004**, *47*, 2071. (d) Y. Rajendra Prasad, A. Lakshmana Rao, L. Prasoon, K. Murali, P. Ravi Kumar, *Bioorg. Med. Chem. Lett.* **2005**, *15*, 5030. (e) N. Gökhan-Keleş, S. Koyunoğlu, S. Yabanoğlu, K. Yelekçi, Ö. Özgen, G. Uçar, K. Erol, E. Kendi, A. Yeşilada, *Bioorg. Med. Chem.* **2009**, *17*, 675. (f) C. D. Cox, M. J. Breslin, B. J. Mariano, P. J. Coleman, C. A. Buser, E. S. Walsh, K. Hamilton, H. E. Huber, N. E. Kohl, M. Torrent, Y. Yan, L. C. Kuo, G. D. Hartman, *Bioorg. Med. Chem. Lett.* **2005**, *15*, 2041. (g) C. D. Cox, M. Torrent, M. J. Breslin, B. J. Mariano, D. B. Whitman, P. J. Coleman, C. A. Buser, E. S. Walsh, K. Hamilton, M. D. Schaber, R. B. Lobell, W. Tao, V. J. South, N. E. Kohl, Y. Yan, L. C. Kuo, T. Prueksaritanont, D. E. Slaughter, C. Li, E. Mahan, B. Lu, G. D. Hartman, *Bioorg. Med. Chem. Lett.* **2006**, *16*, 3175. (h) F. Manna, F. Chimenti, A. Bolasco, M. L. Cenicola, M. D'Amico, C. Parrillo, F. Rossi, E. Marmo, *Eur. J. Med. Chem.* **1992**, *27*, 633. (i) F. Chimenti, B. Bizzarri, F. Manna, A. Bolasco, D. Secci, P. Chimenti, A. Granese, D. Rivanera, D. Lilli, M. M. Scaltrito, M. I. Brenciaglia, *Bioorg. Med. Chem. Lett.* **2005**, *15*, 603. (j) J. R. Goodell, F. Puig-Basagoiti, B. M. Forshey, P.-Y. Shi, D. M. Ferguson, *J. Med. Chem.* **2006**, *49*, 2127. (k) X. Zhang, X. Li, G. F. Allan, T. Sbriscia, O. Linton, S. G. Lundeen, Z. Sui, *J. Med. Chem.* **2007**, *50*, 3857. (l) M. E. Camacho, J. León, A. Entrena, G. Velasco, M. D. Carrión, G. Escames, A. Vivó, D. Acuña-Castroviejo, M. A. Gallo, A. Espinosa, *J. Med. Chem.* **2004**, *47*, 5641.
- [106] E. Fischer, O. Knoevenagel, *Liebigs Ann. Chem.* **1887**, *239*, 194.
- [107] E. Buchner, M. Fritsch, A. Papendieck, H. Witter, *Liebigs Ann. Chem.* **1893**, *273*, 214.
- [108] H. von Pechmann, *Ber. Dtsch. Chem. Ges.* **1894**, *27*, 1888
- [109] For a review on the synthesis of pyrazolines, see: A. Lévai, *J. Heterocycl. Chem.* **2002**, *39*, 1.

- [110] L. Gao, G.-S. Hwang, M. Young Lee, D. H. Ryu, *Chem. Commun.* **2009**, 5460.
- [111] (a) S. Kanemasa, T. Kanai, *J. Am. Chem. Soc.* **2000**, *122*, 10710, (b) M. P. Sibi, L. M. Stanley, T. Soeta *Org. Lett.* **2007**, *9*, 1553.
- [112] R. Shintani, G. C. Fu, *J. Am. Chem. Soc.* **2003**, *125*, 10778.
- [113] T. Kano, T. Hashimoto, K. Maruoka, *J. Am. Chem. Soc.* **2006**, *128*, 2174.
- [114] Y. Yamashita, S. Kobayashi, *J. Am. Chem. Soc.* **2004**, *126*, 11279.
- [115] (a) H. Yanagita, S. Kanemasa, *Heterocycles* **2007**, *71*, 699. (b) For an organocatalytic but racemic version, see: O. Mahé, D. Frath, I. Dez, F. Marsais, V. Levacher, J.-F. Brière, *Org. Biomol. Chem.* **2009**, *7*, 3648.
- [116] H. Ferres, M. S. Hamdam, W. R. Jackson, *J. Chem. Soc. B* **1971**, 1892.
- [117] E. Fischer, *Ber. Dtsch. Chem. Ges.* **1875**, *8*, 589.
- [118] G. B. Rowland, H. Zhang, E. B. Rowland, S. Chennamadhavuni, Y. Wang, J. C. Antilla, *J. Am. Chem. Soc.* **2005**, *127*, 15696.
- [119] (a) X. Cheng, S. Vellalath, R. Goddard, B. List, *J. Am. Chem. Soc.* **2008**, *130*, 15786. (b) M. Rueping, A. P. Antonchick, E. Sugiono, K. Grenader, *Angew. Chem.* **2009**, *121*, 925; *Angew. Chem. Int Ed.* **2009**, *48*, 908.
- [120] G. Li, F. R. Fronczek, J. C. Antilla, *J. Am. Chem. Soc.* **2008**, *130*, 12216.
- [121] S. Vellalath, I. Čorić, B. List, *Angew. Chem.* **2010**, *122*, 9943; *Angew. Chem. Int Ed.* **2010**, *49*, 9749.
- [122] I. Čorić, S. Vellalath, B. List, *J. Am. Chem. Soc.* **2010**, *132*, 8536.
- [123] V. B. Birman, A. L. Rheingold, K.-C. Lam, *Tetrahedron: Asymmetry* **1999**, *10*, 125.
- [124] For a review, see: K. Ding, Z. Han, Z. Wang, *Chem. Asian J.* **2009**, *4*, 32.
- [125] M. Jiang, S.-F. Zhu, Y. Yang, L.-Z. Gong, X.-G. Zhou, Q.-L. Zhou, *Tetrahedron: Asymmetry* **2006**, *17*, 384.
- [126] Y. K. Chung, G. C. Fu, *Angew. Chem.* **2009**, *121*, 2259; *Angew. Chem. Int. Ed.* **2009**, *48*, 2225.
- [127] P. García-García, F. Lay, P. García-García, C. Rabalakos, B. List, *Angew. Chem.* **2009**, *121*, 4427; *Angew. Chem. Int. Ed.* **2009**, *48*, 4363.
- [128] L. Li, D. Seidel, *Org. Lett.* **2010**, *12*, 5064.
- [129] R. Huisgen, *Angew. Chem.* **1980**, *92*, 979; *Angew. Chem. Int. Ed.* **1980**, *19*, 947.
- [130] (a) H. Ahlbrecht, U. Beyer, *Synthesis* **1999**, 365. (b) D. Hoppe, T. Hense, *Angew. Chem.* **1997**, *109*, 2376; *Angew. Chem. Int. Ed.* **1997**, *36*, 2282.

- [131] (a) S. S. Sohn, E. L. Rosen, J. W. Bode, *J. Am. Chem. Soc.* **2004**, *126*, 14370. (b) C. Burstein, F. Glorius, *Angew. Chem.* **2004**, *116*, 6331; *Angew. Chem. Int. Ed.* **2004**, *43*, 6205. (c) Review: V. Nair, S. Vellalath, B. P. Babu, *Chem. Soc. Rev.* **2008**, *37*, 2691.
- [132] For examples, see: (a) B. Cardinal-David, D. E. A. Raup, K. A. Scheidt, *J. Am. Chem. Soc.* **2010**, *132*, 5345. (b) Y. Li, Z.-A. Zhao, H. He, S.-L. You, *Adv. Synth. Catal.* **2008**, *350*, 1885. (c) Y. Matsuoka, Y. Ishida, K. Saigo, *Tetrahedron Lett.* **2008**, *49*, 2985.
- [133] (a) E. J. Corey, R. K. Bakshi, S. Shibata, C. P. Chen, V. K. Singh, *J. Am. Chem. Soc.* **1987**, *109*, 7925. (b) T. Ohkuma, M. Kitamura, R. Noyori, *Tetrahedron Lett.* **1990**, *31*, 5509.
- [134] (a) A.-B. L. Runmo, O. Pàmies, K. Faber, J.-E. Bäckvall, *Tetrahedron Lett.* **2002**, *43*, 2983. (b) A.-B. L. Fransson, L. Borén, O. Pàmies, J.-E. Bäckvall, *J. Org. Chem.* **2005**, *70*, 2582.
- [135] J.-H. Zhang, J. Liao, X. Cui, K.-B. Yu, J. Zhu, J.-G. Deng, S.-F. Zhu, L.-X. Wang, Q.-L. Zhou, L. W. Chung, T. Ye, *Tetrahedron: Asymmetry* **2002**, *13*, 1363.
- [136] Y. Yang, S.-F. Zhu, H.-F. Duan, C.-Y. Zhou, L.-X. Wang, Q.-L. Zhou, *J. Am. Chem. Soc.* **2007**, *129*, 2248.
- [137] K. Sivanandan, S. V. Aathimanikandan, C. G. Arges, C. J. Bardeen, S. Thayumanavan, *J. Am. Chem. Soc.* **2005**, *127*, 2020.
- [138] G. Adair, S. Mukherjee, B. List, *Aldrichimica Acta* **2008**, *41*, 31.
- [139] M. Klussmann, L. Ratjen, S. Hoffmann, V. Wakchaure, R. Goddard, B. List, *Synlett* **2010**, *14*, 2189.
- [140] F. Lay, PhD thesis, Mülheim an der Ruhr, Universität zu Köln, expected **2012**.
- [141] M. Treskow, J. Neudörfl, R. Giernoth, *Eur. J. Org. Chem.* **2009**, 3693.
- [142] (a) M. S. Newman, H. A. Karnes, *J. Org. Chem.* **1966**, *31*, 3980. (b) H. Kwart, E. R. Evans *J. Org. Chem.* **1966**, *31*, 410.
- [143] A. Nishiguchi, K. Maeda, S. Miki, *Synthesis* **2006**, 4131.
- [144] M. Rueping, E. Sugiono, C. Azap, T. Theissmann, M. Bolte, *Org. Lett.* **2005**, *7*, 3781.
- [145] B. Alcaide, M. Miranda, J. Pérez-Castells, C. Polanco, M. A. Sierra, *J. Org. Chem.* **1994**, *59*, 8003.
- [146] D. J. Wallace, D. J. Klauber, C.-y. Chen, R. P. Volante, *Org. Lett.* **2003**, *5*, 4749.
- [147] pKa values in DMSO: (a) F. G. Bordwell, *Acc. Chem. Res.* **1988**, *21*, 456. (b) M. R. Crampton, I. A. Robotham, *J. Chem. Res. (S)* **1997**, 22.
- [148] K. Eastman, P. S. Baran, *Tetrahedron* **2009**, *65*, 3149.

- [149] *N*-Phosphinyl phosphoramides **218** was kindly donated by S. Vellalath from our group, who introduced this catalyst for the direct asymmetric *N,O*-acetalization of aldehydes.^[121]
- [150] For selected examples, see: (a) S. Yamada, I. Chibata, R. Tsurui, *Pharm. Bull. (Japan)* **1953**, *1*, 14. (b) B. Wahab, G. Ellames, S. Passey, P. Watts, *Tetrahedron* **2010**, *66*, 3861. (c) For a review on heterogeneous catalysis of the Fischer indole synthesis, see: R. S. Downing, P. J. Kunkeler, in *Fine Chemicals through Heterogeneous Catalysis*; R. A. Sheldon, H. Bekkum (Eds.), Wiley-VCH: New York, **2001**, pp. 178-183.
- [151] For an example of a study of the effect of varying *N*-benzyl groups in tetrahydrocarbazoles upon biological activity, see: L. Li, C. Beaulieu, M.-C. Carriere, D. Denis, G. Greig, D. Guay, G. O'Neill, R. Zamboni, Z. Wang, *Bioorg. Med. Chem. Lett.* **2010**, *20*, 7462.
- [152] For examples of biologically active 3-aminotetrahydrocarbazoles, see: (a) H. Böshagen, U. Rosentreter, F. Lieb, H. Oediger, F. Seuter, E. Perzborn, V. B. Fiedler, Cycloalkano[1,2-*b*]indole-sulfonamides. EP 0242518, **1987**. (b) P. L. Wood, P. S. McQuade, *Prog. Neuro-Psychopharmacol. Biol. Psychiatry* **1984**, *8*, 773. (c) F. D. King, L. M. Gaster, A. J. Kaumann, R. C. Young, Use of tetrahydrocarbazone derivatives as 5HT₁ receptor agonists. WO 9300086, **1993**.
- [153] N. Çelebi-Ölçüm, B. W. Boal, A. D. Hutters, N. K. Garg, K. N. Houk, *J. Am. Chem. Soc.* **2011**, *133*, 5752.
- [154] D. L. Hughes, *J. Phys. Org. Chem.* **1994**, *7*, 625.
- [155] U. Rosentreter, H. Böshagen, F. Seuter, E. Perzborn, V. B. Fiedler, *Arzneim.-Forsch.* **1989**, *39*, 1519.
- [156] S. Müller, M. J. Webber, B. List, *J. Am. Chem. Soc.* **2011**, *133*, 18534.
- [157] The corresponding SPINOL-derived phosphoric acid **145f** was not yet available when the investigations were conducted and thus was not tested.
- [158] R. Cuberes, J. Berrocal, M. Contijoch, J. Frigola, WO 99/62884, 1999.
- [159] (a) M. Behforouz, J. L. Bolan, M. S. Flynt, *J. Org. Chem.* **1985**, *50*, 1186. (b) S. Faramarz Tayyari, J. L. Speakman, M. B. Arnold, W. Cai, M. Behforouz, *J. Chem. Soc., Perkin Trans. 2* **1998**, 2195. (c) S. Uchiyama, M. Ando, S. Aoyagi, *J. Chromatogr. A* **2003**, *996*, 95. (d) S. Uchiyama, E. Matsushima, S. Aoyagi, M. Ando, *Anal. Chim. Acta* **2004**, *523*, 157.

- [160] (a) J. E. Baldwin, *J. Chem. Soc., Chem. Commun.* **1976**, 734. (b) J. E. Baldwin, R. C. Thomas, L. I. Kruse, L. Silberman, *J. Org. Chem.* **1977**, *42*, 3846.
- [161] Theoretical investigations are ongoing in collaboration with B. Hegen (group of Prof. Dr. W. Thiel).
- [162] 2-Pyrazolines in natural product synthesis: (a) G. A. Whitlock, E. M. Carreira, *J. Org. Chem.* **1997**, *62*, 7916. (b) G. A. Whitlock, E. M. Carreira, *Helv. Chim. Acta* **2000**, *83*, 2007. Reduction of activated 2-pyrazolines: (c) J. M. De los Santos, Y. López, D. Aparicio, F. Palacios, *J. Org. Chem.* **2008**, *73*, 550. Alkylation of 1,3,5-triarylpyrazolines: (d) Y. R. Huang, J. A. Katzenellenbogen, *Org. Lett.* **2000**, *2*, 2833. Nucleophilic additions to 3-unsubstituted 2-pyrazolines: (e) F. M. Guerra, M. R. Mish, E. M. Carreira, *Org. Lett.* **2000**, *2*, 4265.
- [163] H. Nishiyama, H. Arai, Y. Kanai, H. Kawashima, K. Itoh, *Tetrahedron Lett.* **1986**, *27*, 361.
- [164] L. A. Bañuelos, P. Cuadrado, A. M. González-Nogal, I. López-Solera, F. J. Pulido, P. R. Raithby, *Tetrahedron* **1996**, *52*, 9193.
- [165] S. Müller, B. List, *Angew. Chem.* **2009**, *121*, 10160; *Angew. Chem. Int. Ed.* **2009**, *48*, 9975.
- [166] Together with our manuscript, another catalytic asymmetric 6π electrocyclization was published: (a) E. E. Maciver, S. Thompson, M. D. Smith, *Angew. Chem.* **2009**, *121*, 10164; *Angew. Chem. Int. Ed.* **2009**, *48*, 9979. See also: (b) J. L. Vicario, D. Badia, *ChemCatChem* **2010**, *2*, 375.
- [167] S. Müller, B. List, *Synthesis* **2010**, 2171.
- [168] J. M. Keith, J. F. Larrow, E. N. Jacobsen, *Adv. Synth. Catal.* **2001**, *343*, 5.
- [169] (a) P. Somfai, *Angew. Chem.* **1997**, *109*, 2849; *Angew. Chem. Int. Ed.* **1997**, *36*, 2731. (b) E. Vedejs, M. Jure, *Angew. Chem.* **2005**, *117*, 4040; *Angew. Chem. Int. Ed.* **2005**, *44*, 3974.
- [170] For a review, see: R. Kourist, P. Domínguez de María, U. T. Bornscheuer, *ChemBioChem* **2008**, *9*, 491.
- [171] B. List, D. Shabat, G. Zhong, J. M. Turner, A. Li, T. Bui, J. Anderson, R. A. Lerner, C. F. Barbas III, *J. Am. Chem. Soc.* **1999**, *121*, 7283.
- [172] (a) D. J. Schipper, S. Rousseaux, K. Fagnou, *Angew. Chem.* **2009**, *121*, 8493; *Angew. Chem. Int. Ed.* **2009**, *48*, 8343. (b) B. Karatas, S. Rendler, R. Fröhlich, M. Oestreich, *Org. Biomol. Chem.* **2008**, *6*, 1435.

- [173] (a) E. R. Jarvo, C. A. Evans, G. T. Copeland, S. J. Miller, *J. Org. Chem.* **2001**, *66*, 5522. (b) M. C. Angione, S. J. Miller, *Tetrahedron* **2006**, *62*, 5254. (c) Y. Zhao, A. W. Mitra, A. H. Hoveyda, M. L. Snapper, *Angew. Chem.* **2007**, *119*, 8623; *Angew. Chem. Int. Ed.* **2007**, *46*, 8471.
- [174] (a) S.-y. Tosaki, K. Hara, V. Gnanadesikan, H. Morimoto, S. Harada, M. Sugita, N. Yamagiwa, S. Matsunaga, M. Shibasaki, *J. Am. Chem. Soc.* **2006**, *128*, 11776. (b) K. Hara, S.-y. Tosaki, V. Gnanadesikan, H. Morimoto, S. Harada, M. Sugita, N. Yamagiwa, S. Matsunaga, M. Shibasaki, *Tetrahedron* **2009**, *65*, 5030. (c) R. Shintani, K. Takatsu, T. Hayashi, *Org. Lett.* **2008**, *10*, 1191.
- [175] (a) E. Vedejs, X. Chen, *J. Am. Chem. Soc.* **1997**, *119*, 2584. (b) J. R. Dehli, V. Gotor, *Chem. Soc. Rev.* **2002**, *31*, 365.
- [176] P. Walden, *Ber. Dtsch. Chem. Ges.* **1896**, *29*, 133.
- [177] H. C. Brown, S. V. Kulkarni, U. S. Racherla, *J. Org. Chem.* **1994**, *59*, 365.
- [178] D. A. Mulholland, K. McFarland, M. Randrianarivelosia, *Biochem. Syst. Ecol.* **2006**, *34*, 365.
- [179] X.-X. Xu, H.-Q. Dong, *J. Org. Chem.* **1995**, *60*, 3039.
- [180] D. J. Aldous, A. S. Batsanov, D. S. Yufit, A. J. Dalençon, W. M. Dutton, P. G. Steel, *Org. Biomol. Chem.* **2006**, *4*, 2912.
- [181] (a) D. Tobia, B. Rickborn, *J. Org. Chem.* **1986**, *51*, 3849. (b) G. Stork, J. J. La Clair, P. Spargo, R. P. Nargund, N. Totah, *J. Am. Chem. Soc.* **1996**, *118*, 5304.
- [182] R. D. Miller, D. R. McKean, *Tetrahedron Lett.* **1982**, *23*, 323.
- [183] D. S. Brown, M. Bruno, R. J. Davenport, S. V. Ley, *Tetrahedron* **1989**, *45*, 4293.
- [184] T. Esumi, D. Hojyo, H. Zhai, Y. Fukuyama, *Tetrahedron Lett.* **2006**, *47*, 3979.
- [185] A. Ladépêche, E. Tam, J.-E. Ancel, L. Ghosez, *Synthesis* **2004**, 1375.
- [186] (a) E. Ehlinger, P. Magnus, *J. Am. Chem. Soc.* **1980**, *102*, 5004. (b) R. Pedrosa, S. Sayalero, M. Vicente, *Tetrahedron* **2006**, *62*, 10400.
- [187] I. Čorić,† S. Müller,† B. List, *J. Am. Chem. Soc.* **2010**, *132*, 17370. († these authors contributed equally)
- [188] R. A. Glennon, S.-S. Hong, M. Bondarev, H. Law, M. Dukat, S. Rakhit, P. Power, E. Fan, D. Kinneau, R. Kamboj, M. Teitler, K. Herrick-Davis, C. Smith, *J. Med. Chem.* **1996**, *39*, 314.
- [189] H. E. Zimmerman, G. Jones II, *J. Am. Chem. Soc.* **1970**, *92*, 2753.

- [190] (a) F. R. Japp, J. Knox, *J. Chem. Soc., Trans.* **1905**, 87, 673. (b) D. J. Arriola, M. Bokota, R. E. Campbell Jr., J. Klosin, R. E. LaPointe, O. D. Redwine, R. B. Shankar, F. J. Timmers, K. A. Abboud, *J. Am. Chem. Soc.* **2007**, 129, 7065.
- [191] E. J. Corey, H. Uda, *J. Am. Chem. Soc.* **1963**, 85, 1788.
- [192] I.-K. Park, S.-E. Suh, B.-Y. Lim, C.-G. Cho, *Org. Lett.* **2009**, 11, 5454.
- [193] R. B. Perni, G. W. Gribble, *Org. Prep. Proced. Int.* **1982**, 14, 343.
- [194] U. Lerch, J. König, *Synthesis* **1983**, 157.
- [195] K. Zumbansen, A. Döring, B. List, *Adv. Synth. Catal.* **2010**, 352, 1135.
- [196] M. Stadler, B. List, *Synlett* **2008**, 597.
- [197] (a) M. J. Hearn, S. A. Lebold, A. Sinha, K. Sy, *J. Org. Chem.* **1989**, 54, 4188. (b) M. Harej, D. Dolenc, *J. Org. Chem.* **2007**, 72, 7214.
- [198] J. Barluenga, J. R. Fernández, C. Rubiera, M. Yus, *J. Chem. Soc., Perkin Trans. 1*, **1988**, 3113.
- [199] G. Picotin, P. Miginiac, *Chem. Ber.* **1986**, 119, 1725.
- [200] (a) L. Ratjen, P. García-García, F. Lay, M. E. Beck, B. List, *Angew. Chem.* **2011**, 123, 780; *Angew. Chem. Int. Ed.* **2011**, 50, 754. (b) Y. Zhang, F. Lay, P. García-García, B. List, E. Y.-X. Chen, *Chem. Eur. J.* **2010**, 16, 10462. (c) S. Ban, D.-M. Du, H. Liu, W. Yang, *Eur. J. Org. Chem.* **2010**, 5160. (d) C. Luo, D.-M. Du, *Synthesis* **2011**, 1968. (e) L.-Y. Chen, H. He, W.-H. Chan, A. W. M. Lee, *J. Org. Chem.* **2011**, 76, 7141.
- [201] A. Pinto, Max-Planck-Institut für Kohlenforschung, Mülheim an der Ruhr, *unpublished results*.
- [202] (a) S. Mayer, B. List, *Angew. Chem.* **2006**, 118, 4299; *Angew. Chem. Int. Ed.* **2006**, 45, 4193. (b) G. L. Hamilton, E. J. Kang, M. Mba, F. D. Toste, *Science* **2007**, 317, 496. (c) S. Mukherjee, B. List, *J. Am. Chem. Soc.* **2007**, 129, 11336.
- [203] G. Jiang, B. List, *Chem. Commun.* **2011**, 47, 10022.
- [204] (a) T. Sheradeky, *Tetrahedron Lett.* **1966**, 7, 5225. (b) A. Mooradian, P. E. Dupont, *Tetrahedron Lett.* **1967**, 8, 2867. (c) see also: N. Takeda, O. Miyata, T. Naito, *Eur. J. Org. Chem.* **2007**, 1491 (and references therein).
- [205] (a) T. Akiyama, Y. Tamura, J. Itoh, H. Morita, K. Fuchibe, *Synlett* **2006**, 141. (b) G. Li, J. C. Antilla, *Org. Lett.* **2009**, 11, 1075. (c) N. Momiyama, H. Nishimoto, M. Terada, *Org. Lett.* **2011**, 13, 2126.

- [206] P. M. Dinh, J. A. Howarth, A. R. Hudnott, J. M. J. Williams, W. Harris, *Tetrahedron Lett.* **1996**, *37*, 7623.
- [207] A. L. E. Larsson, B. A. Person, J.-E. Bäckvall, *Angew. Chem.* **1997**, *109*, 1256; *Angew. Chem. Int. Ed.* **1997**, *36*, 1211.
- [208] B. A. Persson, A. L. E. Larsson, M. Le Ray, J.-E. Bäckvall, *J. Am. Chem. Soc.* **1999**, *121*, 1645.
- [209] (a) J. H. Choi, Y. H. Kim, S. H. Nam, S. T. Shin, M.-J. Kim, J. Park, *Angew. Chem.* **2002**, *114*, 2479; *Angew. Chem. Int. Ed.* **2002**, *41*, 2373. (b) J. H. Choi, Y. K. Choi, Y. H. Kim, E. S. Park, E. J. Kim, M.-J. Kim, J. Park, *J. Org. Chem.* **2004**, *69*, 1972. (c) B. Martín-Matute, M. Edin, K. Bogár, J.-E. Bäckvall, *Angew. Chem.* **2004**, *116*, 6697; *Angew. Chem. Int. Ed.* **2004**, *43*, 6535.
- [210] Y. Do, I.-C. Hwang, M.-J. Kim, J. Park, *J. Org. Chem.* **2010**, *75*, 5740.
- [211] W. Francke, W. Kitching, *Curr. Org. Chem.* **2001**, *5*, 233.
- [212] (a) M. F. Jacobs, W. Kitching, *Curr. Org. Chem.* **1998**, *2*, 395. (b) J. E. Aho, P. M. Pihko, T. K. Rissa, *Chem. Rev.* **2005**, *105*, 4406.
- [213] W. L. F. Armarego, C. L. L. Chai, *Purification of Laboratory Chemicals*; 5th Ed., Butterworth-Heinemann, Oxford, **2003**.
- [214] (a) K. B. Simonsen, K. V. Gothelf, K. A. Jørgensen, *J. Org. Chem.* **1998**, *63*, 7536. (b) P. Wipf, J.-K. Jung, *J. Org. Chem.* **2000**, *65*, 6319.
- [215] S. S. Zhu, D. R. Cefalo, D. S. La, J. Y. Jamieson, W. M. Davis, A. H. Hoveyda, R. R. Schrock, *J. Am. Chem. Soc.* **1999**, *121*, 8251.
- [216] G. Pousse, A. Devineau, V. Dalla, L. Humphreys, M.-C. Lasne, J. Rouden, J. Blanchet, *Tetrahedron* **2009**, *65*, 10617.
- [217] D. Kampen, *Brønsted-Säure-katalysierte Hosomi-Sakurai-Reaktionen und Prolin-katalysierte Mannich-Reaktion von Acetaldehyd*, PhD Thesis, Universität zu Köln, **2009**.
- [218] F. Xu, D. Huang, C. Han, W. Shen, X. Lin, Y. Wang, *J. Org. Chem.* **2010**, *75*, 8677.
- [219] H. Jackman, S. P. Marsden, P. Shapland, S. Barrett, *Org. Lett.* **2007**, *9*, 5179.
- [220] The synthesis was performed by B. Bechi.
- [221] The synthesis was performed by Dr. M. J. Webber.
- [222] J. P. Guthrie, X.-P. Wang, *Cand. J. Chem.* **1992**, *70*, 1055.
- [223] The synthesis was performed by I. Čorić.

9 Appendix

9.1 Erklärung

„Ich versichere, dass ich die von mir vorgelegte Dissertation selbständig angefertigt, die benutzten Quellen und Hilfsmittel vollständig angegeben und die Stellen der Arbeit - einschließlich Tabellen, Karten und Abbildungen -, die anderen Werken im Wortlaut oder dem Sinn nach entnommen sind, in jedem Einzelfall als Entlehnung kenntlich gemacht habe; dass diese Dissertation noch keiner anderen Fakultät oder Universität zur Prüfung vorgelegen hat; dass sie - abgesehen von unten angegebenen Teilpublikationen - noch nicht veröffentlicht worden ist sowie, dass ich eine solche Veröffentlichung vor Abschluss des Promotionsverfahrens nicht vornehmen werde. Die Bestimmungen dieser Promotionsordnung sind mir bekannt. Die von mir vorgelegte Dissertation ist von Prof. Dr. Benjamin List betreut worden.“

Mülheim an der Ruhr, Januar 2012

Bisher sind folgende Teilpublikationen veröffentlicht worden:

“A Catalytic Asymmetric 6π Electrocyclization: Enantioselective Synthesis of 2-Pyrazolines”, S. Müller, B. List, *Angew. Chem.* **2009**, *121*, 10160-10163; *Angew. Chem. Int. Ed.* **2009**, *48*, 9975-9978.

“Catalytic Asymmetric 6π -Electrocyclization: Accessing Highly Substituted Optically Active 2-Pyrazolines via Diastereoselective Alkylations”, S. Müller, B. List, *Synthesis* **2010**, 2171-2178.

“Kinetic Resolution of Homoaldols via Catalytic Asymmetric Transacetalization”, I. Čorić,† S. Müller,† B. List, *J. Am. Chem. Soc.* **2010**, *132*, 17370-17373. († these authors contributed equally)

“The Catalytic Asymmetric Fischer Indolization”, S. Müller, M. J. Webber, B. List, *J. Am. Chem. Soc.* **2011**, *133*, 18534-18537.

9.2 Lebenslauf

Steffen Müller

Geboren am 9. August 1982 in Einbeck

Staatsangehörigkeit: Deutsch

Akademischer Werdegang

- 02/2008-01/2012 **Promotion** am Max-Planck-Institut für Kohlenforschung in Mülheim an der Ruhr unter der Anleitung von Prof. Dr. B. List zum Thema: "The Catalytic Asymmetric Fischer Indolization and Beyond"
Kekulé-Stipendium der Stiftung Stipendien-Fonds des Verbandes der Chemischen Industrie e.V.
- 02/2007-11/2007 **Diplomarbeit** an der Bayerischen Julius-Maximilians-Universität in Würzburg unter der Anleitung von Prof. Dr. Dr. h.c. G. Bringmann zum Thema "QSAR-geleitete Synthese vereinfachter Dioncophyllin-C-Derivate mit antiplasmodialer Aktivität"
Fakultätspreis der Fakultät für Chemie und Pharmazie der Bayerischen Julius-Maximilians-Universität Würzburg für "hervorragende Leistungen beim Diplom"
- 04/2003-11/2007 **Studium** der Chemie an der Bayerischen Julius-Maximilians-Universität in Würzburg
Notendurchschnitt Vordiplom: 1,32 (sehr gut)
Notendurchschnitt Diplom: 1,07 (sehr gut)
Jubiläums-Stipendium der Stiftung Stipendien-Fonds des Verbandes der Chemischen Industrie e.V.

Wehrdienst

- 07/2002-03/2003 Wehrdienst im 3./PzPiBtl 1 in Holzminden und im 1./NschBtl 12 in Veitshöchheim

Schulausbildung

- 08/1995-06/2002 Paul-Gerhardt-Schule in Dassel
Allgemeine Hochschulreife, Notendurchschnitt: 1,3
- 08/1989-07/1995 Grundschule in Sievershausen und Orientierungsstufe in Dassel